

Joint
Transportation
Research
Program

JTRP

FHWA/IN/JTRP-98/17

Final Report

**PERFORMANCE OF BRIDGE DECKS AND GIRDERS
WITH LIGHTWEIGHT AGGREGATE CONCRETE**

Volume 2 of 2

**Julio Ramirez
Jan Olek
Eric Rolle
Brian Malone**

October 2000

**Indiana
Department
of Transportation**

**Purdue
University**

Final Report

FHWA/IN/JTRP-98/17

**PERFORMANCE OF BRIDGE DECKS AND GIRDERS WITH
LIGHTWEIGHT AGGREGATE CONCRETE
(Volume 2 of 2)**

Julio A. Ramirez
and
Jan Olek
Principal Investigators

and

Eric Rolle
and
Brian Malone
Research Assistants

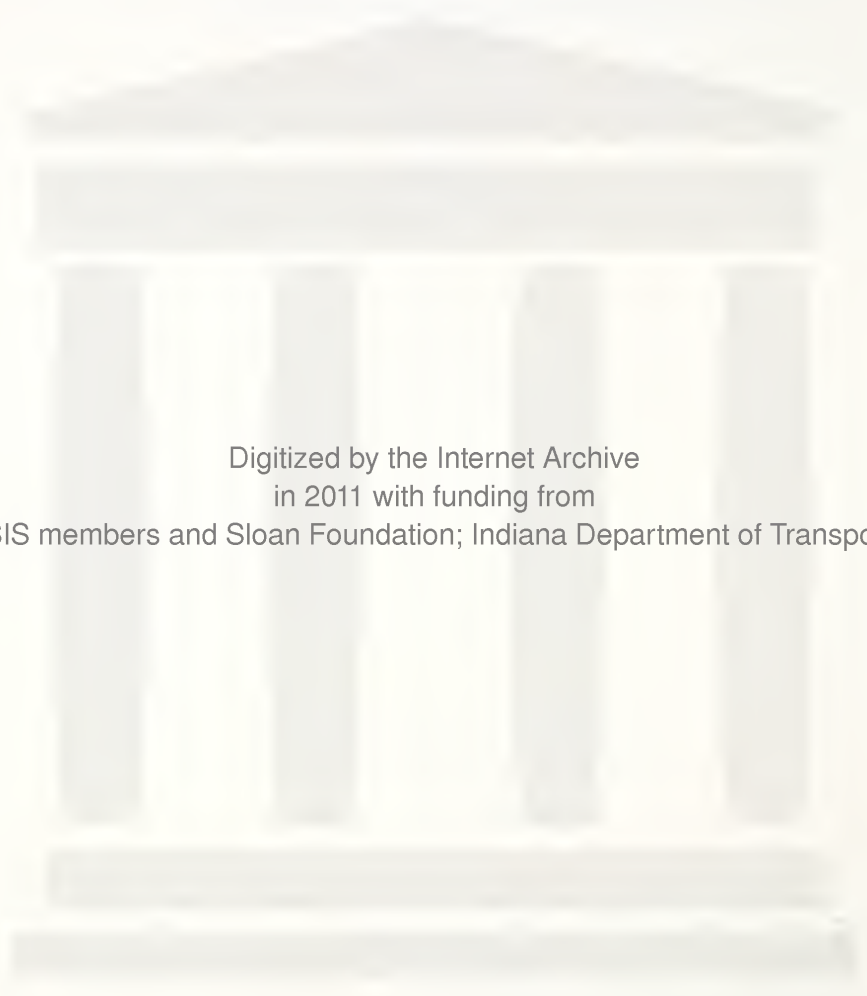
School of Civil Engineering
Purdue University

Joint Highway Research Program
Project Number: C-36-56MM
File Number: 7-4-39

Conducted in Cooperation with the
Indiana Department of Transportation
and the
Federal Highway Administration

The contents of this report reflect the views of the authors, who are responsible for the facts and the accuracy of the data presented herein. The contents do not necessarily reflect the views or policies of the Federal Highway Administration and the Indiana Department of Transportation. This report does not constitute a standard, specification, or regulation.

Purdue University
West Lafayette, IN 47907
October 2000



Digitized by the Internet Archive
in 2011 with funding from
LYRASIS members and Sloan Foundation; Indiana Department of Transportation

1. Report No. FHWA/IN/JTRP-98/17	2. Government Accession No.	3. Recipient's Catalog No.	
4. Title and Subtitle Performance of Bridge Decks and Girders with Lightweight Aggregate Concrete (2 Volumes)		5. Report Date October 2000	
		6. Performing Organization Code	
7. Author(s) Julio Ramirez, Jan Olek, Eric Rolle, and Brian Malone		8. Performing Organization Report No. FHWA/IN/JTRP-98/17	
9. Performing Organization Name and Address Joint Transportation Research Program 1284 Civil Engineering Building Purdue University West Lafayette, Indiana 47907-1284		10. Work Unit No.	
		11. Contract or Grant No. SPR-2131	
12. Sponsoring Agency Name and Address Indiana Department of Transportation State Office Building 100 North Senate Avenue Indianapolis, IN 46204		13. Type of Report and Period Covered Final Report	
		14. Sponsoring Agency Code	
15. Supplementary Notes Prepared in cooperation with the Indiana Department of Transportation and Federal Highway Administration.			
<p>16. Abstract</p> <p>Structural lightweight concrete is a very versatile material and Haydite and Minergy lightweight aggregates can be utilized in the mixture development of concrete for use in girders and decks in bridges. More widespread use of lightweight aggregates (LWA) would result in savings in construction cost due to considerable dead load reduction.</p> <p>The materials phase of this research study evaluated the fresh concrete properties (slump, unit weight, and air content), the mechanical properties of hardened concrete (compressive strength, tensile strength, flexural strength, static and dynamic modulus of elasticity, Poisson's Ratio, and temperature development), and durability related parameters (air void distribution, freeze-thaw resistance, chloride permeability, resistance to scaling, and drying shrinkage). In addition, selected properties (24-hour absorption, bulk specific gravity, size distribution, and internal pore structure) of the lightweight aggregates were also determined.</p> <p>Lightweight aggregate mixes used in this study were proportioned using water-cement ratio/strength method in order to better address the issue of producing mixes that would satisfy both durability and strength requirements. Target compressive strengths for bridge girder concrete were 42 and 69 MPa (6000 and 10,000 psi), and 31 MPa (4500 psi) in the case of bridge deck concrete.</p> <p>In the structural phase of the study the shear strength of reinforced and prestressed concrete lightweight concrete (LWC) beams was evaluated. In the Kettelhut Structural Engineering Laboratory twelve reinforced and four prestressed concrete beams were tested to failure. The experimental shear capacities were compared to calculated shear strength values from the 1995 American Concrete Institute Building Code and the 1994 AASHTO LRFD Standard Specifications.</p> <p>Based on the test results from this study it is recommended that water-cementitious ratio be used for proportioning of lightweight concrete mixes and that trial batches be prepared and tested before actual field application. To ensure adequate durability, lightweight aggregate concrete should be allowed to dry before exposing it to cycles of freezing and thawing. On the structural side, both the ACI and the AASHTO LRFD Specifications were found to yield conservative estimates of the shear strength of LWC reinforced and prestressed beams provided adequate detailing of the reinforcement is provided. More work is needed regarding the minimum amount of shear reinforcement for high strength lightweight concrete beams.</p>			
17. Key Words concrete, lightweight aggregate, shear, strength, durability, freeze-thaw, mix proportioning, properties bridges, beams, reinforced, prestressed.		18. Distribution Statement No restrictions. This document is available to the public through the National Technical Information Service, Springfield, VA 22161	
19. Security Classif. (of this report) Unclassified	20. Security Classif. (of this page) Unclassified	21. No. of Pages 616 (2 volumes)	22. Price

CHAPTER 6. RESULTS AND DISCUSSION

6.1 Properties of Fresh Concrete

From a practical point of view it is desirable that the slump of concrete be in the range of 100-200 mm (4-8 in). The mixture proportions were adjusted accordingly for all the trial batches at the precast plant to procure concrete in the desired slump range. The high strength LWC mixes needed a high dosage of HRWR in order to achieve adequate workability. Because of that, these mixes were stickier than the other mixes. The mixes with silica fume required more HRWR than those with fly ash. Tables 6.1-6.4 shows the fresh concrete properties data of all concrete mixes used in this test program.

Although both lightweight aggregates produced very workable concrete, in general, concrete produced with Minergy aggregate was more workable than concrete produced with Haydite aggregate at the same water-cement ratio and the same dosage of HRWR. The concrete produced using Minergy aggregate also required less HRWR to achieved the same slump. This is because the texture and shape of the aggregates are very different. The Minergy aggregate is round and smooth, whereas the Haydite is angular and rough. Therefore, it would be expected that there would be less frictional resistance between the Minergy aggregate and the other concrete constituents. The average slump of concrete obtained at the precast plant was 150 mm (6 in.) and facilitated easy vibration around rebars and prestressing tendons.

The air contents for the concrete were all within 4-6% range recommended for application where frost resistance is required.

In order to achieve the strength of 69 MPa (10,000 psi) LWC, the unit weight of concrete had to be in the 1928 kg/m³ (120 pcf) range. Concrete with fresh unit weights below 1928 kg/m³ (120 pcf) could not achieve the target compressive strength. Unit weights of concrete made with Minergy lightweight aggregate were much higher than that of concrete made with Haydite aggregate. The specific gravity of Minergy lightweight aggregate is higher and this contributed to higher unit weights of concrete. The semi-lightweight concrete mixes had unit weights in the 2009-2089 kg/m³ (125-130 pcf) range due to the use of the heavier crushed limestone aggregate.

6.2 Properties of Hardened Concrete

This section contains the results of compressive, flexural, and tensile strengths, static and dynamic moduli of elasticity, Poisson's Ratio, density of hardened concrete, and temperature development of all the concrete mixes tested.

6.2.1 Compressive Strength

This section contains the compressive strength results for concrete mixes developed.

6.2.1.1 Girder Mixes

The results for compressive strength of girder mixes are given in Tables 6.5-6.6, and Figures 6.1-6.2.

The LWCH, LWCMI, and NWC concrete mixes achieved the desired 28 day compressive strength of 42 MPa (6000 psi). The NWC, LWCHS, LWCHLS, and LWCHL concrete mixes achieved the desired 28 day compressive strength of 69 MPa

(10,000 psi). In the development of a 69 MPa (10,000 psi) concrete using Minergy LWA, the desired compressive strength was not achieved even at a water-cement ratio of 0.3. The various combinations of silica fume and fly ash in concrete mixes were also unsuccessful in achieving the desired compressive strengths. Based on the compressive strength results for the girder concrete mixes, silica fume was the most effective as a mineral admixture in achieving the high strength desired. Fly ash was effective in providing good workability in the concrete mixes but did not help in strength development (Figure 6.3). From the results we can see that the addition of 10 % silica fume by weight of cement is more effective than replacement of silica fume.

For LWC, the 69 MPa (10,000psi) strength could not be achieved using a water-cement ratio higher 0.33. Some mixes were prepared at a water-cement ratio of 0.35, but the compressive strength results were unsatisfactory.

Comparing the compressive strength results for concrete made with Type III and Type I (using both Haydite and normal weight aggregates) we see that the desired results could not be achieved using Type I cement (Table 6.7 and Figure 6.4). The results for the Type I concrete mixes were based on an average of two trial mixes. In both mixes the 1 day compressive strengths were adequate for releasing of prestressing tendons. The 28 day compressive strengths for the LWC with Type I cement was 26 % lower than its counterpart using Type III cement. In the case of the NWC, the 28 day compressive strength of the concrete using Type I cement was 9% lower than Type III cement mix.

6.2.1.2 Deck Mixes

The compressive strengths for the deck mixes are presented in Table 6.8 and Figure 6.5. The compressive strengths of the newly developed concrete mixes for bridge decks were on average slightly higher than the reference concrete mixes. When a water-cement ratio of 0.42 was used for the LWCHF concrete mix, the 28 day target compressive strength could not be achieved. A water-cement ratio of 0.40 was adopted and resulted in a satisfactory 28 day compressive strength. The LWCHF reference concrete mix did not produce the desired results and fell way below the target compressive strength of 31 MPa (4500 psi).

Based on the results presented, using a water-cement ratio of 0.42 and 0.40 in the case of LWCHF concrete yielded much better results than concrete with a water-cement ratio of 0.443.

6.2.2 Flexural Strength

The flexural strength results are presented in Tables 6.9-6.11 and Figures 6.6-6.8. The flexural strengths for NWC were in the range expected for typical expected and were higher than those for LWC. Concrete made with Minergy LWA showed slightly higher flexural strengths than concrete made with Haydite LWA. The flexural strengths for the reference deck concrete mixes made with Haydite LWA were lower than newly developed deck mixes with the same aggregate. However, the newly developed and reference NWC mixes had similar flexural strengths.

Based on the results it can be concluded that LWC has comparable flexural strengths with that of NWC. The difference in flexural strengths of Haydite and Minergy

aggregate concrete may be due to the maximum size of the aggregate, density, shape, and texture of the two aggregates.

6.2.3 Split Tensile Strength

Determination of split tensile strength was conducted according to ASTM C 496 and the results are presented in Table 6.12-6.14 and Figures 6.9-6.11.

The results indicate that LWC has comparable split tensile strengths to that of NWC. For the 69 MPa (10,000 psi) concrete there is even less of a difference in tensile strengths for LWC and NWC. Bridge girder concrete made with Minergy LWA showed slightly higher tensile strengths than concrete made with Haydite LWA. As expected the NWC produced higher tensile strengths.

The split tensile strengths determined for bridge decks made with LWC and NWC concrete showed some differences. The bridge deck concrete made with Haydite LWA had higher split tensile strengths than concrete made with Minergy LWA. The LWCHS and LWCHF newly developed deck concrete mixes had higher split tensile strengths than the companion reference concrete mixes. The reference NWC mix had a higher tensile strength than the newly developed NWC mix. The split tensile strength results for the LWCH deck mix series were the same. The higher split tensile strength results for the newly developed LWCHS and LWCHF concrete mixes can be explained by the lower water-cementitious ratio.

6.2.4 Static and Dynamic Modulus of Elasticity, and Poisson's Ratio

The results for static and dynamic modulus of elasticity and Poisson's ratio are presented in Tables 6.15-6.17 and Figures 6.13-6.14. The static and dynamic moduli of elasticity for the NWC were higher than the LWC. The static and dynamic moduli of elasticity for Haydite and Minergy LWC were also dissimilar with Minergy LWC producing higher values.

The dynamic moduli for the girder mixes were in general higher than the static modulus. The difference between the dynamic and static moduli for the LWCH, LWCHS, and LWCMI girder mixes were very small. This may have been due to insufficient drying of the samples before determining the static modulus of elasticity. The measured static modulus may have been higher because of the wet condition of the concrete samples. It has been reported that regardless of mixture proportions or curing age, concrete samples that are tested in a wet condition show that the static modulus of elasticity is about 15% higher than the static modulus of elasticity for samples tested in dry condition [Mehta and Monteiro, 1993, Mindess and Young, 1982,].

The dynamic moduli for the deck concrete were in general higher than the static modulus except in the case of the LWCH, NWC, and LWCMI series. The static and dynamic moduli of elasticity for the newly developed mixes were higher than the results for reference mixes. The difference between the dynamic and static modulus was 6.5 % and 8 % for girder and deck concrete mixes respectively.

Poisson's ratio for the girder and deck concrete mixes was in the range 0.13 to 0.22. The NWC mixes had higher values of Poisson's ratio than the LWC mixes. The deck mixes had on average higher values of Poisson's ratio than the girder mixes. There

were no significant differences in the values of Poisson's ratio for concrete made with Haydite and Minergy aggregates.

6.2.5 Density of Hardened Concrete

The densities of the concrete mixes are presented in Tables 6.18-6.20 and Figures 6.15-6.16. In general, the densities of hardened LWC were all within the specified range of 1607-1848 kg/m³ (100-115 pcf). The average density of hardened concrete made with Minergy aggregate was 1944 kg/m³ (121 pcf), only slightly higher than the 1848 kg/m³ (115 pcf) and therefore can find use when LWC is specified with densities in the aforementioned range.

There was on average a 6 % difference between fresh and hardened densities for LWC and a 2 % difference in the case of NWC. There was a 7 % difference between fresh and hardened densities for the newly developed deck mixes made with Haydite aggregate and a 6 % difference in the case of the reference mixes. There was a 7% difference between fresh and hardened densities of concrete made with Minergy aggregate.

6.2.6 Temperature Development

The temperature evolution of high strength LWC samples was evaluated in order to determine the effect of relatively high content of cement in these samples on the potential for thermal cracking. These results obtained from 15 cm x 30 cm (6 in. x 12 in.) samples are given in Figure 6.17. Samples 1 and 2 were sealed in the styrofoam containers and sample 3 was left exposed in the laboratory. The temperature variations

for samples 1 and 2 are very similar with peak temperatures of 69°C and 68°C, respectively. The peak temperature for the laboratory exposed cylinder (sample 3) was 45°C.

Although the experiment did not account for variations in ambient temperature that may be encountered in the field, it does provide a reasonable close approximation of the temperature one can expect inside the beam. Since the recorded temperature development in the high strength LWC mix with 428 kg (950 lbs) of Type III cement did not exceed 70°C it was concluded that the beam produced using these mixes should not experience thermal cracking problems.

6.3 Durability Properties

This section contains the results for air void distribution, drying shrinkage, freeze thaw resistance, rapid chloride ion permeability, and resistance to scaling. Air void distribution and scaling resistance tests were conducted only on bridge deck concrete.

6.3.1 Air Void Distribution

The results for the air void distribution tests in hardened concrete are given in Tables 6.21-6.22 and Figures 6.18-6.20. There was on average a 1 % increase in air content measured for hardened concrete when compared to the air content measured for fresh concrete. The largest increase (3%) occurred for the LWCH and LWCMI mixes. There was a 1.4 % decrease in the air content of hardened concrete when compared to the fresh concrete air content in the NWC-REF mix.

The standard deviation of air content in fresh concrete mixes was 0.41. The standard deviation of air content in hardened concrete was 1.63. The air void-paste ratio for the deck mixes were all within the acceptable limits typically seen for concrete.

The spacing factors calculated for the reference deck mixes were greater than those of the newly developed mixes (Figure 6.18). The greatest difference in spacing factor was observed in the LWCH and NWC concrete series. The specific surface calculated for the newly developed mixes was smaller than that of the reference mixes.

6.3.2 Drying Shrinkage

The test results presented in this section were obtained for both girder and deck concrete. The results are presented in Figures 6.21-6.23. Tests were also performed on the reference deck concrete.

Typical shrinkage results for LWC containing 225 kg - 315 kg (500 lbs-700 lbs) of cement are in the range of 0.055 %-0.061 % [Department of Commerce, 1974]. The values of shrinkage measured for LWC girder mixes were in the 0.0005 % to 0.003 % range. The values of shrinkage measured for the newly developed deck mixes were in the 0.0005 % to 0.004 % range. The values of shrinkage measured for the reference deck mixes were in the 0.01% to 0.04 % range.

A review of the results of concrete for use in bridge girders indicates that the NWC demonstrated more shrinkage than the LWC. In general, the reference deck concrete experienced greater shrinkage than the newly developed deck mixes which had a higher cement/paste content. The LWCHS concrete showed the most shrinkage overall.

There was an increase in shrinkage in the LWCHF reference mix compared to that of the newly developed LWCHF deck mix.

Shrinkage results for NWC in general are expected to be smaller than shrinkage results for LWC. As expected the air-dried samples showed more shrinkage than the samples cured in lime saturated water. The girder concrete mix made with Minergy LWA showed less shrinkage than concrete made with Haydite LWA.

6.3.3 Freeze-Thaw Resistance

The results of freeze-thaw tests obtained in the course of this study are presented in Tables 6.23-6.25 and Figures 6.24-6.30. In general, the results indicate that the resistance of LWC to freezing and thawing is far superior to that of concrete made with the normal weight aggregate used in this research.

6.3.3.1 Girder Mixes

For bridge girder concrete (42 MPa/6000 psi) the LWCH and LWCMII performed well when subjected to cycles of freezing and thawing (Table 6.23 and Figure 6.24). The NWC mix performed unsatisfactorily and reached a durability factor of 0.60 after 294 cycles. Visual examination of the samples revealed numerous pop-out associated with the coarse aggregate. This was linked to the existence of chert in the normal weight aggregate that most likely contributed to the poor performance of the NWC mixes since these particles are susceptible to freezing and thawing damage. The LWCH and LWCMII had durability factors of 0.94 and 0.84 respectively.

The 69 MPa (10,000 psi) mixes performed very satisfactorily when subjected to freezing and thawing cycles. The LWCHS mix had a durability factor of 0.96 compared to 0.94 for the NWC (Table 6.24 and Figure 6.24). In the testing of bridge girder concrete, there was no air-drying of samples prior to subjecting them to cycles of freezing and thawing. Based on the results of durability factors for LWC mixes, if the samples were allowed to dry prior to freezing and thawing, we would expect even better performances from the LWC mixes proposed for use in bridge girders.

6.3.3.2 Deck Mixes

The results for freeze-thaw resistance of deck concrete mixes are given in Tables 6.25-6.26 and Figures 6.26-6.30. When the bridge deck concrete samples were not allowed to dry before subjecting them to cycles of freezing and thawing, the performance in freeze-thaw test was unsatisfactory. Looking at results for this test series (Table 6.25 and Figure 6.26) we see that the LWCHS concrete mix showed the least resistance with a relative dynamic modulus of elasticity of 60 % and durability factor of 0.21 after only 108 cycles of freezing and thawing. Although the LWCH and LWCHF concrete mixes fared better, their durability factors were quite low, reaching values of 0.50 and 0.45, respectively. The NWC concrete mix had a relative dynamic modulus of elasticity of 74% after 300 cycles of freezing and thawing.

The freezing and thawing results (see Table 6.26 and Figure 6.27) were very different when the LWC samples were allowed to air-dry for 14 days after the initial period 14 days of moist curing. The drying took place in the laboratory in which the air temperature was 20°C and relative humidity was maintained at 50 %. The durability

factors after 300 cycles of freezing and thawing for LWC were in the 0.92-0.99 range indicating that LWC has superior freezing and thawing resistance.

Typically, concrete decks are not subjected to freezing and thawing for approximately 2 months after pouring and that means that LWC would have sufficient time to dry out. Because the absorption of the LWA is higher than NWA, subjecting this concrete to harsh conditions such as freezing and thawing without prior drying would causes rapid deterioration.

NWA is not significantly affected by additional drying and therefore was not retested. The durability factor for the NWC mix was 0.74 after 300 cycles of freezing and thawing. There was evidence of pop-outs as in the case with the NWC girder mixes. In both the girder and deck mixes the presence of cherts contributed to the unsatisfactory performance of the NWC. The use of crushed limestone instead of river gravel should produce concrete with better freezing and thawing resistance.

The performance of the reference deck mixes when subjected to freezing and thawing tests were very satisfactory (Table 6.27 and Figure 6.28). The concrete samples were allowed to dry for 14 days after an initial moist curing period of 14 days.

The results for durability factors were very similar and in general, the reference deck mixes had better durability factors after 300 cycles of freezing and thawing. This may be attributed to the higher cement content of the reference deck mixes. The newly developed LWCHF deck mix had a higher durability factor than the companion LWCHF reference deck mix. A water-cementitious ratio of 0.40 was used in the newly developed deck mix compared to a water-cementitious ratio of 0.443 used in the reference deck mix. The durability factor for the NWC reference deck mix was unchanged (0.74 after 300

cycles of freezing and thawing). The reference mix (LWCMI) containing Minergy aggregate performed satisfactorily and had a durability factor of 0.94 after 300 cycles of freezing and thawing. A comparison of durability factors for the newly developed and reference deck mixes are presented in Figures 6.29.

It is interesting to note that the LWC girder mixes performed well in the freezing and thawing test even though the concrete was not dried before the test. The improved performance of girder mixes seems to be related to the higher amount of cementitious materials and the lower water-cementitious ratios.

In conclusion, the results presented here make a very strong case for the use of Haydite and Minergy aggregates where frost resistance is critical. The performance of the LWC was by far superior to that of NWC. It is very important that the LWC be allowed to dry for 7-14 days before subjecting the concrete to cycles of freezing and thawing. Figure 6.30 shows the advantages of allowing LWC samples to dry before subjecting them to cycles of freezing and thawing. As we have seen, the performance is catastrophic if this procedure is not adhered to.

6.3.4 Rapid Chloride Ion Permeability

Rapid chloride ion permeability test results for girder concrete are presented in Tables 6.28-6.29 and Figures 6.31-6.33. For the 42 MPa (6000 psi) girder concrete, the NWC girder mix performed very satisfactorily. The LWCH and LWCMI girder concrete showed border line values (Table 6.28 and Figure 6.31). The tests on LWCH concrete samples were performed at 28 and 56 days and most likely would have been in the moderate range at 90 days. The LWCMI girder concrete mix was tested at 28 and 90

days. The 28 day coulomb reading was unacceptably high but reduced to an acceptable level after 90 days of curing.

The rapid chloride ion permeability results for the high strength (69 MPa /10,000 psi) girder mixes were very satisfactory (Table 6.29 and Figure 6.32). The chloride ion permeability for the LWCHS girder mix was very low and can be attributed to use of the low water-cementitious ratio and silica fume. The permeability of the LWCHS and NWC were 361 and 950 coulombs respectively after 56 days of curing. Measurements of chloride ion permeability were made after 90 days of curing for the NWC girder mix. The coulomb reading for NWC mix after 90 days of curing was 432 coulombs. The 90 day coulomb reading for the NWC mix was comparable to the LWCH reading at 56 days.

The rapid chloride ion permeability tests results for the bridge deck concrete is given in Table 6.30 and Figure 6.32. All the bridge deck concrete mixes developed in the course of this research had satisfactory resistance to chloride ion penetration. The reference deck concrete did not perform well in the chloride ion permeability tests. Significant differences in the rapid chloride-ion permeability value were observed for concrete containing the different types of lightweight aggregate. In particular, mixture containing Minergy (sintered fly ash) aggregate showed unacceptable higher values of permeability. This maybe related to the fact that the Minergy aggregate has a higher absorption and may have a higher degree of internal pore connectivity. Differences in the Interfacial Transition Zone (ITZ) may have contributed to observed differences, but this topic was not included in the scope of this research [Diamond and Huang, 1998].

Silica fume and fly ash were not used in development of bridge deck concrete using Minergy aggregate. The use of this mineral admixture would most likely result in

more impermeable concrete with adequate resistance to the ingress of chloride ions. Time constraints did not allow for the development of these mixes although it would have been beneficial to be able to report these findings.

In general, the use of mineral admixtures resulted in better performing concrete. The performance of silica fume concrete was much better than that of fly ash. The water-cementitious ratio of 0.443 used in the reference deck mixes did not produce concrete that adequately resist the ingress of chloride ions into the concrete.

6.3.5 Resistance to Scaling

Scaling resistance tests were conducted only on the bridge deck concrete and the results are presented in Table 6.31 and Figure 6.34. The LWCMI concrete samples were the only ones that did not perform satisfactorily. The testing on the LWCMI samples was terminated after 20 cycles of freezing and thawing when an ASTM rating of 5 was reached.

It is the author's opinion that a water-cementitious ratio of 0.443 used in the concrete containing Minergy aggregate did not do justice to the potential of the aggregate and the performance of Minergy aggregate concrete can not be justly evaluated. The reference deck concrete mixes containing Haydite aggregate had a higher rating than the newly developed deck concrete.

6.4 Shear Tests

Measurements and observations made throughout the shear tests are described in this section. Test data includes:

- Vertical deflection measurements of LVDTs,
- Steel strain measurements of electrical resistance strain gages (prestressing strands, mild longitudinal steel, and mild transverse steel),
- Mean concrete surface strain calculations from Whittemore strain gage measurements,
- Applied shear force from load cell measurements at all loading increments,
- Maximum applied shear force,
- Applied shear force at flexural and flexure-shear cracking, and
- Failure observations including type of failure and photographs of crack patterns.

The relationships between applied shear force and deflection, steel strains, and mean concrete surface strains are plotted with all of the measurements taken during the tests. In addition, approximately 40 sets of measurements of deflections and steel strains and all sets of concrete strain measurements are listed in tables. A brief description of the each specimen will precede the presentation of test data followed by photographs of the crack patterns at failure. The reinforced concrete beam series will be discussed first followed by the prestressed concrete beam series.

The objective of the reinforced concrete series was to investigate the effect of aggregate type, concrete strength, and amount and distribution of transverse and longitudinal reinforcement on the shear strength of reinforced concrete beams.

The objective of the prestressed concrete series was to investigate the effect of prestressing, concrete strength, and amount of transverse reinforcement on the shear strength of prestressed concrete beams.

6.4.1 Reinforced Concrete Specimens

The reinforced concrete beam series comprised 12 specimens. The objective of the tests conducted in this phase of the research study was to investigate the effect of aggregate type, concrete strength, and amount and distribution of transverse and longitudinal reinforcement on the shear strength of reinforced concrete beams.

This section is divided into 12 subsections; one subsection for each reinforced concrete specimens. Each subsection begins with an introduction that contains specimen details, an explanation of how each specimen relates to the other specimens in the series, and an explanation of how each specimen will be used to investigate the effect of the test variables on the shear capacity. Test variables included aggregate type, concrete strength, and amount and distribution of transverse and longitudinal reinforcement. The presentation of the test data follows the introduction for each specimen. The data presented include vertical deflections, longitudinal steel strains, stirrup strains, concrete surface strains, maximum applied shear force, and cracking observations.

Measurements of deflections and steel strains were recorded at approximately 1 to 2 kN intervals of applied shear for each specimen. Charts that plot the relationships between shear force and deflection and between shear force and strain contain all recorded data points prior to and including the maximum applied load. These charts are shown in Figures 6.35 through 6.106. Tables that summarize these measurements contain approximately 40 sets of readings corresponding to intervals of shear from 10 to 20 kN. These summaries are shown in Tables 6.32 through 6.67. Measurements of vertical deflections with mechanical dial gages were taken at 15 to 40 kN intervals throughout the first part of each test (approximately 60% of the applied load). Because

the deflection measurements with the dial gages corresponded with the deflection measurement with the LVDTs, only measurements of vertical deflection by the LVDTs are reported. Zero slip at the ends of the longitudinal bars for all specimens was measured by the mechanical dial gages. Therefore, no values of slip are reported.

Mean concrete surface strains were determined from the measurements of surface deformation by the Whittemore strain gages. An orthogonal grid of targets and electronic Whittemore strain gages were used to determine surface strains on reinforced concrete specimens 1-NWLA, 2-NWLB, 3-NWLC, 4-NWLD, 5-LWLD, 6-LWLB, 7-LWLC, 8-LWLD, 9-NWLD, and 10-NWHD. The locations of the targets and the measurements are shown in Figures 4.43 – 4.51. The measurements included horizontal, vertical, and diagonal deformation measurements. The horizontal and vertical measurements were taken using the 127-mm gage length strain gage. The diagonal measurements were taken using the 179-mm strain gage. During each test, a steel wide-flange section was used as a calibration check for both electronic Whittemore strain gages. Holes were drilled 127 and 179 apart on the top flange of the section aligned along the web. A calibration reading was taken with each gage at the beginning and end of each set of readings corresponding to each load stage. The difference between the mean calibration reading and each measurement on the grid was taken as the change in length of the particular segment. Strains at each load stage (15 to 40 kN) for each segment were calculated by dividing the change in length by the original length. The original length of each horizontal and vertical segment was taken as 127 mm (gage length) plus the difference in length of the segment from the mean calibration length at zero load. The same procedure applied to the diagonal measurements.

Specimens 11-LWHD and 12-NWHD were instrumented with a series of 45-degree rosettes to measure the concrete surface deformations. The locations of the targets and measurements are shown in Figure 4.52. A 254-mm gage length mechanical Whittemore strain gage was used to measure the deformations between targets. A steel calibration bar was used to establish a 254-mm reference length. The procedure to calculate the experimental strains is the same as the procedure described in the preceding paragraph. Mean Whittemore strains are plotted against the applied shear force for all reinforced concrete specimens in Figures 6.107 through 6.324. The values of mean strain are listed in Tables 6.68 through 6.99.

Visual observations of each test include the sequence of cracking, crack patterns, and modes of failure. The shear force at which flexural cracking occurs is taken as the shear force at which the strain in the longitudinal bars at either end of the test region experienced a significant increase. Similarly, the inclined cracking shear is taken as the shear force at which an instrumented stirrup experienced a significant increase in strain. These increases may be observed in the data shown in the plots and tables. Evidence of crack patterns and failure modes is presented in the form of a series of photographs for each specimen shown in Figures 6.325 through 6.365.

6.4.1.1 Specimen 1-NWLA

6.4.1.1.1 Introduction

Specimen 1-NWLA was made of normal weight aggregate (river gravel) concrete with a concrete compressive strength of 46.2 MPa at the time of the test. The longitudinal reinforcement consisted of an upper and lower layer of five No. 8 bars

distributed evenly across the width of the specimen. The transverse reinforcement consisted of double-leg closed stirrups made of No. 3 bars spaced at 102 mm. This specimen serves as a comparison to specimens 2-NWLB and 3-NWLC with regard to the effect that the amount and distribution of transverse and longitudinal reinforcement has on shear strength. It also serves as a comparison to specimen 5-LWLA in determining the effect of aggregate type on the shear capacity.

6.4.1.1.2 Deflections

The locations of the LVDTs are shown in Figure 4.32. The relationship between the shear force in the test region and the deflections at four locations is shown in Figure 6.35. A maximum deflection of 7.4 mm was measured at location 2. Deflection measurements are shown at approximately 10 to 20 kN intervals of shear force in Table 6.22.

6.4.1.1.3 Longitudinal Mild Steel Strains

The locations of the longitudinal mild steel strain gages are shown in Figure 4.34. The shear force-strain relationships are shown in Figures 6.36 to 6.39. Strain measurements are shown in Table 6.33. The longitudinal reinforcement did not yield prior to failure of specimen 1-NWLA.

6.4.1.1.4 Stirrup Strains

The locations of the stirrup strain gages are shown in Figure 4.34. The shear force-stirrup strain relationship is shown in Figure 6.40. Strain measurements are shown

in Table 6.34. Yielding of the stirrups as indicated by strain gages T2C, T3A, T6A, and T6C precipitated failure of the specimen.

6.4.1.1.5 Concrete Surface Strains

The locations of the concrete surface strain measurements are shown in Figures 4.70 – 4.73. The relationships between applied shear force and mean surface strain are shown in Figures 6.107 – 6.124. These measurements are also listed in Tables 6.68 – 6.70, containing 13 sets of readings, each corresponding to intervals of shear from 28 – 46 kN. Note the significant increase in vertical strain, from 21 microstrain to 599 microstrain, at station V18 between 119 and 150 kN (Refer to Figure 6.118 and Table 6.69). This shear force corresponds to the shear force at flexural-shear cracking (149 kN) determined from the stirrup strain readings.

6.4.1.1.6 Failure Observations

Flexural cracking occurred at a shear of 58 kN. The first inclined crack (flexure-shear crack) occurred at a shear of 149 kN. The maximum applied shear during the test was 436 kN. Photographs of Specimen 1-NWLA after testing are shown in Figures 6.325 to 6.303. At failure, a crack extended through the lower part of the beam into the compression zone near the south support. Spalling was observed in the compression zone near the north load point.

6.4.1.2 Specimen 2-NWLB

6.4.1.2.1 Introduction

Specimen 2-NWLB was made of normal weight aggregate (river gravel) concrete with a concrete compressive strength of 46.2 MPa at the time of the test. The longitudinal reinforcement consisted of an upper and lower layer of five No. 8 bars distributed evenly across the width of the specimen. The transverse reinforcement consisted of triple-leg closed stirrups made of No. 3 bars and spaced at 152 mm. This specimen serves as a comparison to specimens 1-NWLA and 3-NWLC with regard to the effect that the amount and distribution of transverse and longitudinal reinforcement has on shear strength. It also serves as a comparison to specimen 6-LWLB in determining the effect of aggregate type on the shear capacity.

6.4.1.2.2 Deflections

The locations of the LVDTs are shown in Figure 4.32. The relationship between the shear force in the test region and the deflections at four locations is shown in Figure 6.41. A maximum deflection of 9.4 mm was measured at location 2. Deflection measurements are shown at approximately 10 to 20 kN intervals of shear force in Table 6.35.

6.4.1.2.3 Longitudinal Mild Steel Strains

The locations of the longitudinal mild steel strain gages are shown in Figure 4.35. The shear force-strain relationships are shown in Figures 6.42 to 6.45. Figures 6.43 and

6.44 indicate that the longitudinal reinforcement at section 2 yielded prior to the maximum load being reached. Strain measurements are shown in Table 6.36.

6.4.1.2.4 Stirrup Strains

The locations of the stirrup strain gages are shown in Figure 4.35. The shear force-stirrup strain relationship is shown in Figure 6.46. Strain measurements are shown in Table 6.37. Stirrups T2 and T4 yielded prior to failure of the specimen.

6.4.1.2.5 Concrete Surface Strains

The locations of the concrete surface strain measurements are shown in Figures 4.43 – 4.45. The relationships between applied shear force and mean surface strain are shown in Figures 6.125 – 6.142. These measurements are also listed in Tables 6.71 – 6.73, containing 16 sets of readings, each corresponding to intervals of shear from 22 – 45 kN. Note the significant increase in vertical strain, from 56 microstrain to 1071 microstrain, at station V1 between 150 and 172 kN (Refer to Figure 6.131 and Table 6.72). This shear force corresponds to the shear force at flexural-shear cracking (172 kN) determined from the stirrup strain readings.

6.4.1.2.6 Failure Observations

Flexural cracking occurred at a shear of 45 kN. The first inclined crack (flexure-shear crack) occurred at a shear of 172 kN. The maximum applied shear during the test was 485 kN. Photographs of Specimen 2-NWLB after testing are shown in Figures 6.329 to 6.332. At failure, a crack extended through the upper part of the beam into the compression zone near the north load point. Spalling and crushing were observed in the

compression zone near the north load point. Extensive splitting cracks occurred along the upper level of reinforcement.

6.4.1.3 Specimen 3-NWLC

6.4.1.3.1 Introduction

Specimen 3-NWLC was made of normal weight aggregate (river gravel) concrete with a concrete compressive strength of 46.6 MPa at the time of the test. The longitudinal reinforcement consisted of an upper and lower layer of four No. 9 bars bundled in pairs of two in each corner. The transverse reinforcement consisted of double-leg closed stirrups made of No. 3 bars spaced at 102 mm. This specimen serves as a comparison to specimens 1-NWLA and 2-NWLB with regard to the effect of reinforcing details on shear strength. It also serves as a comparison to specimen 7-LWLC in determining the effect of aggregate type on the shear capacity.

6.4.1.3.2 Deflections

The locations of the LVDTs are shown in Figure 4.32. The relationship between the shear force in the test region and the deflections at four locations is shown in Figure 6.47. A maximum deflection of 8.7 mm was measured at location 2. Deflection measurements are shown at approximately 10 to 20 kN intervals of shear force in Table 6.38.

6.4.1.3.3 Longitudinal Mild Steel Strains

The locations of the longitudinal mild steel strain gages are shown in Figure 4.36. The shear force-strain relationships are shown in Figures 6.48 to 6.51. Strain

measurements are shown in Table 6.39. The longitudinal reinforcement did not yield prior to failure of specimen 3-NWLC.

6.4.1.3.4 Stirrup Strains

The locations of the stirrup strain gages are shown in Figure 4.36. The shear force-stirrup strain relationship is shown in Figure 6.52. Strain measurements are shown in Table 6.40. Yielding of the stirrups T2 and T6 precipitated failure of the specimen.

6.4.1.3.5 Concrete Surface Strains

The locations of the concrete surface strain measurements are shown in Figures 4.43 – 4.45. The relationships between applied shear force and mean surface strain are shown in Figures 6.143 – 6.160. These measurements are also listed in Tables 6.74 – 6.76, containing 16 sets of readings, each corresponding to intervals of shear from 22 – 45 kN. Note the significant increase in vertical strain, from 37 microstrain to 261 microstrain, at station V1 between 104 and 127 kN (Refer to Figure 6.149 and Table 6.88). This shear force corresponds to the shear force at flexural-shear cracking (127 kN) determined from the stirrup strain readings.

6.4.1.3.6 Failure Observations

Flexural cracking occurred at a shear of 38 kN. The first inclined crack (flexure-shear crack) occurred at a shear of 127 kN. The maximum applied shear during the test was 421 kN. Photographs of Specimen 3-NWLC after testing are shown in Figures 6.334 to 6.337. At failure, major inclined cracks extended into the compression zones near the

south support and north support. Local concrete crushing along the southern inclined crack was observed indicating a transfer of forces across the crack.

6.4.1.4 Specimen 4-NWLD

6.4.1.4.1 Introduction

Specimen 4-NWLD was made of normal weight aggregate (river gravel) concrete with a concrete compressive strength of 45.8 MPa at the time of the test. The longitudinal reinforcement consisted of an upper and lower layer of four No. 9 bars bundled in pairs of two in each corner. The transverse reinforcement consisted of double-leg closed stirrups made of No. 3 bars spaced at 152 mm. This specimen serves as a comparison to specimen 3-NWLC in determining the effect that the amount of transverse reinforcement has on shear strength. It also serves as a comparison to specimens 8-LWLD and 12-NWHD in determining the effect of aggregate type and concrete compressive strength on the shear capacity, respectively.

6.4.1.4.2 Deflections

The locations of the LVDTs are shown in Figure 4.32. The relationship between the shear force in the test region and the deflections at four locations is shown in Figure 6.53. A maximum deflection of 5.9 mm was measured at location 2. Deflection measurements are shown at approximately 10 to 20 kN intervals of shear force in Table 6.41.

6.4.1.4.3 Longitudinal Mild Steel Strains

The locations of the longitudinal mild steel strain gages are shown in Figure 4.37. The shear force-strain relationships are shown in Figures 6.54 to 6.57. Strain measurements are shown in Table 6.42. The longitudinal reinforcement did not yield prior to failure of specimen 4-NWLD.

6.4.1.4.4 Stirrup Strains

The locations of the stirrup strain gages are shown in Figure 4.37. The shear force-stirrup strain relationship is shown in Figure 6.58. Strain measurements are shown in Table 6.43. Yielding of the stirrups T2 and T4 precipitated failure of the specimen.

6.4.1.4.5 Concrete Surface Strains

The locations of the concrete surface strain measurements are shown in Figures 4.46 – 4.48. The relationships between applied shear force and mean surface strain are shown in Figures 6.161 – 6.185. These measurements are also listed in Tables 6.77 – 6.79, containing 13 sets of readings, each corresponding to intervals of shear from 11 – 30 kN. Note the significant increase in vertical strain, from 10 microstrain to 566 microstrain, at station V15 between 122 and 139 kN (Refer to Figure 6.176 and Table 6.78). This shear force corresponds closely to the shear force at flexural-shear cracking (141 kN) determined from the stirrup strain readings.

6.4.1.4.6 Failure Observations

Flexural cracking occurred at a shear of 39 kN. The first inclined crack (flexure-shear crack) occurred at a shear of 141 kN. The maximum applied shear during the test

was 349 kN. Photographs of Specimen 4-NWLD after testing are shown in Figures 6.338 to 6.340. At failure, two major cracks extended suddenly to the south support and north load point. Spalling and crushing was observed in the compression zones near the south support and north load point.

6.4.1.5 Specimen 5-LWLA

6.4.1.5.1 Introduction

Specimen 5-LWLA was made of sand-lightweight aggregate (Haydite) concrete with a concrete compressive strength of 43.4 MPa at the time of the test. The longitudinal reinforcement consisted of an upper and lower layer of five No. 8 bars distributed evenly across the width of the specimen. The transverse reinforcement consisted of double-leg closed stirrups made of No. 3 bars spaced at 102 mm. This specimen serves as a comparison to specimens 6-LWLB and 7-LWLC with regard to the effect of reinforcing details on shear strength. It also serves as a comparison to specimen 1-NWLA in determining the effect of aggregate type on the shear capacity.

6.4.1.5.2 Deflections

The locations of the LVDTs are shown in Figure 4.32. The relationship between the shear force in the test region and the deflections at four locations is shown in Figure 6.59. A maximum deflection of 6.9 mm was measured at location 2. Deflection measurements are shown at approximately 10 to 20 kN intervals of shear force in Table 6.44.

6.4.1.5.3 Longitudinal Mild Steel Strains

The locations of the longitudinal mild steel strain gages are shown in Figure 4.34. The shear force-strain relationships are shown in Figures 6.60 to 6.63. Strain measurements are shown in Table 6.35. The longitudinal reinforcement did not yield prior to failure of specimen 5-LWLA.

6.4.1.5.4 Stirrup Strains

The locations of the stirrup strain gages are shown in Figure 4.34. The shear force-stirrup strain relationship is shown in Figure 6.64. Strain measurements are shown in Table 6.46. Yielding of the stirrups T2, T3, T4, and T5 precipitated failure of the specimen.

6.4.1.5.5 Concrete Surface Strains

The locations of the concrete surface strain measurements are shown in Figures 4.43 – 4.45. The relationships between applied shear force and mean surface strain are shown in Figures 6.184 – 6.203. These measurements are also listed in Tables 6.80 – 6.82, containing 15 sets of readings, each corresponding to intervals of shear from 22 – 45 kN. Note the increase in vertical strain, from 78 microstrain to 154 microstrain, at station V18 between 74 and 89 kN (Refer to Figure 6.197 and Table 6.81). This shear force corresponds with the shear force at flexural-shear cracking (74 kN) determined from the stirrup strain readings.

6.4.1.5.6 Failure Observations

Flexural cracking occurred at a shear of 21 kN. The first inclined crack (flexure-shear crack) occurred at a shear of 74 kN. The maximum applied shear during the test was 328 kN. Extensive inclined cracking was observed in the entire test region. Failure of the specimen followed the propagation of a crack through the compression zone to the face of the south support. Photographs of Specimen 5-LWLA after testing are shown in Figures 6.341 to 6.344.

6.4.1.6 Specimen 6-LWLB

6.4.1.6.1 Introduction

Specimen 6-LWLB was made of sand-lightweight aggregate (Haydite) concrete with a concrete compressive strength of 43.0 MPa at the time of the test. The longitudinal reinforcement consisted of an upper and lower layer of five No. 8 bars distributed evenly across the width of the specimen. The transverse reinforcement consisted of triple-leg closed stirrups made of No. 3 bars spaced at 152 mm. This specimen serves as a comparison to specimens 5-LWLA and 7-LWLC with regard to the effect of reinforcing details on shear strength. It also serves as a comparison to specimen 2-NWLB in determining the effect of aggregate type on the shear capacity.

6.4.1.6.2 Deflections

The locations of the LVDTs are shown in Figure 4.32. The relationship between the shear force in the test region and the deflections at four locations is shown in Figure 6.65. A maximum deflection of 7.6 mm was measured at location 2. Deflection

measurements are shown at approximately 10 to 20 kN intervals of shear force in Table 6.37.

6.4.1.6.3 Longitudinal Mild Steel Strains

The locations of the longitudinal mild steel strain gages are shown in Figure 4.35. The shear force-strain relationships are shown in Figures 6.66 to 6.69. Strain measurements are shown in Table 6.48. The longitudinal reinforcement did not yield prior to failure of specimen 6-LWLB.

6.4.1.6.4 Stirrup Strains

The locations of the stirrup strain gages are shown in Figure 4.35. The shear force-stirrup strain relationship is shown in Figure 6.70. Strain measurements are shown in Table 6.49. Yielding of the stirrups T1, T2, T3, and T4 precipitated failure of the specimen.

6.4.1.6.5 Concrete Surface Strains

The locations of the concrete surface strain measurements are shown in Figures 4.49 – 4.51. The relationships between applied shear force and mean surface strain are shown in Figures 6.205 – 6.230. These measurements are also listed in Tables 6.81 – 6.85, containing 13 sets of readings, each corresponding to intervals of shear from 21 – 45 kN. Note the significant increase in vertical strain, from -131 microstrain to 354 microstrain, at station V35 between 75 and 104 kN (Refer to Figure 6.131 and Table 6.218). This shear force corresponds to approximately 80% of the shear force at flexural-shear cracking (116 kN) determined from the stirrup strain readings.

6.4.1.6.6 Failure Observations

Flexural cracking occurred at a shear of 23 kN. The first inclined crack (flexure-shear crack) occurred at a shear of 116 kN. The maximum applied shear during the test was 373 kN. Extensive cracking occurred in the south end of the test region. At failure, a crack propagated to the south support. Photographs of Specimen 6-LWLB after testing are shown in Figures 6.345 to 6.349.

6.4.1.7 Specimen 7-LWLC

6.4.1.7.1 Introduction

Specimen 7-LWLC was made of sand-lightweight aggregate (Haydite) concrete with a concrete compressive strength of 43.4 MPa at the time of the test. The longitudinal reinforcement consisted of an upper and lower layer of four No. 9 bars bundled in pairs of two in each corner. The transverse reinforcement consisted of double-leg closed stirrups made of No. 3 bars spaced at 102 mm. This specimen serves as a comparison to specimens 5-LWLA and 6-LWLB with regard to the effect of reinforcing details on shear strength. It also serves as a comparison to specimen 3-NWLC in determining the effect of aggregate type on the shear capacity.

6.4.1.7.2 Deflections

The locations of the LVDTs are shown in Figure 4.32. The relationship between the shear force in the test region and the deflections at four locations is shown in Figure 6.71. A maximum deflection of 6.5 mm was measured at location 2. Deflection

measurements are shown at approximately 10 to 20 kN intervals of shear force in Table 6.50.

6.4.1.7.3 Longitudinal Mild Steel Strains

The locations of the longitudinal mild steel strain gages are shown in Figure 4.36. The shear force-strain relationships are shown in Figures 6.72 to 6.75. Strain measurements are shown in Table 6.51. The longitudinal reinforcement did not yield prior to failure of specimen 7-LWLC.

6.4.1.7.4 Stirrup Strains

The locations of the stirrup strain gages are shown in Figure 4.36. The shear force-stirrup strain relationship is shown in Figure 6.76. Strain measurements are shown in Table 6.52. Yielding of the T2, T3, T4, T5, and T6 precipitated failure of the specimen.

6.4.1.7.5 Concrete Surface Strains

The locations of the concrete surface strain measurements are shown in Figures 4.46 – 4.48. The relationships between applied shear force and mean surface strain are shown in Figures 6.229 – 6.253. These measurements are also listed in Tables 6.86 – 6.88, containing 14 sets of readings, each corresponding to intervals of shear from 15 – 36 kN. Note the significant increase in vertical strain, from 117 microstrain to 402 microstrain, at station V12 between 89 and 105 kN (Refer to Figure 6.242 and Table 6.87). This shear force is approximately 30% larger than the shear force at flexural-shear cracking (75 kN) determined from the stirrup strain readings.

6.4.1.7.6 Failure Observations

Flexural cracking occurred at a shear of 19 kN. The first inclined crack (flexure-shear crack) occurred at a shear of 75 kN. The maximum applied shear during the test was 358 kN. Extensive inclined cracking was observed throughout the entire test region. Major cracks propagated to the south support and to the north load point at failure. Photographs of Specimen 7-LWLC after testing are shown in Figures 6.349 to 6.351.

6.4.1.8 Specimen 8-LWLD

6.4.1.8.1 Introduction

Specimen 8-LWLD was made of sand-lightweight aggregate (Haydite) concrete with a concrete compressive strength of 44.3 MPa at the time of the test. The longitudinal reinforcement consisted of an upper and lower layer of four No. 9 bars bundled in pairs of two in each corner. The transverse reinforcement consisted of double-leg closed stirrups made of No. 3 bars spaced at 152 mm. This specimen serves as a comparison to specimen 7-LWLC with regard to the effect the amount of transverse reinforcement has on shear strength. It also serves as a comparison to specimens 4-LWLD and 11-LWHD in determining the effect of aggregate type and concrete compressive strength on the shear capacity, respectively.

6.4.1.8.2 Deflections

The locations of the LVDTs are shown in Figure 4.32. The relationship between the shear force in the test region and the deflections at four locations is shown in Figure 6.77. A maximum deflection of 6.1 mm was measured at location 2. Deflection

measurements are shown at approximately 10 to 20 kN intervals of shear force in Table 6.53.

6.4.1.8.3 Longitudinal Mild Steel Strains

The locations of the longitudinal mild steel strain gages are shown in Figure 4.37. The shear force-strain relationships are shown in Figures 6.78 to 6.81. Strain measurements are shown in Table 6.54. The longitudinal reinforcement did not yield prior to failure of specimen 8-LWLD.

6.4.1.8.4 Stirrup Strains

The locations of the stirrup strain gages are shown in Figure 4.37. The shear force-stirrup strain relationship is shown in Figure 6.82. Strain measurements are shown in Table 6.55. Yielding of the stirrups T2, T3, and T4 precipitated failure of the specimen.

6.4.1.8.5 Concrete Surface Strains

The locations of the concrete surface strain measurements are shown in Figures 4.46 – 4.48. The relationships between applied shear force and mean surface strain are shown in Figures 6.254 – 6.278. These measurements are also listed in Tables 6.89 – 6.91, containing 13 sets of readings, each corresponding to intervals of shear from 15 – 37 kN. Note the significant increase in vertical strain, from -85 microstrain to 760 microstrain, at station V3 between 89 and 105 kN (Refer to Figure 6.131 and Table 6.90). This shear force is approximately 36% larger than the shear force at flexural-shear cracking (71 kN) determined from the stirrup strain readings.

6.4.1.8.6 Failure Observations

Flexural cracking occurred at a shear of 25 kN. The first inclined crack (flexure-shear crack) occurred at a shear of 71 kN. The maximum applied shear during the test was 280 kN. Cracks extended to both the south support and north load point at failure. Major splitting cracks along the upper level of longitudinal reinforcement caused a buckling failure of the compression zone in the north end of the test region. A photograph of Specimen 8-LWLD after testing is shown in Figure 6.352.

6.4.1.9 Specimen 9-NWLD

6.4.1.9.1 Introduction

Specimen 9-NWLD was made of normal weight aggregate (crushed limestone) concrete with a concrete compressive strength of 40.0 MPa at the time of the test. The longitudinal reinforcement consisted of an upper and lower layer of four No. 9 bars bundled in pairs of two in each corner. The transverse reinforcement consisted of double-leg closed stirrups made of No. 3 bars spaced at 152 mm. This specimen serves as a companion to specimen 4-NWLD.

6.4.1.9.2 Deflections

The locations of the LVDTs are shown in Figure 4.32. The relationship between the shear force in the test region and the deflections at four locations is shown in Figure 6.83. A maximum deflection of 7.5 mm was measured at location 2. Deflection measurements are shown at approximately 10 to 20 kN intervals of shear force in Table 6.56.

6.4.1.9.3 Longitudinal Mild Steel Strains

The locations of the longitudinal mild steel strain gages are shown in Figure 4.37. The shear force-strain relationships are shown in Figures 6.84 to 6.87. Strain measurements are shown in Table 6.57. The longitudinal reinforcement did not yield prior to failure of specimen 9-NWLD.

6.4.1.9.4 Stirrup Strains

The locations of the stirrup strain gages are shown in Figure 4.37. The shear force-stirrup strain relationship is shown in Figure 6.88. Strain measurements are shown in Table 6.80. Yielding of the T4 and T5 precipitated failure of the specimen.

6.4.1.9.5 Concrete Surface Strains

The locations of the concrete surface strain measurements are shown in Figures 4.43 – 4.45. The relationships between applied shear force and mean surface strain are shown in Figures 6.279 – 6.298. These measurements are also listed in Tables 6.92 – 6.94, containing 13 sets of readings, each corresponding to intervals of shear from 22 – 44 kN. Note the significant increase in vertical strain, from 26 microstrain to 256 microstrain, at station V2 between 45 and 74 kN (Refer to Figure 6.285 and Table 6.93). This shear force corresponds to the shear force at flexural-shear cracking (60 kN) determined from the stirrup strain readings.

6.4.1.9.6 Failure Observations

Flexural cracking occurred at a shear of 12 kN. The first inclined crack (flexure-shear crack) occurred at a shear of 60 kN. The maximum applied shear during the test

was 309 kN. Photographs of Specimen 9-NWLA after testing are shown in Figures 6.353 to 6.356. Crushing in both compression zones was observed at a shear of 304 kN. Failure was initiated by the abrupt formation of a crack propagating from the south support plate inclined at a low angle. The major crack on the north end of the test region enlarged at the same time.

6.4.1.10 Specimen 10-NWHD

6.4.1.10.1 Introduction

Specimen 10-NWHD was made of normal weight aggregate (crushed limestone) concrete with a concrete compressive strength of 60.1 MPa at the time of the test. The longitudinal reinforcement consisted of an upper and lower layer of four No. 9 bars bundled in pairs of two in each corner. The transverse reinforcement consisted of double-leg closed stirrups made of No. 3 bars spaced at 152 mm. This specimen serves as a comparison to specimens 4-NWLD and 9-NWLD with regard to the effect of concrete compressive strength on shear strength.

6.4.1.10.2 Deflections

The locations of the LVDTs are shown in Figure 4.32. The relationship between the shear force in the test region and the deflections at four locations is shown in Figure 6.89. A maximum deflection of 5.2 mm was measured at location 2. Deflection measurements are shown at approximately 10 to 20 kN intervals of shear force in Table 6.59.

6.4.1.10.3 Longitudinal Mild Steel Strains

The locations of the longitudinal mild steel strain gages are shown in Figure 4.37. The shear force-strain relationships are shown in Figures 6.90 to 6.93. Strain measurements are shown in Table 6.60. The longitudinal reinforcement did not yield prior to failure of specimen 10-NWHD.

6.4.1.10.4 Stirrup Strains

The locations of the stirrup strain gages are shown in Figure 4.37. The shear force-stirrup strain relationship is shown in Figure 6.93. Strain measurements are shown in Table 6.61. Yielding of the stirrup T2 precipitated failure of the specimen.

6.4.1.10.5 Concrete Surface Strains

The locations of the concrete surface strain measurements are shown in Figures 4.43 – 4.45. The relationships between applied shear force and mean surface strain are shown in Figures 6.296 – 6.314. These measurements are also listed in Tables 6.95 – 6.97, containing 11 sets of readings, each corresponding to intervals of shear from 28 – 45 kN. Note the significant increase in vertical strain, from 32 microstrain to 842 microstrain, at station V18 between 149 and 179 kN (Refer to Figure 6.308 and Table 6.96). This shear force corresponds to approximately 85% of the shear force at flexural-shear cracking (194 kN) determined from the stirrup strain readings.

6.4.1.10.6 Failure Observations

Flexural cracking occurred at a shear of 38 kN. The first inclined crack (flexure-shear crack) occurred at a shear of 194 kN. The maximum applied shear during the test was 359 kN. Major cracking was limited to the north and south ends of the test region. Little cracking occurred in the center of the test region. The major inclined crack extended through the south end of the test region and into the south support. Multiple splitting cracks occurred along the lower row of longitudinal reinforcement. Photographs of Specimen 10-NWHD after testing are shown in Figures 6.357 to 6.359.

6.4.1.11 Specimen 11-LWHD

6.4.1.11.1 Introduction

Specimen 11-LWLD was made of lightweight aggregate (Haydite) concrete with a concrete compressive strength of 72.3 MPa at the time of the test. The longitudinal reinforcement consisted of an upper and lower layer of four No. 9 bars bundled in pairs of two in each corner. The transverse reinforcement consisted of double-leg closed stirrups made of No. 3 bars spaced at 152 mm. This specimen serves as a comparison to specimen 12-NWHD in determining the effect of aggregate type on the shear capacity.

6.4.1.11.2 Deflections

The locations of the LVDTs are shown in Figure 4.32. The relationship between the shear force in the test region and the deflections at four locations is shown in Figure 6.82. A maximum deflection of 7.1 mm was measured at location 2. Deflection

measurements are shown at approximately 10 to 20 kN intervals of shear force in Table 6.62.

6.4.1.11.3 Longitudinal Mild Steel Strains

The locations of the longitudinal mild steel strain gages are shown in Figure 4.37. The shear force-strain relationships are shown in Figures 6.96 to 6.99. Strain measurements are shown in Table 6.63. The longitudinal reinforcement did not yield prior to failure of specimen 11-LWHD.

6.4.1.11.4 Stirrup Strains

The locations of the stirrup strain gages are shown in Figure 4.37. The shear force-stirrup strain relationship is shown in Figure 6.100. Strain measurements are shown in Table 6.64. Yielding of the stirrups T2 and T4 precipitated failure of the specimen.

6.4.1.11.5 Concrete Surface Strains

The locations of the concrete surface strain measurements are shown in Figure 4.52. The relationships between applied shear force and mean surface strain are shown in Figures 6.315 – 6.319. These measurements are also listed in Table 6.98, containing 22 sets of readings, each corresponding to intervals of shear from 14 – 45 kN. Note the significant increase in diagonal strain, from 292 microstrain to 727 microstrain, at station W2 between 133 and 148 kN (Refer to Figure 6.288 and Table 6.84). This shear force corresponds approximately to 5% larger than the shear force at flexural-shear cracking (134 kN) determined from the stirrup strain readings.

6.4.1.11.6 Failure Observations

Flexural cracking occurred at a shear of 25 kN. The first inclined crack (flexure-shear crack) occurred at a shear of 134 kN. The maximum applied shear during the test was 397 kN. Photographs of Specimen 11-LWHD after testing are shown in Figures 6.360 to 6.362. Sudden crushing of the north compression zone initiated failure of this specimen. The two major inclined cracks increased in width. Spalling occurred at the edges of the crack as they moved relative to one another.

6.4.1.12 Specimen 12-NWHD

6.4.1.12.1 Introduction

Specimen 12-NWHD was made of normal weight aggregate (crushed limestone) concrete with a concrete compressive strength of 75.2 MPa at the time of the test. The longitudinal reinforcement consisted of an upper and lower layer of four No. 9 bars bundled in pairs of two in each corner. The transverse reinforcement consisted of double-leg closed stirrups made of No. 3 bars spaced at 152 mm. This specimen serves as a comparison to specimens 4-NWLD, 9-NWLD, and 10-NWHD with regard to the effect of concrete compressive on shear strength. It also serves as a comparison to 11-LWHD in determining the effect of aggregate type on the shear capacity.

6.4.1.12.2 Deflections

The locations of the LVDTs are shown in Figure 4.32. The relationship between the shear force in the test region and the deflections at four locations is shown in Figure 6.101. A maximum deflection of 6.1 mm was measured at location 2. Deflection

measurements are shown at approximately 10 to 20 kN intervals of shear force in Table 6.65.

6.4.1.12.3 Longitudinal Mild Steel Strains

The locations of the longitudinal mild steel strain gages are shown in Figure 4.37. The shear force-strain relationships are shown in Figures 6.102 to 6.105. Strain measurements are shown in Table 6.66. The longitudinal reinforcement did not yield prior to failure of specimen 12-NWHD.

6.4.1.12.4 Stirrup Strains

The locations of the stirrup strain gages are shown in Figure 4.37. The shear force-stirrup strain relationship is shown in Figure 6.106. Strain measurements are shown in Table 6.67. Yielding of the stirrup T2 precipitated failure of the specimen.

6.4.1.12.5 Concrete Surface Strains

The locations of the concrete surface strain measurements are shown in Figure 4.52. The relationships between applied shear force and mean surface strain are shown in Figures 6.320 – 6.324. These measurements are also listed in Table 6.99, containing 24 sets of readings, each corresponding to intervals of shear from 12 – 44 kN. Note the increase in vertical strain, from 7 microstrain to 212 microstrain, at station W1 between 133 and 148 kN (Refer to Figure 6.320 and Table 6.99). This shear force corresponds to approximately 5% larger than the shear force at flexural-shear cracking (134 kN) determined from the stirrup strain readings.

6.4.1.12.6 Failure Observations

Flexural cracking occurred at a shear of 38 kN. The first inclined crack (flexure-shear crack) occurred at a shear of 134 kN. The maximum applied shear during the test was 398 kN. Major inclined cracking was limited to the south and north ends of the test region. There were, however, extensive splitting cracks along the lower level of reinforcement in the center of the test region. Photographs of Specimen 12-NWHD after testing are shown in Figures 6.363 to 6.365.

6.4.2 Prestressed Concrete Specimens

The prestressed concrete beam series comprised 4 specimens. The objective of the tests conducted in this phase of the research study was to investigate the effect of prestressing, concrete strength, and amount of transverse reinforcement on the shear strength of prestressed concrete beams.

This section is divided into 4 subsections; one subsection for each prestressed concrete specimens. Each subsection begins with an introduction that contains specimen details, an explanation of how each specimen relates to the other specimens in the series, and an explanation of how each specimen will be used to investigate the effect of the test variables on the shear capacity. Test variables included concrete compressive strength and the amount of transverse reinforcement. The presentation of the test data follows the introduction for each specimen. The data presented include vertical deflections, prestressing strand strains, longitudinal steel strains, stirrup strains, concrete surface strains, maximum applied shear force, and cracking observations.

The data presented include vertical deflections for all specimens, longitudinal mild steel strains for all specimens, strains in the prestressing strand for specimens PC6N and PC6S, stirrup strains for specimens PC6S and PC10S, mean concrete surface strains for all specimens, and failure observations for all specimens. Measurements of deflection and steel strains were recorded at approximately every 1 to 2 kN of applied shear for each specimen. Charts that plot the relationships between shear force and deflection and between shear force and strain contain all recorded data points prior to and including the maximum applied load. These charts are shown in Figures 6.366 through 6.379. Tables that summarize these measurements contain approximately 40 sets of readings corresponding to intervals of shear from 10 to 20 kN. These summaries are shown in Tables 6.100 through 6.100. Measurements of vertical deflections with mechanical dial gages were taken at 15 to 40 kN intervals throughout the first part of each test (approximately 60% of the applied load). Because the deflection measurements with the dial gages corresponded with the deflection measurement with the LVDTs, only measurements of vertical deflection by the LVDTs are reported. Zero slip at the ends of the prestressing strands for all specimens was measured by the mechanical dial gages. Therefore, no values of slip are reported.

Mean concrete surface strains were determined from the measurements of surface deformation by the mechanical Whittemore strain gage. Each of the prestressed concrete specimens was instrumented with a series of 45-degree rosettes to measure surface deformations in the web. Specimens PC6N and PC6S had three 45-degree rosettes and specimens PC10N and PC10S had five 45-degree rosettes. The additional rosettes on specimens PC10N and PC10S were placed so that measurements across more cracks

could be taken. A 254-mm mechanical Whittemore strain gage was used to measure the surface deformations. Mean strains are plotted against the applied shear force for the prestressed concrete specimens in Figures 6.380 through 6.395. The values of mean strain are listed in Tables 6.112 through 6.115. Calculation of mean strains followed the procedure discussed next. A steel calibration bar was used to establish a 254-mm reference length. A calibration reading was taken with each gage at the beginning and end of each set of readings corresponding to each load stage. The difference between the mean calibration reading and each measurement on the rosette was taken as the change in length of the particular segment. Strains at each load stage (15 to 40 kN) for each segment were calculated by dividing the change in length by the original length. The original length of each horizontal and vertical segment was taken as 254 mm (gage length) plus the difference in length of the segment from the mean calibration length at zero load.

Failure observations of each test include the sequence of cracking, crack patterns, and modes of failure. The web-shear cracking shear was taken as the shear force at which an instrumented stirrup experienced a significant increase in strain and/or an obvious web-shear crack developed. These trends may be observed in the data shown in the plots and tables. Evidence of crack patterns and failure modes is presented in a series of photographs of each specimen shown in Figures 6.396 through 6.412.

6.4.2.1 Specimen PC6N

6.4.2.1.1 Introduction

The lightweight-aggregate concrete girder of Specimen PC6N had a concrete compressive strength of 48.5 MPa at the time of the test. The prestressing consisted of 8 - ½ inch special low-relaxation strands ($A_{ps} = 862 \text{ mm}^2$) in the bottom flange and 2 - ½ inch strands ($A_{ps} = 215 \text{ mm}^2$) in the top flange. Supplemental longitudinal reinforcement consisted of two No. 7 bars ($A_s = 774 \text{ mm}^2$) placed near the centroid of the lower prestressing steel. There was no transverse reinforcement in this specimen. This specimen serves as a comparison with specimen PC6S with regard to the effect that the amount of transverse reinforcement has on shear strength. It also serves as a comparison with specimen PC10N in determining the effect of concrete compressive strength on the shear capacity.

6.4.2.1.2 Deflections

The locations of the LVDTs are shown in Figure 4.53. The relationship between the shear force in the test region and the deflections at four locations is shown in Figure 6.366. A maximum deflection of 8.5 mm was measured at location 3 (midspan). Deflection measurements are shown at approximately 10 to 20 kN intervals of shear force in Table 6.100.

6.4.2.1.3 Longitudinal Mild Steel Strains

The locations of the longitudinal mild steel strain gages on the No. 7 bars are shown in Figure 4.54. The shear force-strain relationship are shown in Figures 6.367.

Strain measurements are shown in Table 6.101. The maximum strain in the longitudinal reinforcement was approximately 1000 microstrain. Also shown in Table 6.101 are the strain readings for the strain gages in the deck.

6.4.2.1.4 Strand Strains

The locations of the prestressing strand strain gages are shown in Figure 4.54. The shear force-strand strain relationship is shown in Figure 6.368. Strain measurements are shown in Table 6.102. Creep in the glue that attached the strain gages to one wire of the strand may have lead to the inconsistent results shown.

6.4.2.1.5 Concrete Surface Strains

The locations of the concrete surface strain measurements are shown in Figure 4.61. The relationships between applied shear force and mean surface strain are shown in Figures 6.380 – 6.382. These measurements are also listed in Table 6.112, containing 6 sets of readings, each corresponding to intervals of shear from 22 – 67 kN. No significant increases in surface strains were calculated because measurements of surface deformations were suspended prior to cracking.

6.4.2.1.6 Failure Observations

Flexural cracking was not observed prior to failure of specimen PC6N. However, strain gages readings on the No. 7 bars indicate that a flexural crack occurred near the maximum applied shear (See Figure 6.367). The first inclined crack (web-shear crack) occurred in the north shear span at a shear of 317 kN. A second web-shear crack also developed in the south shear span. The failure crack was the web-shear crack in the north

shear span that extended from the face of the support to the face of the loading plate. Spalling of the web in the vicinity of the north web-shear crack was noted. The maximum applied shear during the test was 353 kN. Photographs of Specimen PC6N after testing are shown in Figures 6.369 to 6.372.

6.4.2.2 Specimen PC6S

6.4.2.2.1 Introduction

The lightweight-aggregate concrete girder of Specimen PC6S had a concrete compressive strength of 44.8 MPa at the time of the test. The prestressing consisted of 8 - ½ inch special low-relaxation strands ($A_{ps} = 862 \text{ mm}^2$) in the bottom flange and 2 - ½ inch strands ($A_{ps} = 215 \text{ mm}^2$) in the top flange. Supplemental longitudinal reinforcement consisted of two No. 7 bars ($A_s = 774 \text{ mm}^2$) placed near the centroid of the lower prestressing steel. Transverse reinforcement consisted of Grade 60 No. 3 double-leg stirrups spaced at 508 mm on center. This specimen serves as a comparison with specimen PC6N with regard to the effect that the amount of transverse reinforcement has on shear strength. It also serves as a comparison with specimen PC10S in determining the effect of concrete compressive strength on the shear capacity.

6.4.2.2.2 Deflections

The locations of the LVDTs are shown in Figure 4.53. The relationship between the shear force in the test region and the deflections at four locations is shown in Figure 6.369. A maximum deflection of 18.6 mm was measured at location 3 (midspan).

Deflection measurements are shown at approximately 10 to 20 kN intervals of shear force in Table 6.103.

6.4.2.2.3 Longitudinal Mild Steel Strains

The locations of the longitudinal mild steel strain gages are shown in Figure 4.55. The shear force-strain relationships are shown in Figure 6.370. Strain measurements are shown in Table 6.104. The maximum strain in the longitudinal reinforcement was approximately 90 % of yield strain.

6.4.2.2.4 Strand Strains

The locations of the prestressing strand strain gages are shown in Figure 4.55. The shear force-strand strain relationship is shown in Figure 6.371. Strain measurements are shown in Table 6.105. Creep in the glue that attached the strain gages to one wire of the strand may have lead to the inconsistent results shown.

6.4.2.2.5 Stirrup Strains

The locations of the stirrup strain gages are shown in Figure 4.58. The shear force-stirrup strain relationships are shown in Figures 6.372 and 6.373. Strain measurements are shown in Table 6.106. Yielding of the stirrups T2, T7, and T8 precipitated failure of the specimen.

6.4.2.2.6 Concrete Surface Strains

The locations of the concrete surface strain measurements are shown in Figure 4.61. The relationships between applied shear force and mean surface strain are shown in

Figures 6.383 – 6.385. These measurements are also listed in Table 6.113, containing 15 sets of readings, each corresponding to intervals of shear from 7 – 67 kN. Note the significant increase in vertical strain, from 205 microstrain to 2015 microstrain, at station W1 between 267 and 282 kN (Refer to Figure 6.383 and Table 6.113). This shear force is approximately 5% lower than the shear force at web-shear cracking (293 kN) determined from the stirrup strain readings.

6.4.2.2.7 Failure Observations

The first inclined crack (web-shear crack) occurred in the south shear span at a shear of 293 kN. A second web-shear crack developed in the north shear span at 317 kN. Subsequent web-shear cracking occurred near 343 kN. Prior to failure, three web-shear cracks had developed in each shear span. The strain gage readings in the No. 7 bars indicate that flexural cracking occurred after web-shear cracking at approximately 360 kN of shear. The failure crack was the web-shear crack in the south shear span that was closest to midspan. The crack extended from the face of the loading plate to the curtailment of the supplementary No. 7 longitudinal bars. Spalling and crushing of the top flange in the vicinity of the south web-shear crack was noted. A splitting crack extended along the lower layer of prestressing from the end of the mild reinforcing bars to the face of the support. The maximum applied shear during the test was 520 kN. Photographs of Specimen PC6S after testing are shown in Figures 6.400 to 6.403.

6.4.2.3 Specimen PC10N

6.4.2.3.1 Introduction

The lightweight-aggregate concrete girder of Specimen PC10N had a concrete compressive strength of 69.6 MPa at the time of the test. The prestressing consisted of 8 - ½ inch special low-relaxation strands ($A_{ps} = 862 \text{ mm}^2$) in the bottom flange and 2 - ½ inch strands ($A_{ps} = 215 \text{ mm}^2$) in the top flange. Supplemental longitudinal reinforcement consisted of three No. 8 bars ($A_s = 1529 \text{ mm}^2$) placed near the centroid of the lower prestressing steel. No transverse reinforcement was provided in this specimen. Specimen PC10N serves as a comparison with specimen PC10S with regard to the effect that the amount of transverse reinforcement has on shear strength. It also serves as a comparison with specimen PC6N in determining the effect of concrete compressive strength on the shear capacity.

6.4.2.3.2 Deflections

The locations of the LVDTs are shown in Figure 4.53. The relationship between the shear force in the test region and the deflections at four locations is shown in Figure 6.374. A maximum deflection of 10.4 mm was measured at location 3 (midspan). Deflection measurements are shown at approximately 10 to 20 kN intervals of shear force in Table 6.97.

6.4.2.3.3 Longitudinal Mild Steel Strains

The locations of the longitudinal mild steel strain gages are shown in Figure 4.56. The shear force-strain relationships are shown in Figures 6.375. Strain measurements are

shown in Table 6.98. The maximum strain in the longitudinal reinforcement was approximately 40 % of yield strain.

6.4.2.3.4 Concrete Surface Strains

The locations of the concrete surface strain measurements are shown in Figure 4.62. The relationships between applied shear force and mean surface strain are shown in Figures 6.386 – 6.390. These measurements are also listed in Table 6.114, containing 12 sets of readings, each corresponding to intervals of shear from 22 – 68 kN. No significant increases in surface strains were calculated because measurements of surface deformations were suspended prior to cracking.

6.4.2.3.5 Failure Observations

Flexure cracks and flexure-shear cracks at midspan were observed at 180 kN and 195 kN of shear, respectively. However, strain gage readings on the No. 8 bars indicate that flexural cracking occurred at a shear value of 340 kN. The first inclined cracks (web-shear cracks) occurred in the north shear span at a shear of 440 and 445 kN. The failure crack was the web-shear crack in the north shear span. The crack extended from the face of the support to face of the loading plate. The crack was very smooth as shown in the photographs. Spalling and crushing of the top flange in the vicinity of the north web-shear crack was noted. A minor web-shear crack also extended from the load point to the end of the mild longitudinal steel in the lower flange. A splitting crack developed from this crack along the lower layer of prestressing from the end of the mild reinforcing

bars to the face of the support. The maximum applied shear during the test was 466. kN.

Photographs of Specimen PC10N after testing are shown in Figures 6.404 to 6.407.

6.4.2.4 Specimen PC10S

6.4.2.4.1 Introduction

The lightweight-aggregate concrete girder of Specimen PC10S had a concrete compressive strength of 69.6 MPa at the time of the test. The prestressing consisted of 8 - ½ inch special low-relaxation strands ($A_{ps} = 862 \text{ mm}^2$) in the bottom flange and 2 - ½ inch strands ($A_{ps} = 215 \text{ mm}^2$) in the top flange. Supplemental longitudinal reinforcement consisted of three No. 8 bars ($A_s = 1529 \text{ mm}^2$) placed near the centroid of the lower prestressing steel. Transverse reinforcement consisted of Grade 60 No. 3 double-leg stirrups spaced at 508 mm on center. This specimen serves as a comparison with specimen PC10N with regard to the effect that the amount of transverse reinforcement has on shear strength. It also serves as a comparison with specimen PC6S in determining the effect of concrete compressive strength on the shear capacity.

6.4.2.4.2 Deflections

The locations of the LVDTs are shown in Figure 4.53. The relationship between the shear force in the test region and the deflections at four locations is shown in Figure 6.376. A maximum deflection of 15.0 mm was measured at location 3 (midspan). Deflection measurements are shown at approximately 10 to 20 kN intervals of shear force in Table 6.109.

6.4.2.4.3 Longitudinal Mild Steel Strains

The locations of the longitudinal mild steel strain gages are shown in Figure 4.57. The shear force-strain relationships are shown in Figures 6.377. Strain measurements are shown in Table 6.110. The maximum strain in the longitudinal reinforcement was approximately 60 % of yield strain.

6.4.2.4.4 Stirrup Strains

The locations of the stirrup strain gages are shown in Figure 4.58. The shear force-stirrup strain relationships are shown in Figures 6.378 and 6.379. Strain measurements are shown in Table 6.111. Yielding of the stirrups T2, T7, T8, and T9 precipitated failure of the specimen.

6.4.2.4.5 Concrete Surface Strains

The locations of the concrete surface strain measurements are shown in Figure 4.62. The relationships between applied shear force and mean surface strain are shown in Figures 6.391 – 6.395. These measurements are also listed in Tables 6.115, containing 17 sets of readings, each corresponding to intervals of shear from 6 – 68 kN. Note the significant increase in vertical strain, from 255 microstrain to 3823 microstrain, at station W13 between 423 and 429 kN (Refer to Figure 6.394 and Table 6.115). This shear force is approximately 90 % of the shear force at flexural-shear cracking (444 kN) determined from the stirrup strain readings.

6.4.2.4.6 Failure Observations

Flexure cracks and flexure-shear cracks at midspan were observed near 200 kN of shear. However, strain gage readings on the No. 8 bars indicate that flexural cracking occurred at a shear value of 350 kN. The first inclined cracks (web-shear cracks) occurred at a shear of 444 and 451 kN. Subsequent web-shear cracks developed at 500 kN. Near failure, two major web-shear cracks had developed in each shear span. The failure crack was the web-shear crack in the south shear span that was closest to midspan. The crack extended from the face of the loading plate to the curtailment of the supplementary No. 8 longitudinal bars. Spalling and crushing of the top flange in the vicinity of the south web-shear crack was noted. A splitting crack extended along the lower layer of prestressing from the end of the mild reinforcing bars to the face of the support and spalled off the bottom concrete cover. The maximum applied shear during the test was 534 kN. Photographs of Specimen PC10S after testing are shown in Figures 6.408 to 6.412.

6.5 Code-Estimates of Shear Capacities

In this section, the experimental shear capacities are compared with the code-estimated shear capacities. The code methods include the AASHTO LRFD Simplified Method, AASHTO LRFD General Method, ACI 318-95 Simplified Method, and ACI 318-95 Detailed Method. The methods to estimate the shear capacity according to the AASHTO 16th Edition are the same as the methods in ACI 318-95.

6.5.1 Reinforced Concrete Specimens

Measured shear capacities are compared to code-estimated shear capacities of the reinforced concrete beams in this section. The AASHTO LRFD Simplified Method, AASHTO LRFD Detailed Method, ACI 318-95 Simplified Method, and ACI 318-95 Detailed Method are used to determine the code estimates of shear capacity. For each specimen, values of shear strength are plotted with respect to distance from the centerline of the south load plate. One half of the symmetrical test region is shown in each chart. For each specimen the values of measured and calculated shear strength at the critical locations are summarized in a table. The critical location for shear according to the AASHTO LRFD is at a different section than the critical location according to the ACI 318-95. The critical location of shear and the calculated shear capacity according to the AASHTO 16th Edition are the same as those according to the ACI 318-95.

The measured shear capacity was taken as the maximum applied shear force during the test. The shear force due to self-weight of the concrete specimen and steel spreader beam was ignored. The maximum shear force in the test region due to the self-weight was calculated as 5.3 kN which is approximately 2 % of the lowest measured shear capacity of 280 kN for specimen 8-LWLD. On average, the maximum calculated shear force due to self-weight was lower than 1 ½ % of the measured shear capacities.

The code-estimates of shear strength were calculated using measured material properties for the concrete and steel, not specified values. Values of $\sqrt{f'_c}$ larger than 25/3 MPa were allowed because adequate transverse reinforcement was provided. Values of steel yield strength larger than 420 MPa were also used. The material

properties are discussed in Chapter 4 of this report. Neither resistance factors nor load factors were included in the code-estimated calculations.

Charts are shown for each specimen, which illustrate the shear strength at various locations within the test region. The critical locations for shear strength are shown in the charts. The critical location according to AASHTO LRFD is a distance d_c from the face of the support. This distance corresponds to approximately 350 mm from the center of the support or load plate. The critical section according to ACI 318-95 is a distance d from the face of the support. This distance corresponds to approximately 380 mm from the center of the support or load plate. The critical sections are shown in Figure 6.413.

The estimate of shear strength according to the AASHTO LRFD General Procedure is shown in the charts. The general procedure of calculating θ and β involved the use of Table 5.8.3.2-1 of the AASHTO LRFD Bridge Design Specifications. Table 5.8.3.2-1 is reproduced in Appendix A as Table A.1. The procedure used to calculate the shear strength at a single section is summarized in the following steps:

- Assume a value of shear strength ($V_u = V_n$)
- Calculate shear stress, v
- Calculate v/f'_c
- Calculate M_u corresponding to V_u
- Assume a value of theta, θ
- Calculate ϵ_x
- Interpolate from Table A.1 to determine theta, θ
- Iterate until the assumed value of θ equals theta determined from Table A.1
- Interpolate from Table A.1 to determine β
- Calculate V_c
- Calculate V_s

- Calculate V_n
- If calculated V_n equals assumed value of V_n , stop, otherwise assume a new value of V_n and repeat the steps listed above
- This process must be repeated for each section

Shear strength values are plotted in Figures 6.414 to 6.425. Values of shear strength at the critical locations are summarized in Table 6.116.

In the AASHTO LRFD simplified procedure for determining shear strength, θ is assumed to be 45 degrees and β is assumed to be 2.0. Shear capacity calculated using this procedure is constant along the test region because it is not a function of the bending moment. Values of shear strength calculated by the AASHTO LRFD simplified procedure is approximately 90 % of the values of shear strength calculated by the ACI 318-95 simple method. The reason for this reduction is that the AASHTO LRFD calculates V_c and V_s as a function of d_v as opposed to d (ACI 318-95). For these specimens, d_e was approximately 90 % of d . The values of shear strength at each section are not plotted. However, code-estimated shear strengths at the critical location are summarized in Table 6.116.

Two estimates of shear capacity are produced from ACI 318-95. The shear capacity is calculated as the sum of a concrete contribution and a steel contribution. Two values for the concrete contribution were determined at each section from equations (11-3) and (11-5) of ACI 318-95. For the specimens made of sand-lightweight concrete, the value of $\sqrt{f'_c}$ was replaced with $0.85\sqrt{f'_c}$. The steel contribution to the shear strength is calculated as shown in Chapter 2.

6.5.2 Prestressed Concrete Specimens

Measured shear capacities are compared to code-estimated shear capacities of the prestressed concrete beams in this section. The AASHTO LRFD General Method and ACI 318-95 are used to determine the code-calculated values of shear capacity. For each specimen, values of shear strength are shown along the length of the beam measured from the centerline of the south support to the midspan of the beam. One half of the symmetrical test region is shown in each chart. For each specimen, the values of measured and calculated shear strengths at the critical locations are summarized in Table 6.117. The critical location for shear according to the AASHTO LRFD is at a different section than the critical location according to the ACI 318-95. The measured shear capacity was taken as the maximum applied shear force during the test.

Charts are shown for each specimen, which illustrate the shear strength at various locations within the test region. The critical locations for shear strength are shown in the charts. The critical location according to AASHTO LRFD is the larger of $0.5d_v \cot \theta$ and d_v from the face of the support. This distance corresponds to approximately 710 mm from the center of the support. The critical section according to ACI 318-95 is a distance $h/2$ from the face of the support. This distance corresponds to approximately 405 mm from the center of the support. The critical locations for shear are shown in Figure 6.426.

The estimate of shear strength according to the AASHTO LRFD General Procedure is shown in the charts. The general procedure of calculating θ and β for specimen PC6N and PC10N (members without transverse reinforcement) involved the use of Table 5.8.3.2-2 of the AASHTO LRFD Bridge Design Specifications. The values

in Table 5.8.3.2-2 are reproduced in Table A.2 in Appendix A. The procedure used to calculate the shear strength at a given section is summarized in the following steps:

- Assume a value of shear strength ($V_u = V_n$)
- Calculate shear stress, v
- Calculate v/f'_c
- Calculate M_u corresponding to V_u
- Assume a value of theta, θ
- Calculate ϵ_x
- Determine s_x from AASHTO LRFD Figure C5.8.3.4.2-1 ($s_x = d_v$)
- Interpolate from Table A.2 to determine θ
- Iterate until the assumed value of θ equals the value obtained from Table A.2
- Interpolate from Table A.2 to determine β
- Calculate V_c
- Calculate V_s
- Calculate V_n
- If calculated V_n equals assumed value of V_n , stop, otherwise assume a new value of V_n and repeat the steps listed above

The general procedure of calculating θ and β for specimen PC6S and PC10S (members with transverse reinforcement) involved the use of Table 5.8.3.2-1 of the AASHTO LRFD Bridge Design Specifications. The values of Table 5.8.3.2-1 are reproduced in Table A.1 in Appendix A. The procedure used to calculate the shear strength at a given section (same as that for reinforced concrete specimens) is summarized in the following steps:

- Assume a value of shear strength ($V_u = V_n$)
- Calculate shear stress, v
- Calculate v/f'_c

- Calculate M_u corresponding to V_u
- Assume a value of theta, θ
- Calculate ϵ_x
- Interpolate from Table A.1 to determine θ
- Iterate until the assumed value of θ equals the value obtained from Table A.1
- Interpolate from Table A.1 to determine β
- Calculate V_c
- Calculate V_s
- Calculate V_n
- If calculated V_n equals assumed value of V_n , stop, otherwise assume a new value of V_n and repeat the steps listed above

Shear strength values are plotted for the four prestressed concrete specimens in Figures 6.403 To 6.430. Values of shear strength at the critical locations are summarized in Table 6.117.

Two calculations of the concrete contribution (V_{ci} and V_{cw}) are determined from ACI 318-95. The smaller of the two values of V_c and V_s are summed to determine V_n . Web-shear cracking (V_{cw}) governed the value of the concrete contribution for all prestressed specimens. Calculated values of shear strength for the four prestressed concrete specimens are shown in Figures 6.403 to 6.430 and summarized in Table 6.117.

Table 6.1 Slump, Unit Weight and Air Content for Girder Mixes, 42 MPa (6000psi)

Mix	Slump (mm)	Unit Weight (kg/m^3)	Air Content (%)
LWCH	100	1721	5
NWC	150	2355	6
LWCM1	200	1965	5

Table 6.2 Slump, Unit Weight and Air Content for Girder Mixes, 69 MPa (6000psi)

Mix	Slump (mm)	Unit Weight (kg/m^3)	Air Content (%)
NWC	150	2339	5
LWCH	270	1884	4
LWCHS	150	1965	5.5
LWCMIS	190	2014	5.5
SM-LWCHLS	150	2095	5
SM-LWCHL	230	2144	5
LWCHSF	240	1933	5.5
LWCHF	220	1949	4.5

Table 6.3 Slump, Unit Weight and Air Content for Deck Mixes

Mix	Slump (mm)	Unit Weight (kg/m^3)	Air Content (%)
LWCH	150	1819	6
LWCH-REF	160	1835	5.5
LWCHS	150	1884	5.5
LWCHS-REF	150	1819	5.5
LWCHF	200	1884	6
LWCHF-REF	180	1804	6.5
LWCM1-REF	220	2095	5
NWC	160	2339	6.5
NWC-REF	200	2371	6

Table 6.4 Comparison of Slump, Unit Weight and Air Content for 69 MPa (10,000psi)

Girder Mixes with Type III and Type I Cements

Mix	Slump (mm)	Unit Weight (kg/m ³)	Air Content (%)
LWCHS Type III Cement	150	1965	5.5
LWCHS Type I Cement	190	1949	5.5
NWC Type III Cement	150	2339	5
NWC Type I Cement	250	2339	5.5

Table 6.5 Compressive Strength for 42 MPa (6000 psi) Girder Mixes

Mix	7 days (MPa)	14 days (MPa)	28 days (MPa)
LWCH	45	52	54
LWCMi	32	39	40
NWC	41	45	45

Table 6.6 Compressive Strength for 69 MPa (10,000 psi) Girder Mixes

Mix	7 days (MPa)	14 days (MPa)	28 days (MPa)
LWCHS	55	63	70
LWCMIS	52	57	60
NWC	62	65	66
LWCHSF	47	57	59
LWCHF	48	55	54
SM-LWCHLS	60	66	68
SM-LWCHL	63	67	72

Table 6.7 Compressive Strength of Concrete with Type III and Type I Cements.

69 MPa (10,000 psi) Girder Mixes

Mix	1 day (MPa)	7 day (MPa)	14 day (MPa)	28 day (MPa)
LWCHS Type III Cement	*	55	63	70
LWCHS Type I Cement	36	47	52	52
NWC Type III Cement	*	62	65	66
NWC Type I Cement	31	44	49	60

Table 6.8 Compressive Strength for Deck Mixes

Mix	7 days (MPa)	14 days (MPa)	28 days (MPa)
LWCH	25	33	36
LWCH-REF	30	34	33
LWCHS	34	41	43
LWCHS-REF	25	32	35
LWCHF	22	29	46
LWCHF-REF	22	24	26
LWCMI-REF	31	33	35
NWC	24	29	33
NWC-REF	27	30	36

Table 6.9 Flexural Strength of 42 MPa (6000 psi) Girder Mixes

Property	LWCH	NWC	LWCMI
Flexural Strength (MPa)	4	6.3	4.4

Table 6.10 Flexural Strength of 69 MPa (10,000 psi) Girder Mixes

Property	LWCHS	NWC
Flexural Strength (MPa)	5.2	7.0

Table 6.11 Flexural Strength for Deck Mixes

Mixes	Flexural Strength (MPa)
LWCH	3.3
LWCH-REF	3.2
LWCHS	4.7
LWCHS-REF	3.3
LWCHF	4.8
LWCHF-REF	3.3
LWCMI-REF	4.3
NWC	4.3
NWC-REF	4.4

Table 6.12 Split Tensile Strength of 42 MPa (6000 psi) Girder Mixes

Property	LWCH	NWC	LWCMI
Split Tensile Strength (MPa)	2.2	3.2	2.9

Table 6.13 Split Tensile Strength of 69 MPa (10,000 psi) Girder Mixes

Property	LWCHS	NWC
Split Tensile Strength (MPa)	3.6	3.5

Table 6.14 Split Tensile Strength for Deck Mixes

Mix	Split Tensile Strength (MPa)
LWCH	3.0
LWCH-REF	3.0
LWCHS	3.3
LWCHS-REF	2.8
LWCHF	3.0
LWCHF-REF	2.0
LWCMI-REF	2.6
NWC	2.7
NWC-REF	3.0

Table 6.15 Static and Dynamic Moduli of Elasticity, and Poisson's Ratio.

42 MPa (6000 psi) Girder Mixes

Property	LWCH	NWC	LWCMI
Static E, (GPa)	20	35	24
Dynamic E, (GPa)	18	41	26
Poisson's Ratio	0.14	0.22	0.16

Table 6.16 Static and Dynamic Moduli of Elasticity, and Poisson's Ratio.

69 MPa (10,000 psi) Girder Mixes

Property	LWCHS	NWC
Static E, (GPa)	26	52
Dynamic E, (GPa)	26	56
Poisson's Ratio	0.16	0.21

Table 6.17 Static and Dynamic Moduli of Elasticity, Poisson's Ratio for Deck Mixes

Mix	Static E (GPa)	Dynamic E (GPa)	Poisson's Ratio
LWCH	25	20	0.19
LWCH-REF	17	20	0.17
LWCHS	25	25	0.13
LWCHS-REF	17	19	0.17
LWCHF	19	22	0.19
LWCHF-REF	14	20	0.14
LWCMI-REF	32	33	0.2
NWC	37	41	0.16
NWC-REF	38	37	0.18

Table 6.18 Density of Hardened Concrete, 42 Mpa (6000 psi) Girder Mixes

Mix	Density (kg/m ³)	Density (pcf)
LWCH	1672	103
LWCMI	1949	120
NWC	2355	145

Table 6.19 Density of Hardened Concrete, 69 MPa (10,000 psi) Girder Mixes

Mix	Density (kg/m ³)	Density (pcf)
LWCHS	1868	115
NWC	2533	156

Table 6.20 Density of Hardened Concrete, Deck Mixes

Mix	Density (kg/m ³)	Density (pcf)
LWCH	1657	102
LWCH-REF	1705	106
LWCHS	1788	109
LWCHS-REF	1673	104
LWCHF	1788	108
LWCHF-REF	1705	106
LWCMI-REF	1950	121
NWC	2319	141
NWC-REF	2369	144

Table 6.21 Data from Modified Point Count Experiment (Deck Mixes)

Mix	Lines Traverse d	No. of Stops Air	No. of Stops Paste	No. of Stops FA	No. of Stops CA	IA	Total Stops
LWCH	21	123	260	369	425	590	1176
LWCHS	21	76	332	347	440	416	1199
LWCHF	21	92	354	274	493	561	1197
NWC	24	90	347	401	534	448	1368
LWCH- REF	22	60	440	260	415	248	1124
LWCHS- REF	22	84	378	285	494	326	1154
LWCHF- REF	22	81	352	277	409	426	1143
LWCMI- REF	22	99	510	379	243	416	1231
NWC- REF	23	54	396	218	520	181	1188

Table 6.22 Air Void Parameters of Hardened Concrete and Air Content of Fresh Concrete (Deck Mixes)

Mix	%Air Content of Fresh Concrete	% Air Void Calculated	Air-Paste Ratio	Specific Surface (in ⁻¹)	Spacing Factor
LWCH	6	9	0.37	222	0.012
LWCHS	5.5	5.3	0.24	174	0.042
LWCHF	5.5	6.3	0.22	222	0.020
NWC	5.5	7.3	0.22	160	0.27
LWCH- REF	6	7.7	0.26	250	0.015
LWCHS- REF	6.5	7.1	0.23	211	0.020
LWCHF- REF	5	8	0.19	174	0.27
LWCMI- REF	6.5	6.6	0.26	211	0.019
NWC- REF	6	4.6	0.14	138	0.039

Table 6.23 Freeze-Thaw Resistance of Bridge Girder Mixes, 42 MPa (6000psi)

Mix	LWCH	LWCM I	NWC
W/C	0.42	0.42	0.33
No. of Cycles	300	300	300
Initial Wt. (kg)	17	21	26
Final Wt. (kg)	17	21	25
Initial Freq. (khz)	1.576	1.608	2.08
Final Freq. (khz)	1.495	1.486	1.734
Pc (%)	94	84	51
D.F	0.94	0.84	0.51**

** Pc =60% @ 294 cycles: Calculated by Interpolation.

Table 6.24 Freeze-Thaw Resistance of Bridge Girder Mixes, 69 MPa (10,000psi)

Mix	LWCHS	NWC
W/C	0.33	0.33
No. of Cycles	300	300
Initial Wt. (kg)	4.13	5.58
Final Wt. (kg)	4.13	5.58
Initial Freq. (khz)	1.76	2.16
Final Freq. (khz)	1.731	2.138
Pc (%)	96	94
D.F	0.96	0.94

Table 6.25 Freeze-Thaw Resistance for Newly Developed Bridge Deck Mixes with No Air Drying Prior to Testing

Mix	LWCH	LWCHS	LWCHF	NWC
W/C	0.42	0.42	0.42	0.42
No. of Cycles	216	108	216	300
Initial Wt. (kg)	3.93	4.34	4.34	5.37
Final Wt. (kg)	3.93	4.33	4.13	5.17
Initial Freq. (khz)	1.604	1.772	1.772	1.888
Final Freq. (khz)	1.341	1.374	1.404	1.62
Pc (%)	70	60	63	74
D.F	0.50	0.21	0.45	0.74

Table 6.26 Freeze-Thaw Resistance for Newly Developed LWC for Bridge Deck Application with Air Drying Prior to Testing

Mix	LWCH	LWCHS	LWCHF
W/C	0.42	0.42	0.40
No. of Cycles	304	304	304
Initial Wt. (kg)	3.93	3.93	3.93
Final Wt. (kg)	3.93	3.93	3.93
Initial Freq. (khz)	1.594	1.653	1.594
Final Freq. (khz)	1.575	1.586	1.590
Pc (%)	96	92	99
D.F	0.96	0.92	0.99

Table 6.27 Freeze-Thaw Resistance for Reference Mixes for Bridge Deck Application
with Air Drying Prior to Testing

Mix	LWCH-REF	LWCHS-REF	LWCHF-REF	NWC-REF	LWCMI-REF
W/C	0.443	0.443	0.443	0.443	0.443
No. of Cycles	300	300	300	300	300
Initial Wt. (kg)	3.92	3.72	3.92	5.17	4.34
Final Wt. (kg)	3.72	3.72	3.72	4.96	4.34
Initial Freq. (khz)	1.583	1.493	1.525	1.844	1.564
Final Freq. (khz)	1.572	1.478	1.491	1.589	1.513
Pc (%)	98	98	96	74	94
D.F	0.98	0.98	0.96	0.74	0.94

Table 6.28 Rapid Chloride Ion Permeability Results for Bridge Girder Mixes, 42 MPa
(6000 psi)

Mix	28 -Day Coulomb Reading	56-Day Coulomb Reading	90-Day Coulomb Reading
LWCH	4146	4057	None
LWCMI	8842	None	4215
NWC	1973	1601	None

Table 6.29 Rapid Chloride Ion Permeability Results for Bridge Girder Mixes, 69 MPa
(10,000 psi)

Mix	28 -Day Coulomb Reading	56-Day Coulomb Reading	90-Day Coulomb Reading
LWCHS	644	361	None
NWC	1388	950	432

Table 6.30 Rapid Chloride Ion Permeability for Bridge Deck Mixes

Mix	28 Day Coulomb Reading	56 Day Coulomb Reading	90 Day Coulomb Reading
LWCH	3561	2064	None
LWCH-REF	10,140	6697	6273
LWCHS	1842	784	None
LWCHS-REF	3116	2025	1544
LWCHF	6600	4258	3200
LWCHF-REF	16,573	9187	6614
LWCMI-REF	15, 770	12,482	9030
NWC	3800	3500	None
NWC-REF	4158	3293	3306

Table 6.31 Scaling Resistance for Bridge Deck Mixes

Mix	No. of Cycles	ASTM Rating of Surface
LWCH	50	1
LWCH-REF	50	2
LWCHS	50	2
LWCHS- REF	50	2
LWCHF	50	1
LWCHF- REF	50	2
LWCMI- REF	20	5
NWC	50	1
NWC- REF	50	1

Table 6.32 Deflection Data for Specimen 1-NWLA

Shear (kN)	Δ_2 (mm)	Δ_3 (mm)	Δ_4 (mm)	Δ_6 (mm)
0	0.0	0.0	0.0	0.0
12	0.1	0.1	0.1	0.1
32	0.2	0.2	0.2	0.4
55	0.3	0.3	0.3	0.6
74	0.5	0.5	0.4	0.9
95	0.7	0.7	0.5	1.2
105	0.8	0.8	0.6	1.3
126	1.1	1.0	0.7	1.6
135	1.3	1.1	0.8	1.8
146	1.4	1.2	0.8	1.9
155	1.7	1.5	1.0	2.1
166	1.8	1.7	1.1	2.3
175	1.9	1.8	1.1	2.4
185	2.1	1.9	1.2	2.6
196	2.2	2.0	1.2	2.7
205	2.4	2.2	1.3	3.0
215	2.5	2.3	1.4	3.1
225	2.6	2.4	1.4	3.2
235	2.8	2.6	1.5	3.4
246	3.0	2.8	1.6	3.7
256	3.1	2.9	1.7	3.8
266	3.3	3.0	1.7	3.9
275	3.5	3.2	1.8	4.2
286	3.6	3.3	1.9	4.3
296	3.8	3.4	2.0	4.4
306	4.1	3.7	2.2	4.9
315	4.2	3.8	2.2	5.0
326	4.4	4.0	2.3	5.2
335	4.6	4.3	2.5	5.5
345	4.8	4.4	2.6	5.6
356	5.0	4.7	2.7	5.8
375	5.5	5.2	2.9	6.3
386	5.6	5.3	3.0	6.5
395	6.0	5.7	3.2	6.8
406	6.2	5.9	3.3	7.1
415	6.5	6.3	3.6	7.7
426	6.8	6.7	3.8	8.2
431	7.0	6.8	3.9	8.4
436	7.4	7.4	4.6	8.9

Table 6.33 Longitudinal Steel Strain Data for Specimen 1-NWLA

Shear (kN)	ϵ_{L1B1} ($\times 10^{-6}$)	ϵ_{L1B5} ($\times 10^{-6}$)	ϵ_{L2B1} ($\times 10^{-6}$)	ϵ_{L2B2} ($\times 10^{-6}$)	ϵ_{L2B3} ($\times 10^{-6}$)	ϵ_{L2B4} ($\times 10^{-6}$)	ϵ_{L2B5} ($\times 10^{-6}$)	ϵ_{L2T1} ($\times 10^{-6}$)	ϵ_{L2T3} ($\times 10^{-6}$)	ϵ_{L2T5} ($\times 10^{-6}$)
0	0	0	0	0	0	0	0	0	0	0
12	5	2	22	14	17	11	11	-11	-13	-11
32	16	15	53	39	47	35	35	-27	-36	-30
55	33	30	128	99	110	88	90	-47	-67	-59
74	43	41	520	399	420	397	400	-38	-90	-85
95	63	57	681	522	556	531	562	-32	-106	-96
105	70	65	734	571	608	580	623	-39	-119	-106
126	140	106	836	702	751	723	775	-38	-127	-98
135	256	336	891	756	801	764	811	-45	-131	-101
146	343	449	939	803	854	817	872	-48	-140	-109
155	628	637	991	850	921	876	940	-43	-146	-105
166	668	678	1045	896	972	926	999	-51	-156	-113
175	727	738	1094	939	1023	974	1055	-47	-160	-114
185	823	842	1159	996	1094	1039	1129	-38	-162	-109
196	865	888	1213	1042	1148	1091	1187	-42	-171	-113
205	915	945	1264	1088	1199	1139	1245	-40	-177	-115
215	990	1031	1323	1136	1264	1194	1299	-36	-181	-108
225	1032	1082	1375	1182	1313	1240	1350	-38	-188	-111
235	1090	1157	1434	1231	1372	1292	1405	-38	-190	-106
246	1144	1254	1503	1277	1446	1348	1476	-17	-190	-92
256	1178	1298	1553	1320	1496	1393	1527	-18	-195	-94
266	1220	1355	1609	1369	1551	1444	1585	-16	-200	-90
275	1269	1423	1663	1411	1610	1492	1646	-8	-203	-84
286	1309	1474	1719	1459	1665	1543	1706	-9	-208	-84
296	1347	1533	1773	1506	1718	1591	1764	-6	-213	-82
306	1404	1616	1831	1556	1774	1640	1833	3	-233	-78
315	1437	1662	1879	1597	1821	1684	1886	4	-239	-78
326	1480	1718	1935	1647	1876	1733	1943	7	-243	-74
335	1544	1790	1996	1689	1934	1782	2014	16	-249	-68
345	1581	1837	2049	1734	1983	1829	2067	16	-254	-68
356	1626	1891	2099	1780	2034	1877	2128	23	-254	-63
375	1724	2000	2203	1864	2132	1967	2246	32	-260	-56
386	1771	2054	2259	1910	2183	2014	2304	36	-260	-50
395	1838	2115	2315	1956	2229	2059	2377	53	-253	-43
406	1883	2167	2370	2002	2278	2106	2438	62	-250	-41
415	1927	2221	2425	2045	2324	2151	2497	66	-242	-41
426	1988	2287	2486	2094	2379	2205	2569	73	-223	-42
431	2013	2315	2514	2118	2406	2228	2600	75	-221	-42
436	2035	2345	2540	2140	2428	2250	2635	82	-202	-41

Continued

Table 6.33 Longitudinal Steel Strain Data for Specimen 1-NWLA (Concluded)

Shear (kN)	ϵ_{L3B1} ($\times 10^{-6}$)	ϵ_{L3B3} ($\times 10^{-6}$)	ϵ_{L3B5} ($\times 10^{-6}$)	ϵ_{L3T5} ($\times 10^{-6}$)	ϵ_{L4B1} ($\times 10^{-6}$)	ϵ_{L4B3} ($\times 10^{-6}$)	ϵ_{L4B5} ($\times 10^{-6}$)	ϵ_{L4T1} ($\times 10^{-6}$)	ϵ_{L4T3} ($\times 10^{-6}$)	ϵ_{L4T5} ($\times 10^{-6}$)
0	0	0	0	0	0	0	0	0	0	0
12	12	11	2	-16	-10	-14	-9	12	16	11
32	31	27	15	-35	-31	-36	-31	36	45	40
55	61	47	36	-57	-70	-72	-60	129	150	205
74	82	74	53	-74	-86	-88	-65	406	406	458
95	231	171	129	-101	-107	-106	-63	565	559	623
105	274	212	175	-111	-120	-119	-73	616	610	689
126	414	376	377	-122	-142	-140	-86	756	747	816
135	481	471	498	-122	-153	-151	-95	808	794	869
146	618	583	599	-127	-164	-162	-102	865	849	927
155	803	702	724	-111	-173	-171	-110	927	913	994
166	851	740	766	-117	-185	-183	-120	981	963	1059
175	953	797	839	-117	-194	-192	-126	1051	1016	1119
185	1033	844	906	-120	-203	-199	-129	1126	1081	1183
196	1088	883	955	-128	-214	-211	-137	1181	1134	1242
205	1142	919	1009	-133	-223	-219	-141	1237	1184	1292
215	1201	959	1072	-142	-233	-226	-145	1299	1240	1358
225	1249	993	1117	-148	-241	-237	-152	1351	1288	1414
235	1307	1030	1165	-154	-246	-243	-155	1410	1341	1472
246	1346	1072	1236	-166	-250	-251	-157	1479	1404	1531
256	1382	1107	1279	-172	-257	-259	-162	1532	1451	1587
266	1408	1145	1319	-180	-261	-265	-162	1591	1505	1645
275	1471	1189	1367	-188	-260	-268	-157	1649	1555	1700
286	1505	1227	1412	-194	-264	-274	-159	1703	1606	1759
296	1534	1268	1458	-201	-267	-279	-157	1760	1654	1816
306	1603	1313	1510	-208	-271	-277	-150	1822	1702	1863
315	1620	1349	1553	-214	-277	-285	-152	1874	1747	1917
326	1741	1389	1584	-217	-282	-287	-151	1932	1798	1978
335	1772	1439	1645	-212	-291	-287	-152	1997	1848	2034
345	1819	1478	1693	-215	-294	-291	-151	2049	1894	2085
356	1869	1513	1773	-192	-292	-291	-150	2110	1945	2148
375	1962	1603	1873	-144	-307	-295	-158	2225	2037	2249
386	1996	1653	1926	-130	-311	-298	-160	2284	2087	2304
395	-	1709	1986	-69	-333	-302	-179	2349	2138	2362
406	-	1757	2041	-64	-348	-330	-208	2418	2195	2426
415	-	1813	2103	-24	-391	-366	-279	2486	2254	2490
426	-	1860	2174	7	-413	-370	-308	2547	2306	2562
431	-	1883	2203	9	-420	-370	-318	2575	2332	2594
436	-	1899	2269	35	-473	-343	-389	2603	2362	2637

Table 6.34 Stirrup Strain Data for Specimen 1-NWLA

Shear (kN)	ϵ_{T1A} ($\times 10^{-6}$)	ϵ_{T1C} ($\times 10^{-6}$)	ϵ_{T2A} ($\times 10^{-6}$)	ϵ_{T2C} ($\times 10^{-6}$)	ϵ_{T3A} ($\times 10^{-6}$)	ϵ_{T3C} ($\times 10^{-6}$)	ϵ_{T4A} ($\times 10^{-6}$)	ϵ_{T4C} ($\times 10^{-6}$)
0	0	0	0	0	0	0	0	0
12	-1	0	-1	5	-3	-2	-1	2
32	1	0	1	10	-3	-4	-1	5
55	2	-1	4	14	-2	-7	-1	6
74	5	2	2	14	-4	-11	-1	8
95	-8	-1	30	26	-4	-12	3	13
105	-9	-5	37	28	-3	-13	4	15
126	41	-27	26	20	5	-10	9	20
135	72	-21	26	24	7	-9	9	22
146	170	34	30	29	12	-5	13	26
155	362	238	146	361	23	2	21	34
166	400	264	160	415	24	3	23	36
175	566	397	389	668	32	5	27	42
185	671	514	576	885	39	8	35	48
196	722	554	627	966	42	8	36	51
205	782	607	710	1080	46	9	39	52
215	853	705	868	1279	54	12	43	56
225	897	739	908	1351	55	13	44	58
235	949	792	989	1495	60	13	47	64
246	1025	848	1181	1678	71	19	52	68
256	1072	875	1225	1729	76	21	54	72
266	1134	924	1372	1897	105	26	57	77
275	1194	968	1632	2041	142	38	63	79
286	1242	998	1701	2098	150	43	67	83
296	1289	1028	1782	2162	157	47	71	87
306	1345	1070	1910	2257	199	66	104	124
315	1392	1096	1970	2297	203	68	107	128
326	1458	1152	2117	2325	233	188	113	137
335	1525	1198	2262	2371	743	288	139	169
345	1574	1231	2314	2387	803	296	144	172
356	1681	1287	2648	2521	2235	454	217	208
375	1740	1317	2593	2858	3028	637	286	262
386	1755	1332	2647	2990	3312	679	298	272
395	1702	1333	2694	3090	4278	813	374	326
406	1721	1348	2731	3139	4617	840	399	337
415	1733	1358	2755	3169	4935	880	460	359
426	1773	1375	2818	3269	5369	972	595	418
431	1800	1386	2846	3325	5575	985	633	427
436	1868	1402	3003	6490	8857	1140	1066	479

Continued

Table 6.34 Stirrup Strain Data for Specimen 1-NWLA (*Concluded*)

Shear (kN)	ϵ_{T5A} ($\times 10^{-6}$)	ϵ_{T5C} ($\times 10^{-6}$)	ϵ_{T6A} ($\times 10^{-6}$)	ϵ_{T6C} ($\times 10^{-6}$)	ϵ_{T7A} ($\times 10^{-6}$)	ϵ_{T7C} ($\times 10^{-6}$)
0	0	0	0	0	0	0
12	-4	2	0	4	-1	-3
32	-5	1	2	10	2	-3
55	-3	1	4	17	1	-3
74	-4	-1	4	22	26	2
95	2	6	-5	8	14	-27
105	3	7	0	10	13	-31
126	15	11	30	45	1	-13
135	15	13	35	81	-5	-5
146	16	16	63	160	-8	14
155	20	20	121	298	-18	33
166	22	21	181	346	-21	35
175	23	24	290	435	-26	43
185	31	28	513	612	-26	61
196	32	28	573	656	-31	61
205	35	28	699	747	-26	64
215	41	30	986	933	7	74
225	43	31	1063	980	14	75
235	47	35	1231	1077	26	76
246	57	42	1444	1268	39	87
256	60	45	1504	1312	40	87
266	66	49	1589	1370	46	89
275	78	60	1846	1523	77	112
286	84	65	2027	1579	95	122
296	90	70	2237	1626	120	135
306	294	645	3008	3469	200	188
315	300	666	3102	3651	207	194
326	316	699	3382	3973	226	208
335	415	866	6136	5805	288	287
345	427	897	6457	6651	289	297
356	464	1001	6428	8271	638	363
375	553	1164	6819	9504	777	456
386	568	1180	7587	10254	836	485
395	751	1424	8663	12513	928	572
406	801	1435	9525	14951	966	595
415	935	1485	13599	7545	978	624
426	1084	1638	15134	6394	998	681
431	1111	1672	15673	6406	994	700
436	1273	1775	15765	6584	888	698

Table 6.35 Deflection Data for Specimen 2-NWLB

Shear (kN)	Δ_2 (mm)	Δ_3 (mm)	Δ_4 (mm)	Δ_6 (mm)
0	0.0	0.0	0.0	0.0
20	0.1	0.1	0.1	0.1
41	0.2	0.2	0.1	0.2
61	0.3	0.3	0.2	0.4
80	0.5	0.5	0.3	0.6
100	0.7	0.7	0.4	0.8
120	0.9	0.9	0.5	1.0
140	1.2	1.1	0.7	1.3
161	1.6	1.4	0.9	1.6
180	1.9	1.7	1.0	2.0
201	2.3	2.1	1.2	2.4
221	2.6	2.4	1.4	2.7
240	2.8	2.6	1.5	2.9
260	3.2	3.0	1.7	3.2
280	3.6	3.4	1.9	3.5
300	4.0	3.8	2.1	3.9
311	4.2	4.1	2.2	4.1
320	4.3	4.2	2.3	4.2
330	4.5	4.3	2.3	4.4
341	4.7	4.5	2.5	4.6
350	4.8	4.7	2.5	4.7
360	5.0	4.9	2.7	4.9
370	5.4	5.2	2.8	5.2
381	5.5	5.4	2.9	5.3
391	5.7	5.6	2.9	5.5
400	6.1	5.9	3.1	5.9
410	6.2	6.1	3.2	6.0
420	6.4	6.3	3.3	6.2
430	6.7	6.7	3.3	6.4
440	7.0	7.0	3.5	6.6
450	7.3	7.3	3.6	6.8
459	7.7	7.8	3.7	7.0
472	8.4	8.6	4.0	7.4
475	8.5	8.8	4.1	7.5
480	8.8	9.1	4.2	7.6
481	8.9	9.3	4.2	7.7
485	9.4	10.1	4.3	8.0

Table 6.36 Longitudinal Strain Data for Specimen 2-NWLB

Shear (kN)	ϵ_{L1B1} ($\times 10^{-6}$)	ϵ_{L1B5} ($\times 10^{-6}$)	ϵ_{L2B1} ($\times 10^{-6}$)	ϵ_{L2B2} ($\times 10^{-6}$)	ϵ_{L2B3} ($\times 10^{-6}$)	ϵ_{L2B4} ($\times 10^{-6}$)	ϵ_{L2B5} ($\times 10^{-6}$)	ϵ_{L2T1} ($\times 10^{-6}$)	ϵ_{L2T3} ($\times 10^{-6}$)	ϵ_{L2T5} ($\times 10^{-6}$)
0	0	0	0	0	0	0	0	0	0	0
20	8	7	29	26	21	24	22	-16	-23	-19
41	20	19	70	66	58	55	51	-37	-44	-42
61	35	34	216	227	176	222	197	-63	-74	-71
80	50	47	426	472	401	473	419	-71	-88	-78
100	59	57	580	619	547	651	598	-72	-86	-67
120	77	72	705	746	675	787	754	-75	-88	-65
140	153	204	836	879	793	905	862	-84	-95	-69
161	330	447	971	1015	916	1034	989	-94	-104	-78
180	495	651	1092	1135	1020	1143	1104	-100	-110	-81
201	858	938	1224	1272	1144	1274	1237	-102	-113	-80
221	1007	1056	1342	1403	1258	1393	1357	-96	-113	-78
240	1084	1132	1440	1500	1344	1487	1455	-102	-119	-81
260	1228	1243	1560	1624	1452	1607	1570	-94	-115	-71
280	1336	1323	1675	1739	1557	1722	1681	-70	-107	-56
300	1434	1392	1791	1855	1658	1835	1795	-45	-92	-34
311	1500	1430	1864	1926	1721	1905	1864	-15	-78	-11
320	1532	1461	1909	1972	1761	1949	1909	-16	-80	-11
330	1571	1497	1962	2023	1808	2000	1961	-13	-78	-7
341	1627	1537	2032	2090	1866	2066	2028	20	-66	9
350	1661	1569	2077	2137	1907	2109	2075	26	-61	16
360	1703	1604	2134	2190	1957	2161	2127	47	-51	37
370	1752	1638	2201	2251	2006	2216	2184	88	-36	57
381	1793	1675	2256	2306	2055	2269	2238	99	-29	65
391	1838	1714	2305	2358	2101	2319	2293	134	-16	76
400	1885	1757	2368	2418	2148	2378	2351	193	-2	92
410	1923	1789	2418	2467	2190	2423	2397	207	5	100
420	1973	1827	2480	2526	2241	2476	2445	206	-5	86
430	2019	1862	2546	2586	2294	2531	2498	189	-29	58
440	2065	1898	2655	2646	2346	2590	2586	182	-40	47
450	2107	1933	2796	2712	2405	2651	2678	168	-53	32
459	2133	1963	2900	2786	2463	2723	2829	64	-124	-9
472	2181	2003	3085	2971	2557	2899	3027	-36	-213	-62
475	2192	2013	3115	3059	2577	2927	3069	-49	-223	-69
480	2211	2030	3186	3137	2624	3039	3175	-88	-248	-89
481	2216	2034	3226	3157	2638	3064	3204	-101	-254	-97
485	2227	2045	3341	3280	2799	3211	3337	-181	-285	-129

Continued

Table 6.36 Longitudinal Steel Strain Data (*Concluded*)

Shear (kN)	ϵ_{L3B1} ($\times 10^{-6}$)	ϵ_{L3B3} ($\times 10^{-6}$)	ϵ_{L3B5} ($\times 10^{-6}$)	ϵ_{L3T1} ($\times 10^{-6}$)	ϵ_{L3T5} ($\times 10^{-6}$)	ϵ_{L4B1} ($\times 10^{-6}$)	ϵ_{L4B3} ($\times 10^{-6}$)	ϵ_{L4B5} ($\times 10^{-6}$)	ϵ_{L4T1} ($\times 10^{-6}$)	ϵ_{L4T3} ($\times 10^{-6}$)	ϵ_{L4T5} ($\times 10^{-6}$)
0	0	0	0	0	0	0	0	0	0	0	0
20	16	15	11	-10	-17	-20	-19	-18	21	24	-215
41	34	29	25	-21	-33	-42	-39	-39	57	57	-136
61	57	50	43	-33	-46	-66	-47	-59	346	364	322
80	92	82	73	-44	-59	-71	-31	-60	481	508	474
100	221	192	146	-51	-80	-89	-35	-75	589	617	626
120	406	429	426	-65	-84	-100	-36	-88	695	730	783
140	523	564	586	-73	-92	-116	-41	-98	799	832	920
161	672	725	782	-70	-98	-129	-43	-107	912	945	1041
180	766	838	896	-80	-102	-136	-34	-108	1006	1039	1209
201	882	956	1005	-95	-109	-140	-11	-103	1130	1148	1376
221	983	1060	1100	-109	-116	-120	19	-104	1225	1249	1481
240	1052	1136	1173	-121	-125	-129	18	-113	1307	1331	1598
260	1153	1221	1242	-136	-137	-138	34	-116	1412	1429	1719
280	1263	1298	1299	-150	-131	-140	53	-116	1509	1527	1825
300	1353	1363	1373	-165	-145	-146	75	-113	1620	1623	1972
311	1430	1382	1413	-174	-157	-150	91	-108	1689	1683	2065
320	1462	1411	1442	-180	-161	-154	91	-111	1729	1723	2225
330	1506	1439	1477	-186	-167	-157	93	-114	1778	1767	2193
341	1580	1450	1501	-196	-176	-163	109	-109	1844	1824	2178
350	1621	1476	1531	-201	-182	-166	112	-111	1886	1863	2230
360	1694	1491	1558	-207	-190	-168	123	-108	1940	1910	2285
370	1784	1479	1587	-218	-202	-174	145	-103	1997	1957	2335
381	1841	1506	1630	-226	-208	-177	149	-104	2048	2003	2400
391	1932	1506	1681	-233	-214	-177	157	-105	2099	2050	2460
400	2044	1489	1695	-235	-221	-184	180	-103	2152	2095	2533
410	2099	1509	1727	-242	-227	-186	182	-106	2201	2138	2583
420	2190	1510	1747	-246	-223	-188	192	-106	2257	2185	2647
430	2286	1538	1793	-233	-212	-184	205	-103	2314	2231	2695
440	2362	1578	1841	-223	-208	-184	219	-103	2368	2278	2753
450	2435	1613	1901	-215	-207	-187	231	-106	2428	2327	2813
459	2521	1645	1987	-222	-215	-187	242	-105	2491	2374	2891
472	2650	1714	2117	-218	-247	-190	255	-105	2636	2449	3026
475	2693	1730	2151	-220	-251	-189	259	-105	2663	2463	3060
480	2765	1769	2245	-232	-264	-190	267	-101	2727	2495	3111
481	2787	1776	2274	-243	-269	-191	270	-100	2743	2504	3111
485	3045	1805	2435	-341	-323	-191	284	-88	2809	2540	3181

Table 6.37 Stirrup Strain Data for Specimen 2-NWLB

Shear (kN)	ϵ_{T1A} ($\times 10^{-6}$)	ϵ_{T1B} ($\times 10^{-6}$)	ϵ_{T1C} ($\times 10^{-6}$)	ϵ_{T2A} ($\times 10^{-6}$)	ϵ_{T2B} ($\times 10^{-6}$)	ϵ_{T2C} ($\times 10^{-6}$)	ϵ_{T3A} ($\times 10^{-6}$)	ϵ_{T3B} ($\times 10^{-6}$)	ϵ_{T3C} ($\times 10^{-6}$)
0	0	0	0	0	0	0	0	0	0
20	2	2	-2	0	2	3	-1	0	-2
41	5	5	-1	3	5	7	0	0	0
61	5	11	-2	6	7	14	2	3	4
80	16	32	17	9	10	17	4	4	7
100	-5	16	20	8	10	21	3	2	7
120	-11	8	16	27	28	25	3	2	8
140	0	23	27	20	27	39	5	5	13
161	80	76	69	17	29	26	14	10	21
180	129	109	98	50	49	29	26	21	34
201	175	157	137	108	80	53	31	24	42
221	239	202	180	239	271	111	36	28	49
240	261	219	192	265	362	132	38	31	51
260	354	276	239	381	581	223	40	33	56
280	479	333	284	791	1638	1276	46	37	66
300	637	407	326	1683	2314	1939	46	43	68
311	756	477	381	1962	2551	2179	48	51	78
320	770	488	388	2009	2614	2239	50	52	79
330	801	510	409	2090	2707	2321	52	54	80
341	890	587	482	2336	2973	2521	62	62	88
350	909	616	513	2424	3072	2598	64	63	89
360	963	675	691	2595	3369	2824	74	72	91
370	1070	770	828	2742	4462	3068	99	95	106
381	1105	800	872	2769	4699	3189	103	98	109
391	1179	870	956	2801	5104	3422	109	106	112
400	1334	1002	1092	2854	5547	6915	187	131	138
410	1382	1034	1141	2880	5582	7842	192	135	140
420	1465	1108	1233	2963	5791	9244	202	143	149
430	1474	1175	1244	3438	8291	10607	219	155	161
440	1496	1229	1280	4798	9894	11773	246	175	178
450	1516	1283	1316	7984	11222	12934	270	197	196
459	1511	1334	1354	15197	10991	16831	303	221	233
472	1582	1413	1406	4031	5992	17410	492	464	479
475	1597	1428	1421	3704	5714	15520	512	488	504
480	1641	1468	1446	3422	4913	11794	542	528	553
481	1656	1480	1456	3336	4776	11405	547	538	564
485	1728	1527	1492	2938	3531	10297	570	577	613

Continued

Table 6.37 Stirrup Strain Data for Specimen 2-NWLB (Concluded)

Shear (kN)	ϵ_{T4A} ($\times 10^{-6}$)	ϵ_{T4B} ($\times 10^{-6}$)	ϵ_{T4C} ($\times 10^{-6}$)	ϵ_{T5A} ($\times 10^{-6}$)	ϵ_{T5B} ($\times 10^{-6}$)	ϵ_{T5C} ($\times 10^{-6}$)
0	0	0	0	0	0	0
20	2	0	1	1	-1	0
41	4	2	5	3	1	2
61	6	4	8	7	9	5
80	8	7	13	6	9	12
100	5	5	11	-9	-7	-1
120	8	5	14	-25	-15	-18
140	29	16	16	-32	-16	-37
161	21	10	13	46	20	-12
180	339	91	58	287	273	292
201	507	144	84	368	364	432
221	682	234	110	453	469	576
240	737	254	119	484	502	628
260	914	345	150	571	586	745
280	1076	425	198	652	679	878
300	1273	505	375	735	791	1042
311	1450	809	688	827	880	1175
320	1465	820	698	843	894	1201
330	1469	831	717	878	922	1241
341	1501	933	823	965	1000	1330
350	1506	943	839	1001	1026	1369
360	1518	965	875	1068	1076	1424
370	1566	1093	1037	1134	1165	1486
381	1576	1108	1069	1176	1201	1521
391	1592	1137	1137	1225	1253	1569
400	2271	1412	1543	1299	1355	1639
410	2340	1428	1583	1329	1383	1663
420	2531	1466	1651	1373	1437	1699
430	2622	1505	1707	1414	1508	1739
440	2704	1546	1755	1453	1569	1788
450	2797	1588	1811	1496	1617	1834
459	2831	1631	1871	1543	1660	1866
472	2867	1692	1954	1607	1731	1906
475	2873	1703	1964	1620	1750	1919
480	2902	1743	2003	1648	1801	1936
481	2910	1756	2016	1657	1813	1938
485	2966	1830	2086	1706	1917	1928

Table 6.38 Deflection Data for Specimen 3-NWLC

Shear (kN)	Δ_2 (mm)	Δ_3 (mm)	Δ_4 (mm)	Δ_6 (mm)
0	0.0	0.0	0.0	0.0
20	0.1	0.1	0.0	0.1
40	0.2	0.2	0.1	0.2
60	0.3	0.3	0.1	0.4
80	0.5	0.5	0.3	0.8
100	0.8	0.7	0.5	1.1
120	1.0	0.9	0.6	1.4
130	1.2	1.0	0.7	1.7
140	1.4	1.2	0.8	1.7
150	1.6	1.4	0.9	2.0
160	1.7	1.5	1.0	2.1
170	1.9	1.7	1.1	2.2
180	2.0	1.8	1.2	2.4
190	2.1	1.9	1.2	2.5
200	2.3	2.1	1.3	2.8
210	2.4	2.2	1.4	2.9
220	2.5	2.3	1.5	3.1
230	2.7	2.5	1.6	3.3
240	2.9	2.6	1.6	3.4
250	3.1	2.8	1.8	3.9
261	3.2	2.9	1.9	4.2
271	3.5	3.1	2.1	4.5
280	3.6	3.2	2.1	4.6
290	3.8	3.4	2.3	4.9
300	3.9	3.5	2.3	5.0
310	4.3	3.9	2.6	5.4
320	4.4	4.0	2.7	5.5
330	4.5	4.1	2.7	5.7
340	4.8	4.4	3.0	6.0
350	5.0	4.5	3.1	6.2
360	5.3	4.9	3.3	6.4
370	5.6	5.2	3.5	6.7
381	5.8	5.3	3.6	6.9
390	5.9	5.5	3.8	7.1
400	6.3	5.9	4.0	7.4
411	6.5	6.1	4.2	7.7
416	6.7	6.3	4.3	7.9
421	8.7	9.2	6.6	9.1

Table 6.39 Longitudinal Steel Strain Data for Specimen 3-NWLC

Shear (kN)	ϵ_{L1B5} ($\times 10^{-6}$)	ϵ_{L2B1} ($\times 10^{-6}$)	ϵ_{L2B2} ($\times 10^{-6}$)	ϵ_{L2B3} ($\times 10^{-6}$)	ϵ_{L2B4} ($\times 10^{-6}$)	ϵ_{L2B5} ($\times 10^{-6}$)	ϵ_{L2T1} ($\times 10^{-6}$)	ϵ_{L2T3} ($\times 10^{-6}$)	ϵ_{L2T5} ($\times 10^{-6}$)
0	0	0	0	0	0	0	0	0	0
20	14	70	69	79	66	-18	-19	-16	-16
40	26	147	144	170	142	-39	-41	-35	-36
60	40	242	242	281	240	-59	-58	-54	-52
80	57	365	360	422	363	-66	-67	-65	-58
100	70	473	457	533	463	-74	-77	-67	-59
120	109	584	563	661	577	-78	-81	-67	-57
130	215	643	622	726	637	-76	-78	-63	-55
140	237	693	668	781	685	-81	-84	-68	-60
150	388	758	730	851	750	-80	-83	-67	-57
160	416	801	772	900	794	-87	-89	-73	-63
170	770	850	821	969	854	-85	-88	-74	-64
180	861	904	871	1032	912	-85	-88	-73	-59
190	907	954	917	1091	963	-89	-94	-77	-63
200	1020	1016	974	1165	1030	-81	-89	-70	-51
210	1060	1064	1019	1218	1078	-86	-96	-74	-56
220	1114	1112	1065	1272	1127	-87	-98	-75	-55
230	1196	1174	1122	1341	1190	-84	-100	-69	-47
240	1242	1221	1167	1396	1239	-83	-100	-69	-45
250	1314	1279	1220	1464	1301	-76	-98	-62	-33
261	1362	1330	1268	1522	1352	-78	-102	-62	-31
271	1442	1392	1320	1593	1418	-70	-102	-55	-17
280	1487	1437	1364	1648	1467	-72	-105	-56	-17
290	1553	1493	1413	1708	1525	-66	-105	-46	-2
300	1590	1539	1458	1762	1572	-68	-109	-49	-4
310	1645	1600	1513	1833	1641	-57	-108	-37	16
320	1680	1647	1557	1884	1687	-60	-111	-41	14
330	1723	1695	1602	1940	1734	-60	-113	-40	16
340	1780	1755	1654	2008	1799	-54	-114	-27	36
350	1824	1804	1700	2063	1848	-54	-116	-27	38
360	1874	1858	1748	2121	1900	-45	-109	-3	57
370	1933	1915	1796	2188	1967	-39	-113	21	80
381	1976	1962	1841	2243	2017	-40	-115	24	85
390	2019	2013	1886	2297	2066	-37	-116	31	94
400	2084	2070	1939	2366	2131	-31	-121	58	125
411	2133	2125	1988	2428	2185	-30	-125	63	134
416	2158	2159	2019	2462	2214	-30	-130	60	127
421	2187	2232	2076	2569	2295	-136	-268	78	112

Continued

Table 6.39 Longitudinal Steel Strain Data for Specimen 3-NWLC (Concluded)

Shear (kN)	ϵ_{L3B2} ($\times 10^{-6}$)	ϵ_{L3B3} ($\times 10^{-6}$)	ϵ_{L3T2} ($\times 10^{-6}$)	ϵ_{L3T3} ($\times 10^{-6}$)	ϵ_{L4B2} ($\times 10^{-6}$)	ϵ_{L4B3} ($\times 10^{-6}$)	ϵ_{L4T2} ($\times 10^{-6}$)	ϵ_{L4T3} ($\times 10^{-6}$)
0	0	0	0	0	0	0	0	0
20	0	19	-11	-13	-19	-25	66	76
40	0	36	-24	-27	-40	-54	138	154
60	0	57	-39	-41	-56	-79	226	249
80	0	117	-51	-56	-65	-107	357	370
100	0	247	-60	-63	-77	-133	484	484
120	0	405	-71	-74	-86	-160	616	601
130	0	505	-77	-79	-86	-171	690	667
140	0	580	-62	-61	-92	-183	748	720
150	0	651	-41	-52	-92	-192	828	782
160	0	680	-47	-58	-98	-202	875	827
170	0	730	-51	-63	-99	-212	938	888
180	0	788	-54	-70	-96	-223	998	944
190	0	830	-59	-77	-99	-233	1051	999
200	0	908	-63	-87	-93	-244	1126	1067
210	0	945	-68	-93	-97	-254	1175	1115
220	0	989	-74	-99	-95	-262	1227	1165
230	0	1050	-80	-111	-89	-271	1294	1222
240	0	1097	-85	-119	-91	-280	1344	1272
250	0	1167	-89	-131	-80	-279	1409	1315
261	0	1221	-81	-129	-74	-284	1455	1366
271	0	1291	-58	-104	-68	-293	1520	1415
280	0	1335	-63	-109	-69	-303	1570	1464
290	0	1401	-17	-69	-62	-314	1632	1508
300	0	1441	-20	-73	-64	-320	1680	1554
310	0	1528	106	95	-50	-320	1753	1608
320	0	1569	103	92	-52	-326	1798	1651
330	0	1620	116	119	-50	-334	1852	1695
340	0	1697	185	220	-41	-341	1917	1741
350	0	1745	190	226	-41	-347	1968	1786
360	0	1795	271	233	-33	-350	2026	1833
370	0	1855	342	268	-26	-363	2088	1877
381	0	1903	353	273	-22	-368	2138	1922
390	0	1956	380	285	-16	-373	2186	1967
400	0	2023	460	319	-16	-394	2247	2013
411	0	2081	496	317	-16	-404	2300	2061
416	0	2120	543	322	-16	-406	2327	2085
421	0	2363	606	329	-24	-410	2385	2103

Table 6.40 Stirrup Strain Data for Specimen 3-NWLC

Shear (kN)	ϵ_{T1A} ($\times 10^{-6}$)	ϵ_{T1C} ($\times 10^{-6}$)	ϵ_{T2A} ($\times 10^{-6}$)	ϵ_{T2C} ($\times 10^{-6}$)	ϵ_{T3A} ($\times 10^{-6}$)	ϵ_{T3C} ($\times 10^{-6}$)	ϵ_{T4A} ($\times 10^{-6}$)	ϵ_{T4C} ($\times 10^{-6}$)
0	0	0	0	0	0	0	0	0
20	3	5	3	6	4	5	4	5
40	5	5	5	8	7	8	5	8
60	11	6	7	11	11	9	7	13
80	-3	-16	12	16	16	13	13	16
100	6	48	12	15	24	16	16	19
120	99	241	12	18	32	17	20	23
130	195	412	12	19	38	19	24	26
140	233	458	57	83	29	19	33	31
150	327	543	140	233	57	31	41	40
160	348	569	149	243	60	32	43	41
170	413	628	182	296	72	35	47	44
180	493	709	249	415	92	38	51	45
190	532	754	268	440	97	40	54	47
200	657	866	381	611	127	47	61	49
210	688	902	397	636	132	48	63	51
220	734	949	436	687	146	52	65	51
230	825	1034	539	834	210	65	73	57
240	889	1091	609	928	234	70	76	58
250	999	1178	748	1076	323	99	93	59
261	1047	1233	792	1134	343	113	130	75
271	1156	1311	876	1218	409	135	165	95
280	1200	1355	913	1257	421	140	168	98
290	1297	1433	1049	1411	535	175	200	115
300	1332	1473	1080	1449	548	181	204	118
310	1459	1558	1238	1605	751	266	281	154
320	1495	1592	1263	1627	761	270	285	156
330	1548	1637	1312	1672	792	284	296	160
340	1659	1739	1443	1800	949	384	382	196
350	1706	1784	1504	1862	982	394	391	201
360	1775	1834	2159	2590	1612	1788	429	253
370	1850	1902	2380	2741	1922	2027	520	298
381	1896	1932	2490	2788	1962	2104	530	303
390	1944	1974	2618	2834	2003	2210	543	315
400	2031	2042	2758	2930	2108	2421	624	369
411	2086	2058	2941	2975	2171	2625	643	388
416	2100	2009	3135	2987	2231	2669	663	430
421	1599	1394	8252	3223	2623	2675	3075	1089

Continued

Table 6.40 Stirrup Strain Data for Specimen 3-NWLC (*Concluded*)

Shear (kN)	ϵ_{T5A} ($\times 10^{-6}$)	ϵ_{T5C} ($\times 10^{-6}$)	ϵ_{T6A} ($\times 10^{-6}$)	ϵ_{T6C} ($\times 10^{-6}$)	ϵ_{T7A} ($\times 10^{-6}$)	ϵ_{T7C} ($\times 10^{-6}$)
0	0	0	0	0	0	0
20	4	6	5	5	2	5
40	5	8	6	13	-1	5
60	6	7	31	15	-8	1
80	15	18	56	2	-13	-5
100	20	22	111	-6	-14	-8
120	26	26	190	-8	-14	-9
130	34	23	273	0	-7	-9
140	37	25	278	-2	-9	-10
150	51	31	353	37	8	6
160	53	31	361	35	6	5
170	60	33	404	51	11	18
180	78	36	523	77	24	55
190	85	38	552	84	26	71
200	127	50	698	195	56	126
210	131	52	714	200	57	132
220	139	55	778	275	77	208
230	164	66	895	429	125	294
240	171	69	932	457	145	320
250	212	97	1086	1710	302	432
261	1032	128	1439	2381	466	506
271	1356	164	1663	3002	580	576
280	1389	167	1728	3158	595	593
290	1553	184	1932	3598	656	664
300	1583	190	1988	3687	667	689
310	1809	227	2189	3805	862	890
320	1833	231	2242	3869	885	912
330	1889	239	2367	3896	968	982
340	1985	278	2620	4077	1132	1092
350	1997	285	2729	4126	1188	1151
360	2015	295	2868	4168	1272	1229
370	2073	321	2973	4365	1388	1294
381	2088	326	3007	4434	1455	1353
390	2106	336	3020	4477	1545	1440
400	2194	360	5295	4864	1661	1555
411	2223	374	6276	5126	1749	1630
416	2247	378	6581	5297	1804	1675
421	2895	699	8026	11562	2180	2058

Table 6.41 Deflection Data for Specimen 4-NWLD

Shear (kN)	Δ_2 (mm)	Δ_3 (mm)	Δ_4 (mm)	Δ_6 (mm)
0	0.0	0.0	0.0	0.0
16	0.1	0.1	0.0	0.1
20	0.1	0.1	0.0	0.1
41	0.2	0.2	0.1	0.2
52	0.3	0.3	0.2	0.3
61	0.4	0.3	0.2	0.5
71	0.5	0.4	0.3	0.5
81	0.6	0.5	0.3	0.6
91	0.8	0.6	0.4	0.8
103	0.9	0.7	0.4	0.9
111	1.0	0.8	0.5	1.1
120	1.1	0.9	0.5	1.2
132	1.2	1.0	0.6	1.3
141	1.3	1.1	0.7	1.5
150	1.5	1.2	0.7	1.6
161	1.6	1.4	0.8	1.7
161	1.7	1.5	0.8	1.8
166	1.7	1.5	0.9	1.8
177	1.9	1.6	0.9	1.9
182	2.0	1.8	1.0	2.1
191	2.1	1.9	1.1	2.2
200	2.3	2.0	1.1	2.3
209	2.5	2.2	1.2	2.5
220	2.6	2.4	1.3	2.6
230	2.8	2.5	1.4	2.8
241	3.0	2.7	1.5	3.0
250	3.1	2.8	1.5	3.2
260	3.3	3.1	1.7	3.5
272	3.5	3.2	1.8	3.7
280	3.7	3.5	2.0	3.8
289	3.9	3.7	2.1	4.0
301	4.2	4.0	2.3	4.3
310	4.5	4.4	2.6	4.6
319	4.7	4.6	2.8	4.8
330	5.0	4.9	2.9	5.0
340	5.4	5.5	3.5	5.5
345	5.6	5.7	3.7	5.7
349	5.9	6.0	3.9	5.9

Table 6.42 Longitudinal Steel Strain Data for Specimen 4-NWLD

Shear (kN)	ϵ_{L1B2} ($\times 10^{-6}$)	ϵ_{L1B3} ($\times 10^{-6}$)	ϵ_{L2B1} ($\times 10^{-6}$)	ϵ_{L2B2} ($\times 10^{-6}$)	ϵ_{L2B3} ($\times 10^{-6}$)	ϵ_{L2B4} ($\times 10^{-6}$)	ϵ_{L2T1} ($\times 10^{-6}$)	ϵ_{L2T2} ($\times 10^{-6}$)	ϵ_{L2T3} ($\times 10^{-6}$)	ϵ_{L2T4} ($\times 10^{-6}$)
0	0	0	0	0	0	0	0	0	0	0
16	13	15	25	39	24	27	-15	-11	-17	-19
20	14	15	35	45	28	32	-20	-14	-23	-24
41	25	25	142	156	135	145	-52	-36	-59	-64
52	32	32	209	226	204	217	-64	-46	-79	-86
61	36	37	327	350	309	330	-67	-46	-91	-99
71	44	44	399	425	375	395	-73	-50	-100	-112
81	48	50	469	498	441	459	-75	-52	-105	-119
91	63	66	540	568	511	519	-78	-55	-110	-124
103	84	87	592	626	573	584	-85	-57	-122	-140
111	102	105	638	676	623	628	-92	-63	-126	-148
120	134	142	690	726	676	679	-100	-66	-134	-158
132	207	212	755	798	748	747	-111	-71	-144	-172
141	364	308	801	845	804	801	-119	-74	-153	-182
150	481	389	852	897	859	852	-130	-82	-163	-195
161	549	447	912	954	912	904	-143	-90	-171	-206
161	591	479	926	965	919	904	-143	-92	-155	-194
166	611	498	949	987	941	925	-146	-93	-160	-201
177	668	555	1005	1043	990	974	-160	-101	-170	-213
182	753	629	1042	1080	1018	1005	-158	-93	-163	-209
191	797	667	1088	1124	1063	1045	-162	-92	-162	-213
200	842	706	1133	1173	1109	1093	-166	-88	-166	-221
209	913	766	1182	1220	1159	1140	-155	-69	-153	-218
220	962	809	1238	1278	1214	1196	-163	-67	-160	-230
230	1017	862	1287	1327	1260	1245	-164	-61	-164	-238
241	1088	919	1346	1387	1318	1298	-168	-56	-167	-247
250	1135	959	1395	1438	1362	1341	-172	-53	-173	-257
260	1186	1011	1452	1495	1418	1394	-172	-46	-179	-267
272	1234	1059	1513	1559	1478	1455	-178	-43	-188	-280
280	1267	1099	1551	1600	1524	1501	-167	-22	-193	-289
289	1295	1138	1590	1639	1571	1543	-167	-15	-196	-296
301	1333	1193	1648	1699	1632	1607	-168	-8	-203	-307
310	1367	1236	1693	1745	1683	1655	-167	0	-205	-314
319	1397	1267	1734	1785	1727	1698	-170	2	-211	-321
330	1438	1308	1785	1837	1781	1753	-167	15	-208	-327
340	1479	1347	1834	1889	1832	1805	-169	23	-202	-330
345	1498	1367	1859	1915	1857	1828	-170	26	-198	-331
349	1512	1380	1878	1929	1870	1841	-163	42	-181	-321

Continued

Table 6.42 Longitudinal Steel Strain Data for Specimen 4-NWLD (*Concluded*)

Shear (kN)	ϵ_{L1B2} ($\times 10^{-6}$)	ϵ_{L1B3} ($\times 10^{-6}$)	ϵ_{L2B1} ($\times 10^{-6}$)	ϵ_{L2B2} ($\times 10^{-6}$)	ϵ_{L2B3} ($\times 10^{-6}$)	ϵ_{L2B4} ($\times 10^{-6}$)	ϵ_{L2T1} ($\times 10^{-6}$)	ϵ_{L2T2} ($\times 10^{-6}$)
0	0	0	0	0	0	0	0	0
16	18	18	-7	-8	-11	-5	18	26
20	19	20	-9	-11	-15	-11	21	31
41	44	39	-22	-28	-39	-35	163	189
52	61	58	-29	-37	-37	-35	322	346
61	102	87	-35	-46	-30	-26	418	441
71	150	133	-42	-52	-27	-26	477	504
81	226	194	-49	-60	-22	-26	533	563
91	326	278	-55	-68	-20	-28	590	626
103	388	341	-60	-72	-15	-27	656	700
111	452	393	-64	-78	-17	-31	705	745
120	550	478	-64	-80	-18	-30	751	795
132	627	549	-69	-86	-21	-33	814	863
141	681	605	-74	-90	-19	-33	862	915
150	734	658	-81	-99	-21	-37	911	967
161	812	718	-89	-103	-24	-39	966	1028
161	856	749	-84	-95	-19	-40	971	1034
166	875	765	-85	-95	-21	-40	994	1060
177	922	804	-92	-102	-25	-44	1045	1116
182	960	856	-87	-96	-18	-38	1075	1149
191	998	900	-91	-102	-20	-41	1117	1194
200	1037	942	-95	-104	-21	-41	1163	1242
209	1079	1005	-100	-107	-18	-40	1211	1292
220	1119	1049	-105	-111	-18	-40	1267	1352
230	1154	1091	-110	-114	-14	-34	1315	1398
241	1197	1136	-117	-123	-7	-30	1372	1460
250	1229	1172	-121	-125	-4	-26	1414	1505
260	1267	1218	-126	-131	9	-20	1465	1561
272	1312	1268	-132	-133	12	-14	1524	1621
280	1336	1310	-131	-133	21	-5	1565	1663
289	1363	1342	-132	-134	25	-1	1609	1706
301	1405	1395	-133	-132	31	13	1671	1766
310	1435	1434	-120	-105	46	30	1717	1811
319	1463	1470	-118	-97	51	35	1759	1856
330	1500	1516	-106	-76	59	44	1812	1909
340	1540	1552	30	146	84	55	1863	1951
345	1561	1566	83	215	94	58	1887	1974
349	1574	1567	146	269	97	57	1906	1993

Table 6.43 Stirrup Strain Data for Specimen 4-NWLD

Shear (kN)	ϵ_{T1A} ($\times 10^{-6}$)	ϵ_{T1C} ($\times 10^{-6}$)	ϵ_{T2A} ($\times 10^{-6}$)	ϵ_{T2C} ($\times 10^{-6}$)	ϵ_{T3A} ($\times 10^{-6}$)	ϵ_{T3C} ($\times 10^{-6}$)	ϵ_{T4A} ($\times 10^{-6}$)	ϵ_{T4C} ($\times 10^{-6}$)	ϵ_{T5A} ($\times 10^{-6}$)	ϵ_{T5C} ($\times 10^{-6}$)
0	0	0	0	0	0	0	0	0	0	0
16	5	6	2	8	1	7	1	9	0	1
20	5	5	0	8	1	6	1	9	0	-1
41	14	5	0	9	1	9	0	10	-2	-5
52	32	7	4	9	2	10	-2	6	-7	-8
61	24	2	3	9	2	11	-1	6	-4	-10
71	20	-5	5	9	3	12	1	9	0	-9
81	10	-16	7	9	2	11	2	10	2	-9
91	0	-26	16	10	2	9	12	10	1	-12
103	-4	-19	18	15	3	12	16	16	-2	-23
111	-14	-5	23	16	5	12	30	43	-4	-30
120	-18	64	27	22	7	15	41	64	-16	-37
132	-19	129	34	26	11	19	68	119	-22	-41
141	-16	178	36	32	15	23	112	167	-25	-43
150	-16	230	41	27	16	23	154	228	-28	-47
161	-3	316	38	25	20	27	197	276	-33	-49
161	25	475	35	51	16	26	270	323	-29	-49
166	28	491	37	57	18	29	283	337	-28	-49
177	33	540	39	65	19	30	391	410	-28	-53
182	86	674	94	168	20	36	506	533	-22	-49
191	143	781	167	232	21	34	555	589	-20	-53
200	206	875	232	270	20	36	596	633	-20	-55
209	409	1076	710	452	24	36	714	756	-12	-55
220	448	1137	802	478	26	41	769	808	-12	-57
230	502	1206	978	515	28	42	900	918	-4	-55
241	556	1281	1190	576	29	42	1089	1091	26	-54
250	598	1343	1326	608	31	44	1248	1218	46	-53
260	663	1419	1527	670	38	48	1848	1541	144	-36
272	728	1500	1692	709	44	56	2030	1589	171	-43
280	852	1581	1790	784	47	67	2149	1637	198	-44
289	926	1634	1947	853	56	78	2242	1701	230	-42
301	1018	1714	2034	887	67	94	2367	1778	243	-12
310	1083	1782	2083	899	88	130	2495	1885	269	45
319	1127	1837	2132	907	104	146	2565	1932	285	65
330	1188	1946	2221	919	160	170	2649	1978	311	109
340	1218	2040	2298	935	226	285	2973	2116	402	282
345	1242	2097	2341	1310	244	310	3187	2175	459	332
349	1309	2191	2460	2679	288	377	3571	2226	511	380

Table 6.44 Deflection Data for Specimen 5-LWLA

Shear (kN)	Δ_2 (mm)	Δ_3 (mm)	Δ_4 (mm)	Δ_6 (mm)
0	0.0	0.0	0.0	0.0
10	0.1	0.1	0.0	0.1
21	0.1	0.1	0.1	0.1
31	0.2	0.2	0.1	0.2
41	0.3	0.3	0.2	0.3
50	0.4	0.4	0.2	0.4
60	0.5	0.5	0.3	0.5
71	0.7	0.6	0.4	0.6
81	0.8	0.8	0.5	0.8
93	1.0	0.9	0.6	1.0
100	1.1	1.0	0.6	1.1
110	1.3	1.2	0.7	1.2
120	1.4	1.3	0.8	1.4
130	1.7	1.6	1.0	1.7
140	1.8	1.7	1.1	1.8
151	2.1	2.0	1.1	2.1
160	2.2	2.1	1.2	2.2
170	2.4	2.3	1.3	2.4
180	2.5	2.4	1.4	2.6
190	2.7	2.6	1.5	2.7
200	3.0	2.8	1.7	3.1
211	3.2	3.0	1.8	3.3
221	3.4	3.1	1.9	3.4
230	3.6	3.4	2.0	3.7
240	3.8	3.5	2.1	3.9
251	4.1	3.8	2.3	4.2
260	4.3	4.0	2.4	4.4
271	4.6	4.3	2.5	4.7
280	4.8	4.5	2.7	4.9
290	5.3	5.0	2.9	5.2
300	5.5	5.2	3.0	5.4
306	5.7	5.4	3.4	5.6
310	5.9	5.6	3.5	5.7
315	6.3	6.0	3.9	6.0
319	6.4	6.2	4.1	6.1
324	6.5	6.3	4.1	6.2
326	6.6	6.5	4.4	6.5
328	6.9	6.9	4.8	6.8

Table 6.45 Longitudinal Steel Strain Data for Specimen 5-LWLA

Shear (kN)	ϵ_{L1B1} ($\times 10^{-6}$)	ϵ_{L1B5} ($\times 10^{-6}$)	ϵ_{L2B1} ($\times 10^{-6}$)	ϵ_{L2B2} ($\times 10^{-6}$)	ϵ_{L2B3} ($\times 10^{-6}$)	ϵ_{L2B4} ($\times 10^{-6}$)	ϵ_{L2B5} ($\times 10^{-6}$)	ϵ_{L2T1} ($\times 10^{-6}$)	ϵ_{L2T3} ($\times 10^{-6}$)	ϵ_{L2T5} ($\times 10^{-6}$)
0	0	0	0	0	0	0	0	0	0	0
10	10	9	26	21	23	22	28	-16	-18	-16
21	16	16	166	174	127	165	154	-5	-32	-28
31	26	25	222	234	179	222	218	-17	-50	-41
41	35	32	282	303	236	285	285	-34	-74	-57
50	42	40	349	370	297	354	382	-44	-100	-68
60	50	55	378	421	347	408	458	-52	-123	-87
71	74	97	432	483	408	465	538	-76	-154	-105
81	105	166	476	536	470	521	616	-86	-177	-120
93	176	274	549	603	562	590	724	-105	-206	-139
100	202	307	586	638	602	626	774	-115	-220	-147
110	329	383	654	696	668	685	823	-131	-243	-163
120	369	430	705	748	728	737	893	-135	-263	-176
130	445	512	757	797	790	791	971	-142	-285	-187
140	476	545	806	847	843	842	1040	-154	-303	-198
151	578	636	871	906	907	896	1117	-169	-322	-212
160	607	668	915	950	952	940	1175	-178	-336	-217
170	641	710	966	1003	1008	992	1247	-186	-352	-225
180	683	768	1015	1048	1058	1036	1308	-194	-368	-227
190	720	826	1076	1105	1113	1091	1372	-202	-382	-225
200	798	904	1145	1157	1163	1134	1427	-200	-392	-194
211	828	939	1198	1207	1213	1185	1491	-208	-407	-200
221	869	981	1254	1258	1262	1235	1557	-213	-419	-200
230	916	1032	1310	1306	1311	1282	1628	-220	-434	-204
240	954	1068	1362	1354	1361	1330	1692	-226	-447	-208
251	1004	1119	1424	1409	1412	1381	1772	-239	-460	-217
260	1041	1156	1473	1454	1455	1424	1830	-243	-469	-220
271	1094	1209	1540	1511	1506	1469	1906	-256	-472	-229
280	1130	1245	1590	1559	1553	1514	1970	-264	-479	-230
290	1185	1292	1651	1603	1591	1551	2040	-276	-476	-245
300	1219	1327	1703	1651	1638	1597	2104	-283	-483	-253
306	1246	1353	1735	1679	1663	1623	2142	-284	-481	-255
310	1262	1367	1766	1693	1672	1632	2156	-262	-468	-239
315	1297	1398	1808	1708	1684	1646	2199	-276	-471	-258
319	1314	1419	1836	1733	1707	1669	2231	-281	-472	-260
324	1330	1435	1861	1757	1730	1692	2262	-285	-474	-264
326	1337	1445	1872	1765	1737	1700	2275	-293	-468	-266
328	1342	1453	1879	1772	1747	1707	2289	-318	-435	-275

Continued

Table 6.45 Longitudinal Steel Strain Data for Specimen 5-LWLA (Concluded)

Shear (kN)	ϵ_{L3B1} ($\times 10^{-6}$)	ϵ_{L3B3} ($\times 10^{-6}$)	ϵ_{L3B5} ($\times 10^{-6}$)	ϵ_{L3T5} ($\times 10^{-6}$)	ϵ_{L4B1} ($\times 10^{-6}$)	ϵ_{L4B3} ($\times 10^{-6}$)	ϵ_{L4B5} ($\times 10^{-6}$)	ϵ_{L4T1} ($\times 10^{-6}$)	ϵ_{L4T3} ($\times 10^{-6}$)	ϵ_{L4T5} ($\times 10^{-6}$)	ϵ_{L4T3} ($\times 10^{-6}$)
0	0	0	0	0	0	0	0	0	0	0	0
10	15	15	17	-11	-13	-20	-20	-22	32	45	2
21	35	29	36	-20	-29	-50	-41	-48	92	138	4
31	52	45	53	-27	-40	-66	-56	-67	139	202	5
41	95	69	78	-37	-58	-88	-70	-91	198	289	8
50	191	145	133	-37	-78	-105	-86	-122	236	374	12
60	243	201	173	-38	-88	-120	-99	-140	279	430	26
71	308	259	212	-48	-101	-146	-119	-171	337	516	43
81	364	306	254	-55	-109	-166	-134	-197	386	587	67
93	438	372	316	-61	-114	-180	-149	-235	444	678	88
100	470	406	349	-66	-111	-192	-159	-245	481	723	94
110	554	487	466	-82	-88	-209	-171	-267	544	795	118
120	599	530	506	-90	-98	-223	-182	-285	599	861	154
130	654	589	573	-98	-112	-245	-193	-307	656	932	203
140	695	629	610	-107	-120	-260	-208	-319	705	997	217
151	833	701	673	-117	-31	-272	-212	-339	767	1072	268
160	869	737	707	-126	-37	-280	-219	-350	809	1126	285
170	913	782	746	-136	-47	-293	-231	-363	859	1188	323
180	957	830	786	-147	-64	-310	-240	-383	902	1243	381
190	1011	900	834	-159	-78	-322	-247	-393	955	1309	418
200	1071	1020	926	-176	-111	-328	-233	-402	1002	1363	572
211	1113	1068	966	-189	-121	-338	-242	-412	1052	1424	597
221	1165	1125	1019	-200	-136	-349	-247	-420	1102	1483	642
230	1222	1178	1076	-212	-159	-367	-250	-434	1151	1539	714
240	1277	1235	1131	-218	-173	-375	-252	-443	1197	1593	754
251	1353	1301	1198	-207	-178	-396	-253	-463	1250	1642	828
260	1405	1357	1255	-207	-167	-407	-252	-471	1293	1693	869
271	1488	1428	1334	-175	-114	-437	-251	-494	1345	1746	957
280	1533	1476	1385	-179	-115	-450	-254	-503	1390	1797	990
290	1600	1528	1461	-212	-59	-488	-249	-539	1438	1843	1110
300	1643	1575	1517	-227	-57	-502	-254	-554	1484	1896	1204
306	1682	1601	1562	-235	-40	-514	-251	-568	1514	1930	1271
310	1739	1628	1665	-240	-47	-522	-249	-578	1532	1951	1598
315	1765	1648	1682	-275	7	-561	-247	-622	1562	1969	1680
319	1790	1671	1708	-284	14	-574	-256	-632	1589	1997	1700
324	1812	1693	1729	-293	13	-579	-257	-637	1612	2022	1719
326	1827	1703	1740	-312	36	-599	-279	-660	1633	2034	1714
328	1859	1715	1769	-336	98	-622	-284	-678	1661	2042	1646

Table 6.46 Stirrup Strain Data for Specimen 5-LWLA

Shear (kN)	ϵ_{T1A} ($\times 10^{-6}$)	ϵ_{T1C} ($\times 10^{-6}$)	ϵ_{T2A} ($\times 10^{-6}$)	ϵ_{T2C} ($\times 10^{-6}$)	ϵ_{T3A} ($\times 10^{-6}$)	ϵ_{T3C} ($\times 10^{-6}$)	ϵ_{T4A} ($\times 10^{-6}$)	ϵ_{T4C} ($\times 10^{-6}$)
0	0	0	0	0	0	0	0	0
10	2	5	4	3	0	2	0	1
21	2	12	11	3	-3	2	0	0
31	0	16	15	4	-2	3	0	0
41	2	31	18	5	0	3	0	0
50	0	92	24	11	-5	3	-2	-2
60	3	124	32	18	-2	6	1	1
71	-2	161	43	22	-4	8	1	5
81	-14	195	57	28	0	13	4	14
93	-27	313	89	35	9	16	7	15
100	-27	346	128	38	16	18	11	16
110	-27	490	474	43	49	17	14	16
120	-34	555	543	43	59	22	20	17
130	-38	794	648	62	117	64	51	547
140	-38	893	704	72	134	72	57	581
151	-27	1476	955	172	1058	86	71	679
160	-26	1542	989	182	1120	91	78	712
170	-23	1607	1032	198	1203	100	85	764
180	-16	1699	1082	222	1297	112	88	866
190	-3	1771	1117	237	1372	129	98	974
200	389	1824	1141	307	1463	166	128	1296
211	440	1892	1179	325	1538	175	136	1357
221	536	1971	1229	353	1639	185	153	1464
230	653	2060	1300	462	1761	206	196	1630
240	729	2123	1345	494	1839	219	212	1711
251	843	2211	1426	635	1948	274	258	1946
260	906	2277	1478	671	2007	290	274	2040
271	1026	2417	1762	833	2039	461	309	2195
280	1069	2507	1846	889	2099	552	324	2258
290	1165	3303	2055	1233	2203	822	378	2322
300	1208	3549	2131	1299	2262	867	395	2364
306	1252	3744	2200	1402	2434	928	416	2397
310	1397	3764	2335	1455	2484	947	430	2407
315	1431	3894	2371	1596	2498	1098	477	2443
319	1450	3932	2402	1610	2523	1135	485	2459
324	1462	3960	2422	1616	2544	1154	490	2470
326	1469	3997	2441	1638	2562	1176	493	2484
328	1443	4167	2472	3056	2676	1186	516	2518

Continued

Table 6.46 Stirrup Strain Data for Specimen 5-LWLA (Concluded)

Shear (kN)	ϵ_{T5A} ($\times 10^{-6}$)	ϵ_{T5C} ($\times 10^{-6}$)	ϵ_{T6A} ($\times 10^{-6}$)	ϵ_{T6C} ($\times 10^{-6}$)	ϵ_{T7A} ($\times 10^{-6}$)	ϵ_{T7C} ($\times 10^{-6}$)
0	0	0	0	0	0	0
10	0	-2	2	-4	0	40
21	-1	-5	3	-11	0	128
31	0	-5	4	-15	-1	181
41	1	-6	5	-19	-2	258
50	-2	-2	7	0	-3	349
60	1	7	12	0	-1	404
71	6	54	30	-9	-1	489
81	16	191	208	-5	6	558
93	23	247	285	-10	26	652
100	26	264	309	-15	61	689
110	32	330	371	-26	134	750
120	38	380	469	-29	180	813
130	658	558	813	-32	264	879
140	699	574	841	-35	300	939
151	787	615	885	-38	387	1022
160	829	631	913	-37	418	1079
170	896	650	957	-36	465	1144
180	1004	689	1025	-32	528	1209
190	1092	761	1144	-29	583	1278
200	1332	1374	1695	455	758	1351
211	1392	1426	1765	478	791	1415
221	1506	1517	1858	513	840	1480
230	1669	1651	1993	567	916	1549
240	1751	1736	2105	595	976	1613
251	1956	1950	2234	653	1117	1693
260	2060	2092	2289	687	1176	1753
271	2184	2267	2426	748	1283	1831
280	2219	2344	2520	779	1348	1890
290	2359	2392	2631	881	1473	1964
300	2449	2432	2687	922	1521	2028
306	2531	2469	2760	963	1559	2074
310	2551	2486	2796	996	1569	2100
315	2604	2562	2929	1088	1599	2141
319	2657	2661	2987	1125	1622	2179
324	2679	2687	3019	1165	1643	2209
326	2753	3153	3133	1244	1651	2228
328	2816	5772	3396	1283	1674	2242

Table 6.47 Deflection Data for Specimen 6-LWLB

Shear (kN)	Δ_2 (mm)	Δ_3 (mm)	Δ_4 (mm)	Δ_6 (mm)
0	0.0	0.0	0.0	0.0
23	0.1	0.1	0.1	0.1
40	0.3	0.3	0.1	0.3
60	0.4	0.4	0.2	0.5
70	0.6	0.5	0.3	0.7
81	0.7	0.7	0.4	0.8
90	0.8	0.8	0.4	0.9
100	1.0	0.9	0.5	1.0
111	1.2	1.1	0.6	1.2
120	1.4	1.3	0.7	1.4
130	1.5	1.5	0.8	1.6
140	1.7	1.6	0.8	1.7
150	1.8	1.7	0.9	1.9
160	2.0	1.9	1.0	2.1
171	2.2	2.1	1.1	2.3
180	2.3	2.2	1.1	2.5
191	2.5	2.4	1.3	2.7
200	2.6	2.5	1.3	2.8
211	2.9	2.8	1.4	3.0
220	3.1	2.9	1.5	3.2
231	3.3	3.1	1.7	3.5
241	3.4	3.3	1.7	3.6
252	3.7	3.5	1.9	3.9
261	3.8	3.6	2.0	4.0
270	4.0	3.8	2.0	4.2
280	4.3	4.1	2.2	4.4
290	4.4	4.2	2.3	4.6
300	4.6	4.5	2.4	4.8
310	4.8	4.7	2.6	5.0
321	5.2	5.0	2.8	5.4
330	5.4	5.1	2.9	5.5
340	5.6	5.5	3.1	5.9
350	6.1	6.1	3.7	6.7
355	6.4	6.5	4.1	7.1
361	6.8	7.0	4.6	7.7
365	7.0	7.2	4.8	8.0
370	7.2	7.5	5.1	8.3
373	7.6	8.0	5.7	8.7

Table 6.48 Longitudinal Steel Strain Data for Specimen 6-LWLB

Shear (kN)	ϵ_{L1B1} ($\times 10^{-6}$)	ϵ_{L1B5} ($\times 10^{-6}$)	ϵ_{L2B1} ($\times 10^{-6}$)	ϵ_{L2B2} ($\times 10^{-6}$)	ϵ_{L2B3} ($\times 10^{-6}$)	ϵ_{L2B4} ($\times 10^{-6}$)	ϵ_{L2B5} ($\times 10^{-6}$)	ϵ_{L2T1} ($\times 10^{-6}$)	ϵ_{L2T3} ($\times 10^{-6}$)	ϵ_{L2T5} ($\times 10^{-6}$)
0	0	0	0	0	0	0	0	0	0	0
23	19	16	99	68	69	67	99	-36	-36	-46
40	32	31	299	260	238	240	285	-48	-51	-71
60	55	56	442	388	376	340	443	-71	-69	-104
70	79	79	534	475	453	403	503	-81	-77	-112
81	104	95	590	536	513	451	571	-90	-90	-135
90	129	130	644	585	561	490	622	-102	-100	-150
100	199	247	707	652	625	537	688	-116	-113	-167
111	264	334	769	714	686	588	755	-128	-128	-185
120	297	373	827	765	731	628	800	-141	-137	-196
130	368	465	896	826	793	678	865	-156	-149	-210
140	439	544	960	886	851	720	924	-165	-158	-220
150	470	579	1019	940	900	765	979	-178	-168	-232
160	533	645	1086	1003	960	813	1045	-187	-177	-243
171	612	709	1148	1067	1020	859	1110	-195	-185	-250
180	654	749	1199	1117	1068	900	1165	-202	-192	-258
191	837	863	1259	1183	1134	958	1248	-192	-198	-265
200	873	899	1303	1229	1176	1004	1303	-188	-202	-270
211	920	965	1374	1289	1224	1065	1374	-176	-193	-212
220	953	1009	1429	1338	1267	1106	1428	-181	-198	-212
231	1002	1075	1498	1402	1321	1154	1498	-184	-204	-212
241	1036	1114	1557	1452	1367	1198	1555	-189	-211	-217
252	1085	1175	1630	1520	1424	1248	1627	-192	-218	-220
261	1113	1211	1682	1565	1466	1288	1677	-196	-224	-224
270	1145	1263	1738	1618	1514	1330	1734	-199	-230	-228
280	1198	1325	1804	1678	1566	1373	1802	-196	-232	-228
290	1232	1363	1862	1731	1614	1418	1859	-200	-239	-232
300	1275	1411	1925	1792	1673	1460	1925	-202	-244	-233
310	1319	1452	1987	1854	1733	1499	1986	-199	-246	-232
321	1370	1494	2056	1920	1794	1540	2055	-193	-245	-229
330	1403	1530	2110	1970	1838	1580	2107	-194	-250	-232
340	1449	1578	2171	2027	1891	1624	2171	-179	-245	-226
350	1496	1618	2237	2086	1948	1667	2236	-165	-244	-229
355	1519	1634	2269	2116	1973	1688	2264	-169	-248	-227
361	1551	1664	2315	2157	2009	1716	2304	-172	-259	-225
365	1568	1681	2339	2179	2028	1729	2324	-170	-265	-221
370	1587	1700	2370	2206	2052	1749	2355	-170	-270	-221
373	1601	1714	2395	2225	2069	1761	2373	-168	-274	-214

Continued

Table 6.48 Longitudinal Steel Strain Data for Specimen 6-LWLB (Concluded)

Shear (kN)	ϵ_{L3B1} ($\times 10^{-6}$)	ϵ_{L3B3} ($\times 10^{-6}$)	ϵ_{L3B5} ($\times 10^{-6}$)	ϵ_{L3T1} ($\times 10^{-6}$)	ϵ_{L3T5} ($\times 10^{-6}$)	ϵ_{L4B1} ($\times 10^{-6}$)	ϵ_{L4B3} ($\times 10^{-6}$)	ϵ_{L4B5} ($\times 10^{-6}$)	ϵ_{L4T1} ($\times 10^{-6}$)	ϵ_{L4T3} ($\times 10^{-6}$)	ϵ_{L4T5} ($\times 10^{-6}$)
0	0	0	0	0	0	0	0	0	0	0	0
23	24	26	27	-26	-21	-43	-42	-45	97	82	3
40	53	60	57	-46	-39	-53	-63	-64	274	243	9
60	105	119	113	-74	-64	-81	-89	-100	384	369	4
70	158	196	191	-88	-72	-98	-105	-117	439	434	-21
81	241	314	288	-103	-77	-120	-123	-137	492	492	-36
90	280	350	320	-111	-82	-134	-135	-150	538	539	-32
100	351	411	376	-121	-90	-155	-152	-171	593	605	-13
111	440	489	433	-127	-102	-176	-171	-186	651	667	9
120	585	647	586	-106	-78	-189	-183	-202	702	716	18
130	628	693	634	-119	-86	-205	-198	-220	755	780	18
140	675	731	678	-135	-95	-221	-212	-236	809	833	17
150	712	772	719	-144	-102	-234	-225	-250	862	885	19
160	759	823	769	-159	-112	-247	-239	-265	919	942	22
171	815	878	822	-181	-126	-265	-256	-282	976	998	40
180	857	917	861	-189	-133	-275	-266	-293	1026	1048	108
191	930	974	921	-207	-146	-291	-280	-305	1092	1113	372
200	974	1009	967	-217	-151	-301	-291	-312	1139	1155	586
211	977	1134	1097	-228	-172	-319	-305	-324	1206	1215	1029
220	1015	1189	1143	-235	-179	-328	-314	-332	1255	1262	1108
231	1082	1258	1187	-256	-189	-344	-327	-345	1320	1316	1223
241	1126	1310	1232	-264	-192	-351	-336	-352	1371	1365	1280
252	1193	1385	1286	-284	-203	-365	-350	-365	1436	1422	1369
261	1228	1432	1325	-292	-210	-372	-358	-373	1483	1465	1413
270	1273	1486	1370	-301	-219	-379	-368	-381	1534	1514	1462
280	1330	1554	1415	-322	-232	-393	-383	-396	1595	1564	1545
290	1375	1609	1461	-332	-239	-400	-393	-405	1648	1612	1597
300	1425	1676	1514	-350	-251	-408	-408	-420	1701	1664	1659
310	1470	1736	1563	-357	-256	-412	-416	-430	1755	1716	1719
321	1516	1812	1617	-370	-256	-427	-429	-449	1817	1771	1806
330	1557	1864	1656	-377	-258	-430	-435	-456	1864	1818	1857
340	1612	1939	1689	-356	-243	-441	-448	-470	1921	1875	1926
350	1671	2018	1743	-281	-171	-519	-535	-531	1997	1966	1949
355	1699	2053	1767	-173	-80	-539	-570	-564	2039	2003	1958
361	1738	2098	1799	-36	29	-559	-594	-589	2079	2049	1975
365	1759	2122	1813	-14	67	-573	-607	-606	2101	2074	1997
370	1785	2150	1830	-4	77	-584	-620	-619	2128	2103	2023
373	1807	2172	1838	6	84	-599	-642	-635	2149	2132	2041

Table 6.49 Stirrup Strain Data for Specimen 6-LWLB

Shear (kN)	ϵ_{T1A} ($\times 10^{-6}$)	ϵ_{T1B} ($\times 10^{-6}$)	ϵ_{T1C} ($\times 10^{-6}$)	ϵ_{T2A} ($\times 10^{-6}$)	ϵ_{T2B} ($\times 10^{-6}$)	ϵ_{T2C} ($\times 10^{-6}$)	ϵ_{T3A} ($\times 10^{-6}$)	ϵ_{T3B} ($\times 10^{-6}$)	ϵ_{T3C} ($\times 10^{-6}$)
0	0	0	0	0	0	0	0	0	0
23	0	2	5	-1	4	4	2	-1	5
40	4	7	8	-1	4	7	2	0	9
60	13	14	17	-4	4	14	2	0	31
70	14	18	23	-5	4	19	5	5	33
81	-3	18	22	-3	5	26	2	7	5
90	-8	20	26	-1	7	30	6	10	12
100	-26	26	26	0	11	37	7	16	23
111	-40	5	9	-15	12	44	9	28	34
120	-31	15	87	317	138	60	31	47	43
130	-34	13	121	457	221	70	34	58	86
140	-42	-1	164	598	300	73	34	65	122
150	-45	-1	177	653	331	78	40	69	132
160	-47	-1	242	783	430	83	42	75	169
171	-45	6	383	949	546	88	42	81	254
180	-43	10	435	1032	602	92	47	84	280
191	4	16	611	1210	720	98	52	92	384
200	103	26	673	1295	772	102	56	98	425
211	630	616	1566	1580	908	116	74	108	563
220	704	723	1669	1647	948	124	86	113	642
231	814	868	1929	1896	1242	146	116	125	854
241	859	919	2023	1991	1320	154	125	133	898
252	944	1018	2193	2199	1520	192	154	160	1586
261	978	1056	2269	2277	1593	202	164	166	1681
270	1020	1102	2362	2379	1672	217	178	177	1803
280	1097	1182	2530	2904	1740	253	249	218	1982
290	1139	1226	2632	3421	1822	264	263	229	2045
300	1200	1288	2821	4205	1925	285	323	265	2152
310	1252	1340	2894	4630	2023	305	357	287	2207
321	1346	1425	3013	5159	2104	347	443	338	2297
330	1391	1474	3078	5358	2171	361	465	357	2344
340	1470	1550	3194	6176	3099	390	593	397	2479
350	1518	1527	3469	7664	4974	543	603	484	3215
355	1526	1536	3603	8066	5298	571	648	789	8236
361	1530	1550	3828	8306	5495	618	677	1082	9364
365	1548	1567	4075	8464	5520	638	712	1489	9691
370	1568	1582	4256	8616	5573	648	747	1910	10142
373	1589	1609	4447	8846	5702	651	811	2113	10759

Continued

Table 6.49 Stirrup Strain Data for Specimen 6-LWLB (*Concluded*)

Shear (kN)	ϵ_{T4A} ($\times 10^{-6}$)	ϵ_{T4B} ($\times 10^{-6}$)	ϵ_{T4C} ($\times 10^{-6}$)	ϵ_{T5A} ($\times 10^{-6}$)	ϵ_{T5B} ($\times 10^{-6}$)	ϵ_{T5C} ($\times 10^{-6}$)
0	0	0	0	0	0	0
23	5	-1	-9	-3	2	-24
40	7	-2	-11	2	6	-44
60	24	2	7	-4	14	-69
70	30	6	25	0	15	-88
81	8	10	34	5	11	-99
90	13	16	37	9	13	-107
100	21	10	44	16	15	-117
111	56	23	46	21	17	-118
120	89	77	47	25	22	-72
130	130	129	49	24	21	-80
140	165	194	47	25	25	-79
150	180	221	51	27	26	-87
160	229	336	51	32	26	-93
171	528	532	61	39	27	-92
180	624	590	68	46	24	-103
191	896	766	88	54	17	-111
200	980	844	98	60	17	-113
211	1203	1046	119	83	25	-91
220	1349	1159	128	100	32	-96
231	1551	1335	182	158	59	-109
241	1630	1402	197	175	67	-118
252	1890	1827	265	233	91	-136
261	1965	1960	275	245	96	-147
270	2059	2129	303	264	104	-158
280	2190	2397	407	354	162	-174
290	2262	2521	430	381	186	-182
300	2315	2741	521	461	244	-195
310	2345	2918	554	508	271	-209
321	2401	3194	616	748	341	-224
330	2434	3267	647	813	374	-240
340	2489	3369	752	1070	449	-277
350	2770	4089	762	1560	709	-311
355	7963	9738	770	1635	769	-299
361	2551	16973	764	1619	841	-274
365	2345	19141	767	1605	885	-270
370	2239	20878	765	1604	915	-276
373	2286	25204	751	1556	952	-300

Table 6.50 Deflection Data for Specimen 7-LWLC

Shear (kN)	Δ_2 (mm)	Δ_3 (mm)	Δ_4 (mm)	Δ_6 (mm)
0	0.0	0.0	0.0	0.0
10	0.1	0.1	0.0	0.1
19	0.1	0.1	0.1	0.1
31	0.2	0.2	0.1	0.3
41	0.3	0.3	0.2	0.3
51	0.5	0.5	0.3	0.4
60	0.6	0.5	0.3	0.6
70	0.7	0.7	0.4	0.7
81	0.9	0.8	0.5	0.9
90	1.0	0.9	0.5	1.0
100	1.1	1.0	0.6	1.1
111	1.3	1.2	0.7	1.3
120	1.4	1.3	0.7	1.4
130	1.5	1.4	0.8	1.6
141	1.7	1.6	0.9	1.8
150	1.8	1.7	1.0	1.9
160	2.0	1.9	1.0	2.1
171	2.2	2.1	1.1	2.3
180	2.3	2.2	1.2	2.4
190	2.6	2.4	1.3	2.6
201	2.7	2.5	1.4	2.8
210	2.9	2.7	1.4	2.9
220	3.0	2.9	1.5	3.1
231	3.2	3.0	1.6	3.3
240	3.4	3.2	1.7	3.6
252	3.7	3.6	2.0	3.9
260	4.1	4.0	2.1	4.2
270	4.2	4.1	2.1	4.4
281	4.4	4.3	2.3	4.6
290	4.6	4.5	2.4	4.8
300	4.8	4.7	2.5	5.0
312	5.1	5.0	2.7	5.2
320	5.3	5.2	2.8	5.5
330	5.5	5.5	3.0	5.8
341	5.9	5.9	3.3	6.2
351	6.2	6.3	3.6	6.5
354	6.4	6.5	3.8	6.8
358	6.5	6.7	3.9	7.0

Table 6.51 Longitudinal Steel Strain Data for Specimen 7-LWLC

Shear (kN)	ϵ_{L1B1} ($\times 10^{-6}$)	ϵ_{L1B5} ($\times 10^{-6}$)	ϵ_{L2B1} ($\times 10^{-6}$)	ϵ_{L2B2} ($\times 10^{-6}$)	ϵ_{L2B3} ($\times 10^{-6}$)	ϵ_{L2B4} ($\times 10^{-6}$)	ϵ_{L2B5} ($\times 10^{-6}$)	ϵ_{L2T1} ($\times 10^{-6}$)	ϵ_{L2T3} ($\times 10^{-6}$)	ϵ_{L2T5} ($\times 10^{-6}$)
0	0	0	0	0	0	0	0	0	0	0
10	10	13	29	25	24	32	-15	-18	-15	-22
19	16	22	64	48	47	65	-28	-36	-34	-43
31	30	36	129	102	94	126	-51	-64	-64	-78
41	49	57	319	262	298	296	-50	-74	-65	-95
51	102	127	396	340	384	375	-55	-83	-71	-110
60	128	154	442	384	432	426	-68	-99	-88	-130
70	172	211	507	443	493	490	-85	-123	-106	-155
81	258	286	572	507	561	560	-98	-143	-120	-179
90	300	326	626	557	611	616	-109	-159	-132	-196
100	362	385	690	622	675	678	-122	-177	-140	-215
111	421	438	754	682	736	728	-138	-198	-154	-239
120	465	481	804	729	783	779	-147	-210	-161	-254
130	533	552	865	783	846	838	-160	-229	-171	-273
141	575	599	921	834	904	898	-168	-242	-181	-288
150	628	666	978	891	960	958	-171	-251	-184	-298
160	667	709	1032	943	1016	1014	-180	-264	-193	-314
171	723	768	1094	999	1080	1074	-181	-277	-194	-326
180	756	804	1138	1049	1127	1123	-185	-285	-193	-336
190	806	857	1194	1109	1184	1182	-184	-293	-177	-338
201	853	901	1253	1167	1237	1241	-191	-302	-182	-351
210	904	944	1306	1220	1287	1296	-192	-309	-182	-361
220	951	985	1358	1273	1340	1351	-198	-318	-178	-371
231	994	1024	1416	1330	1396	1410	-202	-326	-167	-374
240	1041	1065	1468	1381	1446	1464	-211	-341	-160	-387
252	1094	1113	1534	1442	1510	1532	-216	-350	-159	-396
260	1141	1157	1580	1487	1558	1587	-212	-347	-128	-394
270	1178	1195	1633	1538	1608	1641	-218	-355	-130	-404
281	1231	1251	1702	1602	1669	1707	-224	-366	-129	-418
290	1268	1287	1752	1651	1715	1755	-233	-378	-130	-430
300	1304	1324	1804	1700	1765	1808	-236	-385	-129	-440
312	1361	1382	1876	1773	1834	1883	-241	-392	-120	-451
320	1398	1420	1921	1816	1875	1931	-245	-397	-115	-458
330	1439	1462	1973	1867	1926	1984	-247	-400	-108	-467
341	1497	1521	2039	1931	1991	2055	-245	-400	-90	-473
351	1539	1561	2089	1978	2036	2107	-247	-405	-76	-476
354	1560	1580	2109	1998	2056	2128	-244	-402	-57	-473
358	1576	1598	2129	2017	2076	2150	-244	-402	-51	-473

Continued

Table 6.51 Longitudinal Steel Strain Data for Specimen 7-LWLC (*Concluded*)

Shear (kN)	ϵ_{L3B2} ($\times 10^{-6}$)	ϵ_{L3B3} ($\times 10^{-6}$)	ϵ_{L3T2} ($\times 10^{-6}$)	ϵ_{L3T3} ($\times 10^{-6}$)	ϵ_{L4B2} ($\times 10^{-6}$)	ϵ_{L4B3} ($\times 10^{-6}$)	ϵ_{L4T2} ($\times 10^{-6}$)	ϵ_{L4T3} ($\times 10^{-6}$)
0	0	0	0	0	0	0	0	0
10	16	16	-11	-11	-14	-16	31	26
19	28	29	-21	-25	-22	-30	119	104
31	60	57	-33	-45	-33	-40	213	190
41	97	96	-42	-58	-44	-56	275	252
51	247	289	-40	-53	-51	-63	359	325
60	282	336	-50	-64	-61	-77	423	372
70	324	399	-59	-78	-77	-92	490	432
81	374	467	-66	-87	-90	-111	562	496
90	403	513	-73	-95	-100	-127	617	545
100	440	567	-75	-96	-105	-147	689	603
111	478	612	-76	-80	-106	-171	760	660
120	507	653	-81	-83	-111	-185	813	705
130	536	701	-88	-89	-116	-206	879	758
141	570	746	-97	-95	-122	-222	938	807
150	606	792	-78	-58	-122	-232	997	860
160	651	833	-78	-53	-129	-245	1059	909
171	707	874	-65	-16	-131	-261	1126	964
180	760	912	-64	-9	-135	-274	1178	1007
190	849	965	-53	13	-140	-290	1243	1061
201	896	1011	-52	16	-145	-301	1304	1113
210	943	1059	-44	29	-147	-311	1359	1161
220	991	1113	-42	39	-152	-324	1414	1209
231	1051	1208	-46	36	-159	-336	1476	1264
240	1090	1269	-56	42	-166	-353	1532	1310
252	1140	1334	-53	100	-166	-355	1601	1361
260	1188	1415	-36	113	-175	-375	1651	1408
270	1224	1460	-38	113	-177	-383	1705	1458
281	1268	1518	-30	121	-177	-397	1767	1519
290	1299	1562	-21	122	-182	-413	1814	1564
300	1335	1610	-15	124	-186	-423	1863	1610
312	1387	1685	22	150	-187	-440	1932	1677
320	1419	1736	57	179	-186	-448	1973	1719
330	1457	1790	127	238	-183	-458	2023	1765
341	1506	1861	173	309	-185	-471	2085	1827
351	1540	1916	208	348	-167	-491	2126	1874
354	1554	1943	243	381	-174	-520	2149	1893
358	1567	1967	260	397	-194	-551	2175	1915

Table 6.52 Stirrup Strain Data for Specimen 7-LWLC

Shear (kN)	ϵ_{T1A} ($\times 10^{-6}$)	ϵ_{T1C} ($\times 10^{-6}$)	ϵ_{T2A} ($\times 10^{-6}$)	ϵ_{T2C} ($\times 10^{-6}$)	ϵ_{T3A} ($\times 10^{-6}$)	ϵ_{T3C} ($\times 10^{-6}$)	ϵ_{T4A} ($\times 10^{-6}$)	ϵ_{T4C} ($\times 10^{-6}$)
0	0	0	0	0	0	0	0	0
10	-1	3	5	5	4	2	4	3
19	-2	5	6	7	5	5	6	3
31	-5	4	5	7	6	4	8	3
41	-4	5	6	11	11	5	12	5
51	16	6	21	10	22	16	20	13
60	17	5	24	9	24	17	23	13
70	19	4	27	10	75	17	31	11
81	20	5	39	21	192	3	46	16
90	19	3	48	26	226	4	54	18
100	20	7	65	41	365	15	65	26
111	10	1	72	55	526	389	69	33
120	8	-1	79	60	560	445	75	39
130	3	-12	87	64	632	528	80	41
141	-8	-14	93	67	678	595	85	45
150	-8	-6	108	81	886	817	98	57
160	-14	5	118	96	975	914	104	61
171	-9	25	137	125	1144	1128	109	63
180	-3	88	150	160	1217	1211	115	67
190	106	446	202	291	1351	1349	130	67
201	119	488	219	311	1429	1426	143	73
210	147	556	241	343	1568	1541	154	77
220	203	635	284	410	1680	1659	194	83
231	403	784	449	548	1714	1714	211	92
240	503	855	594	652	1801	1800	254	126
252	554	898	648	692	1870	1884	436	370
260	741	1051	2275	2045	1939	2172	561	447
270	755	1071	2367	2142	1962	2207	658	470
281	769	1095	2472	2274	1995	2271	1160	503
290	782	1112	2552	2386	2007	2325	1577	544
300	795	1131	2623	2491	2031	2372	1725	565
312	822	1164	2717	2647	2071	2489	2065	606
320	845	1189	2764	2749	2098	2560	2272	630
330	875	1217	2836	2842	2113	2630	2612	663
341	931	1275	3235	3014	2161	2731	2874	716
351	964	1336	3712	3192	2203	2792	3034	769
354	989	1368	4026	3322	2224	2833	3671	801
358	1000	1385	4169	3409	2242	2854	4247	825

Continued

Table 6.52 Stirrup Strain Data for Specimen 7-LWLC (Concluded)

Shear (kN)	ϵ_{T5A} ($\times 10^{-6}$)	ϵ_{T5C} ($\times 10^{-6}$)	ϵ_{T6A} ($\times 10^{-6}$)	ϵ_{T6C} ($\times 10^{-6}$)	ϵ_{T7A} ($\times 10^{-6}$)	ϵ_{T7C} ($\times 10^{-6}$)
0	0	0	0	0	0	0
10	3	3	5	4	2	3
19	4	4	8	5	0	4
31	2	-1	6	10	-2	5
41	4	-1	5	15	1	8
51	13	4	7	29	2	19
60	14	5	6	31	-9	26
70	17	10	6	1	-16	26
81	27	14	54	5	-20	30
90	32	15	171	9	-24	34
100	47	16	530	19	-17	26
111	56	19	790	42	-17	18
120	60	23	918	59	-16	16
130	70	27	1102	160	-16	21
141	79	33	1217	278	-16	34
150	127	58	1506	473	-1	91
160	141	66	1613	524	1	133
171	181	88	1783	679	15	200
180	199	96	1886	737	21	225
190	270	134	2055	896	47	287
201	294	153	2169	961	56	313
210	326	216	2313	1080	74	369
220	422	310	2479	1249	102	440
231	516	350	2626	1363	118	481
240	710	453	2806	1565	158	552
252	2438	1946	2904	1930	203	621
260	2545	2048	3497	2022	235	678
270	2648	2123	4128	2085	254	709
281	2893	2250	6022	2193	289	789
290	3271	2342	6754	2258	316	844
300	4544	2437	7048	2332	335	914
312	6003	2613	7722	2510	378	1021
320	7013	2720	8899	2638	431	1077
330	8182	2718	10261	2838	502	1141
341	10173	2765	12147	3059	616	1236
351	11982	6001	13207	5269	886	1312
354	13023	8369	13920	7946	979	1323
358	13912	9378	14817	9633	1008	1324

Table 6.53 Deflection Data for Specimen 8-LWLD

Shear (kN)	Δ_2 (mm)	Δ_3 (mm)	Δ_4 (mm)	Δ_6 (mm)
0	0.0	0.0	0.0	0.0
12	0.1	0.1	0.0	0.1
25	0.2	0.2	0.1	0.3
32	0.2	0.2	0.1	0.3
50	0.5	0.4	0.3	0.5
59	0.6	0.5	0.3	0.6
71	0.8	0.7	0.4	0.7
80	0.9	0.8	0.5	0.8
90	1.0	0.9	0.6	1.0
101	1.2	1.0	0.7	1.1
110	1.4	1.3	0.7	1.3
121	1.6	1.4	0.8	1.4
130	1.7	1.6	0.9	1.6
140	1.9	1.7	1.0	1.7
150	2.0	1.9	1.1	1.9
161	2.2	2.1	1.3	2.3
170	2.4	2.2	1.4	2.5
176	2.5	2.3	1.4	2.5
180	2.6	2.4	1.5	2.6
185	2.7	2.5	1.5	2.7
193	2.9	2.7	1.6	2.9
200	3.0	2.8	1.7	3.1
205	3.1	2.9	1.7	3.2
210	3.1	2.9	1.8	3.2
214	3.3	3.1	1.9	3.4
220	3.3	3.1	1.9	3.5
225	3.5	3.2	2.0	3.6
230	3.5	3.3	2.0	3.7
235	3.8	3.6	2.2	4.0
241	3.9	3.7	2.2	4.1
245	4.0	3.8	2.3	4.2
250	4.1	3.9	2.4	4.4
255	4.2	4.1	2.5	4.5
260	4.9	5.0	3.2	5.2
265	5.0	5.1	3.3	5.3
271	5.1	5.3	3.4	5.5
275	5.3	5.4	3.5	5.6
280	6.1	6.6	4.2	6.4

Table 6.54 Longitudinal Steel Strain Data for Specimen 8-LWLD

Shear (kN)	ϵ_{L1B2} ($\times 10^{-6}$)	ϵ_{L1B3} ($\times 10^{-6}$)	ϵ_{L2B1} ($\times 10^{-6}$)	ϵ_{L2B2} ($\times 10^{-6}$)	ϵ_{L2B3} ($\times 10^{-6}$)	ϵ_{L2B4} ($\times 10^{-6}$)	ϵ_{L2T1} ($\times 10^{-6}$)	ϵ_{L2T2} ($\times 10^{-6}$)	ϵ_{L2T3} ($\times 10^{-6}$)	ϵ_{L2T4} ($\times 10^{-6}$)
0	0	0	0	0	0	0	0	0	0	0
12	15	13	23	27	33	28	-15	-15	-16	-12
25	21	27	94	88	92	113	-41	-43	-41	-25
32	28	37	131	130	128	153	-52	-54	-54	-33
50	54	69	241	271	258	278	-69	-84	-84	-47
59	79	97	302	381	468	417	-74	-85	-86	-36
71	102	123	352	459	567	490	-85	-97	-103	-46
80	135	159	391	535	655	557	-93	-107	-117	-55
90	177	206	439	626	753	631	-100	-116	-133	-65
101	209	241	488	693	823	689	-110	-127	-144	-73
110	251	291	527	759	886	735	-118	-142	-154	-82
121	376	363	571	831	962	800	-123	-149	-170	-92
130	466	460	609	898	1031	854	-130	-160	-182	-100
140	555	572	653	966	1103	914	-137	-170	-194	-106
150	605	641	695	1034	1179	972	-143	-182	-207	-114
161	648	694	739	1108	1254	1035	-146	-189	-216	-118
170	696	745	778	1174	1311	1079	-145	-196	-206	-106
176	718	770	801	1209	1350	1113	-138	-193	-201	-98
180	740	796	818	1239	1381	1139	-137	-194	-201	-96
185	756	815	836	1267	1410	1162	-137	-197	-203	-98
193	799	863	866	1323	1465	1206	-132	-198	-198	-92
200	834	896	893	1369	1511	1246	-128	-198	-198	-87
205	853	921	912	1404	1548	1276	-126	-199	-199	-86
210	870	939	931	1434	1577	1301	-126	-201	-202	-87
214	902	963	942	1459	1603	1319	-121	-201	-195	-82
220	922	988	962	1494	1641	1351	-121	-202	-198	-82
225	952	1020	986	1532	1678	1383	-116	-200	-199	-80
230	971	1042	1002	1559	1708	1407	-113	-200	-200	-78
235	1006	1080	1018	1596	1745	1439	-89	-182	-173	-47
241	1028	1104	1043	1632	1782	1469	-86	-182	-173	-44
245	1045	1120	1059	1657	1808	1491	-84	-182	-174	-44
250	1073	1144	1080	1691	1839	1518	-75	-175	-167	-31
255	1087	1163	1098	1721	1869	1543	-70	-172	-160	-23
260	1120	1188	1119	1762	1900	1563	-14	-115	-68	75
265	1141	1207	1139	1793	1932	1590	-9	-113	-66	80
271	1163	1230	1161	1829	1968	1621	-2	-105	-55	92
275	1183	1246	1177	1853	1993	1641	13	-90	-44	104
280	1210	1268	1195	1887	2036	1681	88	15	32	195

Continued

Table 6.54 Longitudinal Steel Strain Data for Specimen 8-LWLD (*Concluded*)

Shear (kN)	ϵ_{L3B2} ($\times 10^{-6}$)	ϵ_{L3B3} ($\times 10^{-6}$)	ϵ_{L3T2} ($\times 10^{-6}$)	ϵ_{L3T3} ($\times 10^{-6}$)	ϵ_{L4B2} ($\times 10^{-6}$)	ϵ_{L4B3} ($\times 10^{-6}$)	ϵ_{L4T2} ($\times 10^{-6}$)	ϵ_{L4T3} ($\times 10^{-6}$)
0	0	0	0	0	0	0	0	0
12	15	18	-14	-9	-21	-21	19	27
25	33	46	-32	-22	-57	-43	165	194
32	51	65	-40	-29	-71	-50	209	242
50	133	137	-60	-49	-112	-85	309	350
59	192	186	-65	-55	-137	-105	354	400
71	232	226	-78	-67	-153	-120	409	459
80	301	284	-84	-74	-173	-141	452	507
90	372	352	-88	-83	-200	-163	508	568
101	417	396	-95	-91	-215	-180	554	623
110	510	508	-26	-32	-233	-200	595	674
121	549	545	-35	-44	-249	-208	651	727
130	587	581	-48	-61	-264	-225	692	774
140	636	624	-62	-74	-279	-241	738	827
150	683	666	-78	-95	-301	-261	785	882
161	739	715	-97	-117	-306	-270	831	934
170	799	789	-108	-136	-328	-291	873	979
176	847	834	-115	-144	-338	-300	902	1011
180	873	853	-121	-155	-345	-308	922	1033
185	893	871	-128	-163	-352	-314	944	1056
193	939	907	-144	-187	-370	-330	986	1091
200	987	945	-155	-201	-380	-340	1021	1128
205	1019	971	-164	-209	-390	-347	1047	1153
210	1044	995	-174	-216	-397	-353	1070	1175
214	1077	1012	-184	-211	-413	-365	1090	1189
220	1106	1037	-193	-219	-419	-371	1117	1218
225	1139	1068	-204	-222	-426	-378	1146	1247
230	1164	1088	-210	-226	-432	-383	1165	1267
235	1261	1132	-119	9	-449	-390	1192	1287
241	1299	1160	-119	13	-454	-397	1220	1317
245	1327	1179	-119	17	-459	-400	1238	1334
250	1371	1213	7	114	-466	-402	1261	1359
255	1406	1232	54	149	-474	-406	1279	1383
260	1489	1276	435	418	-494	-409	1307	1405
265	1516	1298	458	432	-497	-411	1328	1430
271	1553	1331	536	459	-505	-419	1355	1458
275	1583	1356	636	485	-508	-423	1373	1477
280	1745	1488	1119	600	-499	-420	1387	1504

Table 6.55 Stirrup Strain Data for Specimen 8-LWLD

Shear (kN)	ϵ_{T1A} ($\times 10^{-6}$)	ϵ_{T1C} ($\times 10^{-6}$)	ϵ_{T2A} ($\times 10^{-6}$)	ϵ_{T2C} ($\times 10^{-6}$)	ϵ_{T3A} ($\times 10^{-6}$)	ϵ_{T3C} ($\times 10^{-6}$)	ϵ_{T4A} ($\times 10^{-6}$)	ϵ_{T4C} ($\times 10^{-6}$)	ϵ_{T5A} ($\times 10^{-6}$)	ϵ_{T5C} ($\times 10^{-6}$)
0	0	0	0	0	0	0	0	0	0	0
12	1	4	2	0	1	0	4	0	4	0
25	3	9	4	-1	5	0	7	-1	2	-4
32	3	13	4	-1	5	0	11	1	0	-3
50	-1	21	0	1	5	0	32	2	-16	-2
59	0	26	4	7	10	0	44	3	-16	3
71	1	28	5	16	11	3	56	8	-19	78
80	8	27	10	25	13	5	68	10	5	128
90	21	28	17	33	19	9	80	11	50	171
101	29	33	23	44	24	14	88	14	68	193
110	34	44	946	985	37	20	107	11	182	255
121	38	48	1075	1092	47	26	122	25	279	431
130	39	44	1218	1238	52	25	133	35	430	533
140	42	34	1354	1392	57	26	146	48	494	577
150	43	32	1526	1574	63	24	160	61	570	626
161	46	37	1694	1765	98	17	1636	1042	741	740
170	181	365	1827	1911	111	26	1800	1211	795	770
176	409	546	1865	1972	117	30	1862	1262	816	790
180	476	615	1916	2041	119	35	1923	1315	840	805
185	511	652	1980	2113	122	37	1972	1350	856	822
193	668	797	2114	2273	167	144	2304	1693	915	883
200	766	896	2207	2396	173	166	2398	1774	974	936
205	817	946	2273	2469	182	183	2467	1839	1001	977
210	854	983	2341	2542	188	193	2534	1890	1028	1020
214	940	1054	2408	2627	202	222	2633	2019	1071	1080
220	986	1097	2502	2733	209	228	2698	2062	1103	1122
225	1054	1153	2605	2877	218	236	2779	2105	1142	1182
230	1102	1191	2694	2994	224	241	2838	2119	1168	1227
235	1315	1351	2874	3032	298	270	2934	2196	1229	1341
241	1367	1402	2961	3062	307	276	2975	2226	1257	1382
245	1404	1441	3048	3082	310	280	2995	2239	1278	1416
250	1465	1498	3592	3111	417	289	3033	2274	1321	1491
255	1520	1558	4685	3166	506	293	3056	2294	1331	1551
260	1684	1699	6901	4107	8627	712	3130	2773	1348	1616
265	1707	1714	6952	4248	9086	740	3177	2802	1371	1645
271	1749	1736	7051	4509	10259	794	3232	2836	1408	1683
275	1776	1755	7156	4752	11093	829	3273	2860	1434	1717
280	1708	1721	10069	8501	13694	1025	4567	7710	1509	1814

Table 6.56 Deflection Data for Specimen 9-NWLD

Shear (kN)	Δ_2 (mm)	Δ_3 (mm)	Δ_4 (mm)	Δ_6 (mm)
0	0.0	0.0	0.0	0.0
12	0.1	0.1	0.1	0.1
20	0.1	0.1	0.1	0.2
30	0.2	0.2	0.1	0.3
40	0.2	0.2	0.2	0.4
50	0.3	0.3	0.2	0.6
61	0.4	0.4	0.2	0.8
70	0.5	0.5	0.3	0.9
80	0.7	0.6	0.4	1.1
91	0.8	0.7	0.4	1.3
100	0.9	0.8	0.5	1.4
110	1.0	0.9	0.6	1.6
120	1.1	1.0	0.6	1.7
130	1.4	1.2	0.7	2.0
141	1.4	1.3	0.8	2.1
150	1.6	1.5	0.9	2.3
160	1.8	1.7	1.0	2.5
171	2.0	1.9	1.1	2.7
180	2.2	2.1	1.2	3.0
190	2.3	2.2	1.3	3.1
201	2.7	2.6	1.5	3.6
210	2.8	2.7	1.5	3.8
220	2.9	2.8	1.6	4.0
230	3.2	3.2	1.7	4.4
240	3.4	3.3	1.8	4.6
251	3.7	3.7	2.0	5.1
262	4.3	4.4	2.6	6.0
271	4.6	4.8	2.9	6.5
275	4.7	4.9	2.9	6.6
280	4.8	5.0	3.0	6.7
285	4.9	5.1	3.1	6.9
290	5.9	6.4	3.9	7.7
296	6.0	6.6	4.0	7.8
301	6.3	6.9	4.2	8.0
303	7.1	8.0	4.9	8.5
306	7.2	8.1	4.9	8.5
309	7.5	8.5	5.2	8.8

Table 6.57 Longitudinal Steel Strain Data for Specimen 9-NWLD

Shear (kN)	ϵ_{L1B2} ($\times 10^{-6}$)	ϵ_{L1B3} ($\times 10^{-6}$)	ϵ_{L2B1} ($\times 10^{-6}$)	ϵ_{L2B2} ($\times 10^{-6}$)	ϵ_{L2B3} ($\times 10^{-6}$)	ϵ_{L2B4} ($\times 10^{-6}$)	ϵ_{L2T1} ($\times 10^{-6}$)	ϵ_{L2T2} ($\times 10^{-6}$)	ϵ_{L2T3} ($\times 10^{-6}$)	ϵ_{L2T4} ($\times 10^{-6}$)
0	0	0	0	0	0	0	0	0	0	0
12	13	19	33	22	21	25	-6	5	-11	-16
20	16	23	54	35	34	36	-13	-3	-21	-30
30	22	28	86	54	50	57	-23	-16	-34	-50
40	28	35	195	129	98	120	-27	-26	-54	-79
50	36	46	323	264	212	243	-5	-12	-53	-88
61	43	52	404	343	298	318	-10	-21	-58	-103
70	50	59	486	415	380	394	-6	-20	-57	-109
80	86	107	549	484	461	466	-6	-25	-65	-121
91	104	129	613	537	522	524	-14	-36	-74	-140
100	127	157	660	581	572	573	-21	-43	-81	-154
110	193	226	735	643	648	642	-23	-47	-86	-165
120	209	242	785	686	692	682	-33	-57	-91	-176
130	289	324	866	749	775	751	-28	-57	-83	-176
141	316	346	917	792	826	799	-36	-67	-91	-191
150	472	496	974	834	883	847	-38	-69	-94	-199
160	626	668	1034	884	949	910	-29	-61	-88	-200
171	679	734	1094	931	1013	968	-17	-50	-72	-197
180	733	819	1153	976	1072	1022	-13	-46	-63	-196
190	772	867	1210	1021	1125	1073	-16	-54	-66	-204
201	855	1025	1290	1082	1206	1149	7	-34	-32	-181
210	885	1058	1341	1119	1248	1188	2	-41	-36	-190
220	921	1102	1389	1162	1299	1238	-2	-47	-36	-195
230	967	1175	1462	1217	1367	1302	15	-36	-15	-184
240	1002	1218	1515	1258	1414	1347	14	-40	-12	-189
251	1047	1291	1584	1314	1484	1411	21	-41	12	-180
262	1095	1351	1668	1376	1539	1459	50	-19	150	-91
271	1131	1409	1731	1425	1593	1511	79	0	257	-25
275	1146	1426	1750	1441	1613	1528	78	-3	256	-27
280	1163	1448	1772	1463	1635	1552	78	-5	263	-26
285	1185	1475	1807	1489	1665	1579	83	-2	286	-11
290	1206	1508	1884	1546	1709	1615	283	169	545	217
296	1227	1533	1921	1574	1741	1642	285	168	550	219
301	1245	1553	1972	1612	1783	1681	295	179	575	239
303	1249	1567	2025	1653	1858	1759	336	228	613	278
306	1257	1577	2035	1665	1871	1773	336	227	614	278
309	1269	1596	2069	1691	1906	1807	369	258	643	305

Continued

Table 6.57 Longitudinal Steel Strain Data for Specimen 9-NWLD (*Concluded*)

Shear (kN)	ϵ_{L3B2} ($\times 10^{-6}$)	ϵ_{L3B3} ($\times 10^{-6}$)	ϵ_{L3T2} ($\times 10^{-6}$)	ϵ_{L3T3} ($\times 10^{-6}$)	ϵ_{L4B2} ($\times 10^{-6}$)	ϵ_{L4B3} ($\times 10^{-6}$)	ϵ_{L4T2} ($\times 10^{-6}$)	ϵ_{L4T3} ($\times 10^{-6}$)
0	0	0	0	0	0	0	0	0
12	15	14	-5	-10	-8	-12	26	21
20	22	18	-9	-19	-16	-23	44	36
30	32	26	-17	-30	-26	-32	102	75
40	44	38	-23	-44	-27	-50	205	151
50	65	54	-30	-55	-31	-53	301	240
61	78	67	-38	-67	-37	-61	381	308
70	151	116	-46	-78	-32	-70	455	374
80	260	199	-49	-95	-27	-75	532	436
91	328	255	-53	-105	-32	-84	589	486
100	389	313	-57	-113	-36	-86	638	526
110	513	453	-58	-119	-31	-98	710	589
120	571	526	-63	-124	-37	-103	755	627
130	676	614	-65	-128	-26	-98	829	692
141	714	649	-73	-137	-31	-106	878	734
150	749	685	-78	-145	-23	-109	929	777
160	722	737	-84	-152	-10	-95	989	830
171	724	846	-85	-158	-5	-95	1047	881
180	782	898	-90	-161	4	-93	1102	930
190	832	949	-98	-169	3	-98	1154	978
201	934	1018	-96	-148	52	-72	1234	1055
210	969	1056	-102	-154	49	-77	1274	1092
220	1015	1103	-109	-156	53	-78	1326	1138
230	1069	1175	-89	-81	73	-64	1395	1197
240	1110	1219	-91	-73	76	-72	1442	1241
251	1160	1273	-6	59	87	-77	1506	1302
262	1212	1327	387	419	132	-34	1563	1340
271	1233	1363	469	456	130	-36	1617	1385
275	1247	1378	473	463	130	-36	1634	1401
280	1264	1396	485	474	130	-31	1658	1421
285	1286	1423	510	496	132	-36	1687	1447
290	1344	1488	732	606	140	-24	1722	1476
296	1370	1520	749	618	140	-22	1749	1500
301	1417	1587	764	636	144	-23	1775	1523
303	1463	1721	761	645	164	-16	1788	1537
306	1475	1733	766	650	164	-13	1800	1548
309	1493	1782	784	669	176	-12	1817	1563

Table 6.58 Stirrup Strain Data for Specimen 9-NWLD

Shear (kN)	ϵ_{T1A} ($\times 10^{-6}$)	ϵ_{T1C} ($\times 10^{-6}$)	ϵ_{T2A} ($\times 10^{-6}$)	ϵ_{T2C} ($\times 10^{-6}$)	ϵ_{T3A} ($\times 10^{-6}$)	ϵ_{T3C} ($\times 10^{-6}$)	ϵ_{T4A} ($\times 10^{-6}$)	ϵ_{T4C} ($\times 10^{-6}$)	ϵ_{T5A} ($\times 10^{-6}$)	ϵ_{T5C} ($\times 10^{-6}$)
0	0	0	0	0	0	0	0	0	0	0
12	3	3	3	8	3	4	5	5	4	4
20	2	3	2	9	2	5	4	5	4	5
30	-1	3	1	10	3	7	5	5	17	13
40	-1	3	0	11	2	9	8	8	35	30
50	7	5	1	13	2	10	14	10	38	37
61	7	6	0	14	3	13	74	19	40	38
70	5	11	0	14	5	16	150	-3	47	43
80	0	10	5	14	5	16	202	-11	56	49
91	4	16	9	17	7	20	221	-9	62	57
100	13	18	13	19	10	23	243	-6	65	65
110	47	40	23	26	14	27	305	8	78	83
120	57	65	24	27	14	30	313	8	78	88
130	157	227	30	34	16	35	361	34	184	275
141	166	241	30	35	16	36	367	36	246	325
150	195	291	30	35	16	38	375	40	488	524
160	272	390	28	36	24	45	395	60	724	804
171	318	532	33	42	30	50	404	71	829	942
180	368	634	40	57	34	58	433	114	931	1085
190	390	686	43	60	36	60	442	129	989	1173
201	525	877	85	95	63	92	544	270	1190	1509
210	544	912	87	97	64	95	547	274	1234	1567
220	578	972	92	99	71	99	553	284	1289	1652
230	712	1122	167	139	145	131	608	374	1369	1777
240	757	1187	173	145	153	136	616	385	1421	1852
251	854	1290	234	213	230	181	696	623	1506	1984
262	946	1336	554	488	361	268	1840	2418	1640	2148
271	1036	1350	717	545	430	313	2006	2555	1673	2216
275	1044	1357	722	550	432	316	2021	2565	1689	2240
280	1061	1376	735	555	436	318	2045	2574	1712	2272
285	1096	1393	779	568	445	328	2082	2593	1741	2314
290	1444	1424	1739	1266	611	677	2916	2793	1806	2428
296	1456	1434	1754	1297	621	688	3008	2832	1833	2472
301	1474	1468	1777	1389	647	708	3143	2952	1868	2530
303	1473	1478	1844	1775	788	801	3422	3200	1931	2575
306	1475	1481	1851	1792	796	805	3580	3223	1945	2593
309	1503	1500	1878	1905	856	830	4899	3290	1983	2630

Table 6.59 Deflection Data for Specimen 10-NWHD

Shear (kN)	Δ_2 (mm)	Δ_3 (mm)	Δ_4 (mm)	Δ_6 (mm)
0	0.0	0.0	0.0	0.0
10	0.1	0.1	0.1	0.1
20	0.1	0.1	0.1	0.2
32	0.2	0.2	0.1	0.2
42	0.2	0.2	0.2	0.3
50	0.3	0.3	0.2	0.4
60	0.3	0.3	0.2	0.5
71	0.4	0.4	0.2	0.6
80	0.5	0.5	0.3	0.7
91	0.7	0.6	0.4	0.9
100	0.7	0.6	0.4	1.0
110	0.8	0.7	0.4	1.1
120	1.0	0.9	0.5	1.4
130	1.0	0.9	0.5	1.4
140	1.1	1.0	0.6	1.6
150	1.4	1.2	0.7	1.8
160	1.4	1.3	0.8	1.8
170	1.6	1.4	0.8	1.9
180	1.9	1.8	1.0	2.2
190	1.9	1.9	1.0	2.3
201	2.0	2.0	1.1	2.4
210	2.3	2.2	1.2	2.8
220	2.4	2.3	1.3	2.9
230	2.5	2.4	1.4	3.0
240	2.7	2.7	1.5	3.3
250	2.8	2.7	1.5	3.2
260	2.9	2.9	1.6	3.4
270	3.2	3.2	1.8	3.9
281	3.3	3.3	1.9	4.0
290	3.5	3.5	2.0	4.1
300	3.8	3.9	2.3	4.5
310	4.0	4.1	2.4	4.7
320	4.2	4.3	2.5	4.9
331	4.6	4.9	3.0	5.3
340	4.7	5.0	3.1	5.4
350	4.9	5.1	3.1	5.5
355	5.1	5.5	3.4	5.7
359	5.2	5.6	3.5	5.8

Table 6.60 Longitudinal Steel Strain Data for Specimen 10-NWHD

Shear (kN)	ϵ_{L1B2} ($\times 10^{-6}$)	ϵ_{L1B3} ($\times 10^{-6}$)	ϵ_{L2B1} ($\times 10^{-6}$)	ϵ_{L2B2} ($\times 10^{-6}$)	ϵ_{L2B3} ($\times 10^{-6}$)	ϵ_{L2B4} ($\times 10^{-6}$)	ϵ_{L2T1} ($\times 10^{-6}$)	ϵ_{L2T2} ($\times 10^{-6}$)	ϵ_{L2T3} ($\times 10^{-6}$)	ϵ_{L2T4} ($\times 10^{-6}$)
0	0	0	0	0	0	0	0	0	0	0
10	4	5	13	13	13	15	-7	-11	-6	-5
20	8	11	27	29	28	34	-17	-25	-16	-16
32	16	16	54	57	57	66	-29	-40	-26	-26
42	19	22	101	124	122	124	-40	-58	-37	-39
50	34	37	163	218	209	213	-47	-72	-48	-45
60	40	47	247	317	301	305	-55	-93	-58	-54
71	51	59	344	423	401	411	-52	-113	-63	-56
80	65	79	406	497	477	490	-46	-121	-65	-60
91	104	147	481	579	547	570	-42	-129	-66	-64
100	111	160	519	625	586	614	-46	-141	-72	-71
110	131	201	576	682	642	674	-47	-151	-79	-79
120	179	283	651	749	699	746	-46	-162	-84	-86
130	190	298	694	797	746	793	-50	-173	-92	-94
140	219	339	747	852	795	847	-51	-181	-97	-100
150	362	478	813	914	848	912	-47	-187	-102	-103
160	380	502	857	962	894	959	-51	-198	-109	-113
170	439	571	913	1020	942	1012	-54	-209	-113	-115
180	517	661	976	1074	994	1066	-47	-222	-110	-109
190	536	687	1020	1122	1039	1113	-49	-232	-116	-114
201	581	745	1079	1180	1092	1171	-46	-241	-118	-115
210	626	812	1141	1227	1149	1231	-33	-254	-111	-109
220	645	834	1183	1272	1192	1276	-36	-264	-118	-115
230	671	865	1231	1321	1239	1326	-35	-272	-120	-118
240	749	903	1292	1377	1299	1393	-16	-273	-115	-108
250	771	927	1335	1424	1344	1439	-16	-283	-119	-111
260	802	958	1385	1478	1395	1494	-9	-289	-120	-110
270	851	1004	1442	1530	1461	1566	26	-290	-116	-101
281	874	1030	1488	1579	1509	1616	28	-298	-119	-107
290	903	1059	1528	1621	1558	1668	40	-299	-119	-103
300	955	1108	1575	1664	1617	1731	72	-299	-103	-88
310	986	1147	1624	1722	1665	1794	77	-299	-109	-87
320	1010	1177	1667	1766	1712	1843	83	-305	-108	-82
331	1051	1226	1721	1820	1763	1904	122	-298	-67	-41
340	1072	1249	1763	1862	1805	1949	126	-303	-69	-44
350	1101	1281	1807	1909	1853	2002	138	-306	-66	-38
355	1116	1298	1830	1931	1871	2021	172	-290	-31	-5
359	1128	1309	1848	1950	1890	2041	185	-288	-23	0

Continued

Table 6.60 Longitudinal Steel Strain Data for Specimen 10-NWHD (*Concluded*)

Shear (kN)	ϵ_{L3B2} ($\times 10^{-6}$)	ϵ_{L3T2} ($\times 10^{-6}$)	ϵ_{L3T3} ($\times 10^{-6}$)	ϵ_{L4B2} ($\times 10^{-6}$)	ϵ_{L4B3} ($\times 10^{-6}$)	ϵ_{L4T2} ($\times 10^{-6}$)	ϵ_{L4T3} ($\times 10^{-6}$)
0	0	0	0	0	0	0	0
10	6	-6	-6	-7	-9	15	10
20	15	-12	-16	-16	-21	36	27
32	23	-20	-22	-31	-35	113	84
42	35	-26	-29	-46	-47	211	172
50	51	-30	-34	-53	-53	331	273
60	63	-37	-43	-60	-57	430	350
71	86	-49	-53	-67	-63	527	427
80	119	-57	-61	-71	-67	593	485
91	219	-64	-69	-72	-67	681	566
100	239	-70	-76	-78	-72	730	610
110	303	-76	-84	-81	-75	795	662
120	428	-75	-88	-84	-75	875	738
130	455	-80	-95	-90	-81	927	784
140	502	-84	-99	-94	-84	988	839
150	619	-88	-99	-94	-83	1065	904
160	652	-95	-104	-98	-88	1118	950
170	720	-103	-109	-100	-89	1181	1009
180	813	-72	-103	-95	-88	1251	1072
190	840	-76	-109	-97	-91	1304	1118
201	884	-78	-112	-95	-87	1372	1180
210	932	-79	-120	-76	-69	1440	1237
220	961	-84	-127	-79	-73	1490	1280
230	994	-88	-133	-80	-73	1546	1329
240	1038	-91	-136	-63	-53	1590	1382
250	1070	-95	-142	-65	-54	1640	1426
260	1103	-98	-149	-58	-46	1692	1482
270	1142	-99	-118	-36	-17	1754	1536
281	1174	-104	-122	-37	-16	1807	1582
290	1211	-102	-114	-30	-6	1856	1627
300	1262	-85	-7	-10	23	1912	1678
310	1301	-82	16	-9	29	1968	1732
320	1344	-78	74	1	41	2017	1776
331	1401	-28	223	35	85	2077	1827
340	1432	-31	223	37	88	2122	1867
350	1469	-27	246	47	105	2172	1912
355	1498	5	292	46	129	2200	1941
359	1511	14	303	47	140	2219	1954

Table 6.61 Stirrup Strain Data for Specimen 10-NWHD

Shear (kN)	ϵ_{T1A} ($\times 10^{-6}$)	ϵ_{T1C} ($\times 10^{-6}$)	ϵ_{T2A} ($\times 10^{-6}$)	ϵ_{T2C} ($\times 10^{-6}$)	ϵ_{T3A} ($\times 10^{-6}$)	ϵ_{T3C} ($\times 10^{-6}$)	ϵ_{T4A} ($\times 10^{-6}$)	ϵ_{T4C} ($\times 10^{-6}$)	ϵ_{T5A} ($\times 10^{-6}$)	ϵ_{T5C} ($\times 10^{-6}$)
0	0	0	0	0	0	0	0	0	0	0
10	-1	0	0	1	-1	1	3	0	-2	0
20	-2	1	1	1	-1	2	6	2	-3	-1
32	-4	0	1	2	-1	2	9	3	-5	-3
42	-5	-2	2	3	-2	3	11	5	-12	-5
50	-5	-2	6	5	5	6	16	7	-16	-8
60	-8	-5	6	5	4	6	12	4	-24	-14
71	-9	-5	5	3	2	6	15	5	-29	-21
80	-5	-5	5	4	2	8	18	11	-29	-21
91	-11	-7	6	6	5	10	27	17	-19	-14
100	-15	-8	7	6	3	9	31	22	-21	-16
110	-25	-8	8	8	4	11	30	23	-16	-23
120	-35	-16	15	16	6	13	1	5	-2	-44
130	-38	-18	14	16	5	15	1	5	-3	-48
140	-43	-24	14	18	7	16	2	4	-2	-56
150	-42	-15	13	18	9	19	10	37	4	-63
160	-47	-15	13	18	8	19	11	39	0	-67
170	-38	0	4	16	9	24	19	56	-3	-69
180	47	74	38	54	16	32	40	128	11	-70
190	47	77	40	57	16	35	43	134	9	-75
201	61	94	53	75	18	40	56	165	13	-78
210	105	129	142	143	24	45	158	469	58	-54
220	105	130	145	146	23	46	161	477	56	-57
230	110	137	168	152	22	47	170	500	57	-60
240	171	171	390	251	24	52	250	683	77	-46
250	172	174	405	257	25	54	259	700	76	-49
260	189	183	522	282	25	55	300	720	79	-44
270	276	252	1129	468	41	128	533	925	127	-25
281	284	258	1206	480	42	130	545	942	127	-26
290	309	285	1676	546	45	140	573	972	140	-25
300	409	370	2367	666	60	184	668	1247	204	4
310	437	388	2438	700	72	201	708	1471	221	10
320	462	410	2454	710	76	211	722	1675	243	19
331	554	531	2641	2365	109	363	790	2037	346	78
340	568	540	2678	2441	112	368	798	2091	351	78
350	604	562	2711	2574	116	411	808	2160	372	88
355	642	603	2848	5148	150	820	823	2231	404	115
359	653	615	2872	6249	154	860	827	2251	412	120

Table 6.62 Deflection Data for Specimen 11-LWHD

Shear (kN)	Δ_2 (mm)	Δ_3 (mm)	Δ_4 (mm)	Δ_6 (mm)
0	0.0	0.0	0.0	0.0
20	0.2	0.2	0.1	0.2
42	0.3	0.3	0.3	0.5
60	0.4	0.3	0.2	0.4
80	0.5	0.5	0.4	0.7
100	0.7	0.7	0.4	0.9
110	0.8	0.8	0.5	1.1
120	1.0	0.9	0.6	1.3
130	1.1	1.0	0.6	1.4
140	1.2	1.1	0.7	1.5
150	1.4	1.2	0.8	1.7
160	1.5	1.3	0.9	1.8
180	1.8	1.7	1.1	2.1
200	2.1	2.0	1.2	2.4
210	2.3	2.2	1.3	2.6
220	2.5	2.4	1.4	2.7
230	2.8	2.6	1.5	2.8
240	2.9	2.7	1.6	3.0
250	3.0	2.9	1.6	3.1
260	3.2	3.0	1.8	3.4
270	3.4	3.2	1.9	3.6
280	3.6	3.4	2.0	3.8
290	3.8	3.6	2.1	3.9
300	4.0	3.8	2.3	4.1
310	4.1	4.0	2.4	4.3
320	4.6	4.5	2.8	4.6
330	4.8	4.8	2.9	4.9
340	5.0	5.0	3.1	5.1
351	5.2	5.3	3.3	5.3
360	5.5	5.6	3.5	5.6
370	5.9	6.2	4.1	6.3
375	6.1	6.4	4.3	6.5
380	6.2	6.5	4.4	6.6
385	6.3	6.7	4.5	6.7
390	6.5	6.8	4.6	6.9
395	6.9	7.4	5.1	7.4
397	7.1	7.6	5.3	7.5

Table 6.63 Longitudinal Steel Strain Data for Specimen 11-LWHD

Shear (kN)	ϵ_{L1B2} ($\times 10^{-6}$)	ϵ_{L1B3} ($\times 10^{-6}$)	ϵ_{L2B1} ($\times 10^{-6}$)	ϵ_{L2B2} ($\times 10^{-6}$)	ϵ_{L2B3} ($\times 10^{-6}$)	ϵ_{L2B4} ($\times 10^{-6}$)	ϵ_{L2T1} ($\times 10^{-6}$)	ϵ_{L2T2} ($\times 10^{-6}$)	ϵ_{L2T3} ($\times 10^{-6}$)	ϵ_{L2T4} ($\times 10^{-6}$)
0	0	0	0	0	0	0	0	0	0	0
20	17	17	46	44	-32	47	-20	-26	-28	-29
42	34	36	93	90	0	98	-46	-55	-61	-63
60	54	56	146	139	56	150	-63	-80	-90	-92
80	78	83	231	212	119	237	-88	-115	-129	-130
100	101	112	388	373	346	389	-110	-149	-166	-166
110	119	129	452	448	440	463	-120	-167	-185	-185
120	140	154	508	516	475	529	-129	-181	-204	-202
130	153	170	555	565	500	575	-140	-193	-218	-216
140	180	213	616	632	588	636	-149	-206	-231	-229
150	214	276	674	696	613	699	-150	-212	-243	-240
160	238	310	726	748	683	747	-154	-221	-254	-250
180	317	397	849	861	833	865	-155	-232	-274	-268
200	409	492	958	968	964	979	-155	-240	-292	-285
210	528	574	1011	1020	1020	1046	-149	-236	-296	-288
220	582	625	1057	1066	1109	1106	-139	-223	-301	-292
230	654	683	1108	1113	1119	1165	-161	-240	-323	-312
240	720	751	1180	1179	1142	1237	-154	-240	-328	-316
250	758	786	1231	1229	1259	1290	-159	-245	-334	-322
260	804	828	1289	1284	1325	1356	-160	-249	-341	-327
270	844	873	1341	1334	1395	1416	-161	-251	-349	-336
280	885	915	1394	1386	1445	1483	-158	-248	-353	-337
290	923	965	1446	1438	1490	1544	-157	-248	-357	-342
300	958	1001	1498	1488	1553	1606	-160	-254	-365	-348
310	995	1040	1548	1539	1613	1666	-160	-253	-365	-351
320	1044	1084	1612	1591	1667	1716	-137	-225	-346	-334
330	1082	1122	1665	1641	1707	1775	-135	-224	-348	-336
340	1125	1167	1720	1690	1766	1840	-126	-215	-346	-336
351	1169	1209	1773	1738	1855	1907	-120	-209	-344	-338
360	1208	1250	1820	1783	1945	1967	-115	-203	-339	-336
370	1254	1292	1866	1827	1972	2029	-98	-182	-313	-306
375	1279	1317	1891	1848	1950	2055	-89	-173	-273	-270
380	1301	1338	1917	1871	2003	2086	-82	-170	-262	-258
385	1320	1357	1942	1897	2032	2114	-79	-170	-254	-248
390	1340	1376	1968	1919	2045	2139	-67	-160	-231	-223
395	1365	1399	1987	1935	2079	2160	-8	-111	-126	-118
397	1372	1408	1994	1941	2054	2169	6	-97	-91	-82

Continued

Table 6.63 Longitudinal Steel Strain Data for Specimen 11-LWHD (*Concluded*)

Shear (kN)	ϵ_{L3B2} ($\times 10^{-6}$)	ϵ_{L3B3} ($\times 10^{-6}$)	ϵ_{L3T2} ($\times 10^{-6}$)	ϵ_{L3T3} ($\times 10^{-6}$)	ϵ_{L4B2} ($\times 10^{-6}$)	ϵ_{L4B3} ($\times 10^{-6}$)	ϵ_{L4T2} ($\times 10^{-6}$)	ϵ_{L4T3} ($\times 10^{-6}$)
0	0	0	0	0	0	0	0	0
20	25	21	-26	-21	-28	-28	46	47
42	50	44	-47	-45	-59	-60	100	106
60	75	68	-68	-64	-88	-90	178	178
80	108	101	-98	-87	-128	-126	329	324
100	140	131	-116	-108	-161	-157	471	468
110	171	157	-125	-121	-179	-176	536	544
120	255	224	-132	-124	-193	-191	590	608
130	295	273	-140	-130	-206	-205	643	670
140	372	369	-150	-136	-217	-221	699	741
150	495	491	-158	-141	-224	-235	755	815
160	557	546	-171	-149	-234	-247	805	866
180	711	659	-182	-156	-254	-273	922	997
200	812	767	-193	-169	-269	-292	1036	1117
210	872	838	-203	-175	-278	-303	1097	1178
220	927	905	-195	-166	-288	-312	1150	1239
230	962	938	-215	-180	-306	-333	1199	1289
240	1015	996	-223	-181	-308	-336	1266	1357
250	1055	1040	-225	-183	-315	-343	1312	1409
260	1101	1091	-233	-187	-318	-349	1371	1478
270	1140	1138	-243	-194	-327	-358	1422	1531
280	1184	1188	-246	-196	-330	-364	1478	1594
290	1233	1234	-252	-195	-336	-370	1532	1654
300	1280	1276	-262	-198	-345	-378	1585	1711
310	1325	1322	-257	-198	-347	-381	1635	1768
320	1385	1352	-226	-164	-351	-385	1693	1827
330	1431	1394	-202	-128	-351	-386	1740	1878
340	1483	1441	-185	-100	-353	-390	1795	1940
351	1529	1488	-156	-61	-358	-398	1849	1997
360	1573	1532	-94	28	-362	-399	1900	2045
370	1617	1582	291	402	-341	-383	1930	2089
375	1641	1600	366	479	-341	-379	1957	2116
380	1666	1622	389	506	-341	-378	1984	2143
385	1688	1643	413	534	-344	-378	2009	2164
390	1712	1664	453	578	-340	-377	2034	2187
395	1749	1698	535	735	-323	-360	2054	2204
397	1766	1715	529	774	-316	-355	2064	2217

Table 6.64 Stirrup Strain Data for Specimen 11-LWHD

Shear (kN)	ϵ_{T1A} ($\times 10^{-6}$)	ϵ_{T1C} ($\times 10^{-6}$)	ϵ_{T2A} ($\times 10^{-6}$)	ϵ_{T2C} ($\times 10^{-6}$)	ϵ_{T3A} ($\times 10^{-6}$)	ϵ_{T3C} ($\times 10^{-6}$)	ϵ_{T4A} ($\times 10^{-6}$)	ϵ_{T4C} ($\times 10^{-6}$)	ϵ_{T5A} ($\times 10^{-6}$)	ϵ_{T5C} ($\times 10^{-6}$)
0	0	0	0	0	0	0	0	0	0	0
20	-25	1	7	1	1	-2	-2	-1	0	2
42	-16	0	14	2	5	-4	-1	-1	-3	2
60	16	2	22	4	5	-4	12	2	-4	2
80	24	3	28	5	3	-4	16	5	-10	-5
100	24	-5	34	6	7	-3	19	7	-16	-10
110	26	-6	40	8	9	-3	21	20	-15	-5
120	87	-11	44	12	6	-3	16	18	-36	26
130	132	-4	47	16	12	-3	14	18	-43	35
140	292	67	46	16	15	-2	7	18	84	31
150	499	181	41	16	19	2	18	19	354	81
160	566	231	40	12	17	4	23	20	455	109
180	843	434	40	2	22	8	101	26	699	147
200	1019	569	69	15	26	9	276	140	854	182
210	1153	705	119	27	25	11	425	198	947	203
220	1314	829	559	91	23	15	466	243	992	223
230	1359	871	636	119	13	2	617	521	1082	249
240	1384	937	697	150	18	10	772	1030	1217	320
250	1414	981	724	164	21	14	816	1060	1273	344
260	1461	1038	744	187	30	17	893	1072	1381	388
270	1503	1090	754	211	26	17	937	1078	1475	441
280	1570	1125	770	234	29	19	978	1087	1561	499
290	1622	1185	789	245	35	20	1009	1103	1635	553
300	1676	1240	802	243	40	20	1009	1116	1682	622
310	1736	1285	813	244	76	27	1023	1133	1727	671
320	1878	1416	1100	6194	178	203	1030	1158	1709	772
330	1934	1446	1244	7895	284	242	1046	1214	1738	864
340	2027	1508	1480	11909	334	287	1055	1346	1790	930
351	2084	1539	1605	10985	400	326	1077	1524	1825	980
360	2133	1578	1664	5816	505	337	1110	1622	1869	1031
370	2190	1674	1738	5201	4833	415	2410	2924	1949	1147
375	2234	1735	1780	4919	2399	426	2488	8642	1961	1189
380	2246	1766	1807	4756	2241	439	2552	10163	1982	1209
385	2262	1792	1821	4738	2343	448	2588	11276	2003	1235
390	2288	1824	1831	4701	2489	461	2645	12908	2040	1270
395	2316	1872	1857	4592	2870	626	1175	16192	2103	1363
397	2325	1879	1899	4561	2950	670	1052	16994	2124	1393

Table 6.65 Deflection Data for Specimen 12-NWHD

Shear (kN)	Δ_2 (mm)	Δ_3 (mm)	Δ_4 (mm)	Δ_6 (mm)
0	0.0	0.0	0.0	0.0
21	0.1	0.1	0.0	0.1
40	0.1	0.1	0.1	0.1
61	0.2	0.2	0.1	0.3
80	0.4	0.4	0.2	0.5
90	0.5	0.4	0.3	0.7
100	0.6	0.5	0.3	0.8
110	0.7	0.6	0.4	1.0
120	0.9	0.8	0.4	1.1
130	1.0	0.8	0.5	1.2
140	1.1	1.0	0.5	1.4
150	1.3	1.1	0.6	1.5
160	1.4	1.2	0.7	1.6
170	1.5	1.3	0.8	1.8
180	1.6	1.5	0.8	1.9
190	1.8	1.6	0.9	2.0
200	2.0	1.8	1.0	2.2
210	2.2	2.1	1.1	2.6
220	2.4	2.2	1.2	2.8
230	2.5	2.4	1.3	3.0
240	2.7	2.5	1.4	3.2
250	2.8	2.7	1.4	3.3
260	3.0	2.9	1.6	3.5
270	3.2	3.1	1.7	3.7
281	3.3	3.2	1.8	3.9
290	3.6	3.5	1.9	4.1
300	3.7	3.6	2.0	4.3
310	3.9	3.8	2.1	4.5
320	4.1	4.0	2.2	4.7
330	4.3	4.3	2.4	4.9
340	4.5	4.5	2.5	5.1
350	4.8	4.7	2.6	5.4
360	5.1	5.1	2.8	5.8
370	5.4	5.6	2.9	6.0
380	5.7	5.8	3.0	6.2
390	5.9	6.0	3.1	6.5
395	6.0	6.2	3.2	6.7
398	6.1	6.3	3.3	6.8

Table 6.66 Longitudinal Steel Strain Data for Specimen 12-NWHD

Shear (kN)	ϵ_{L1B2} ($\times 10^{-6}$)	ϵ_{L1B3} ($\times 10^{-6}$)	ϵ_{L2B1} ($\times 10^{-6}$)	ϵ_{L2B2} ($\times 10^{-6}$)	ϵ_{L2B3} ($\times 10^{-6}$)	ϵ_{L2B4} ($\times 10^{-6}$)	ϵ_{L2T1} ($\times 10^{-6}$)	ϵ_{L2T2} ($\times 10^{-6}$)	ϵ_{L2T3} ($\times 10^{-6}$)	ϵ_{L2T4} ($\times 10^{-6}$)
0	0	0	0	0	0	0	0	0	0	0
21	13	28	10	26	25	25	-20	-18	-17	-22
40	22	63	19	57	54	57	-40	-37	-36	-45
61	36	153	34	116	118	137	-72	-68	-63	-82
80	49	298	44	212	250	290	-101	-94	-88	-117
90	58	397	55	296	324	370	-114	-103	-97	-132
100	68	454	65	341	365	416	-127	-115	-106	-146
110	96	519	92	399	422	478	-138	-124	-114	-161
120	148	595	148	470	494	539	-149	-131	-121	-178
130	165	635	166	509	539	582	-159	-139	-131	-192
140	210	687	224	562	603	637	-168	-147	-138	-204
150	266	756	305	635	669	698	-177	-152	-141	-213
160	292	805	342	680	715	743	-187	-160	-148	-224
170	357	870	445	750	778	801	-193	-165	-150	-233
180	474	929	616	810	822	843	-199	-168	-151	-238
190	533	998	683	875	879	898	-204	-171	-154	-247
200	616	1062	759	943	936	949	-206	-171	-152	-250
210	740	1141	851	1022	997	1003	-196	-162	-140	-246
220	792	1188	894	1065	1039	1045	-202	-167	-144	-254
230	921	1247	975	1124	1100	1101	-202	-165	-142	-260
240	1001	1307	1038	1185	1158	1155	-203	-163	-141	-267
250	1053	1361	1085	1237	1204	1199	-207	-166	-143	-274
260	1126	1432	1142	1310	1261	1251	-202	-163	-138	-279
270	1196	1497	1198	1373	1321	1307	-205	-165	-139	-289
281	1249	1553	1242	1425	1370	1356	-208	-167	-137	-295
290	1321	1613	1294	1482	1426	1407	-212	-168	-134	-307
300	1382	1670	1343	1537	1478	1459	-212	-167	-129	-311
310	1434	1720	1385	1587	1524	1504	-211	-164	-123	-316
320	1499	1783	1437	1646	1582	1558	-212	-159	-116	-325
330	1573	1839	1499	1703	1636	1610	-209	-152	-108	-331
340	1631	1895	1548	1755	1683	1656	-210	-150	-103	-337
350	1691	1958	1599	1816	1739	1709	-210	-142	-96	-349
360	1746	2020	1646	1874	1785	1755	-212	-137	-88	-358
370	1800	2056	1689	1912	1827	1797	-186	-97	-55	-352
380	1854	2108	1736	1963	1879	1849	-189	-90	-50	-368
390	1901	2160	1783	2014	1930	1898	-190	-85	-47	-379
395	1929	2193	1807	2045	1957	1925	-190	-83	-47	-386
398	1942	2209	1822	2060	1972	1941	-190	-79	-46	-388

Continued

Table 6.66 Longitudinal Steel Strain Data for Specimen 12-NWHD (*Concluded*)

Shear (kN)	ϵ_{L3B2} ($\times 10^{-6}$)	ϵ_{L3B3} ($\times 10^{-6}$)	ϵ_{L3T2} ($\times 10^{-6}$)	ϵ_{L3T3} ($\times 10^{-6}$)	ϵ_{L4B2} ($\times 10^{-6}$)	ϵ_{L4B3} ($\times 10^{-6}$)	ϵ_{L4T2} ($\times 10^{-6}$)	ϵ_{L4T3} ($\times 10^{-6}$)
0	0	0	0	0	0	0	0	0
21	16	16	-11	-15	-23	-17	32	32
40	30	28	-25	-30	-52	-38	150	140
61	52	53	-40	-47	-94	-65	383	358
80	80	81	-55	-65	-119	-78	581	556
90	122	131	-62	-72	-129	-77	674	634
100	149	162	-70	-78	-140	-82	742	697
110	209	232	-76	-86	-150	-86	816	767
120	286	315	-79	-91	-161	-88	893	842
130	325	350	-83	-96	-171	-93	948	897
140	436	464	-86	-98	-182	-96	1011	963
150	552	571	-88	-99	-191	-98	1082	1036
160	604	615	-93	-106	-201	-101	1142	1095
170	665	664	-96	-110	-207	-98	1207	1161
180	708	693	-101	-116	-212	-97	1264	1217
190	748	720	-105	-121	-222	-98	1328	1280
200	813	799	-107	-113	-226	-95	1382	1341
210	910	870	-95	-104	-226	-88	1444	1403
220	941	900	-99	-109	-229	-88	1495	1455
230	982	944	-104	-114	-232	-81	1552	1517
240	1024	984	-109	-119	-233	-75	1609	1574
250	1061	1020	-114	-125	-239	-72	1663	1629
260	1096	1052	-116	-128	-237	-55	1720	1683
270	1144	1095	-120	-133	-243	-47	1781	1745
281	1185	1133	-125	-137	-246	-44	1835	1800
290	1233	1171	-128	-140	-254	-35	1890	1853
300	1286	1212	-130	-143	-257	-24	1944	1906
310	1339	1248	-131	-145	-260	-18	1997	1959
320	1398	1289	-133	-146	-264	-6	2052	2013
330	1456	1330	-132	-143	-267	4	2108	2066
340	1506	1367	-132	-141	-270	9	2159	2115
350	1566	1410	-112	-129	-272	23	2212	2173
360	1634	1444	69	16	-271	41	2262	2221
370	1682	1491	118	69	-274	44	2314	2271
380	1735	1527	147	112	-281	52	2366	2323
390	1785	1565	178	150	-285	57	2420	2377
395	1813	1585	215	237	-319	50	2450	2419
398	1825	1597	238	276	-325	46	2468	2437

Table 6.67 Stirrup Strain Data for Specimen 12-NWHD

Shear (kN)	ϵ_{T1A} ($\times 10^{-6}$)	ϵ_{T1C} ($\times 10^{-6}$)	ϵ_{T2A} ($\times 10^{-6}$)	ϵ_{T2C} ($\times 10^{-6}$)	ϵ_{T3A} ($\times 10^{-6}$)	ϵ_{T3C} ($\times 10^{-6}$)	ϵ_{T4A} ($\times 10^{-6}$)	ϵ_{T4C} ($\times 10^{-6}$)	ϵ_{T5A} ($\times 10^{-6}$)	ϵ_{T5C} ($\times 10^{-6}$)
0	0	0	0	0	0	0	0	0	0	0
21	0	1	0	-1	1	2	3	0	0	1
40	-2	2	-1	-3	2	3	5	0	-4	-2
61	-6	-5	-2	-4	4	5	6	0	-16	-11
80	2	-16	-4	-7	3	5	1	0	-27	-19
90	6	-25	-5	-7	5	5	10	0	-29	-18
100	8	-26	-5	-8	5	6	14	0	-30	-16
110	8	-28	-1	-3	5	5	20	0	-24	-10
120	12	-25	4	2	9	8	-8	0	-2	8
130	16	-26	5	2	10	10	-7	0	4	10
140	66	-16	8	-3	14	12	-5	0	15	20
150	78	18	8	-2	20	16	5	0	31	29
160	84	26	5	-5	22	16	8	0	35	31
170	95	36	4	-5	26	20	15	0	45	38
180	104	44	4	-5	31	25	20	0	52	39
190	110	50	2	-5	32	26	26	0	60	39
200	128	75	-3	-6	41	31	36	0	85	38
210	197	155	59	182	49	38	57	0	140	49
220	204	163	68	207	51	40	140	0	197	55
230	231	193	103	295	54	40	240	0	297	79
240	258	217	140	399	56	40	297	0	357	91
250	272	228	154	457	59	41	340	0	389	100
260	316	277	266	782	62	44	552	0	544	207
270	345	305	310	919	67	43	714	0	603	258
281	364	321	333	1008	70	44	777	0	621	271
290	411	356	389	1189	75	43	956	0	673	302
300	456	389	408	1286	78	42	1020	0	715	326
310	495	423	419	1335	79	43	1052	0	745	341
320	553	472	446	1430	83	47	1136	0	798	378
330	604	518	463	1493	87	55	1183	0	835	412
340	640	548	477	1537	93	69	1212	0	863	434
350	734	626	928	1616	108	99	1294	0	917	479
360	798	707	1173	1701	157	184	1371	0	941	532
370	989	975	2821	1742	284	212	1407	0	962	552
380	1055	1118	2820	1774	343	229	1450	0	981	587
390	1096	1202	2934	1796	370	240	1480	0	1001	618
395	1119	1237	3024	1809	393	245	1519	0	975	656
398	1133	1257	3091	1815	450	250	1532	0	981	669

Table 6.68 Horizontal Whittemore Strain Data for Specimen 1-NWLA

Shear (kN)	Mean Whittemore Strain ($\mu\epsilon$)									
	1	2	3	4	5	6	7	8	9	10
0	0	0	0	0	0	0	0	0	0	0
45	71	13	14	-3	32	83	29	56	22	41
89	28	-23	-12	36	10	69	29	26	13	9
119	-18	-52	-61	-36	-20	104	28	2	-37	-44
149	516	-58	-60	-39	-29	63	6	-7	-12	-33
179	1040	-41	-42	-36	1	6	-37	-25	-39	-44
208	1465	-70	-73	-35	17	138	5	-5	-49	-37
238	1908	-38	-103	-73	-27	214	-71	-67	-35	0
267	2254	-59	-114	-153	-81	227	-130	-114	-112	-44
296	2797	1502	523	-166	-21	974	-190	-158	-97	-7
327	2970	2002	1009	-225	-85	1582	-263	-212	-164	-75
356	3453	2056	882	-244	-80	2031	-209	-210	-211	-29
386	3945	2421	795	-361	-126	2493	-293	-294	-306	-69

Shear (kN)	Mean Whittemore Strain ($\mu\epsilon$)									
	11	12	13	14	15	16	17	18	19	20
0	0	0	0	0	0	0	0	0	0	0
45	79	44	-54	52	-8	30	-14	44	-27	13
89	75	58	25	63	-20	63	29	85	-34	21
119	71	21	-79	2	-23	17	-31	31	-58	-2
149	55	33	-52	12	-1	64	34	72	-4	85
179	7	-29	-93	42	-78	7	-40	15	-102	21
208	35	-21	-89	10	-82	47	-25	5	-60	41
238	37	-35	-95	46	-30	25	-90	6	-89	43
267	51	-62	-153	-30	-65	-9	-130	-60	-167	176
296	96	-150	-220	-99	-36	-21	-151	-72	-128	302
327	-36	-195	-262	-125	-107	-108	-205	-205	18	413
356	-33	-147	-306	-171	104	-47	-207	-169	1153	1096
386	-88	-160	-344	-256	124	-129	-228	-217	1434	1138

Continued

Table 6.68 Horizontal Whittemore Strain Data for Specimen 1-NWLA (Concluded)

Shear (kN)	Mean Whittemore Strain ($\mu\epsilon$)									
	21	22	23	24	25	26	27	28	29	30
0	0	0	0	0	0	0	0	0	0	0
45	32	-48	0	68	43	-64	-67	-62	73	73
89	50	39	79	53	56	-17	-7	-17	48	14
119	29	-34	-13	17	23	-60	-15	-79	4	17
149	45	-6	-7	71	202	-91	-98	-96	-83	370
179	29	-69	-37	7	347	-80	-105	-150	-139	668
208	75	-17	-41	-27	463	-29	-70	-122	-249	901
238	2	-54	-75	-41	690	-67	-114	-186	-178	1104
267	0	-106	-102	-98	909	-83	-225	11	256	1249
296	-28	-115	-155	-61	1191	-150	-218	93	469	1425
327	-87	-215	-152	-245	1394	-207	-283	155	590	1492
356	-66	-197	778	-210	1752	-193	327	194	814	1678
386	-71	-319	950	-323	2049	-277	507	306	955	1751

Table 6.69 Vertical Whittemore Strain Data for Specimen 1-NWLA

Shear (kN)	Mean Whittemore Strain ($\mu\epsilon$)								
	1	2	3	4	5	6	7	8	9
0	0	0	0	0	0	0	0	0	0
46	8	-14	-68	41	33	25	27	33	-2
89	10	-9	-29	26	45	6	15	39	7
119	14	17	-22	44	76	76	40	16	5
150	-30	25	-65	51	73	-32	-6	29	27
180	121	22	-48	76	73	24	19	-16	-5
207	259	16	10	284	78	13	33	63	30
237	510	35	14	530	94	16	59	48	49
267	790	128	-42	784	28	56	45	71	17
297	2645	1465	-116	1933	35	-65	-68	-3	-29
327	3454	2299	-131	2783	81	0	-154	-6	54
356	4312	2866	-151	3888	1	-39	-200	-59	538
386	6074	3168	-103	5719	-27	-38	-173	11	813

Shear (kN)	Mean Whittemore Strain ($\mu\epsilon$)								
	10	11	12	13	14	15	16	17	18
0	0	0	0	0	0	0	0	0	0
46	16	3	79	22	22	14	2	54	35
89	56	39	36	29	21	26	23	47	33
119	6	27	14	-8	-40	0	3	25	21
150	-27	2	13	-11	-16	2	-21	25	599
180	21	98	57	96	65	116	21	51	1340
207	85	57	72	27	30	230	10	25	1810
237	66	10	94	36	-40	570	87	146	2294
267	23	6	355	28	-25	1134	-4	651	2929
297	-62	2	380	-13	-113	1266	-44	847	3080
327	-41	-52	855	5	316	1884	32	1330	3444
356	-83	767	2331	-157	1905	3744	1102	2643	3577
386	19	885	2854	-125	2405	4558	1390	3211	3873

Table 6.70 Diagonal Whittemore Strain Data for Specimen 1-NWLA

Shear (kN)	Mean Whittemore Strain ($\mu\epsilon$)								
	1	2	3	4	5	6	7	8	9
0	0	0	0	0	0	0	0	0	0
46	39	-10	-4	-18	-22	-20	29	-1	6
89	34	-18	-12	-28	-25	-49	41	7	17
119	60	-20	-12	-31	-28	-50	87	31	18
149	811	-10	-12	-116	-108	-101	76	30	12
180	1702	8	13	-171	-131	-104	41	24	32
208	2548	14	26	-148	-112	-104	287	91	83
238	3460	6	-3	-56	-204	-159	653	56	37
267	4299	223	37	-7	-242	-189	922	98	68
296	6783	2741	1384	-202	-410	-284	2599	86	75
326	8088	3620	2289	-346	-505	-351	3497	37	46
357	9985	3856	2317	-351	-556	-390	4396	46	138
385	12390	5046	2559	112	-682	-466	5988	-23	307

Shear (kN)	Mean Whittemore Strain ($\mu\epsilon$)								
	10	11	12	13	14	15	16	17	18
0	0	0	0	0	0	0	0	0	0
46	-10	-39	-31	7	30	26	23	20	1
89	-23	-34	-56	33	55	41	2	12	-25
119	-52	-60	-76	49	52	10	-50	-32	-55
149	-118	-99	-109	36	66	70	-51	-39	-47
180	-119	-108	-102	75	93	78	-68	-57	-52
208	-126	-92	-84	86	91	78	-103	-60	-55
238	-237	-184	-146	82	88	14	-128	-111	-119
267	-274	-187	-147	119	69	103	-140	-112	-131
296	-527	-280	-200	110	83	98	-260	-178	-157
326	-628	-310	-196	50	81	141	-315	-163	-173
357	-732	-433	-327	7	28	936	-463	-349	-394
385	-881	-552	-464	2	41	1263	-545	-432	-503

Continued

Table 6.70 Diagonal Whittemore Strain Data for Specimen 1-NWLA (Concluded)

Shear (kN)	Mean Whittemore Strain ($\mu\epsilon$)								
	19	20	21	22	23	24	25	26	27
0	0	0	0	0	0	0	0	0	0
46	41	31	27	35	39	7	57	12	45
89	39	39	23	5	-23	9	30	-10	37
119	46	44	51	-23	-34	-13	41	6	57
149	60	92	80	4	-40	-28	42	34	369
180	93	88	122	-22	-38	-30	46	22	739
208	95	115	149	-19	-54	-32	77	48	1112
238	80	74	233	-42	-74	-55	83	21	1573
267	104	139	800	-62	-108	-118	89	-15	2289
296	63	104	947	-176	-169	-205	29	-51	2572
326	82	761	1641	-198	-161	-294	233	253	3399
357	177	2663	3485	-362	-398	-159	2042	2117	5521
385	275	3260	4075	-439	-491	-238	2619	2633	6454

Shear (kN)	Mean Whittemore Strain ($\mu\epsilon$)								
	28	29	30	31	32	33	34	35	36
0	0	0	0	0	0	0	0	0	0
46	6	-1	25	22	41	83	18	40	58
89	-47	-47	-25	33	51	58	2	29	61
119	-61	-53	-31	17	6	42	-29	9	9
149	-12	-55	-44	33	14	908	-37	-58	-42
180	-49	-100	-123	10	-75	1751	-60	-121	-29
208	-52	-111	-133	50	-167	2399	-82	-154	6
238	-79	-146	-142	50	-151	3128	-112	-241	41
267	-128	-205	-9	308	479	4034	-157	-337	-90
296	-187	-239	24	527	734	4537	-230	-422	-238
326	-219	-118	145	864	1255	5367	-191	-501	-365
357	-402	1	-89	2241	3077	5669	75	-559	-448
385	-544	-52	-173	2728	3843	6281	62	-688	-520

Table 6.71 Horizontal Whittemore Strain Data for Specimen 2-NWLB

Shear (kN)	Mean Whittemore Strain ($\mu\epsilon$)									
	1	2	3	4	5	6	7	8	9	10
0	0	0	0	0	0	0	0	0	0	0
45	9	-30	35	-6	-8	33	-2	2	-11	-70
75	17	-35	79	-38	-51	13	-21	-32	-46	-85
104	46	-40	46	-62	-93	27	-22	-48	-76	-101
127	192	42	82	-77	-96	69	-58	-31	-40	-96
150	388	178	37	-105	-135	-40	-134	-217	-167	-170
172	753	915	-157	-159	-173	333	-168	-180	-147	-131
197	839	1134	-214	-224	-227	471	-269	-198	-178	-203
220	877	1373	-34	-200	-135	675	-277	-285	-173	-176
241	1011	1664	-181	-226	-142	946	-201	-183	-153	-112
264	973	1840	-96	-230	-181	1172	-290	-234	-197	-202
286	976	2075	-108	-237	-141	1450	-247	-262	-217	-169
308	899	2352	-126	-275	-188	1871	-273	-299	-192	-153
331	972	2700	-117	-256	-196	2209	-261	-232	-187	-160
361	912	3019	-127	-340	-207	2577	-282	-288	-308	-297
391	866	3569	-248	-385	-243	2901	-318	-353	-330	-286

Shear (kN)	Mean Whittemore Strain ($\mu\epsilon$)									
	11	12	13	14	15	16	17	18	19	20
0	0	0	0	0	0	0	0	0	0	0
45	-13	-3	14	22	-32	-84	-24	-33	-30	-6
75	-52	-11	6	-32	-52	-138	-84	-95	-78	-50
104	-19	22	13	5	28	-81	-54	-40	-22	-2
127	-34	-2	15	15	-73	-128	-34	-47	-47	-37
150	-118	31	-61	-48	-147	-155	-102	-116	-71	-15
172	-112	-133	-106	-59	-125	-169	-118	-161	-145	-86
197	-159	-127	-141	-143	-218	-240	-183	-221	-164	-67
220	-126	-129	-108	-99	-135	-193	-194	-202	-136	-10
241	-161	-137	-135	-73	-91	-159	-156	-188	-158	40
264	-256	-234	-166	-149	-171	-202	-240	-289	-253	73
286	-272	-211	-191	-192	-113	-201	-204	-307	-352	224
308	-241	-226	-210	-192	-73	-248	-324	-330	-335	304
331	-206	-211	-161	-191	-125	-244	-237	-306	-219	478
361	-161	-297	-248	-261	-12	-348	-342	-389	-66	678
391	59	-335	-313	-240	128	-288	-411	-418	31	705

Continued

Table 6.71 Horizontal Whittemore Strain Data for Specimen 2-NWLB (*Concluded*)

Shear (kN)	Mean Whittemore Strain ($\mu\epsilon$)									
	21	22	23	24	25	26	27	28	29	30
0	0	0	0	0	0	0	0	0	0	0
45	-22	-29	25	-27	13	-46	-60	-22	16	-33
75	-90	-73	14	-27	-8	-108	-75	-35	8	41
104	-71	-48	29	2	89	-65	-98	-35	14	106
127	-97	-71	20	-68	14	-89	-61	-31	45	145
150	-135	-125	-115	-138	109	-151	-207	247	446	462
172	-149	-158	-153	-227	171	-214	-213	454	714	540
197	-184	-210	-226	-274	339	-245	-278	694	988	624
220	-192	-190	-161	-274	599	-232	-288	895	1342	630
241	-151	-203	-199	-276	812	-178	-264	1151	1641	814
264	-149	-245	-224	-324	977	-248	-316	1303	1939	898
286	-188	-234	-322	420	1204	-234	-289	1749	1730	1002
308	-255	-290	-375	652	1409	-271	-335	1910	1672	1121
331	-242	-272	-368	886	1642	-223	-274	2071	1699	1254
361	-258	-390	-424	1145	1610	-317	-361	2400	1606	1335
391	-342	-476	-482	1412	1779	-358	-537	2494	1841	1446

Table 6.72 Vertical Whittemore Strain Data for Specimen 2-NWLB

Shear (kN)	Mean Whittemore Strain ($\mu\epsilon$)								
	1	2	3	4	5	6	7	8	9
0	0	0	0	0	0	0	0	0	0
45	-54	7	-3	5	-26	19	4	40	35
74	-16	21	48	35	30	19	-14	172	113
104	-43	50	61	-5	-13	6	3	-138	65
127	-24	-54	33	-28	-51	-35	6	399	44
150	56	-49	-32	-68	-93	-85	-121	446	-82
172	1071	501	-124	-183	-137	-131	-163	-695	-32
197	1419	839	-242	-236	-222	-197	-125	-753	-212
219	1658	1069	-251	-200	-301	-248	-203	-849	-249
242	1962	1278	-318	-185	-306	-344	-312	-867	-369
264	2182	1463	-428	-251	-420	-392	-325	-932	-301
286	2389	1654	-521	-288	-507	-527	-440	-1053	-478
308	2802	2045	-654	-215	-674	-699	-607	-1119	-600
331	3160	2308	-806	-247	-786	-751	-746	-1265	-606
361	3730	2467	-1054	-91	-1051	-1001	-799	-1631	-475
392	4643	2973	-1444	411	-1228	-1389	-465	-1928	-765

Shear (kN)	Mean Whittemore Strain ($\mu\epsilon$)								
	10	11	12	13	14	15	16	17	18
0	0	0	0	0	0	0	0	0	0
45	-68	-38	-20	21	84	34	32	-28	-84
74	-51	-62	-56	-82	29	33	-71	-94	-132
104	-40	-21	3	-7	92	34	-35	-135	-73
127	-105	-20	-44	-48	15	-32	-43	-10	-72
150	-101	-24	-46	-152	22	-35	-141	312	295
172	-155	-101	-170	-176	-79	-73	-204	532	530
197	-262	-188	-207	-234	-131	-215	-201	850	771
219	-283	-192	-282	-381	-265	-351	-293	1171	1079
242	-320	-264	-313	-416	-283	-460	-385	1413	1364
264	-435	-413	-403	-503	-398	-315	-434	1713	1761
286	-541	-483	-514	-681	-562	545	-306	2210	1907
308	-692	-591	-372	-782	-651	814	-151	2455	1913
331	-780	-732	-181	-839	-739	998	20	2671	1989
361	-1075	-1084	321	-1120	-781	1545	645	3222	1959
392	-1033	-1393	374	-1438	-961	1843	946	3590	2546

Table 6.73 Diagonal Whittemore Strain Data for Specimen 2-NWLB

Shear (kN)	Mean Whittemore Strain ($\mu\epsilon$)								
	1	2	3	4	5	6	7	8	9
0	0	0	0	0	0	0	0	0	0
45	28	-52	-12	-34	-53	-126	37	21	-34
74	38	-62	8	-56	-59	-168	44	33	-30
104	23	-157	10	-60	-107	-150	50	39	4
127	289	37	3	-70	-62	-182	67	57	-30
149	467	220	-54	-98	-87	-230	78	40	-10
172	1851	1518	-23	-10	-174	-261	1007	1	-44
198	2435	1990	-34	55	-250	-321	1348	-28	-69
220	2761	2403	-20	120	-277	-258	1751	-13	4
242	3155	2829	25	201	-295	-305	2177	1	31
264	3565	3033	-6	252	-339	-516	2613	-15	-33
286	3961	3495	34	342	-360	-376	3084	20	42
308	4463	3911	23	430	-389	-273	3737	17	47
331	4957	4513	-26	569	-391	-363	4330	41	-154
361	5871	5300	-42	735	-474	-493	5193	2	-3
391	7177	6513	102	1052	-610	-552	6682	-51	1

Shear (kN)	Mean Whittemore Strain ($\mu\epsilon$)								
	10	11	12	13	14	15	16	17	18
0	0	0	0	0	0	0	0	0	0
45	-4	-49	-54	-62	43	29	-48	-37	-23
74	-56	-72	-85	33	70	37	-65	-78	-40
104	-1	-92	-114	28	66	33	-95	-74	-61
127	-67	-94	-106	47	81	59	-87	-76	-70
149	-61	-115	-98	52	85	59	-102	-92	-78
172	-116	-143	-103	77	105	25	-131	-109	-64
198	-139	-162	-119	102	100	55	-141	-139	-93
220	-246	-204	-167	64	115	66	-145	-136	-93
242	-261	-228	-157	6	72	68	-196	-173	-138
264	-304	-274	-153	-39	67	72	-206	-179	-157
286	-334	-255	-221	-70	12	166	-199	-197	-174
308	-380	-284	-249	-103	47	203	-241	-216	-203
331	-507	-309	-227	-115	46	197	-257	-241	-243
361	-524	-337	-307	-3	109	458	-324	-309	-318
391	-323	-364	-336	875	108	546	-354	-367	-394

Continued

Table 6.73 Diagonal Whittemore Strain Data for Specimen 2-NWLB (*Concluded*)

Shear (kN)	Mean Whittemore Strain ($\mu\epsilon$)								
	19	20	21	22	23	24	25	26	27
0	0	0	0	0	0	0	0	0	0
45	21	42	41	-15	-32	-31	39	9	29
74	22	46	40	-56	-49	-61	47	29	43
104	20	46	37	-60	-72	-80	42	33	36
127	33	65	53	-75	-92	-81	41	32	65
149	45	73	72	-86	-101	-105	13	19	339
172	36	69	91	-96	-103	-136	13	-17	606
198	41	66	84	-125	-115	-135	-7	-55	953
220	79	74	298	-139	-129	-166	-2	-53	1501
242	58	66	349	-176	-162	-198	-12	-60	1895
264	39	39	687	-176	-175	-221	-13	-74	2520
286	56	30	1339	-211	-228	-280	-12	1283	3518
308	44	58	1602	-231	-235	-313	-42	1657	4001
331	38	222	1866	-257	-256	-355	-40	2059	4511
361	35	861	2753	-307	-298	-534	-65	3078	5638
391	373	1103	3207	-400	-364	-638	-118	3825	6608

Shear (kN)	Mean Whittemore Strain ($\mu\epsilon$)								
	28	29	30	31	32	33	34	35	36
0	0	0	0	0	0	0	0	0	0
45	-33	-23	-6	29	17	46	-26	-20	10
74	-58	-53	-29	16	27	59	-65	-64	-19
104	-81	-87	-44	-6	4	84	-74	-67	-25
127	-81	-88	-49	3	86	235	-81	-52	6
149	-81	-81	-83	508	675	847	-102	-111	-13
172	-105	-117	-130	856	1034	1218	-125	-150	20
198	-125	-152	-144	1186	1428	1656	-180	-195	28
220	-127	-176	-125	1595	1914	2218	-191	-241	18
242	-175	-214	-101	1888	2300	2711	-225	-263	37
264	-212	-255	-36	2276	2791	3397	-274	-339	13
286	-255	-329	68	2864	3495	4450	-274	-207	4
308	-252	-319	175	3138	3831	5133	-279	-198	9
331	-280	-288	233	3410	4179	5825	-311	-184	35
361	-319	-86	302	4097	5145	7241	-390	-164	-36
391	-375	-74	404	4635	6957	8940	-477	-88	33

Table 6.74 Horizontal Whittemore Strain Data for Specimen 3-NWLC

Shear (kN)	Mean Whittemore Strain ($\mu\epsilon$)									
	1	2	3	4	5	6	7	8	9	10
0	0	0	0	0	0	0	0	0	0	0
45	45	28	9	-36	-23	-1	43	29	-25	-25
74	40	5	43	11	-24	9	39	19	-25	-62
104	37	6	-1	-29	-63	-15	20	18	-18	-34
127	261	16	-49	-84	-117	-72	-22	-49	-78	-115
149	472	24	-25	-19	-35	0	-22	3	5	-17
172	570	-20	-69	-74	-92	-79	-13	-50	-51	-47
198	534	-195	-168	-172	-188	-156	-60	-126	-90	-71
220	468	-245	-218	-210	-204	-175	-83	-147	-119	-118
242	605	-196	-175	-217	-271	-227	-78	-203	-172	-159
264	729	-266	694	-254	-228	72	938	-204	-174	-95
287	819	-216	922	-226	-160	106	1129	-206	-157	-97
309	862	-310	1119	-323	-240	68	1373	-287	-218	-156
332	894	-371	1414	-330	-232	131	1757	-255	-211	-136
362	1063	-401	1702	-426	-289	206	2101	-307	-294	-158
392	1084	-505	2038	-535	-370	230	2583	-390	-386	-226

Shear (kN)	Mean Whittemore Strain ($\mu\epsilon$)									
	11	12	13	14	15	16	17	18	19	20
0	0	0	0	0	0	0	0	0	0	0
45	6	1	-15	-15	-23	-33	-37	-25	2	26
74	-13	-11	-3	3	-49	-26	-19	-27	-22	-2
104	2	1	-21	-52	-29	-55	-25	-22	-7	9
127	-35	-59	-47	-57	-65	-81	-83	-67	-70	-35
149	38	-17	-27	-13	-22	-35	-75	-85	-51	-10
172	53	-110	-89	-82	-77	-76	-129	-124	-93	-66
198	146	-124	-98	-81	-65	-100	-156	-171	-159	-88
220	136	-187	-190	-155	-113	-187	-237	-228	-190	-93
242	115	-207	-206	-171	-125	-112	-226	-237	-195	9
264	579	-164	-208	-175	-89	46	-256	-238	-182	54
287	642	-139	-204	-155	-74	76	-266	-261	-248	45
309	882	-91	-255	-201	-109	-130	-339	-279	-218	147
332	1209	10	-275	-229	-117	-199	-386	-289	-198	242
362	1650	124	-294	-275	-65	-287	-433	-323	-250	429
392	2022	141	-393	-389	-135	-439	-544	-409	-308	612

Continued

Table 6.74 Horizontal Whittemore Strain Data for Specimen 3-NWLC (*Concluded*)

Shear (kN)	Mean Whittemore Strain ($\mu\epsilon$)									
	21	22	23	24	25	26	27	28	29	30
0	0	0	0	0	0	0	0	0	0	0
45	31	1	14	-7	-26	-48	-29	39	2	32
74	-22	-18	6	-32	-10	-36	-21	-14	-10	2
104	-4	-10	14	-33	6	-63	-69	-53	6	34
127	-96	-65	-13	-6	38	-75	-103	-88	-67	5
149	-41	-76	-73	620	478	-109	199	449	-27	270
172	-26	-80	-102	751	650	-48	338	662	-32	262
198	-80	-180	-181	895	819	-106	375	752	-63	236
220	-144	-238	-242	1046	997	-169	423	875	-78	210
242	-163	-260	-260	1264	1221	-174	533	1036	-105	156
264	-274	-328	-310	1350	1361	-216	524	1070	-116	157
287	-243	-359	-315	1499	1519	-243	589	1178	-99	179
309	-15	-381	-328	1652	1713	-388	541	1222	-175	312
332	115	-395	-326	1796	1892	-411	534	1268	-195	652
362	194	-460	-353	2443	2291	-523	686	1658	-246	950
392	218	-586	-445	2602	2318	-523	612	1683	-272	1241

Table 6.75 Vertical Whittemore Strain Data for Specimen 3-NWLC

Shear (kN)	Mean Whittemore Strain ($\mu\epsilon$)								
	1	2	3	4	5	6	7	8	9
0	0	0	0	0	0	0	0	0	0
45	-60	-44	-41	31	32	17	-7	-14	-7
74	-31	-47	-32	30	25	27	-2	17	39
104	-19	-48	-36	-3	0	15	3	24	-9
127	218	-23	-73	-3	30	-36	7	15	-11
149	520	-64	-133	-35	-62	-96	-56	-31	-53
172	861	-41	-105	25	-78	-142	-148	-151	-126
198	1134	-122	-181	139	-144	-164	-147	-221	-149
220	1208	-181	-226	184	-191	-233	-261	-248	-228
242	1381	-245	-333	291	-299	-309	-293	-289	-298
264	1216	902	849	1563	-527	-543	-186	-583	-580
287	1117	1051	1049	1757	-689	-695	-171	-683	-636
309	1245	1349	1352	2292	-870	-890	-103	-852	-809
332	1328	1809	1827	2976	-990	-1045	-71	-1053	-1015
363	1238	2291	2311	3770	-1474	-1503	-248	-1517	-1588
391	1538	3272	3327	5208	-1944	-1959	-387	-2023	-2087

Shear (kN)	Mean Whittemore Strain ($\mu\epsilon$)								
	10	11	12	13	14	15	16	17	18
0	0	0	0	0	0	0	0	0	0
45	-9	18	7	5	31	64	2	-6	-48
74	26	36	-13	-19	-1	-50	33	-45	-61
104	24	-30	-20	-16	15	7	30	2	-4
127	-3	27	1	100	12	-41	-14	-44	-77
149	-89	-59	-99	-160	-94	177	327	359	-21
172	-133	-151	-148	-157	-164	310	433	457	-158
198	-186	-168	-184	-176	-189	510	577	571	-257
220	-213	-219	-229	-249	-269	762	791	814	-283
242	-256	-310	-367	-292	-358	1110	1053	1103	-303
264	-259	-594	-654	-518	-643	1088	984	1045	-517
287	-125	-669	-779	-645	-669	1311	1151	1193	-599
309	228	-849	-967	-801	-867	1543	1300	1298	-665
332	540	-1036	-1145	-781	-1111	1679	1361	1272	-1000
363	610	-1523	-1316	-1273	-1535	3443	3006	2888	-1665
391	912	-2049	-1688	-1701	-1838	4163	3682	3552	-2167

Table 6.76 Diagonal Whittemore Strain Data for Specimen 3-NWLC

Shear (kN)	Mean Whittemore Strain ($\mu\epsilon$)								
	1	2	3	4	5	6	7	8	9
0	0	0	0	0	0	0	0	0	0
45	4	31	7	-25	-54	-20	23	9	6
74	-8	0	-5	-82	-56	-135	-5	-8	-32
104	62	33	3	-93	-71	-90	65	48	0
127	532	52	40	-144	-136	-90	45	46	13
149	855	53	2	-281	-182	-118	29	36	15
172	1131	16	-32	-478	-299	-261	35	14	-14
198	1445	18	-47	-581	-238	-192	203	76	-17
220	1676	62	3	-654	-321	-204	291	146	24
242	2101	117	18	-706	-351	-297	415	235	26
264	4046	1759	1474	-667	-209	-402	2312	2167	37
287	4613	2150	1838	-731	-201	-455	2724	2584	38
308	5505	2599	2223	-802	-209	-511	3391	3210	46
332	6709	3339	2864	-829	-28	-571	4366	4126	52
362	8421	4270	3698	-802	431	-606	5642	5286	232
392	10822	5546	4791	-794	1063	-723	7396	6933	304

Shear (kN)	Mean Whittemore Strain ($\mu\epsilon$)								
	10	11	12	13	14	15	16	17	18
0	0	0	0	0	0	0	0	0	0
45	-25	-83	-33	-10	7	4	-13	7	9
74	-68	-102	-82	-19	-18	-18	-71	-24	-19
104	-84	-132	-82	19	21	-11	-64	-51	-38
127	-135	-151	-113	58	16	8	-86	-72	-73
149	-158	-169	-103	110	29	22	-117	-87	-75
172	-240	-260	-198	233	-41	-61	-208	-177	-171
198	-178	-306	-207	455	-17	-9	-193	-177	-140
220	-178	-318	-211	675	-19	16	-224	-205	-167
242	-153	-363	-221	904	-20	30	-247	-216	-169
264	211	-484	-280	2439	22	51	-135	-255	-205
287	259	-539	-316	2868	63	54	-107	-305	-228
308	409	-599	-346	3670	132	102	7	-336	-291
332	713	-634	-431	4716	307	159	102	-403	-356
362	1233	-653	-452	6070	485	701	271	-465	-396
392	2041	-704	-528	7869	623	823	564	-529	-454

Continued

Table 6.76 Diagonal Whittemore Strain Data for Specimen 3-NWLC (Concluded)

Shear (kN)	Mean Whittemore Strain ($\mu\epsilon$)								
	19	20	21	22	23	24	25	26	27
0	0	0	0	0	0	0	0	0	0
45	23	-2	-23	-50	-10	15	1	12	12
74	0	-34	-66	-93	-32	-47	-37	-13	29
104	35	18	-32	-111	-64	-51	-8	10	53
127	86	48	13	-122	-89	-75	14	34	93
149	52	17	23	-153	-80	-105	2	928	923
172	10	-61	-43	-208	-165	-167	-69	1158	1158
198	30	-60	-34	-251	-195	-203	-65	1504	1503
220	66	-29	-22	-231	-189	-183	-61	1848	1911
242	235	-42	113	-273	-211	-181	-44	2346	2443
264	785	-59	125	-396	-259	-222	-50	2533	2715
287	1015	-66	174	-369	-293	-243	157	2841	3092
308	1412	-81	313	-280	-369	-314	743	3160	3515
332	1756	-73	434	-182	-450	-381	1149	3465	3867
362	2254	-41	1505	62	-511	-237	1663	5628	6099
392	2866	-50	2154	430	-606	-243	2430	6601	7173

Shear (kN)	Mean Whittemore Strain ($\mu\epsilon$)								
	28	29	30	31	32	33	34	35	36
0	0	0	0	0	0	0	0	0	0
45	12	21	10	-23	9	-21	-26	-6	1
74	-59	-40	-32	-54	-27	-27	-70	-37	-34
104	-70	-35	-59	-29	21	19	-62	-46	-46
127	-106	-73	-60	-8	8	21	-64	-64	-56
149	-128	-142	-190	536	746	938	-119	-135	28
172	-195	-227	-292	684	927	1162	-226	-215	-59
198	-220	-240	-325	941	1219	1454	-241	-225	-65
220	-251	-255	-397	1184	1513	1798	-298	-269	-115
242	-291	-318	-473	1531	1905	2245	-334	-264	-138
264	-357	-344	-494	1692	2059	2437	-378	-266	-160
287	-396	-378	-549	1896	2290	2722	-418	-316	-192
308	-541	-454	-595	2013	2405	3348	-453	-361	-242
332	-665	-507	-637	2165	2550	4015	-477	-364	-307
362	-777	-578	-255	3828	4393	6493	-504	-439	-355
392	-919	-654	-42	4592	5204	7845	-405	-508	-453

Table 6.77 Horizontal Whittemore Strain Data for Specimen 4-NWLD

Shear (kN)	Mean Whittemore Strain ($\mu\epsilon$)									
	1	2	3	4	5	6	7	8	9	10
0	0	0	0	0	0	0	0	0	0	0
18	146	122	77	75	-61	66	212	72	9	-47
44	356	395	342	91	9	21	176	48	-158	-147
55	325	481	282	164	-97	89	126	-40	-6	-111
66	315	334	163	346	-65	284	193	28	-116	-204
78	543	647	349	145	-66	254	181	42	-80	-167
92	537	401	293	222	-121	503	400	-17	-39	-222
122	887	616	385	168	32	1236	1070	722	378	-141
139	868	581	497	111	123	1721	1661	1073	728	-45
157	819	547	254	-69	-85	1958	1754	1229	833	-283
175	1050	545	304	-221	25	2253	2171	1307	1011	-100
193	1315	514	228	402	-10	2965	2743	1902	528	-300
210	1295	472	70	711	-119	3291	3184	2254	469	-304

Shear (kN)	Mean Whittemore Strain ($\mu\epsilon$)									
	11	12	13	14	15	16	17	18	19	20
0	0	0	0	0	0	0	0	0	0	0
18	21	-9	-23	-85	53	-81	-141	-140	-168	-210
44	105	-7	47	72	203	74	6	-45	-26	-59
55	74	-126	77	-15	58	-44	-48	-66	-67	-89
66	166	-30	63	-72	27	-110	-81	-125	-153	-207
78	94	-45	-33	-99	-10	-85	-155	-116	-100	-150
92	-1	-159	-144	-1	18	-111	-185	-165	-105	-153
122	69	-13	20	-44	55	-1	-125	-96	-61	-34
139	204	-40	82	36	179	113	21	74	-20	-16
157	77	-145	-137	-153	20	6	-155	-169	-109	-100
175	59	-127	-13	-51	83	40	-133	-128	-72	-20
193	-102	-145	-74	-85	61	245	-198	-169	-149	-169
210	5	-325	-257	-261	-52	356	-303	-295	-287	-251

Continued

Table 6.77 Horizontal Whittemore Strain Data for Specimen 4-NWLD (*Concluded*)

Shear (kN)	Mean Whittemore Strain ($\mu\epsilon$)									
	21	22	23	24	25	26	27	28	29	30
0	0	0	0	0	0	0	0	0	0	0
18	-238	-180	-280	-82	-123	-151	-282	-154	-25	-162
44	-251	-122	-141	-36	-109	-184	-190	-77	-132	-138
55	-240	-33	-151	9	-21	-122	-69	-114	-69	-69
66	-326	-169	-265	-111	-182	-137	-161	-201	-67	-110
78	-299	-271	-263	-56	-98	-156	-100	-105	-169	-113
92	-422	-293	-298	-149	-130	-51	-10	1	9	-9
122	-378	-284	-323	-133	-103	15	91	40	40	17
139	-238	-140	-204	26	-88	143	212	178	140	343
157	-286	-154	-338	-160	-112	-173	-286	-252	-232	542
175	-296	-155	-243	-67	-38	133	96	25	-74	1018
193	-321	-271	-342	-133	-4	-56	-53	-143	-222	1108
210	-448	-256	-377	-210	287	5	-103	-92	-71	1625

Shear (kN)	Mean Whittemore Strain ($\mu\epsilon$)									
	21	22	23	24	25	26	27	28	29	30
0	0	0	0	0	0	0	0	0	0	0
18	-117	-201	-223	-153	-103	-328	-144	-139	-227	-26
44	-349	-372	-247	-278	-117	-382	-283	-420	-504	-176
55	-261	-387	-350	-90	-76	-357	-187	-286	-220	2
66	-264	-308	-203	-48	18	-366	-252	-225	-63	252
78	-290	-368	-312	2	-18	-397	-232	-113	114	401
92	-209	-342	-296	-140	98	-416	-96	121	353	675
122	-285	-266	-234	183	439	-446	42	467	618	1084
139	-352	-406	274	648	638	-370	490	428	727	1356
157	-266	-368	1032	1315	727	-493	845	188	650	1316
175	-251	-374	1449	1806	846	-545	1029	57	611	1311
193	-272	-468	1702	2178	942	-453	1299	207	729	1544
210	-238	-473	1659	2929	1004	-508	1703	821	808	1604

Table 6.78 Vertical Whittemore Strain Data for Specimen 4-NWLD

Shear (kN)	Mean Whittemore Strain ($\mu\epsilon$)								
	1	2	3	4	5	6	7	8	9
0	0	0	0	0	0	0	0	0	0
18	228	157	218	126	76	-35	30	121	297
44	83	73	-24	232	164	223	107	306	236
55	56	-63	141	306	-10	-17	-216	17	37
66	66	115	129	133	200	104	97	38	124
78	73	116	207	296	212	253	187	378	291
92	95	122	197	256	126	62	59	153	166
122	-34	-60	92	429	-178	20	62	116	108
139	162	142	88	984	-230	69	-49	-8	93
157	151	323	93	1237	-201	64	176	184	251
175	340	457	310	1891	-124	284	666	295	355
193	537	1325	279	3253	-15	33	1071	141	200
210	659	1638	206	4816	995	45	1612	267	154

Shear (kN)	Mean Whittemore Strain ($\mu\epsilon$)								
	10	11	12	13	14	15	16	17	18
0	0	0	0	0	0	0	0	0	0
18	171	127	128	-74	88	192	32	102	158
44	247	219	291	-34	196	105	181	107	284
55	82	163	-60	-304	-283	-177	-275	-184	44
66	109	154	145	-281	-348	-8	-197	-172	-35
78	302	317	364	-28	124	165	-35	24	106
92	82	-29	-41	-299	-2	59	-115	-114	-49
122	116	15	65	-114	-87	10	-141	146	94
139	18	-68	53	-256	163	566	-237	329	-126
157	134	35	165	-221	1156	1545	-304	968	-59
175	310	421	714	-86	1760	2210	-302	1410	58
193	141	67	564	-227	2162	2563	-357	1792	-180
210	-8	57	1371	-661	3313	2474	862	2767	-90

Table 6.79 Diagonal Whittemore Strain Data for Specimen 4-NWLD

Shear (kN)	Mean Whittemore Strain ($\mu\epsilon$)							
	1	2	3	4	5	6	7	8
0	0	0	0	0	0	0	0	0
18	-23	22	-41	106	-5	62	-57	61
44	142	73	-7	-22	-12	19	-53	-34
55	243	174	16	72	51	33	24	25
66	189	116	18	37	98	102	-74	48
78	235	55	16	40	175	52	-14	8
106	195	474	-211	-59	394	82	208	258
122	497	186	329	31	904	67	459	62
139	516	124	711	5	1470	-103	978	17
157	458	52	798	-7	1677	-281	1183	-71
175	740	185	1067	45	2183	-353	1543	-47
193	1084	269	2004	544	3255	-741	2613	244
210	885	346	2911	1046	4609	-661	3809	196

Shear (kN)	Mean Whittemore Strain ($\mu\epsilon$)							
	9	10	11	12	13	14	15	16
0	0	0	0	0	0	0	0	0
18	-43	38	-39	37	-13	66	-138	33
44	-57	84	-32	-8	-97	78	-108	34
55	27	52	-5	95	-54	58	-80	57
66	4	58	-66	46	-17	69	-92	37
78	74	-43	-49	-22	21	-17	-47	8
106	63	373	143	271	306	142	306	321
122	-43	-24	-24	-42	-8	-47	-99	-74
139	57	90	79	1	90	34	-61	-51
157	-9	-33	20	-45	157	-28	0	-60
175	141	72	129	15	457	29	121	-13
193	361	390	129	301	795	33	92	50
210	1092	647	221	47	1202	51	-1837	-80

Continued

Table 6.79 Diagonal Whittemore Strain Data for Specimen 4-NWLD (*Concluded*)

Shear (kN)	Mean Whittemore Strain ($\mu\epsilon$)							
	17	18	19	20	21	22	23	24
0	0	0	0	0	0	0	0	0
18	-193	58	-60	13	-60	-14	-120	-16
44	-140	37	-90	-57	-101	-45	16	9
55	-81	-1	-36	-52	67	131	-9	119
66	-129	-7	-114	-55	18	-17	-173	26
78	-60	-42	4	-60	-25	2	13	16
106	378	198	311	178	511	161	626	282
122	-133	-88	-68	-119	170	34	81	114
139	-133	31	-153	-175	89	232	525	261
157	-124	-89	-95	-183	-97	-135	991	-130
175	8	-126	-14	-225	17	16	1617	-3
193	16	-73	379	-49	198	60	2086	194
210	-92	-222	951	-248	165	-15562	3063	288

Shear (kN)	Mean Whittemore Strain ($\mu\epsilon$)							
	25	26	27	28	29	30	31	32
0	0	0	0	0	0	0	0	0
18	-201	-11	-266	-36	-27	-6	-82	-20
44	-194	-18	-61	-19	-112	20	62	54
55	-183	-3	-138	-87	-161	-26	-85	-20
66	-208	24	-196	14	-153	37	29	46
78	-72	-83	-7	5	-32	-5	165	67
106	201	176	359	222	561	59	905	310
122	-68	-113	184	-137	347	-112	734	51
139	512	-102	770	-21	847	-90	680	70
157	1363	-137	1601	-81	1399	-106	649	28
175	1956	-138	2076	-197	1829	47	585	63
193	2457	-89	2618	-112	2045	173	-31	-314
210	2437	-210	3777	-80	3042	-162	1635	-33

Table 6.80 Horizontal Whittemore Strain Data for Specimen 5-LWLA

Shear (kN)	Mean Whittemore Strain ($\mu\epsilon$)									
	1	2	3	4	5	6	7	8	9	10
0	0	0	0	0	0	0	0	0	0	0
45	37	35	81	-19	-104	41	-33	-2	-25	-21
59	-33	-92	-123	-9	-64	17	-84	44	-52	-68
74	176	-118	-133	-108	-122	23	-72	-76	-69	-7
89	262	-209	-157	-163	-102	-59	-154	-10	-72	-64
104	366	-130	-64	-80	-112	-44	-108	-123	-164	-27
126	479	-391	649	-132	-214	594	867	-257	-278	-169
149	478	-519	639	-295	-291	668	913	-358	-312	-188
171	545	-506	693	-361	-285	828	1036	-362	-396	-228
197	794	-636	813	-336	-277	1139	1430	-429	-206	-208
220	813	-768	929	-347	-306	1102	1503	-502	-445	-283
242	943	-837	915	-447	-433	1316	1795	-476	-447	-327
264	1389	-977	979	-463	-432	1302	1856	-523	-544	-256
286	1819	-981	1137	-571	-482	1300	1899	-576	-595	-393
308	2865	-1053	1086	-738	-619	802	1509	-678	-667	-474

Shear (kN)	Mean Whittemore Strain ($\mu\epsilon$)									
	11	12	13	14	15	16	17	18	19	20
0	0	0	0	0	0	0	0	0	0	0
45	49	17	71	-63	-87	3	13	-29	-95	21
59	77	50	119	-96	-64	-67	12	-31	-63	23
74	79	6	-65	-123	-24	-39	-65	-133	-142	-5
89	134	61	14	-112	-24	-23	-9	-107	-72	-109
104	16	-55	-117	-95	-128	-115	-145	-127	-152	-31
126	-26	-413	-320	-232	-96	-115	-150	-316	-241	-50
149	30	-260	-300	-350	-216	-191	-235	-360	-434	-119
171	-82	-502	-445	-297	-169	-221	-326	-385	-477	-23
197	63	-541	-471	-436	-259	-136	-409	-502	-546	29
220	125	-588	-492	-447	-246	-179	-293	-473	-582	99
242	237	-687	-597	-513	-244	-55	-512	-536	-597	281
264	369	-569	-532	-581	-280	-71	-490	-553	-626	328
286	407	-254	-523	-618	-330	-172	-618	-584	-727	435
308	491	-62	-702	-688	-494	-125	-547	-593	-751	950

Continued

Table 6.80 Horizontal Whittemore Strain Data for Specimen 5-LWLA (*Concluded*)

Shear (kN)	Mean Whittemore Strain ($\mu\epsilon$)									
	21	22	23	24	25	26	27	28	29	30
0	0	0	0	0	0	0	0	0	0	0
45	103	-41	-19	-98	-17	-20	-131	85	165	180
59	76	-99	-68	-138	-67	81	-10	237	315	318
74	63	-124	-51	-76	23	-2	-4	297	467	492
89	40	-143	-125	-160	-10	-21	-42	361	500	598
104	32	-120	-108	-126	-79	-58	-73	501	710	761
126	-171	-291	-252	-347	179	-147	-259	638	933	621
149	-62	-276	-346	-422	433	-167	-328	1159	1460	590
171	-168	-356	-382	-386	560	-108	-315	1182	1582	690
197	-316	-507	-474	-561	498	-233	-444	1079	1705	705
220	-284	-529	-415	-491	574	-268	-423	1224	1704	789
242	-450	-655	-442	-449	675	-312	-478	1170	1689	814
264	-483	-664	-506	-549	672	-356	-520	1038	1619	1071
286	-470	-844	-639	-472	810	-565	-639	999	1641	1220
308	-384	-1034	-669	-87	925	-644	-704	896	1304	1529

Table 6.81 Vertical Whittemore Strain Data for Specimen 5-LWLA

Shear (kN)	Mean Whittemore Strain ($\mu\epsilon$)								
	1	2	3	4	5	6	7	8	9
0	0	0	0	0	0	0	0	0	0
45	56	-36	-4	-64	-199	-71	-89	-217	83
59	20	6	-68	-83	-93	-52	-149	-95	79
74	99	79	46	-13	-287	-20	-166	-124	38
89	42	55	35	-24	-235	-63	-133	-20	173
104	76	-35	-99	-79	-120	-75	-248	-122	-51
126	-98	722	791	962	-350	-199	-332	-310	-255
149	-287	786	859	926	-502	-415	-561	-410	-260
171	-332	1039	1096	1035	-567	-515	-483	-564	-406
198	-475	1422	1424	1289	-760	-605	-166	-738	-543
219	-797	1677	1723	1783	-1004	-742	106	-631	-522
242	-790	1863	2025	2304	-1215	-925	163	-890	-709
263	-444	2175	2320	2925	-1402	-1119	301	-1056	-884
286	-227	2798	2912	3686	-1732	-1513	577	-1405	-1286
309	839	4158	4153	5278	-2239	-2114	325	-2236	-1766

Shear (kN)	Mean Whittemore Strain ($\mu\epsilon$)								
	10	11	12	13	14	15	16	17	18
0	0	0	0	0	0	0	0	0	0
45	58	29	71	-105	68	238	37	-9	106
59	73	-67	17	13	67	232	42	81	85
74	133	-104	92	77	67	98	-71	104	78
89	38	1	58	53	7	81	-150	-55	154
104	53	-11	94	-13	14	263	-35	153	298
126	-118	-113	-139	-258	-165	292	-344	53	392
149	-354	-431	-270	-287	-280	740	-405	790	1159
171	-360	-440	-193	-297	-454	704	-475	881	1325
198	-577	-568	-423	-657	-558	867	-697	1316	1464
219	-648	-755	-415	-607	-714	848	-838	1266	1718
242	-954	-696	-327	-862	-725	1005	-979	1405	1913
263	-975	-943	-322	-951	-977	971	-1347	1420	2254
286	-922	-1198	-683	-1092	-1273	1111	-1680	1759	2596
309	-698	-1702	-1015	-1854	-1984	1450	-2202	2088	3227

Table 6.82 Diagonal Whittemore Strain Data for Specimen 5-LWLA

Shear (kN)	Mean Whittemore Strain ($\mu\epsilon$)								
	1	2	3	4	5	6	7	8	9
0	0	0	0	0	0	0	0	0	0
45	95	38	6	-53	-162	-21	47	70	35
59	62	-58	-54	-111	-108	-43	96	65	-90
74	510	-82	-146	-156	-223	-118	83	63	3
89	661	-78	-129	-267	-252	-195	63	11	-65
104	915	-23	-62	-288	-289	-197	-43	-51	-113
126	2521	1167	798	-566	-640	-541	1586	1560	-275
149	2835	1282	966	-715	-780	-760	1860	1748	-472
171	3228	1556	1205	-848	-901	-930	2262	2113	-507
198	4525	2002	1405	-1176	-909	-1097	2978	2741	-638
220	5202	2225	1562	-1297	-873	-1224	3524	3083	-687
242	6225	2520	1827	-1472	-843	-1433	4250	3559	-823
264	7478	2743	2056	-1779	-789	-1638	4810	3991	-905
286	9063	3238	2463	-2057	-622	-2037	5582	4632	-1178
308	12059	3997	3369	-2399	496	-2594	6582	5550	-1476

Shear (kN)	Mean Whittemore Strain ($\mu\epsilon$)								
	10	11	12	13	14	15	16	17	18
0	0	0	0	0	0	0	0	0	0
45	-64	-43	-69	-10	-40	-23	-62	-99	-24
59	-46	-64	-35	77	28	-9	-9	-92	-98
74	-69	-56	-60	50	-5	-24	-162	-110	-132
89	-133	-112	-74	-28	-20	-27	-103	-138	-153
104	-207	-181	-167	92	8	-30	-151	-143	-136
126	-681	-529	-425	30	-188	-279	-595	-516	-405
149	-936	-683	-589	-52	-338	-373	-749	-737	-617
171	-1121	-815	-736	61	-475	-430	-846	-813	-686
198	-1404	-1002	-855	200	-555	-511	-1019	-979	-823
220	-1532	-1162	-969	382	-548	-504	-1257	-1099	-1004
242	-1823	-1342	-1159	636	-654	-505	-1529	-1275	-1123
264	-1862	-1519	-1323	1050	-738	-690	-1754	-1504	-1392
286	-2223	-1865	-1721	1394	-523	-876	-2073	-1827	-1757
308	-2643	-2385	-2442	1693	-536	-1192	-2433	-2381	-2491

Continued

Table 6.82 Diagonal Whittemore Strain Data for Specimen 5-LWLA (*Concluded*)

Shear (kN)	Mean Whittemore Strain ($\mu\epsilon$)								
	19	20	21	22	23	24	25	26	27
0	0	0	0	0	0	0	0	0	0
45	61	5	22	-84	-91	-75	61	38	40
59	37	0	-16	-85	-24	-92	10	42	13
74	29	-68	-84	-170	-128	-154	95	88	93
89	23	-6	-19	-184	-109	-149	43	15	89
104	46	-59	10	-179	-176	-174	65	44	126
126	-115	-272	-151	-429	-470	-367	-193	-304	377
149	-303	-468	111	-631	-679	-655	-403	-451	1218
171	-317	-557	125	-702	-731	-735	-415	-479	1534
198	-251	-602	151	-988	-916	-903	-521	-619	1767
220	-263	-685	333	-1156	-1082	-1033	-574	-644	2014
242	-195	-738	511	-1480	-1292	-1217	-711	-781	2356
264	-167	-892	641	-1699	-1445	-1481	-702	-854	2631
286	119	-1124	925	-1948	-1854	-1881	-526	-728	3335
308	379	-1445	1572	-2285	-2418	-2624	-307	-557	4110

Shear (kN)	Mean Whittemore Strain ($\mu\epsilon$)								
	28	29	30	31	32	33	34	35	36
0	0	0	0	0	0	0	0	0	0
45	-115	-104	-24	274	168	209	44	-58	87
59	-83	-146	-135	381	322	362	-4	-72	80
74	-110	-110	-88	433	457	429	-36	-79	113
89	-91	-175	-120	542	596	680	-43	-76	77
104	-168	-212	-213	737	816	887	-52	-213	-135
126	-342	-456	-426	851	1033	1178	-401	-567	-417
149	-514	-680	-589	1807	2065	2358	-556	-813	-796
171	-652	-836	-775	1971	2269	2633	-632	-1010	-1041
198	-824	-989	-912	1993	2388	2919	-901	-1173	-1229
220	-1062	-1161	-1079	2104	2482	3216	-1061	-1351	-1401
242	-1311	-1398	-1265	2122	2487	3610	-1196	-1455	-1559
264	-1637	-1591	-1376	2190	2532	4119	-1395	-1597	-1767
286	-2154	-1909	-1605	2322	2821	4827	-1786	-1884	-2186
308	-2689	-2395	-1888	2173	2777	5746	-2420	-2422	-2860

Table 6.83 Horizontal Whittemore Strain Data for Specimen 6-LWLB

Shear (kN)	Mean Whittemore Strain ($\mu\epsilon$)									
	1	2	3	4	5	6	7	8	9	10
0	0	0	0	0	0	0	0	0	0	0
44	86	-47	-17	-147	-104	7	-91	-34	-28	-80
74	368	183	46	-80	-191	32	-92	-129	-54	-175
89	714	495	-129	-115	-199	-25	-141	-197	-38	-150
104	1101	822	-80	-119	-160	-7	-182	-160	9	-106
119	1095	1187	-142	-117	-136	227	-266	-198	-74	-103
134	1069	1532	-128	-123	-153	575	-179	-69	-56	-133
149	1122	1625	-188	-150	-151	602	-220	-222	-84	-166
164	1034	1798	-248	-232	-216	734	-273	-277	-105	-159
179	1161	2056	-105	-172	-184	874	-297	-269	-141	-153
203	1293	2419	-119	-134	-197	1032	-286	-262	-33	-89
224	1256	2584	-163	-289	-188	1195	-223	-330	-199	-222
246	1249	2773	-48	-277	-243	1359	-240	-304	-175	-118
269	1367	2203	576	-257	-196	1475	1050	-371	-158	-158
291	1345	2252	668	-328	-307	1506	1101	-423	-294	-221
314	1536	2561	849	-343	-258	1773	1386	-430	-350	-225

Shear (kN)	Mean Whittemore Strain ($\mu\epsilon$)									
	11	12	13	14	15	16	17	18	19	20
0	0	0	0	0	0	0	0	0	0	0
44	47	18	-150	18	42	12	-210	-71	20	56
74	-3	-89	-182	-40	-108	-21	-246	-154	-68	-39
89	24	-147	-205	-82	-142	-162	-402	-244	-97	-70
104	10	-63	-137	-36	6	-46	-229	-182	-68	-15
119	-100	-104	-255	-58	-72	-79	-461	-263	-101	-56
134	9	-140	-270	-145	-85	-31	-449	-296	-120	-26
149	-33	-252	-247	-108	-60	-21	-69	-246	-126	-77
164	21	-378	-257	-176	-151	-85	-378	-289	-180	-55
179	125	-345	-328	-162	-121	-86	-477	-308	-172	52
203	315	-222	-260	-159	-167	-78	-511	-289	-259	528
224	325	-319	-327	-191	-200	-78	-309	-351	-258	652
246	429	-324	-411	-270	-247	18	-554	-401	-367	697
269	800	-316	-312	-254	-282	119	-497	-418	-415	854
291	853	-467	-441	-336	-363	-11	-691	-489	-442	889
314	1032	-499	-470	-283	-181	41	-427	-493	-463	1045

Continued

Table 6.83 Horizontal Whittemore Strain Data for Specimen 2-NWLB (*Concluded*)

Shear (kN)	Mean Whittemore Strain ($\mu\epsilon$)									
	21	22	23	24	25	26	27	28	29	30
0	0	0	0	0	0	0	0	0	0	0
44	-2	-67	12	86	45	-17	-50	45	29	158
74	-109	-133	-49	25	30	-165	-98	-46	153	208
89	-71	-117	-105	-62	-78	-178	-100	-32	64	167
104	-7	-145	-28	42	-1	-133	-34	69	286	410
119	-45	-180	-195	-155	-151	-185	-246	698	914	1068
134	-37	-202	-179	-201	-227	-64	-153	845	1150	1312
149	6	-148	-153	-108	-177	-145	-158	987	1221	1480
164	-27	-243	-189	-209	-255	-197	-283	1067	1393	1636
179	-17	-173	-221	-176	-253	-57	-209	1167	1582	1922
203	-52	-168	-281	503	-194	-153	-260	1325	1141	1720
224	-42	-272	-293	792	-41	-213	-344	1528	1104	1800
246	-68	-222	-348	980	162	-183	-321	1530	1076	1706
269	-130	-321	-385	1413	338	-303	-376	1692	1003	1762
291	-217	-395	-448	1543	379	-337	-461	1720	926	1710
314	-164	-347	-433	1998	683	-352	-425	1947	912	1760

Table 6.84 Vertical Whittemore Strain Data for Specimen 6-LWLB

Shear (kN)	Mean Whittemore Strain ($\mu\epsilon$)								
	1	2	3	4	5	6	7	8	9
0	0	0	0	0	0	0	0	0	0
45	-5	29	27	29	65	75	10	88	-22
75	171	244	45	275	57	-20	91	28	-98
104	714	859	-126	817	-2	198	275	128	63
134	1558	1555	-39	1716	316	48	887	-104	-119
164	2098	2052	-73	2300	684	54	1607	-29	-48
179	2358	2373	77	2701	916	-125	1860	2	-2
202	2789	2806	-17	3104	1152	-15	2364	31	-44
225	3260	3314	103	3481	1518	445	2832	30	19
247	3645	3868	259	3510	2064	1032	3476	1086	-64
269	3660	4565	805	3615	2674	1756	4254	2071	2
291	4025	5133	1025	3857	2904	2025	4567	2264	-118
313	5184	6468	1132	5008	3975	2282	5527	2720	-52

Shear (kN)	Mean Whittemore Strain ($\mu\epsilon$)								
	10	11	12	13	14	15	16	17	18
0	0	0	0	0	0	0	0	0	0
45	10	48	48	50	22	-10	25	-41	29
75	-52	-75	-123	57	-6	15	29	-58	-74
104	246	150	143	265	263	193	225	40	158
134	638	-40	-123	-19	-58	10	12	-75	-29
164	1107	-41	-76	336	10	51	62	-49	-16
179	1268	69	-7	577	-4	69	52	-50	-31
202	1577	124	27	736	102	21	17	-31	12
225	1923	119	50	983	56	145	-62	2	16
247	2498	125	27	1415	16	64	-27	-73	-11
269	3038	26	-2	2140	41	79	90	29	99
291	3336	51	-23	2287	-199	0	25	10	-37
313	3973	64	70	2885	-44	147	276	-185	243

Continued

Table 6.84 Vertical Whittemore Strain Data for Specimen 6-LWLB

Shear (kN)	Mean Whittemore Strain ($\mu\epsilon$)								
	19	20	21	22	23	24	25	26	27
0	0	0	0	0	0	0	0	0	0
45	-10	-29	-70	49	-59	-78	-54	33	-70
75	-10	-113	-147	-61	-91	-95	-26	-51	-60
104	77	61	126	85	116	95	158	124	168
134	-2	-52	-82	-42	-75	-45	-20	-40	7
164	6	-97	-81	5	-60	-26	-24	-44	73
179	-52	-85	-93	-85	-96	-101	-15	-32	233
202	92	-50	-60	-36	-97	-127	-55	-51	927
225	258	-8	-3	-13	-44	-77	89	16	1128
247	462	-132	-97	-128	-196	-238	-49	-96	1110
269	780	47	-1	147	-67	-202	15	-28	1228
291	945	-107	-151	375	-97	-622	40	-139	1299
313	1256	-10	163	769	-97	-87	102	-34	1727

Shear (kN)	Mean Whittemore Strain ($\mu\epsilon$)								
	28	29	30	31	32	33	34	35	36
0	0	0	0	0	0	0	0	0	0
45	14	36	-6	11	-115	16	-73	-82	-88
75	23	32	-34	-34	-138	-22	-68	-131	-232
104	285	279	182	167	100	213	100	354	229
134	65	62	34	-30	-108	-153	-28	1168	1010
164	18	102	64	-62	-181	-172	-102	1736	1533
179	-1	86	80	36	-103	-317	-100	1968	1889
202	-17	139	1301	14	1154	980	-71	2912	2731
225	85	193	1786	-53	1659	1538	-48	3470	3290
247	48	142	2154	-117	1974	1899	-72	3761	3586
269	65	150	2676	-69	2557	2409	-159	4432	4293
291	-18	142	3067	-37	2976	2769	-161	4769	4698
313	17	234	3990	50	3880	3679	-117	5596	5547

Continued

Table 6.84 Vertical Whittemore Strain Data for Specimen 6-LWLB (*Concluded*)

Shear (kN)	Mean Whittemore Strain ($\mu\epsilon$)							
	37	38	39					
0	0	0	0					
45	-24	-90	-66					
75	-70	-180	-75					
104	158	193	151					
134	930	864	-7					
164	1452	1397	-66					
179	1697	1618	-2					
202	2358	2357	175					
225	2647	2488	229					
247	2898	2844	82					
269	3378	3327	398					
291	3622	3611	61					
313	4375	4422	27					

Table 6.85 Diagonal Whittemore Strain Data for Specimen 6-LWLB

Shear (kN)	Mean Whittemore Strain ($\mu\epsilon$)								
	1	2	3	4	5	6	7	8	9
0	0	0	0	0	0	0	0	0	0
44	45	61	60	-10	-12	-42	120	21	28
75	371	328	1	-38	-84	-96	135	-21	-17
104	1073	992	-27	-123	-81	-112	128	12	-7
134	1765	1646	-44	-130	-175	-159	895	-50	-36
164	2298	2139	-81	-90	-276	-192	1496	-38	-30
179	2596	2398	-51	-46	-238	-187	1726	-46	-14
202	3015	2771	-59	-14	-313	-224	2115	-51	-51
225	3467	3204	50	59	-287	-223	2506	-25	-50
247	4046	3658	311	38	-182	-330	3083	901	-72
269	4696	4222	770	19	-52	-355	3717	1604	-62
291	5194	4720	967	54	-3	-283	4079	1887	-33
314	6129	5685	1150	167	25	-395	4769	2151	-9

Shear (kN)	Mean Whittemore Strain ($\mu\epsilon$)								
	10	11	12	13	14	15	16	17	18
0	0	0	0	0	0	0	0	0	0
44	-10	-39	14	66	66	50	-69	-60	-4
75	-72	-77	-47	84	38	14	-68	-90	-29
104	-106	-90	-40	93	96	59	-105	-64	-13
134	-159	-166	-107	120	40	2	-138	-116	-77
164	-125	-163	-108	359	23	52	-172	-129	-56
179	-155	-170	-110	433	7	-11	-174	-120	-41
202	-179	-236	-187	571	-38	-42	-161	-182	-127
225	-170	-223	-144	758	-46	-29	-199	-164	-95
247	-94	-308	-222	1186	-99	-82	-167	-191	-175
269	-35	-261	-219	1686	-48	-66	-57	-260	-202
291	64	-253	-194	1962	-62	-46	64	-198	-221
314	132	-291	-163	2416	-66	174	81	-278	-266

Continued

Table 6.85 Diagonal Whittemore Strain Data for Specimen 6-LWLB (*Concluded*)

Shear (kN)	Mean Whittemore Strain ($\mu\epsilon$)								
	19	20	21	22	23	24	25	26	27
0	0	0	0	0	0	0	0	0	0
44	102	71	87	-25	-35	11	75	40	28
75	72	125	61	-71	-45	-35	74	77	58
104	100	125	122	-54	-59	-65	61	50	118
134	76	-112	80	-90	-91	-78	37	-11	-31
164	87	127	137	-69	-96	-87	42	11	-76
179	100	69	265	-100	-94	-104	55	54	-9
202	67	22	938	-203	-224	-204	-25	1044	976
225	228	27	1023	-136	-205	-214	54	1495	1413
247	346	2	1076	-231	-308	-271	-35	1762	1704
269	533	-30	1204	-312	-350	-336	-37	2188	2136
291	728	-49	1429	-284	-338	-402	1	2556	2505
314	948	-102	1772	-356	-364	-391	95	3194	3189

Shear (kN)	Mean Whittemore Strain ($\mu\epsilon$)								
	28	29	30	31	32	33	34	35	36
0	0	0	0	0	0	0	0	0	0
44	-21	-11	-11	69	93	102	-32	-23	39
75	-76	-82	-43	73	107	136	-87	-55	-13
104	-67	-82	-94	198	324	376	-93	-51	-5
134	-69	-139	-145	1120	1262	1422	-179	-232	-282
164	-90	-118	-106	1486	1674	1913	-174	-234	-424
179	-43	-125	-126	1659	1899	2228	-186	-257	-546
202	-152	-269	-182	2019	2413	2915	-330	-141	-767
225	-153	-243	-187	2361	2806	3378	-315	-11	-746
247	-232	-317	-259	2505	2984	3611	-437	-75	-856
269	-218	-347	-302	2802	3318	3974	-432	31	-948
291	-207	-353	-269	3099	3617	4315	-440	106	-933
314	-240	-391	-233	3585	4200	4895	-482	234	-1010

Table 6.86 Horizontal Whittemore Strain Data for Specimen 7-LWLC

Shear (kN)	Mean Whittemore Strain ($\mu\epsilon$)									
	1	2	3	4	5	6	7	8	9	10
0	0	0	0	0	0	0	0	0	0	0
24	268	-623	-235	-792	-721	-194	-522	-524	-276	-363
60	654	-115	1	-604	-307	-29	-167	-158	-83	-241
74	714	-259	-386	-1208	-854	-217	-427	-619	-578	-576
90	727	22	366	-399	-495	187	142	-378	-447	-401
105	687	-229	392	-291	-627	365	493	-407	-316	-466
123	838	-733	569	-392	-774	407	530	-693	-803	-759
140	652	-813	781	-112	-859	375	1016	-748	-774	-611
163	723	-522	1045	-30	-629	792	1255	-642	-596	-599
186	567	-276	1615	441	-557	985	1823	-474	-210	-161
210	1217	-116	1785	606	-636	1314	2085	-455	-309	-153
233	925	-194	2125	926	-676	1346	2386	-445	-402	-401
257	1191	-97	1901	438	-565	1527	2373	-483	244	-457
281	1057	-450	1825	435	-476	1445	2427	-123	666	-337

Shear (kN)	Mean Whittemore Strain ($\mu\epsilon$)									
	11	12	13	14	15	16	17	18	19	20
0	0	0	0	0	0	0	0	0	0	0
24	-416	-282	-342	-324	-349	-386	-134	-333	-435	-360
60	88	-52	-207	-132	-32	-112	-178	-231	-201	-67
74	-147	-272	-446	-544	-511	-197	-645	-692	-582	-592
90	-21	44	-229	-219	-139	-189	-288	-443	-271	-249
105	57	-184	-360	-456	-388	-434	-397	-493	-484	-442
123	-25	-363	-378	-612	-460	-347	-504	-655	-704	-517
140	61	-379	-708	-735	-549	-306	-562	-521	-499	-447
163	375	-270	-365	-562	-475	-237	-466	-602	-504	-483
186	495	-191	-353	-385	-329	-45	-463	-638	-642	-459
210	638	-199	-304	-566	-283	161	-327	-370	-404	-340
233	744	-181	-450	-611	-461	142	-467	-530	-533	-386
257	1287	889	676	-607	-451	202	-394	-676	-766	-311
281	1531	1006	755	-410	-307	412	-522	-153	-578	-105

Continued

Table 6.86 Horizontal Whittemore Strain Data for Specimen 7-LWLC (*Concluded*)

Shear (kN)	Mean Whittemore Strain ($\mu\epsilon$)									
	21	22	23	24	25	26	27	28	29	30
0	0	0	0	0	0	0	0	0	0	0
24	-440	-565	-425	-519	-561	-692	-598	-668	-437	-596
60	-454	-391	-484	-308	-298	-620	-475	-542	-331	-306
74	-472	-565	-536	-630	-288	-562	-311	-425	-246	-585
90	-178	-383	-425	-482	1	-323	-128	-165	120	-221
105	-436	-624	-477	-512	-11	-167	-5	50	175	-296
123	-598	-724	-616	-515	129	-402	-158	62	136	-234
140	-569	-733	-520	-275	377	-227	-7	221	176	-308
163	-529	-1046	-826	-98	289	-440	-87	69	-228	-379
186	-554	-746	-525	440	783	103	212	528	44	-272
210	-437	-714	-298	622	1211	147	411	243	-399	-334
233	-463	-715	-474	897	1214	-13	426	636	42	43
257	-429	-893	-722	790	1094	-156	226	83	520	501
281	-354	-345	-578	823	1077	223	-14	153	1176	946

Shear (kN)	Mean Whittemore Strain ($\mu\epsilon$)									
	21	22	23	24	25	26	27	28	29	30
0	0	0	0	0	0	0	0	0	0	0
24	-777	-632	-521	-373	-593	-573	-612	-313	-261	-368
60	-614	-856	-799	-608	-534	-658	-975	-288	-246	-221
74	-328	-738	-809	-614	-562	-476	-607	37	40	-13
90	-352	-624	-632	-474	-45	-424	-507	126	349	161
105	-424	-609	-626	-538	-196	-698	-835	121	315	-8
123	-683	-885	-827	-688	-200	-645	-846	172	408	79
140	-572	-799	-669	-603	61	-614	-784	89	444	18
163	-914	-1054	-934	-874	-31	-1030	-1198	-130	391	-14
186	-679	-765	-675	-580	378	-657	-814	408	920	366
210	-615	-1012	-840	-830	305	-634	-1106	359	1005	424
233	-377	-503	-428	-601	920	-595	-810	762	1569	565
257	-606	-879	329	-914	1021	-798	-539	445	1365	552
281	-329	-859	737	-488	1182	-621	-494	410	1516	634

Table 6.87 Vertical Whittemore Strain Data for Specimen 7-LWLC

Shear (kN)	Mean Whittemore Strain ($\mu\epsilon$)								
	1	2	3	4	5	6	7	8	9
0	0	0	0	0	0	0	0	0	0
24	-36	-198	-297	-188	7	-362	-243	-455	-316
60	-65	-98	-249	138	78	-218	-221	2	-66
75	185	-167	-560	-210	-143	-169	-341	-245	-405
89	-193	-78	0	-533	147	-342	-536	-479	-194
105	-69	136	300	-181	308	-244	-219	-296	-79
122	-189	513	884	-122	582	-31	-75	-252	-193
140	-93	570	1074	-327	920	-232	-247	-517	-516
163	-25	977	1762	11	1323	46	309	6	148
187	-263	843	2070	-311	1434	-86	294	-396	-600
209	-136	1495	3143	147	2337	361	980	224	429
233	4	2304	3937	246	2456	394	1083	-199	306
256	-225	2651	4250	1137	3046	2605	3412	553	797
281	257	3316	4885	1626	3007	3234	3334	1017	1397

Shear (kN)	Mean Whittemore Strain ($\mu\epsilon$)								
	10	11	12	13	14	15	16	17	18
0	0	0	0	0	0	0	0	0	0
24	-596	-507	-479	-511	-315	-522	-500	-308	-332
60	-57	-79	31	37	524	403	186	302	104
75	-400	-400	-67	-238	-145	-168	-31	152	10
89	-535	-586	117	-390	-305	-284	-202	257	-115
105	-429	-324	402	-62	-186	-266	35	156	-285
122	-283	-159	624	-34	-199	-216	221	322	-73
140	-545	-779	589	-184	-184	-120	121	255	-133
163	-93	74	1646	-143	116	-31	501	619	23
187	-613	-231	1823	-274	144	9	940	1360	296
209	282	292	2530	305	525	301	1360	1422	460
233	330	187	3120	727	637	205	1901	2171	489
256	959	851	4020	1683	2834	2155	1932	2678	44
281	961	698	4179	1699	2930	2586	2158	2751	-3

Table 6.88 Diagonal Whittemore Strain Data for Specimen 7-LWLC

Shear (kN)	Mean Whittemore Strain ($\mu\epsilon$)							
	1	2	3	4	5	6	7	8
0	0	0	0	0	0	0	0	0
24	-4	138	3	3	-258	-56	-105	38
60	381	153	74	43	205	-258	155	7
75	433	-146	154	-381	-261	-610	276	-733
90	1461	116	834	89	918	-811	759	198
105	1224	-1077	573	-1131	696	-963	478	-1086
122	2206	-866	1478	-556	1952	-795	1046	129
141	2812	-7	2043	351	2147	-697	1346	420
163	2698	-1379	1604	-1230	1860	-1452	153	-1010
186	2344	-1183	1945	-1073	2361	-1009	352	-1290
210	3123	-1804	2583	-582	2542	-1586	1094	-163
233	4178	-1189	2706	-515	3488	-508	828	-728
257	4440	-530	4180	-579	4503	1113	2976	1076
282	4737	-138	4818	-714	4847	210	2730	212

Shear (kN)	Mean Whittemore Strain ($\mu\epsilon$)							
	9	10	11	12	13	14	15	16
0	0	0	0	0	0	0	0	0
24	24	-206	-147	-156	-264	-316	-220	-341
60	227	-253	147	-61	65	-197	146	-548
75	331	-775	282	-591	326	-707	295	-887
90	901	-818	858	-979	1061	-791	597	-1141
105	396	-1295	661	-1053	58	-1132	219	-1359
122	999	-946	1055	-767	613	-898	661	-936
141	1520	-211	1478	-701	1026	-170	1098	-564
163	1476	-1673	375	-681	250	-1397	211	-1237
186	1300	-1221	882	-1418	865	-1373	285	-1254
210	2541	-1349	942	-1536	1453	-1309	487	-1303
233	2375	-1238	1069	-1380	1306	-1580	509	-1206
257	5190	-544	3155	-570	3334	-771	2184	-774
282	5437	-393	3790	-582	4030	-507	2374	-202

Continued

Table 6.88 Diagonal Whittemore Strain Data for Specimen 7-LWLC (*Concluded*)

Shear (kN)	Mean Whittemore Strain ($\mu\epsilon$)							
	17	18	19	20	21	22	23	24
0	0	0	0	0	0	0	0	0
24	-218	-459	-354	-365	-245	-233	-304	-342
60	-237	-280	89	-50	-109	-522	28	-577
75	197	-929	459	-592	-148	-506	589	-884
90	1011	-517	1333	-64	1275	-121	850	-409
105	-144	-1274	810	-1098	947	-748	821	-1265
122	543	-291	1284	-791	1346	-280	1716	-891
141	1142	95	2083	183	2535	-839	2232	-647
163	376	-1322	1590	-656	1305	-1630	1893	-1088
186	142	-1122	1471	-1329	1434	-2043	2051	-869
210	579	-1290	2689	-1379	2200	-2137	2740	-1558
233	595	-1468	3091	-1316	1991	-2050	2745	-1370
257	2614	-167	4184	478	4147	-948	5476	11
282	2716	-432	4242	19	4268	-1375	5680	-668

Shear (kN)	Mean Whittemore Strain ($\mu\epsilon$)							
	25	26	27	28	29	30	31	32
0	0	0	0	0	0	0	0	0
24	-518	-272	-334	-444	-305	24	-323	-453
60	-4	-776	343	-650	-57	636	619	-670
75	-502	-725	344	-615	628	789	807	-1080
90	363	-692	1250	-1038	1408	1120	1578	-709
105	-512	-669	974	-521	125	841	1416	-506
122	-39	-245	1463	-196	1153	1255	2095	-618
141	237	39	2125	186	2063	1648	2505	-605
163	-467	-741	1521	-742	1495	830	2162	-816
186	-532	-1393	1874	-821	679	815	2388	-1158
210	881	-1528	2179	-1292	958	843	2637	-1763
233	326	-1000	2729	-1212	2488	898	3292	-1871
257	3401	-97	5474	550	5147	1795	4370	-949
282	3467	-540	5751	-81	3739	1615	4018	-760

Table 6.89 Horizontal Whittemore Strain Data for Specimen 8-LWLD

Shear (kN)	Mean Whittemore Strain ($\mu\epsilon$)									
	1	2	3	4	5	6	7	8	9	10
0	0	0	0	0	0	0	0	0	0	0
37	-252	172	-250	47	-172	-286	-547	-158	-255	-230
58	-29	-117	-345	-39	-257	-142	-397	-273	-292	-208
74	118	87	-85	210	93	76	9	53	165	45
89	212	98	-292	14	-217	134	-358	-155	-319	-415
105	258	730	213	73	-321	575	-246	-53	-164	-118
122	541	1074	742	135	-231	644	-468	-417	-317	-321
140	546	1586	1009	-116	-163	1167	-424	-294	-399	-321
162	460	1639	1356	605	-113	1278	-461	608	-348	-154
186	613	1734	1112	645	-318	1041	-696	788	-731	-460
209	733	1965	1492	552	-337	1351	-875	1161	-554	-347
233	885	2213	1710	643	-331	2141	-952	1362	-682	-403
257	957	2586	1844	564	-790	2344	-1549	1359	-935	379

Shear (kN)	Mean Whittemore Strain ($\mu\epsilon$)									
	11	12	13	14	15	16	17	18	19	20
0	0	0	0	0	0	0	0	0	0	0
37	-216	-151	-314	-284	-477	-253	-248	-258	-231	-169
58	-152	-48	20	-28	-116	-219	-166	-124	-143	-109
74	369	327	150	-39	38	114	142	70	123	150
89	-211	-28	-91	-248	-172	-154	-206	-251	-205	-35
105	54	152	-72	-31	-127	-34	-225	-196	58	74
122	-34	-56	-98	-170	-176	-76	-379	-110	-248	-55
140	-117	89	-73	-130	-290	-15	-258	-177	-271	6
162	428	1473	-101	-76	-70	205	-419	-343	-135	65
186	681	1605	-428	-333	-333	-2	-626	-582	-420	-262
209	1206	2486	-257	-110	-93	-71	-477	-255	-178	122
233	1578	3020	-376	-391	-271	339	-428	-327	-168	61
257	2220	3780	-527	1292	-358	1039	-533	1578	-402	-118

Continued

Table 6.89 Horizontal Whittemore Strain Data for Specimen 8-LWLD (*Concluded*)

Shear (kN)	Mean Whittemore Strain ($\mu\epsilon$)									
	21	22	23	24	25	26	27	28	29	30
0	0	0	0	0	0	0	0	0	0	0
37	-313	-340	-324	-319	-172	-228	-179	-224	-207	16
58	-85	-170	-262	-167	-80	-205	-275	-152	-218	48
74	109	-23	-55	58	179	51	63	135	-17	237
89	-216	-522	-427	-159	-86	-234	24	134	-27	127
105	-34	-180	-315	-288	-206	-130	-113	-227	-545	136
122	-141	-183	-475	-198	-50	-140	-263	-353	-583	130
140	-260	-210	-277	-271	-224	-26	-110	-252	-628	416
162	132	-280	-438	-262	-126	-160	-141	-278	-519	409
186	-239	-583	-810	-566	-505	-603	-583	-520	-813	355
209	-48	-636	-540	-461	-205	-382	-461	-643	-928	361
233	134	-499	-494	-337	232	-236	-278	-432	-707	543
257	-161	1142	-720	-490	195	145	-464	-812	-868	153

Shear (kN)	Mean Whittemore Strain ($\mu\epsilon$)									
	21	22	23	24	25	26	27	28	29	30
0	0	0	0	0	0	0	0	0	0	0
37	-113	-186	-181	-229	39	-195	-215	-158	-118	-201
58	-132	-67	-12	-169	-149	-136	-148	-175	-171	49
74	26	74	116	236	240	-198	-149	-108	257	258
89	16	20	25	-58	203	36	-93	-145	416	682
105	-49	423	661	907	447	93	-157	-303	312	657
122	-62	449	635	812	439	188	-266	-361	308	569
140	-101	533	750	1255	591	40	-296	-282	412	762
162	-158	542	1008	1212	521	71	-128	-217	726	1059
186	-283	276	688	1057	543	-234	-537	-385	982	1439
209	-520	142	660	1071	440	-234	-585	-709	1358	1774
233	-529	222	885	1444	705	-169	-473	-916	1868	2440
257	-529	-878	253	1132	771	-736	-836	-867	2164	3039

Table 6.90 Vertical Whittemore Strain Data for Specimen 8-LWLD

Shear (kN)	Mean Whittemore Strain ($\mu\epsilon$)								
	1	2	3	4	5	6	7	8	9
0	0	0	0	0	0	0	0	0	0
37	-175	-200	-187	-207	-141	32	-262	61	-88
58	-25	276	-630	-499	-610	-168	-71	-73	-223
74	-71	-164	-68	-119	-133	7	-96	52	42
89	-233	-409	-85	-563	-418	58	-255	55	-121
105	148	444	760	-110	-94	69	344	201	84
122	-271	771	976	-65	-158	146	13	9	-20
140	129	1290	1787	62	-89	327	406	345	224
162	-266	1826	1340	1139	1760	-390	1023	153	-34
186	6	2294	1804	1882	2872	173	1718	-26	143
209	181	3195	2461	2304	3733	238	2038	53	257
233	141	4322	3727	3098	5116	261	2690	31	18
257	318	5819	4722	3878	6699	5043	3030	5850	5344

Shear (kN)	Mean Whittemore Strain ($\mu\epsilon$)								
	10	11	12	13	14	15	16	17	18
0	0	0	0	0	0	0	0	0	0
37	-81	-103	-135	-49	-196	-63	-142	-221	-298
58	-168	-190	-198	9	-466	-309	-433	-457	-415
74	-214	126	306	-18	169	137	-113	4	-77
89	-157	-104	6	-132	-283	-198	-91	-270	-96
105	121	79	35	-129	752	674	-49	-190	0
122	56	60	177	-65	1208	719	91	-123	158
140	185	283	443	323	1794	848	178	-110	251
162	-114	-129	-104	-326	2028	1149	-101	-156	279
186	-33	-94	250	151	2783	1834	77	-104	1382
209	162	98	260	-79	3053	1849	-168	-406	1723
233	-107	268	507	6	3652	2479	-179	-117	2663
257	-229	4588	647	2023	4758	4036	-278	-661	3228

Table 6.91 Diagonal Whittemore Strain Data for Specimen 8-LWLD

Shear (kN)	Mean Whittemore Strain ($\mu\epsilon$)							
	1	2	3	4	5	6	7	8
0	0	0	0	0	0	0	0	0
37	-13	-116	-116	-220	15	-70	-76	-15
58	108	-97	-68	-78	97	66	83	40
74	362	-88	-91	-103	104	-9	-28	-52
89	585	-64	16	-59	438	64	-33	-93
105	1018	-93	392	-105	822	-130	-83	-66
122	1595	-132	894	-138	1267	-135	-31	-56
140	1975	-146	1255	-66	1674	-213	44	15
162	2145	-224	2221	165	3363	-294	1289	-170
186	2531	-266	2735	68	4322	-435	1803	-229
209	3015	-396	3321	119	5219	-418	2083	-267
233	4148	-322	4386	209	6906	-611	2525	-405
257	4947	-609	5319	313	8763	-726	6520	-719

Shear (kN)	Mean Whittemore Strain ($\mu\epsilon$)							
	9	10	11	12	13	14	15	16
0	0	0	0	0	0	0	0	0
37	-22	-38	-101	-103	-110	-89	-111	-125
58	95	-3	68	-31	-40	-71	11	-20
74	94	-2	-7	-43	-11	-139	-31	-119
89	10	8	19	-76	-18	-106	-103	-108
105	104	45	44	-70	66	-90	-1	-62
122	119	4	-2	30	59	-135	-37	-77
140	165	-19	52	-25	201	-33	16	-74
162	1913	182	18	-66	1115	-251	47	-104
186	2837	149	42	-169	1328	-320	14	-150
209	3446	104	55	-222	1460	-582	-29	-197
233	4526	63	-29	-247	2080	-867	43	-170
257	6019	72	3899	1478	7089	-1406	4154	-456

Continued

Table 6.91 Diagonal Whittemore Strain Data for Specimen 8-LWLD (*Concluded*)

Shear (kN)	Mean Whittemore Strain ($\mu\epsilon$)							
	17	18	19	20	21	22	23	24
0	0	0	0	0	0	0	0	0
37	-61	-153	-114	-141	-70	-115	-85	-66
58	-7	-80	45	-127	-18	-38	34	15
74	36	-58	56	-65	-24	-48	13	-50
89	-49	3	-36	-59	-59	37	3	12
105	4	-103	16	-128	-106	-39	459	-137
122	120	-95	63	-127	-43	-13	722	-85
140	76	-120	84	-223	-91	-106	969	-201
162	271	-190	132	-134	-63	-94	1237	-170
186	279	-358	51	-209	-160	-230	1495	-180
209	314	-474	187	-260	-150	-202	1820	-228
233	341	-662	391	-259	-69	-469	2189	-303
257	4224	730	600	-561	3429	-99	2893	-425

Shear (kN)	Mean Whittemore Strain ($\mu\epsilon$)							
	25	26	27	28	29	30	31	32
0	0	0	0	0	0	0	0	0
37	-26	-129	-61	-151	-77	-83	-17	-52
58	23	-150	55	-58	-22	-71	234	-35
74	-37	-167	-12	-121	-67	-93	310	-64
89	-56	-92	-42	-83	-139	-55	416	-108
105	577	-154	810	53	175	-185	423	-22
122	877	-225	1077	156	387	-133	560	14
140	997	-276	1304	124	400	-184	614	-87
162	1276	-398	1590	110	568	-265	823	-92
186	1482	-389	1811	24	563	-251	1537	-284
209	1698	-451	1992	127	849	-272	2181	-356
233	1808	-542	2150	43	1135	-378	2842	-458
257	3592	-478	2570	15	2036	-856	3476	-449

Table 6.92 Horizontal Whittemore Strain Data for Specimen 9-NWLD

Shear (kN)	Mean Whittemore Strain ($\mu\epsilon$)									
	1	2	3	4	5	6	7	8	9	10
0	0	0	0	0	0	0	0	0	0	0
44	57	58	-26	-12	69	51	53	48	31	34
74	661	632	453	180	36	86	40	66	36	42
104	843	861	608	356	18	99	47	10	40	74
127	1103	943	688	417	138	104	44	30	36	54
150	991	850	631	453	131	67	39	-10	-12	17
172	1592	848	514	277	103	106	19	14	68	54
198	2147	601	422	174	81	136	-8	-87	-70	-21
220	2461	577	387	195	64	82	54	-108	-55	29
243	2898	475	432	289	231	139	143	-111	-52	16
265	4553	433	2390	-134	-66	754	2762	-280	-183	-52
287	5461	-348	3660	-283	-239	1188	5814	-325	-284	-97
309	6313	-971	6711	-532	-531	1728	11235	-492	-595	6

Shear (kN)	Mean Whittemore Strain ($\mu\epsilon$)									
	11	12	13	14	15	16	17	18	19	20
0	0	0	0	0	0	0	0	0	0	0
44	47	58	69	105	47	47	54	50	69	67
74	87	42	29	83	93	95	70	81	131	116
104	111	69	31	108	80	92	76	103	167	127
127	113	48	69	127	114	104	59	104	160	164
150	176	-1	42	101	115	63	42	93	155	168
172	286	11	24	85	119	54	21	35	132	125
198	404	-141	-55	-14	65	129	-80	-33	62	100
220	337	-181	-43	57	67	271	-114	-35	59	142
243	324	-231	-87	6	102	329	-150	-57	-6	173
265	832	-478	-258	-137	112	-92	-456	-294	-142	214
287	1835	-537	-240	-204	213	364	-405	-231	-62	804
309	3579	-910	-520	-435	-398	1007	-634	-506	-264	1572

Continued

Table 6.92 Horizontal Whittemore Strain Data for Specimen 9-NWLD (*Concluded*)

Shear (kN)	Mean Whittemore Strain ($\mu\epsilon$)									
	21	22	23	24	25	26	27	28	29	30
0	0	0	0	0	0	0	0	0	0	0
44	26	220	49	106	152	42	69	79	151	166
74	70	247	101	152	219	91	118	148	185	250
104	42	226	34	114	174	25	45	47	161	333
127	53	241	88	132	128	70	87	114	240	377
150	28	231	47	86	236	52	76	101	205	473
172	42	214	21	24	321	35	38	24	113	1013
198	-46	129	-40	-29	510	22	-13	6	99	1181
220	-67	109	-33	-16	766	14	-41	-49	128	1531
243	-86	63	-95	-72	824	16	-68	-38	161	1747
265	-307	-239	-297	-205	874	-233	-524	-212	236	2024
287	-19	-160	-196	-445	2296	-520	-564	881	2546	2500
309	587	-520	-509	-1467	2991	-820	-1338	1092	4556	3223

Table 6.93 Vertical Whittemore Strain Data for Specimen 9-NWLD

Shear (kN)	Mean Whittemore Strain ($\mu\epsilon$)								
	1	2	3	4	5	6	7	8	9
0	0	0	0	0	0	0	0	0	0
45	-33	26	-47	-14	42	56	-26	112	53
74	61	256	207	63	66	36	76	147	53
104	73	391	343	32	68	52	33	129	33
127	177	564	468	135	63	89	105	110	57
150	387	630	480	220	101	126	84	118	17
172	397	589	482	727	123	134	28	163	49
198	780	642	504	1457	123	132	401	158	17
220	867	607	495	2034	127	125	1135	168	103
242	935	548	481	2778	86	49	1981	16	-17
265	6561	6072	371	7321	314	141	5427	13	326
287	9842	9407	673	11371	3062	728	8506	-78	1282
309	16126	16980	1805	21522	8870	3102	17373	221	2291

Shear (kN)	Mean Whittemore Strain ($\mu\epsilon$)								
	10	11	12	13	14	15	16	17	18
0	0	0	0	0	0	0	0	0	0
45	75	102	78	101	23	23	44	-10	-47
74	87	123	46	195	102	79	133	68	-2
104	103	117	78	116	62	22	106	65	41
127	68	11	48	92	65	95	122	110	119
150	41	85	44	26	-1	44	126	80	265
172	176	180	98	190	138	112	207	144	1034
198	234	138	65	149	103	121	204	110	1550
220	856	106	96	175	39	273	187	234	2132
242	1346	-47	-102	175	-112	294	81	10	2338
265	3654	22	279	3077	-32	1002	1275	332	3032
287	6562	28	1822	5053	-81	3444	2907	2499	5471
309	14607	19	5004	13155	2	8847	9904	5253	9634

Table 6.94 Diagonal Whittemore Strain Data for Specimen 9-NWLD

Shear (kN)	Mean Whittemore Strain ($\mu\epsilon$)								
	1	2	3	4	5	6	7	8	9
0	0	0	0	0	0	0	0	0	0
44	76	75	41	8	11	37	50	40	24
74	432	387	295	151	92	61	104	31	-9
104	755	574	489	134	80	12	111	52	25
127	866	586	441	55	122	-1	86	43	2
150	790	612	473	-111	-40	-5	128	33	-5
172	1554	572	447	-163	-27	-21	391	73	31
197	2616	542	385	-232	-68	-10	826	55	-6
220	3535	592	457	-344	-189	-32	1094	157	66
242	4828	568	416	-431	-149	-153	1362	215	63
265	10029	4514	3953	-514	436	-264	5530	3956	47
286	13513	7251	6420	-84	1163	-266	9531	8087	282
309	20323	12062	10760	613	3107	-322	16830	15070	1496

Shear (kN)	Mean Whittemore Strain ($\mu\epsilon$)								
	10	11	12	13	14	15	16	17	18
0	0	0	0	0	0	0	0	0	0
44	20	-5	24	83	61	41	1	19	32
74	-31	1	29	77	56	55	-14	-7	26
104	-45	37	73	131	93	86	-1	66	56
127	-49	-10	24	138	73	28	-69	-11	44
150	-109	-27	-5	270	73	49	-91	5	43
172	-132	-105	-55	507	78	93	-102	-40	-1
197	-86	-135	-91	888	34	97	-207	-128	3
220	129	-118	-81	1400	89	147	13	-97	-8
242	474	-126	-111	2076	49	164	416	-131	-19
265	1447	-173	-128	4945	9	329	1811	-201	-137
286	2375	-243	-285	8736	-175	581	3124	-331	-289
309	5040	-389	-464	16163	-295	985	6636	-429	108

Continued

Table 6.94 Diagonal Whittemore Strain Data for Specimen 9-NWLD (Concluded)

Shear (kN)	Mean Whittemore Strain ($\mu\epsilon$)								
	19	20	21	22	23	24	25	26	27
0	0	0	0	0	0	0	0	0	0
44	66	41	28	-9	34	43	-5	40	27
74	60	50	25	-21	-15	-5	-7	38	28
104	69	51	23	-23	-14	35	11	40	37
127	51	38	30	-21	-43	-27	-2	40	42
150	68	46	61	-73	-57	-52	3	40	103
172	101	59	59	-81	-82	-63	26	33	302
197	173	43	72	-108	-62	-59	49	20	524
220	787	75	230	-211	-97	-41	40	54	900
242	1453	43	398	-380	-161	-156	151	14	1038
265	3925	19	803	-270	-302	-212	1398	32	1597
286	7007	24	2300	-84	-410	-418	2746	-421	4088
309	13245	83	5432	1278	-575	-555	5934	-716	7253

Shear (kN)	Mean Whittemore Strain ($\mu\epsilon$)								
	28	29	30	31	32	33	34	35	36
0	0	0	0	0	0	0	0	0	0
44	-5	3	-13	16	43	46	6	-22	50
74	-1	-28	-1	19	61	81	-49	-20	-23
104	-35	-38	-27	29	94	172	-9	8	60
127	-39	-7	43	27	90	158	-42	-11	59
150	-59	-76	-51	-19	41	443	-82	-118	-78
172	-77	-95	-70	62	78	1324	-82	-126	-121
197	-134	-150	-72	39	86	1910	-102	-185	-183
220	-131	-149	-97	120	146	2570	-133	-198	-167
242	-194	-261	-141	278	71	3009	-252	-283	-254
265	894	-355	-63	2349	196	3725	275	-443	-175
286	2304	-473	386	6118	1950	6026	1811	-591	-286
309	7100	-655	1873	12880	3576	9245	8360	-333	-238

Table 6.95 Horizontal Whittemore Strain Data for Specimen 10-NWHD

Shear (kN)	Mean Whittemore Strain ($\mu\epsilon$)									
	1	2	3	4	5	6	7	8	9	10
0	0	0	0	0	0	0	0	0	0	0
45	101	86	39	21	-14	110	61	85	-1	-60
89	65	-3	-25	-55	-105	116	60	56	-43	-52
119	626	416	-40	-54	-108	103	-6	64	-30	-6
149	1225	996	-119	-81	-83	54	-3	27	-68	-19
179	1878	1625	-117	-108	-103	17	-67	-8	-108	-27
209	2919	2469	-173	-162	-121	-65	-125	-49	-86	-17
238	3417	2851	-165	-130	-106	-48	-90	29	-54	32
268	4233	3674	-264	-267	-222	-20	-220	-52	-102	-10
298	5050	4499	-215	-257	-141	83	-215	-104	-134	-45
326	6029	5198	-263	-325	-206	21	-171	-117	-224	-108

Shear (kN)	Mean Whittemore Strain ($\mu\epsilon$)									
	11	12	13	14	15	16	17	18	19	20
0	0	0	0	0	0	0	0	0	0	0
45	44	-7	-20	39	25	28	6	40	79	82
89	33	-14	-43	2	36	6	-5	-17	2	11
119	78	27	-25	8	86	24	17	25	24	24
149	48	-29	-60	0	78	2	-16	-22	24	65
179	-6	-44	-90	-33	16	-13	-3	-32	11	22
209	-40	-79	-87	-40	24	-65	-91	-111	-35	-3
238	-40	-81	-78	14	59	-48	-49	-24	-17	33
268	-71	-185	-179	-94	-20	-174	-155	-136	-75	-99
298	13	-193	-182	-104	-2	-187	-228	-183	-204	93
326	40	-203	-232	-155	-21	-243	-259	-229	-186	489

Continued

Table 6.95 Horizontal Whittemore Strain Data for Specimen 10-NWHD (*Concluded*)

Shear (kN)	Mean Whittemore Strain ($\mu\epsilon$)									
	21	22	23	24	25	26	27	28	29	30
0	0	0	0	0	0	0	0	0	0	0
45	-21	26	100	95	120	56	50	34	36	118
89	-70	-27	67	33	105	-67	-6	44	46	129
119	-68	-48	25	21	119	-60	-11	29	48	167
149	-81	-38	41	49	135	-73	-13	16	63	279
179	-48	-43	13	-43	409	-59	-73	623	824	603
209	-82	-98	-70	-132	755	-95	-130	936	1220	648
238	-44	-81	-32	-79	1227	-79	-78	1299	1703	737
268	-170	-191	-136	-276	1802	-117	4	1663	2245	722
298	-182	-190	-147	957	2412	-118	-162	2186	2059	718
326	-176	-214	-209	1844	3049	-222	-271	1922	2312	734

Table 6.96 Vertical Whittemore Strain Data for Specimen 10-NWHD

Shear (kN)	Mean Whittemore Strain ($\mu\epsilon$)								
	1	2	3	4	5	6	7	8	9
0	0	0	0	0	0	0	0	0	0
45	-13	30	41	32	16	-16	32	75	-14
89	-20	-6	-2	-44	-29	-9	21	-1	-85
119	230	-10	66	52	36	63	67	-6	12
149	835	-52	14	52	21	22	29	-3	-44
179	1956	-105	16	54	24	22	84	-48	-70
209	3828	-204	2	-128	-82	-42	-61	-63	-82
237	4865	-172	35	-108	-41	17	-73	-29	-46
268	7499	-188	42	142	-74	29	-77	-131	-67
298	10415	-180	51	499	-48	30	-49	-67	-25
328	13818	-285	28	439	-118	6	-117	-157	115

Shear (kN)	Mean Whittemore Strain ($\mu\epsilon$)								
	10	11	12	13	14	15	16	17	18
0	0	0	0	0	0	0	0	0	0
45	6	3	-22	87	-2	40	-16	37	10
89	-15	-18	-61	29	-10	58	-66	-71	-64
119	36	72	20	66	10	61	-58	-15	25
149	-25	-2	-21	-13	-38	21	-57	-5	32
179	5	70	-3	-3	51	41	-125	-146	842
209	-37	-17	-4	12	-107	-55	-169	-104	1361
237	-8	-29	-19	51	-35	-100	-160	-133	1952
268	-2	-37	-105	2	-96	6	-72	104	2881
298	-27	-117	141	43	-73	1343	-402	2214	5251
328	-102	-261	1061	-29	-102	2969	-345	3519	7673

Table 6.97 Diagonal Whittemore Strain Data for Specimen 10-NWHD

Shear (kN)	Mean Whittemore Strain ($\mu\epsilon$)								
	1	2	3	4	5	6	7	8	9
0	0	0	0	0	0	0	0	0	0
45	68	61	65	10	7	-17	89	66	51
89	187	68	61	13	2	-27	149	105	89
119	633	454	41	-23	-8	-48	163	76	73
149	1267	1061	2	-128	-80	-68	106	47	45
179	2207	1946	16	-217	-125	-107	76	39	32
209	3643	3310	14	-276	-148	-128	49	51	60
238	4369	3971	-18	-326	-203	-156	36	26	47
268	6291	5758	3	-287	-200	-157	320	19	64
298	8251	7596	-15	-328	-264	-193	509	16	56
326	10477	9672	9	-292	-289	-211	463	-2	40

Shear (kN)	Mean Whittemore Strain ($\mu\epsilon$)								
	10	11	12	13	14	15	16	17	18
0	0	0	0	0	0	0	0	0	0
45	-6	0	-9	26	36	35	-19	19	-17
89	26	14	-7	76	73	79	-28	-21	-14
119	-10	-7	-28	58	57	45	-56	-18	-33
149	-37	-36	-28	80	72	65	-52	-41	-34
179	-93	-79	-58	57	45	64	-74	-55	-37
209	-178	-109	-60	15	41	52	-100	-63	-38
238	-256	-157	-99	-14	11	7	-139	-122	-83
268	-341	-177	-116	-24	-22	-6	-232	-146	-132
298	-391	-187	-129	56	-28	-19	-320	-189	-135
326	-425	-184	-157	85	-9	15	-354	-229	-217

Continued

Table 6.97 Diagonal Whittemore Strain Data for Specimen 10-NWHD (*Concluded*)

Shear (kN)	Mean Whittemore Strain ($\mu\epsilon$)								
	19	20	21	22	23	24	25	26	27
0	0	0	0	0	0	0	0	0	0
45	27	57	48	-1	13	-11	49	56	41
89	70	96	71	-14	-13	-35	64	76	51
119	69	100	73	-32	-18	-25	61	78	59
149	86	102	75	-40	-36	-53	52	69	63
179	59	90	68	-42	-32	-55	9	13	381
209	23	55	48	-42	-35	-61	19	-15	814
238	-7	18	-11	-88	-90	-91	28	-24	1321
268	-81	-28	-63	-163	-135	-157	-20	49	2163
298	-93	-15	135	-204	-208	-230	-48	1634	3593
326	-62	-11	778	-273	-227	-370	-46	3018	5512

Shear (kN)	Mean Whittemore Strain ($\mu\epsilon$)								
	28	29	30	31	32	33	34	35	36
0	0	0	0	0	0	0	0	0	0
45	-27	-15	-1	25	52	58	-16	3	-9
89	-59	-21	-3	34	82	79	-48	-35	-13
119	-79	-38	-25	3	65	61	-73	-24	-26
149	-84	-69	-42	1	70	92	-70	-35	-37
179	-92	-109	-66	720	873	940	-96	-101	-195
209	-88	-112	-98	1163	1340	1425	-108	-119	-286
238	-112	-137	-148	1591	1803	1931	-118	-129	-310
268	-164	-223	-216	2233	2519	2710	-146	-122	-401
298	-181	-194	-305	3166	4181	4329	-156	294	-326
326	-216	-220	-303	3330	5981	6229	-169	760	-77

Table 6.98 Whittemore Strain Data for Specimen 11-LWHD

Shear (kN)	Mean Whittemore Strain ($\mu\epsilon$)									
	1	2	3	4	5	6	7	8	9	10
0	0	0	0	0	0	0	0	0	0	0
45	32	52	2	-37	-2	42	-7	-27	13	33
60	32	62	12	-47	17	42	2	-47	23	43
74	22	82	12	-97	7	62	12	-37	23	63
89	42	82	-7	-67	27	72	12	-47	43	63
104	7	107	7	-82	2	87	37	-72	18	68
119	22	152	-17	-117	17	102	22	-77	23	73
133	12	292	-47	-117	7	82	-27	-117	3	83
148	37	727	-72	-122	42	97	-2	-102	18	98
164	127	1017	-92	-162	122	57	-52	-112	28	98
178	217	1177	-122	-222	152	37	-52	-142	28	98
192	627	1496	-132	-272	352	7	-82	-172	18	78
207	892	1781	-177	-297	557	12	-107	-217	43	53
223	1102	2061	-197	-327	697	42	-137	-227	43	-18
238	1417	2446	-222	-352	922	37	-152	-262	38	-3
252	1322	2681	-237	-407	1047	2	-207	-317	13	-48
267	1282	2940	-267	-407	1127	52	-207	-317	3	-28
282	1362	3270	-307	-457	1337	2	-237	-357	-18	-58
297	1537	3625	-332	-492	1502	57	-252	-382	-23	-43
311	1687	3945	-392	-512	1512	17	-312	-412	128	-63
341	2172	4649	-447	-567	1877	2	-357	-417	493	-8
374	5490	-	-607	812	5847	3992	832	1242	5095	3533

Continued

Table 6.98 Whittemore Strain Data for Specimen 11-LWHD (*Concluded*)

Shear (kN)	Mean Whittemore Strain ($\mu\epsilon$)									
	11	12	13	14	15	16	17	18	19	20
0	0	0	0	0	0	0	0	0	0	0
45	13	-32	13	58	-2	-28	12	37	7	-12
60	-8	-52	3	78	-22	-38	12	47	-22	-32
74	13	-62	23	88	-2	-38	12	77	-12	-42
89	13	-62	13	88	-32	-58	12	87	-2	-52
104	-3	-87	18	103	-17	-73	27	82	-7	-67
119	-28	-82	13	88	-32	-78	2	77	-22	-92
133	-28	-102	23	108	-72	-88	22	57	-12	-102
148	-23	-107	28	133	-67	-83	17	52	-27	-87
164	-33	-127	28	153	-87	-103	47	52	-27	-107
178	-53	-157	38	123	-87	-133	7	42	-77	-147
192	-63	-147	38	113	-97	-133	37	32	-97	-167
207	-128	-172	83	78	-162	-178	422	247	-92	-212
223	-168	-222	613	98	-252	-218	1172	1146	-192	-312
238	-183	-217	698	424	-237	-213	1317	1320	-197	-317
252	-228	-262	723	620	-282	-278	1452	1415	-242	-372
267	-198	-262	823	901	-312	-268	1662	1585	-242	-382
282	-258	-342	1003	1322	-342	-328	2032	1974	-282	-432
297	-263	-327	1128	1598	-357	-343	2347	2259	-307	-427
311	-313	-477	2168	3013	-417	-403	3796	3486	-347	-457
341	-358	-642	3173	4463	-492	-468	5180	4200	-472	-582
374	863	877	-	9048	-642	-678	-	-	-532	-772

Table 6.99 Whittemore Strain Data for Specimen 12-NWHD

Shear (kN)	Mean Whittemore Strain ($\mu\epsilon$)									
	1	2	3	4	5	6	7	8	9	10
-1	0	0	0	0	0	0	0	0	0	0
44	12	27	7	-22	-17	2	-2	-2	13	2
58	7	12	22	-37	-2	17	-7	-17	8	17
74	2	17	37	-42	-27	22	7	-22	-8	2
88	-22	2	-17	-57	-22	27	-7	-37	-3	-2
103	-32	62	-27	-57	-29	27	-17	-37	-33	17
118	-2	232	-27	-67	-22	17	-7	-47	-13	37
133	7	382	-67	-77	-2	37	-27	-57	-3	-12
148	212	607	-82	-82	-27	22	-62	-62	-8	42
163	332	717	-112	-92	-7	22	-52	-72	-8	22
178	467	912	-97	-107	-2	37	-37	-77	-13	47
193	712	1117	-112	-142	-17	2	-82	-82	-8	12
208	1052	1426	-132	-152	2	2	-62	-72	3	12
222	1552	2036	-112	-172	132	22	-82	-102	33	-7
238	1786	2271	-147	-197	127	17	-117	-147	-3	-72
252	2046	2810	-147	-217	187	27	-127	-147	-3	-62
267	2331	3255	-162	-222	242	42	-132	-152	13	-87
282	-	3925	-182	-212	322	52	-152	-182	63	-77
297	-	4264	-212	-232	342	52	-192	-222	53	-97
312	-	4754	-202	-222	392	72	-162	-222	193	-77
326	-	5184	-232	-262	412	82	-202	-252	313	-47
341	-	5199	-	-227	626	147	-217	-277	688	237
356	-	-	-	-272	671	152	-232	-312	1093	372
371	-	-	-	-257	686	317	-267	-377	1898	1066

Continued

Table 6.99 Whittemore Strain Data for Specimen 12-NWHD (*Concluded*)

Shear (kN)	Mean Whittemore Strain ($\mu\epsilon$)									
	11	12	13	14	15	16	17	18	19	20
-1	0	0	0	0	0	0	0	0	0	0
44	-22	-17	-	17	12	-22	17	17	-2	-37
58	2	-22	-	12	-2	-27	-7	52	2	-42
74	-22	-27	-	7	-7	-22	-22	47	-22	-27
88	-27	-72	-	12	-2	-37	-27	12	2	-72
103	-7	-72	-	32	-2	-77	-27	22	-7	-72
118	-7	-72	-	52	7	-67	-27	62	-17	-62
133	-17	-72	-	32	-2	-67	-27	32	-17	-82
148	-42	-77	-	37	-27	-82	-2	7	-42	-107
163	-22	-87	-	77	-27	-82	-2	7	-42	-107
178	-37	-82	-	42	-22	-97	-27	12	-47	-102
193	-52	-107	-	67	-27	-102	-32	37	-52	-107
208	-82	-87	-	67	-87	-92	407	787	207	-147
222	-82	-97	-	87	-57	-82	537	907	177	-167
238	-137	-132	-	52	-102	-117	592	1032	162	-212
252	-137	-142	-	82	-122	-127	792	1282	132	-222
267	-122	-117	-	77	-107	-142	877	1396	97	-227
282	-132	-157	-	57	-107	-152	1027	1606	47	-227
297	-162	-167	-	47	-147	-192	1157	1786	27	-267
312	-162	-177	-	37	-137	-202	1447	2126	-92	-267
326	-202	-207	-	37	-187	-212	1697	2346	-232	-277
341	-207	-232	-	282	-182	-277	2301	2781	-367	-302
356	-252	-297	-	657	-227	-342	2586	3055	-512	-347
371	-267	-372	-	2331	-272	-217	4500	4979	212	117

Table 6.100 Deflection Data for Specimen PC6N

Shear (kN)	Δ_2 (mm)	Δ_3 (mm)	Δ_4 (mm)	Δ_5 (mm)
0	0.0	0.0	0.0	0.0
21	0.0	0.1	0.4	0.0
40	0.0	0.2	0.7	0.0
66	0.2	0.3	1.0	0.2
80	0.3	0.5	1.2	0.3
102	0.4	0.7	1.4	0.4
121	0.5	0.9	1.6	0.5
130	0.6	1.0	1.7	0.6
140	0.6	1.1	1.8	0.7
150	0.7	1.2	1.9	0.7
160	0.8	1.3	2.0	0.8
170	0.9	1.4	2.1	0.9
180	0.9	1.5	2.2	0.9
190	1.0	1.6	2.3	1.0
201	1.1	1.8	2.5	1.1
210	1.2	1.9	2.7	1.2
221	1.2	2.0	2.8	1.2
230	1.3	2.1	2.9	1.3
240	1.4	2.2	3.0	1.4
250	1.5	2.3	3.1	1.5
261	1.5	2.5	3.2	1.6
270	1.6	2.6	3.4	1.6
281	1.7	2.7	3.5	1.7
290	1.8	2.8	3.6	1.8
301	1.9	3.0	3.8	1.9
310	1.9	3.1	3.9	2.0
317	2.0	3.2	4.1	2.1
247	2.3	4.0	4.8	4.0
259	2.5	4.4	5.1	4.5
272	2.8	4.9	5.6	5.1
290	3.1	5.5	6.3	5.8
303	3.4	6.1	6.9	6.4
317	3.7	6.7	7.5	7.2
324	3.9	7.0	7.8	7.5
331	4.0	7.3	8.1	7.9
340	4.3	7.8	8.6	8.5
348	4.5	8.2	9.0	9.0
353	4.7	8.5	9.3	9.3

Table 6.101 Longitudinal Strain Data for Specimen PC6N

Shear (kN)	ϵ_{L1A} ($\times 10^{-6}$)	ϵ_{L1B} ($\times 10^{-6}$)	ϵ_{L2A} ($\times 10^{-6}$)	ϵ_{L2B} ($\times 10^{-6}$)	ϵ_{D1} ($\times 10^{-6}$)	ϵ_{D2} ($\times 10^{-6}$)
0	0	0	0	0	0	0
21	44	45	31	26	4	-14
40	86	86	65	53	-1	-28
66	145	144	113	98	-14	-50
80	167	166	133	115	-21	-57
102	211	209	172	152	-30	-71
121	254	252	214	189	-42	-84
130	270	268	231	205	-45	-89
140	289	286	249	221	-48	-96
150	311	308	271	242	-53	-103
160	341	336	296	265	-61	-112
170	359	355	317	282	-64	-118
180	379	374	336	302	-68	-124
190	402	398	358	322	-73	-131
201	426	421	383	343	-78	-139
210	461	453	412	369	-88	-150
221	482	475	433	389	-93	-156
230	512	504	458	415	-98	-164
240	533	524	479	432	-103	-171
250	558	549	502	454	-108	-178
261	586	577	529	477	-114	-186
270	615	606	556	502	-119	-194
281	647	640	585	527	-125	-202
290	710	734	616	549	-131	-210
301	794	833	653	576	-139	-219
310	850	897	686	602	-146	-227
317	908	954	716	626	-150	-233
247	604	621	505	453	8	-110
259	625	643	524	468	19	-106
272	667	689	554	497	57	-71
290	728	756	599	532	96	-30
303	785	818	634	561	187	42
317	834	869	667	589	254	91
324	856	894	684	604	278	119
331	877	916	701	620	300	150
340	908	948	729	644	332	193
348	949	988	759	670	352	232
353	998	1035	791	696	369	257

Table 6.102 Strand Strain Data for Specimen PC6N

Shear (kN)	ϵ_{S1} ($\times 10^{-6}$)	ϵ_{S2} ($\times 10^{-6}$)	ϵ_{S3} ($\times 10^{-6}$)	ϵ_{S4} ($\times 10^{-6}$)	ϵ_{S5} ($\times 10^{-6}$)	ϵ_{S6} ($\times 10^{-6}$)	ϵ_{S7} ($\times 10^{-6}$)	ϵ_{S8} ($\times 10^{-6}$)
0	0	0	0	0	0	0	0	0
21	51	55	45	25	28	20	42	26
40	95	106	85	52	55	39	77	48
66	150	165	136	83	98	70	126	86
80	176	197	159	85	108	78	146	103
102	218	228	198	112	143	104	182	136
121	262	287	237	126	165	123	217	166
130	278	297	251	136	178	135	232	179
140	297	316	271	150	195	147	247	194
150	319	346	293	163	212	161	267	210
160	348	363	315	165	213	166	291	232
170	367	396	334	176	228	180	306	246
180	385	408	353	189	245	193	324	262
190	408	427	374	204	263	206	343	280
201	434	467	398	217	279	220	364	297
210	462	490	424	214	266	221	390	321
221	485	513	445	227	283	236	408	338
230	510	549	469	232	283	242	432	356
240	531	571	489	245	299	255	449	373
250	556	585	511	260	318	269	472	391
261	584	620	540	276	336	285	497	413
270	614	644	567	291	352	297	522	433
281	654	680	598	308	368	313	551	456
290	822	784	655	327	381	322	640	477
301	980	868	722	354	399	334	762	505
310	1074	930	769	373	413	346	841	531
317	1154	977	817	393	426	357	912	555
247	673	629	538	235	242	227	567	402
259	701	661	559	253	264	243	589	416
272	761	695	593	276	293	265	632	439
290	861	777	649	307	328	290	703	470
303	951	829	697	332	358	309	768	498
317	1027	888	741	354	384	328	826	523
324	1061	920	761	365	396	338	852	536
331	1092	938	779	377	409	349	877	549
340	1133	963	807	392	428	364	915	573
348	1184	1001	845	410	449	382	961	599
353	1238	1047	896	434	470	397	1011	624

Table 6.103 Deflection Data for Specimen PC6S

Shear (kN)	Δ_2 (mm)	Δ_3 (mm)	Δ_4 (mm)	Δ_5 (mm)
0	0.0	0.0	0.0	0.0
22	0.2	0.3	0.1	0.2
46	0.4	0.5	0.2	0.4
61	0.5	0.7	0.4	0.5
80	0.6	0.9	0.6	0.6
100	0.8	1.1	0.8	0.7
120	0.9	1.3	1.0	0.9
140	1.0	1.5	1.2	1.0
161	1.2	1.7	1.4	1.2
181	1.3	1.9	1.6	1.3
200	1.4	2.1	1.8	1.4
220	1.5	2.3	2.0	1.5
242	1.7	2.5	2.3	1.7
261	1.8	2.8	2.5	1.8
281	2.0	3.0	2.7	2.0
293	2.1	3.1	2.9	2.1
282	2.2	3.4	3.2	2.5
290	2.3	3.6	3.3	2.6
300	2.5	3.9	3.6	2.9
317	2.6	4.1	3.9	3.1
300	2.5	4.1	3.9	3.1
310	2.6	4.3	4.1	3.2
321	2.7	4.4	4.2	3.3
343	2.9	5.0	4.8	3.7
330	3.7	5.4	5.2	3.9
350	4.0	5.8	5.6	4.2
369	4.4	6.5	6.2	4.7
380	4.7	6.9	6.7	5.1
401	5.4	8.1	-	6.0
420	6.3	9.4	-	6.9
441	7.1	10.8	-	7.9
460	8.0	12.2	-	8.9
480	9.1	13.8	-	10.2
502	10.9	16.2	-	11.9
511	11.5	17.0	-	12.6
518	12.1	17.8	-	13.2
514	12.2	18.0	-	13.8
520	12.6	18.6	-	14.4

Table 6.104 Longitudinal Steel Strain Data for Specimen PC6S

Shear (kN)	ϵ_{L1A} ($\times 10^{-6}$)	ϵ_{L2A} ($\times 10^{-6}$)	ϵ_{L2B} ($\times 10^{-6}$)	ϵ_{D1} ($\times 10^{-6}$)	ϵ_{D2} ($\times 10^{-6}$)
0	0	0	0	0	0
22	47	122	22	-2	-12
46	89	157	46	-12	-35
61	119	190	50	-18	-43
80	161	264	52	-26	-57
100	197	335	51	-36	-70
120	227	378	44	-49	-88
140	263	364	44	-63	-108
161	308	436	64	-72	-124
181	348	496	67	-84	-140
200	382	526	87	-96	-157
220	420	567	94	-108	-176
242	467	606	97	-124	-196
261	513	664	88	-138	-210
281	567	710	95	-151	-230
293	603	738	100	-158	-234
282	575	628	72	-173	-250
290	594	718	93	-184	-268
300	612	742	85	-195	-278
317	662	771	102	-206	-293
300	624	740	75	-210	-296
310	643	756	85	-215	-303
321	665	772	92	-223	-308
343	754	821	115	-242	-336
330	721	771	88	-239	-338
350	786	820	103	-253	-352
369	974	919	126	-273	-368
380	1116	1056	178	-284	-386
401	1412	1446	415	-293	-409
420	1568	1597	450	-298	-430
441	1752	1796	463	-295	-435
460	1927	1962	505	-293	-441
480	2102	2151	553	-261	-418
502	2279	2359	597	-236	-403
511	2359	2452	614	-231	-391
518	2427	2527	626	-223	-384
514	2388	2487	589	-210	-372
520	2431	2538	599	-205	-353

Table 6.105 Strand Strain Data for Specimen PC6S

Shear (kN)	ϵ_{S1} ($\times 10^{-6}$)	ϵ_{S2} ($\times 10^{-6}$)	ϵ_{S3} ($\times 10^{-6}$)	ϵ_{S4} ($\times 10^{-6}$)	ϵ_{S5} ($\times 10^{-6}$)	ϵ_{S6} ($\times 10^{-6}$)	ϵ_{S7} ($\times 10^{-6}$)	ϵ_{S8} ($\times 10^{-6}$)
0	0	0	0	0	0	0	0	0
22	120	46	49	29	28	23	37	17
46	166	85	78	59	62	55	64	42
61	182	117	106	83	85	77	90	51
80	293	160	133	122	120	117	106	60
100	255	202	163	158	153	148	130	69
120	301	242	196	190	182	180	155	74
140	351	272	219	211	214	203	177	75
161	353	318	249	255	257	254	200	89
181	353	362	287	283	293	291	228	98
200	386	391	312	314	324	320	248	112
220	325	432	345	348	362	357	268	118
242	392	480	371	376	399	378	288	125
261	-203	535	415	407	437	435	310	130
281	-130	610	444	438	479	475	332	140
293	-70	666	493	462	504	499	359	147
282	-102	625	460	433	472	466	337	124
290	-159	642	461	440	486	479	338	134
300	-135	670	479	454	500	495	353	137
317	-26	724	518	480	533	520	395	151
300	-113	683	477	455	503	497	355	131
310	-86	704	492	467	518	512	369	141
321	-47	731	519	487	536	527	388	149
343	94	822	575	520	579	554	467	166
330	26	777	528	493	551	529	410	144
350	120	844	577	530	585	557	465	161
369	326	1008	771	618	644	592	590	179
380	441	1089	802	750	750	646	645	200
401	471	1225	819	973	1039	1110	709	257
420	481	1301	832	1055	1129	1199	739	264
441	511	1427	900	1152	1226	1292	801	277
460	559	1537	828	1230	1306	1376	861	291
480	586	1651	749	1313	1385	1461	915	307
502	504	1729	744	1399	1443	1468	960	321
511	480	1779	756	1437	1461	1484	987	326
518	374	1819	755	1465	1471	1499	1001	328
514	294	1772	693	1428	1429	1453	952	307
520	267	1802	731	1457	1447	1481	977	327

Table 6.106 Stirrup Strain Data for Specimen PC6S

Shear (kN)	ϵ_{T1A} ($\times 10^{-6}$)	ϵ_{T1B} ($\times 10^{-6}$)	ϵ_{T2A} ($\times 10^{-6}$)	ϵ_{T2B} ($\times 10^{-6}$)	ϵ_{T3A} ($\times 10^{-6}$)	ϵ_{T3B} ($\times 10^{-6}$)	ϵ_{T4A} ($\times 10^{-6}$)	ϵ_{T4B} ($\times 10^{-6}$)	ϵ_{T5A} ($\times 10^{-6}$)	ϵ_{T5B} ($\times 10^{-6}$)
0	0	0	0	0	0	0	0	0	0	0
22	2	12	-5	10	-10	17	-8	10	-18	-14
46	-8	5	-11	8	-16	14	-16	7	-31	-16
61	-12	10	-12	11	-18	17	-19	10	-40	-23
80	-14	5	-12	13	-18	28	-22	10	-49	-28
100	-16	5	-12	16	-23	31	-26	10	-57	-41
120	-24	5	-16	16	-26	23	-31	11	-70	-55
140	-34	-5	-19	10	-31	17	-35	7	-80	-58
161	-35	-14	-16	12	-30	15	-35	5	-86	-62
181	-37	-9	-14	16	-31	15	-36	7	-94	-75
200	-41	-22	-16	12	-34	12	-40	2	-102	-81
220	-47	-26	-14	12	-35	12	-42	1	-111	-88
242	-51	-32	-13	12	-36	10	-45	3	-120	-96
261	-55	-24	-6	16	-34	19	-47	8	-129	-107
281	-58	-35	-5	14	-36	15	-47	8	-138	-114
293	-60	-30	-4	18	-36	17	-47	11	-143	-118
282	-58	-28	-1	18	-33	14	-48	11	-147	-119
290	-61	-38	-2	15	-36	11	-52	5	-154	-129
300	-62	-33	-2	19	-36	17	-54	10	-160	-134
317	-66	-45	-1	16	-39	12	-56	9	-167	-137
300	-64	-33	6	26	8	47	446	461	-83	-52
310	-66	-35	7	26	10	48	451	469	-82	-52
321	-68	-38	8	28	14	52	611	626	-79	-50
343	-72	-51	18	61	17	47	971	1012	-74	-47
330	47	71	2463	2406	1337	1435	1096	1138	-60	-33
350	47	68	2672	2606	1837	1512	1126	1174	-61	-36
369	46	77	2929	2838	727	745	1248	1260	-63	-45
380	45	68	3097	2970	583	656	1341	1333	-59	-44
401	53	85	3310	2920	588	592	1555	1538	-21	-18
420	69	96	932	2898	678	671	1616	1591	-15	-21
441	89	129	893	3021	629	708	1636	1634	-18	-29
460	118	157	901	1635	701	866	1643	1650	-29	-42
480	171	211	937	1206	1163	1137	1659	1665	-34	-44
502	212	254	904	1187	1028	1330	1707	1704	-38	-48
511	213	264	906	1167	1124	1444	1706	1709	-42	-55
518	215	264	909	1143	1224	1538	1707	1706	-45	-58
514	216	256	896	1131	1122	1454	1701	1693	-47	-59
520	215	264	907	1114	1208	1538	1708	1705	-48	-64

Continued

Table 6.106 Stirrup Strain Data for Specimen PC6S (*Concluded*)

Shear (kN)	ϵ_{T6A} ($\times 10^{-6}$)	ϵ_{T6B} ($\times 10^{-6}$)	ϵ_{T7A} ($\times 10^{-6}$)	ϵ_{T7B} ($\times 10^{-6}$)	ϵ_{T8A} ($\times 10^{-6}$)	ϵ_{T8B} ($\times 10^{-6}$)	ϵ_{T9A} ($\times 10^{-6}$)	ϵ_{T9B} ($\times 10^{-6}$)	ϵ_{T10A} ($\times 10^{-6}$)	ϵ_{T10B} ($\times 10^{-6}$)
0	0	0	0	0	0	0	0	0	0	0
22	-22	11	-3	5	16	5	3	7	-12	709
46	-37	5	-11	5	12	2	3	2	-22	732
61	-47	3	-12	5	9	5	3	8	-31	692
80	-58	-1	-16	8	17	3	1	4	-36	-23
100	-69	-7	-17	8	21	3	-2	5	-44	269
120	-83	-16	-22	5	16	2	-9	7	-57	203
140	-98	-26	-26	4	-5	-1	-14	4	-65	99
161	-105	-30	-36	8	15	2	-14	1	-65	181
181	-115	-36	-21	10	12	4	-18	9	-72	285
200	-125	-46	-37	8	11	-2	-26	0	-78	370
220	-135	-53	-36	10	12	-2	-30	-2	-83	490
242	-145	-60	-36	16	10	0	-36	-1	-89	555
261	-156	-67	-19	26	9	3	-42	6	-96	586
281	-165	-74	-31	57	12	2	-47	-1	-99	533
293	-171	-78	-16	72	10	5	-51	5	-104	527
282	-69	11	2224	2227	1299	1848	-35	88	-101	530
290	-71	5	2307	2313	1457	1988	-37	87	-103	727
300	-71	7	2649	2648	1731	2319	19	1147	-53	1556
317	-74	5	2811	2828	1796	2407	23	1289	-49	1668
300	-80	5	2674	2684	1765	2364	22	1301	-51	1553
310	-81	5	2740	2745	1786	2389	21	1312	-52	1569
321	-83	2	2832	2835	1818	2430	21	1349	-52	1604
343	-88	-5	3094	3183	1937	2567	16	1521	-55	1803
330	-92	-5	2956	3040	2542	2544	17	1517	-54	1721
350	-92	-8	3695	2954	2649	2611	16	1578	-57	1827
369	-94	-5	2148	1620	2697	2621	11	1643	-63	1962
380	-94	0	1783	1275	2718	2631	5	1673	-65	2055
401	-58	32	1358	440	2749	2645	-1	1735	-73	2063
420	-61	32	1162	474	2751	2682	-8	1783	-74	2128
441	-64	19	1125	375	2788	2722	-12	1860	-79	2220
460	-54	16	967	337	2841	2769	-18	1919	-79	2261
480	-48	16	960	310	2931	2849	-24	2014	-81	2329
502	-16	43	977	392	2997	2980	-31	2107	-86	2417
511	-10	48	1020	416	3049	3038	-36	2154	-92	2442
518	-4	52	1008	428	3091	3118	-38	2176	-93	2464
514	-2	52	966	386	3256	3207	-32	2075	-83	2387
520	4	59	1185	363	3289	3105	-35	2079	-88	2393

Table 6.107 Deflection Data for Specimen PC10N

Shear (kN)	Δ_2 (mm)	Δ_3 (mm)	Δ_4 (mm)	Δ_5 (mm)
0	0.0	0.0	0.0	0.0
20	0.1	0.2	0.1	0.1
41	0.2	0.4	0.2	0.2
60	0.3	0.5	0.4	0.3
80	0.4	0.7	0.6	0.4
100	0.5	0.8	0.7	0.5
121	0.6	1.0	0.9	0.6
141	0.7	1.1	1.1	0.8
161	0.8	1.3	1.2	0.9
180	1.0	1.5	1.4	1.0
200	1.1	1.6	1.6	1.1
220	1.2	1.8	1.7	1.2
241	1.3	2.0	1.9	1.3
261	1.4	2.2	2.1	1.4
280	1.5	2.3	2.3	1.5
300	1.6	2.5	2.4	1.6
320	1.7	2.7	2.6	1.7
340	1.9	2.9	2.8	1.8
328	1.8	2.8	2.7	1.8
340	1.9	2.9	2.8	1.9
360	2.0	3.1	3.0	2.0
380	2.1	3.3	3.2	2.1
400	2.3	3.5	3.5	2.3
420	2.5	3.9	3.9	2.5
431	2.7	4.2	4.2	2.6
440	2.8	4.5	4.4	2.8
421	2.9	4.7	4.6	2.9
440	3.4	5.2	5.1	3.2
445	3.5	5.3	5.2	3.2
375	6.3	6.1	6.0	3.5
391	6.7	6.4	6.3	3.7
412	7.4	7.2	7.1	4.1
420	7.8	7.5	7.4	4.3
431	8.4	8.1	8.0	4.6
444	9.5	8.9	8.8	5.0
452	10.1	9.5	9.4	5.3
461	10.8	10.1	10.0	5.6
466	11.3	10.4	10.4	5.8

Table 6.108 Longitudinal Steel Strain Data for Specimen PC10N

Shear (kN)	ϵ_{8-1} ($\times 10^{-6}$)	ϵ_{8-2} ($\times 10^{-6}$)	ϵ_{8-3} ($\times 10^{-6}$)	ϵ_{8-4} ($\times 10^{-6}$)	ϵ_{3-1} ($\times 10^{-6}$)	ϵ_{3-2} ($\times 10^{-6}$)	ϵ_{3-3} ($\times 10^{-6}$)	ϵ_{D1} ($\times 10^{-6}$)	ϵ_{D2} ($\times 10^{-6}$)
0	0	0	0	0	0	0	0	0	0
20	27	19	25	17	-5	-3	0	-18	-15
41	56	45	51	45	-6	-4	5	-35	-31
60	80	68	76	68	-9	-5	6	-50	-45
80	109	98	106	98	-12	-7	10	-67	-60
100	134	125	132	125	-16	-10	12	-84	-76
121	159	154	162	153	-19	-13	15	-102	-93
141	182	179	186	178	-22	-15	16	-116	-107
161	205	208	216	207	-26	-19	16	-137	-128
180	228	234	240	235	-30	-22	18	-151	-141
200	250	262	268	261	-33	-24	20	-167	-156
220	270	291	297	290	-36	-27	23	-186	-176
241	295	319	326	320	-40	-31	25	-203	-191
261	316	349	357	350	-45	-33	26	-222	-210
280	337	378	385	378	-47	-36	28	-238	-227
300	356	409	418	411	-53	-40	31	-260	-247
320	378	439	448	441	-57	-42	33	-277	-264
340	407	475	484	473	-60	-45	35	-297	-282
328	388	459	469	460	-59	-44	33	-290	-276
340	404	479	492	479	-64	-48	35	-303	-290
360	464	523	559	520	-67	-52	37	-323	-307
380	557	614	650	610	-68	-53	45	-346	-328
400	628	703	749	692	-68	-53	55	-368	-348
420	645	890	827	901	-57	-36	92	-402	-380
431	664	943	921	955	-45	-24	127	-426	-403
440	689	973	955	983	-24	2	181	-449	-426
421	532	816	830	814	74	90	243	-475	-452
440	613	882	886	887	129	143	309	-520	-498
445	630	902	903	908	138	151	320	-528	-506
375	267	525	586	519	455	422	672	-490	-448
391	362	564	624	558	472	437	676	-506	-459
412	444	651	699	644	522	485	697	-520	-473
420	475	687	731	681	544	511	708	-528	-478
431	514	734	773	730	580	552	730	-539	-479
444	560	789	822	786	667	640	790	-548	-481
452	590	828	857	825	701	677	818	-554	-484
461	629	868	899	867	743	731	857	-560	-490
466	650	893	924	893	771	761	878	-569	-495

Table 6.109 Deflection Data for Specimen PC10S

Shear (kN)	Δ_2 (mm)	Δ_3 (mm)	Δ_4 (mm)	Δ_5 (mm)
0	0.0	0.0	0.0	0.0
45	0.3	0.5	0.2	0.3
60	0.4	0.6	0.3	0.4
80	0.5	0.8	0.5	0.5
100	0.7	1.0	0.7	0.7
140	0.9	1.3	1.0	0.9
160	1.0	1.5	1.2	1.0
180	1.1	1.7	1.3	1.1
200	1.2	1.8	1.5	1.2
220	1.4	2.0	1.7	1.4
240	1.5	2.2	1.9	1.5
261	1.6	2.4	2.1	1.6
280	1.7	2.6	2.2	1.7
300	1.9	2.8	2.4	1.9
320	2.0	3.0	2.6	2.0
340	2.1	3.2	2.8	2.1
360	2.3	3.4	3.0	2.3
380	2.4	3.6	3.2	2.4
400	2.6	3.9	3.5	2.6
420	2.8	4.2	3.9	2.8
440	3.0	4.6	4.3	3.0
444	3.2	5.1	4.7	3.2
426	3.3	5.3	4.9	3.8
441	3.5	5.7	5.3	4.2
450	3.7	6.1	5.7	4.6
460	3.9	6.4	6.0	4.8
468	4.1	6.7	6.3	5.0
451	4.6	6.8	6.4	5.1
460	4.9	7.2	6.7	5.3
480	5.6	8.0	7.5	5.8
500	6.8	9.3	8.9	6.7
511	7.4	10.1	9.7	7.4
502	7.9	10.3	9.8	7.4
517	8.6	11.1	10.6	8.0
494	8.6	11.3	10.8	9.3
520	9.7	13.1	12.6	10.8
530	10.7	14.4	14.0	12.2
534	11.1	15.0	14.5	12.7

Table 6.110 Longitudinal Steel Strain Data for Specimen PC10S

Shear (kN)	ϵ_{8-1} ($\times 10^{-6}$)	ϵ_{8-2} ($\times 10^{-6}$)	ϵ_{8-3} ($\times 10^{-6}$)	ϵ_{8-4} ($\times 10^{-6}$)	ϵ_{3-1} ($\times 10^{-6}$)	ϵ_{3-2} ($\times 10^{-6}$)	ϵ_{3-3} ($\times 10^{-6}$)	ϵ_{3-4} ($\times 10^{-6}$)	ϵ_{D1} ($\times 10^{-6}$)	ϵ_{D2} ($\times 10^{-6}$)
0	0	0	0	0	0	0	0	0	0	0
45	72	47	70	46	-6	-10	32	19	-46	-43
60	91	65	90	65	-8	-12	41	32	-61	-58
80	122	92	118	95	-14	-17	55	40	-84	-83
100	149	116	146	120	-17	-23	67	53	-105	-105
140	207	167	206	175	-26	-32	93	83	-149	-153
160	237	195	236	202	-31	-39	108	96	-175	-178
180	265	222	265	231	-36	-44	120	109	-197	-202
200	292	247	291	258	-39	-49	132	119	-215	-223
220	321	276	323	287	-46	-55	147	135	-239	-248
240	351	304	353	318	-49	-60	160	147	-262	-272
261	385	335	386	350	-56	-67	174	164	-287	-299
280	415	363	418	380	-60	-73	190	177	-310	-325
300	448	393	449	411	-65	-79	203	188	-335	-351
320	483	426	484	445	-70	-87	219	204	-362	-380
340	519	462	521	488	-74	-91	234	219	-386	-405
360	579	529	583	559	-78	-99	252	235	-416	-436
380	659	629	705	660	-82	-103	280	262	-441	-463
400	793	775	843	822	-83	-106	349	343	-471	-495
420	991	879	996	914	-78	-102	506	608	-509	-535
440	1095	966	1088	1020	-67	-92	628	788	-549	-577
444	1114	960	1095	1009	-19	-40	614	680	-592	-620
426	988	852	972	891	33	17	559	588	-590	-620
441	1053	912	1035	957	57	42	589	637	-630	-660
450	1091	946	1072	993	112	80	598	659	-644	-670
460	1137	992	1119	1044	130	97	628	711	-667	-682
468	1078	934	1057	979	165	144	622	704	-687	-688
451	1073	931	1053	975	167	147	620	701	-689	-689
460	1125	973	1104	1023	176	156	647	739	-721	-725
480	1218	1060	1196	1118	207	198	710	825	-746	-747
500	1336	1184	1315	1245	242	239	833	988	-813	-777
511	1406	1255	1386	1320	247	240	902	1079	-814	-667
502	1357	1211	1338	1271	251	246	874	1042	-809	-654
517	1447	1293	1427	1359	263	261	947	1136	-836	-668
494	1304	1161	1285	1215	309	306	870	1008	-813	-622
520	1497	1321	1473	1386	261	276	994	1185	-882	-736
530	1566	1384	1544	1453	265	283	1067	1276	-896	-760
534	1593	1407	1570	1478	267	280	1099	1312	-900	-762

Table 6.111 Stirrup Strain Data for Specimen PC10S

Shear (kN)	ϵ_{T1A} ($\times 10^{-6}$)	ϵ_{T1B} ($\times 10^{-6}$)	ϵ_{T2A} ($\times 10^{-6}$)	ϵ_{T2B} ($\times 10^{-6}$)	ϵ_{T3A} ($\times 10^{-6}$)	ϵ_{T3B} ($\times 10^{-6}$)	ϵ_{T4A} ($\times 10^{-6}$)	ϵ_{T4B} ($\times 10^{-6}$)	ϵ_{T5A} ($\times 10^{-6}$)	ϵ_{T5B} ($\times 10^{-6}$)
0	0	0	0	0	0	0	0	0	0	0
45	5	-21	3	-10	33	1	29	-2	-30	-4
60	-4	-24	9	-11	33	3	36	0	-36	-7
80	-3	-30	4	-13	42	1	29	-3	-44	-15
100	-7	-36	4	-14	43	1	30	-3	-52	-21
140	-19	-45	8	-16	40	1	33	-2	-67	-33
160	-24	-49	8	-17	40	1	34	-2	-76	-40
180	-28	-54	8	-18	41	1	34	-3	-82	-47
200	-36	-59	6	-18	42	1	33	-3	-89	-53
220	-37	-62	7	-19	41	2	33	-2	-96	-59
240	-44	-67	7	-21	40	1	33	-2	-103	-67
261	-47	-72	6	-22	42	1	33	-1	-110	-73
280	-51	-75	7	-22	41	3	32	0	-116	-80
300	-51	-80	0	-22	41	3	27	-3	-122	-88
320	-53	-84	0	-23	44	5	27	-1	-129	-96
340	-58	-88	1	-22	46	10	28	0	-135	-101
360	-62	-92	1	-21	44	10	28	0	-142	-109
380	-72	-95	9	-22	43	15	32	1	-147	-115
400	-71	-99	22	-21	41	16	24	-5	-152	-124
420	-73	-103	26	-20	39	17	21	-7	-159	-129
440	-86	-108	35	-22	38	21	28	-2	-184	-152
444	-81	-109	30	-22	49	28	29	1	-37	316
426	-76	-104	32	-18	50	29	26	-4	-51	238
441	-76	-108	33	-19	47	30	23	-5	-48	252
450	-78	-109	34	-18	48	30	22	-6	-47	255
460	-89	-112	38	-18	47	32	28	-5	-44	269
468	-91	-114	39	-18	50	34	28	-7	-31	310
451	-78	-107	74	20	69	52	337	832	22	437
460	-87	-108	91	31	43	57	316	945	48	479
480	-79	-109	93	35	46	61	331	1002	123	592
500	-79	-108	102	44	54	77	-243	-588	166	644
511	-87	-109	109	47	54	80	-235	-539	192	690
502	20	-3	2284	2490	150	186	-257	-603	223	747
517	25	6	3645	3008	153	225	-153	-471	264	799
494	36	9	3466	2831	146	212	-245	-492	235	664
520	26	8	3765	3008	152	235	-112	-470	322	906
530	35	12	3374	3048	154	244	0	-445	393	1006
534	31	12	3380	3040	154	249	-160	-543	400	1010

Continued

Table 6.111 Stirrup Strain Data for Specimen PC10S (Concluded)

Shear (kN)	ϵ_{T6A} ($\times 10^{-6}$)	ϵ_{T6B} ($\times 10^{-6}$)	ϵ_{T7A} ($\times 10^{-6}$)	ϵ_{T7B} ($\times 10^{-6}$)	ϵ_{T8A} ($\times 10^{-6}$)	ϵ_{T8B} ($\times 10^{-6}$)	ϵ_{T9A} ($\times 10^{-6}$)	ϵ_{T9B} ($\times 10^{-6}$)	ϵ_{T10A} ($\times 10^{-6}$)	ϵ_{T10B} ($\times 10^{-6}$)
0	0	0	0	0	0	0	0	0	0	0
45	9	-22	5	-10	34	-9	1	-16	1	-9
60	7	-26	5	-6	31	-9	1	-10	-1	-11
80	4	-32	5	-11	39	-11	0	-19	-4	-16
100	0	-38	5	-12	40	-11	-2	-21	-6	-25
140	-8	-49	5	-8	37	-14	-3	-17	-13	-34
160	-12	-54	3	-8	37	-15	-4	-19	-16	-38
180	-16	-59	5	-8	37	-16	-5	-19	-18	-44
200	-23	-65	3	-8	36	-16	-5	-22	-22	-47
220	-27	-69	4	-7	37	-17	-6	-22	-24	-53
240	-33	-75	3	-8	34	-19	-7	-23	-29	-57
261	-37	-80	3	-6	36	-20	-8	-23	-32	-62
280	-43	-85	4	-5	35	-21	-8	-23	-34	-65
300	-50	-90	4	-13	37	-21	-9	-30	-36	-75
320	-55	-96	5	-12	38	-23	-10	-29	-41	-78
340	-59	-100	5	-11	39	-22	-10	-29	-42	-80
360	-70	-108	7	-10	40	-22	-10	-29	-45	-85
380	-77	-115	5	-6	39	-22	-9	-22	-48	-88
400	-86	-121	2	-15	43	-22	-9	-29	-51	-95
420	-98	-131	-1	-18	45	-22	-8	-29	-54	-98
440	-110	-147	1	-11	44	-21	-8	-22	-57	-101
444	-18	-147	11	-9	52	-19	-6	-27	-57	-105
426	59	-71	840	316	103	20	29	7	-54	-99
441	61	-63	1150	363	112	28	34	10	-54	-100
450	64	-56	2992	149	121	33	38	14	-53	-100
460	67	-56	2987	407	119	36	38	21	-53	-100
468	69	-56	2896	430	119	34	40	22	-52	-98
451	55	-58	2663	488	122	33	40	15	-52	-100
460	57	-59	2847	351	127	37	41	22	-53	-99
480	60	-57	2672	343	133	39	43	16	-53	-103
500	69	-57	2678	32	143	45	45	18	-54	-106
511	69	-59	526	-326	147	49	47	25	-53	-104
502	65	-59	464	-337	146	47	47	26	-53	-103
517	72	-57	1055	-576	159	54	48	25	-53	-104
494	90	-40	2258	-732	2821	2975	2715	2057	47	0
520	80	-55	6246	-680	3282	3112	2581	1214	45	9
530	100	5	7461	-690	3350	1036	2392	915	41	12
534	116	36	8889	-539	3269	407	2311	899	41	16

Table 6.112 Whittemore Strain Data for Specimen PC6N

Shear (kN)	Mean Whittemore Strain ($\mu\epsilon$)											
	1	2	3	4	5	6	7	8	9	10	11	12
0	0	0	0	0	0	0	0	0	0	0	0	0
67	75	65	18	-72	85	65	28	-58	38	68	22	-62
111	115	105	48	-92	125	125	58	-98	98	118	52	-82
156	125	145	48	-122	165	135	58	-128	138	148	52	-122
200	190	170	63	-157	230	220	83	-133	203	203	87	-147
222	210	210	73	-167	240	220	83	-163	213	223	87	-157

Table 6.113 Whittemore Strain Data for Specimen PC6S

Shear (kN)	Mean Whittemore Strain ($\mu\epsilon$)											
	1	2	3	4	5	6	7	8	9	10	11	12
0	0	0	0	0	0	0	0	0	0	0	0	0
67	40	50	5	0	40	35	15	0	45	55	20	-5
89	60	60	15	-20	30	25	55	-30	55	45	10	-25
111	65	55	50	-35	65	70	20	-15	70	70	35	-30
133	100	90	45	-30	100	95	45	-20	95	105	50	-25
156	105	105	50	-45	115	120	50	-35	110	120	55	-40
178	110	120	45	-60	120	125	45	-50	125	135	60	-55
200	155	155	70	-55	155	160	70	-35	160	170	75	-60
222	170	160	35	-70	160	155	55	-70	165	175	70	-85
245	195	185	70	-65	205	190	90	-75	200	220	95	-90
267	205	205	80	-105	215	210	80	-95	210	240	95	-100
282	2015	1755	-70	-235	2065	1720	-130	-315	1990	1650	735	420
289	3110	2640	-195	-210	3140	1665	-225	-310	2285	1785	620	795
302	3445	2895	-250	-265	3465	1750	-290	-385	2410	1880	625	790
325	4030	3430	-275	-300	4030	1925	-335	-407	2695	2085	710	875

Table 6.114 Whittemore Strain Data for Specimen PC10N

Shear (kN)	Mean Whittemore Strain ($\mu\epsilon$)									
	1	2	3	4	5	6	7	8	9	10
0	0	0	0	0	0	0	0	0	0	0
68	30	30	10	-35	30	10	15	-40	25	45
111	50	40	10	-65	30	50	25	-60	55	45
156	65	75	5	-80	65	45	20	-85	70	50
200	110	100	40	-95	90	110	35	-90	95	95
245	125	105	35	-110	125	115	50	-115	120	130
289	155	145	45	-140	145	125	40	-135	140	140
334	180	190	40	-165	180	170	45	-160	185	155
356	205	195	45	-160	215	175	70	-155	200	180
378	210	200	40	-155	190	180	65	-170	235	195
400	230	210	50	-175	200	220	75	-180	225	245
423	220	200	50	-205	220	210	65	-210	215	205

Shear (kN)	Mean Whittemore Strain ($\mu\epsilon$)									
	11	12	13	14	15	16	17	18	19	20
0	0	0	0	0	0	0	0	0	0	0
68	5	-30	45	10	5	-40	25	20	10	-35
111	-5	-50	55	30	25	-60	55	60	40	-45
156	-10	-75	90	45	20	-85	60	65	15	-70
200	35	-80	125	80	55	-90	115	100	50	-75
245	40	-105	140	115	50	-115	140	165	75	-110
289	20	-135	170	135	30	-145	150	135	45	-120
334	45	-150	195	140	45	-160	185	170	70	-145
356	60	-155	210	165	70	-165	180	175	55	-150
378	45	-160	245	200	85	-160	215	220	70	-145
400	65	-170	245	210	75	-170	235	220	100	-165
423	55	-190	215	180	75	-200	215	230	60	-195

Table 6.115 Whittemore Strain Data for Specimen PC10S

Shear (kN)	Mean Whittemore Strain ($\mu\epsilon$)									
	1	2	3	4	5	6	7	8	9	10
0	0	0	0	0	0	0	0	0	0	0
68	-10	25	-20	-25	20	30	-10	-15	20	20
112	40	85	30	-15	50	90	20	-15	60	70
156	35	60	-15	-60	45	85	-5	-60	55	75
202	70	85	10	-75	60	100	20	-75	90	100
245	90	115	-10	-95	60	110	10	-105	100	110
267	125	120	25	-100	125	145	25	-100	135	145
289	120	155	10	-105	140	160	30	-105	180	130
311	140	165	40	-125	130	160	20	-115	150	150
334	140	175	30	-135	140	170	10	-135	170	140
356	165	170	15	-140	155	175	25	-150	195	185
378	170	175	50	-145	150	190	20	-155	220	180
400	165	190	5	-170	175	195	45	-170	225	195
423	225	230	35	-170	185	245	55	-160	245	205
429	195	170	-65	-210	135	125	-95	-230	145	105
452	205	170	-65	-220	185	145	-105	-250	165	95
490	215	150	-125	-260	175	125	-165	-310	155	65

Shear (kN)	Mean Whittemore Strain ($\mu\epsilon$)									
	11	12	13	14	15	16	17	18	19	20
0	0	0	0	0	0	0	0	0	0	0
68	-10	-30	30	5	10	-20	50	50	-5	10
112	0	-30	90	65	40	-10	80	70	35	-10
156	-5	-65	65	60	15	-55	75	75	10	-45
202	30	-80	100	85	20	-70	120	100	25	-50
245	20	-110	110	85	30	-90	130	120	35	-80
267	25	-95	135	100	45	-85	155	175	30	-75
289	20	-120	150	135	60	-100	170	160	35	-80
311	40	-120	150	145	60	-110	190	180	35	-90
334	10	-150	170	145	40	-130	170	160	55	-100
356	45	-155	175	180	65	-135	195	185	50	-105
378	60	-150	230	185	60	-130	220	220	55	-120
400	45	-175	215	190	45	-155	225	225	50	-145
423	45	-175	255	220	95	-155	245	245	80	-135
429	-125	-285	3823	3019	-135	-335	3772	3013	637	2144
452	-165	-315	-	3748	-185	-395	-	4881	119	3163
490	-204	-365	-	4288	-255	-455	-	-	70	3573

Table 6.116 Comparison of Measured Shear Capacities and Code-Estimated Nominal Shear Capacities, Reinforced Concrete Specimens

Specimen	V_{Measured} kN	$V_{\text{AASHTO LRFD}}$ General Method kN	$V_{\text{ACI 318-95}}$ Simple Method kN	$\frac{V_{\text{Measured}}}{V_{\text{AASHTO LRFD}}}$	$\frac{V_{\text{Measured}}}{V_{\text{ACI 318-95}}}$
1-NWLA	436	332	321	1.31	1.36
2-NWLB	485	332	321	1.46	1.51
3-NWLC	421	332	322	1.27	1.31
4-NWLD	348	274	254	1.27	1.37
5-LWLA	328	318	300	1.03	1.09
6-LWLB	372	318	299	1.17	1.24
7-LWLC	357	319	302	1.12	1.18
8-LWLD	280	259	234	1.08	1.20
9-NWLD	310	268	246	1.16	1.26
10-NWHD	359	288	271	1.25	1.32
11-LWHD	396	281	262	1.41	1.51
12-NWHD	397	299	288	1.33	1.38

Table 6.117 Comparison of Measured Shear Capacities and Code-Estimated Nominal Shear Capacities, Prestressed Concrete Specimens

Specimen	V_{Measured} kN	$V_{\text{AASHTO LRFD}}$ General Method kN	$V_{\text{ACI 318-95}}$ kN	$\frac{V_{\text{Measured}}}{V_{\text{AASHTO LRFD}}}$	$\frac{V_{\text{Measured}}}{V_{\text{ACI 318-95}}}$
PC6N	356	301	316	1.18	1.13
PC6S	520	435	413	1.20	1.26
PC10N	465	322	353	1.44	1.32
PC10S	534	496	458	1.08	1.16

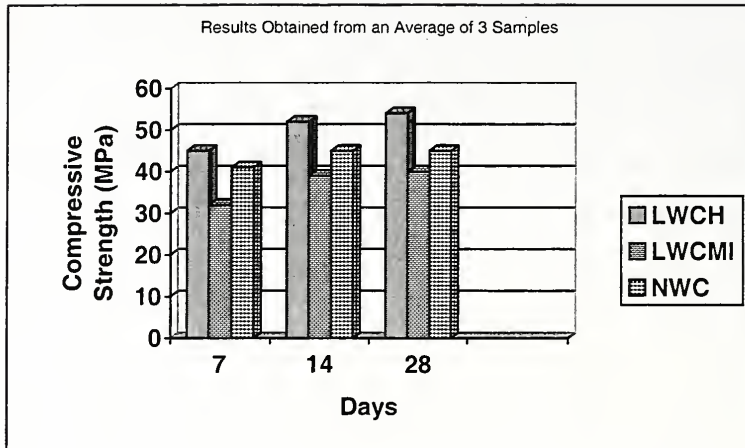


Figure 6.1 Compressive Strength of 42 MPa (6000 psi) Girder Mixes

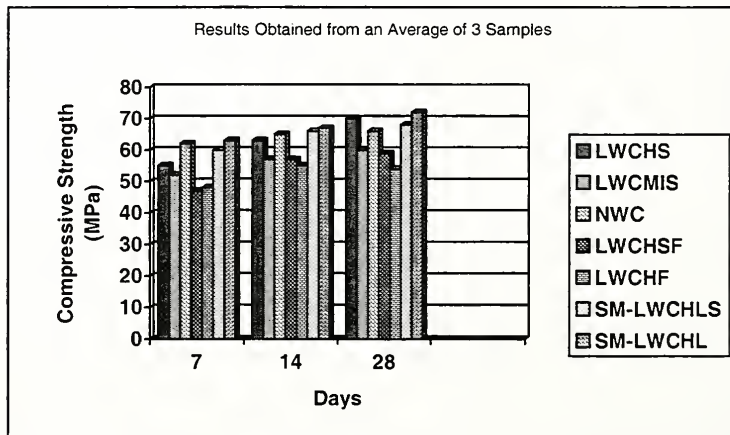


Figure 6.2 Compressive Strength of 69 MPa (10,000 psi) Girder Mixes

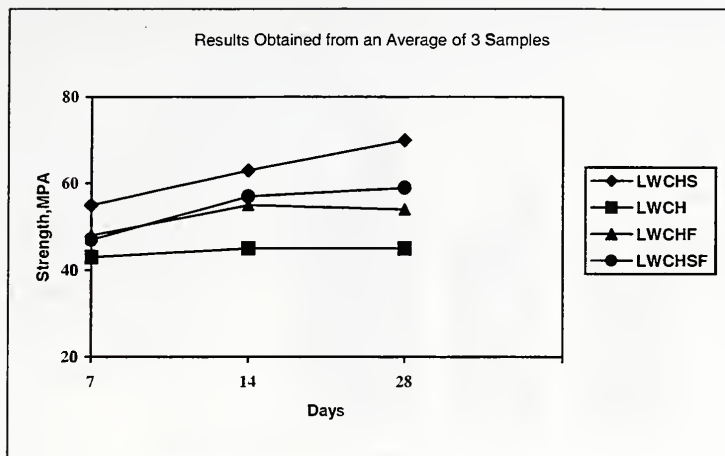


Figure 6.3 Effect of Mineral Admixtures on Compressive Strength of 69 MPa (10,000 psi) Girder Mixes

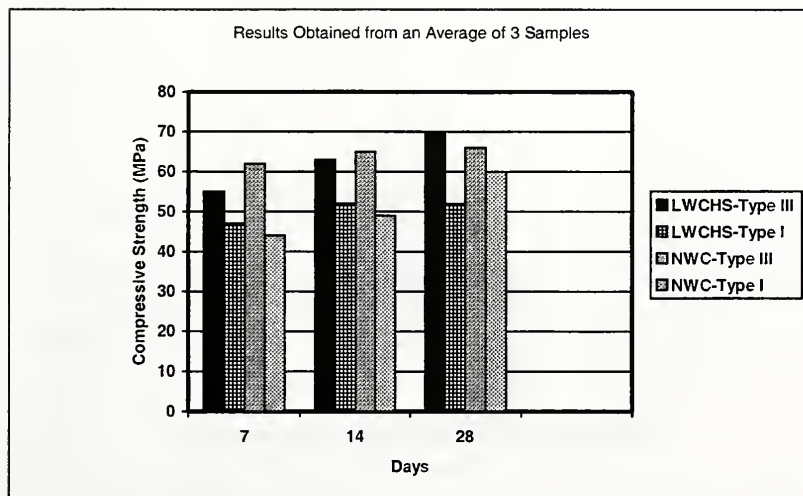


Figure 6.4 Comparison of Compressive Strength of Concrete Made with Type III And Type I Cements, 69 MPa (6000 psi) Girder Mixes

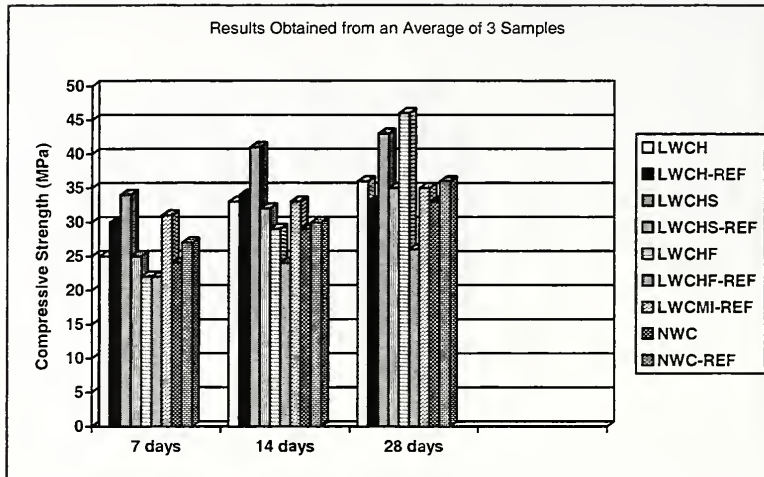


Figure 6.5 Compressive Strength Comparison for Newly Developed Mixes and Reference Mixes for Use in Bridge Decks

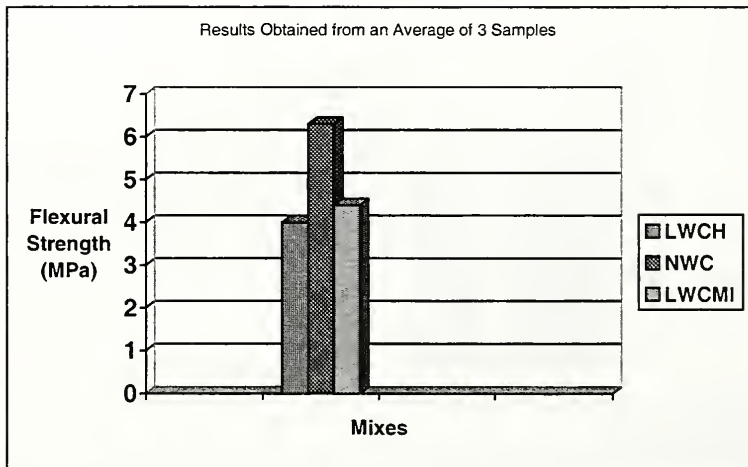


Figure 6.6 Flexural Strength of 42 MPa (6000 psi) Girder Mixes

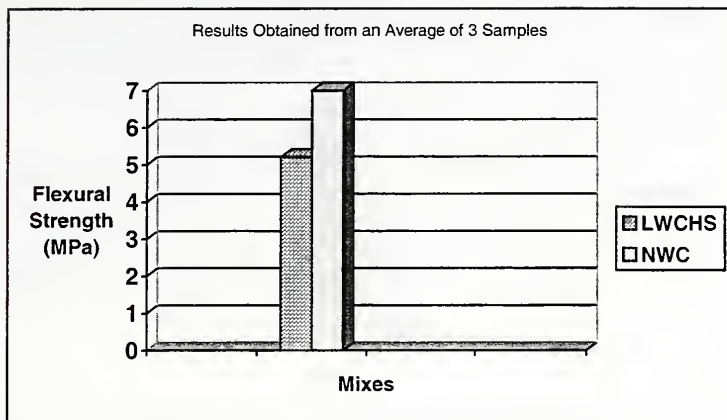


Figure 6.7 Flexural Strength of 69 MPa (10,000 psi) Girder Mixes

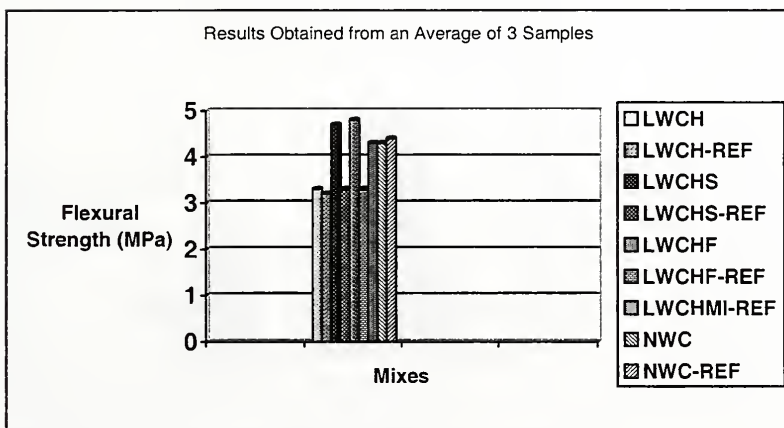


Figure 6.8 Flexural Strength for Deck Mixes

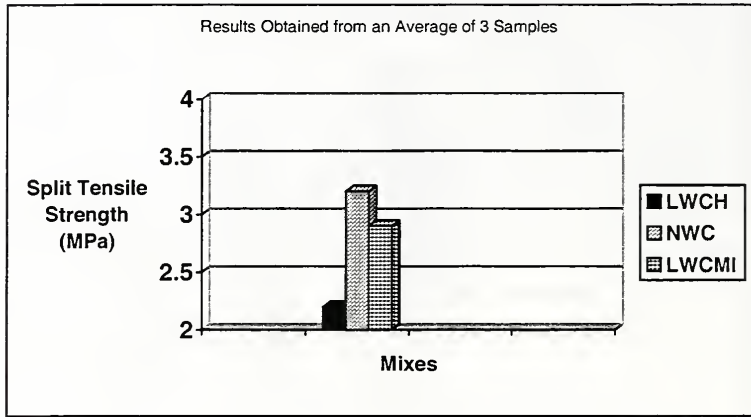


Figure 6.9 Split Tensile Strength of 42 MPa (6000 psi) Girder Mixes

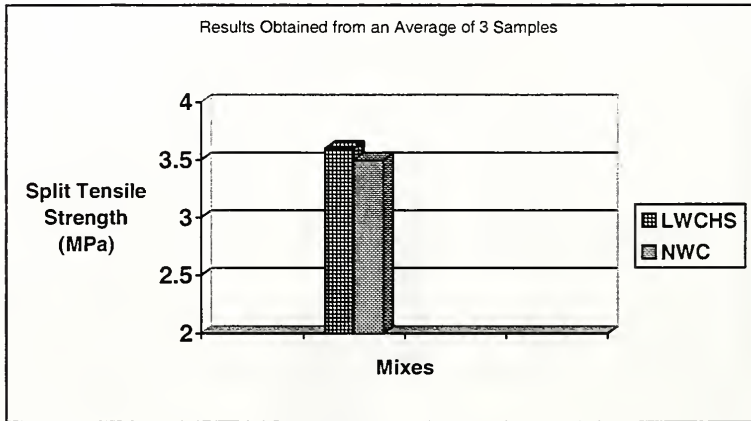


Figure 6.10 Split Tensile Strength of 69 MPa (10,000 psi) Girder Mixes

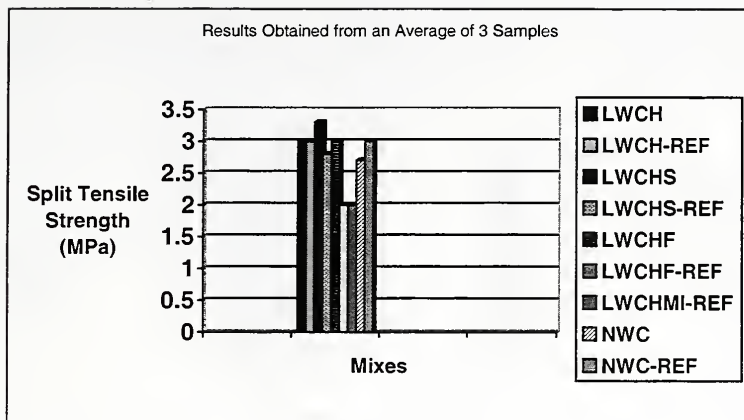


Figure 6.11 Split Tensile Strength for Deck Mixes

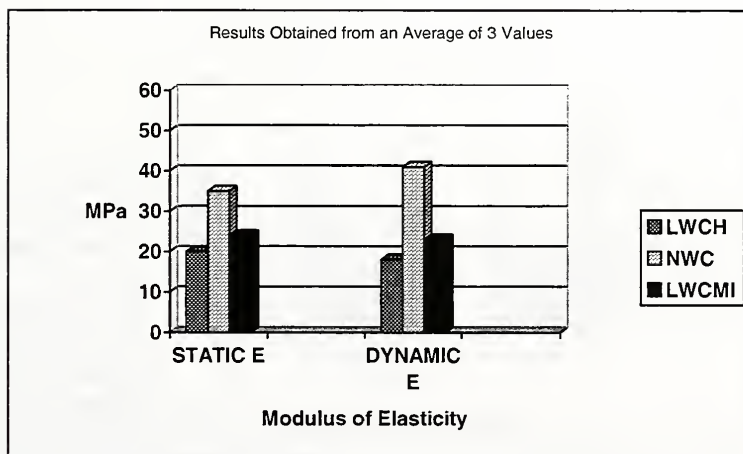


Figure 6.12 Static and Dynamic Moduli of Elasticity for 42 MPa (6000 psi) Girder Mixes

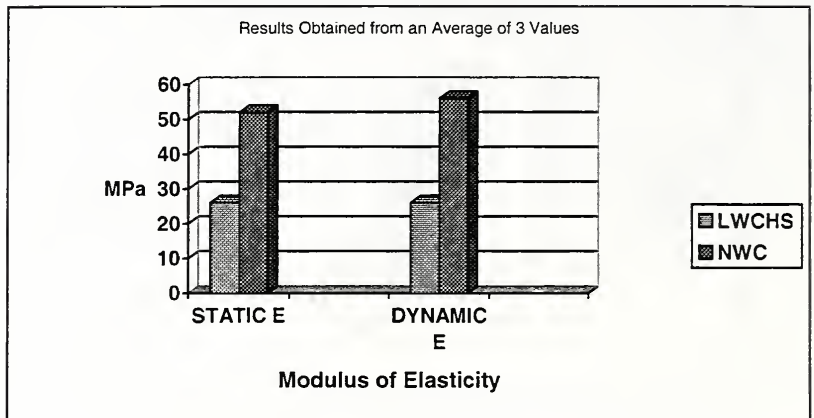


Figure 6.13 Static and Dynamic Moduli of Elasticity 69 MPa (10,000 psi) Girder Mixes

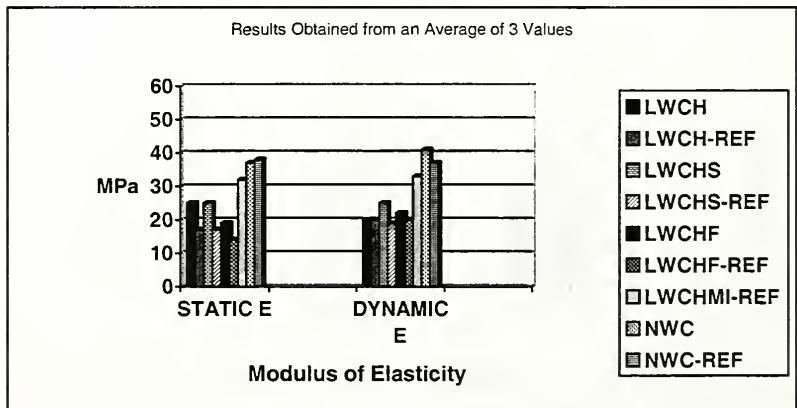


Figure 6.14 Comparison of Moduli of Elasticity for Deck Mixes

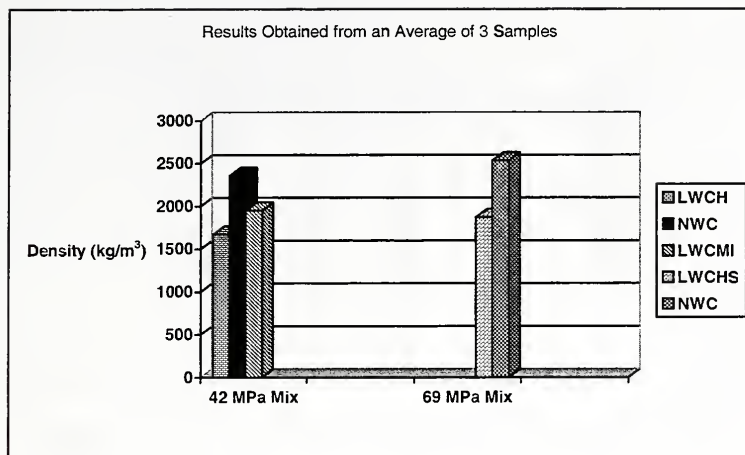


Figure 6.15 Density of Hardened Concrete, Girder Mixes

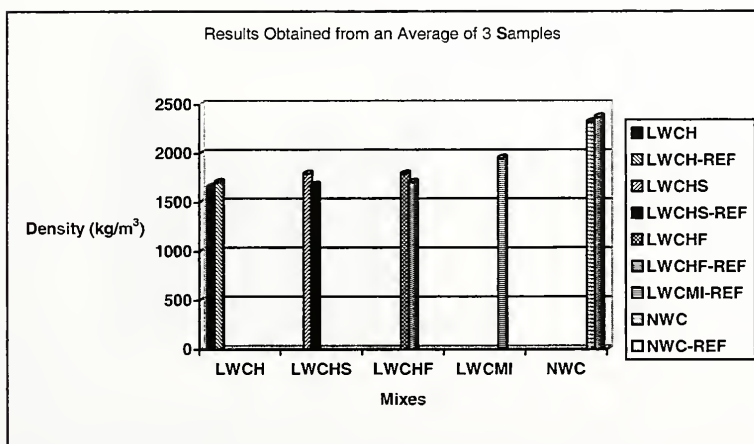


Figure 6.16 Density of Hardened Concrete, Deck Mixes

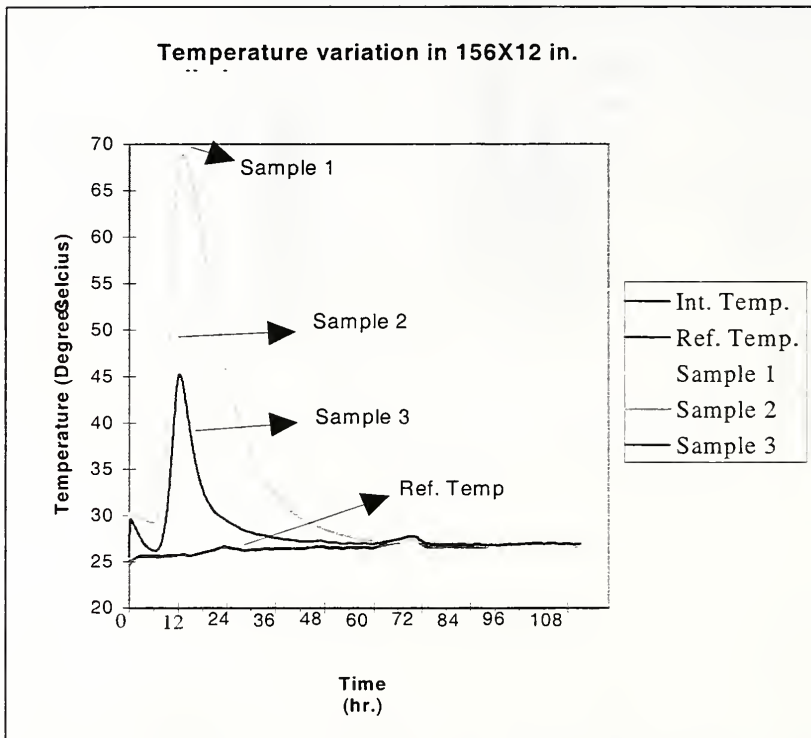


Figure 6.17 Temperature Variation in 69 MPa (10,000 psi) LWC Girder Mixes

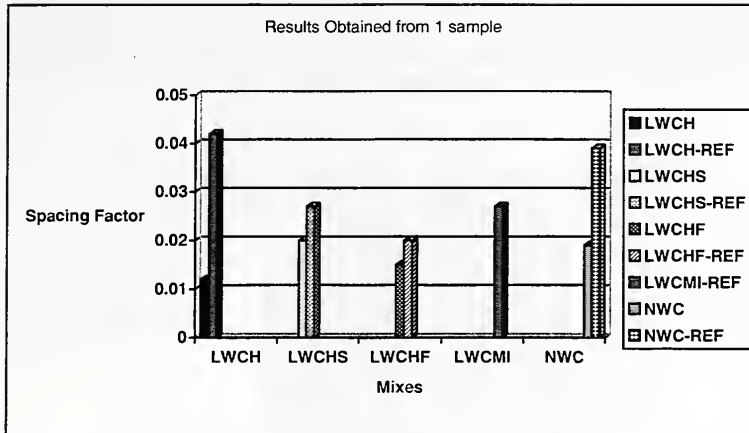


Figure 6.18 Comparison of Spacing Factors for Deck Concrete Mixes

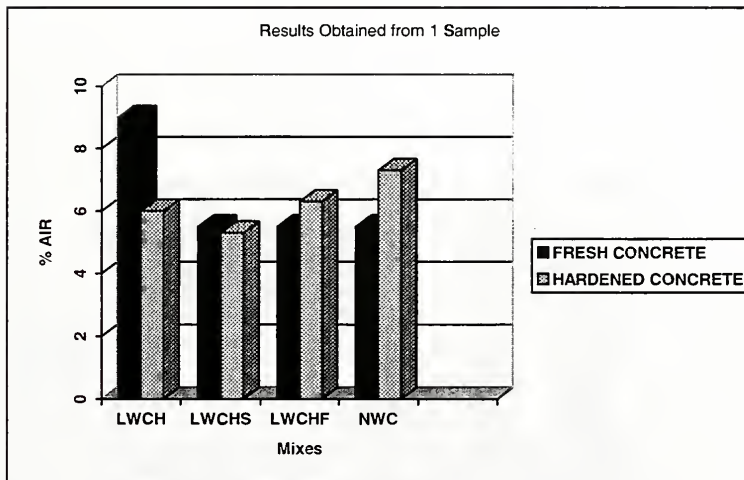


Figure 6.19 Comparison of Air Content for Hardened and Fresh Concrete, Newly Developed Deck Mixes

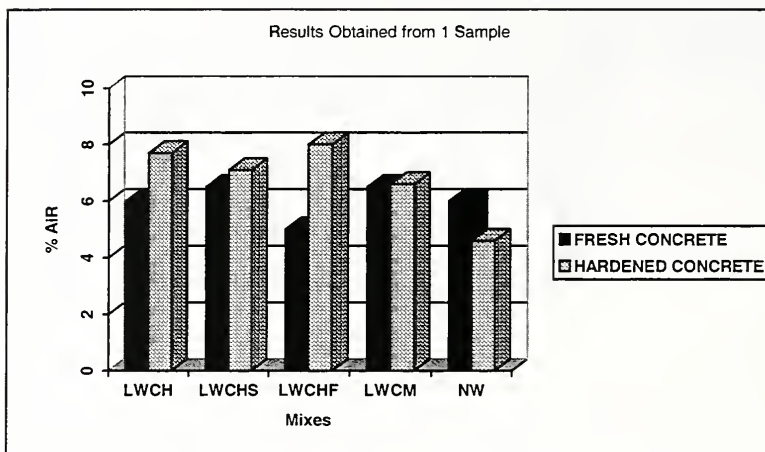


Figure 6.20 Comparison of Air Content for Hardened and Fresh Concrete, Reference Deck Mixes

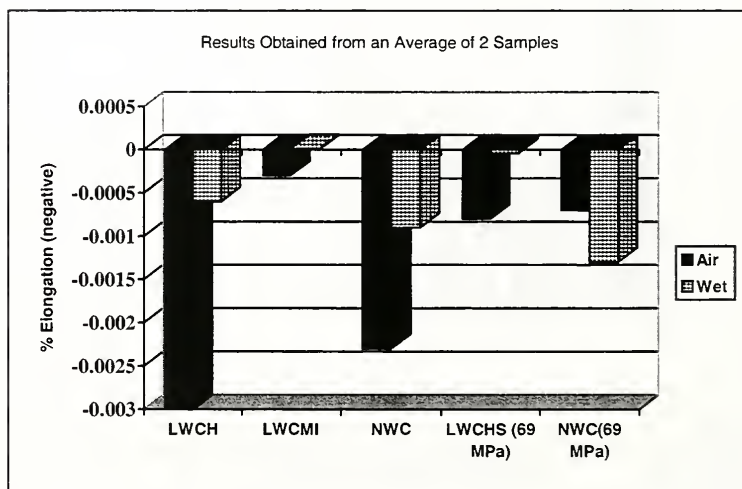


Figure 6.21 Drying Shrinkage for Bridge Girder Mixes

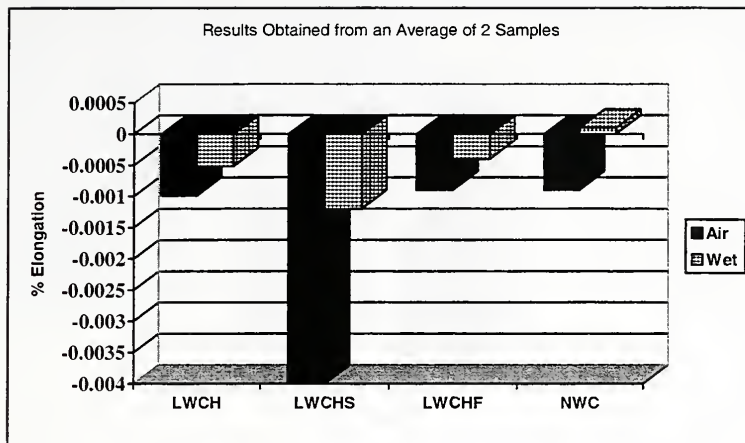


Figure 6.22 Drying Shrinkage for Newly Developed Bridge Deck Mixes

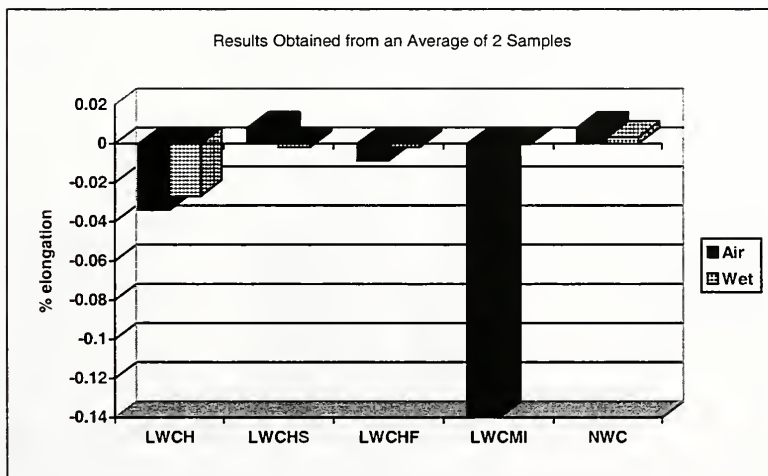


Figure 6.23 Drying Shrinkage for Reference Deck Mixes

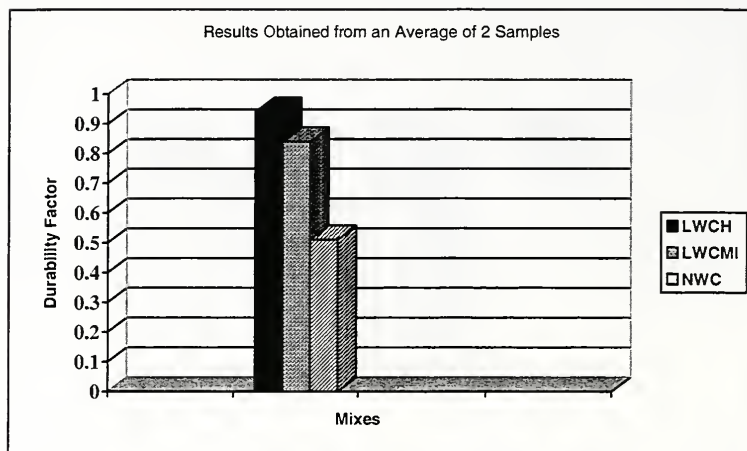


Figure 6.24 Comparison of Durability Factors for 42 MPa (6000 psi) Mixes

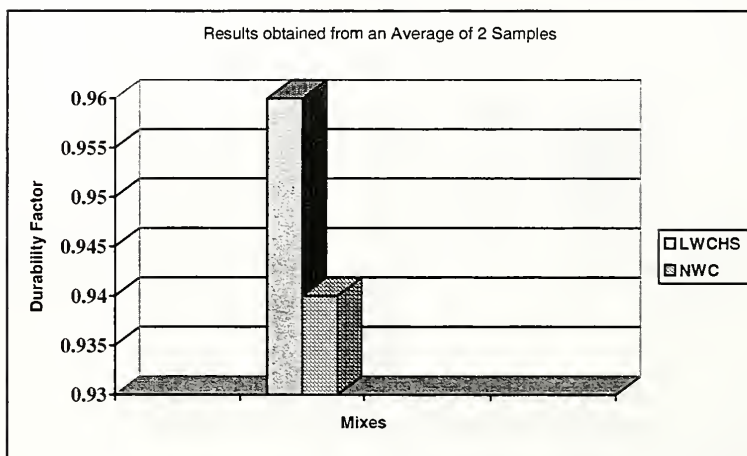


Figure 6.25 Comparison of Durability Factors for 69 MPa (10,000 psi) Mixes

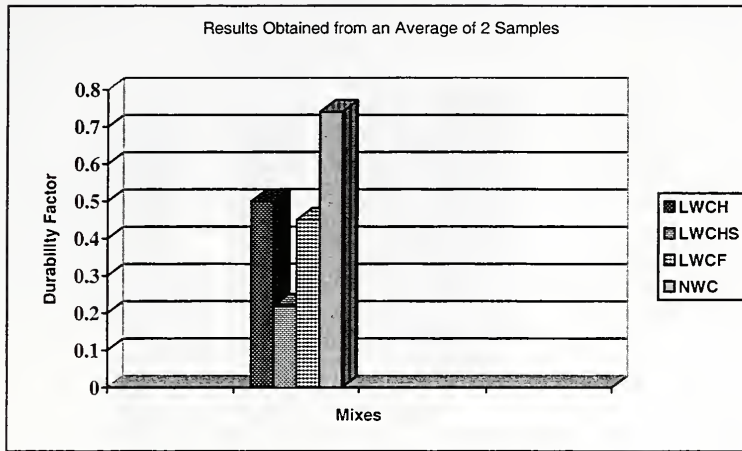


Figure 6.26 Comparison of Durability Factors for Newly Developed Bridge Deck Mixes with No Air Drying Prior to Testing

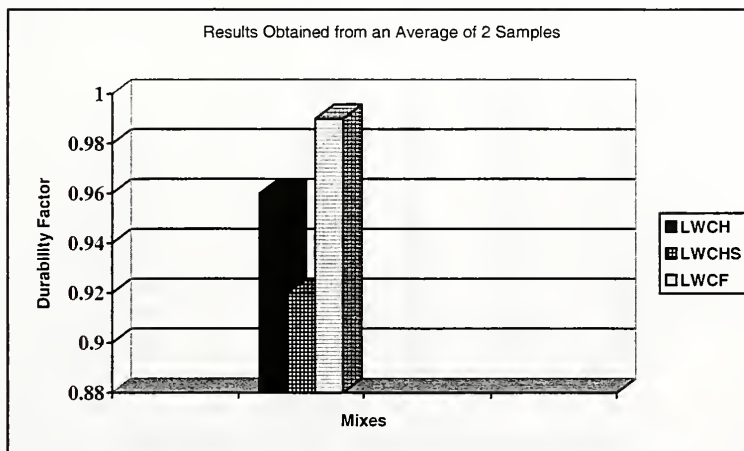


Figure 6.27 Comparison of Durability Factors for Newly Developed LWC For Bridge Deck Application with Air Drying Prior to Testing

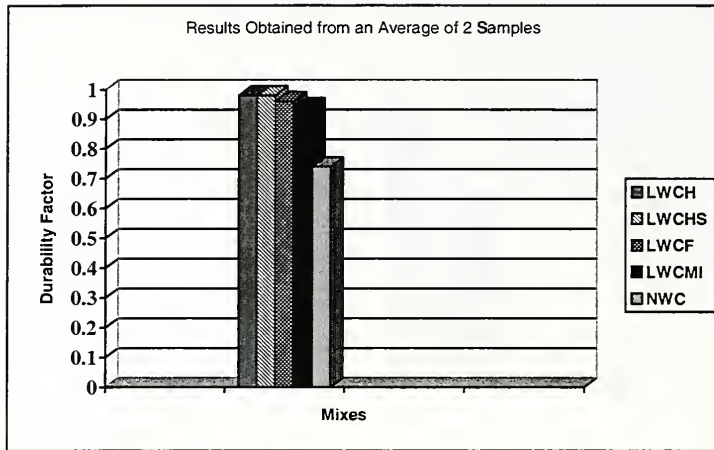


Figure 6.28 Comparison of Durability Factors for Reference Mixes for Bridge Deck Application with Air Drying Prior to Testing

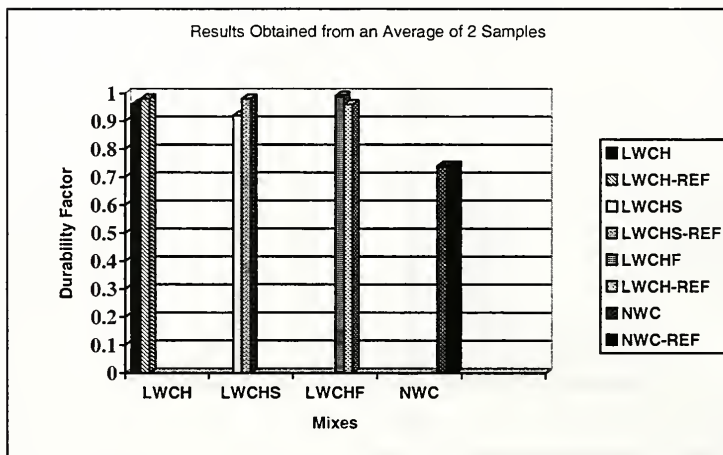


Figure 6.29 Comparison of Durability Factors for Newly Developed and Reference Mixes for Bridge Deck Application

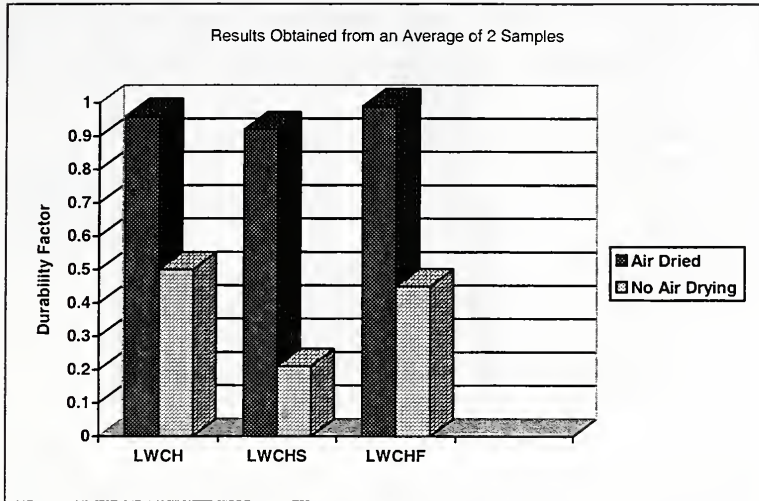


Figure 6.30 Effect of Air Drying period of LWC Samples on Durability Factor

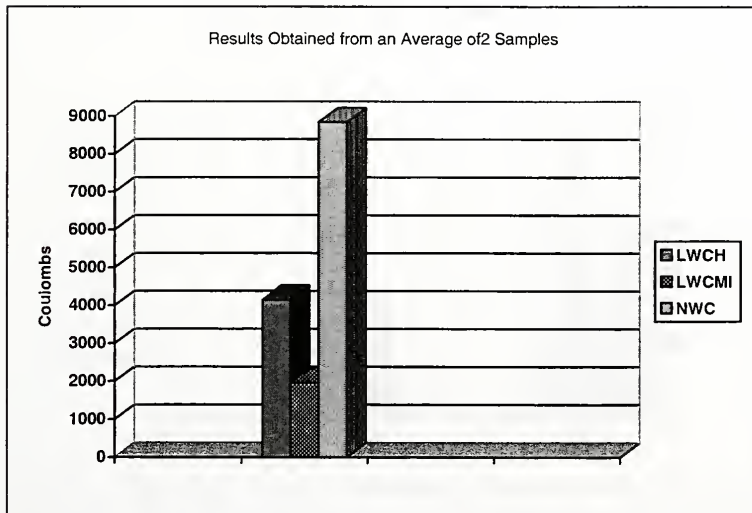


Figure 6.31 Comparison of 28 Day Coulomb Reading For Girder Mixes, 42 MPa(6000 psi)

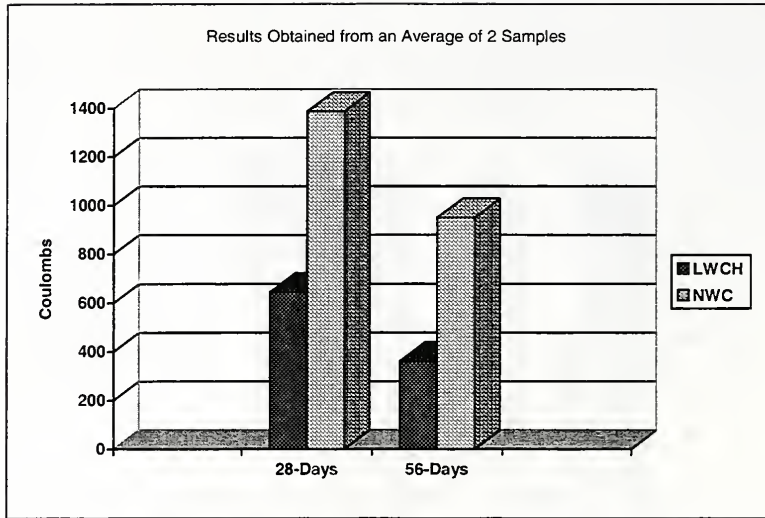


Figure 6.32 Comparison of 28 and 56 Day Coulomb Reading For Girder Mixes, 69 MPa(10,000 psi)

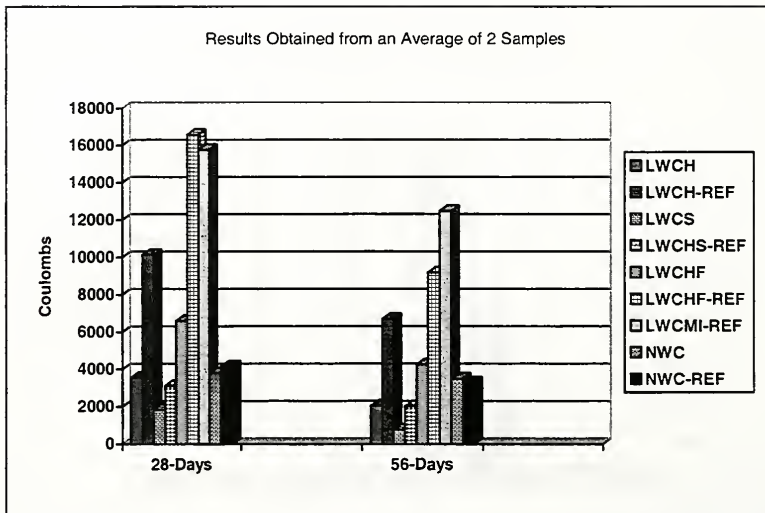


Figure 6.33 Comparison of 28 and 56 Day Coulomb Reading For Deck Mixes

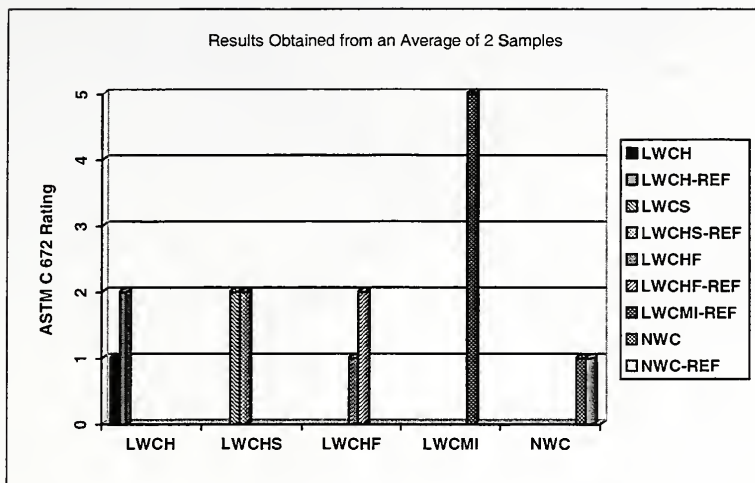


Figure 6.34 Scaling Resistance Ratings Observed for Deck Concrete

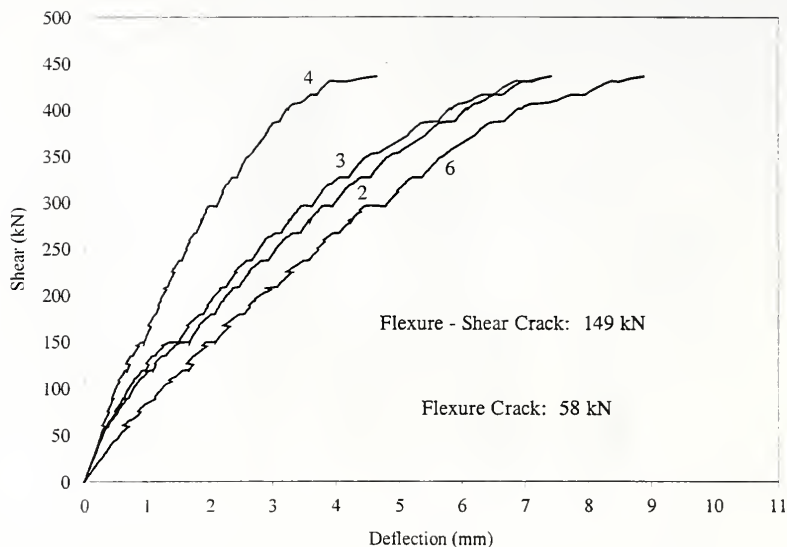


Figure 6.35 Shear-Deflection Relationship, Specimen 1-NWLA

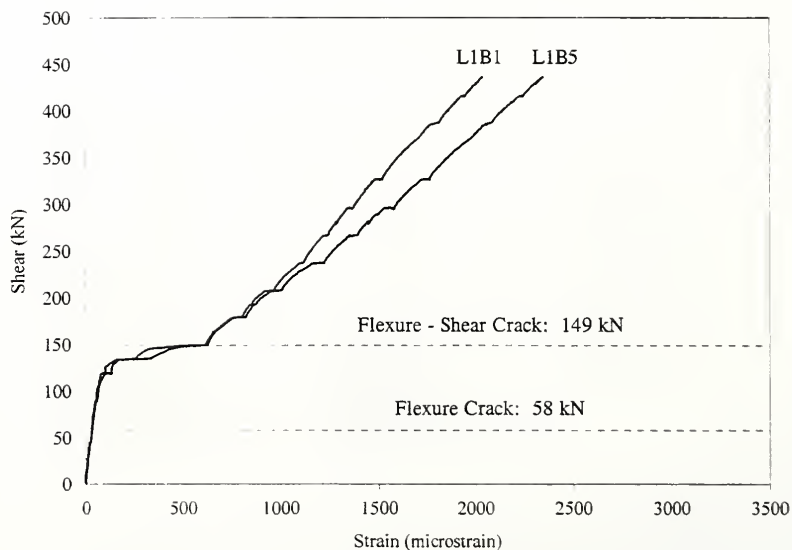


Figure 6.36 Shear-Strain Relationship, Specimen 1-NWLA, Section 1, Bottom Steel

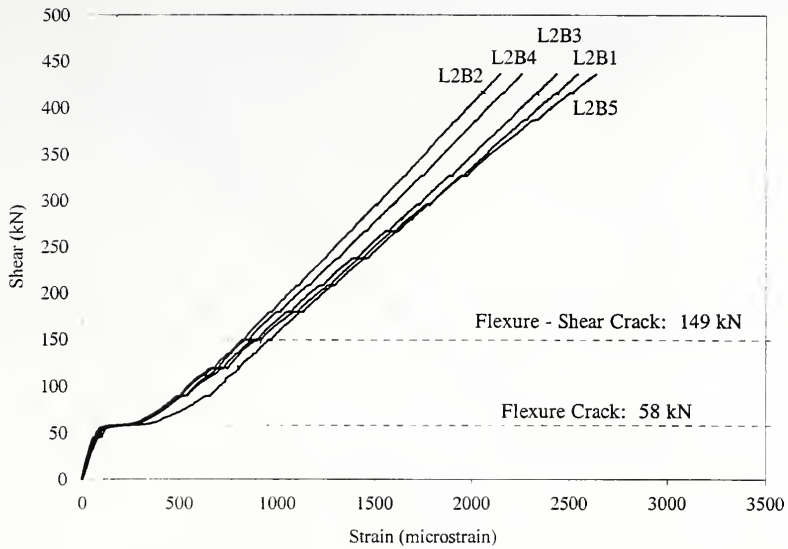


Figure 6.37 Shear-Strain Relationship, Specimen 1-NWLA, Section 2, Bottom Steel

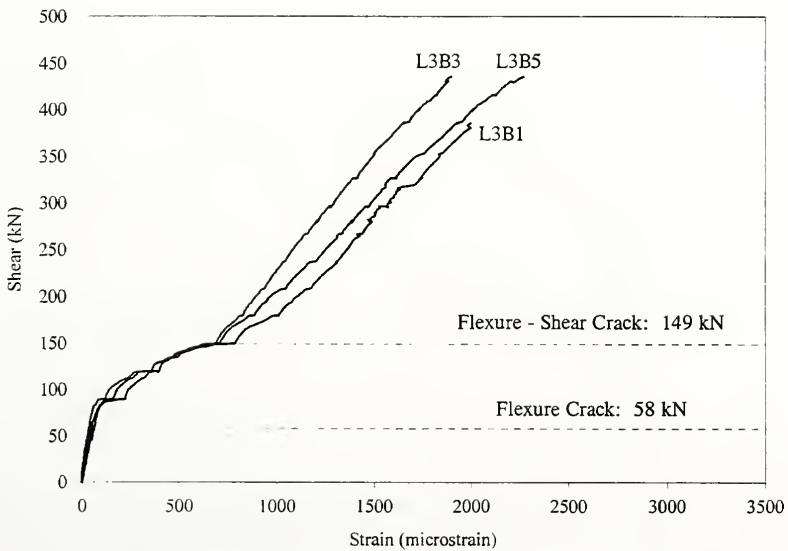


Figure 6.38 Shear-Strain Relationship, Specimen 1-NWLA, Section 3, Bottom Steel

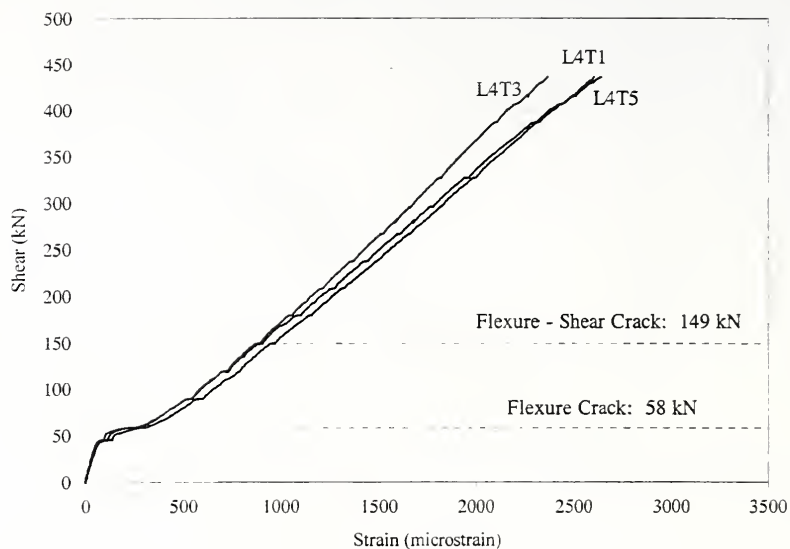


Figure 6.39 Shear-Strain Relationship, Specimen 1-NWLA, Section 4, Top Steel

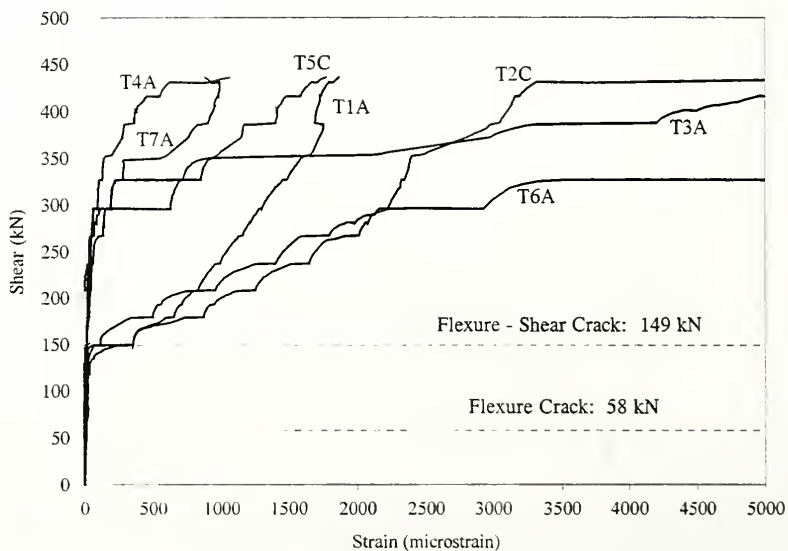


Figure 6.40 Shear-Stirrup Strain Relationship, Specimen 1-NWLA

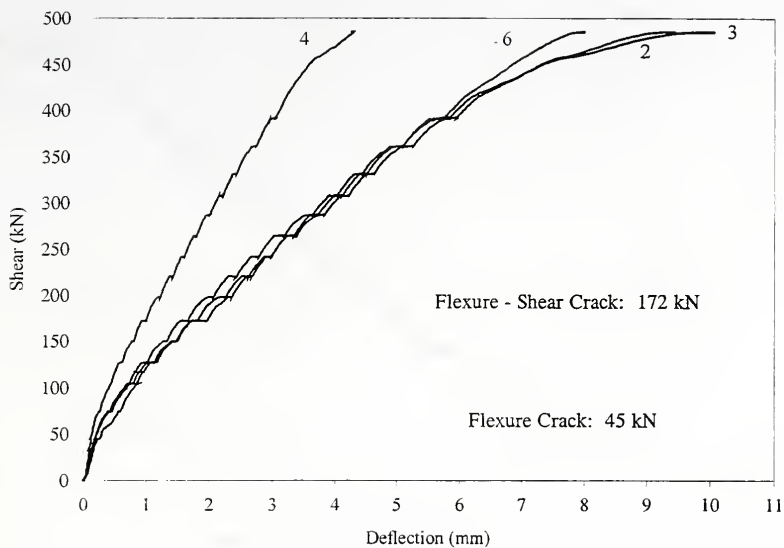


Figure 6.41 Shear-Deflection Relationship, Specimen 2-NWLB

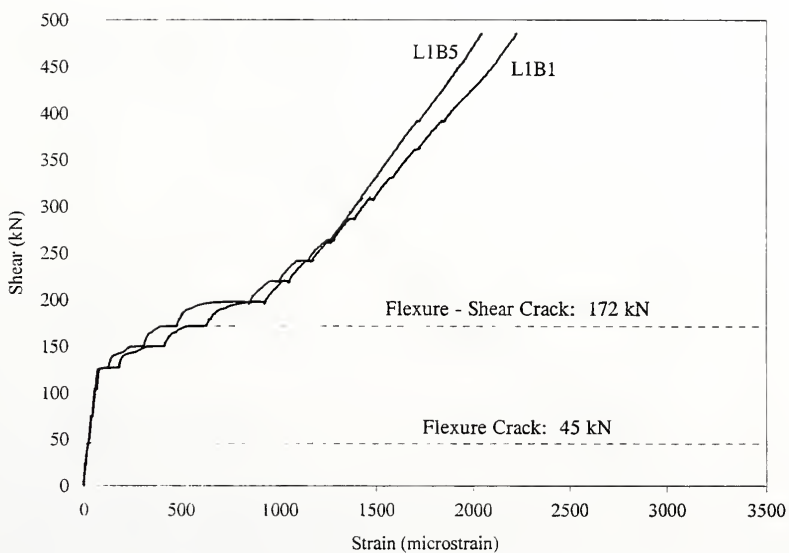


Figure 6.42 Shear-Strain Relationship, Specimen 2-NWLB, Section 1, Bottom Steel

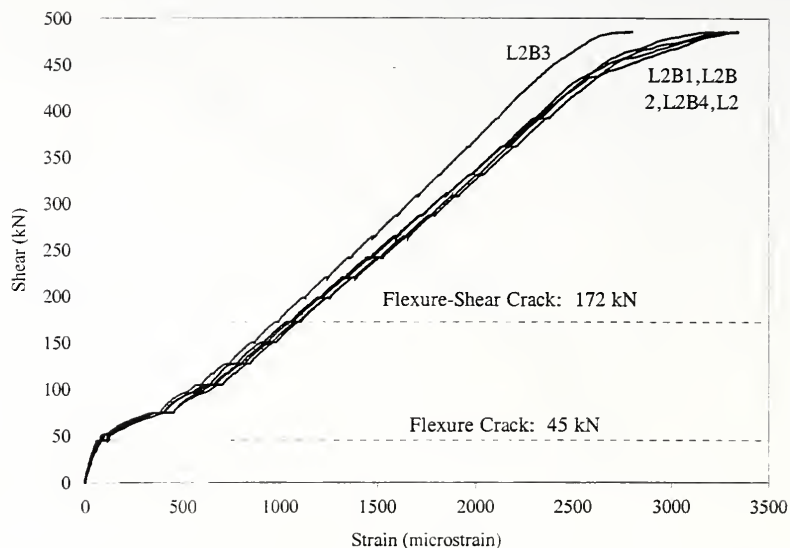


Figure 6.43 Shear-Strain Relationship, Specimen 2-NWLB, Section 2, Bottom Steel

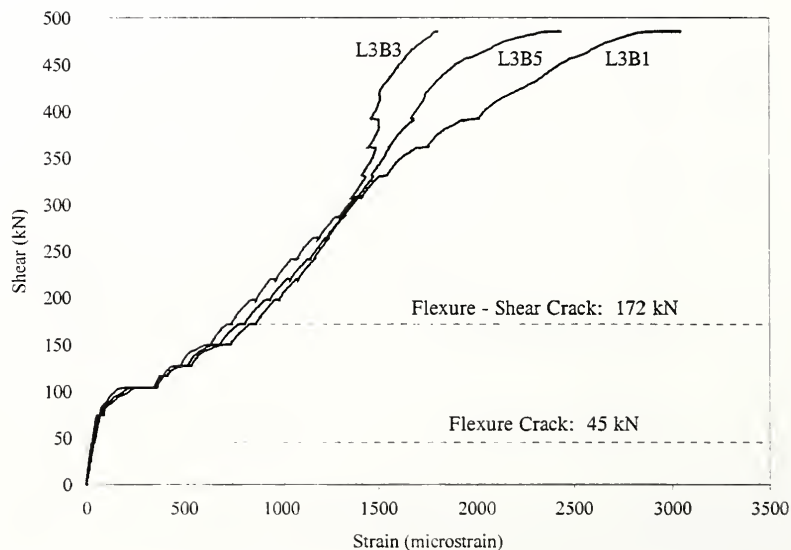


Figure 6.44 Shear-Strain Relationship, Specimen 2-NWLB, Section 3, Bottom Steel

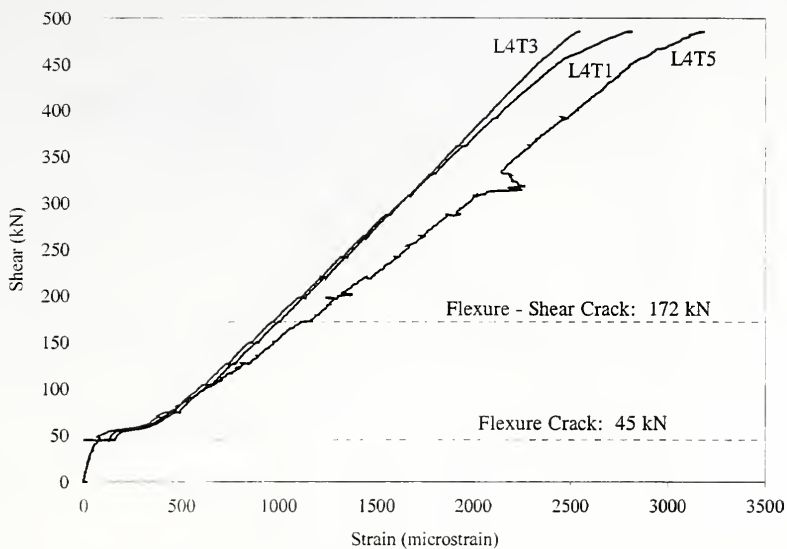


Figure 6.45 Shear-Strain Relationship, Specimen 2-NWLB, Section 4, Top Steel

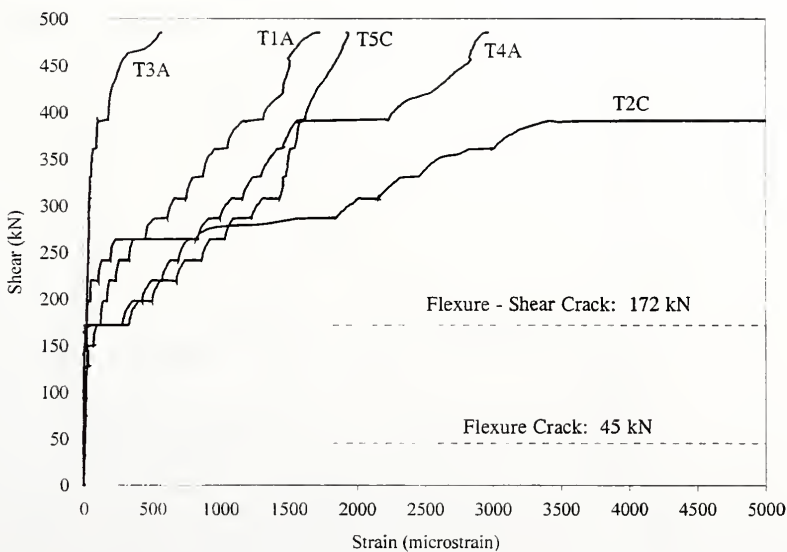


Figure 6.46 Shear-Stirrup Strain Relationship, Specimen 2-NWLB

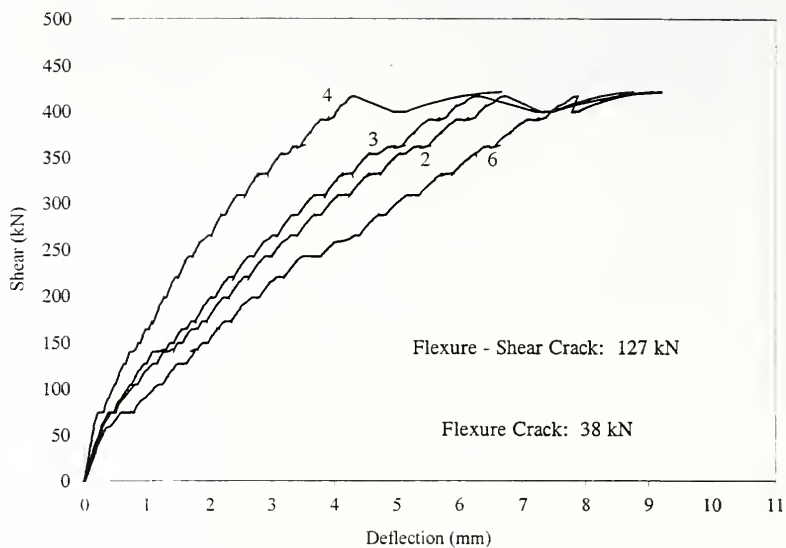


Figure 6.47 Shear-Deflection Relationship, Specimen 3-NWLC

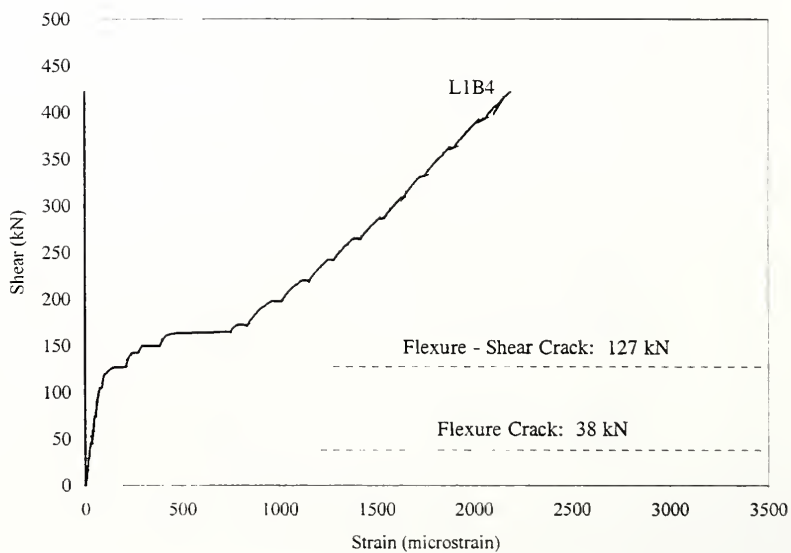


Figure 6.48 Shear-Strain Relationship, Specimen 3-NWLC, Section 1, Bottom Steel

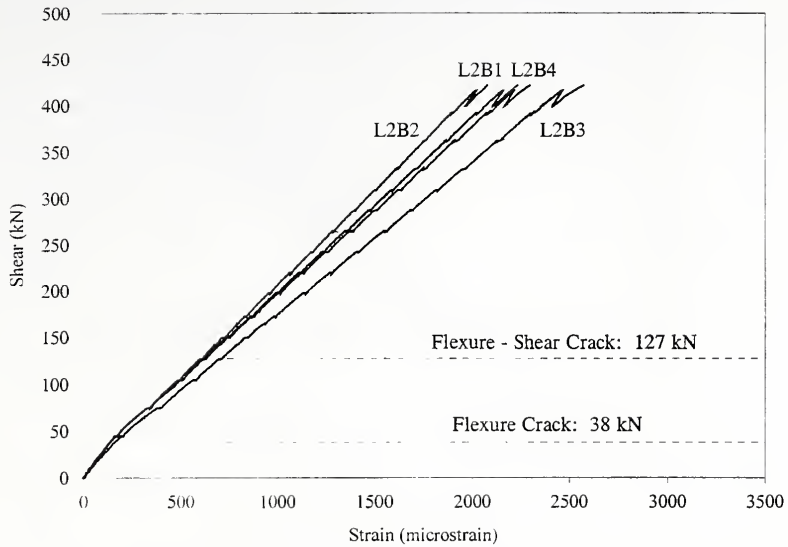


Figure 6.49 Shear-Strain Relationship, Specimen 3-NWLC, Section 2, Bottom Steel

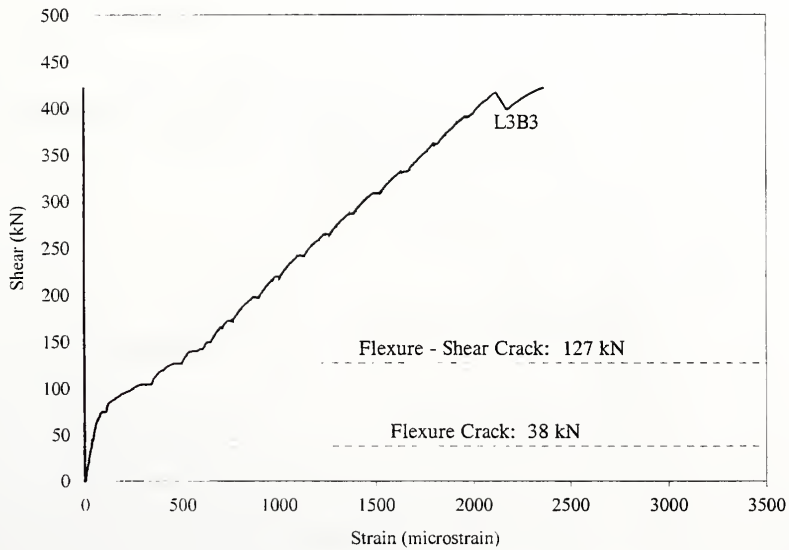


Figure 6.50 Shear-Strain Relationship, Specimen 3-NWLC, Section 3, Bottom Steel

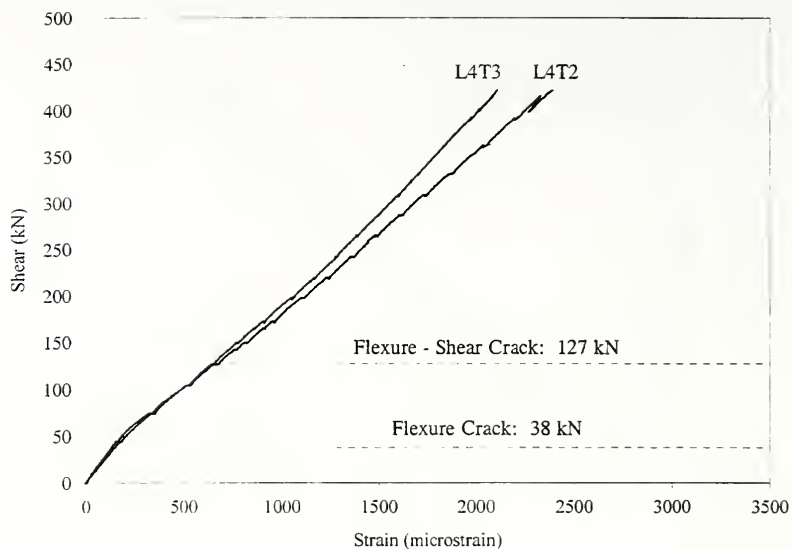


Figure 6.51 Shear-Strain Relationship, Specimen 3-NWLC, Section 4, Top Steel

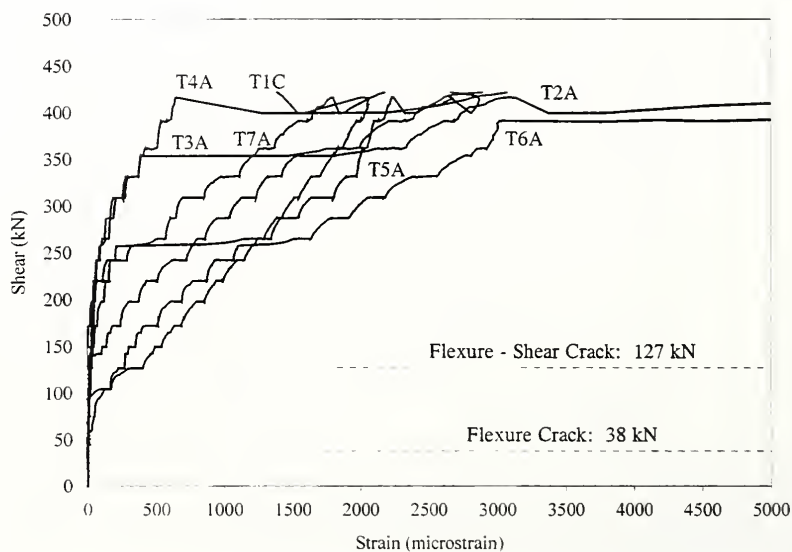


Figure 6.52 Shear-Stirrup Strain Relationship, Specimen 3-NWLC

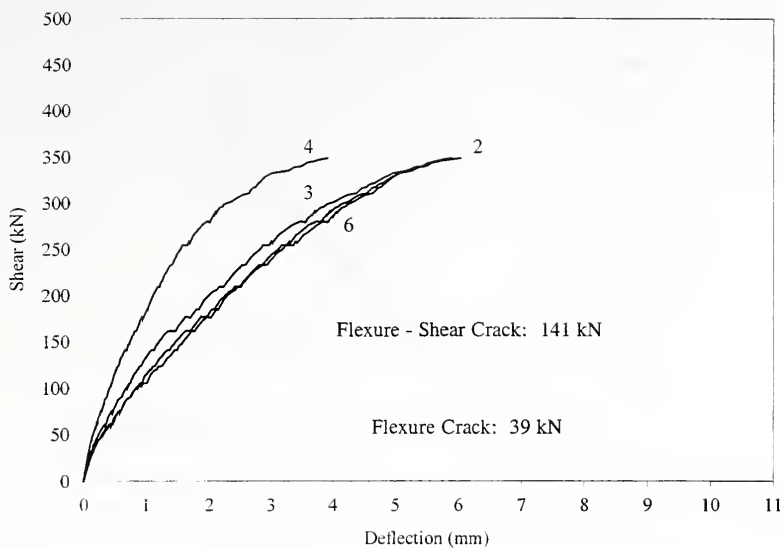


Figure 6.53 Shear-Deflection Relationship, Specimen 4-NWLD

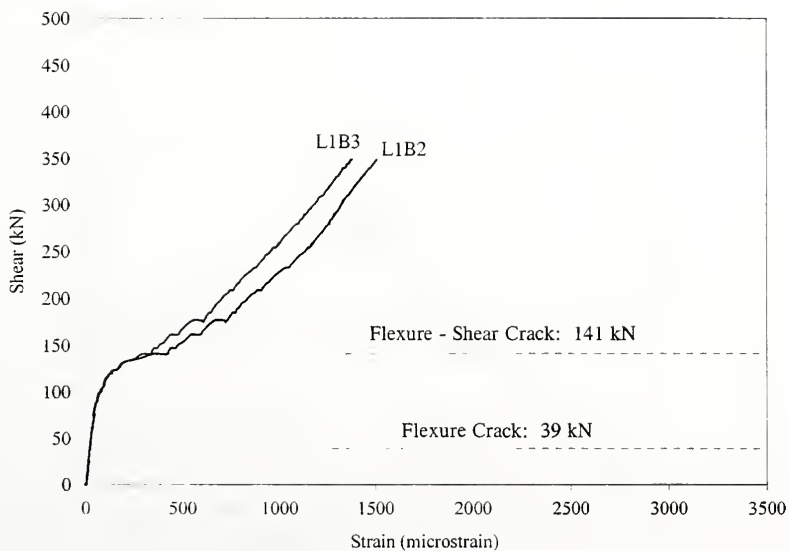


Figure 6.54 Shear-Strain Relationship, Specimen 4-NWLD, Section 1, Bottom Steel

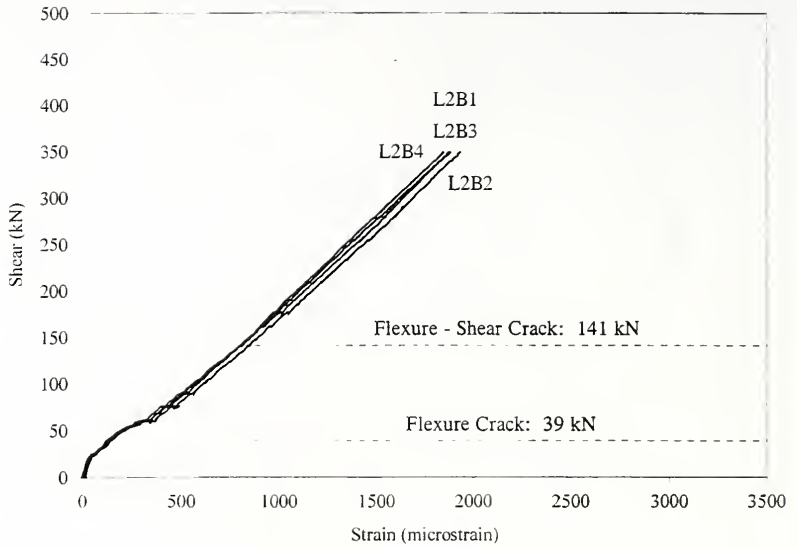


Figure 6.55 Shear-Strain Relationship, Specimen 4-NWLD, Section 2, Bottom Steel

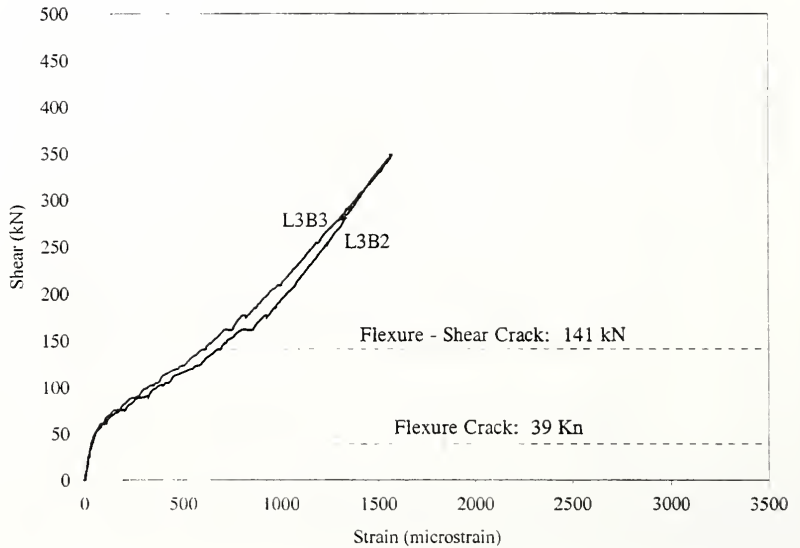


Figure 6.56 Shear-Strain Relationship, Specimen 4-NWLD, Section 3, Bottom Steel

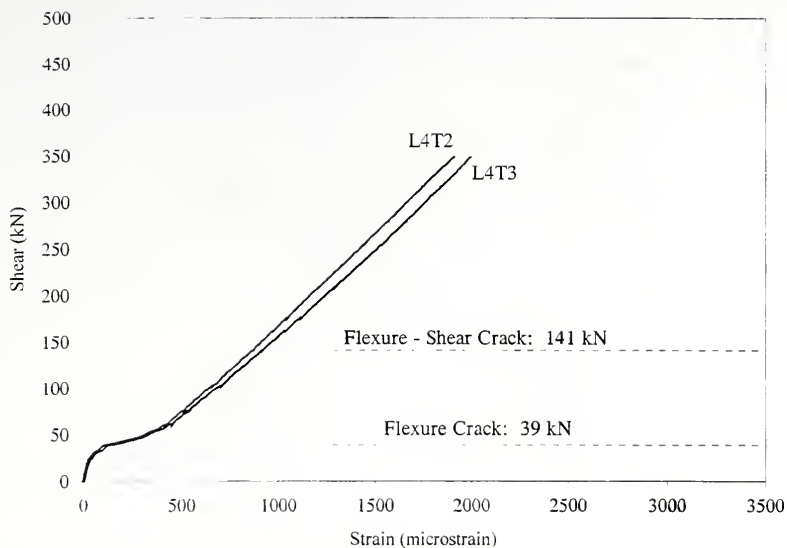


Figure 6.57 Shear-Strain Relationship, Specimen 4-NWLD, Section 4, Top Steel

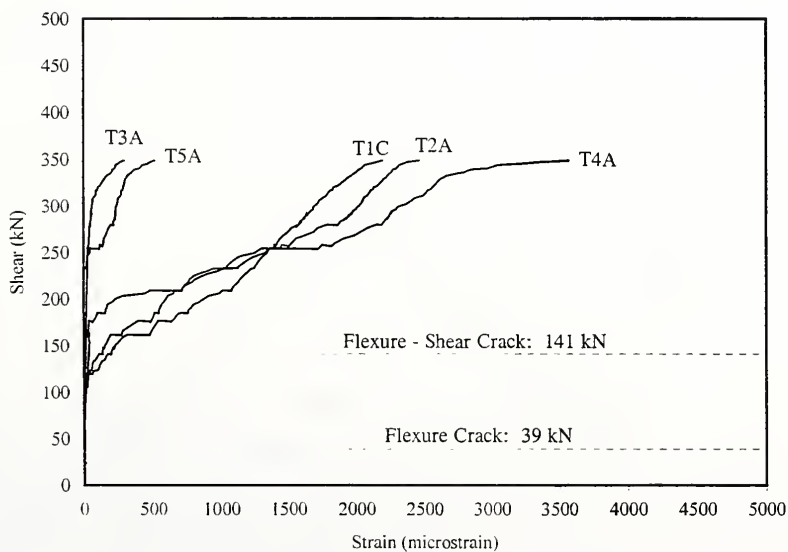


Figure 6.58 Shear-Stirrup Strain Relationship, Specimen 4-NWLD

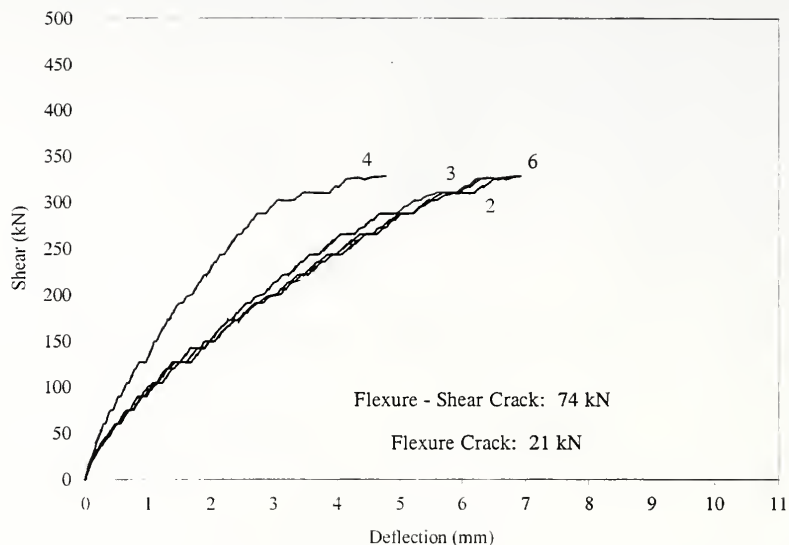


Figure 6.59 Shear-Deflection Relationship, Specimen 5-LWLA

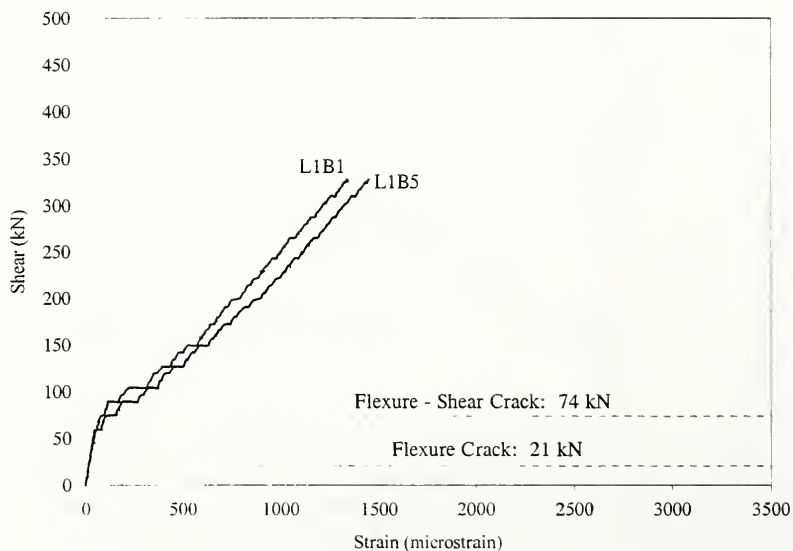


Figure 6.60 Shear-Strain Relationship, Specimen 5-LWLA, Section 1, Bottom Steel

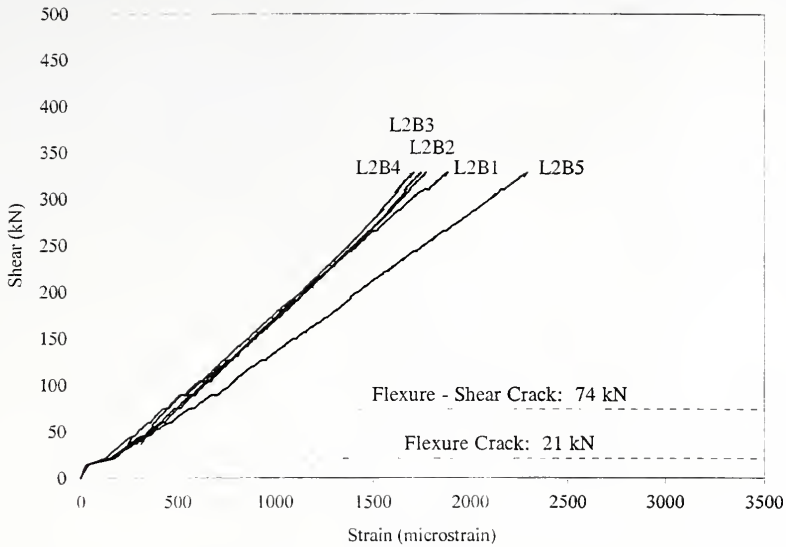


Figure 6.61 Shear-Strain Relationship, Specimen 5-LWLA, Section 2, Bottom Steel

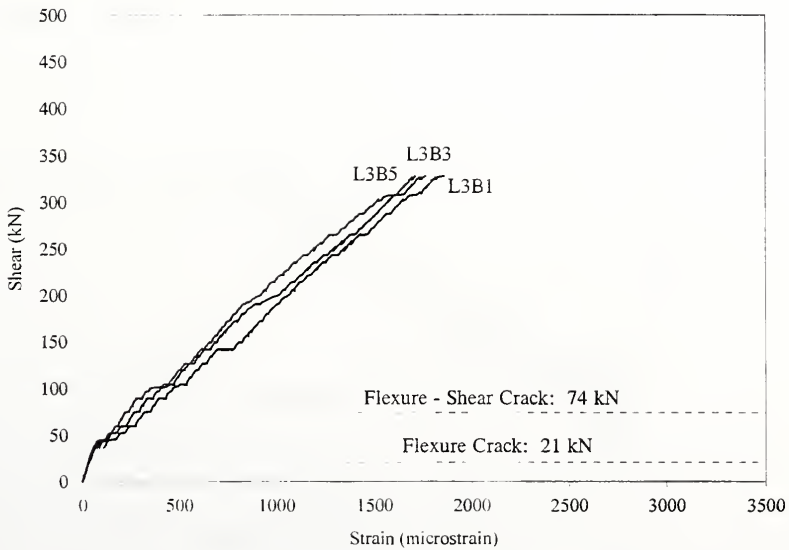


Figure 6.62 Shear-Strain Relationship, Specimen 5-LWLA, Section 3, Bottom Steel

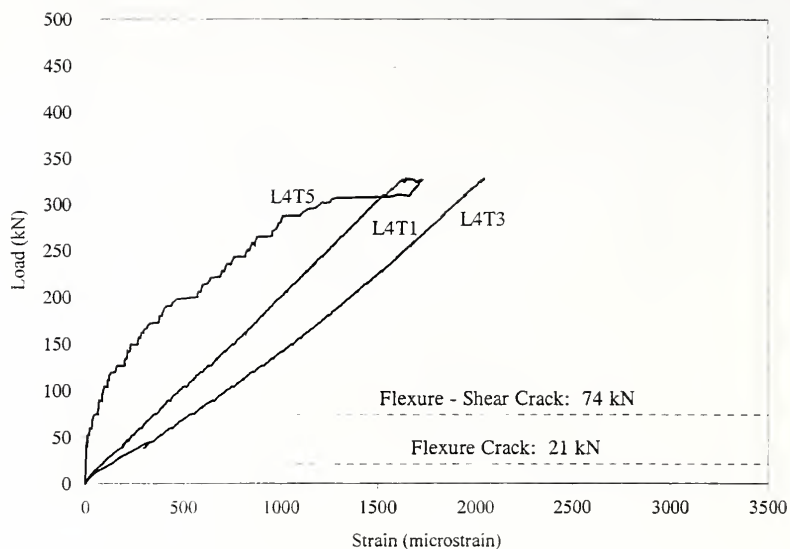


Figure 6.63 Shear-Strain Relationship, Specimen 5-LWLA, Section 4, Top Steel

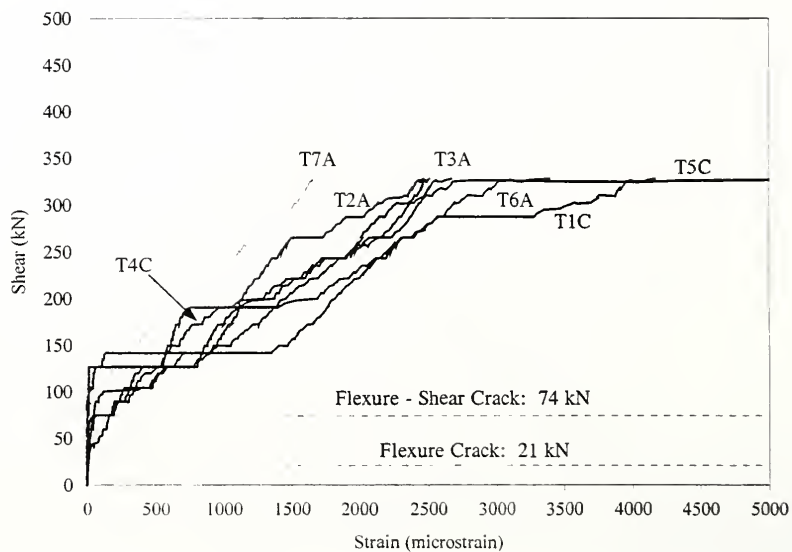


Figure 6.64 Shear-Stirrup Strain Relationship, Specimen 5-LWLA

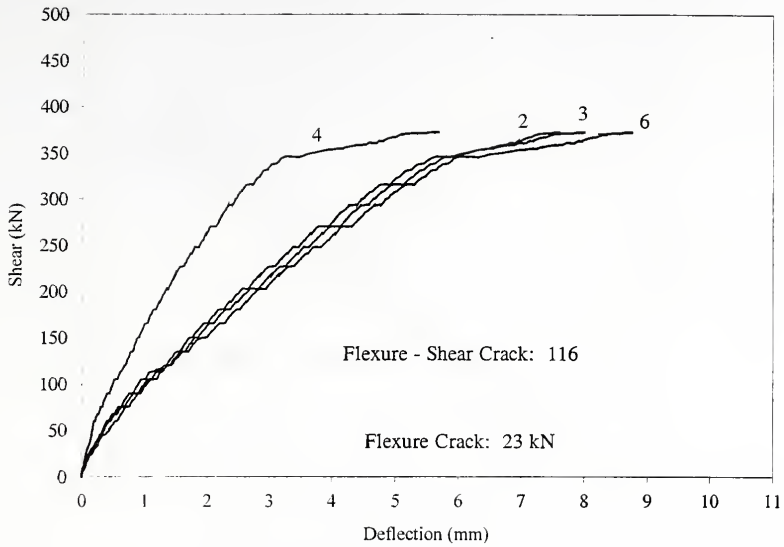


Figure 6.65 Shear-Deflection Relationship, Specimen 6-LWLB

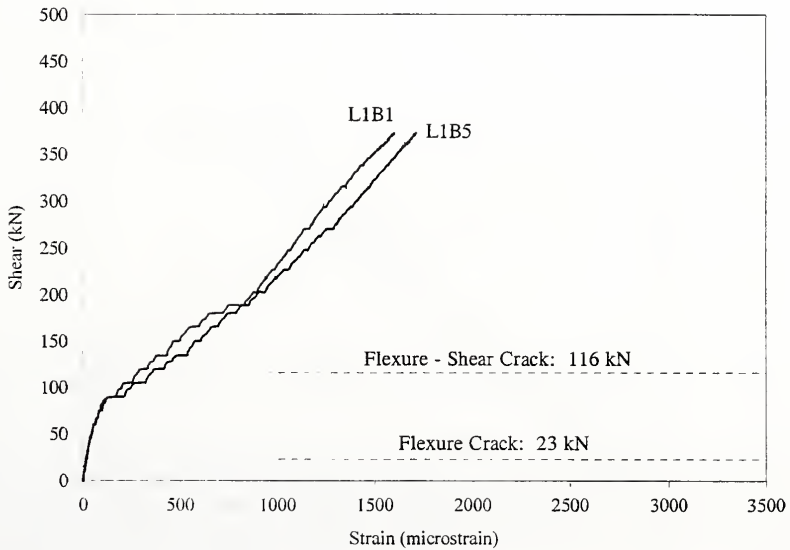


Figure 6.66 Shear-Strain Relationship, Specimen 6-LWLB, Section 1, Bottom Steel

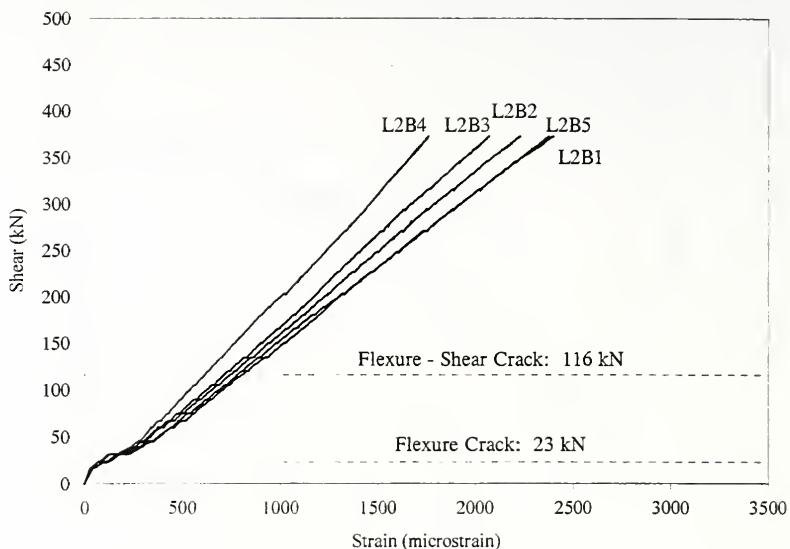


Figure 6.67 Shear-Strain Relationship, Specimen 6-LWLB, Section 2, Bottom Steel

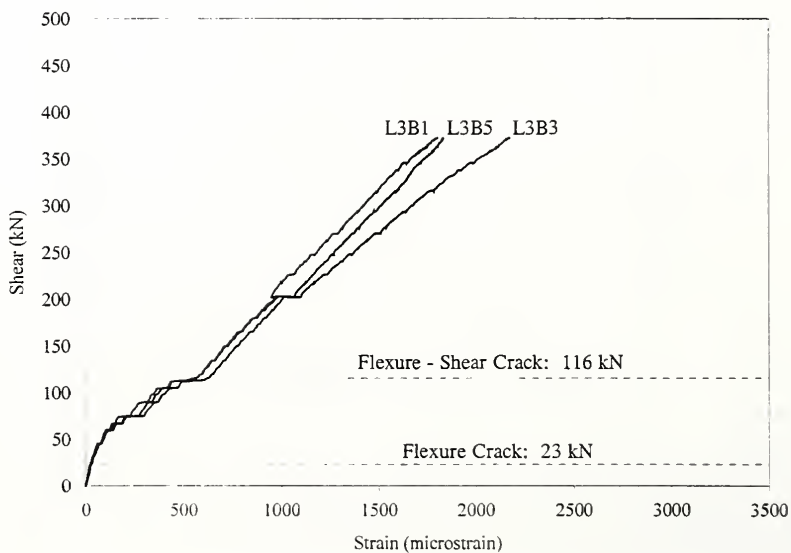


Figure 6.68 Shear-Strain Relationship, Specimen 6-LWLB, Section 3, Bottom Steel

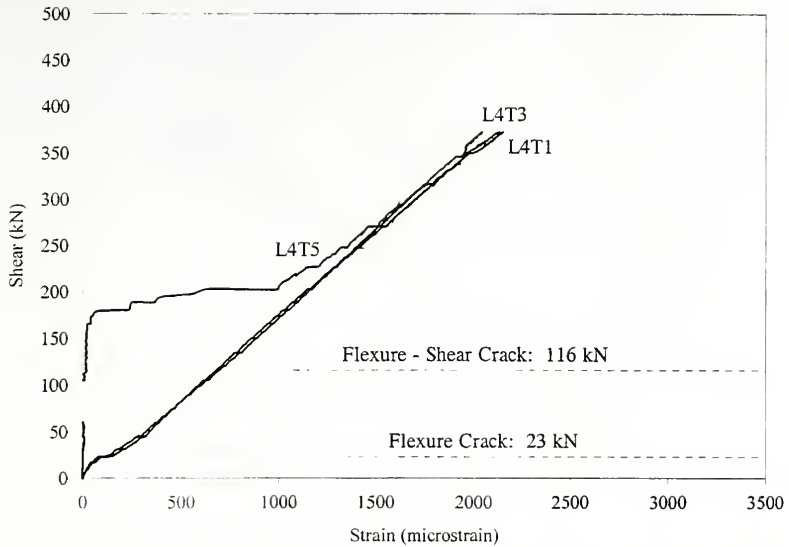


Figure 6.69 Shear-Strain Relationship, Specimen 6-LWLB, Section 4, Top Steel

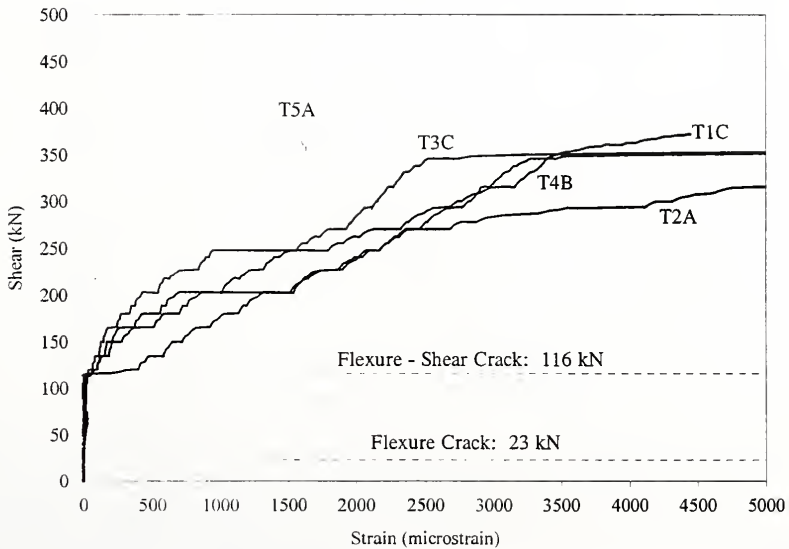


Figure 6.70 Shear-Stirrup Strain Relationship, Specimen 6-LWLB

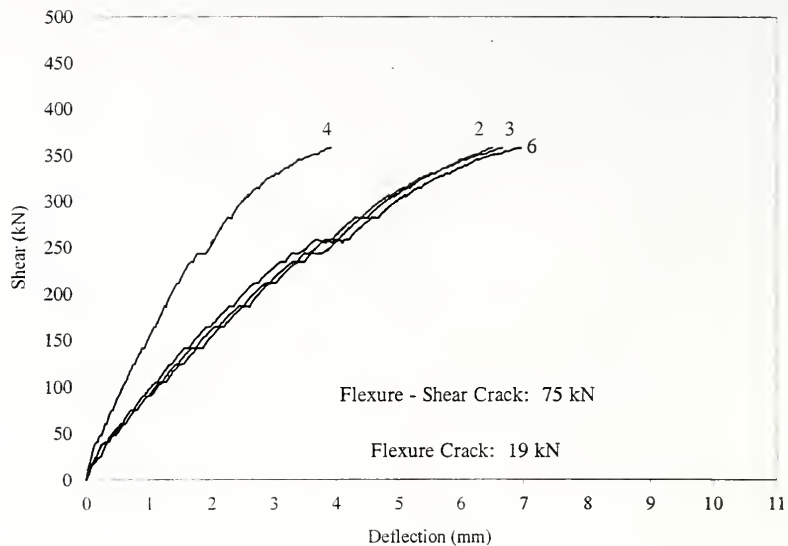


Figure 6.71 Shear-Deflection Relationship, Specimen 7-LWLC

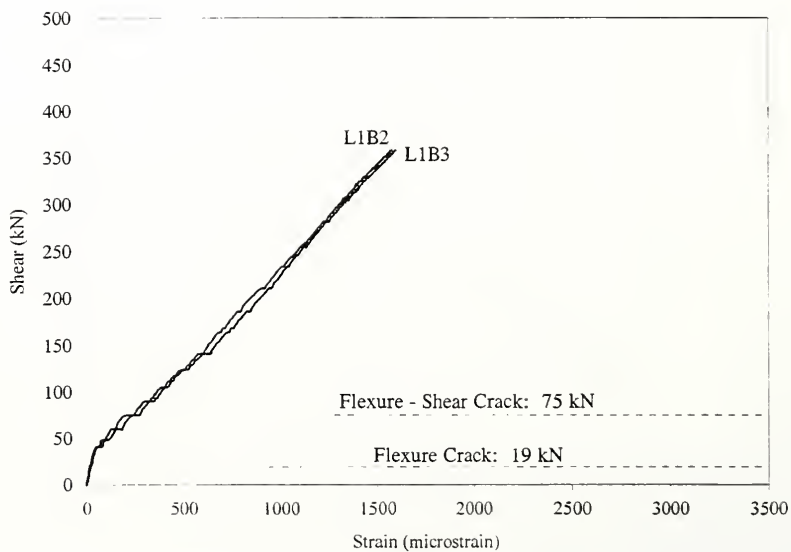


Figure 6.72 Shear-Strain Relationship, Specimen 7-LWLC, Section 1, Bottom Steel

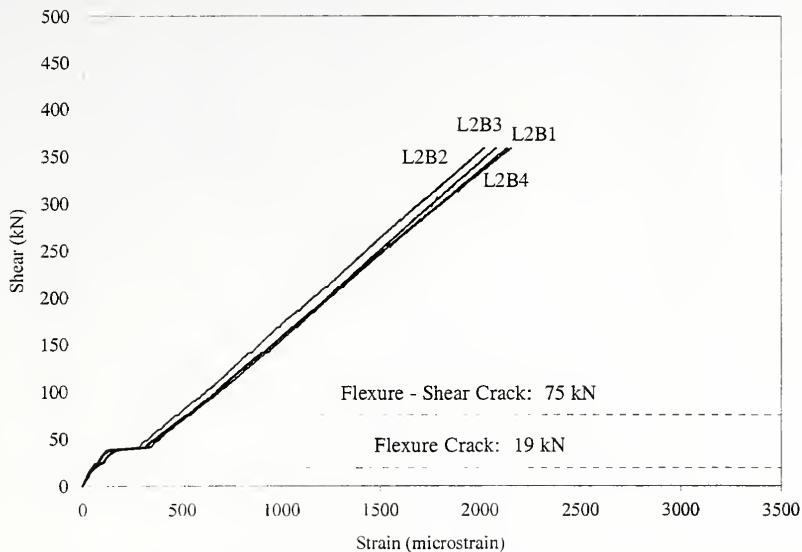


Figure 6.73 Shear-Strain Relationship, Specimen 7-LWLC, Section 2, Bottom Steel

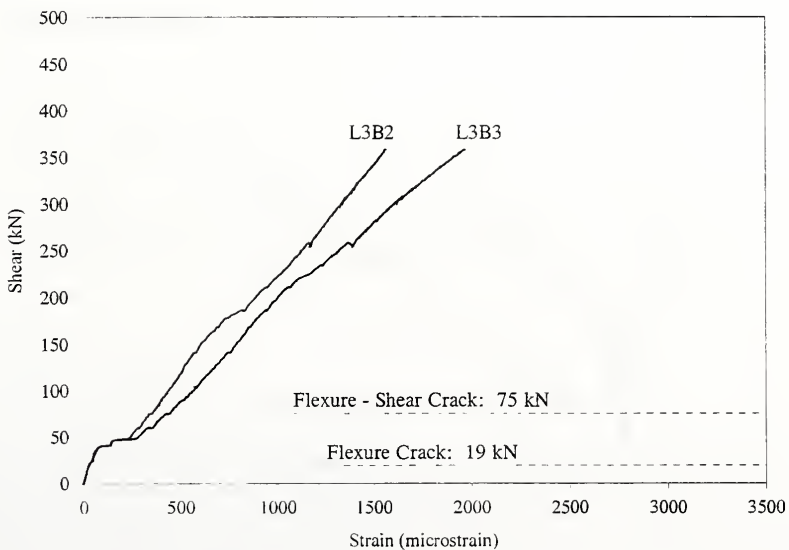


Figure 6.74 Shear-Strain Relationship, Specimen 7-LWLC, Section 3, Bottom Steel

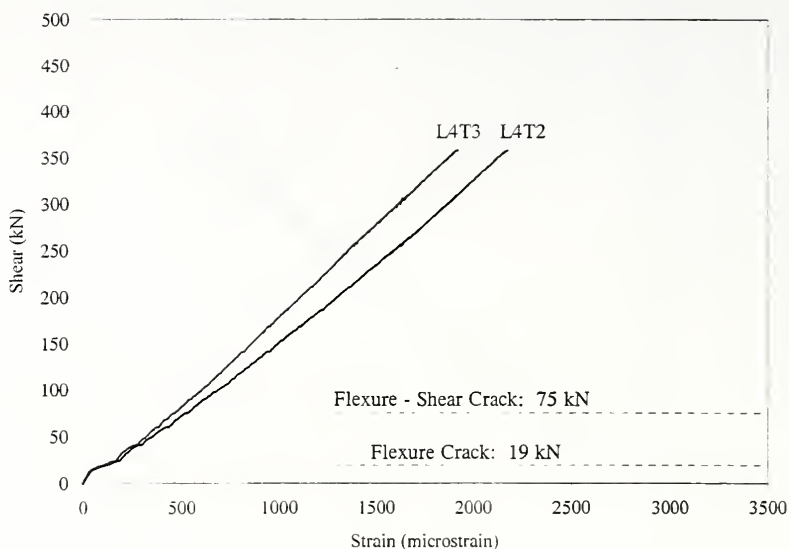


Figure 6.75 Shear-Strain Relationship, Specimen 7-LWLC, Section 4, Top Steel

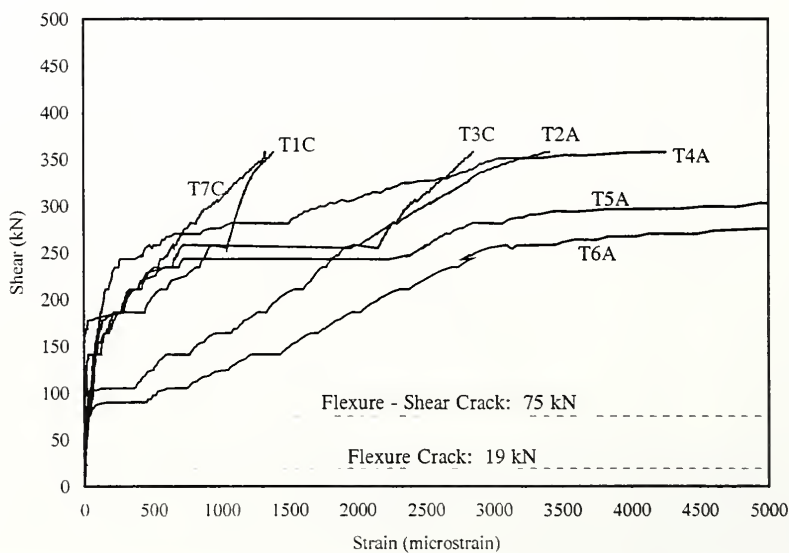


Figure 6.76 Shear-Stirrup Strain Relationship, Specimen 7-LWLC

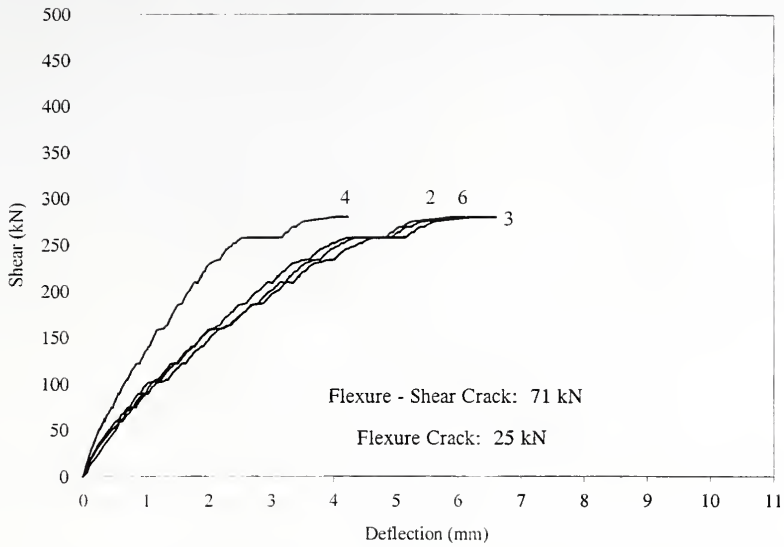


Figure 6.77 Shear-Deflection Relationship, Specimen 8-LWLD

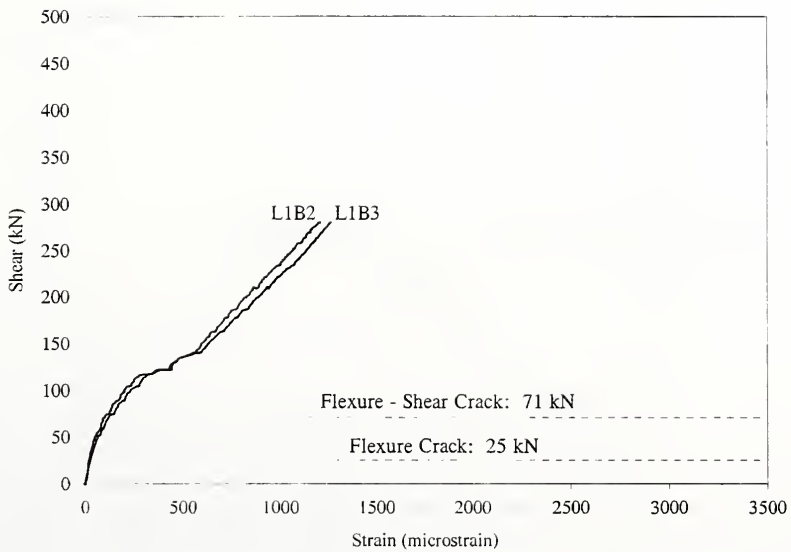


Figure 6.78 Shear-Strain Relationship, Specimen 8-LWLD, Section 1, Bottom Steel

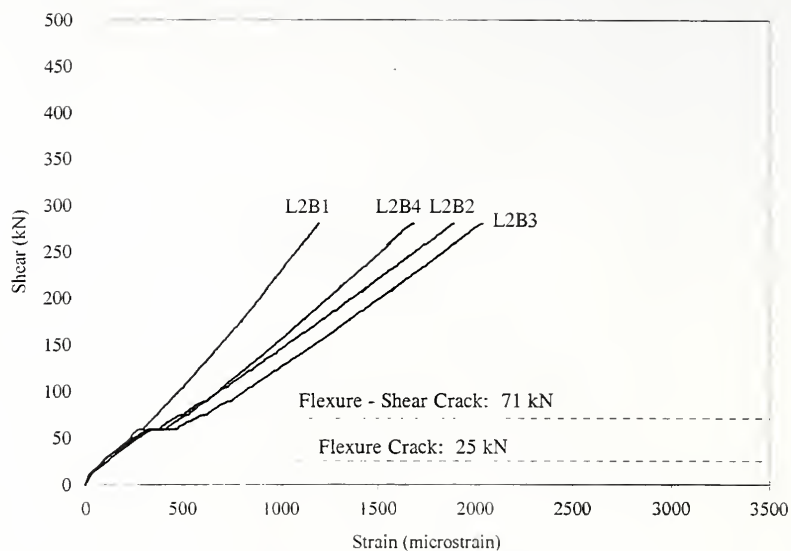


Figure 6.79 Shear-Strain Relationship, Specimen 8-LWLD, Section 2, Bottom

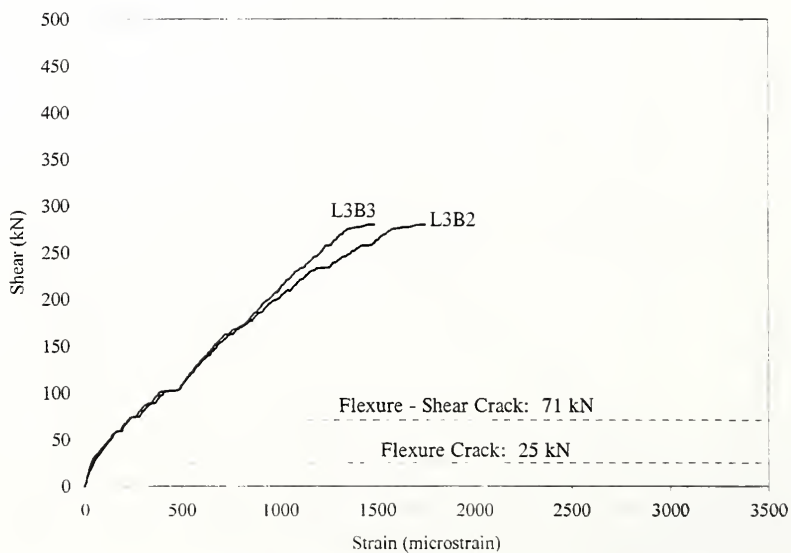


Figure 6.80 Shear-Strain Relationship, Specimen 8-LWLD, Section 3, Bottom Steel

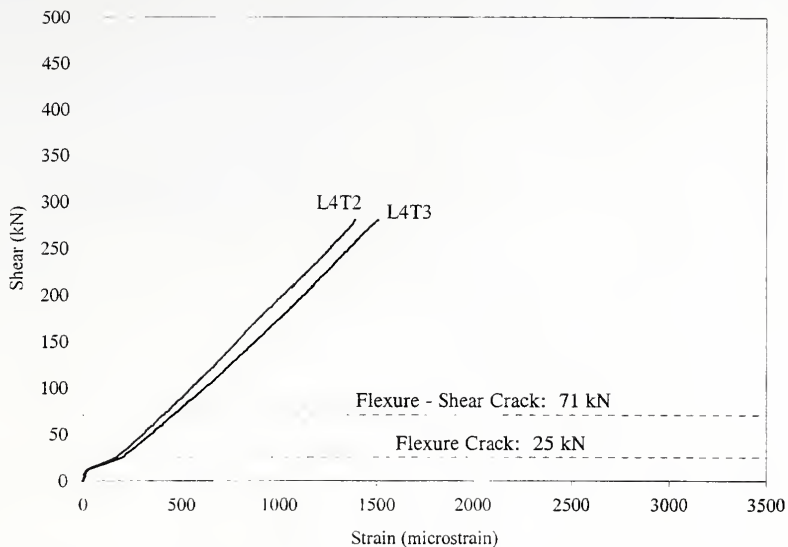


Figure 6.81 Shear-Strain Relationship, Specimen 8-LWLD, Section 4, Top Steel

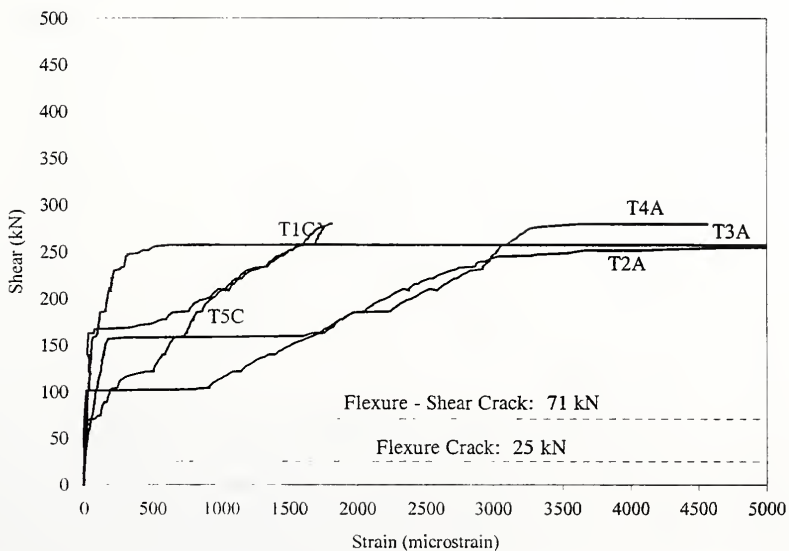


Figure 6.82 Shear-Stirrup Strain Relationship, Specimen 8-LWLD

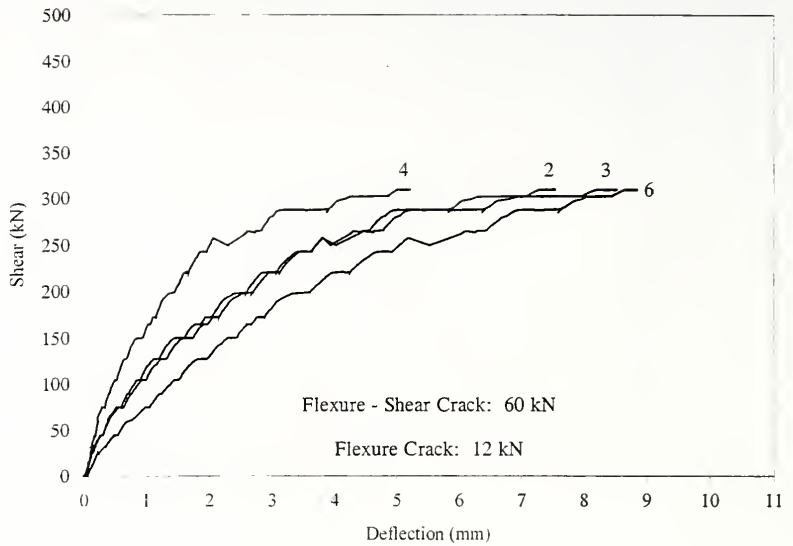


Figure 6.83 Shear-Deflection Relationship, Specimen 9-NWLD

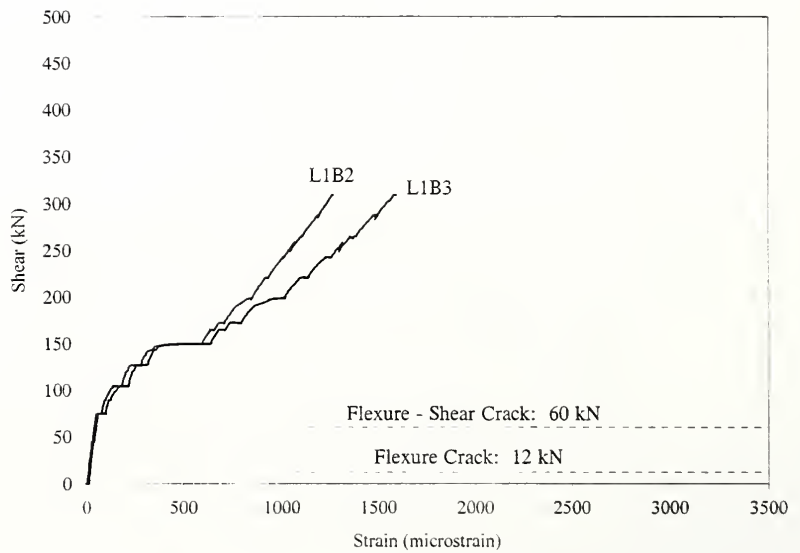


Figure 6.84 Shear-Strain Relationship, Specimen 9-NWLD, Section 1, Bottom Steel

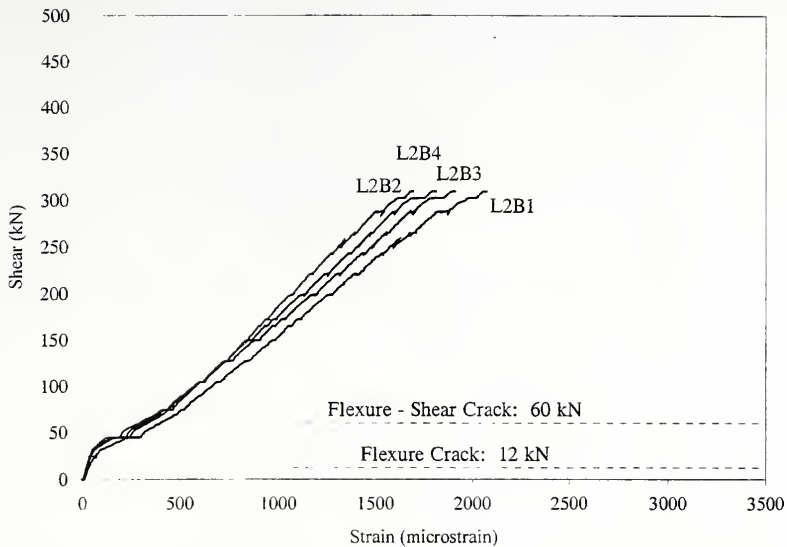


Figure 6.85 Shear-Strain Relationship, Specimen 9-NWLD, Section 2, Bottom Steel

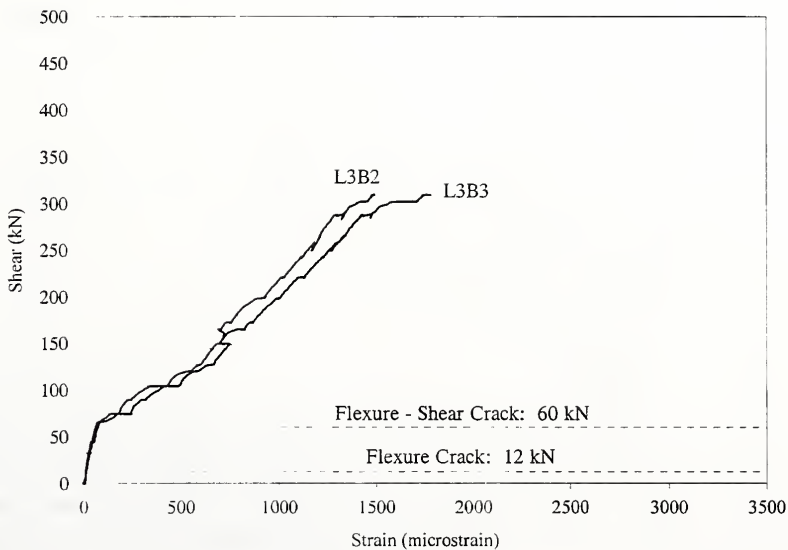


Figure 6.86 Shear-Strain Relationship, Specimen 9-NWLD, Section 3, Bottom Steel

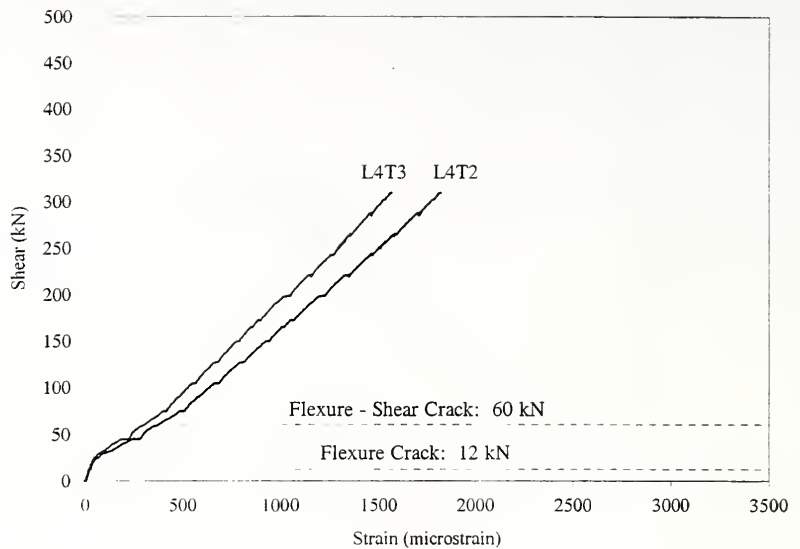


Figure 6.87 Shear-Strain Relationship, Specimen 9-NWLD, Section 4, Top Steel

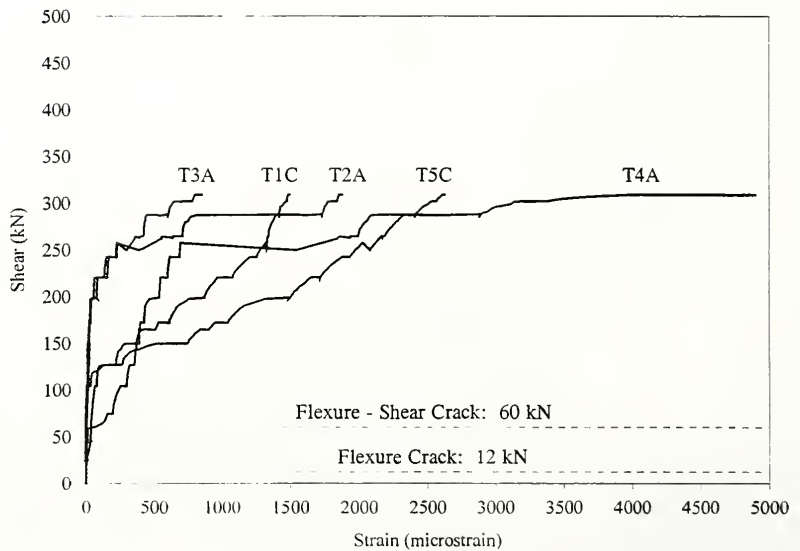


Figure 6.88 Shear-Stirrup Strain Relationship, Specimen 9-NWLD

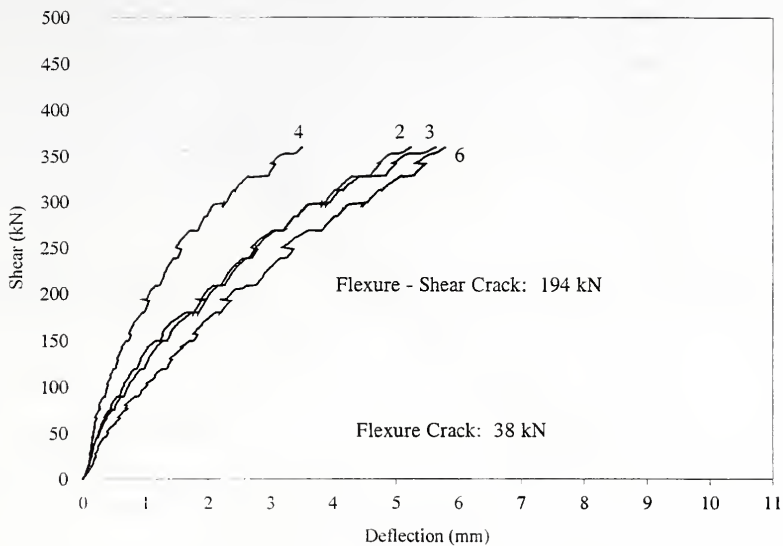


Figure 6.89 Shear-Deflection Relationship, Specimen 10-NWHD

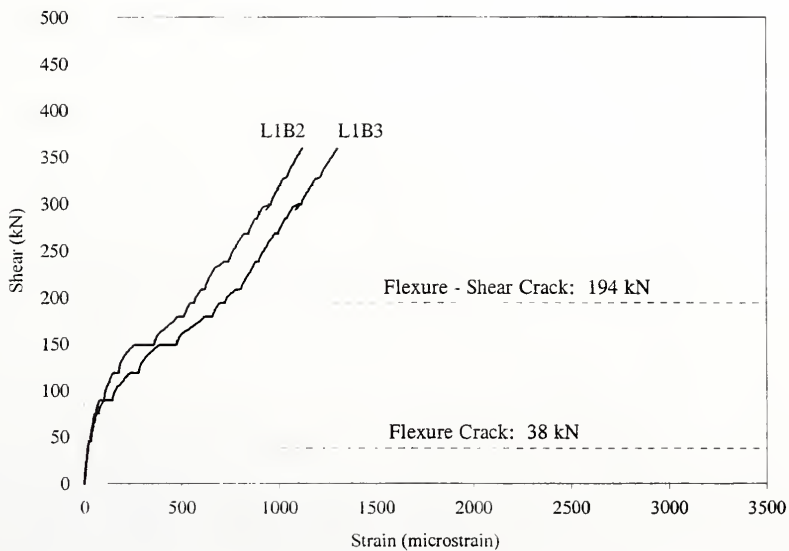


Figure 6.90 Shear-Strain Relationship, Specimen 10-NWHD, Section 1, Bottom Steel

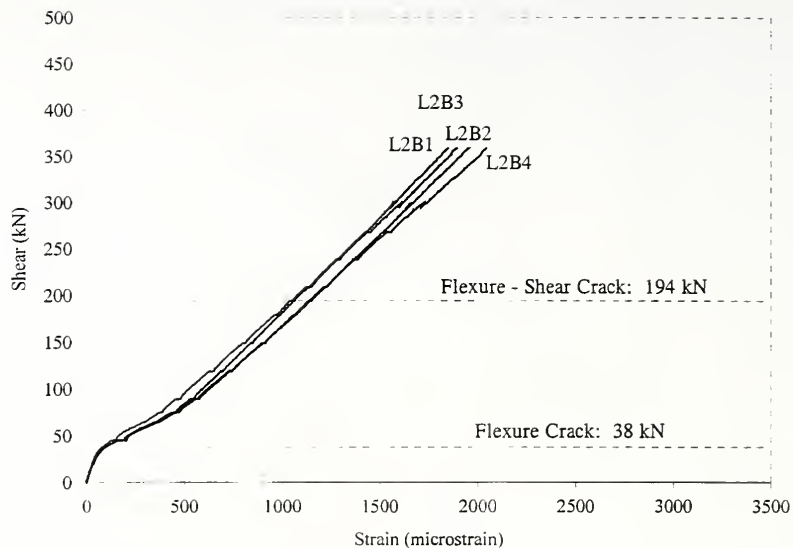


Figure 6.91 Shear-Strain Relationship, Specimen 10-NWHD, Section 2, Bottom Steel

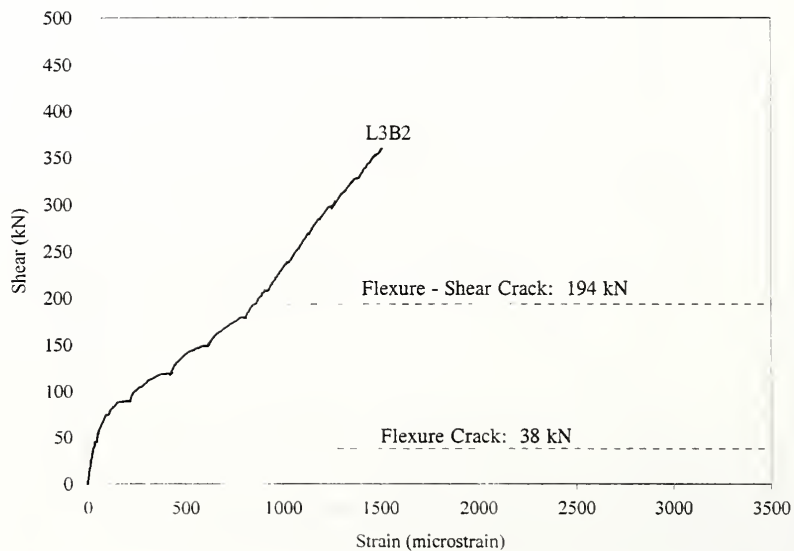


Figure 6.92 Shear-Strain Relationship, Specimen 10-NWHD, Section 3, Bottom Steel

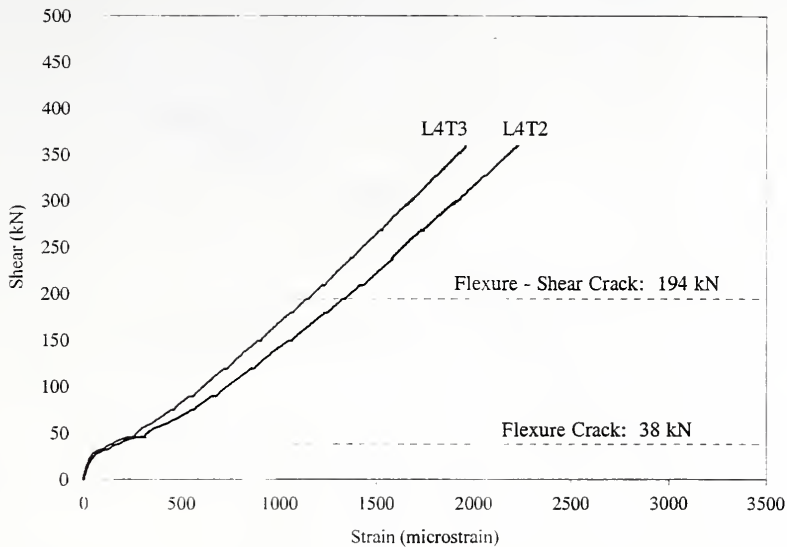


Figure 6.93 Shear-Strain Relationship, Specimen 10-NWHD, Section 4, Top Steel

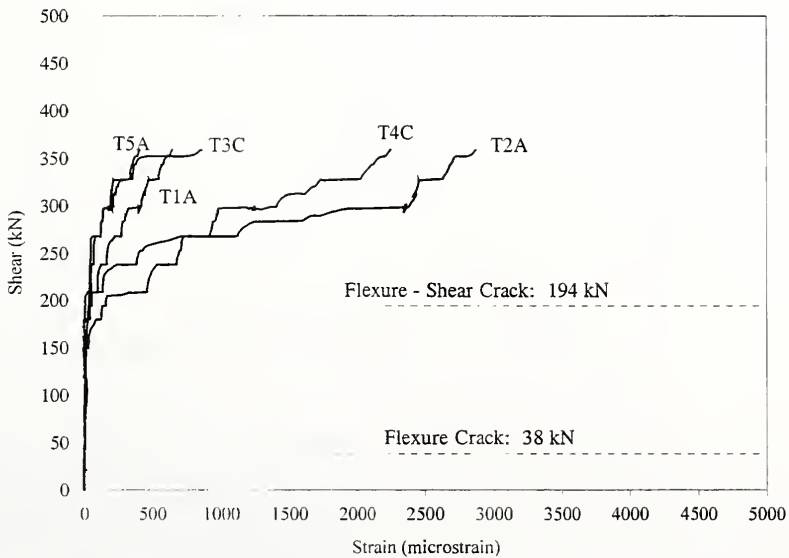


Figure 6.94 Shear-Stirrup Strain Relationship, Specimen 10-NWHD

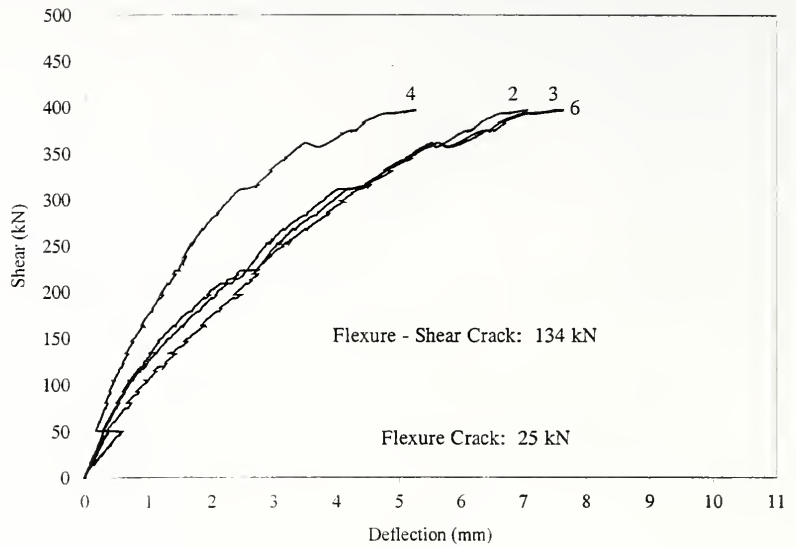


Figure 6.95 Shear-Deflection Relationship, Specimen 11-LWHD

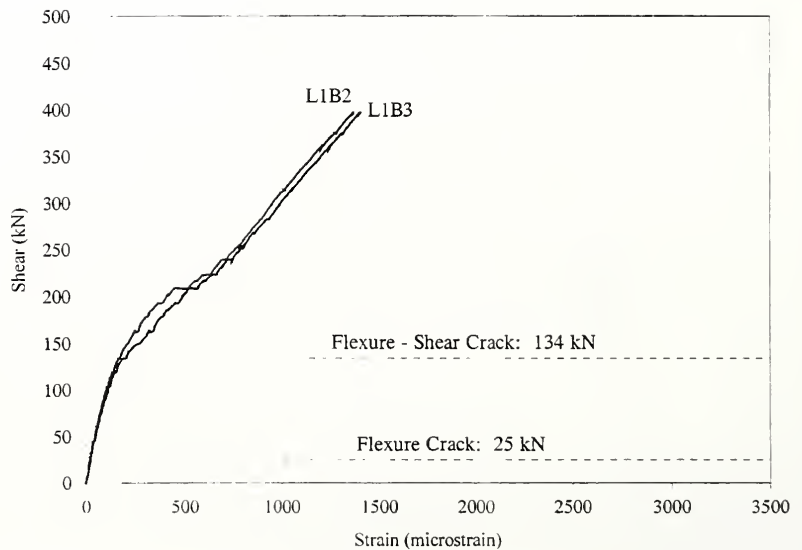


Figure 6.96 Shear-Strain Relationship, Specimen 11-LWHD, Section 1, Bottom Steel

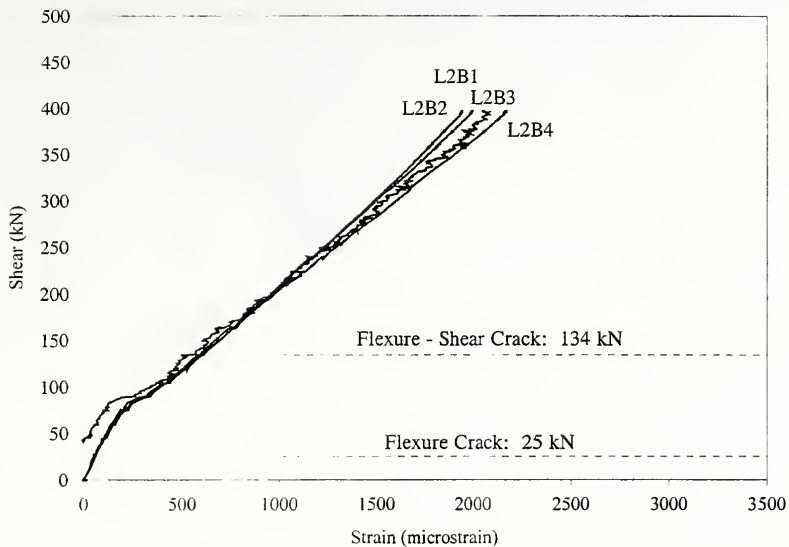


Figure 6.97 Shear-Strain Relationship, Specimen 11-LWHD, Section 2, Bottom Steel

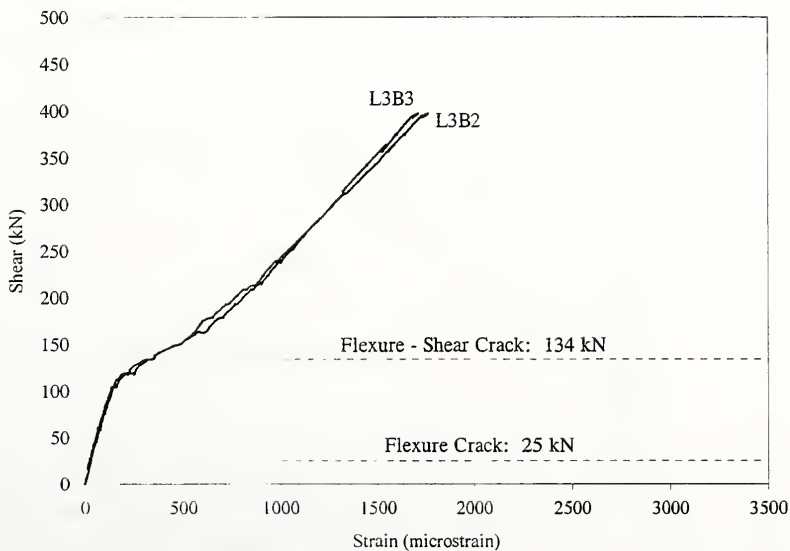


Figure 6.98 Shear-Strain Relationship, Specimen 11-LWHD, Section 3, Bottom Steel

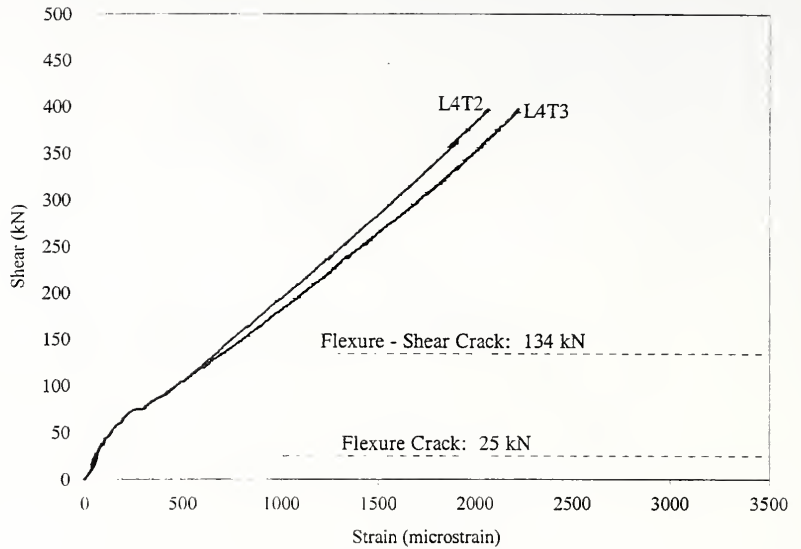


Figure 6.99 Shear-Strain Relationship, Specimen 11-LWHD, Section 4, Top Steel

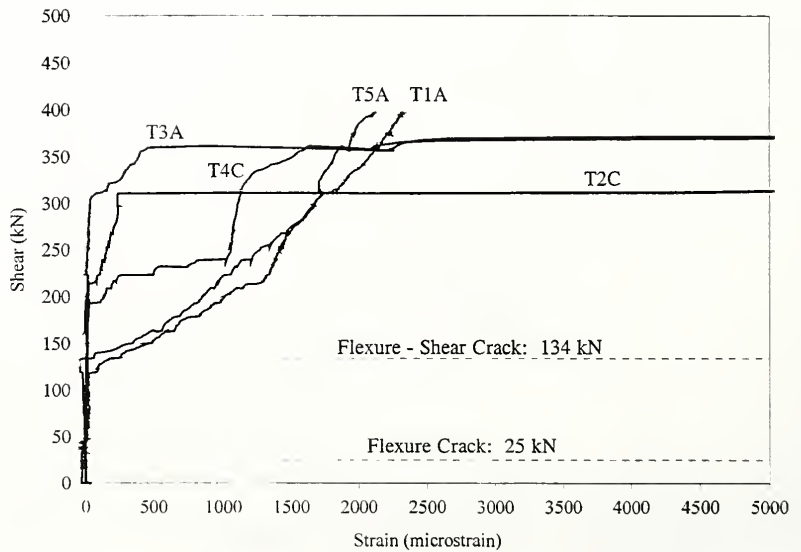


Figure 6.100 Shear-Stirrup Strain Relationship, Specimen 11-LWHD

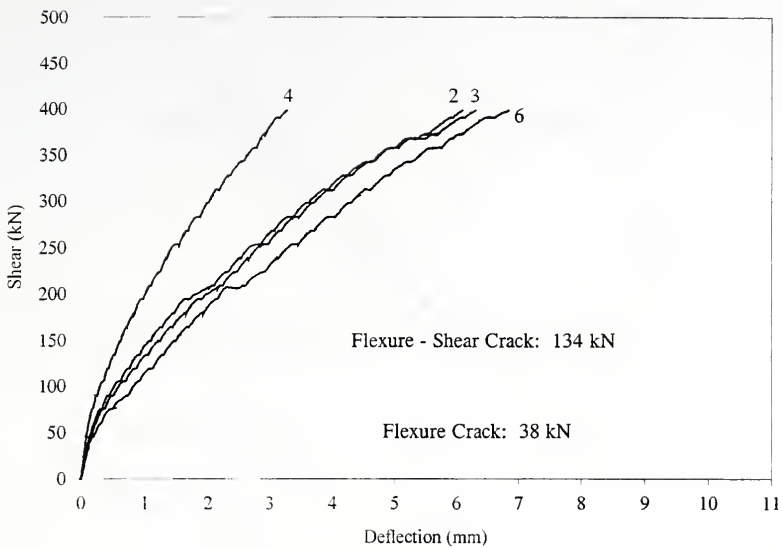


Figure 6.101 Shear-Deflection Relationship, Specimen 12-NWHD

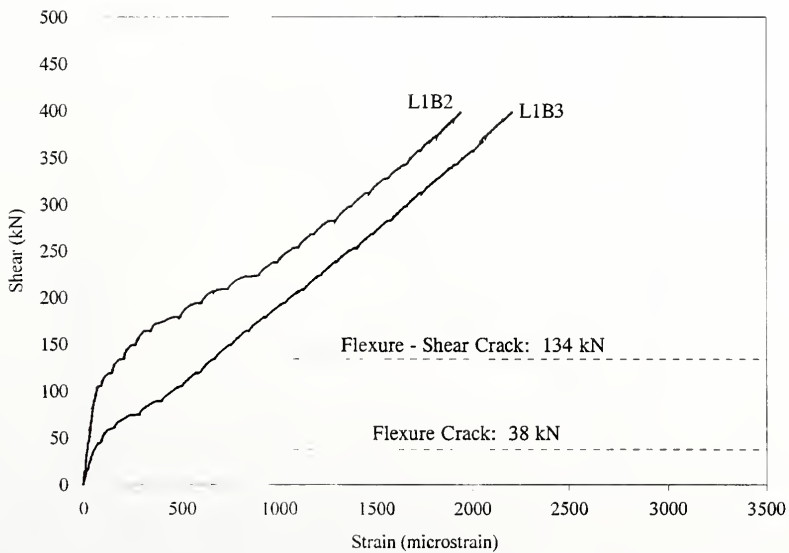


Figure 6.102 Shear-Strain Relationship, Specimen 12-NWHD, Section 1, Bottom Steel

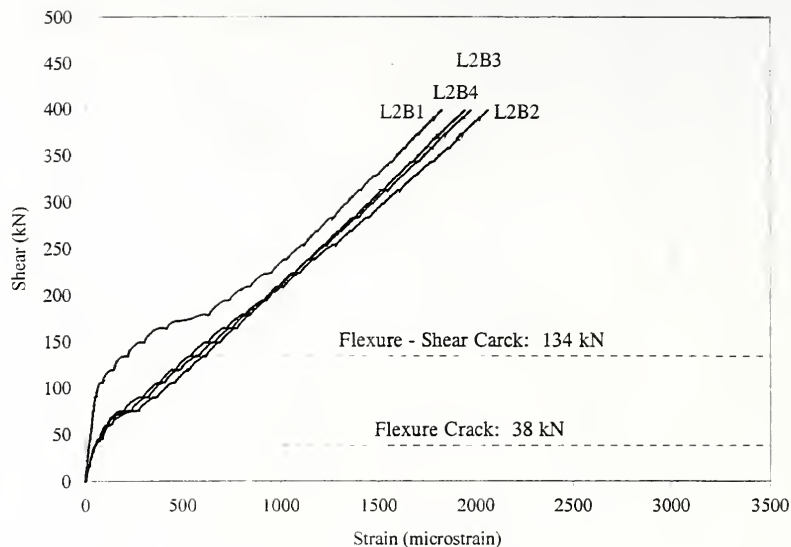


Figure 6.103 Shear-Strain Relationship, Specimen 12-NWHD, Section 2, Bottom Steel

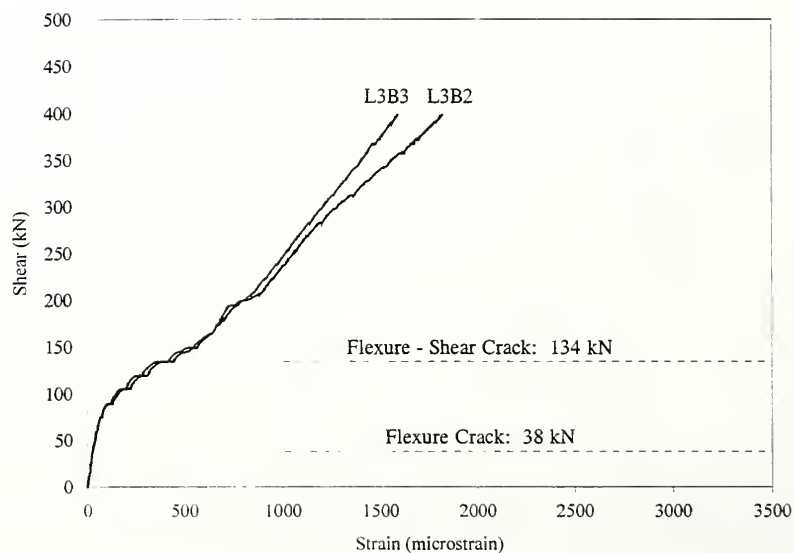


Figure 6.104 Shear-Strain Relationship, Specimen 12-NWHD, Section 3, Bottom Steel

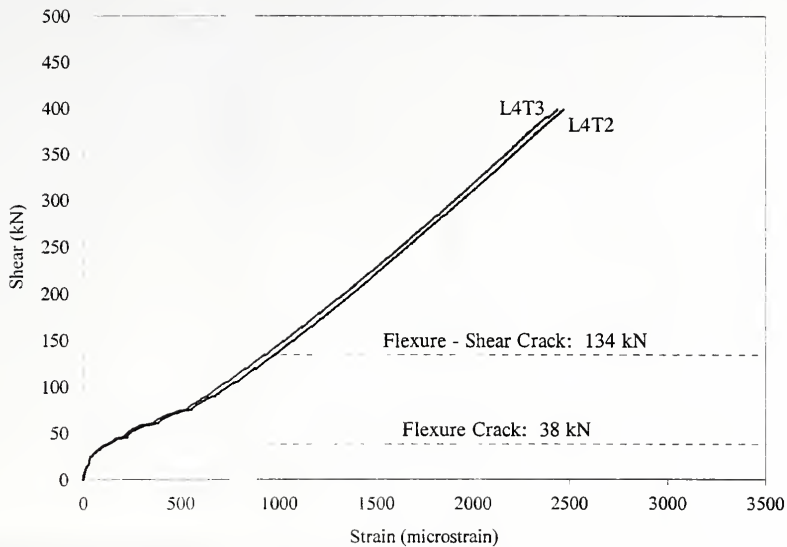


Figure 6.105 Shear-Strain Relationship, Specimen 12-NWHD, Section 4, Top Steel

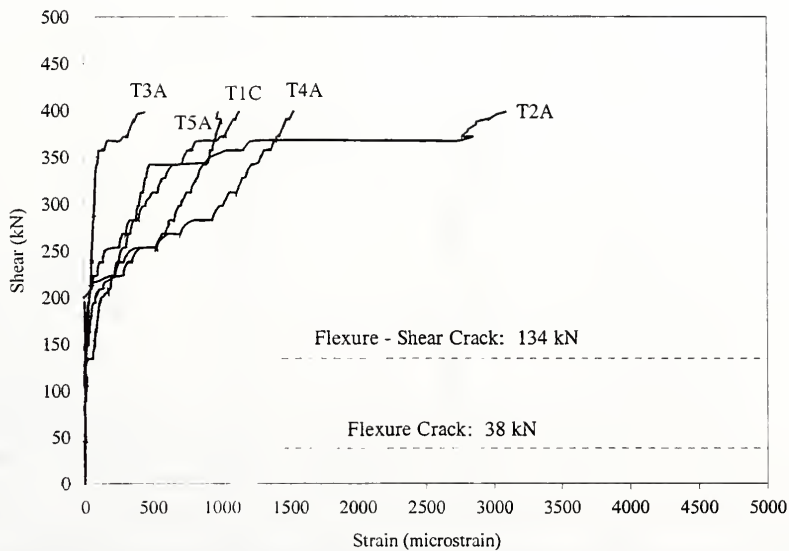


Figure 6.106 Shear-Stirrup Strain Relationship, Specimen 12-NWHD

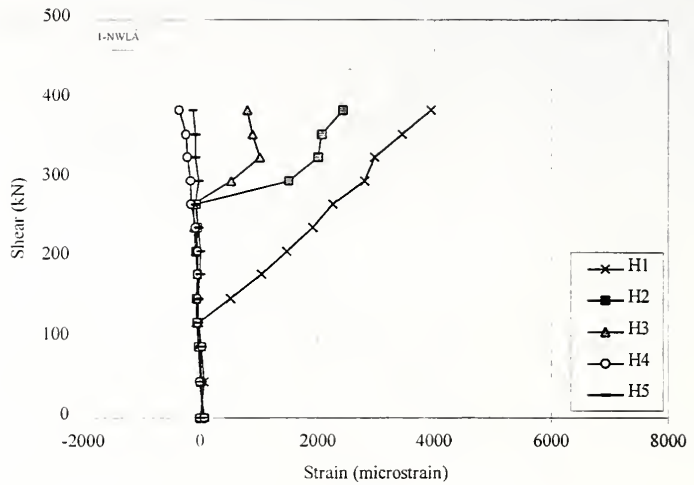


Figure 6.107 Shear-Strain Relationship, Horizontal Whittemore Measurements 1-5, Specimen 1-NWLA

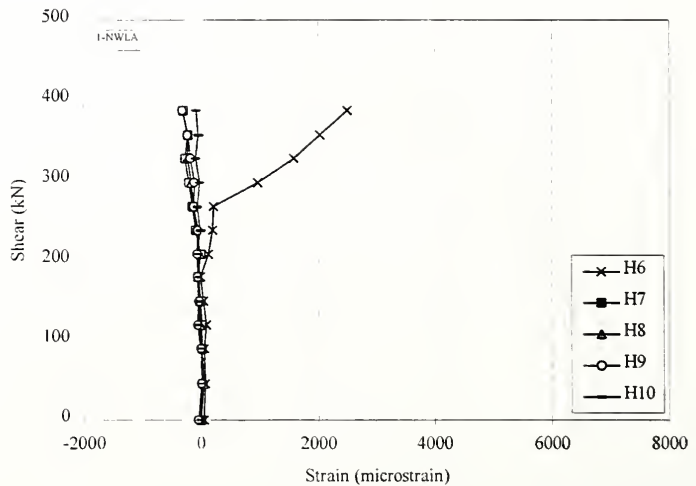


Figure 6.108 Shear-Strain Relationship, Horizontal Whittemore Measurements 6-10, Specimen 1-NWLA

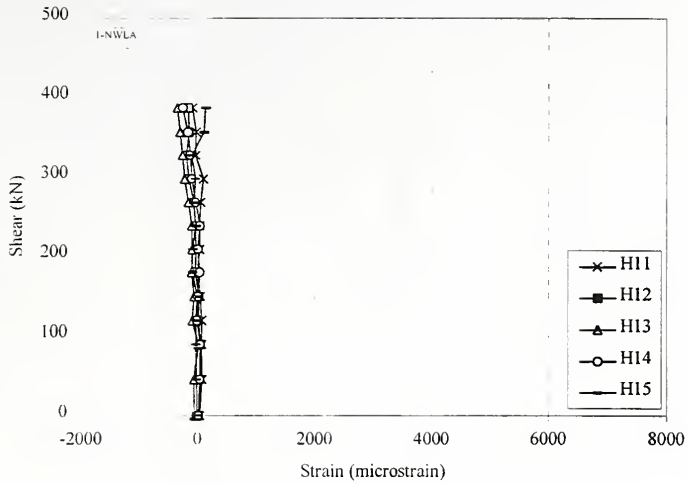


Figure 6.109 Shear-Strain Relationship, Horizontal Whittemore Measurements 11-15, Specimen 1-NWLA

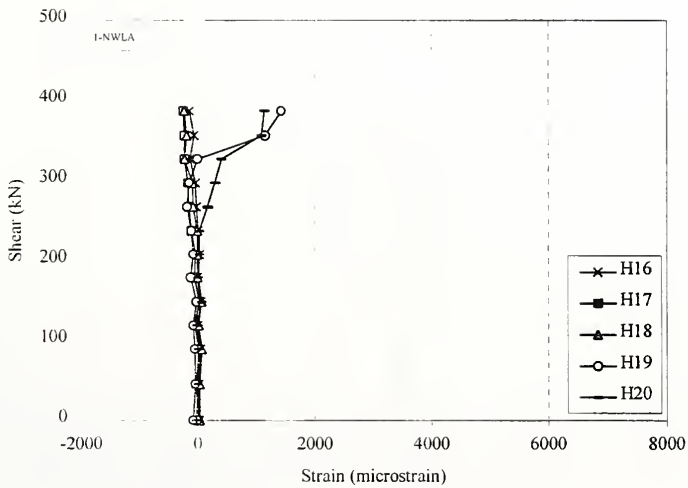


Figure 6.110 Shear-Strain Relationship, Horizontal Whittemore Measurements 16-20, Specimen 1-NWLA

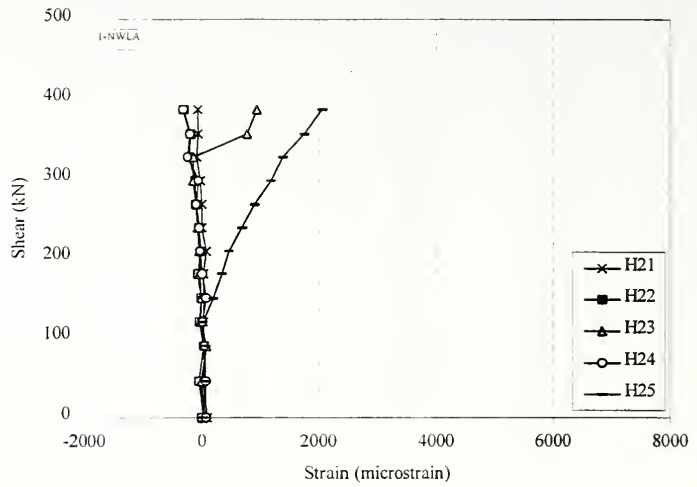


Figure 6.111 Shear-Strain Relationship, Horizontal Whittemore Measurements 21-25, Specimen 1-NWLA

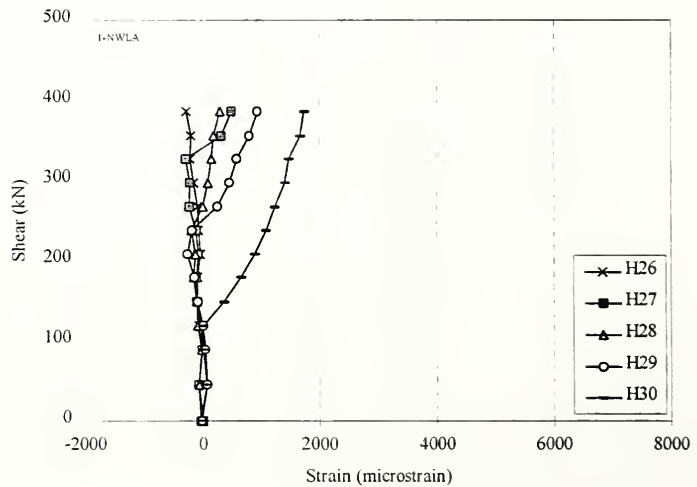


Figure 6.112 Shear-Strain Relationship, Horizontal Whittemore Measurements 26-30, Specimen 1-NWLA

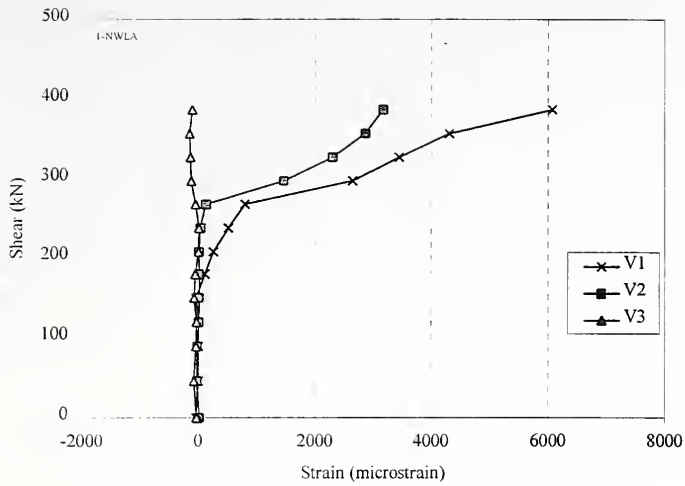


Figure 6.113 Shear-Strain Relationship, Vertical Whittemore Measurements 1-3, Specimen 1-NWLA

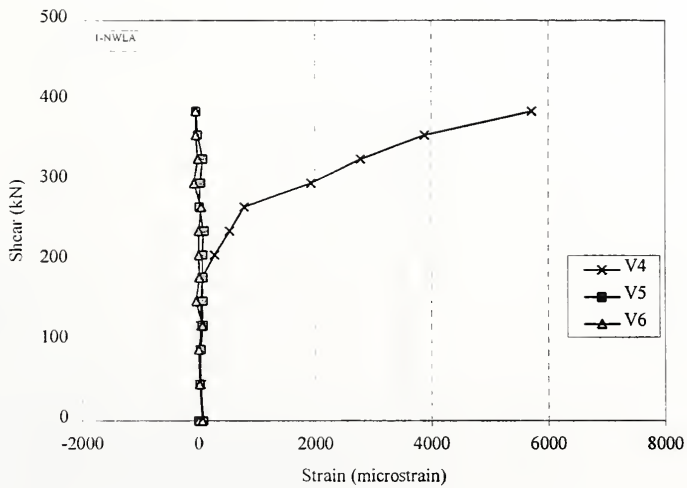


Figure 6.114 Shear-Strain Relationship, Vertical Whittemore Measurements 4-6, Specimen 1-NWLA

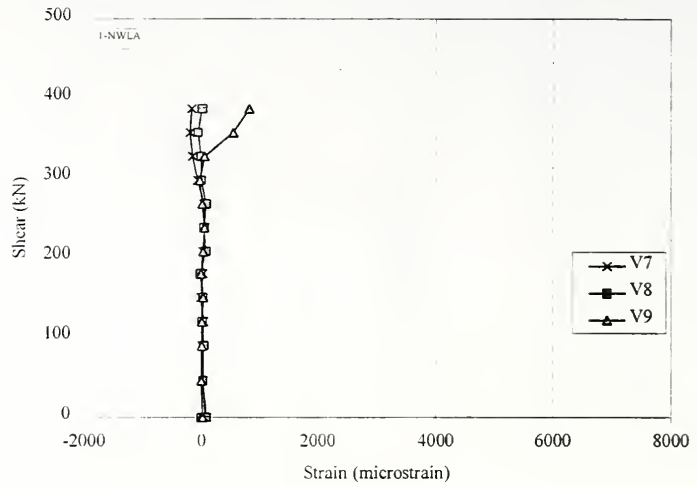


Figure 6.115 Shear-Strain Relationship, Vertical Whittemore Measurements 7-9, Specimen 1-NWLA

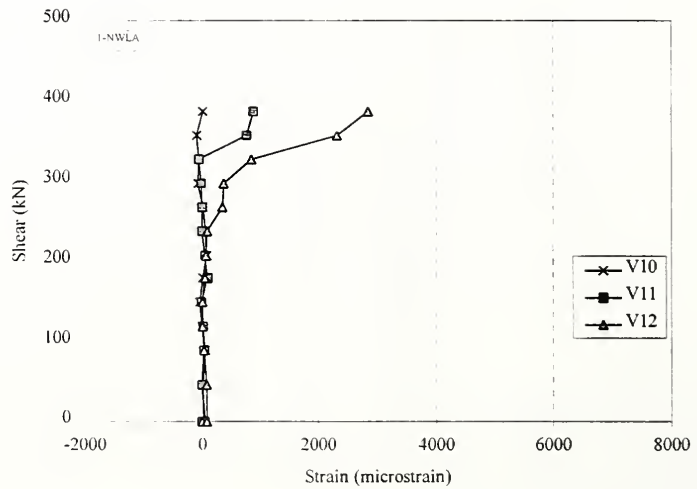


Figure 6.116 Shear-Strain Relationship, Vertical Whittemore Measurements 10-12, Specimen 1-NWLA

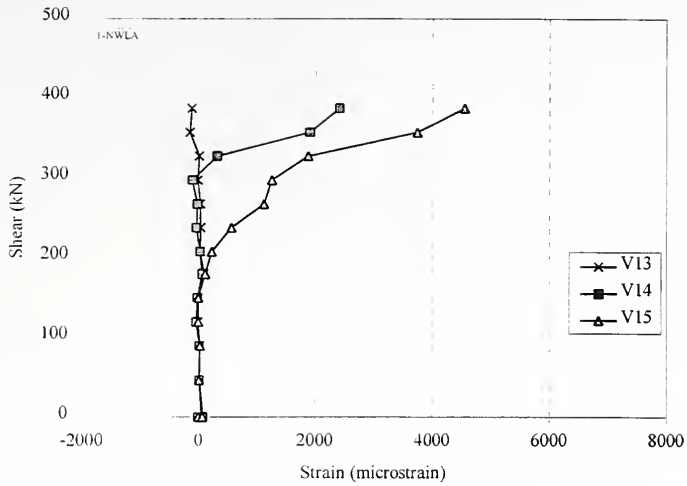


Figure 6.117 Shear-Strain Relationship, Vertical Whittemore Measurements 13-15, Specimen 1-NWLA

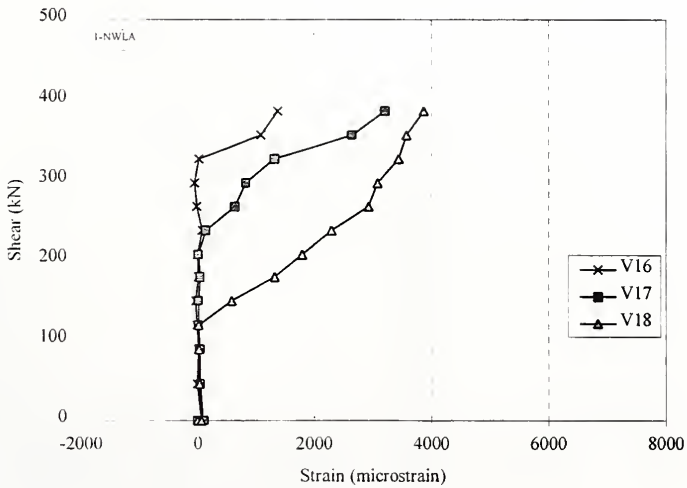


Figure 6.118 Shear-Strain Relationship, Vertical Whittemore Measurements 16-18, Specimen 1-NWLA

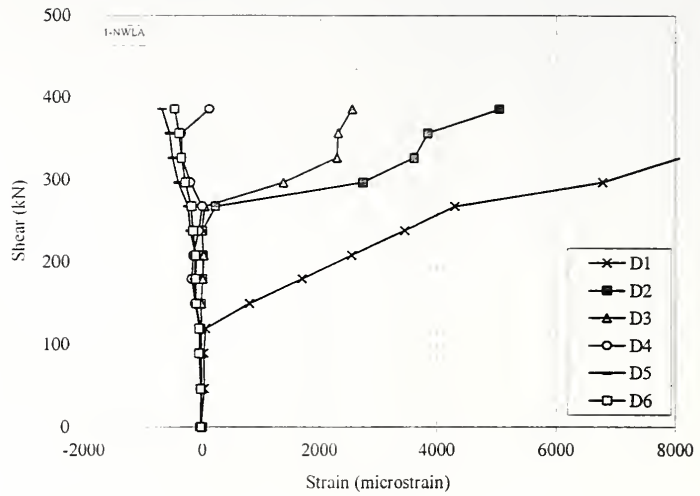


Figure 6.119 Shear-Strain Relationship, Diagonal Whittemore Measurements 1-6, Specimen 1-NWLA

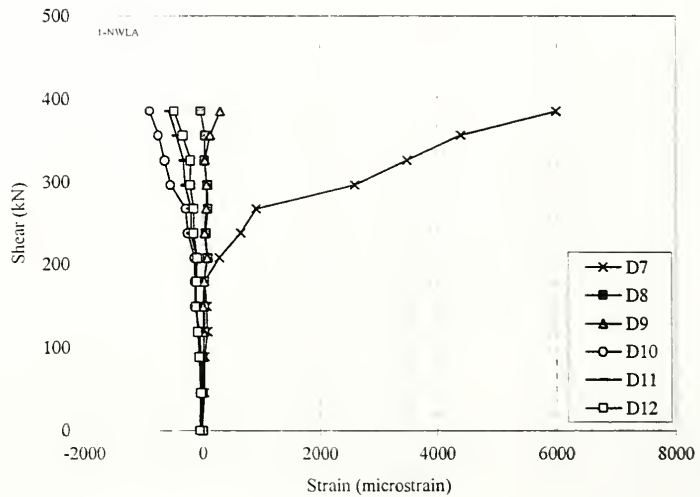


Figure 6.120 Shear-Strain Relationship, Diagonal Whittemore Measurements 7-12, Specimen 1-NWLA

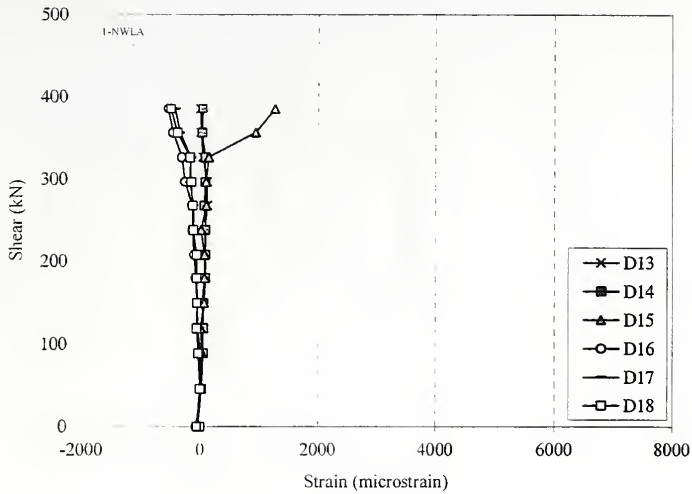


Figure 6.121 Shear-Strain Relationship, Diagonal Whittemore Measurements 13-18, Specimen 1-NWLA

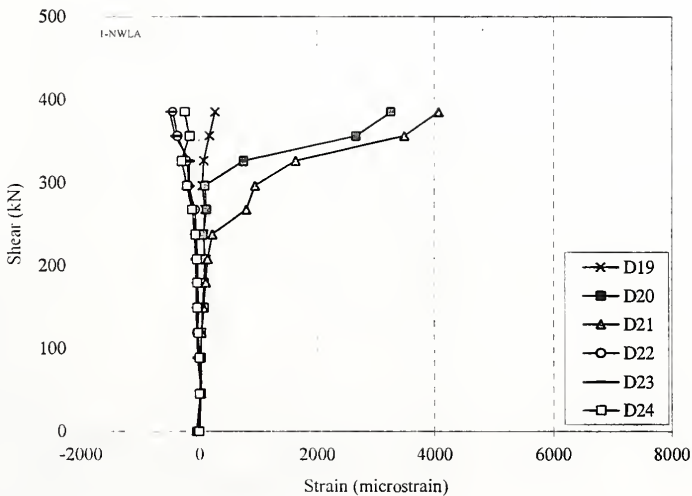


Figure 6.122 Shear-Strain Relationship, Diagonal Whittemore Measurements 19-24, Specimen 1-NWLA

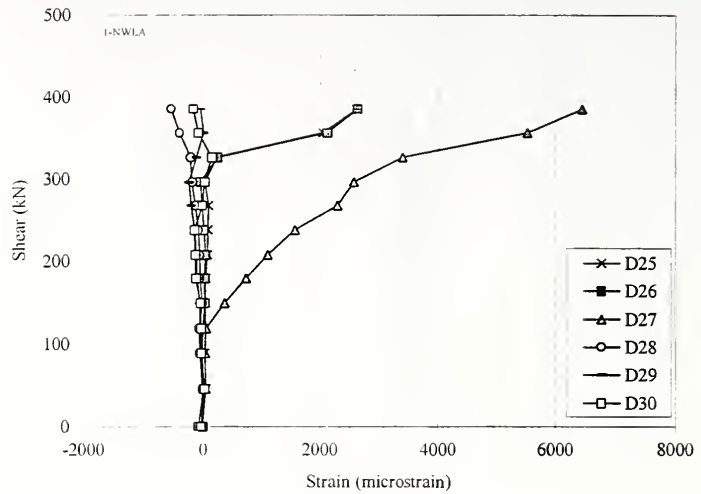


Figure 6.123 Shear-Strain Relationship, Diagonal Whittemore Measurements 25-30, Specimen 1-NWLA

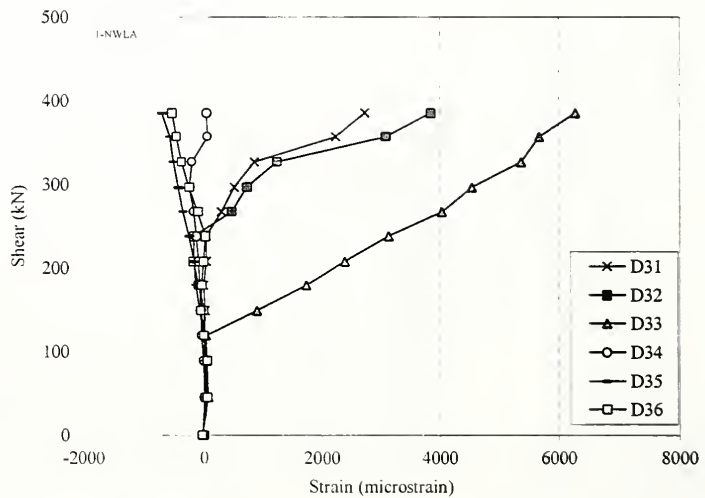


Figure 6.124 Shear-Strain Relationship, Diagonal Whittemore Measurements 31-36, Specimen 1-NWLA

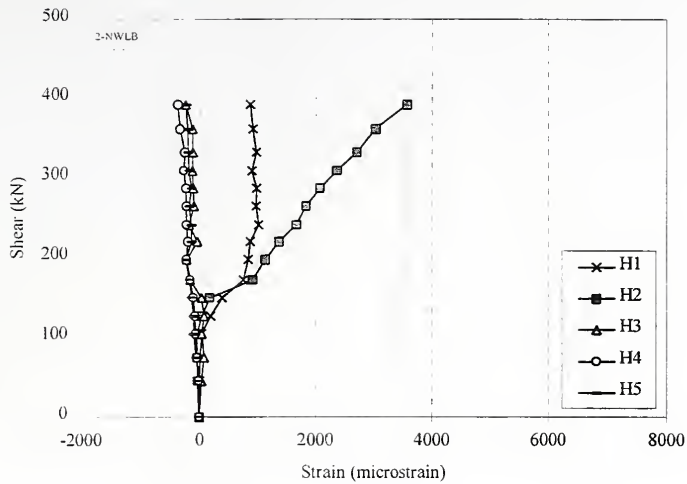


Figure 6.125 Shear-Strain Relationship, Horizontal Whittemore Measurements 1-5, Specimen 2-NWL B

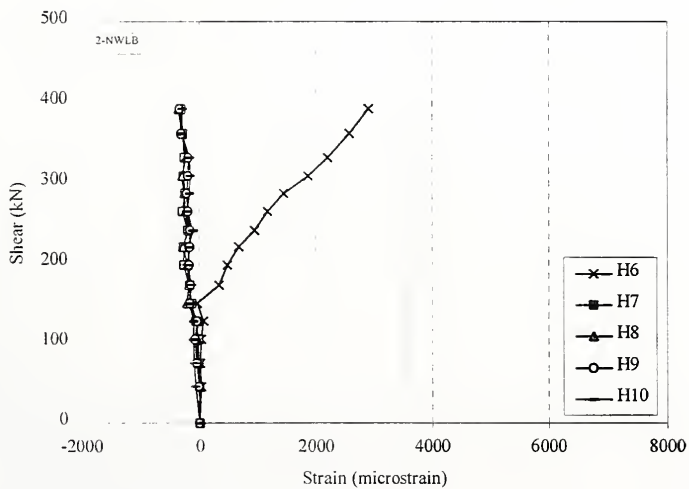


Figure 6.126 Shear-Strain Relationship, Horizontal Whittemore Measurements 6-10, Specimen 2-NWL B

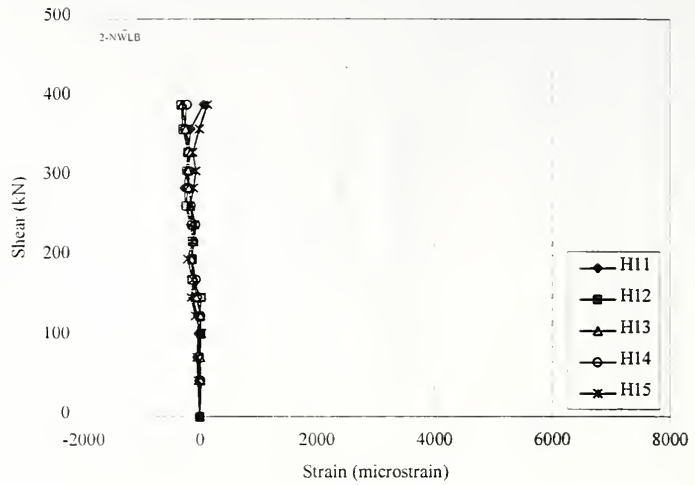


Figure 6.127 Shear-Strain Relationship, Horizontal Whittemore Measurements 11-15, Specimen 2-NWLB

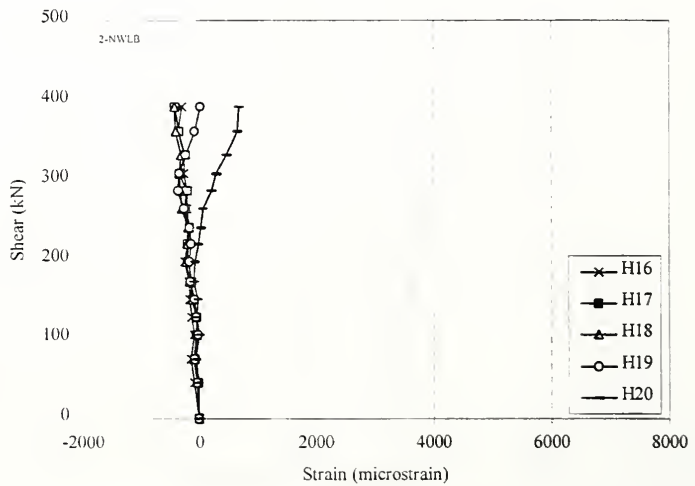


Figure 6.128 Shear-Strain Relationship, Horizontal Whittemore Measurements 16-20, Specimen 2-NWLB

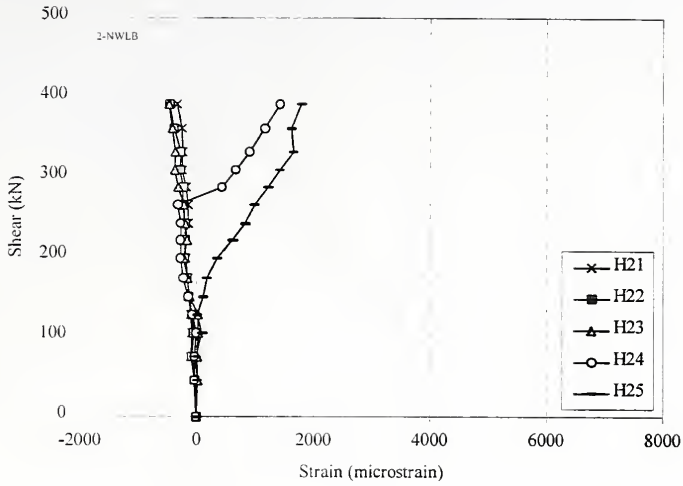


Figure 6.129 Shear-Strain Relationship, Horizontal Whittemore Measurements 21-25, Specimen 2-NWLB

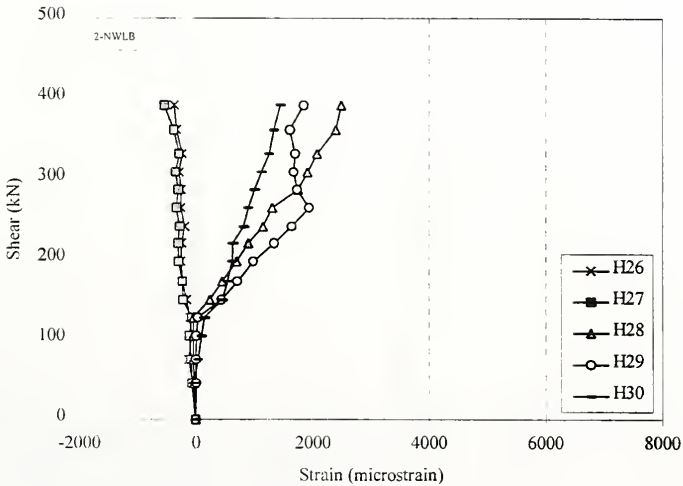


Figure 6.130 Shear-Strain Relationship, Horizontal Whittemore Measurements 26-30, Specimen 2-NWLB

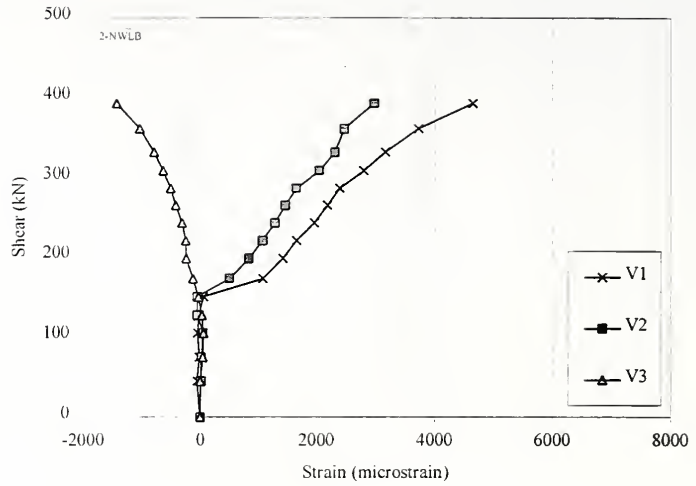


Figure 6.131 Shear-Strain Relationship, Vertical Whittemore Measurements 1-3, Specimen 2-NWLB

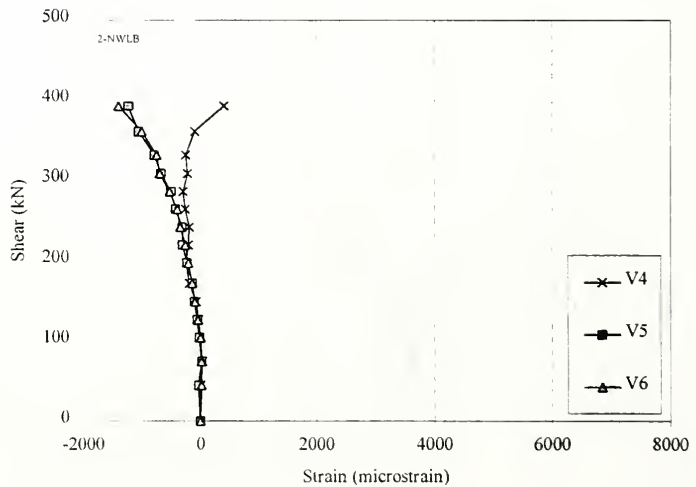


Figure 6.132 Shear-Strain Relationship, Vertical Whittemore Measurements 4-6, Specimen 2-NWLB

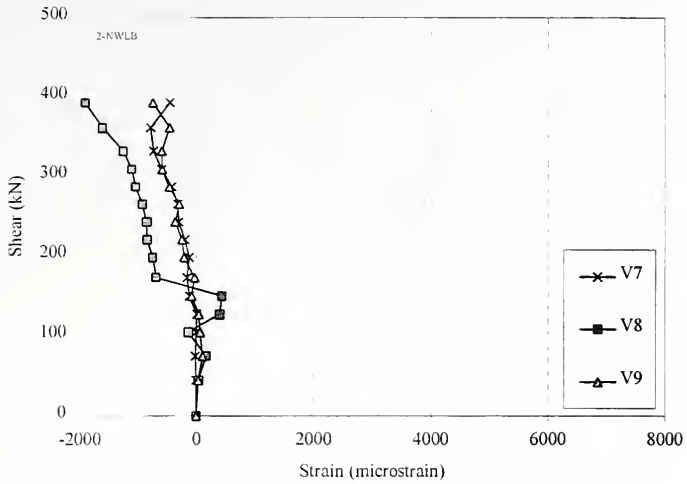


Figure 6.133 Shear-Strain Relationship, Vertical Whittemore Measurements 7-9, Specimen 2-NWLb

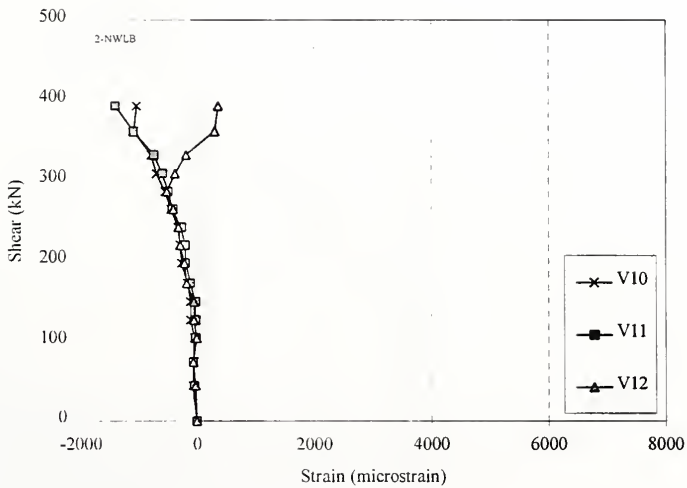


Figure 6.134 Shear-Strain Relationship, Vertical Whittemore Measurements 10-12, Specimen 2-NWLb

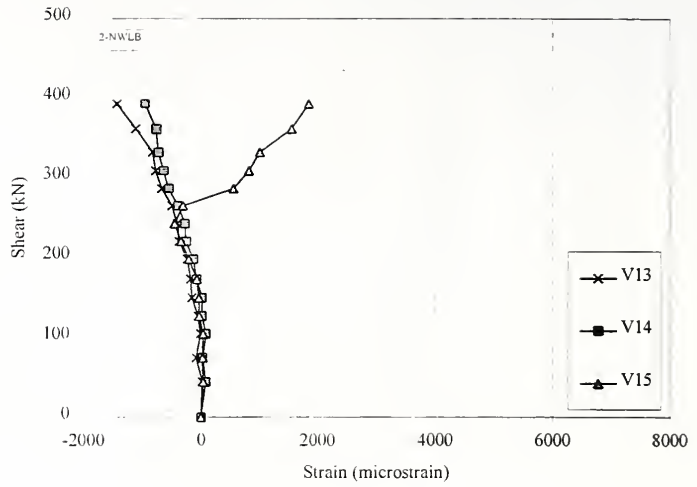


Figure 6.135 Shear-Strain Relationship, Vertical Whittemore Measurements 13-15, Specimen 2-NWLB

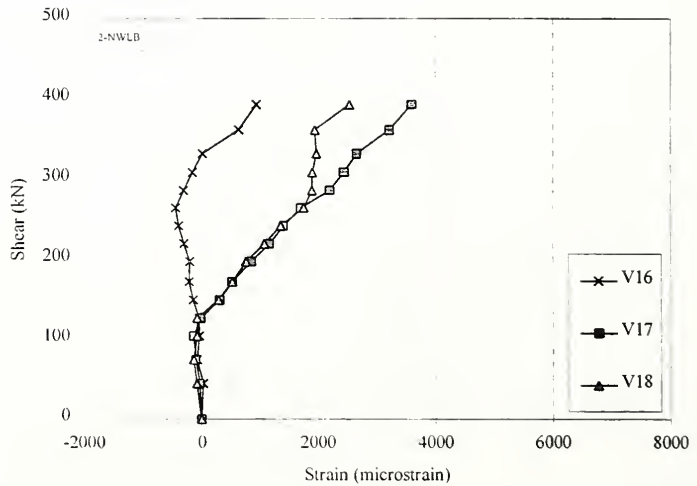


Figure 6.136 Shear-Strain Relationship, Vertical Whittemore Measurements 16-18, Specimen 2-NWLB

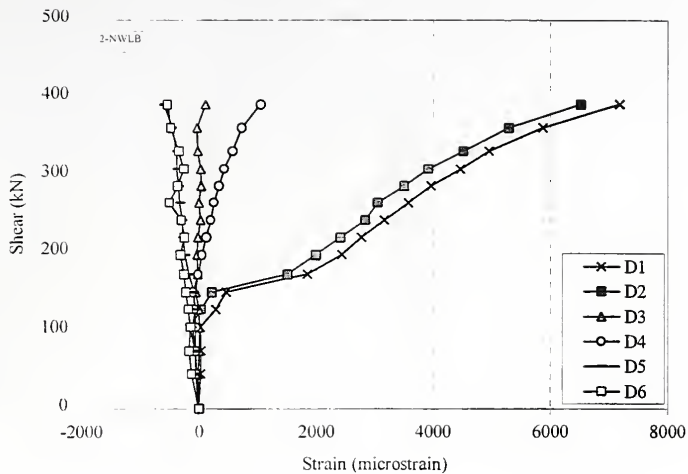


Figure 6.137 Shear-Strain Relationship, Diagonal Whittemore Measurements 1-6, Specimen 2-NWLB

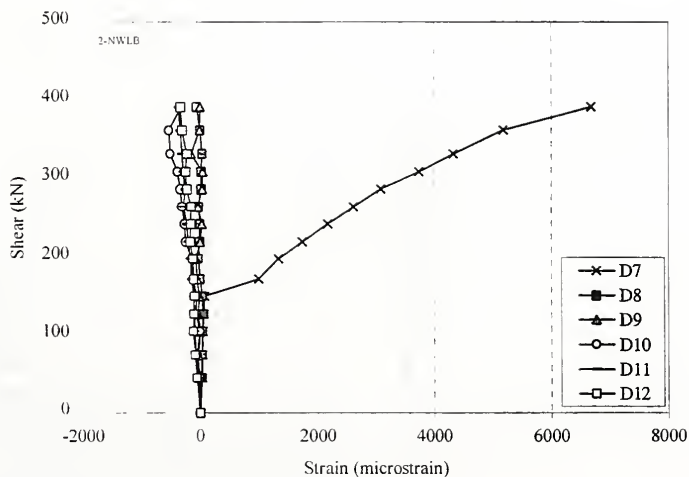


Figure 6.138 Shear-Strain Relationship, Diagonal Whittemore Measurements 7-12, Specimen 2-NWLB

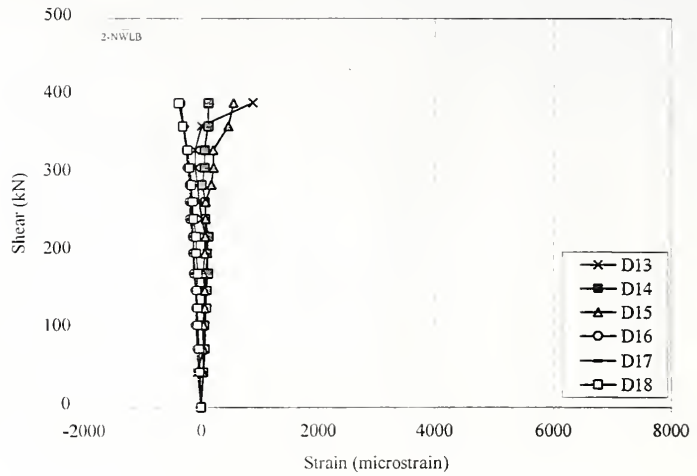


Figure 6.139 Shear-Strain Relationship, Diagonal Whittemore Measurements 13-18, Specimen 2-NWLB

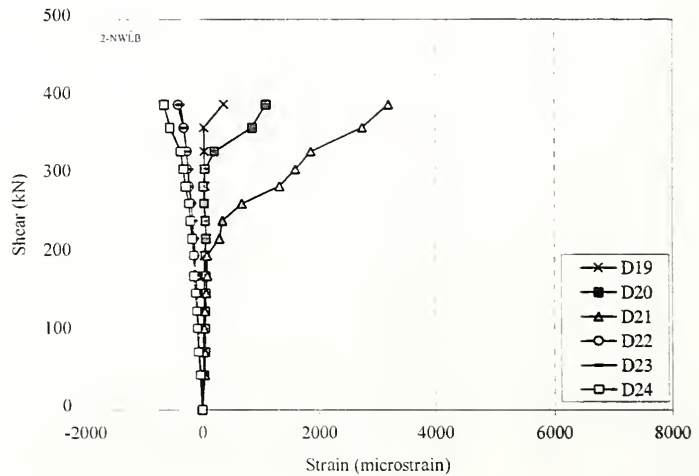


Figure 6.140 Shear-Strain Relationship, Diagonal Whittemore Measurements 19-24, Specimen 2-NWLB

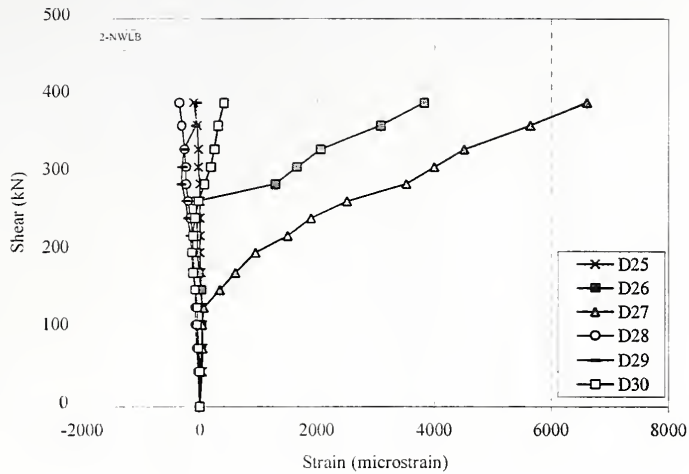


Figure 6.141 Shear-Strain Relationship, Diagonal Whittemore Measurements 25-30, Specimen 2-NWLB

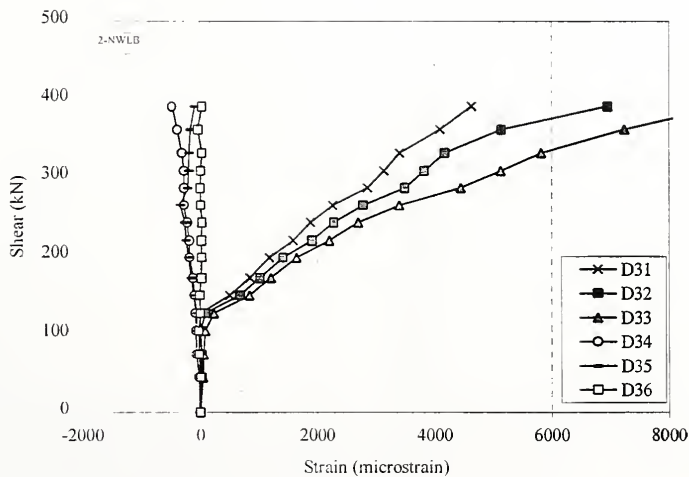


Figure 6.142 Shear-Strain Relationship, Diagonal Whittemore Measurements 31-36, Specimen 2-NWLB

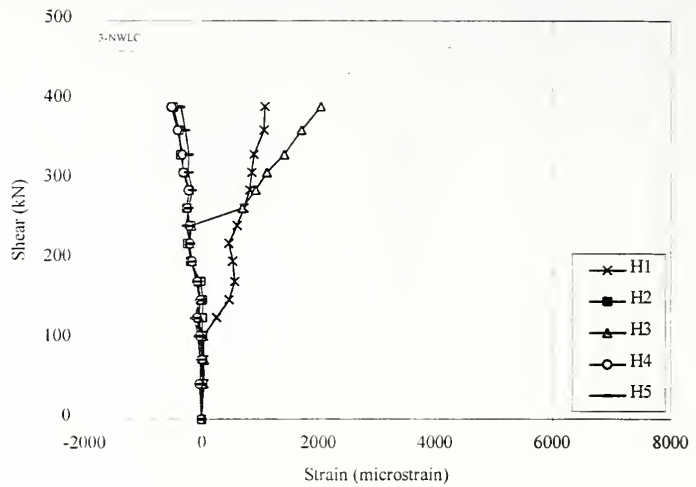


Figure 6.143 Shear-Strain Relationship. Horizontal Whittemore Measurements 1-5, Specimen 3-NWLC

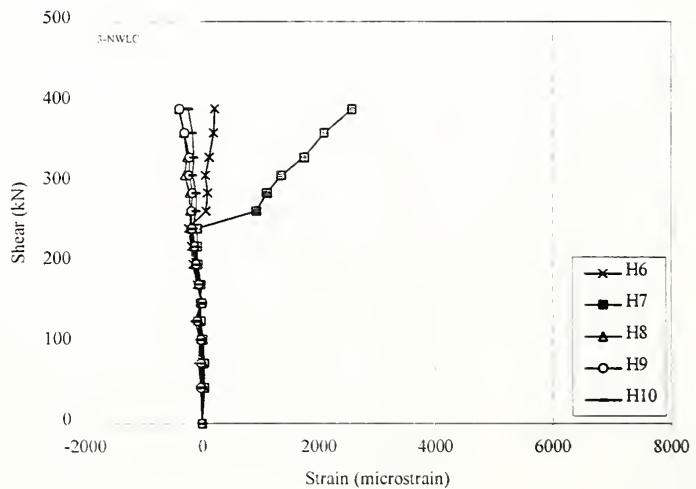


Figure 6.144 Shear-Strain Relationship. Horizontal Whittemore Measurements 6-10, Specimen 3-NWLC

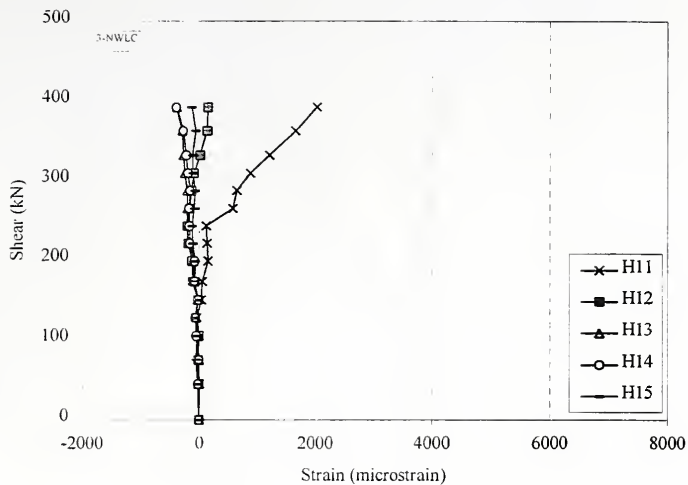


Figure 6.145 Shear-Strain Relationship, Horizontal Whittemore Measurements 11-15, Specimen 3-NWLC

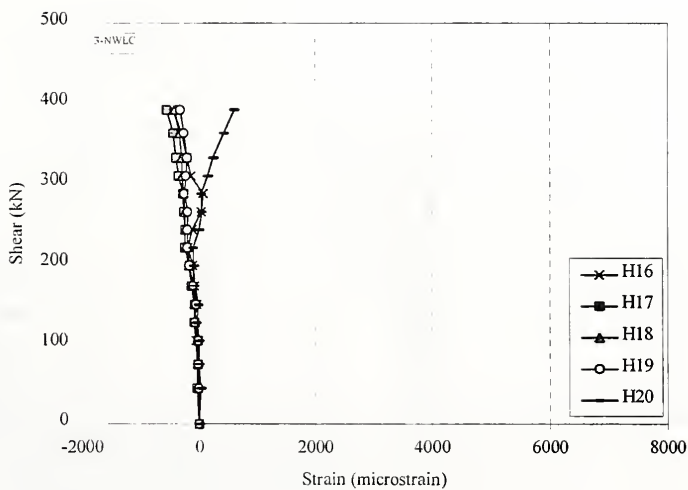


Figure 6.146 Shear-Strain Relationship, Horizontal Whittemore Measurements 16-20, Specimen 3-NWLC

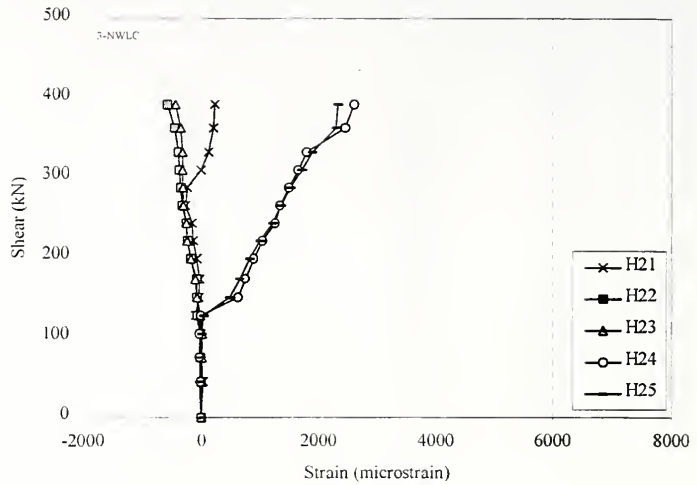


Figure 6.147 Shear-Strain Relationship, Horizontal Whittemore Measurements 21-25, Specimen 3-NWLC

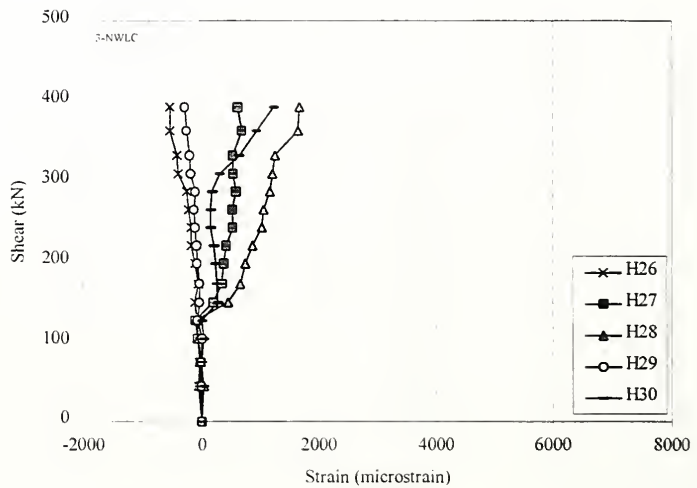


Figure 6.148 Shear-Strain Relationship, Horizontal Whittemore Measurements 26-30, Specimen 3-NWLC

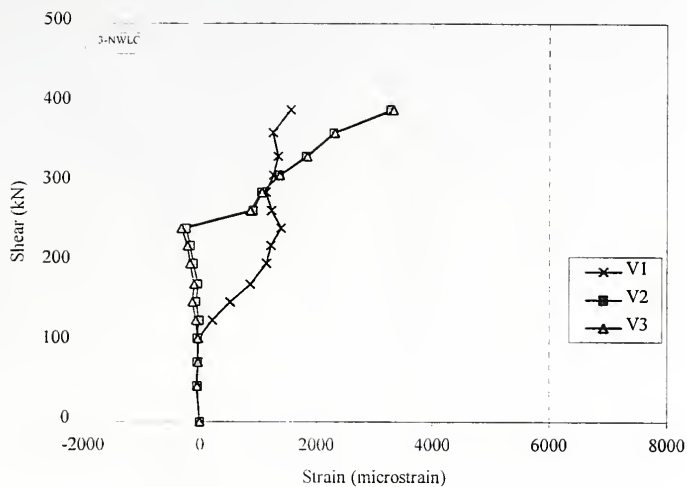


Figure 6.149 Shear-Strain Relationship, Vertical Whittemore Measurements 1-3, Specimen 3-NWLC

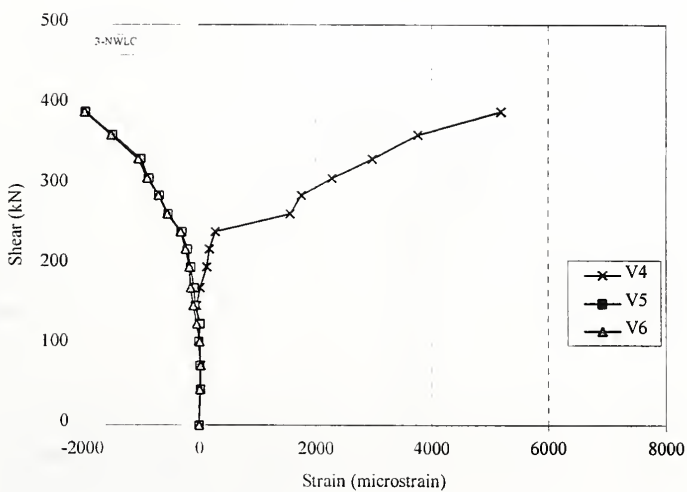


Figure 6.150 Shear-Strain Relationship, Vertical Whittemore Measurements 4-6, Specimen 3-NWLC

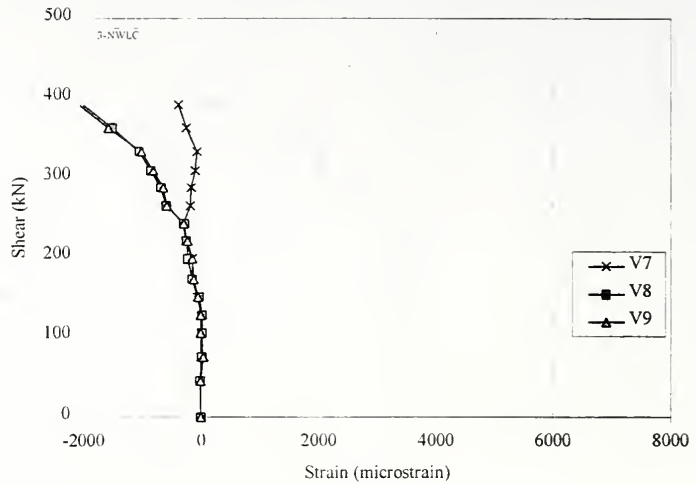


Figure 6.151 Shear-Strain Relationship, Vertical Whittemore Measurements 7-9, Specimen 3-NWLC

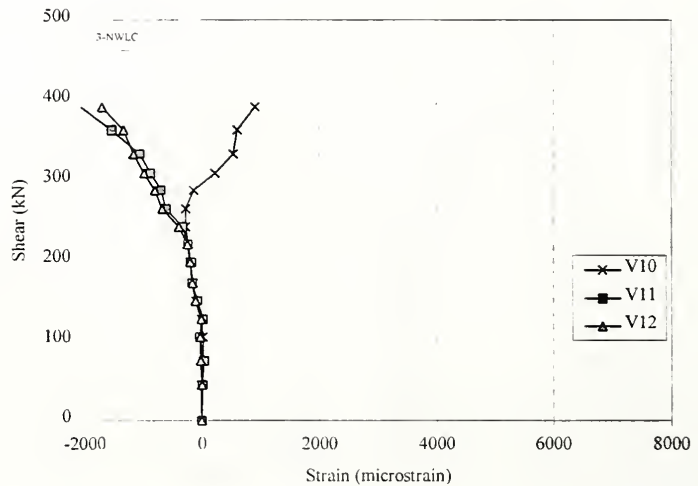


Figure 6.152 Shear-Strain Relationship, Vertical Whittemore Measurements 10-12, Specimen 3-NWLC

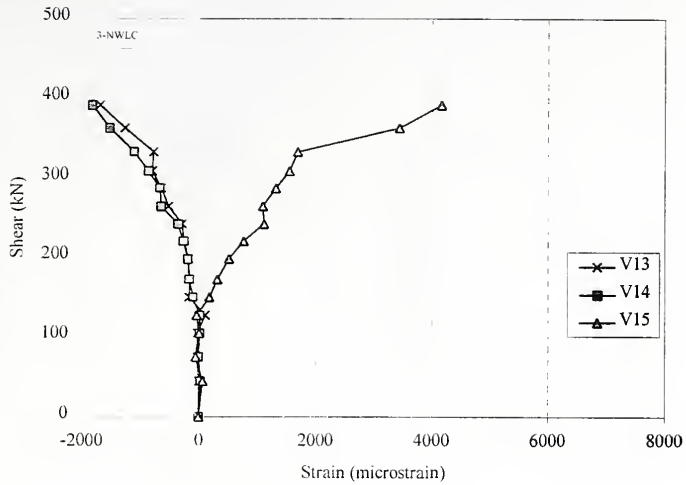


Figure 6.153 Shear-Strain Relationship. Vertical Whittemore Measurements 13-15, Specimen 3-NWLC

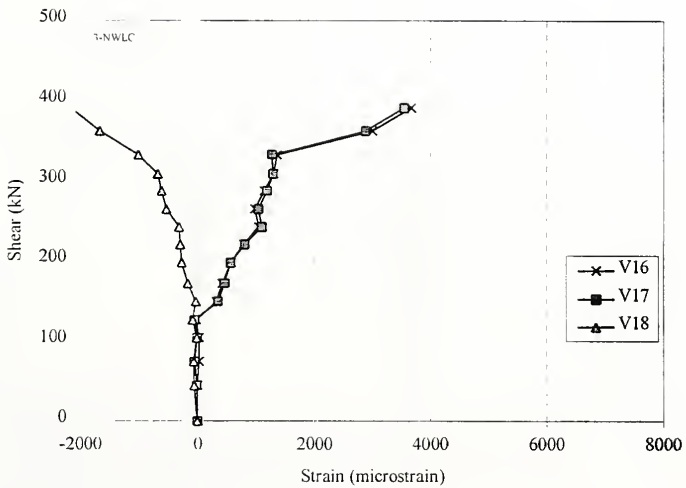


Figure 6.154 Shear-Strain Relationship. Vertical Whittemore Measurements 16-18, Specimen 3-NWLC

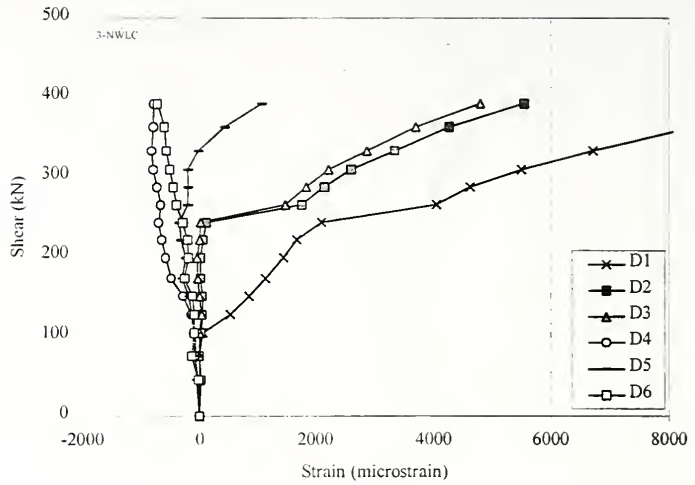


Figure 6.155 Shear-Strain Relationship, Diagonal Whittemore Measurements 1-6, Specimen 3-NWLC

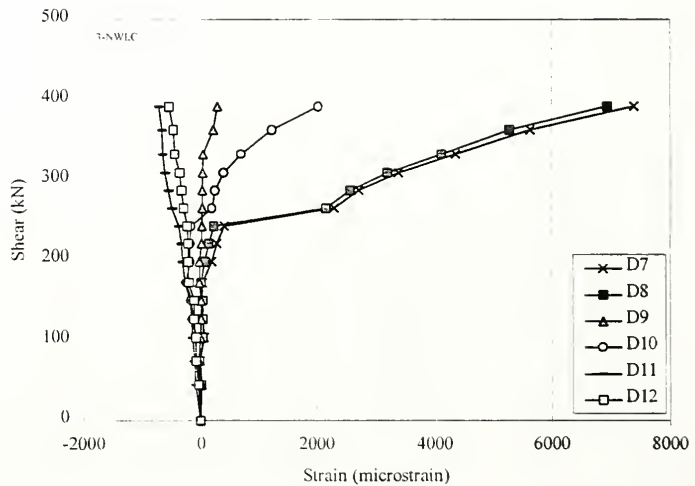


Figure 6.156 Shear-Strain Relationship, Diagonal Whittemore Measurements 7-12, Specimen 3-NWLC

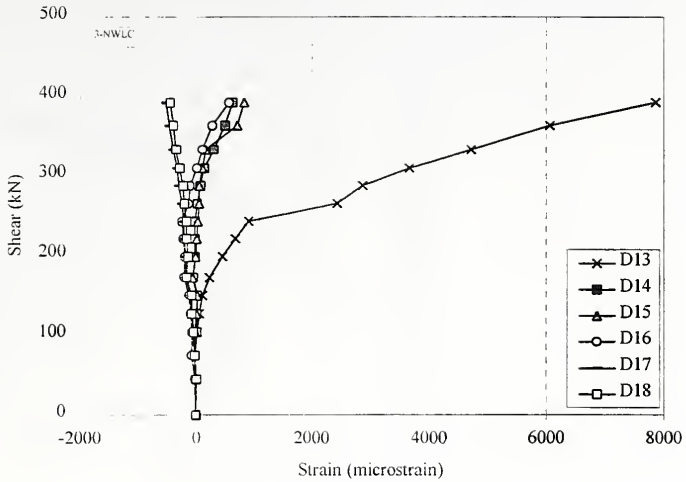


Figure 6.157 Shear-Strain Relationship, Diagonal Whittemore Measurements 13-18, Specimen 3-NWLC

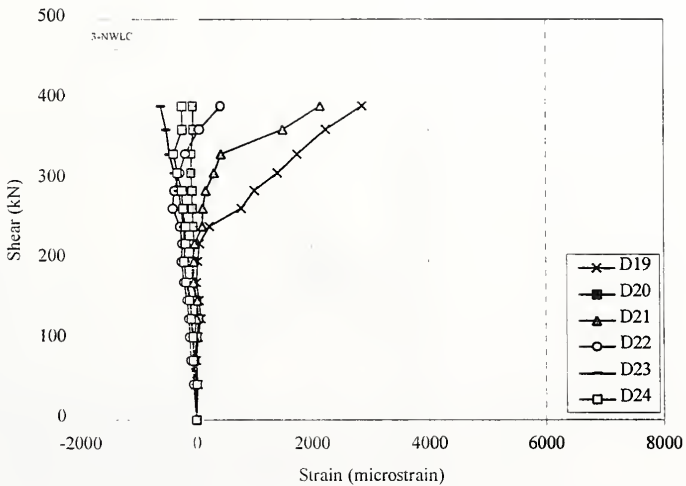


Figure 6.158 Shear-Strain Relationship, Diagonal Whittemore Measurements 19-24, Specimen 3-NWLC

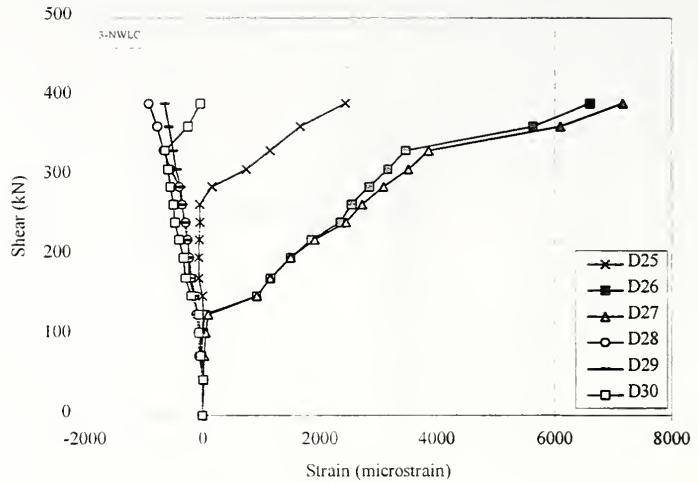


Figure 6.159 Shear-Strain Relationship, Diagonal Whittemore Measurements 25-30, Specimen 3-NWLC

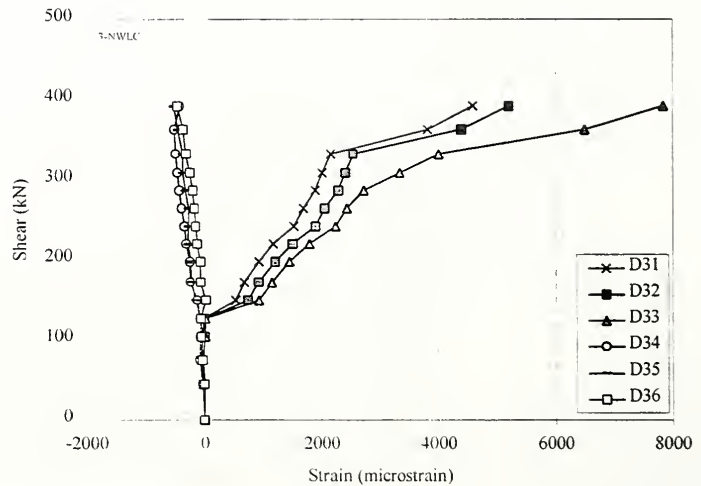


Figure 6.160 Shear-Strain Relationship, Diagonal Whittemore Measurements 31-36, Specimen 3-NWLC

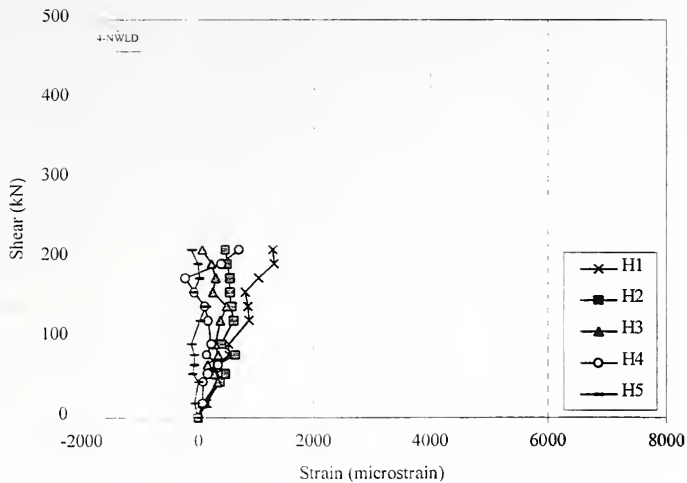


Figure 6.161 Shear-Strain Relationship, Horizontal Whittemore Measurements 1-5, Specimen 4-NWLD

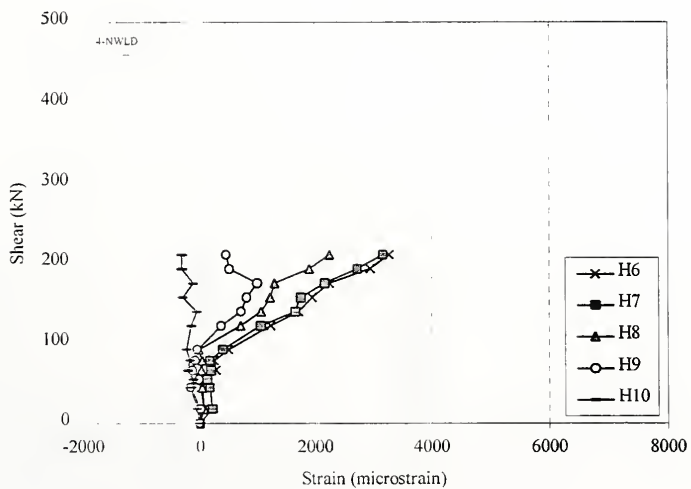


Figure 6.162 Shear-Strain Relationship, Horizontal Whittemore Measurements 6-10, Specimen 4-NWLD

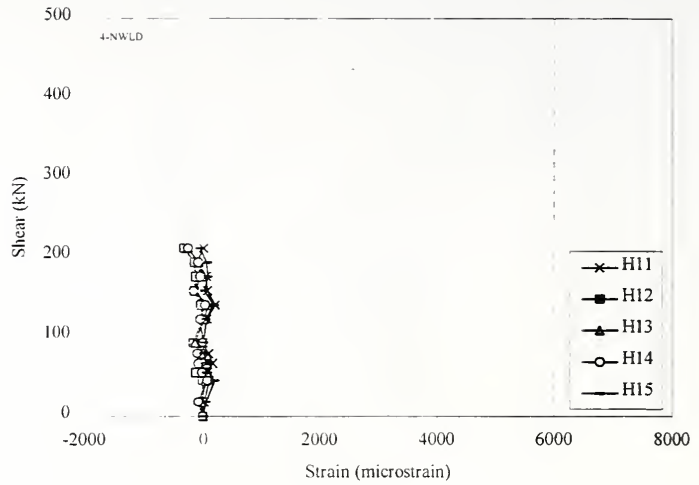


Figure 6.163 Shear-Strain Relationship. Horizontal Whittemore Measurements 11-15, Specimen 4-NWLD

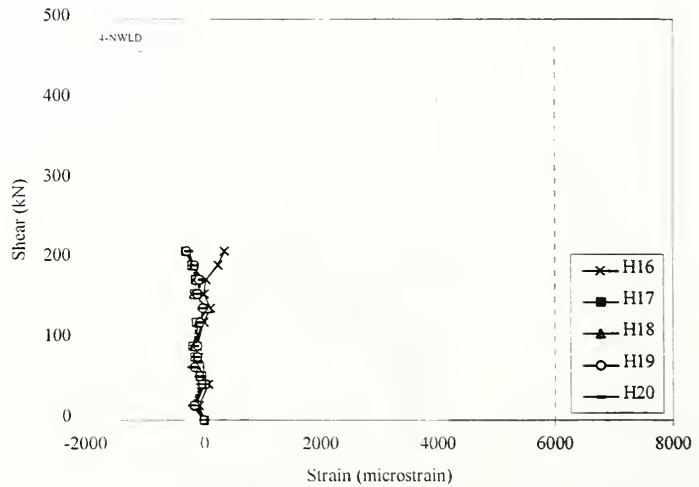


Figure 6.164 Shear-Strain Relationship. Horizontal Whittemore Measurements 16-20, Specimen 4-NWLD

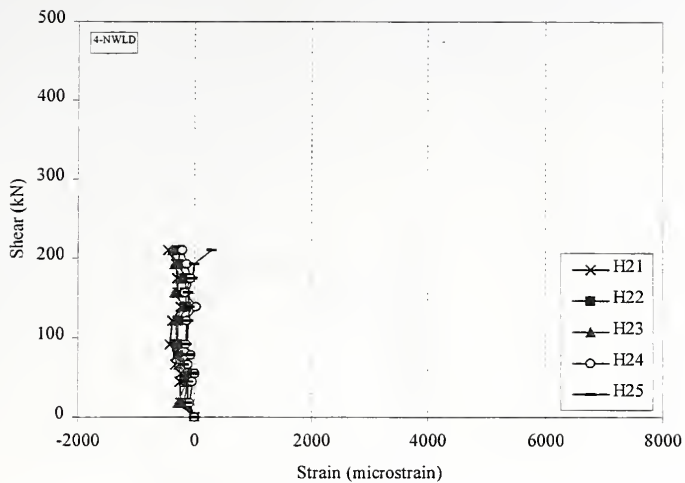


Figure 6.165 Shear-Strain Relationship, Horizontal Whittemore Measurements 21-25, Specimen 4-NWLD

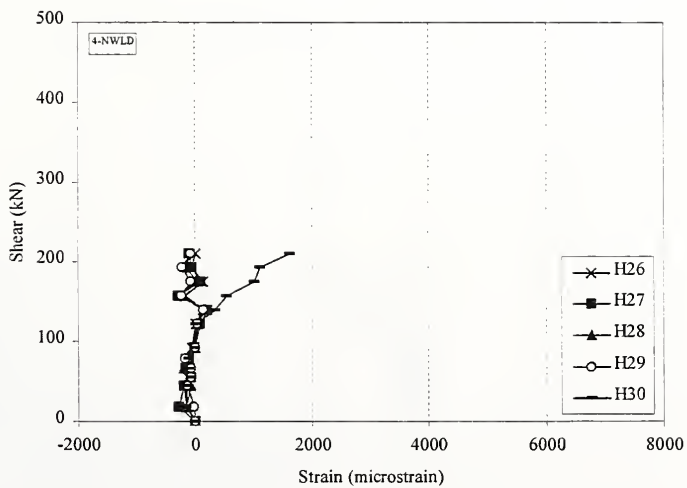


Figure 6.166 Shear-Strain Relationship, Horizontal Whittemore Measurements 26-30, Specimen 4-NWLD

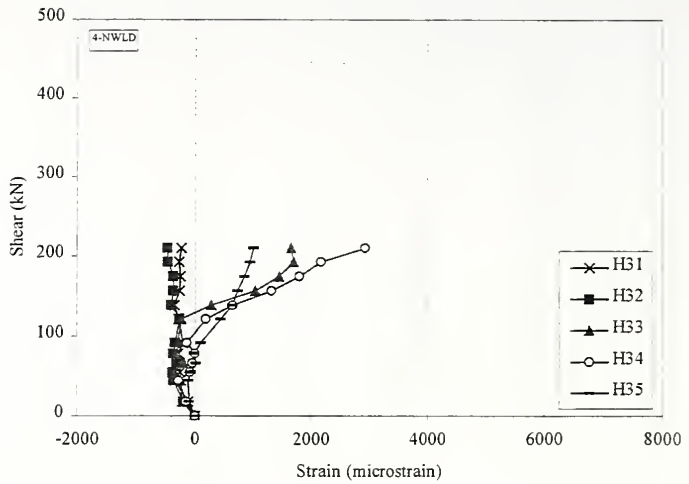


Figure 6.167 Shear-Strain Relationship, Horizontal Whittemore Measurements 31-35, Specimen 4-NWLD

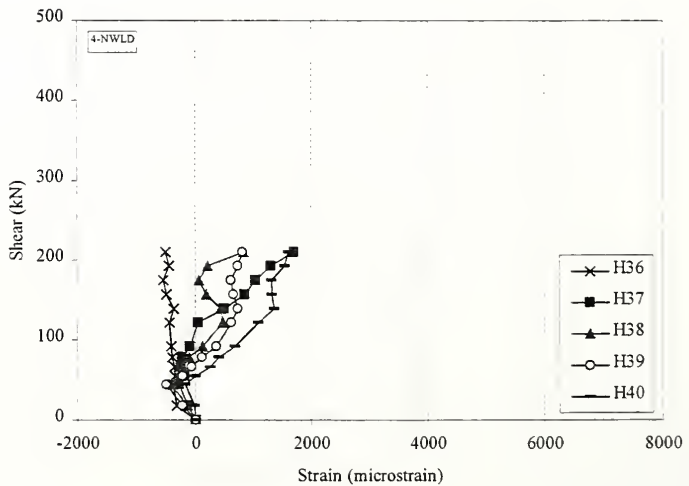


Figure 6.168 Shear-Strain Relationship, Horizontal Whittemore Measurements 36-40, Specimen 4-NWLD

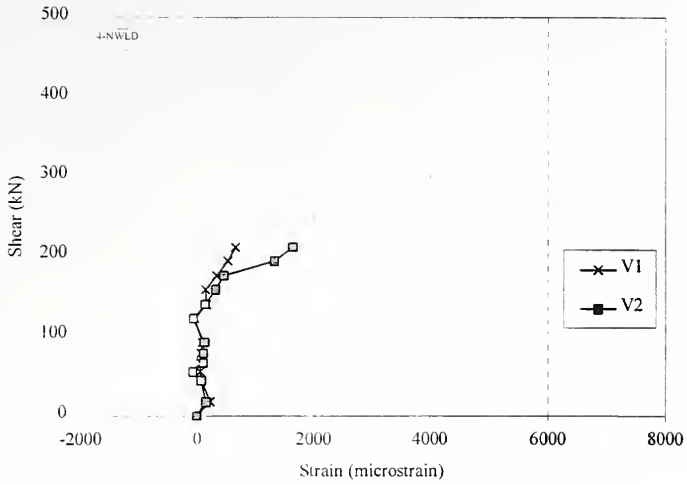


Figure 6.169 Shear-Strain Relationship, Vertical Whittemore Measurements 1-2, Specimen 4-NWLD

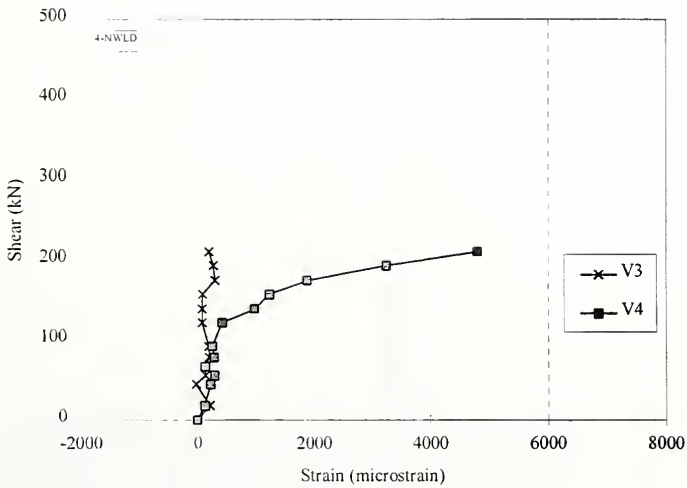


Figure 6.170 Shear-Strain Relationship, Vertical Whittemore Measurements 3-4, Specimen 4-NWLD

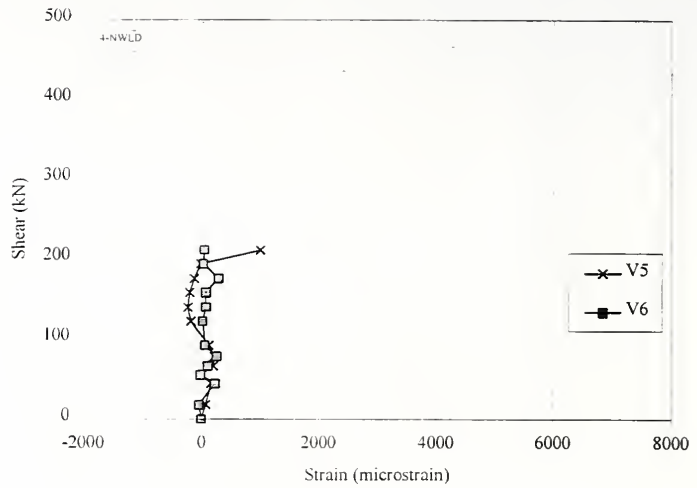


Figure 6.171 Shear-Strain Relationship, Vertical Whittemore Measurements 5-6, Specimen 4-NWLD

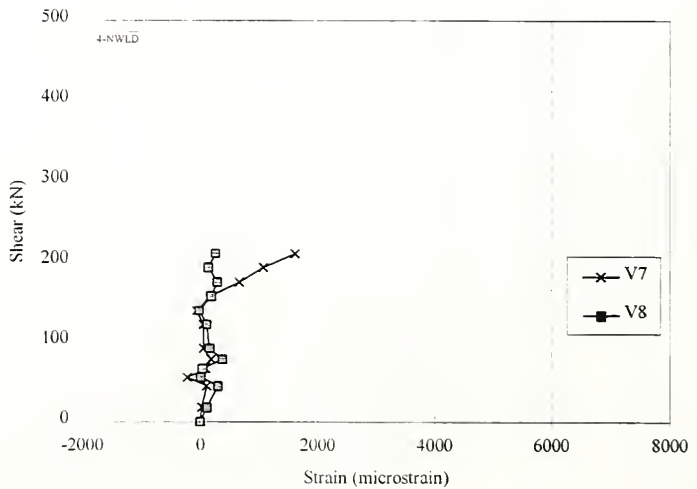


Figure 6.172 Shear-Strain Relationship, Vertical Whittemore Measurements 7-8, Specimen 4-NWLD

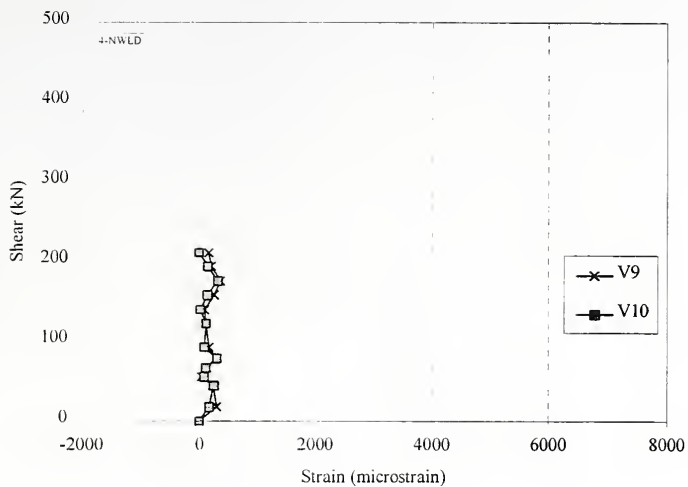


Figure 6.173 Shear-Strain Relationship, Vertical Whittemore Measurements 9-10, Specimen 4-NWLD

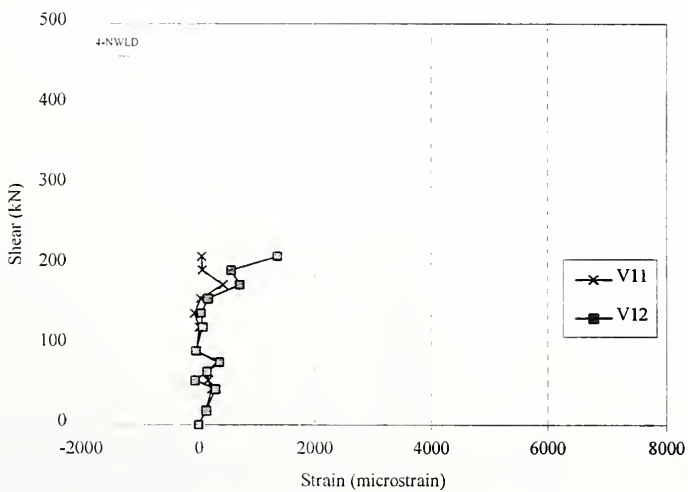


Figure 6.174 Shear-Strain Relationship, Vertical Whittemore Measurements 11-12, Specimen 4-NWLD

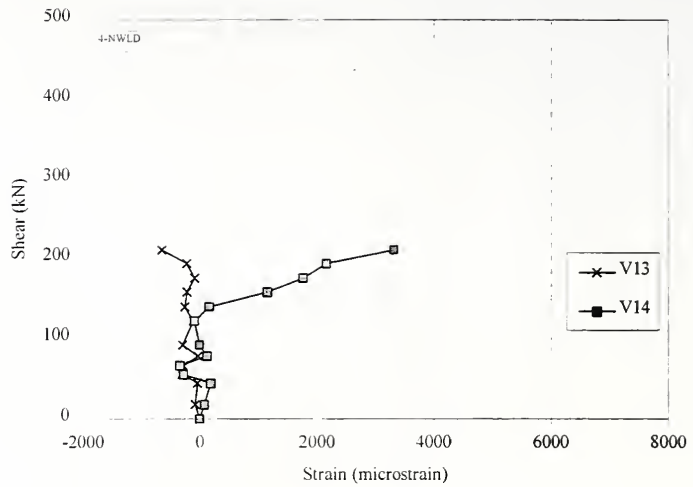


Figure 6.175 Shear-Strain Relationship, Vertical Whittemore Measurements 13-14, Specimen 4-NWLD

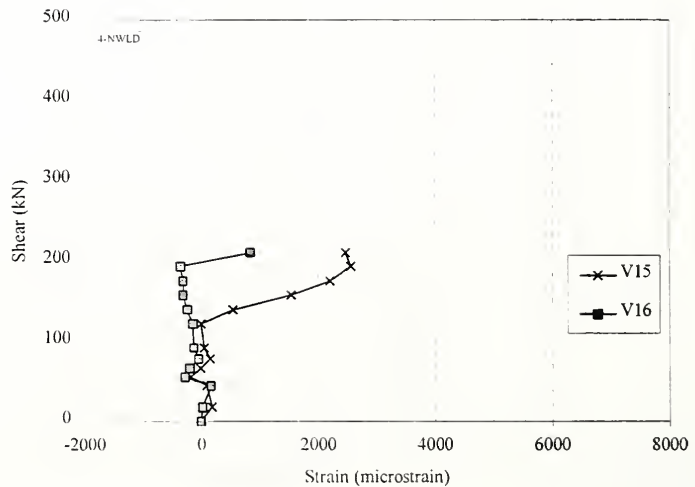


Figure 6.176 Shear-Strain Relationship, Vertical Whittemore Measurements 15-16, Specimen 4-NWLD

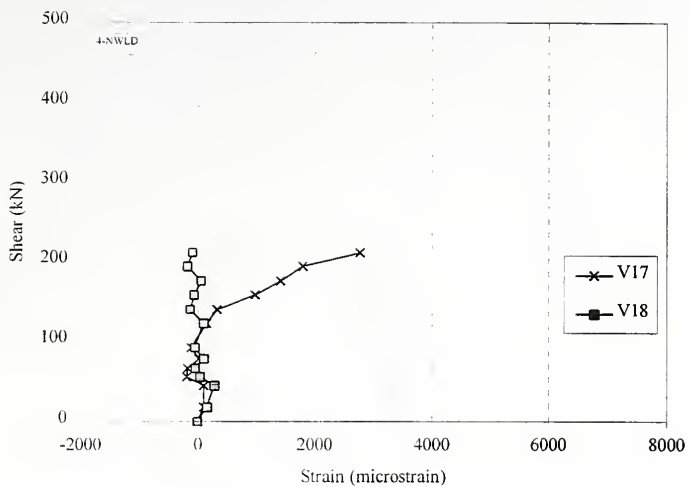


Figure 6.177 Shear-Strain Relationship. Vertical Whittemore Measurements 17-18, Specimen 4-NWLD

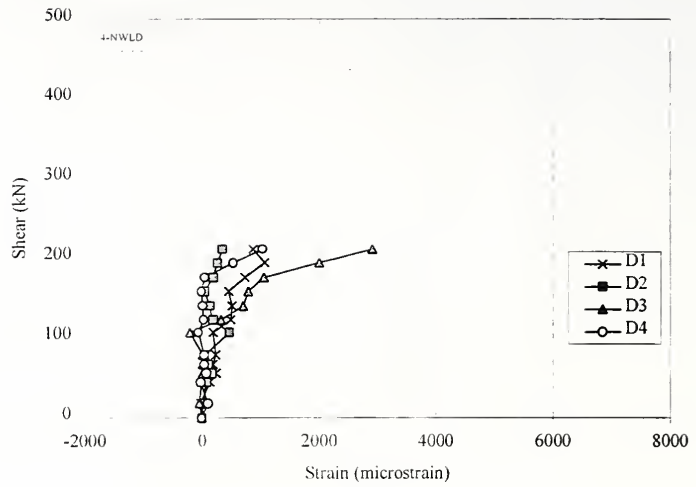


Figure 6.178 Shear-Strain Relationship, Diagonal Whittemore Measurements 1-4, Specimen 4-NWLD

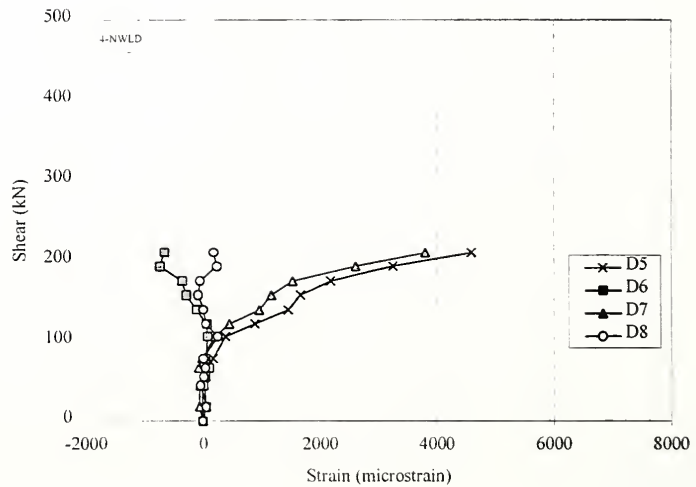


Figure 6.179 Shear-Strain Relationship, Diagonal Whittemore Measurements 5-8, Specimen 4-NWLD

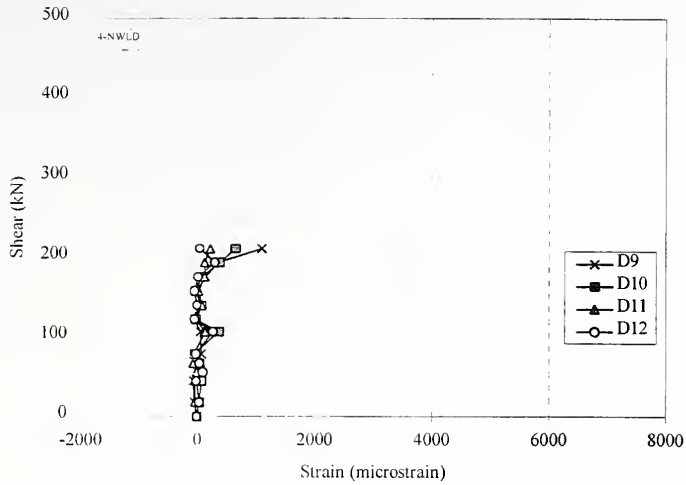


Figure 6.180 Shear-Strain Relationship, Diagonal Whittemore Measurements 9-12, Specimen 4-NWLD

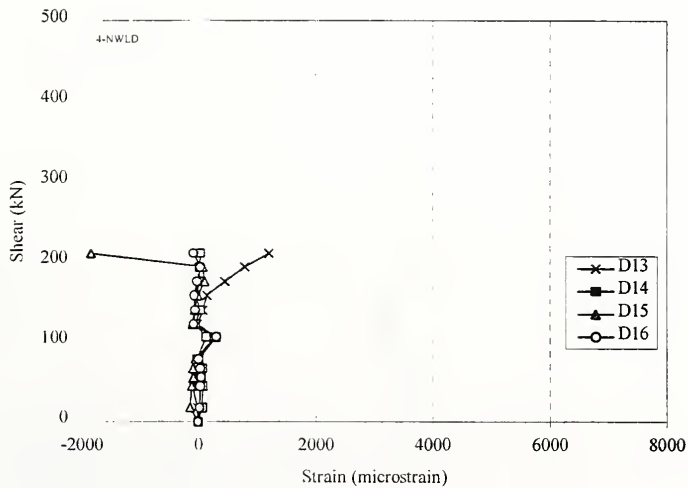


Figure 6.181 Shear-Strain Relationship, Diagonal Whittemore Measurements 13-16, Specimen 4-NWLD

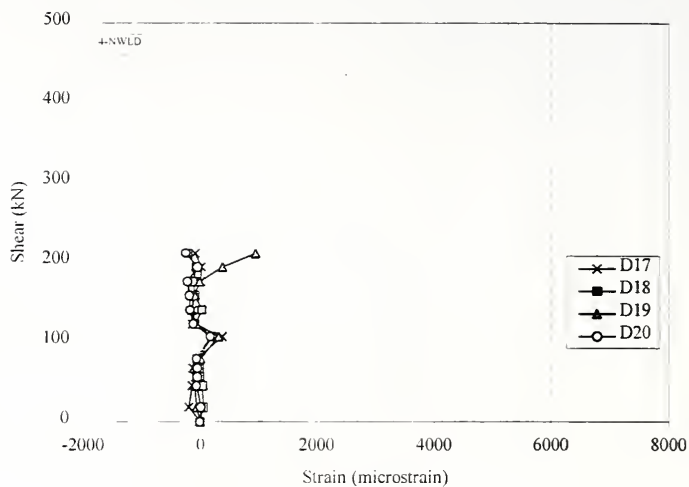


Figure 6.182 Shear-Strain Relationship. Diagonal Whittemore Measurements 17-20, Specimen 4-NWLD

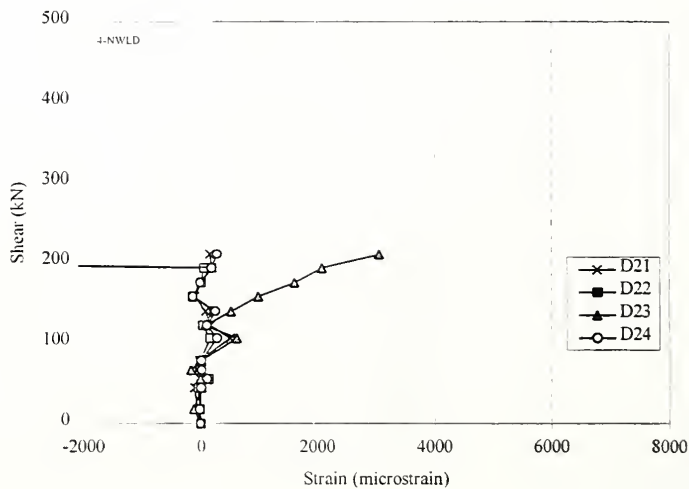


Figure 6.183 Shear-Strain Relationship. Diagonal Whittemore Measurements 21-24, Specimen 4-NWLD

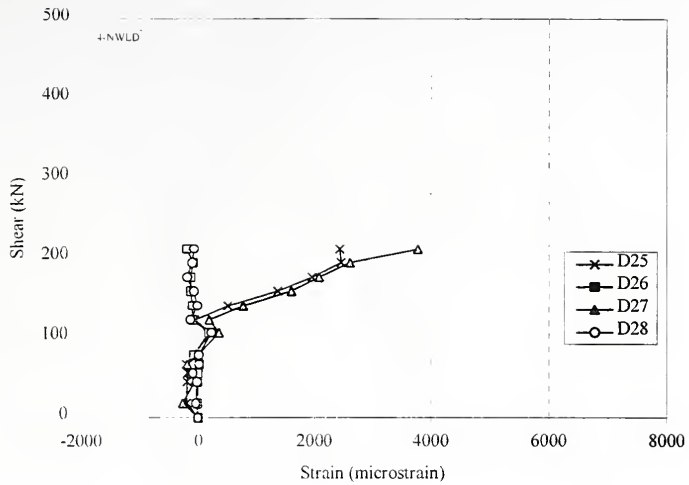


Figure 6.184 Shear-Strain Relationship, Diagonal Whittemore Measurements 25-28, Specimen 4-NWLD

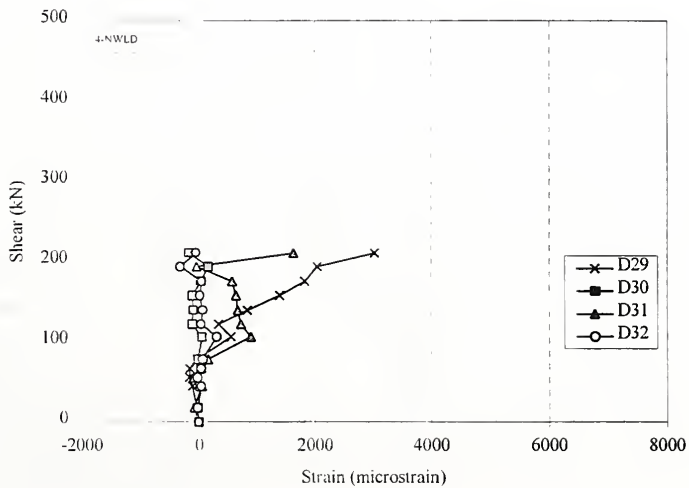


Figure 6.185 Shear-Strain Relationship, Diagonal Whittemore Measurements 29-32, Specimen 4-NWLD

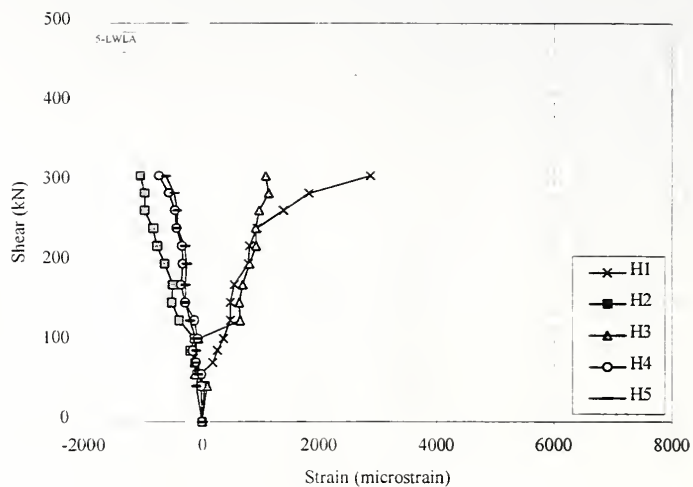


Figure 6.186 Shear-Strain Relationship, Horizontal Whittemore Measurements 1-5, Specimen 5-LWLA

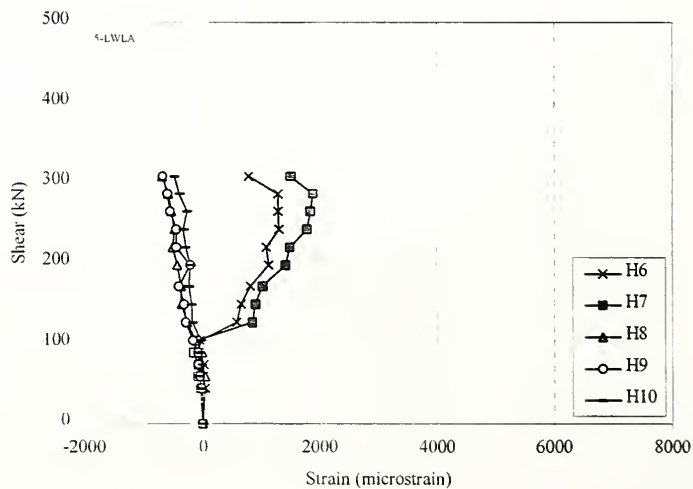


Figure 6.187 Shear-Strain Relationship, Horizontal Whittemore Measurements 6-10, Specimen 5-LWLA

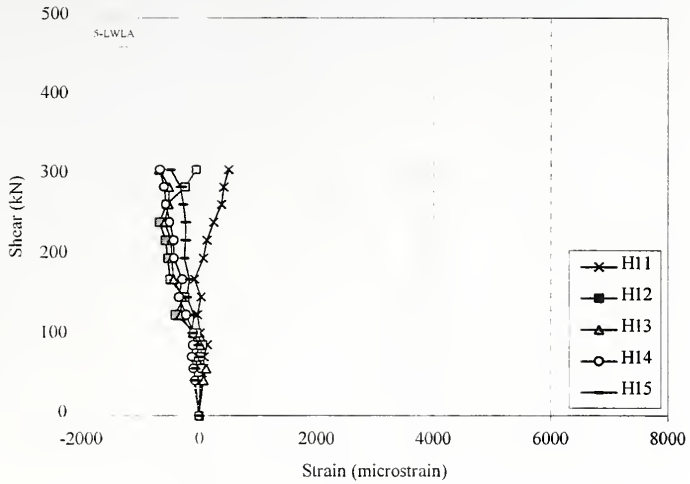


Figure 6.188 Shear-Strain Relationship, Horizontal Whittemore Measurements 11-15, Specimen 5-LWLA

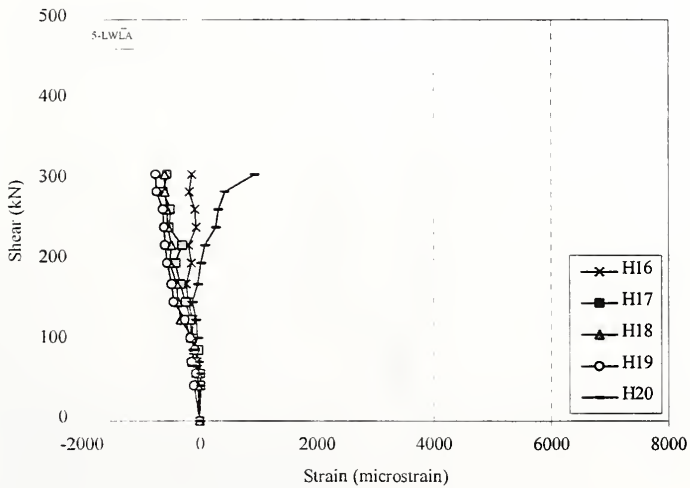


Figure 6.189 Shear-Strain Relationship, Horizontal Whittemore Measurements 16-20, Specimen 5-LWLA

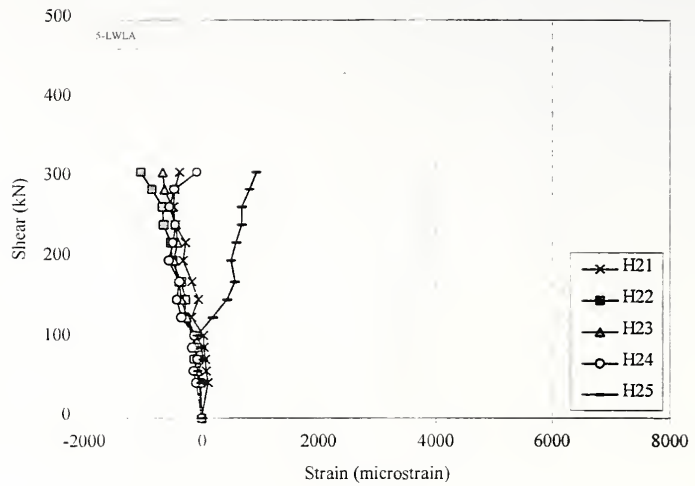


Figure 6.190 Shear-Strain Relationship, Horizontal Whittemore Measurements 21-25, Specimen 5-LWLA

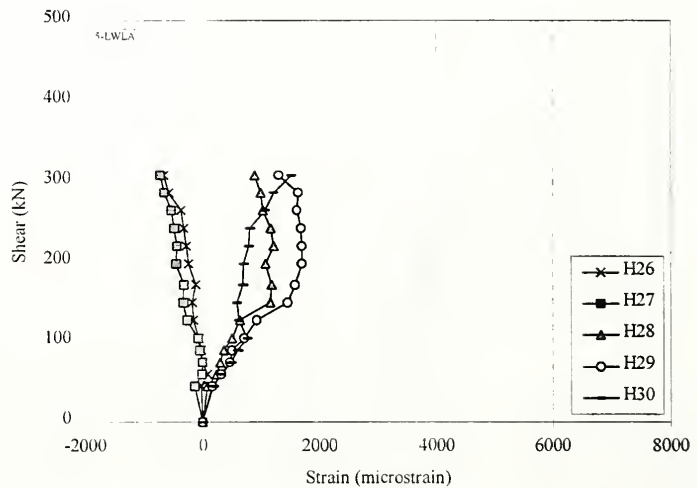


Figure 6.191 Shear-Strain Relationship, Horizontal Whittemore Measurements 26-30, Specimen 5-LWLA

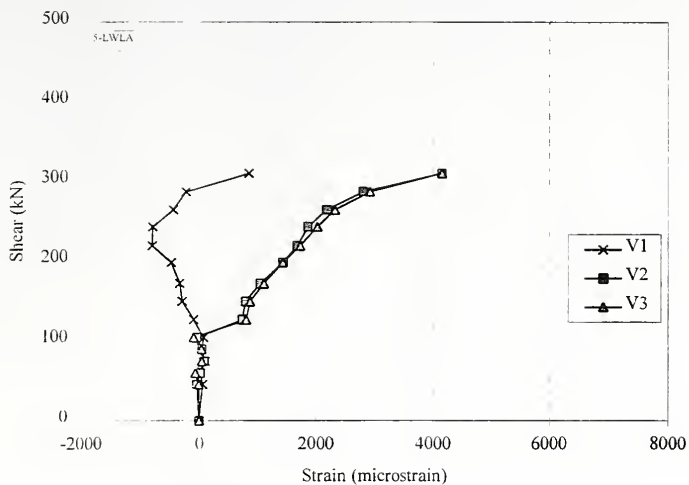


Figure 6.192 Shear-Strain Relationship, Vertical Whittemore Measurements 1-3, Specimen 5-LWLA

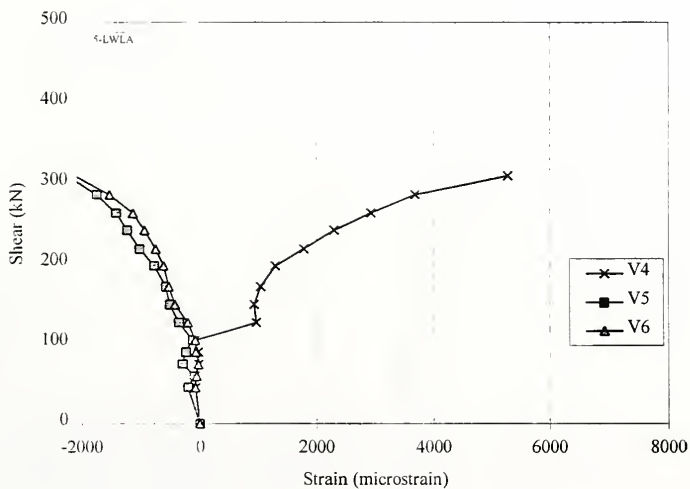


Figure 6.193 Shear-Strain Relationship, Vertical Whittemore Measurements 4-6, Specimen 5-LWLA

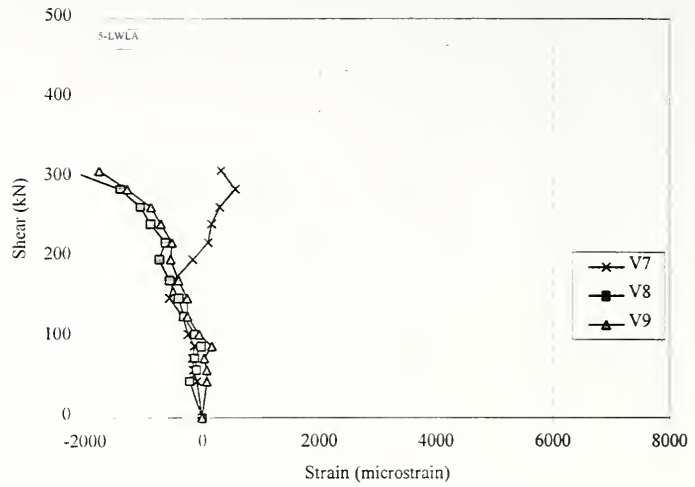


Figure 6.194 Shear-Strain Relationship, Vertical Whittemore Measurements 7-9, Specimen 5-LWLA

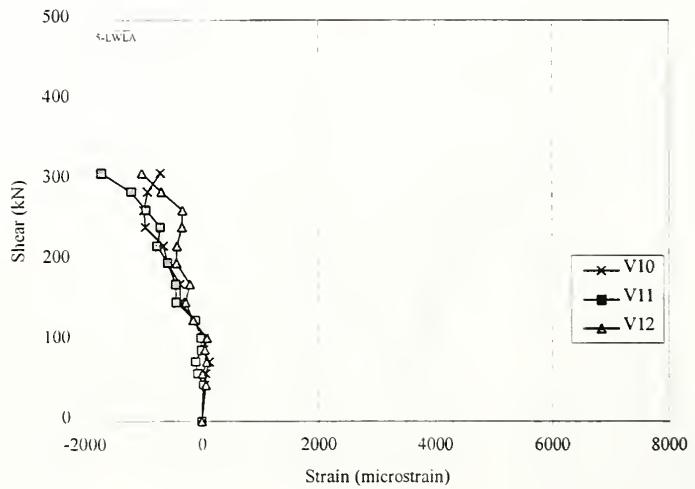


Figure 6.195 Shear-Strain Relationship, Vertical Whittemore Measurements 10-12, Specimen 5-LWLA

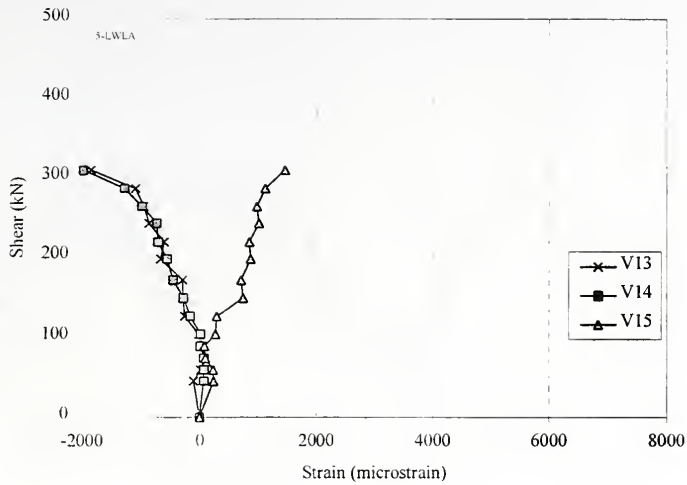


Figure 6.196 Shear-Strain Relationship, Vertical Whittemore Measurements 13-15, Specimen 5-LWLA

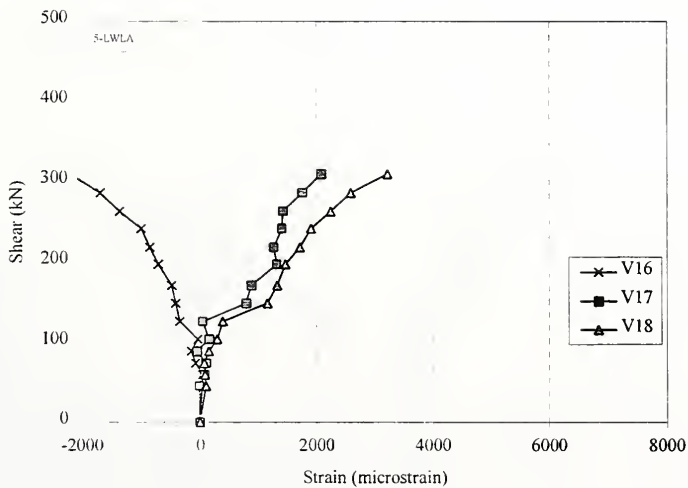


Figure 6.197 Shear-Strain Relationship, Vertical Whittemore Measurements 16-18, Specimen 5-LWLA

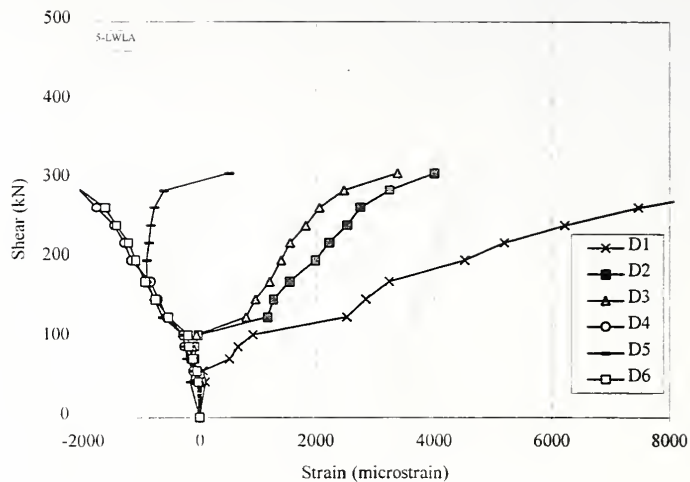


Figure 6.198 Shear-Strain Relationship, Diagonal Whittemore Measurements 1-6, Specimen 5-LWLA

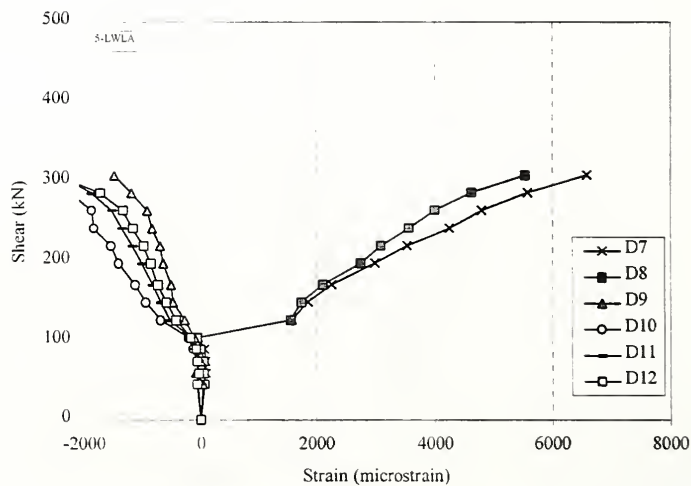


Figure 6.199 Shear-Strain Relationship, Diagonal Whittemore Measurements 7-12, Specimen 5-LWLA

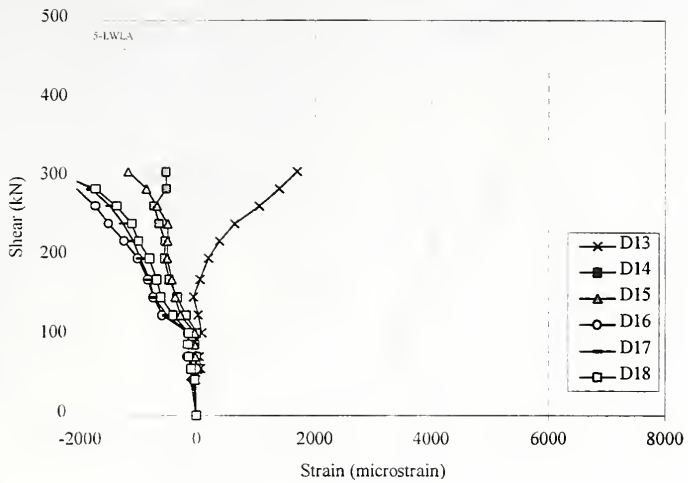


Figure 6.200 Shear-Strain Relationship, Diagonal Whittemore Measurements 13-18, Specimen 5-LWLA

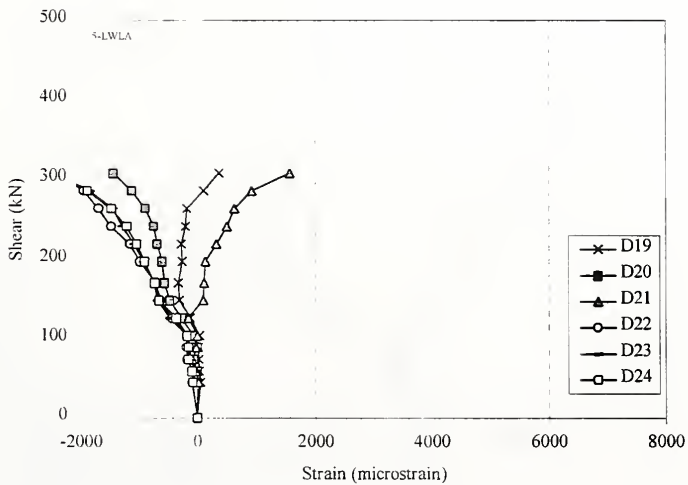


Figure 6.201 Shear-Strain Relationship, Diagonal Whittemore Measurements 19-24, Specimen 5-LWLA

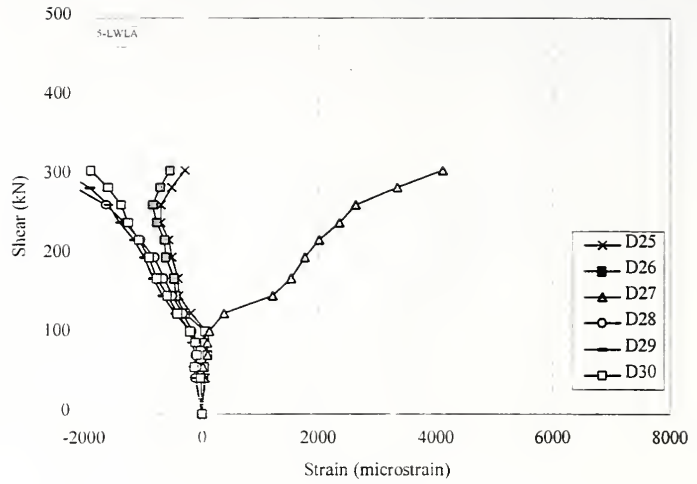


Figure 6.202 Shear-Strain Relationship, Diagonal Whittemore Measurements 25-30, Specimen 5-LWLA

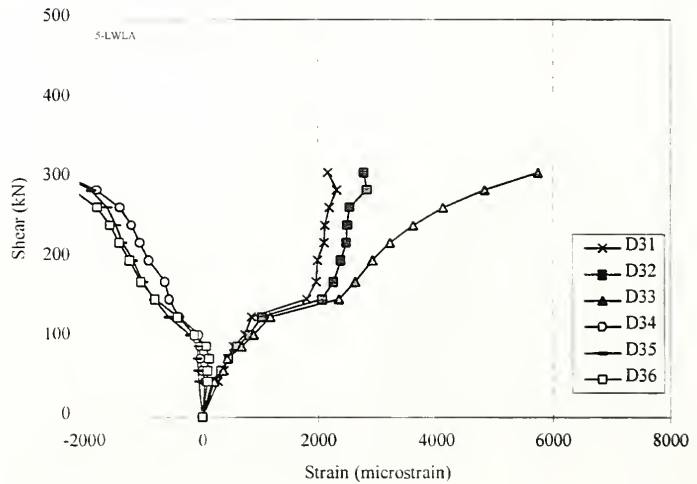


Figure 6.203 Shear-Strain Relationship, Diagonal Whittemore Measurements 31-36, Specimen 5-LWLA

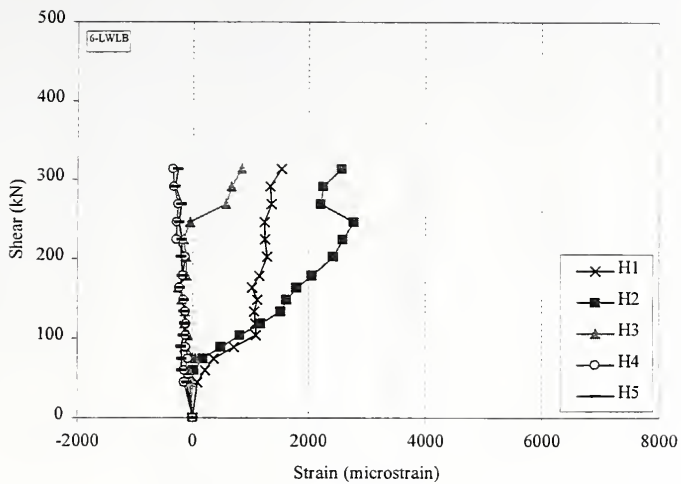


Figure 6.204 Shear-Strain Relationship, Horizontal Whittemore Measurements 1-5, Specimen 6-LWLB

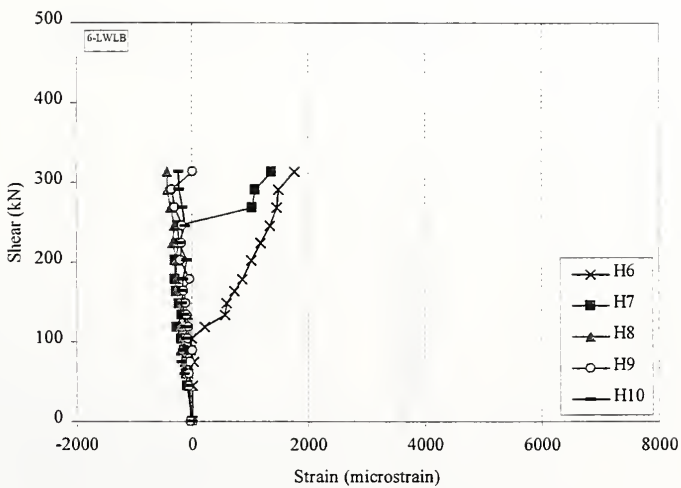


Figure 6.205 Shear-Strain Relationship, Horizontal Whittemore Measurements 6-10, Specimen 6-LWLB

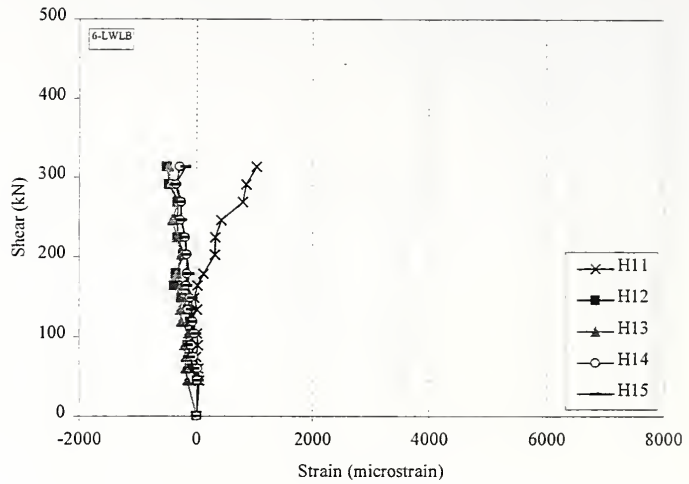


Figure 6.206 Shear-Strain Relationship, Horizontal Whittemore Measurements 11-15, Specimen 6-LWLB

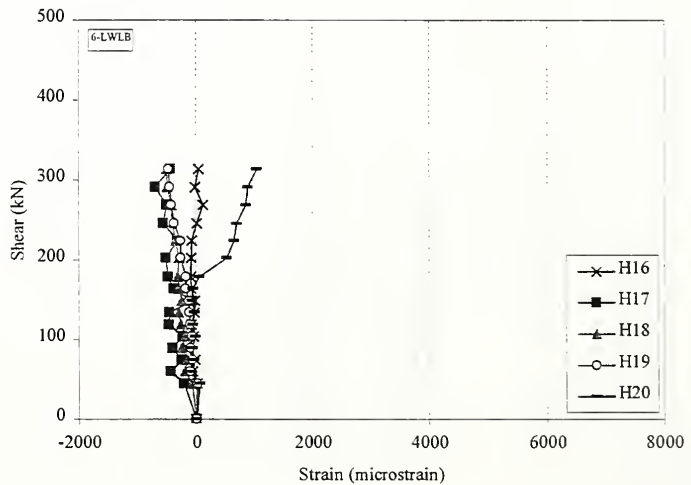


Figure 6.207 Shear-Strain Relationship, Horizontal Whittemore Measurements 16-20, Specimen 6-LWLB

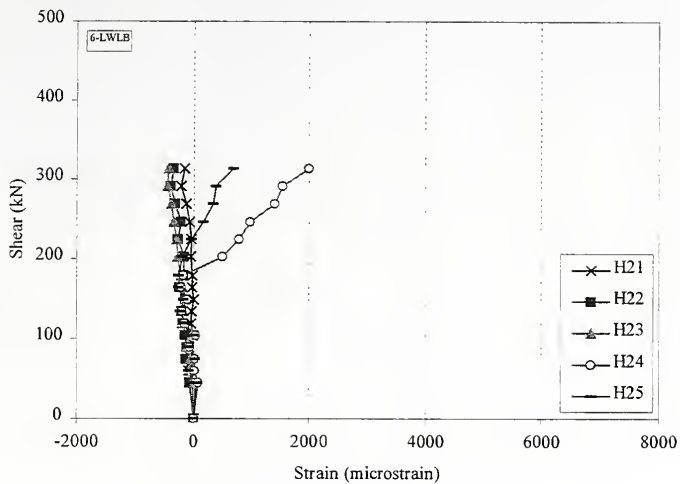


Figure 6.208 Shear-Strain Relationship, Horizontal Whittemore Measurements 21-25, Specimen 6-LWLB

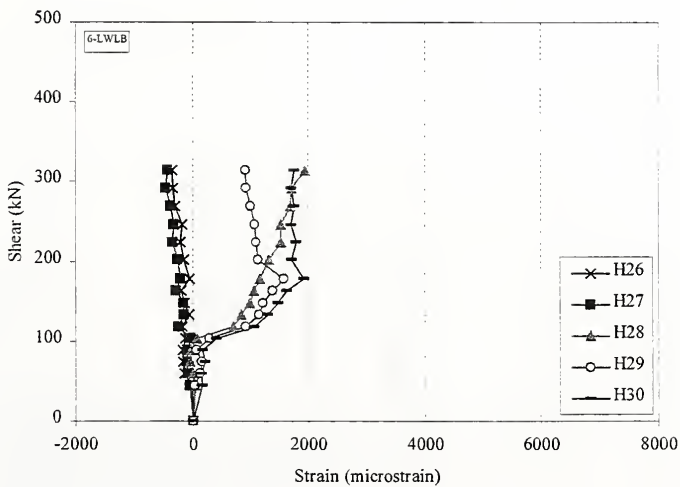


Figure 6.209 Shear-Strain Relationship, Horizontal Whittemore Measurements 26-30, Specimen 6-LWLB

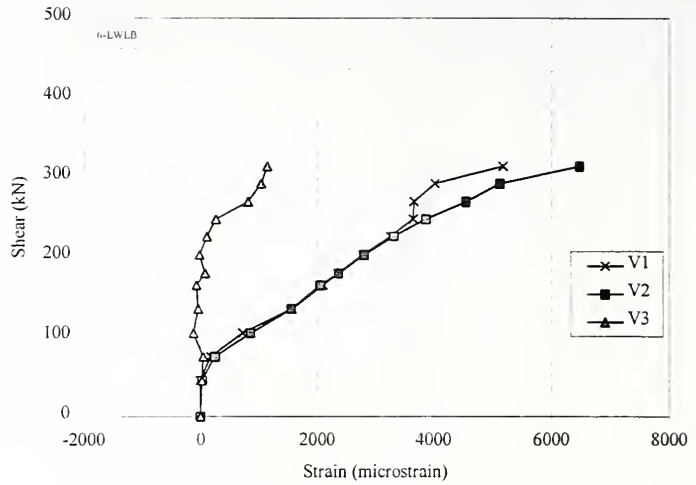


Figure 6.210 Shear-Strain Relationship, Vertical Whittemore Measurements 1-3, Specimen 6-LWLB

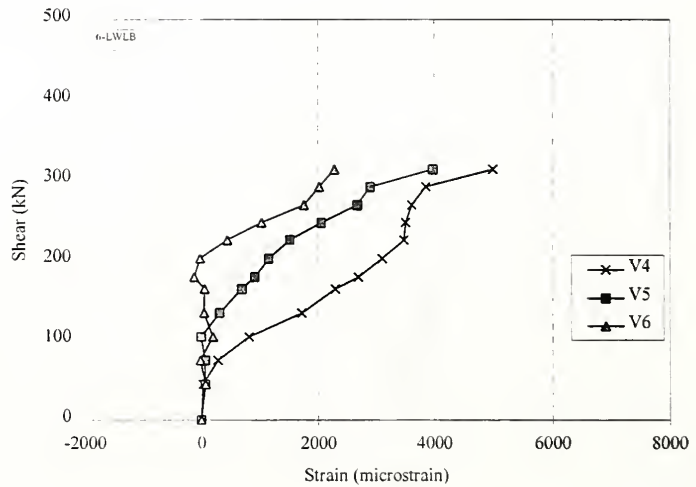


Figure 6.211 Shear-Strain Relationship, Vertical Whittemore Measurements 4-6, Specimen 6-LWLB

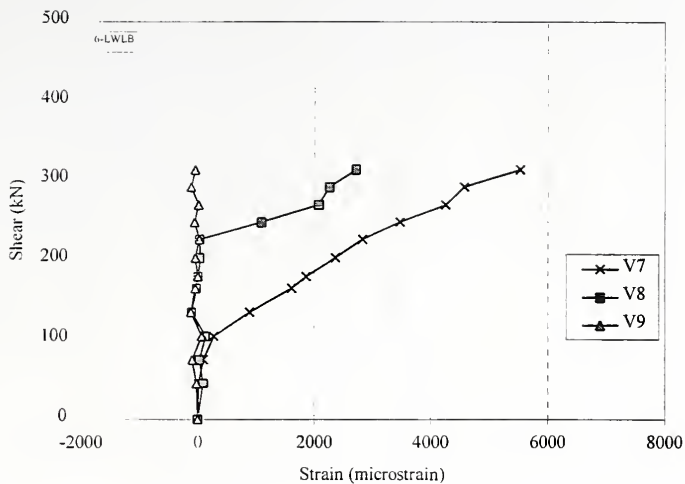


Figure 6.212 Shear-Strain Relationship, Vertical Whittemore Measurements 7-9, Specimen 6-LWLB

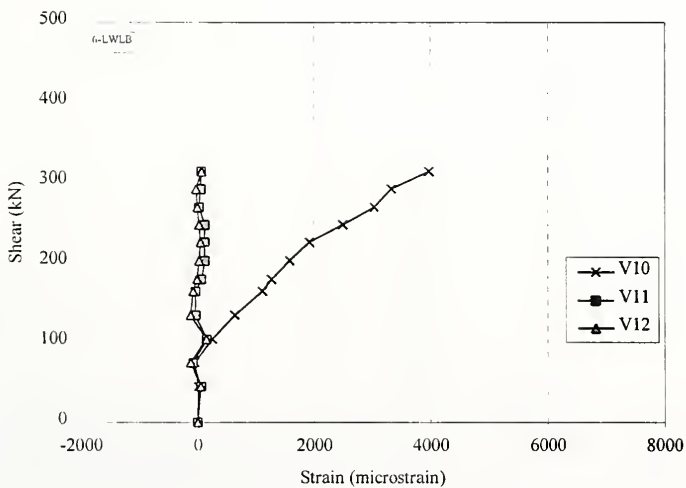


Figure 6.213 Shear-Strain Relationship, Vertical Whittemore Measurements 10-12, Specimen 6-LWLB

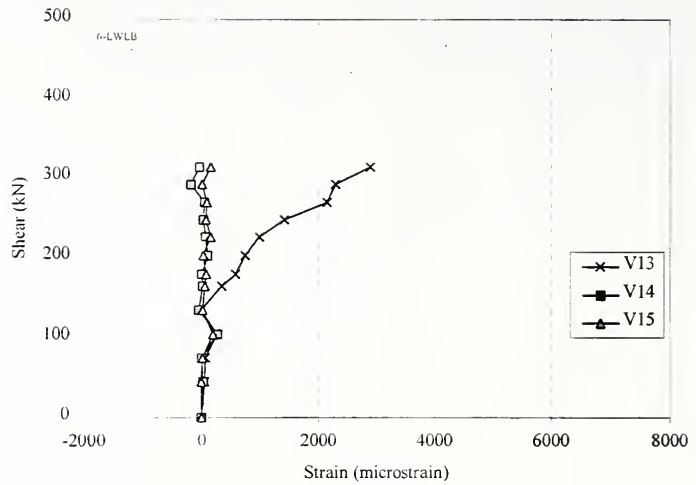


Figure 6.214 Shear-Strain Relationship, Vertical Whittemore Measurements 13-15, Specimen 6-LWLB

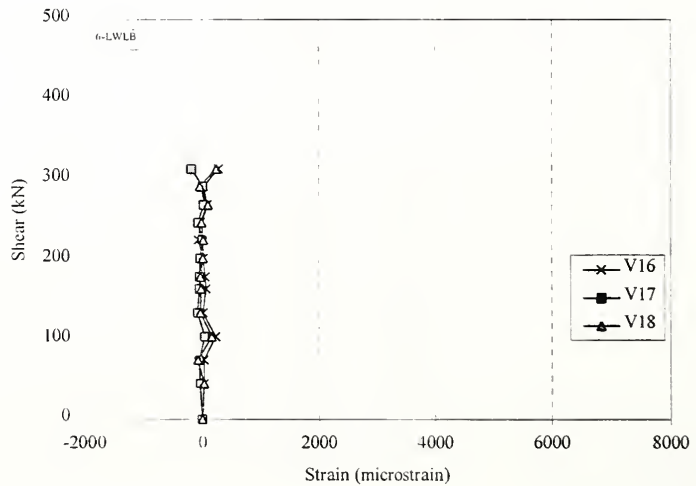


Figure 6.215 Shear-Strain Relationship, Vertical Whittemore Measurements 16-18, Specimen 6-LWLB

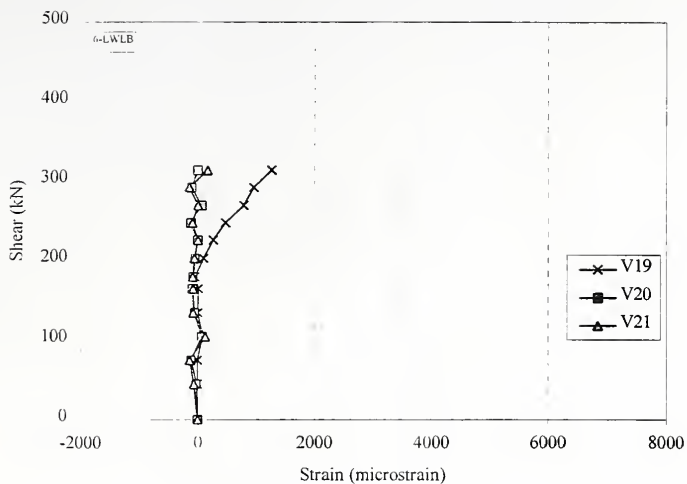


Figure 6.216 Shear-Strain Relationship, Vertical Whittemore Measurements 19-21, Specimen 6-LWLB

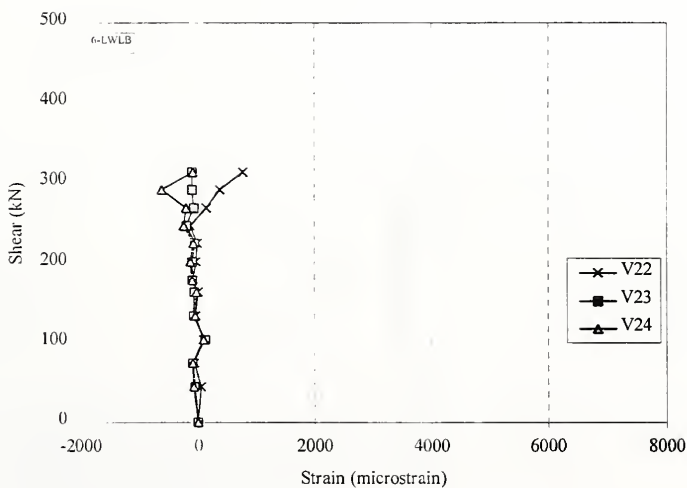


Figure 6.217 Shear-Strain Relationship, Vertical Whittemore Measurements 22-24, Specimen 6-LWLB

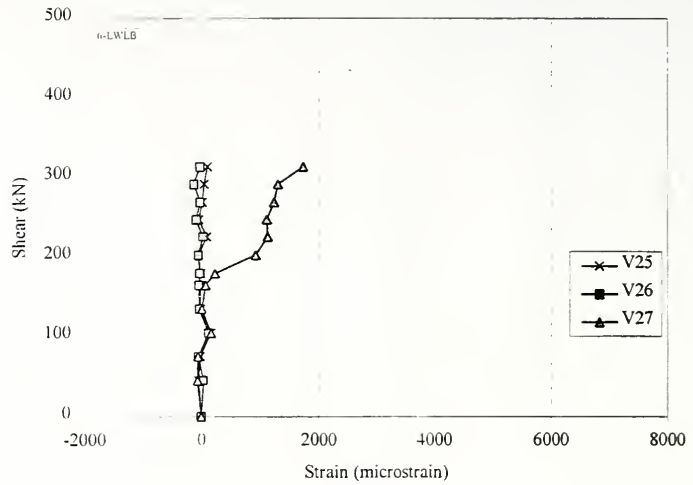


Figure 6.218 Shear-Strain Relationship, Vertical Whittemore Measurements 25-27, Specimen 6-LWLB

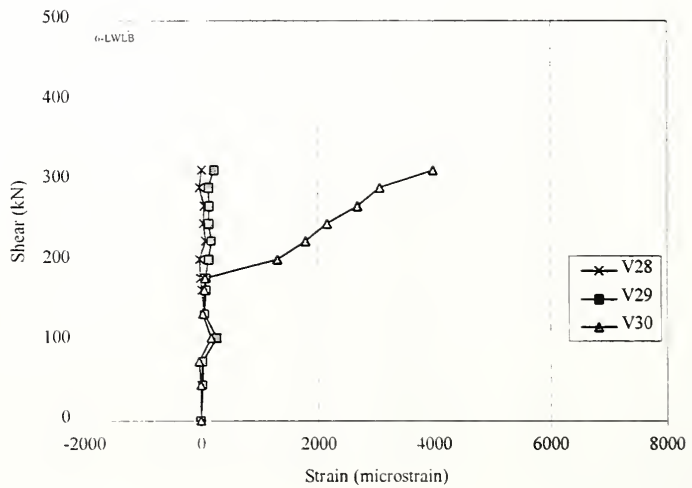


Figure 6.219 Shear-Strain Relationship, Vertical Whittemore Measurements 28-30, Specimen 6-LWLB

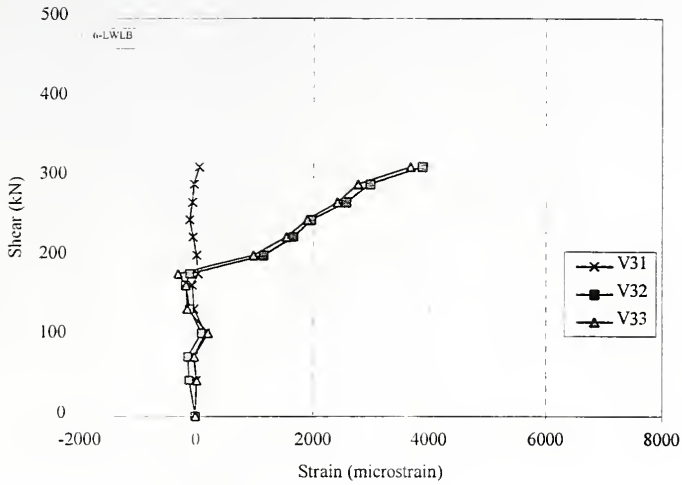


Figure 6.220 Shear-Strain Relationship, Vertical Whittemore Measurements 31-33, Specimen 6-LWLB

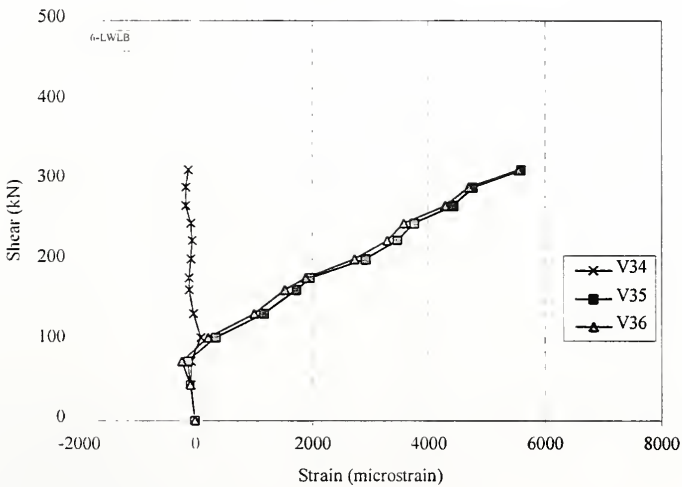


Figure 6.221 Shear-Strain Relationship, Vertical Whittemore Measurements 34-36, Specimen 6-LWLB

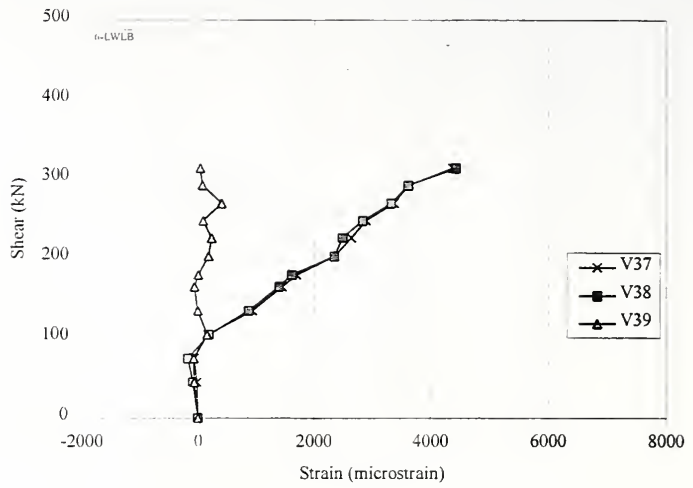


Figure 6.222 Shear-Strain Relationship, Vertical Whittemore Measurements 37-39, Specimen 6-LWLB

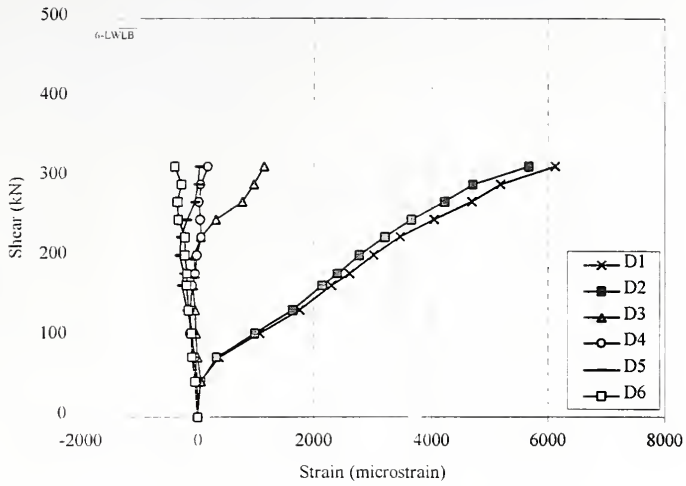


Figure 6.223 Shear-Strain Relationship, Diagonal Whittemore Measurements 1-6, Specimen 6-LWLB

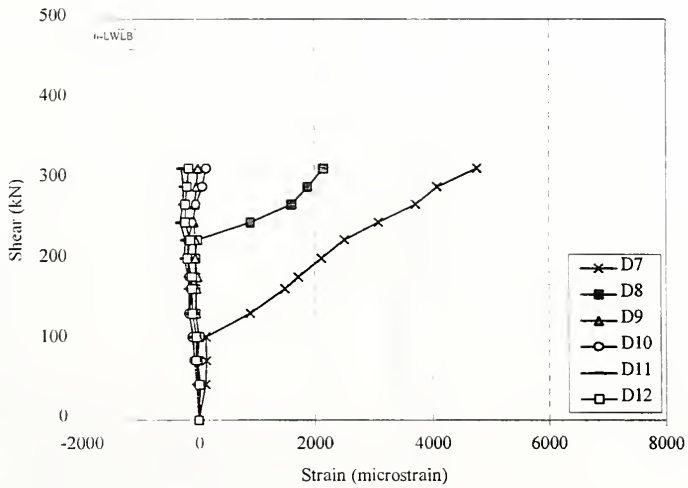


Figure 6.224 Shear-Strain Relationship, Diagonal Whittemore Measurements 7-12, Specimen 6-LWLB

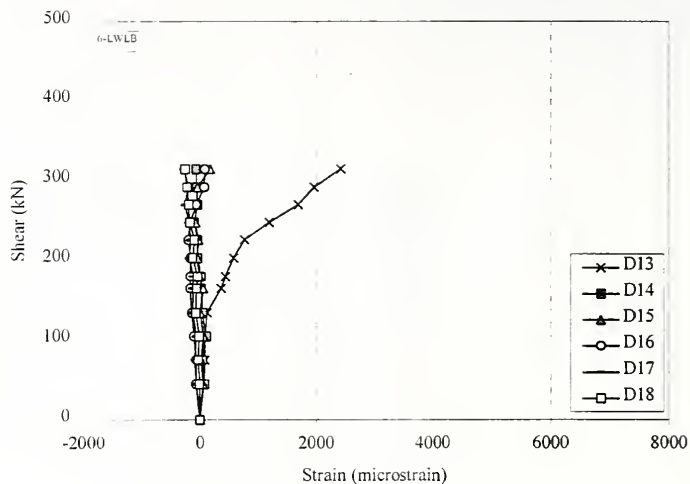


Figure 6.225 Shear-Strain Relationship, Diagonal Whittemore Measurements 13-18, Specimen 6-LWLB

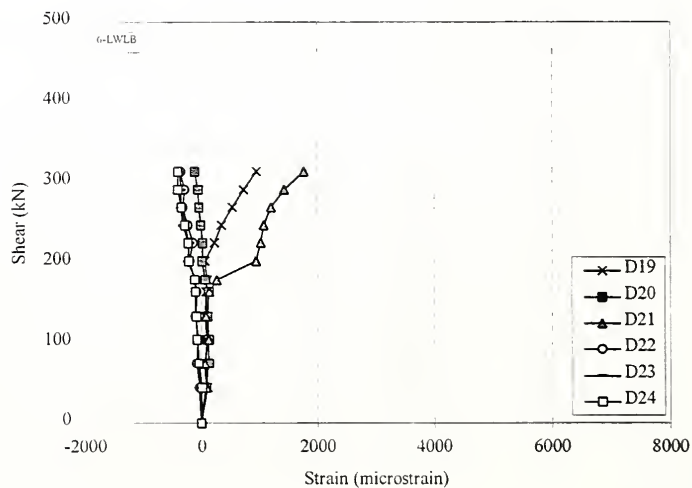


Figure 6.226 Shear-Strain Relationship, Diagonal Whittemore Measurements 19-24, Specimen 6-LWLB

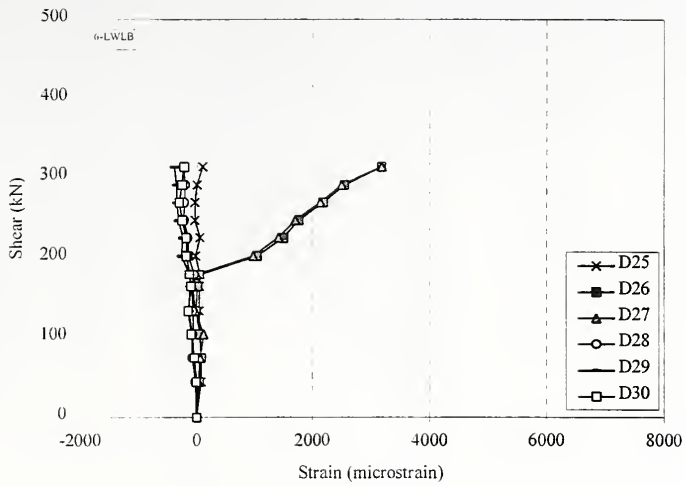


Figure 6.227 Shear-Strain Relationship, Diagonal Whittemore Measurements 25-30, Specimen 6-LWLB

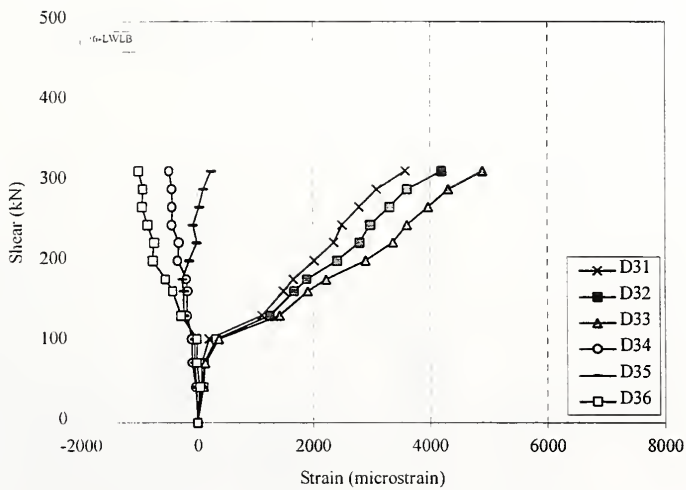


Figure 6.228 Shear-Strain Relationship, Diagonal Whittemore Measurements 31-36, Specimen 6-LWLB

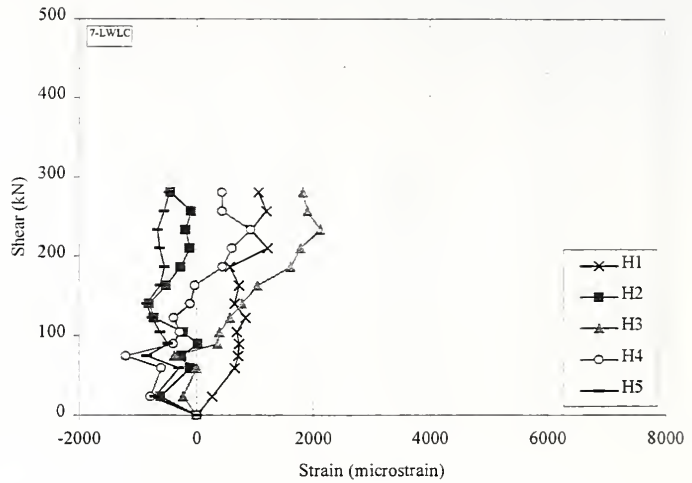


Figure 6.229 Shear-Strain Relationship, Horizontal Whittemore Measurements 1-5, Specimen 7-LWLC

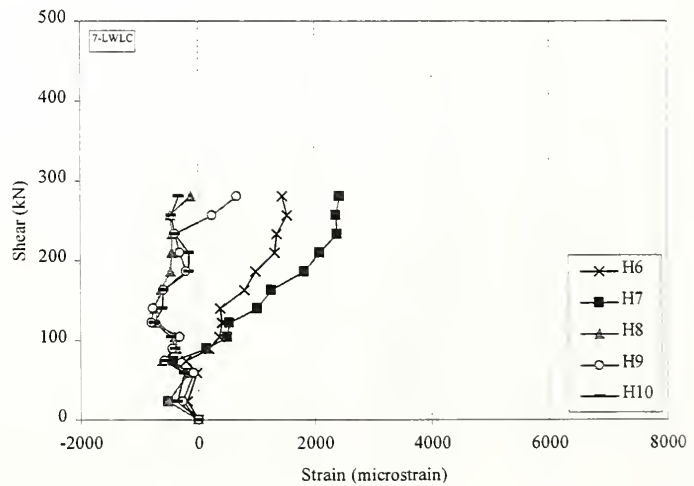


Figure 6.230 Shear-Strain Relationship, Horizontal Whittemore Measurements 6-10, Specimen 7-LWLC

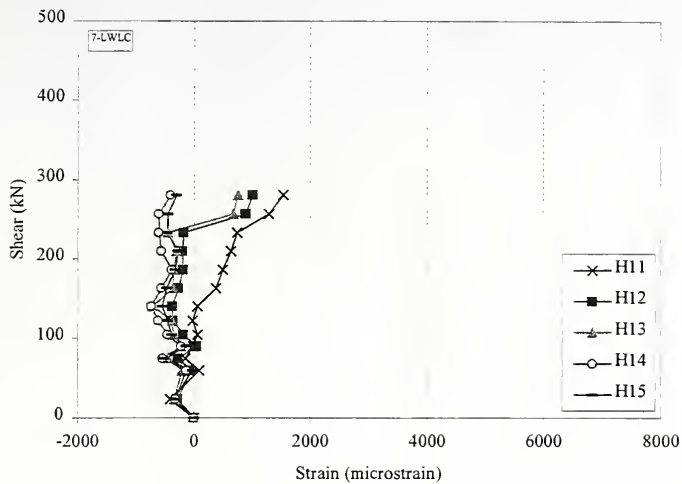


Figure 6.231 Shear-Strain Relationship, Horizontal Whittemore Measurements 11-15, Specimen 7-LWLC

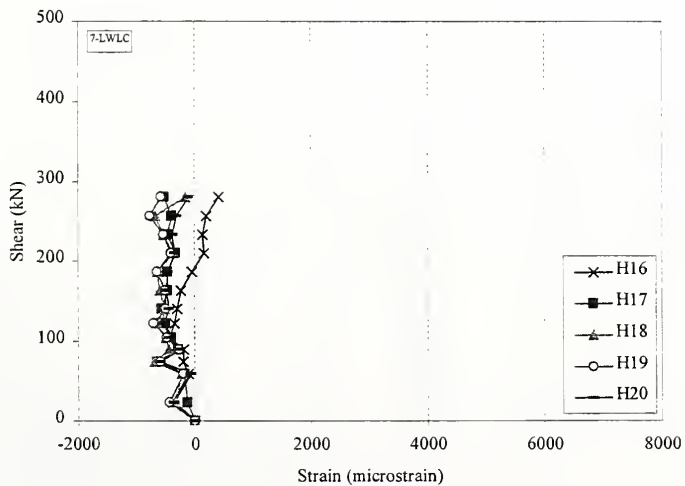


Figure 6.232 Shear-Strain Relationship, Horizontal Whittemore Measurements 16-20, Specimen 7-LWLC

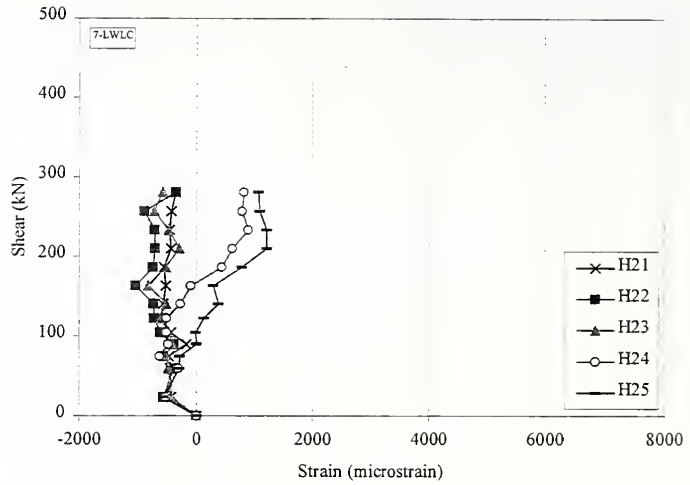


Figure 6.233 Shear-Strain Relationship, Horizontal Whittemore Measurements 21-25, Specimen 7-LWLC

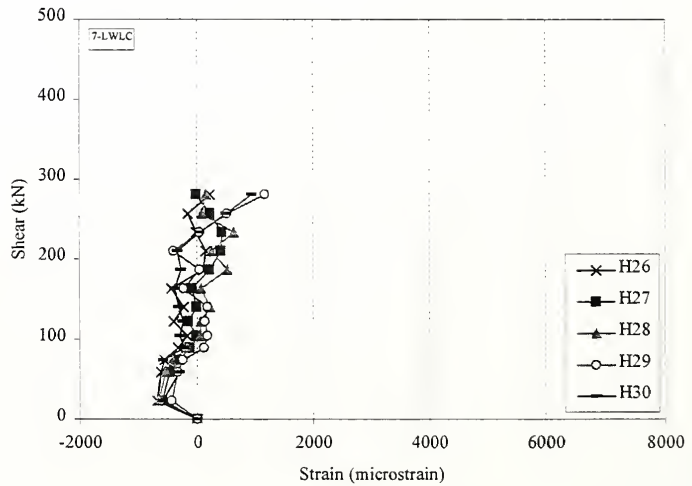


Figure 6.234 Shear-Strain Relationship, Horizontal Whittemore Measurements 26-30, Specimen 7-LWLC

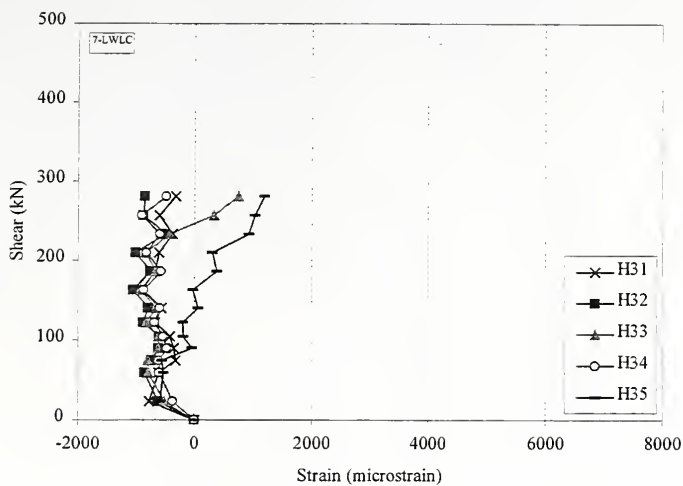


Figure 6.235 Shear-Strain Relationship, Horizontal Whittemore Measurements 31-35, Specimen 7-LWLC

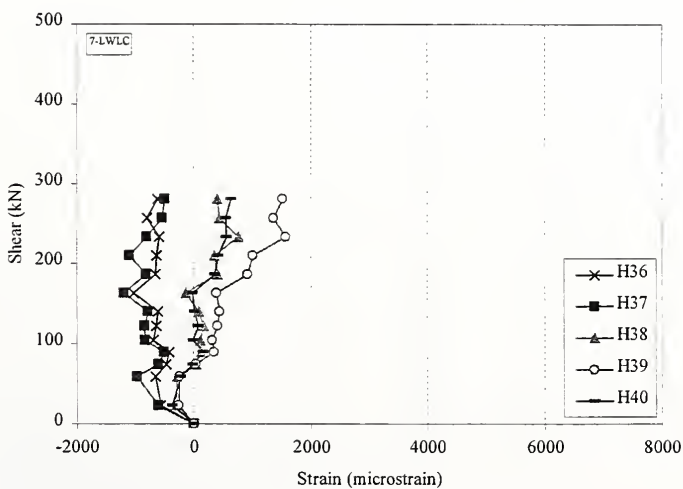


Figure 6.236 Shear-Strain Relationship, Horizontal Whittemore Measurements 36-40, Specimen 7-LWLC

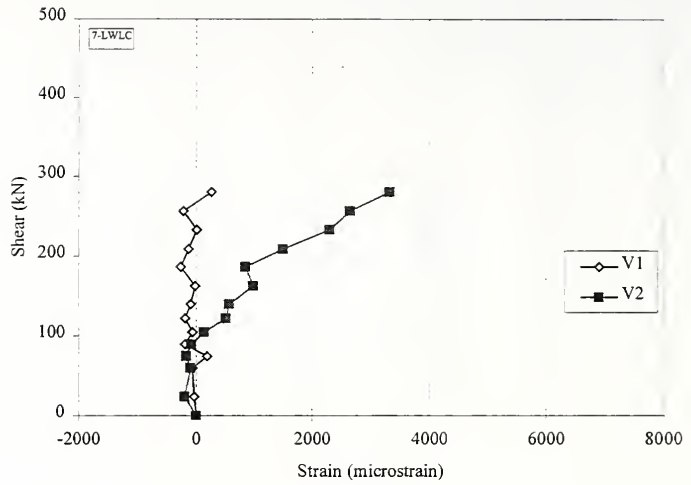


Figure 6.237 Shear-Strain Relationship, Vertical Whittemore Measurements 1-2, Specimen 7-LWLC

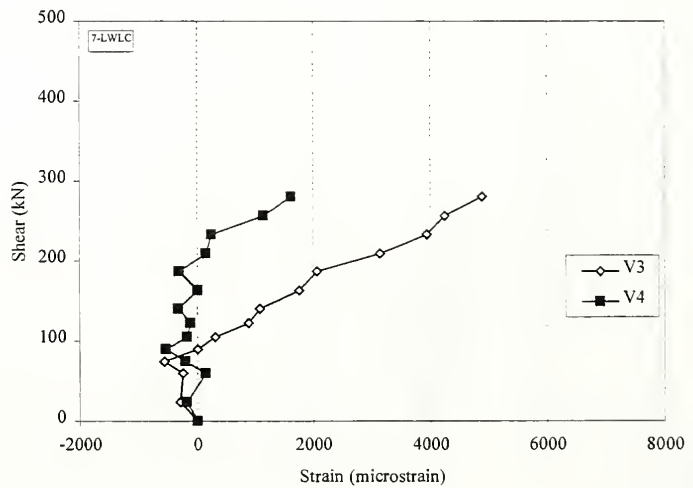


Figure 6.238 Shear-Strain Relationship, Vertical Whittemore Measurements 3-4, Specimen 7-LWLC

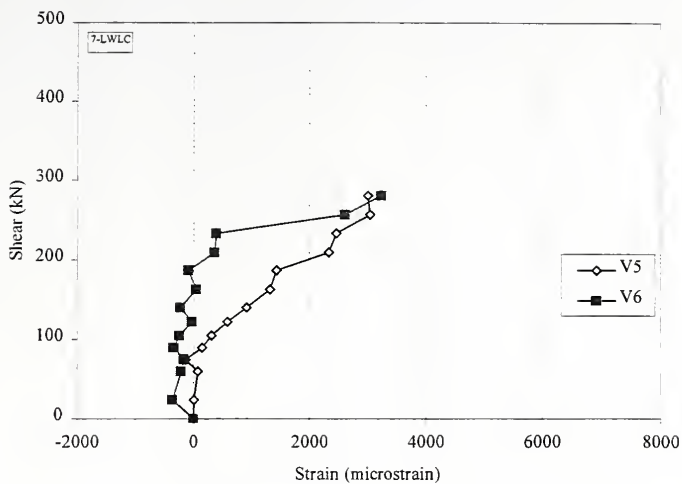


Figure 6.239 Shear-Strain Relationship, Vertical Whittemore Measurements 5-6, Specimen 7-LWLC

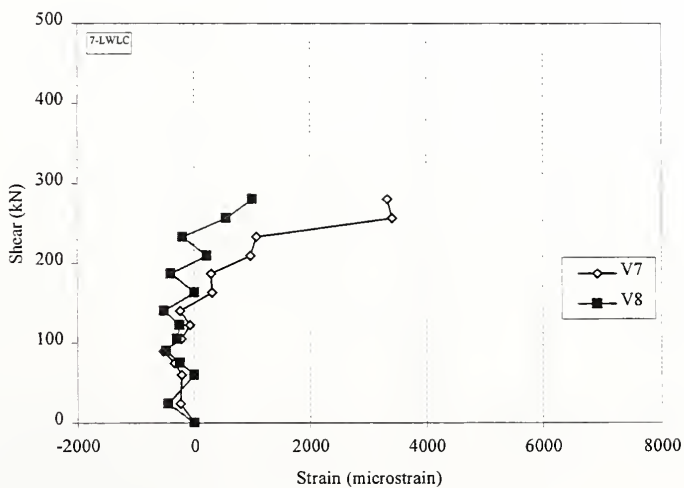


Figure 6.240 Shear-Strain Relationship, Vertical Whittemore Measurements 7-8, Specimen 7-LWLC

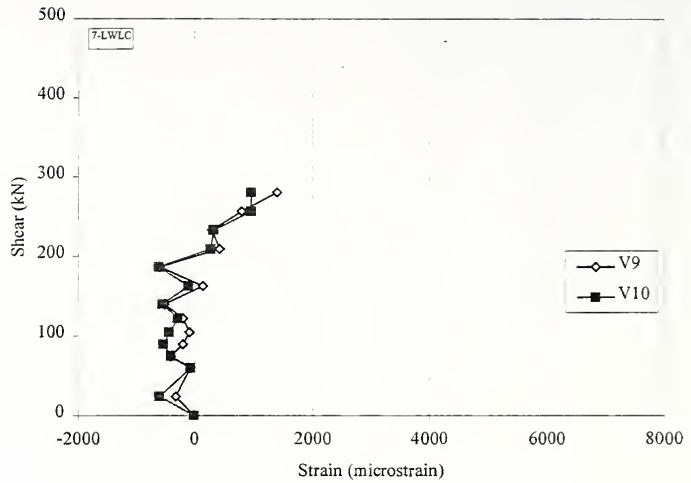


Figure 6.241 Shear-Strain Relationship, Vertical Whittemore Measurements 9-10, Specimen 7-LWLC

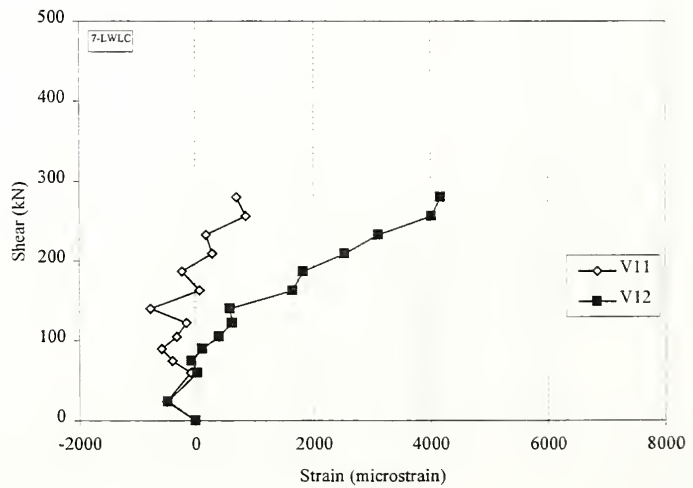


Figure 6.242 Shear-Strain Relationship, Vertical Whittemore Measurements 11-12, Specimen 7-LWLC

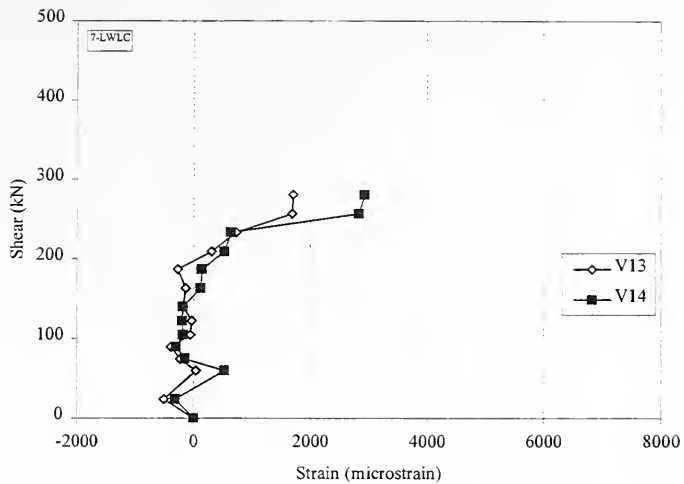


Figure 6.243 Shear-Strain Relationship, Vertical Whittemore Measurements 13-14, Specimen 7-LWLC

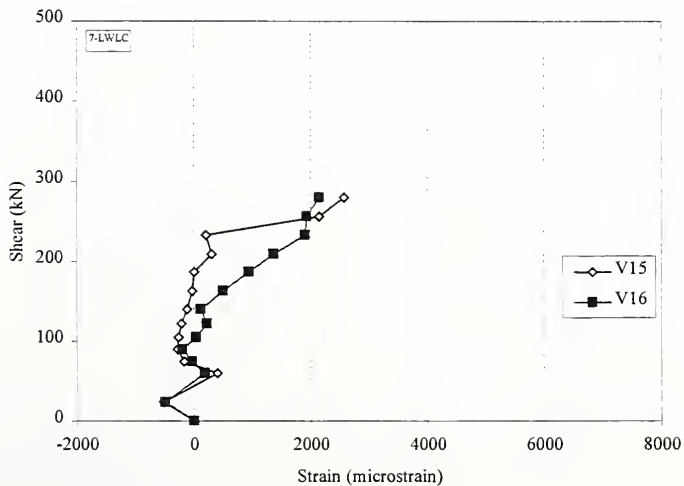


Figure 6.244 Shear-Strain Relationship, Vertical Whittemore Measurements 15-16, Specimen 7-LWLC

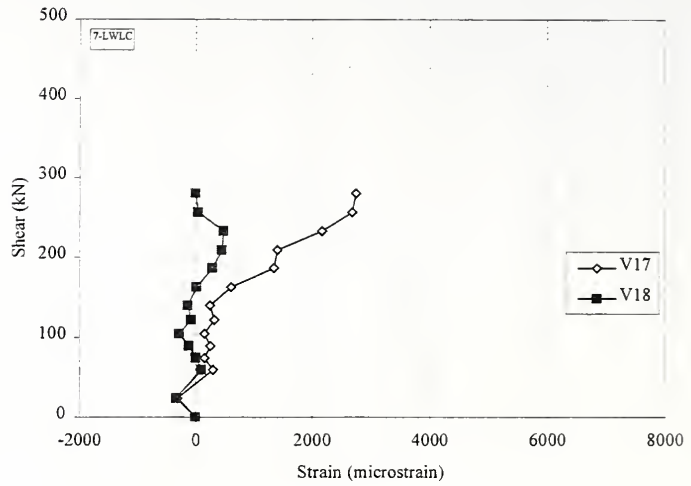


Figure 6.245 Shear-Strain Relationship, Vertical Whittemore Measurements 17-18, Specimen 7-LWLC

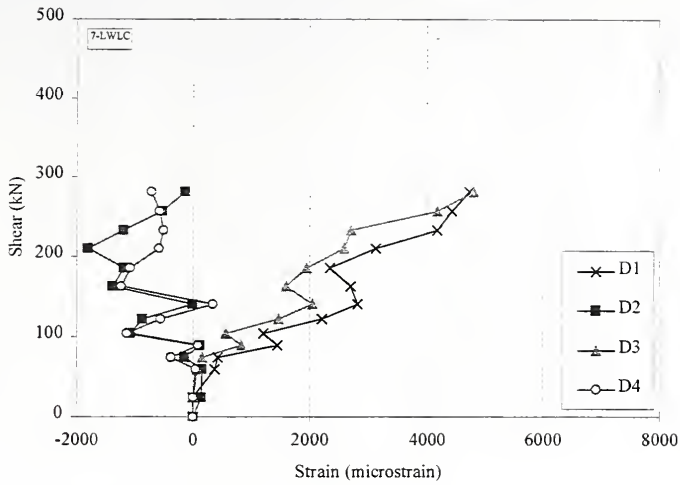


Figure 6.246 Shear-Strain Relationship, Diagonal Whittemore Measurements 1-4, Specimen 7-LWLC

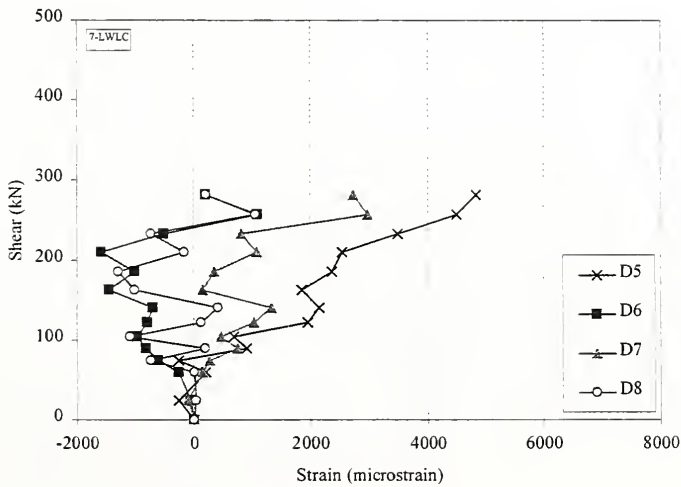


Figure 6.247 Shear-Strain Relationship, Diagonal Whittemore Measurements 5-8, Specimen 7-LWLC

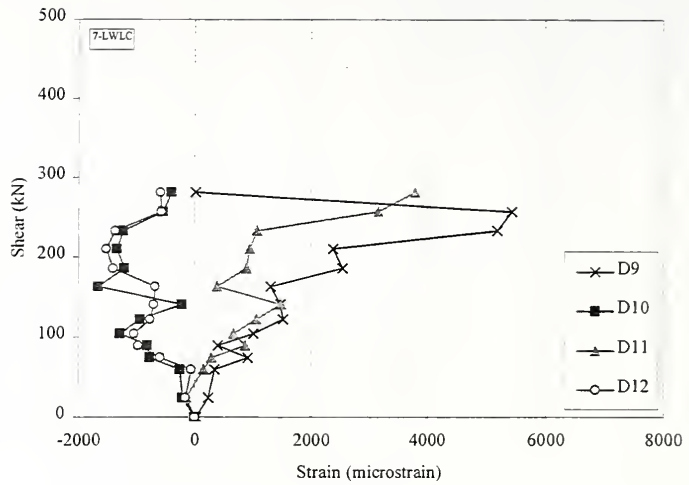


Figure 6.248 Shear-Strain Relationship, Diagonal Whittemore Measurements 9-12, Specimen 7-LWLC

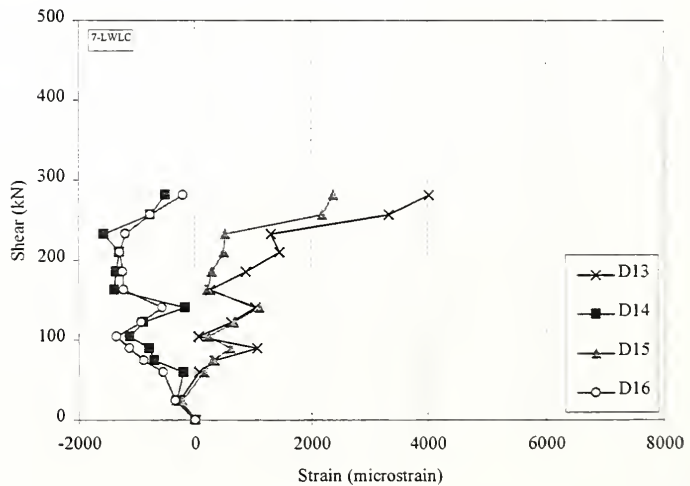


Figure 6.249 Shear-Strain Relationship, Diagonal Whittemore Measurements 13-16, Specimen 7-LWLC

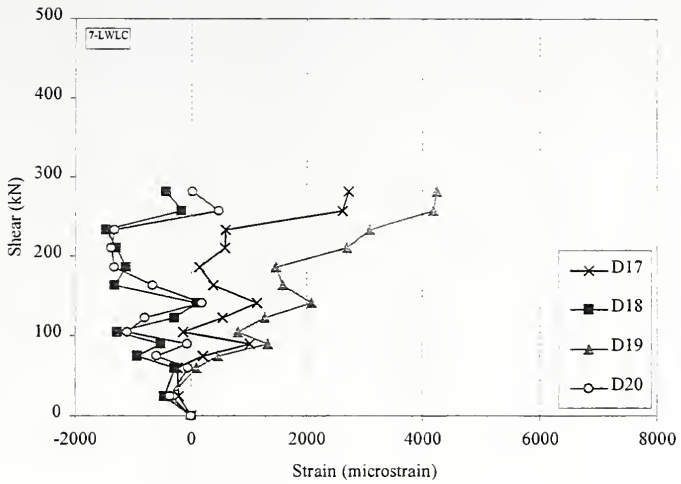


Figure 6.250 Shear-Strain Relationship, Diagonal Whittemore Measurements 17-20, Specimen 7-LWLC

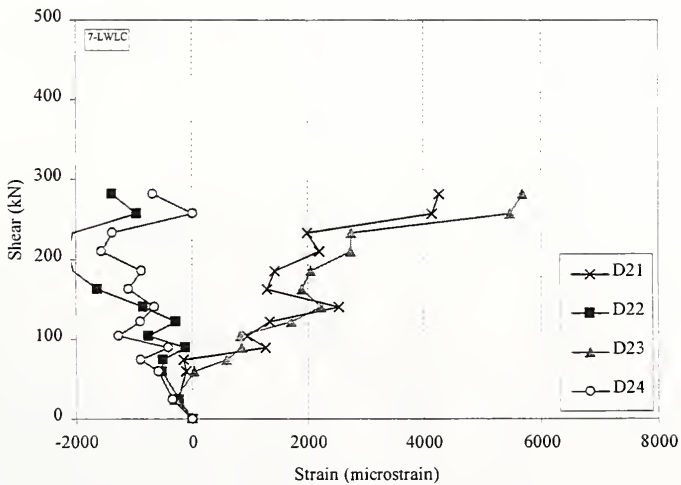


Figure 6.251 Shear-Strain Relationship, Diagonal Whittemore Measurements 21-24, Specimen 7-LWLC

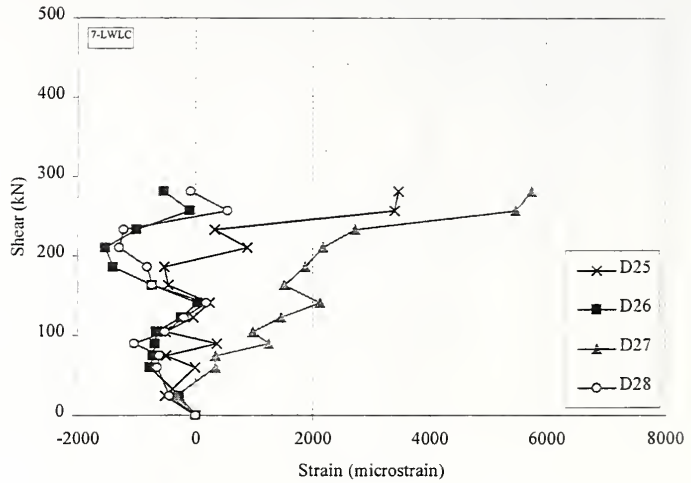


Figure 6.252 Shear-Strain Relationship, Diagonal Whittemore Measurements 25-28, Specimen 7-LWLC

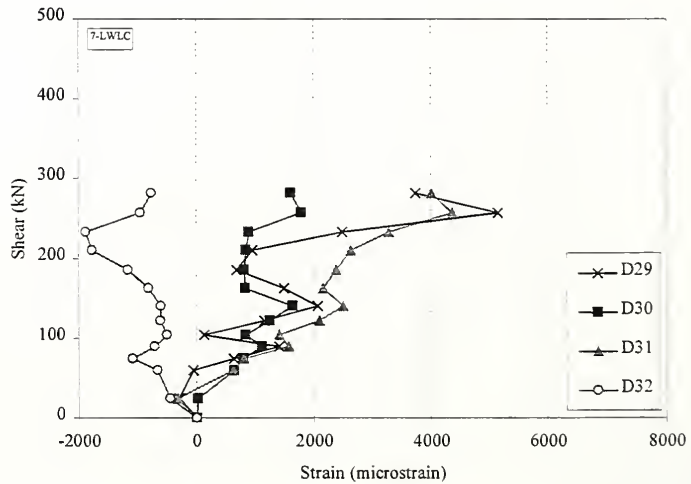


Figure 6.253 Shear-Strain Relationship, Diagonal Whittemore Measurements 29-32, Specimen 7-LWLC

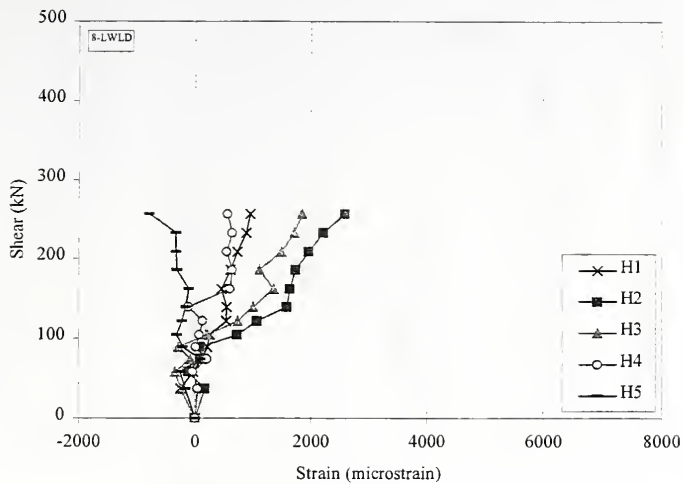


Figure 6.254 Shear-Strain Relationship, Horizontal Whittemore Measurements 1-5, Specimen 8-LWLD

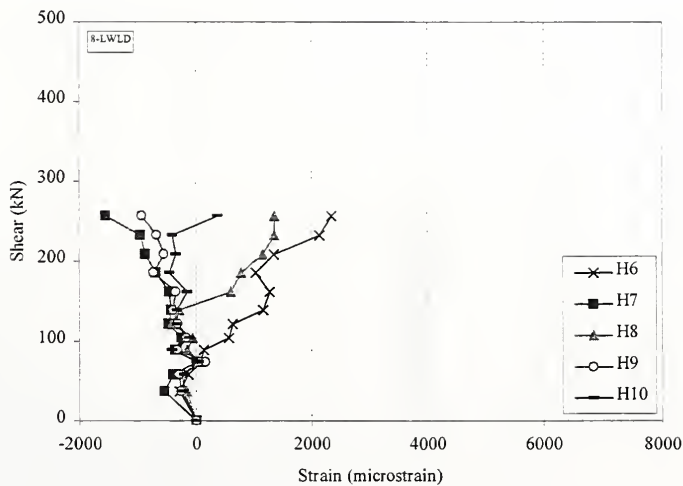


Figure 6.255 Shear-Strain Relationship, Horizontal Whittemore Measurements 6-10, Specimen 8-LWLD

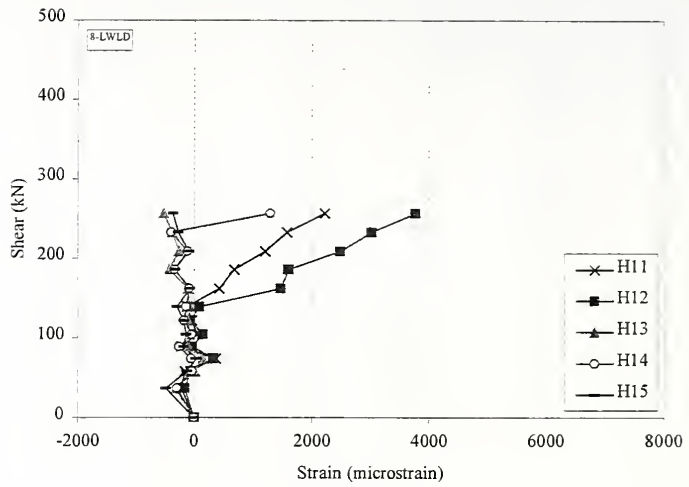


Figure 6.256 Shear-Strain Relationship, Horizontal Whittemore Measurements 11-15, Specimen 8-LWLD

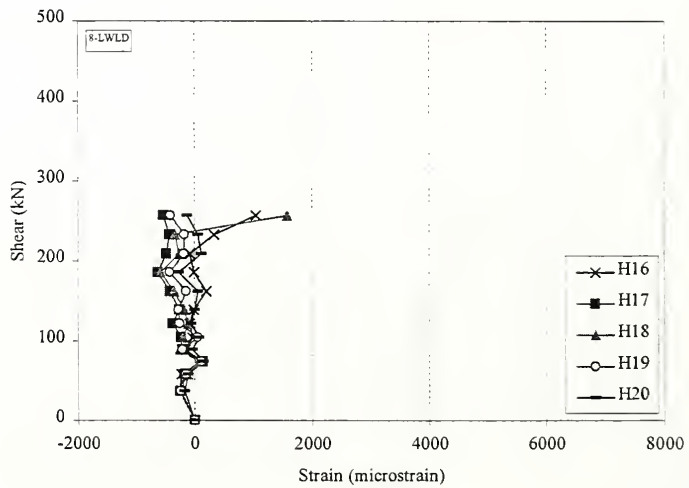


Figure 6.257 Shear-Strain Relationship, Horizontal Whittemore Measurements 16-20, Specimen 8-LWLD

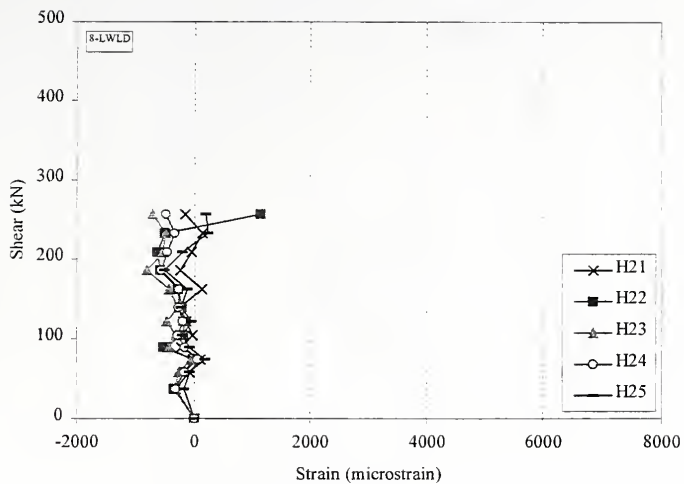


Figure 6.258 Shear-Strain Relationship, Horizontal Whittemore Measurements 21-25, Specimen 8-LWLD

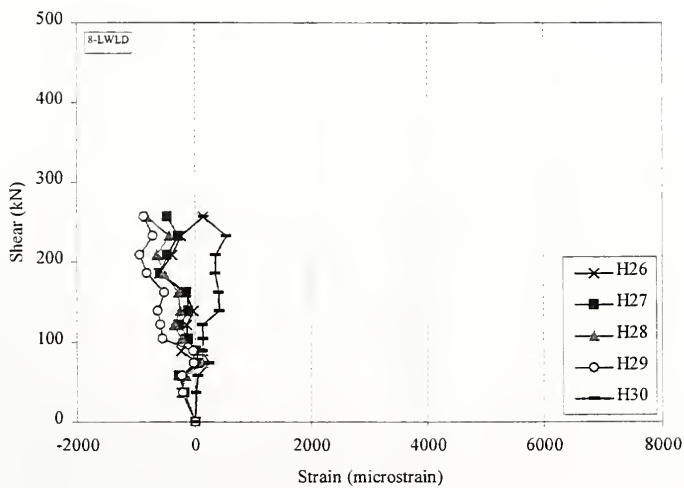


Figure 6.259 Shear-Strain Relationship, Horizontal Whittemore Measurements 26-30, Specimen 8-LWLD

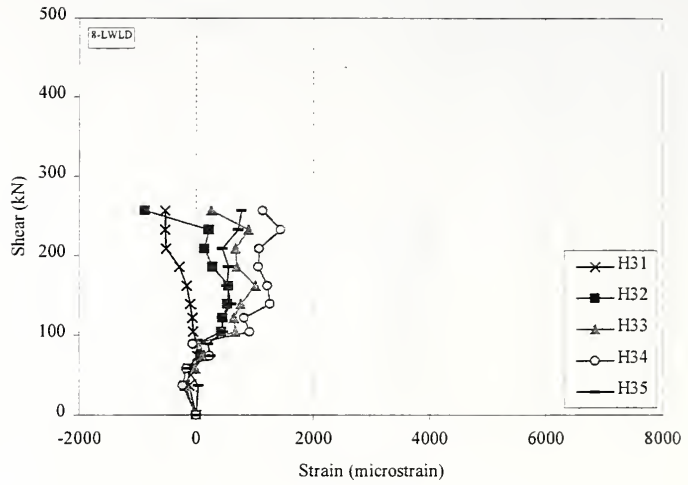


Figure 6.260 Shear-Strain Relationship, Horizontal Whittemore Measurements 31-35, Specimen 8-LWLD

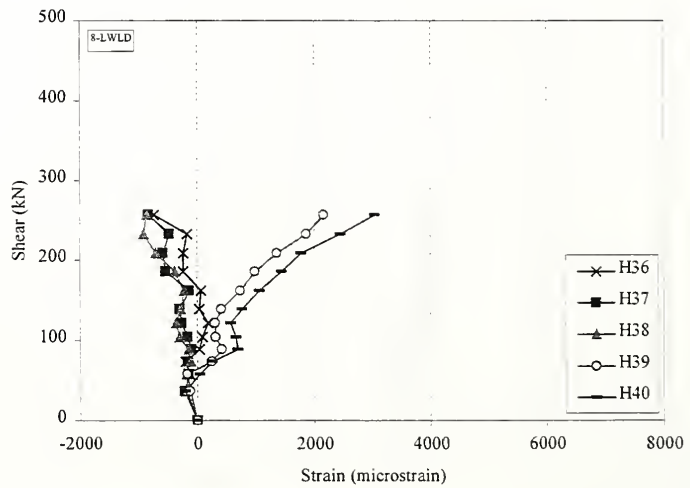


Figure 6.261 Shear-Strain Relationship, Horizontal Whittemore Measurements 36-40, Specimen 8-LWLD

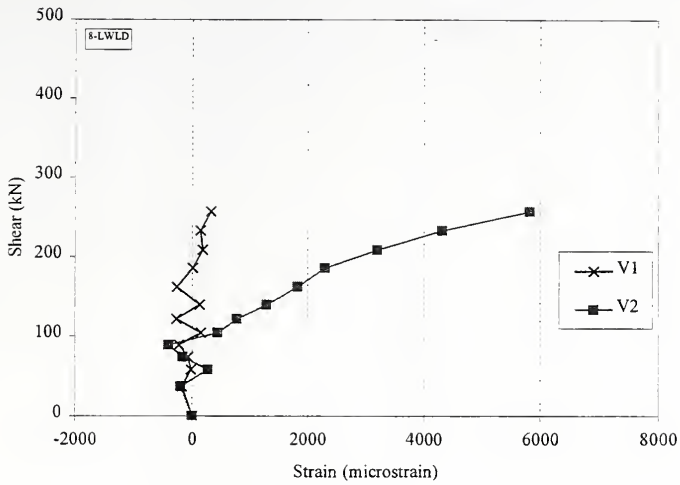


Figure 6.262 Shear-Strain Relationship, Vertical Whittemore Measurements 1-2, Specimen 8-LWLD

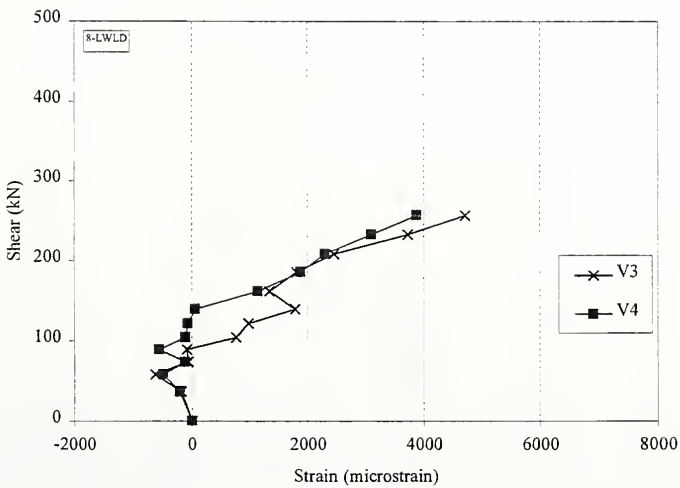


Figure 6.263 Shear-Strain Relationship, Vertical Whittemore Measurements 3-4, Specimen 8-LWLD

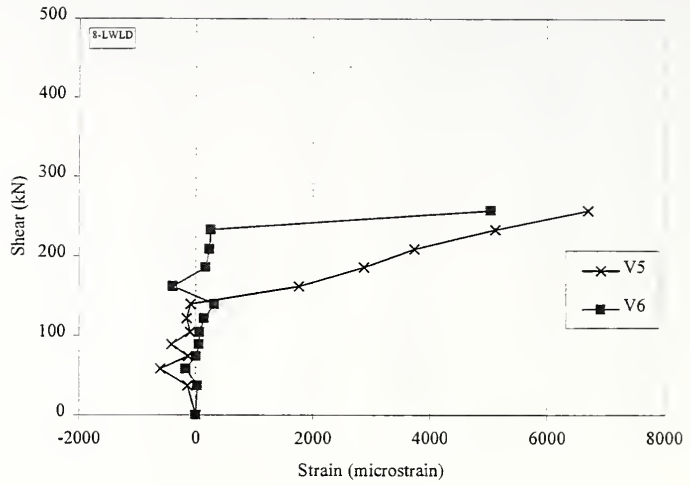


Figure 6.264 Shear-Strain Relationship, Vertical Whittemore Measurements 5-6, Specimen 8-LWLD

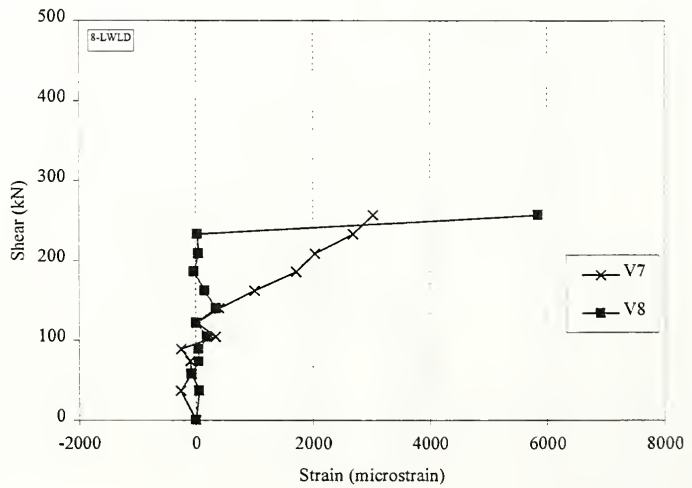


Figure 6.265 Shear-Strain Relationship, Vertical Whittemore Measurements 7-8, Specimen 8-LWLD

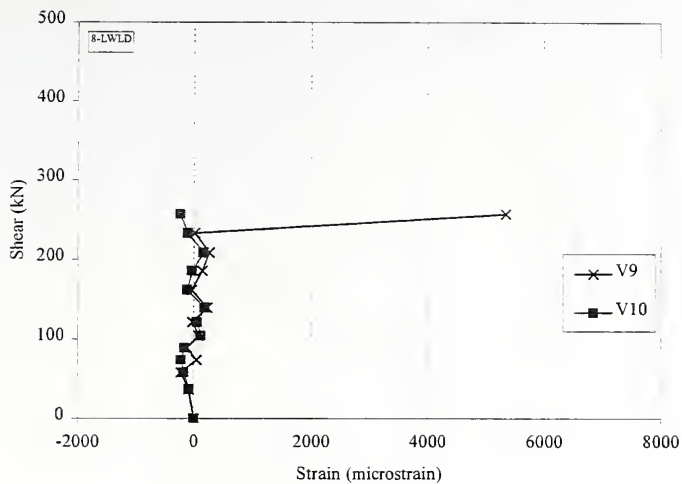


Figure 6.266 Shear-Strain Relationship, Vertical Whittemore Measurements 9-10, Specimen 8-LWLD

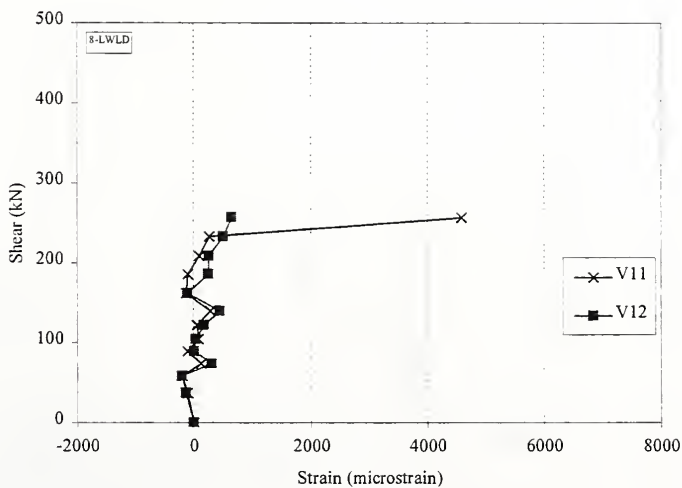


Figure 6.267 Shear-Strain Relationship, Vertical Whittemore Measurements 11-12, Specimen 8-LWLD

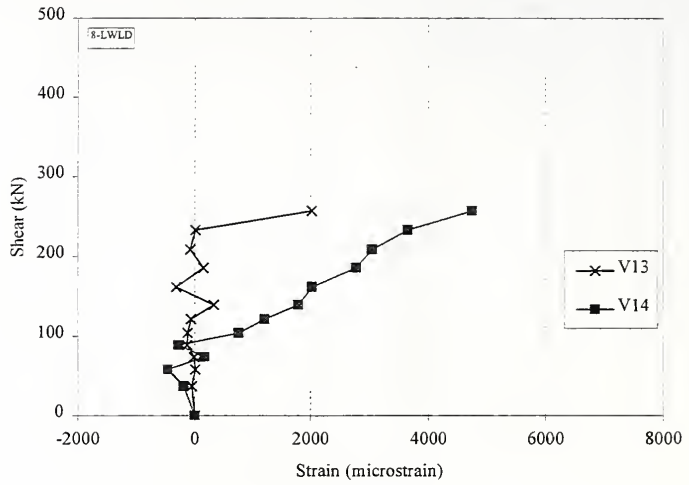


Figure 6.268 Shear-Strain Relationship, Vertical Whittemore Measurements 13-14, Specimen 8-LWLD

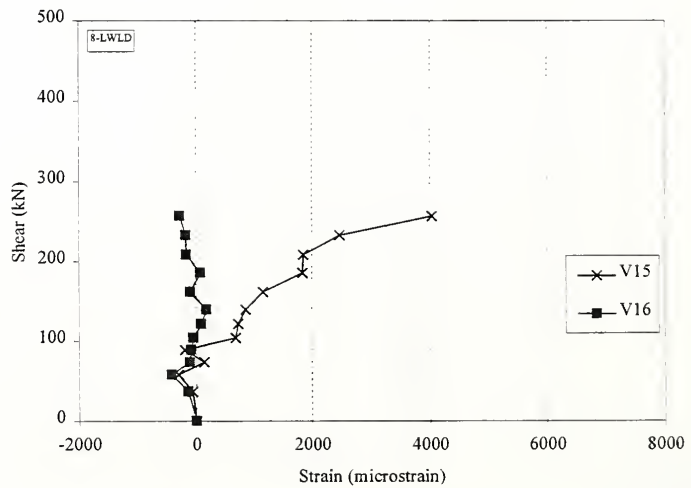


Figure 6.269 Shear-Strain Relationship, Vertical Whittemore Measurements 15-16, Specimen 8-LWLD

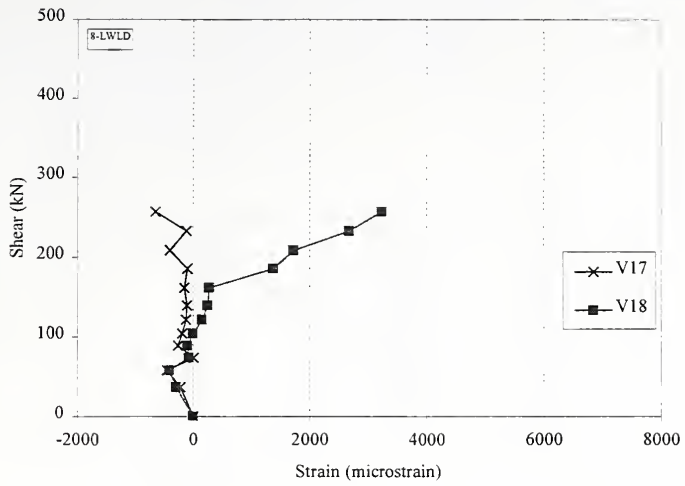


Figure 6.270 Shear-Strain Relationship, Vertical Whittemore Measurements 17-18, Specimen 8-LWLD

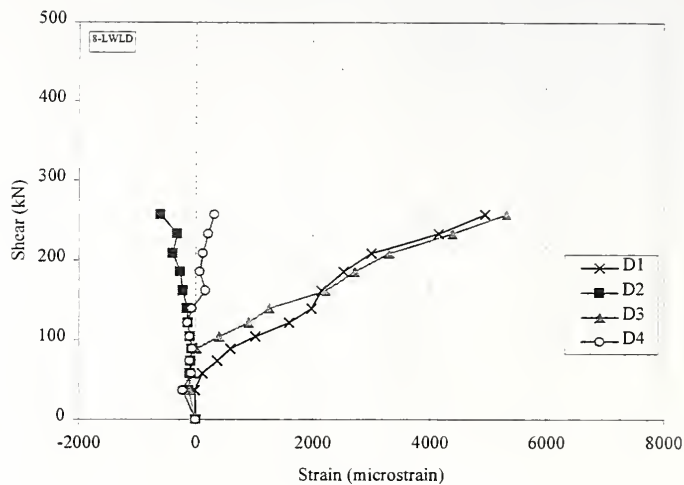


Figure 6.271 Shear-Strain Relationship, Diagonal Whittemore Measurements 1-4, Specimen 8-LWLD

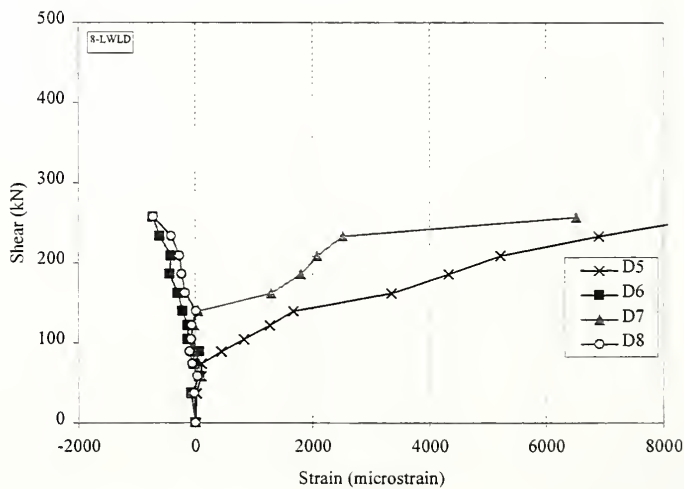


Figure 6.272 Shear-Strain Relationship, Diagonal Whittemore Measurements 5-8, Specimen 8-LWLD

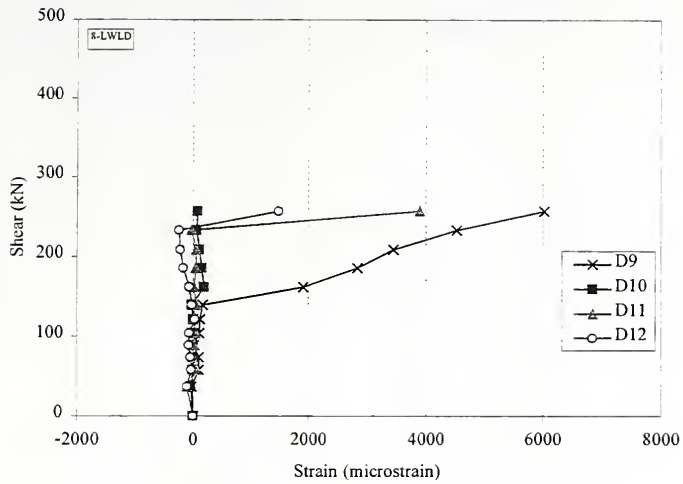


Figure 6.273 Shear-Strain Relationship, Diagonal Whittemore Measurements 9-12, Specimen 8-LWLD

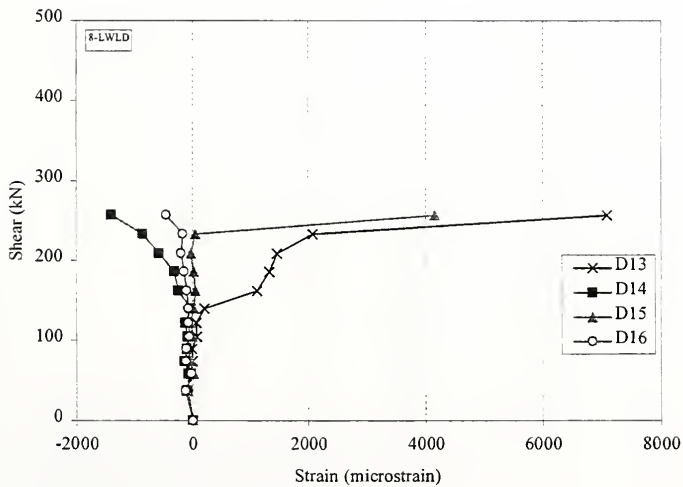


Figure 6.274 Shear-Strain Relationship, Diagonal Whittemore Measurements 13-16, Specimen 8-LWLD

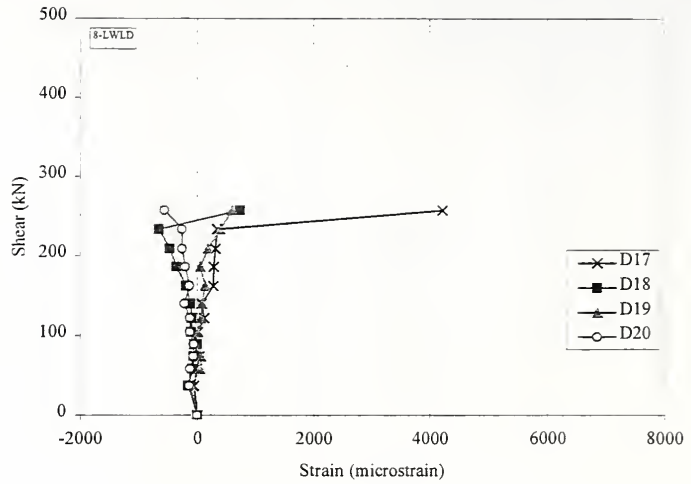


Figure 6.275 Shear-Strain Relationship, Diagonal Whittemore Measurements 17-20, Specimen 8-LWLD

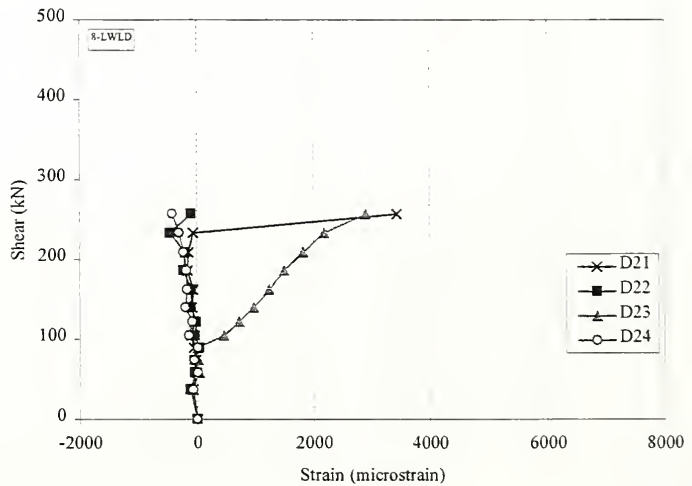


Figure 6.276 Shear-Strain Relationship, Diagonal Whittemore Measurements 21-24, Specimen 8-LWLD

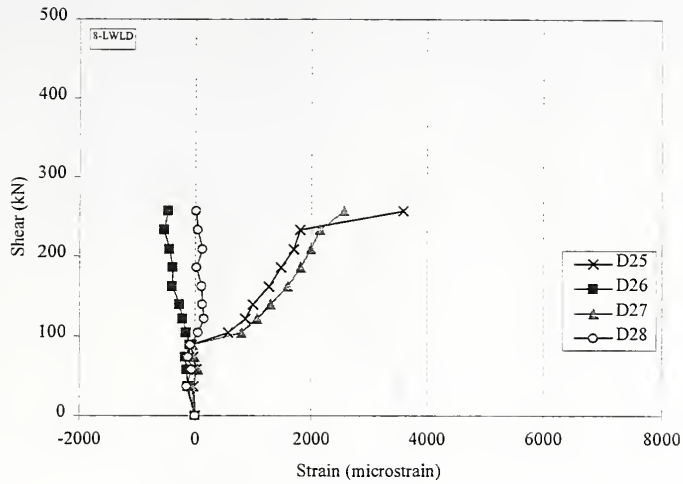


Figure 6.277 Shear-Strain Relationship, Diagonal Whittemore Measurements 25-28, Specimen 8-LWLD

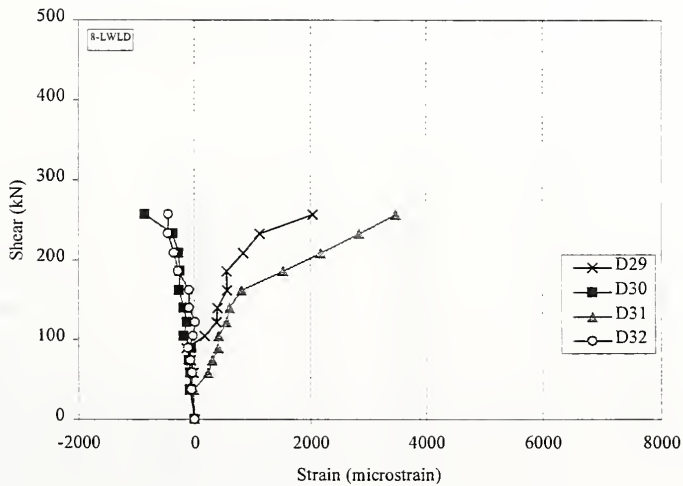


Figure 6.278 Shear-Strain Relationship, Diagonal Whittemore Measurements 29-32, Specimen 8-LWLD

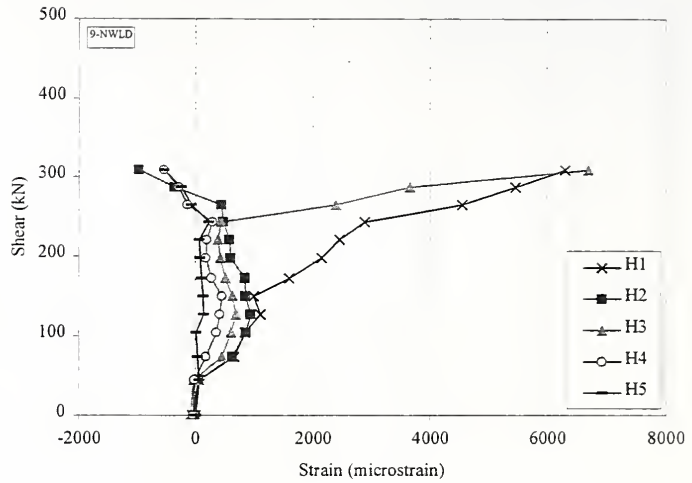


Figure 6.279 Shear-Strain Relationship, Horizontal Whittemore Measurements 1-5, Specimen 9-NWLD

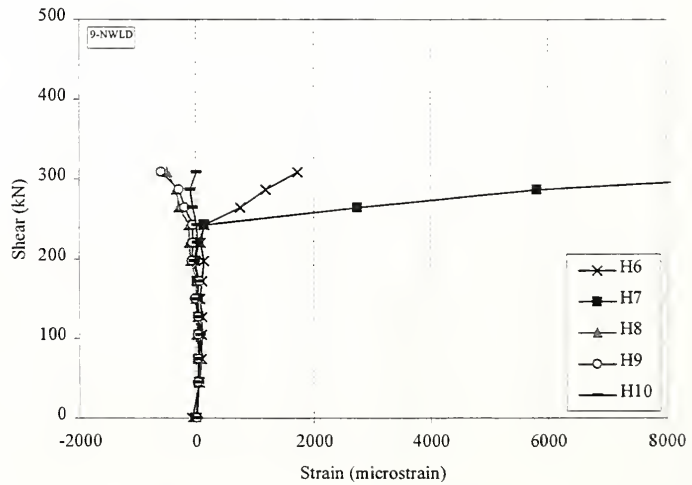


Figure 6.280 Shear-Strain Relationship, Horizontal Whittemore Measurements 6-10, Specimen 9-NWLD

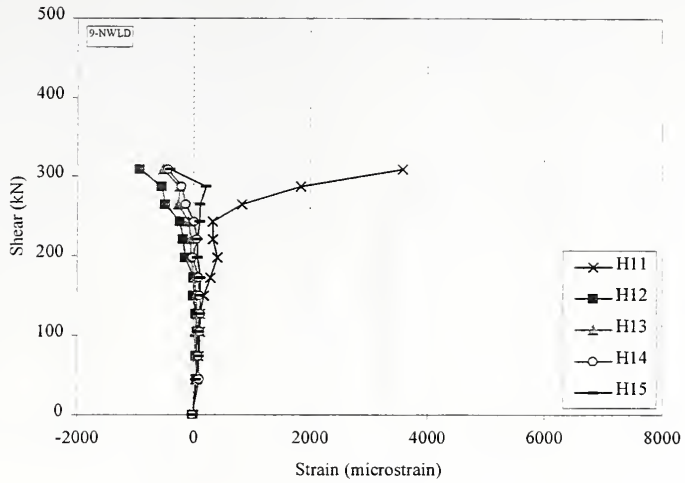


Figure 6.281 Shear-Strain Relationship, Horizontal Whittemore Measurements 11-15, Specimen 9-NWLD

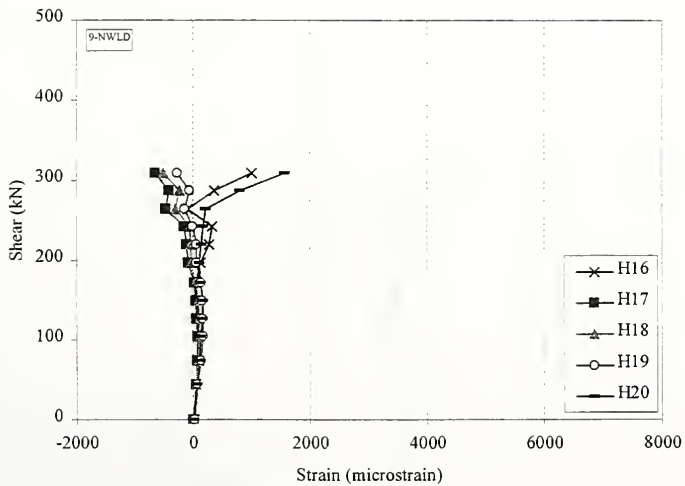


Figure 6.282 Shear-Strain Relationship, Horizontal Whittemore Measurements 16-20, Specimen 9-NWLD

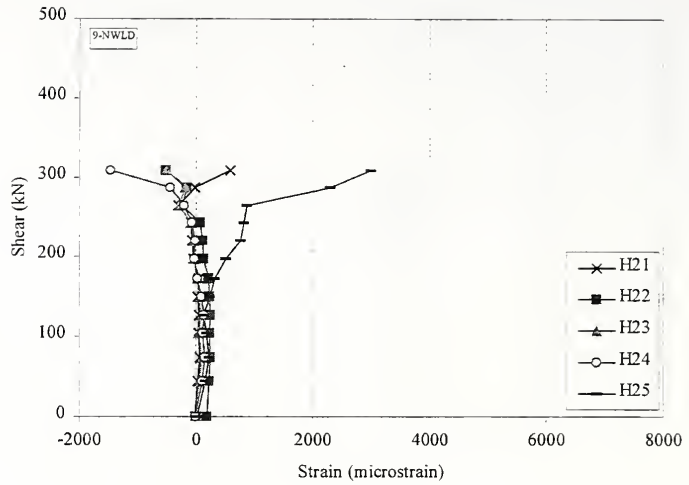


Figure 6.283 Shear-Strain Relationship, Horizontal Whittemore Measurements 21-25, Specimen 9-NWLD

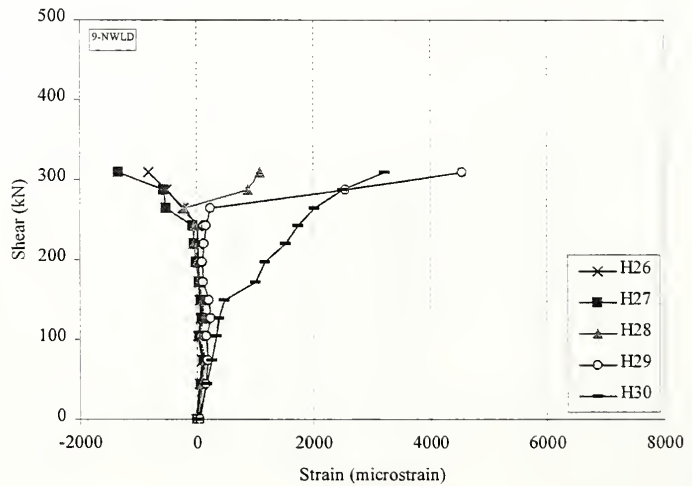


Figure 6.284 Shear-Strain Relationship, Horizontal Whittemore Measurements 26-30, Specimen 9-NWLD

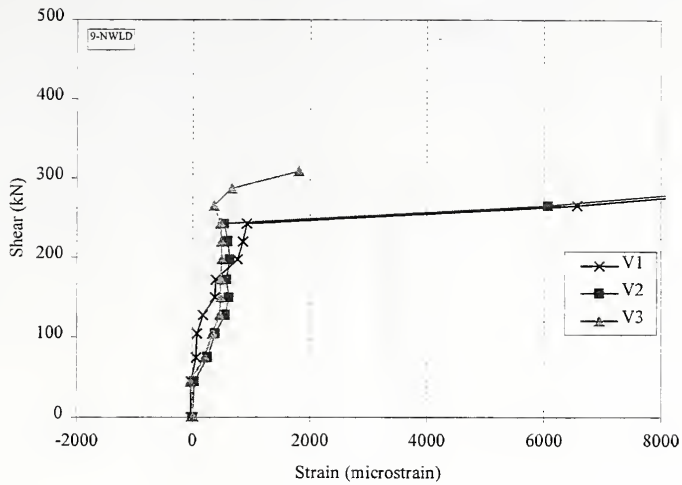


Figure 6.285 Shear-Strain Relationship, Vertical Whittemore Measurements 1-3, Specimen 9-NWLD

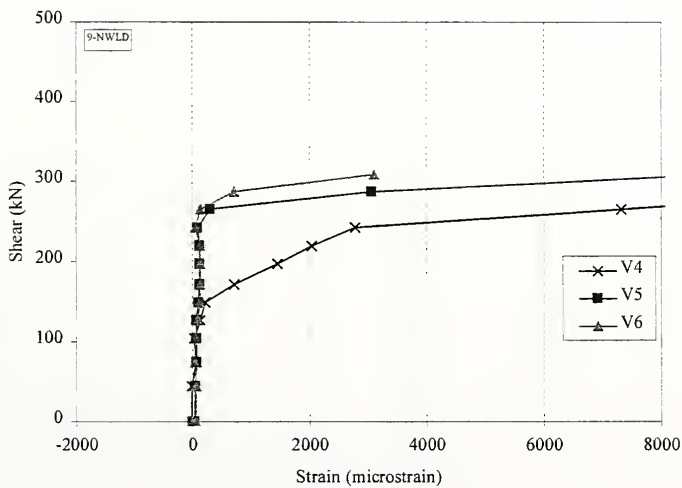


Figure 6.286 Shear-Strain Relationship, Vertical Whittemore Measurements 4-6, Specimen 9-NWLD

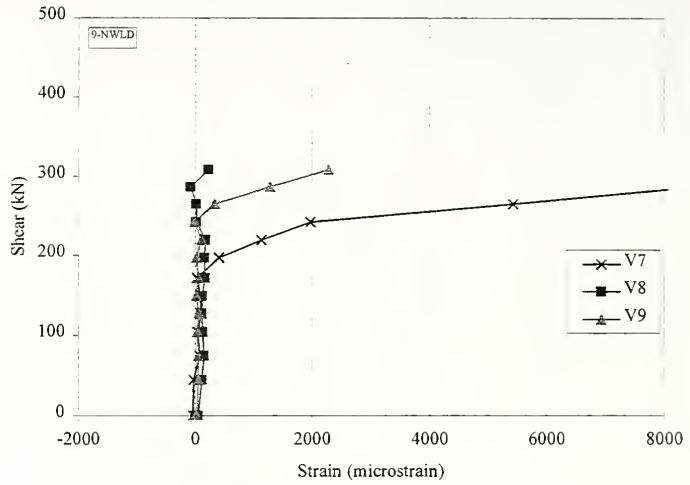


Figure 6.287 Shear-Strain Relationship, Vertical Whittemore Measurements 7-9, Specimen 9-NWLD

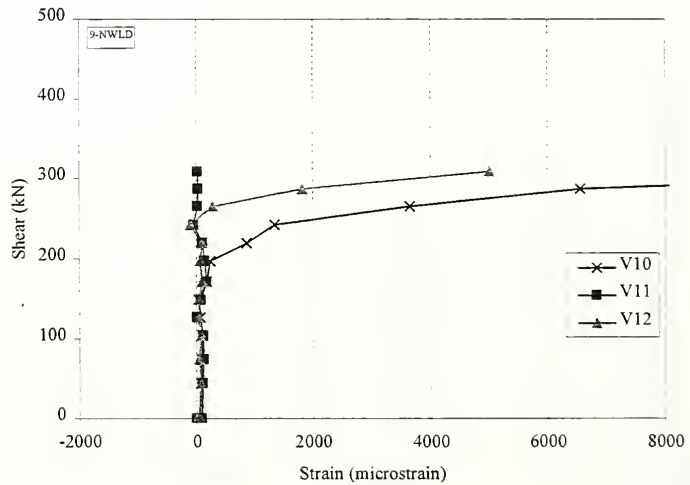


Figure 6.288 Shear-Strain Relationship, Vertical Whittemore Measurements 10-12, Specimen 9-NWLD

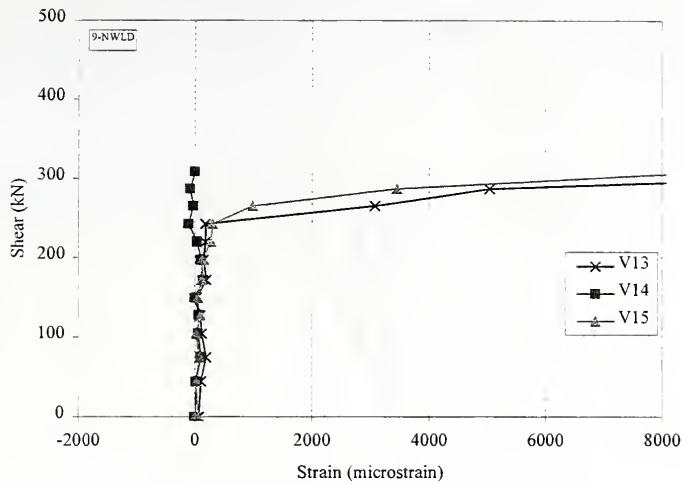


Figure 6.289 Shear-Strain Relationship, Vertical Whittemore Measurements 13-15, Specimen 9-NWLD

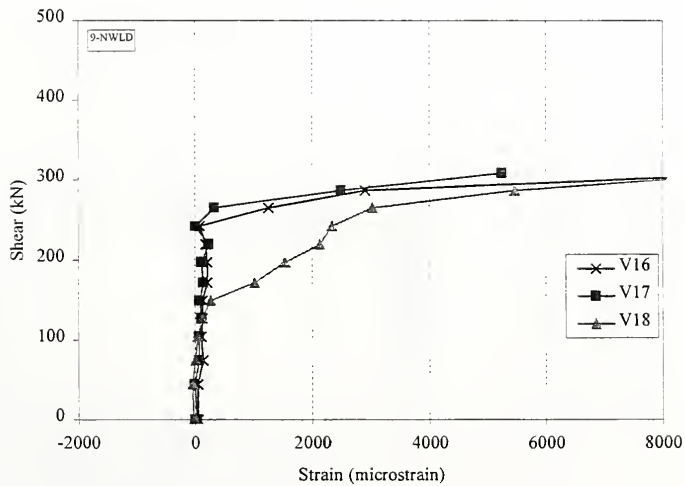


Figure 6.290 Shear-Strain Relationship, Vertical Whittemore Measurements 16-18, Specimen 9-NWLD

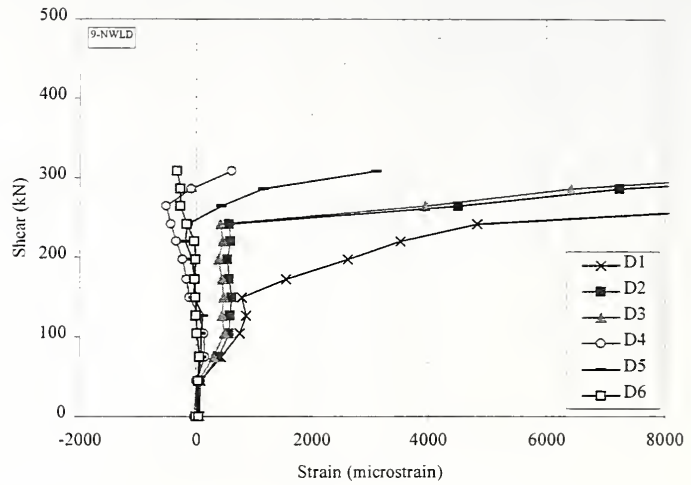


Figure 6.291 Shear-Strain Relationship, Diagonal Whittemore Measurements 1-6, Specimen 9-NWLD

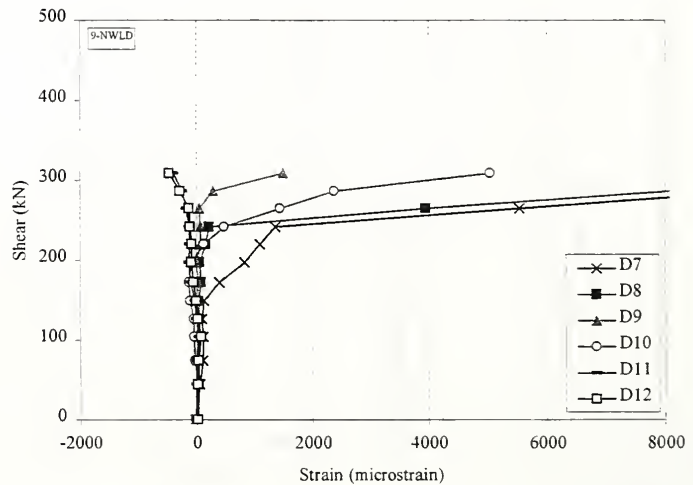


Figure 6.292 Shear-Strain Relationship, Diagonal Whittemore Measurements 7-12, Specimen 9-NWLD

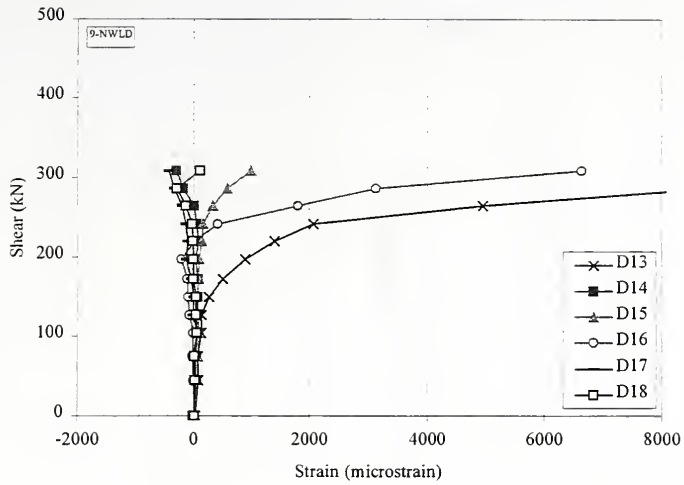


Figure 6.293 Shear-Strain Relationship, Diagonal Whittemore Measurements 13-18, Specimen 9-NWLD

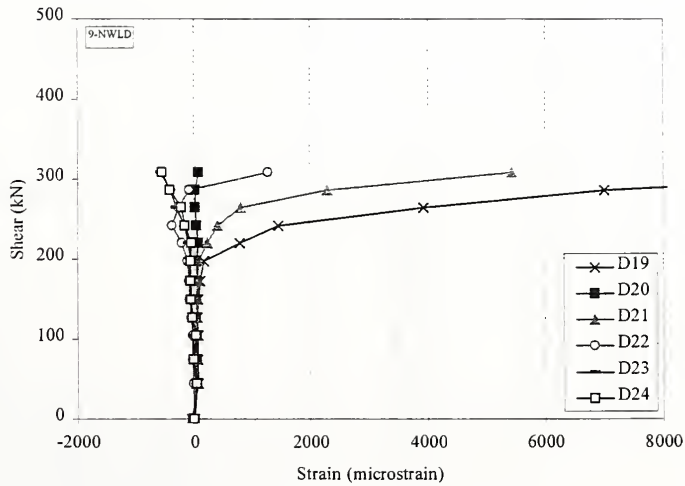


Figure 6.294 Shear-Strain Relationship, Diagonal Whittemore Measurements 19-24, Specimen 9-NWLD

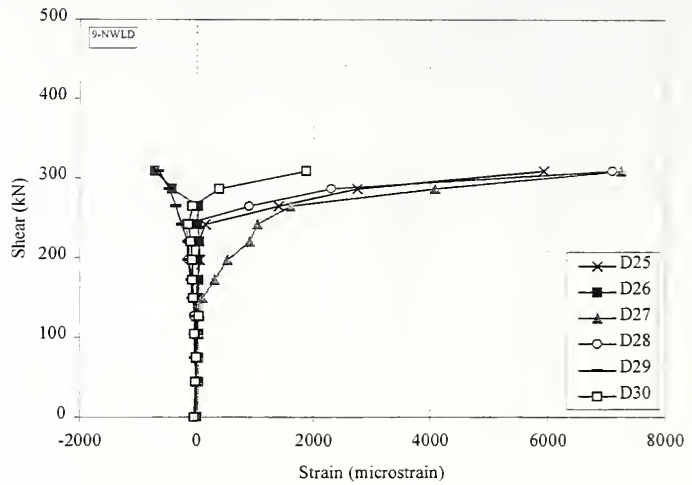


Figure 6.295 Shear-Strain Relationship, Diagonal Whittemore Measurements 25-30, Specimen 9-NWLD

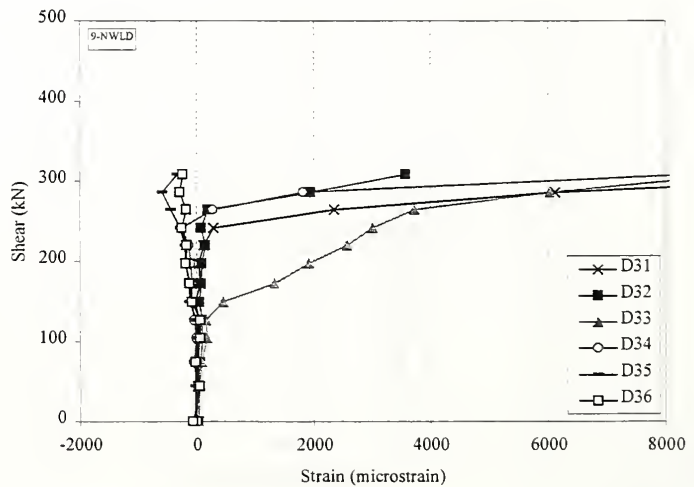


Figure 6.296 Shear-Strain Relationship, Diagonal Whittemore Measurements 31-36, Specimen 9-NWLD

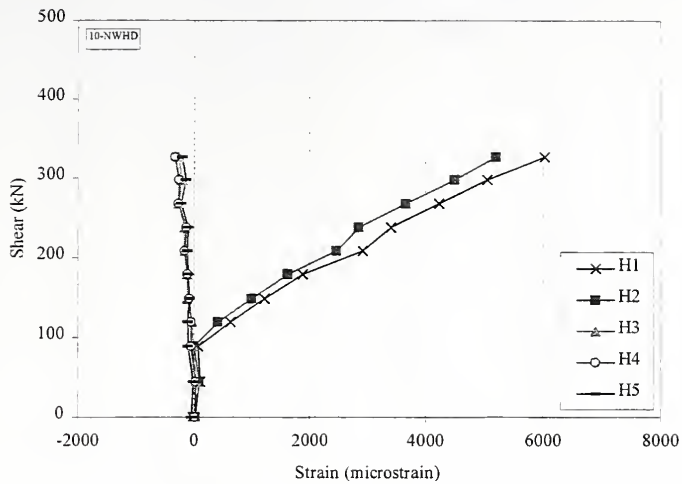


Figure 6.297 Shear-Strain Relationship, Horizontal Whittemore Measurements 1-5, Specimen 10-NWHD

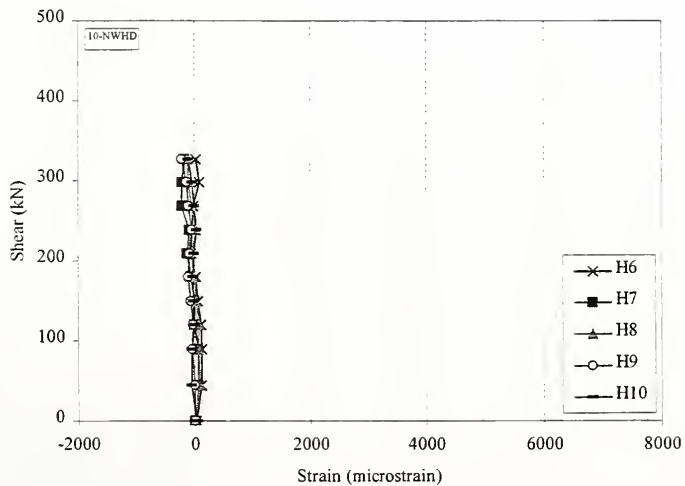


Figure 6.298 Shear-Strain Relationship, Horizontal Whittemore Measurements 6-10, Specimen 10-NWHD

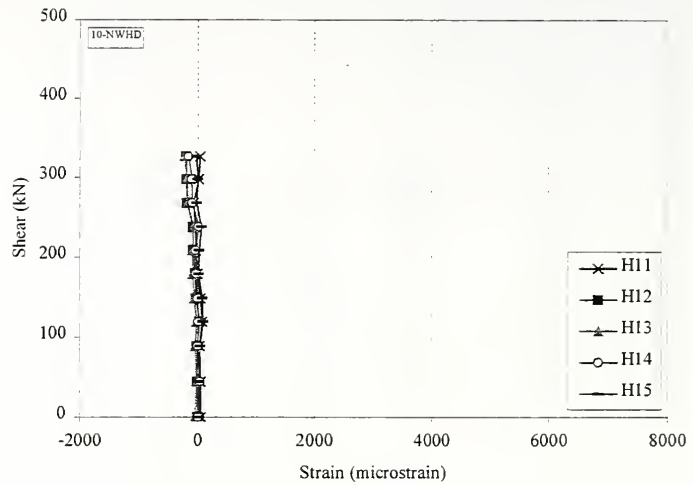


Figure 6.299 Shear-Strain Relationship, Horizontal Whittemore Measurements 11-15, Specimen 10-NWHD

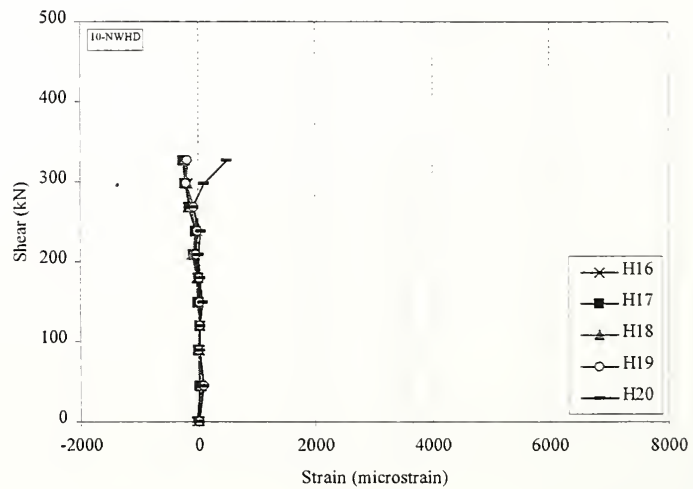


Figure 6.300 Shear-Strain Relationship, Horizontal Whittemore Measurements 16-20, Specimen 10-NWHD

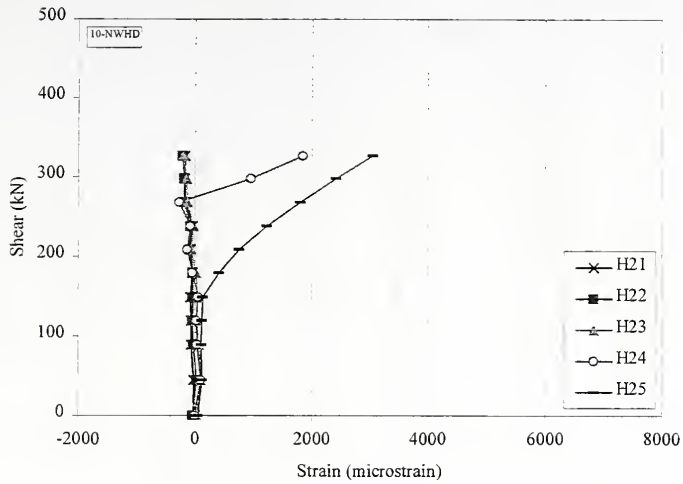


Figure 6.301 Shear-Strain Relationship, Horizontal Whittemore Measurements 21-25, Specimen 10-NWHD

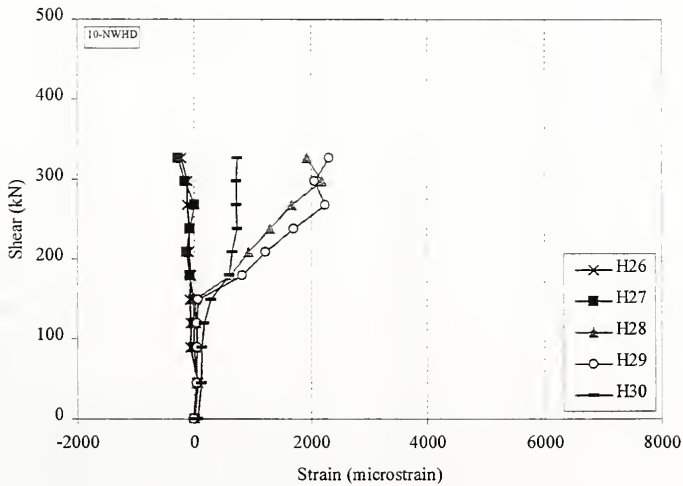


Figure 6.302 Shear-Strain Relationship, Horizontal Whittemore Measurements 26-30, Specimen 10-NWHD

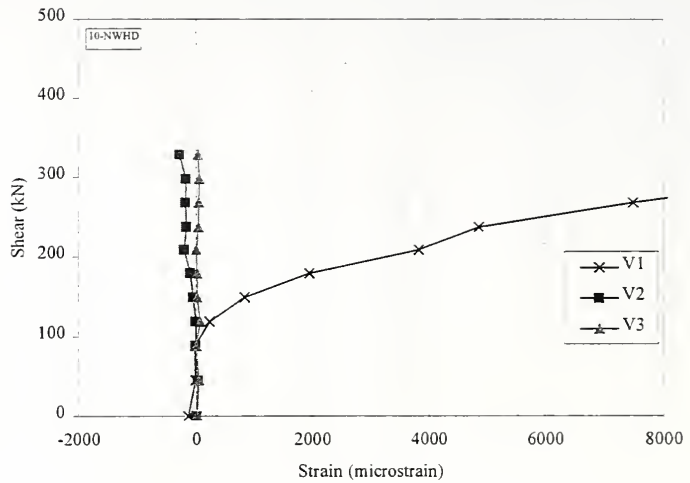


Figure 6.303 Shear-Strain Relationship, Vertical Whittemore Measurements 1-3, Specimen 10-NWHD

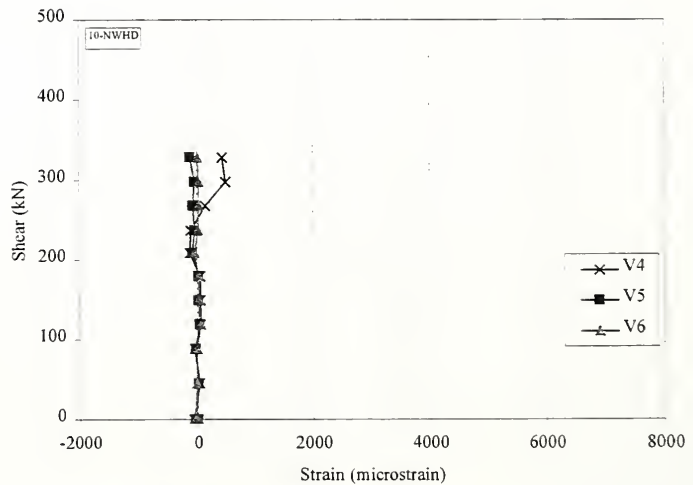


Figure 6.304 Shear-Strain Relationship, Vertical Whittemore Measurements 4-6, Specimen 10-NWHD

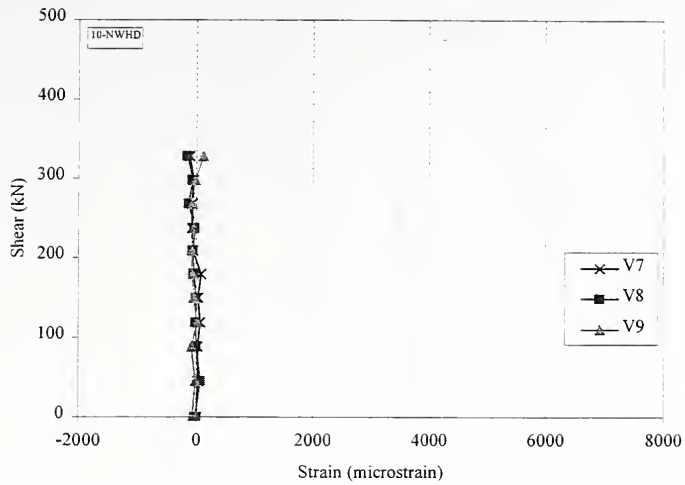


Figure 6.305 Shear-Strain Relationship, Vertical Whittemore Measurements 7-9, Specimen 10-NWHD

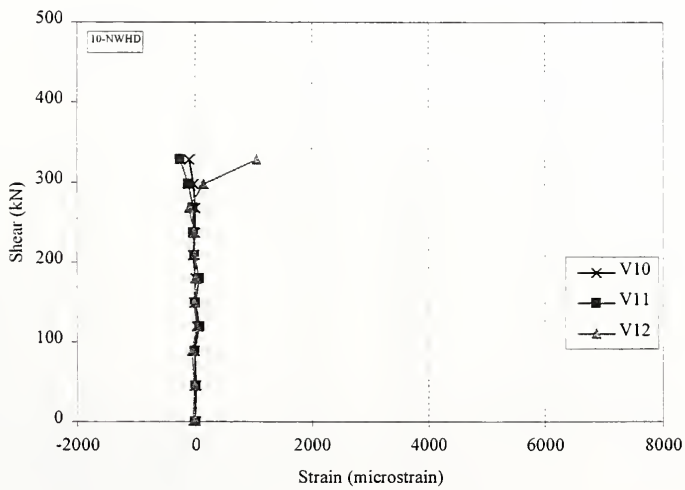


Figure 6.306 Shear-Strain Relationship, Vertical Whittemore Measurements 10-12, Specimen 10-NWHD

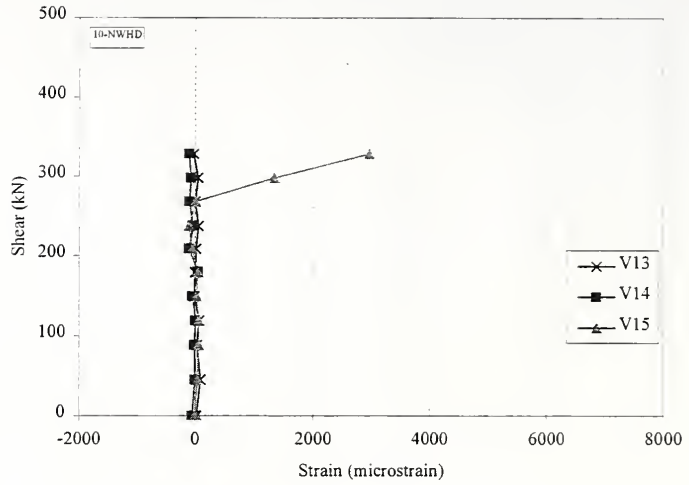


Figure 6.307 Shear-Strain Relationship, Vertical Whittemore Measurements 13-15, Specimen 10-NWHD

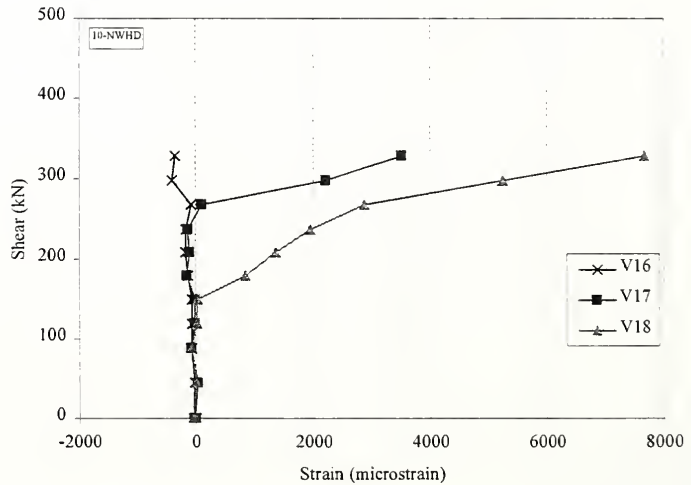


Figure 6.308 Shear-Strain Relationship, Vertical Whittemore Measurements 16-18, Specimen 10-NWHD

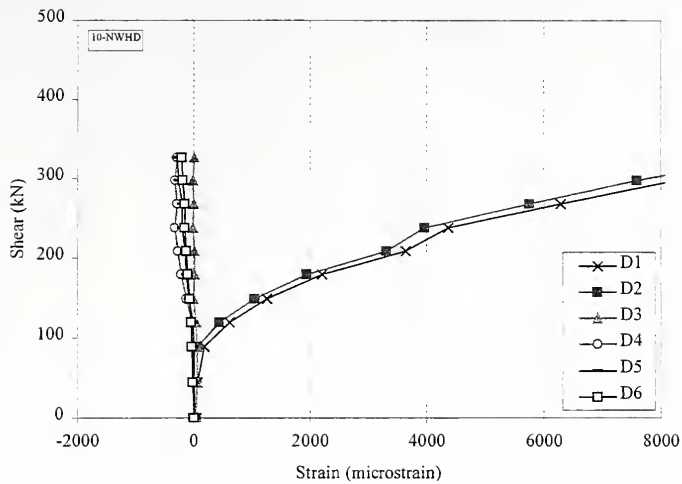


Figure 6.309 Shear-Strain Relationship, Diagonal Whittemore Measurements 1-6, Specimen 10-NWHD

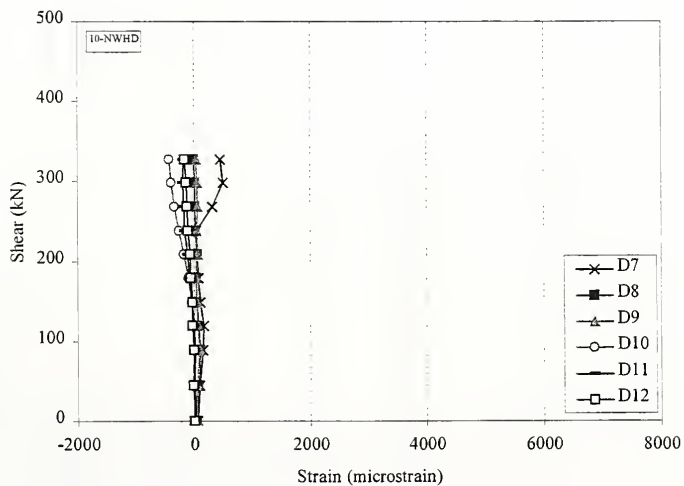


Figure 6.310 Shear-Strain Relationship, Diagonal Whittemore Measurements 7-12, Specimen 10-NWHD

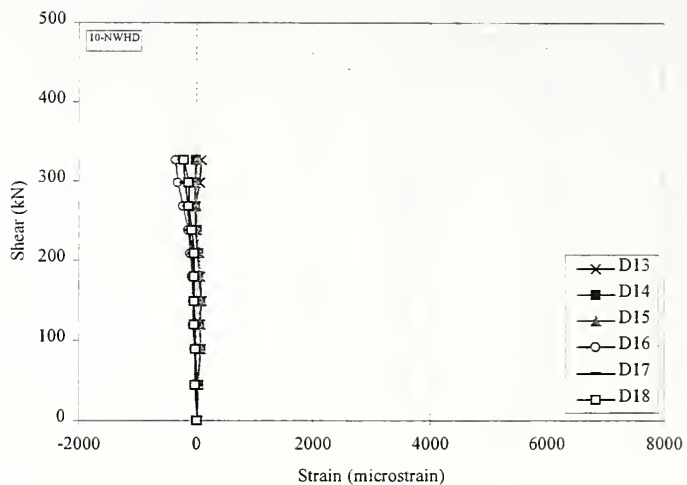


Figure 6.311 Shear-Strain Relationship, Diagonal Whittemore Measurements 13-18, Specimen 10-NWHD

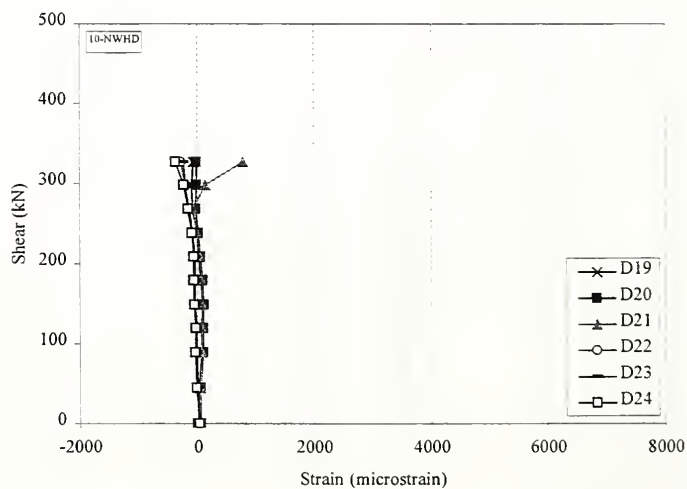


Figure 6.312 Shear-Strain Relationship, Diagonal Whittemore Measurements 19-24, Specimen 10-NWHD

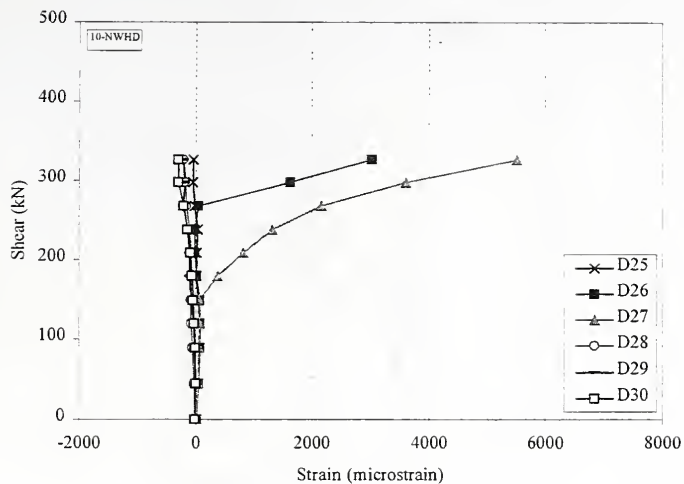


Figure 6.313 Shear-Strain Relationship, Diagonal Whittemore Measurements 25-30, Specimen 10-NWHD

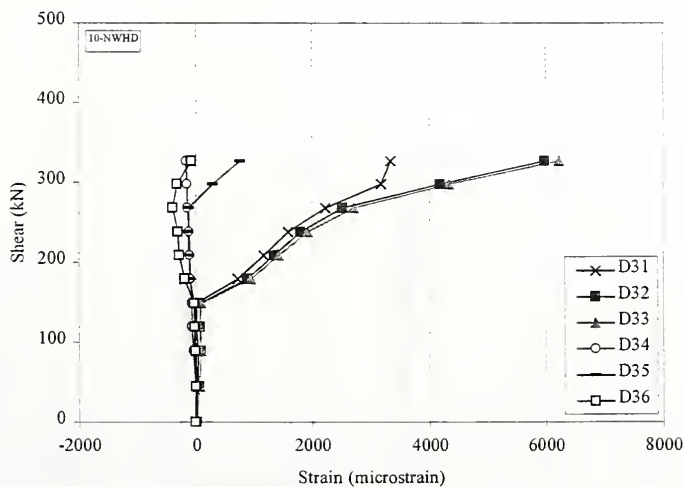


Figure 6.314 Shear-Strain Relationship, Diagonal Whittemore Measurements 31-36, Specimen 10-NWHD

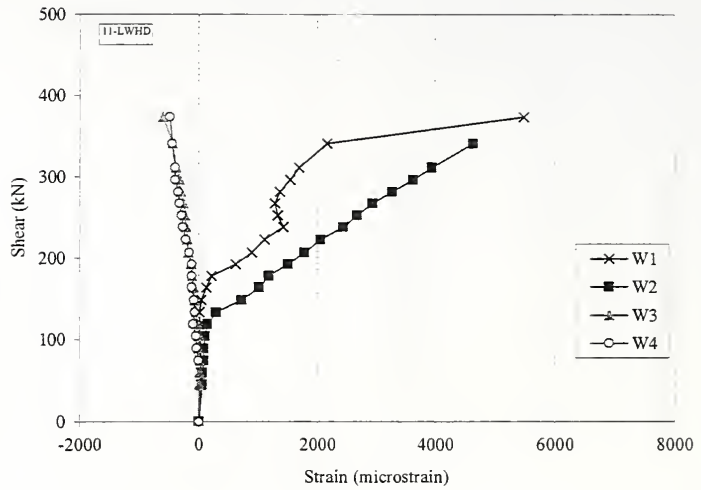


Figure 6.315 Shear-Strain Relationship, Whittemore Strains, Rosette 1, Specimen 11-LWHD

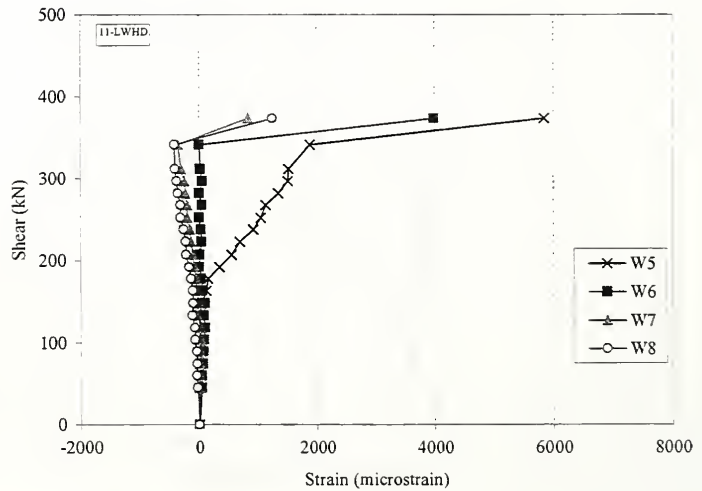


Figure 6.316 Shear-Strain Relationship, Whittemore Strains, Rosette 2, Specimen 11-LWHD

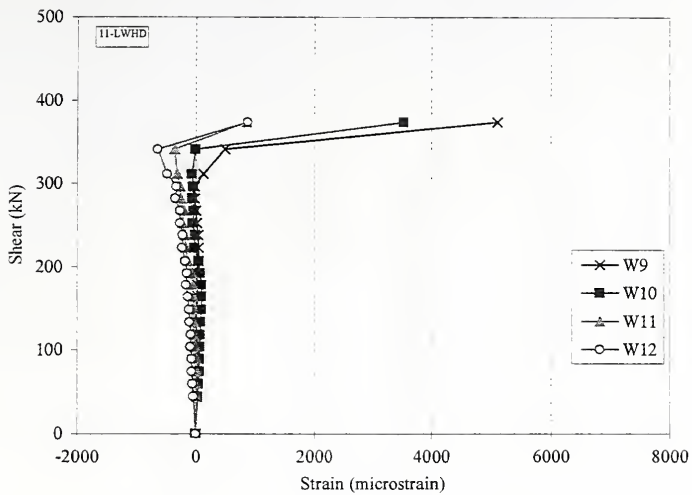


Figure 6.317 Shear-Strain Relationship, Whittemore Strains, Rosette 3, Specimen 11-LWHD

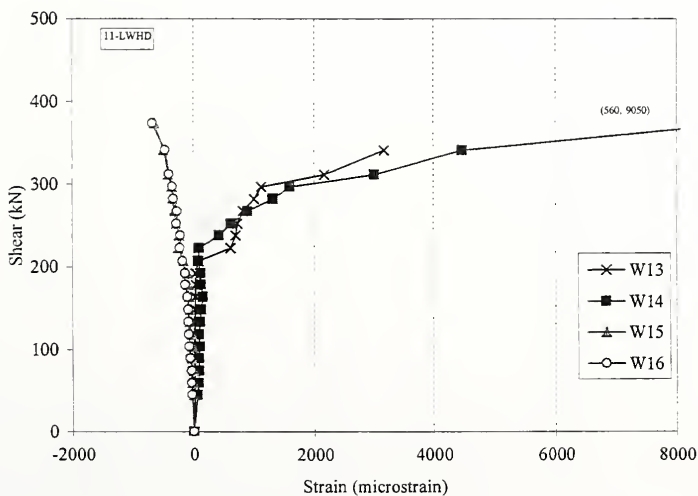


Figure 6.318 Shear-Strain Relationship, Whittemore Strains, Rosette 4, Specimen 11-LWHD

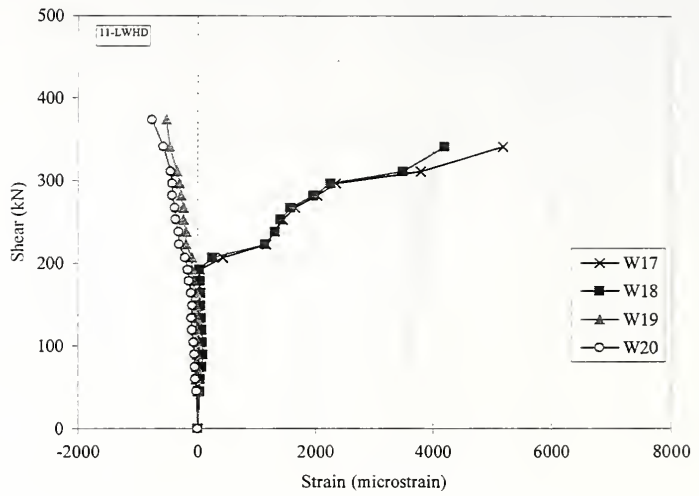


Figure 6.319 Shear-Strain Relationship, Whittemore Strains, Rosette 5, Specimen 11-LWHD

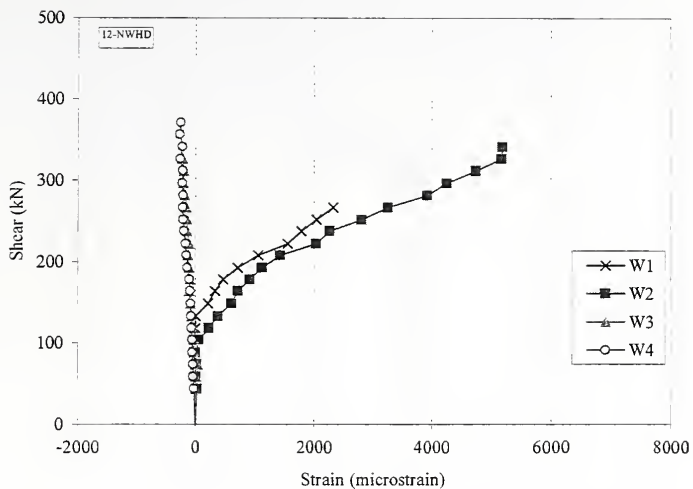


Figure 6.320 Shear-Strain Relationship, Whittemore Strains, Rosette 1, Specimen 12-NWHD

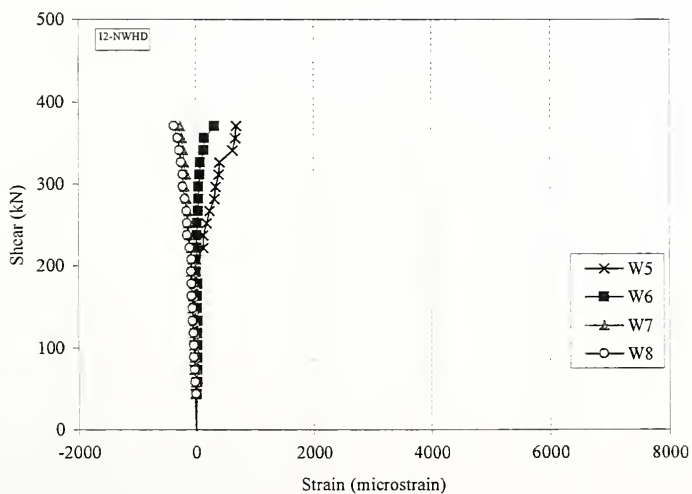


Figure 6.321 Shear-Strain Relationship, Whittemore Strains, Rosette 2, Specimen 12-NWHD

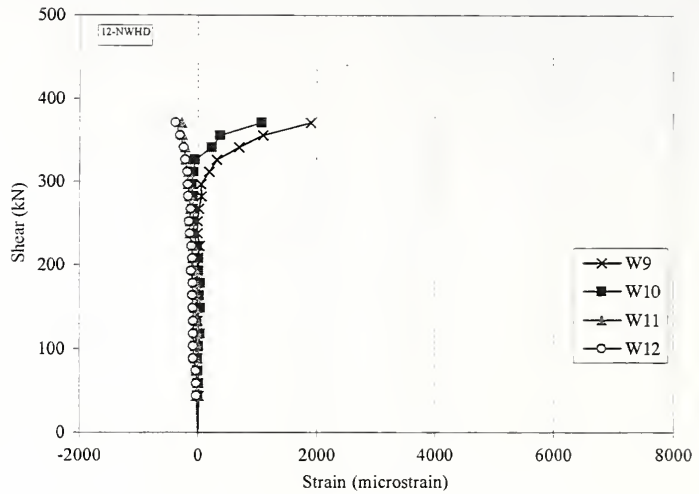


Figure 6.322 Shear-Strain Relationship, Whittemore Strains, Rosette 3, Specimen 12-NWHD

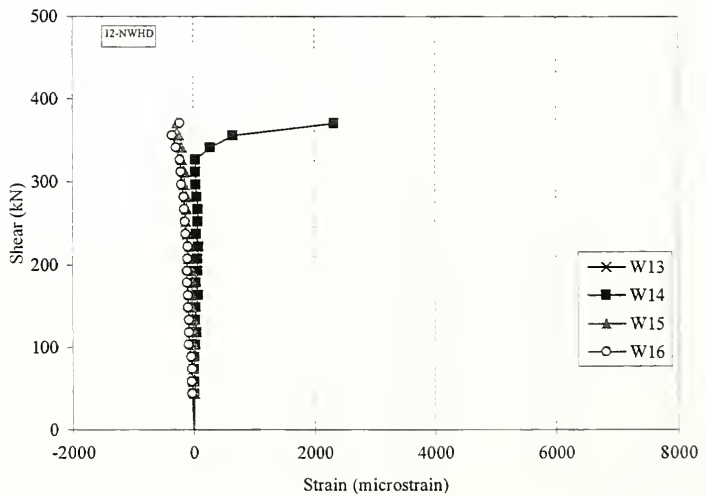


Figure 6.323 Shear-Strain Relationship, Whittemore Strains, Rosette 4, Specimen 12-NWHD

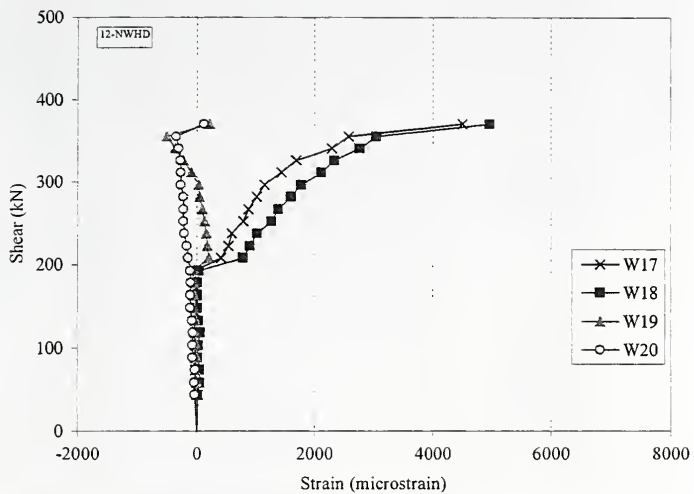


Figure 6.324 Shear-Strain Relationship, Whittemore Strains, Rosette 5, Specimen 12-NWHD

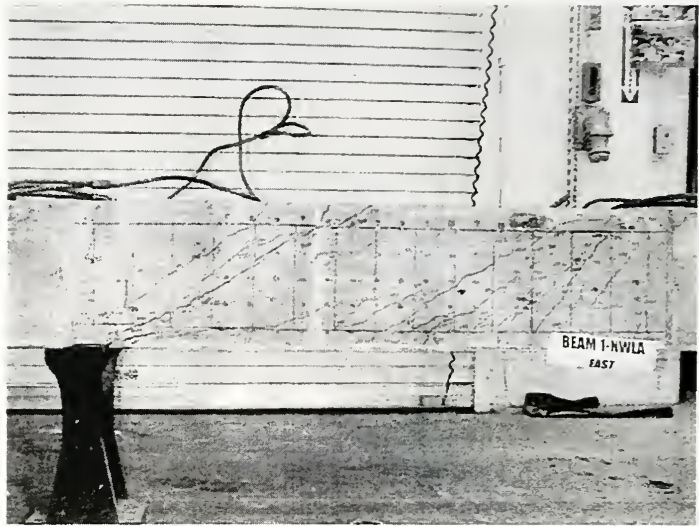


Figure 6.325 Specimen 1-NWLA at Failure

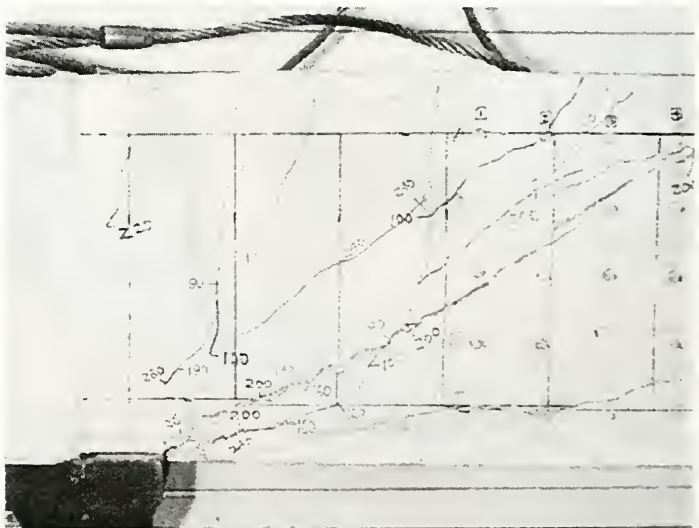


Figure 6.326 Specimen 1-NWLA at Failure (Part 1 of 3)

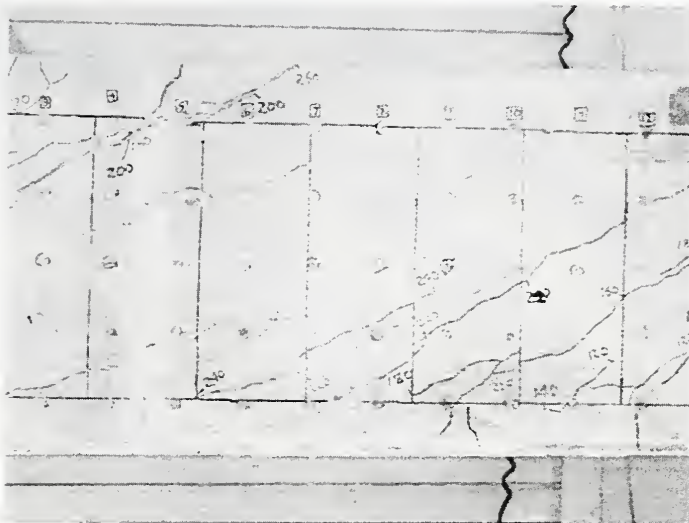


Figure 6.327 Specimen 1-NWLA at Failure (Part 2 of 3)

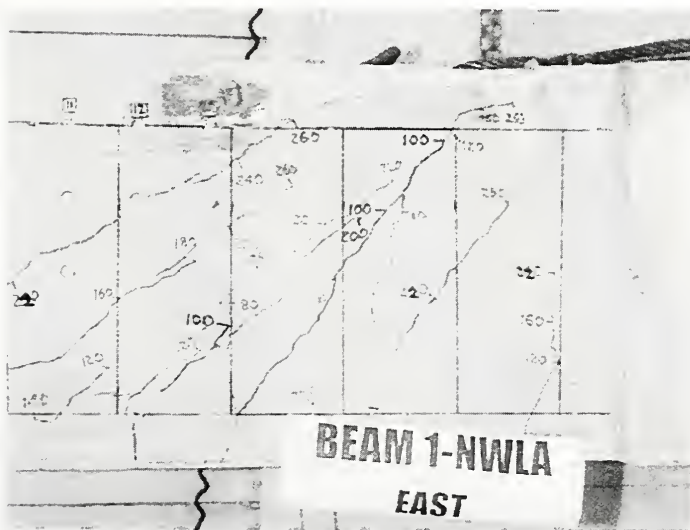


Figure 6.328 Specimen 1-NWLA at Failure (Part 3 of 3)

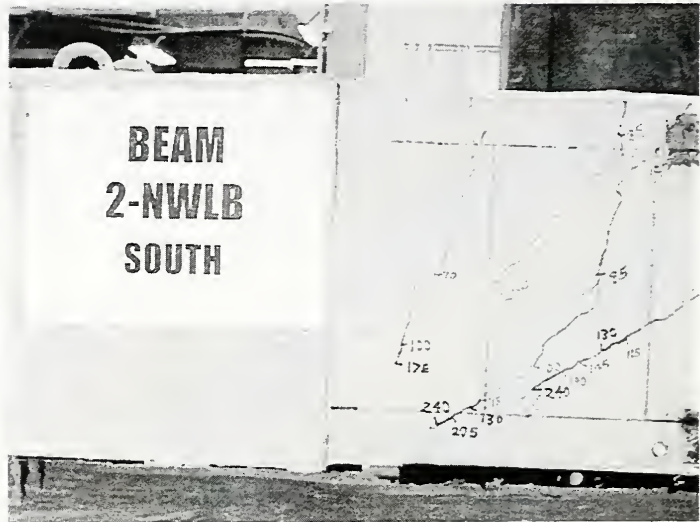


Figure 6.329 Specimen 2-NWLB at Failure, East Face, South End of Test Region

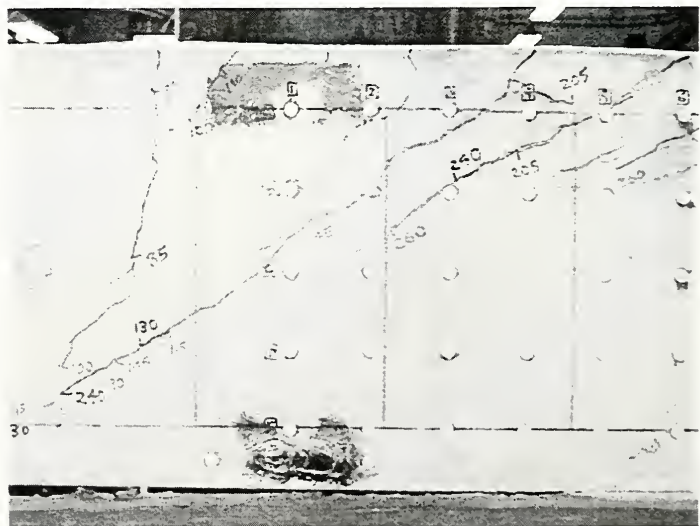


Figure 6.330 Specimen 2-NWLB at Failure, East Face, South Central Test Region

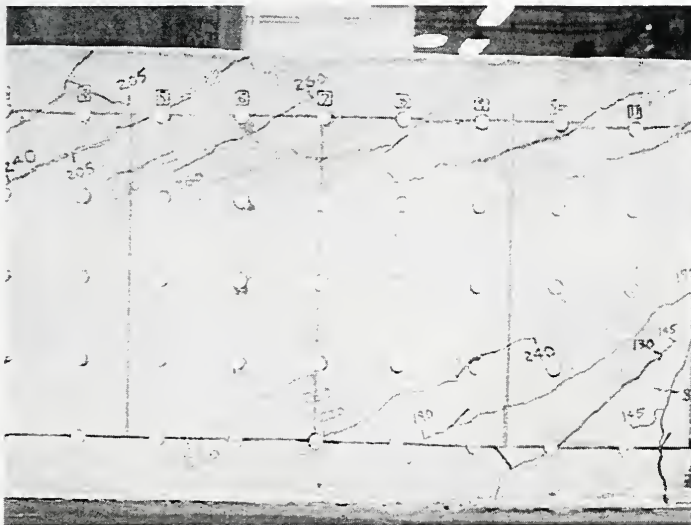


Figure 6.331 Specimen 2-NWLB at Failure, East Face, Center of Test Region



Figure 6.332 Specimen 2-NWL at Failure, East Face, North Central Test Region

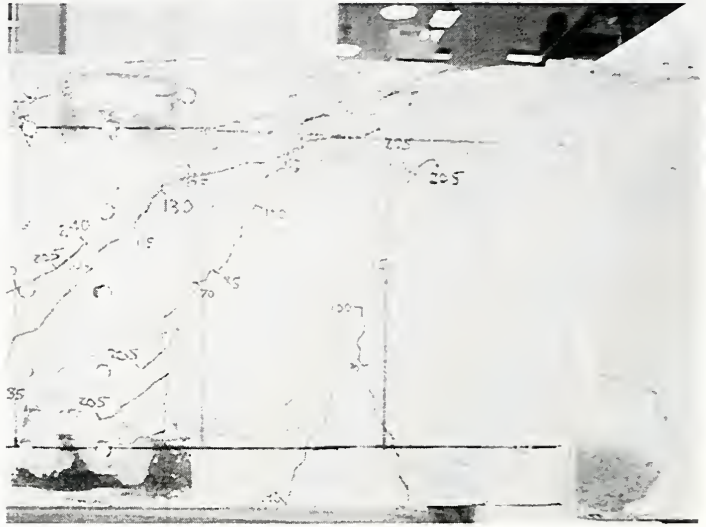


Figure 6.333 Specimen 2-NWLB at Failure, East Face, North End of Test Region

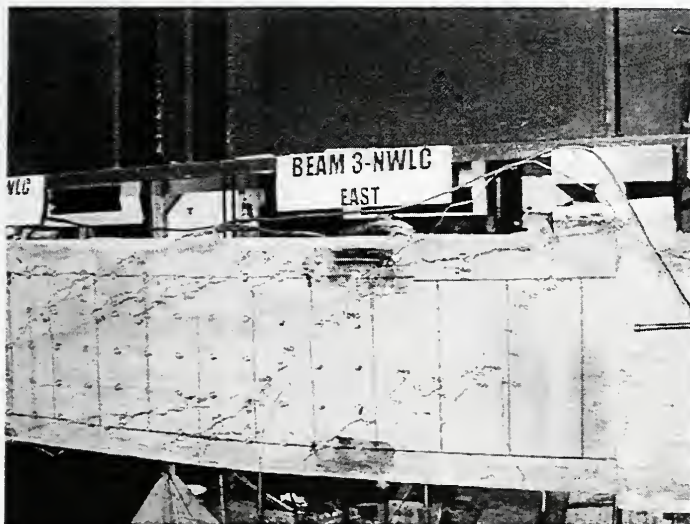


Figure 6.334 Specimen 3-NWLC



Figure 6.335 Specimen 3-NWLC

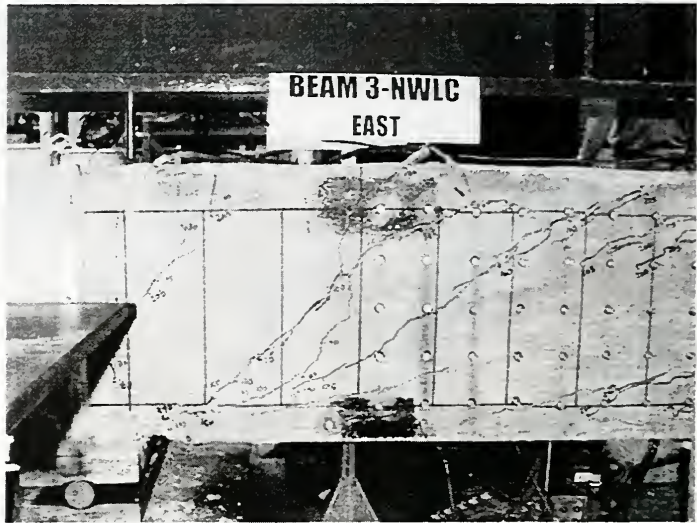


Figure 6.336 Specimen 3-NWLC

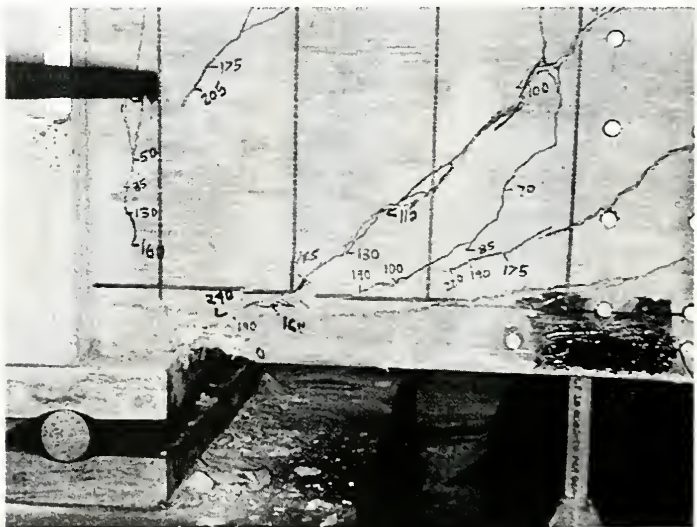


Figure 6.337 Specimen 3-NWLC

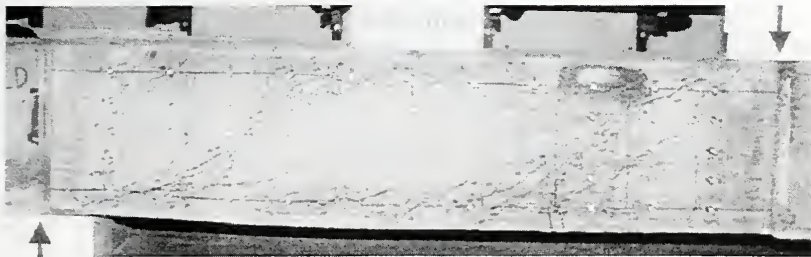


Figure 6.338 Specimen 4-NWLD at Failure

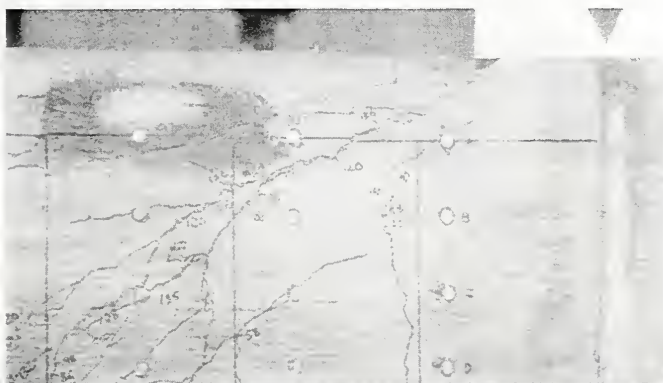


Figure 6.339 Specimen 4-NWLD, South Load Point

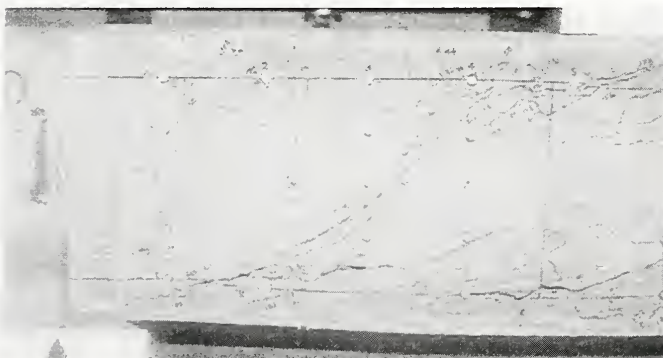


Figure 6.340 Specimen 4-NWLD, North Support Region

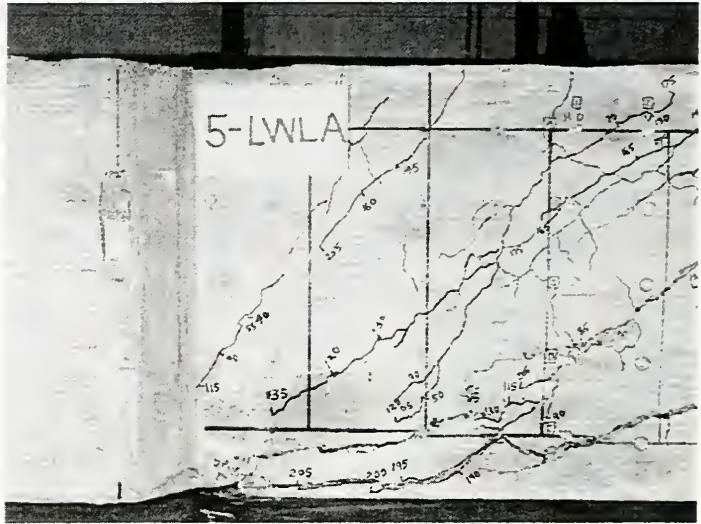


Figure 6.341 Specimen 5-LWLA at Failure (Part 1 of 4)

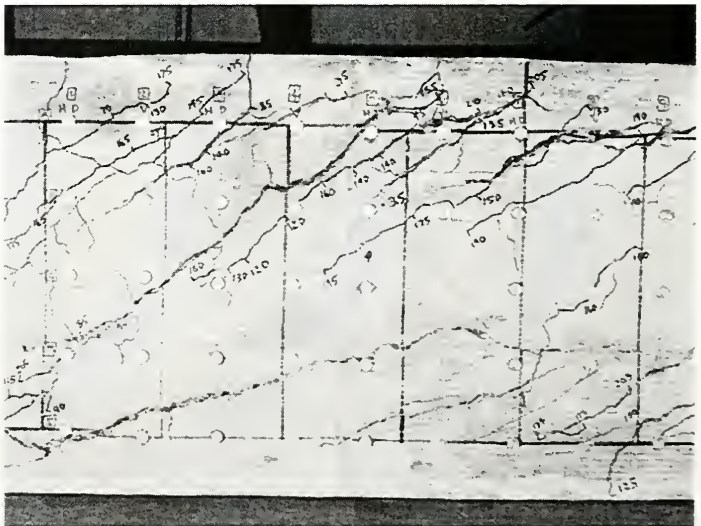


Figure 6.342 Specimen 5-LWLA at Failure (Part 2 of 4)



Figure 6.343 Specimen 5-LWLA at Failure (Part 3 of 4)



Figure 6.344 Specimen 5-LWLA at Failure (Part 4 of 4)

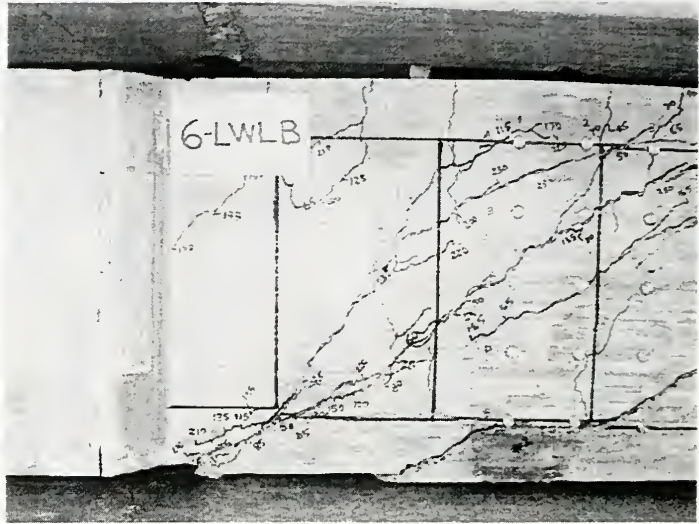


Figure 6.345 Specimen 6-LWLB at Failure (Part 1 of 4)

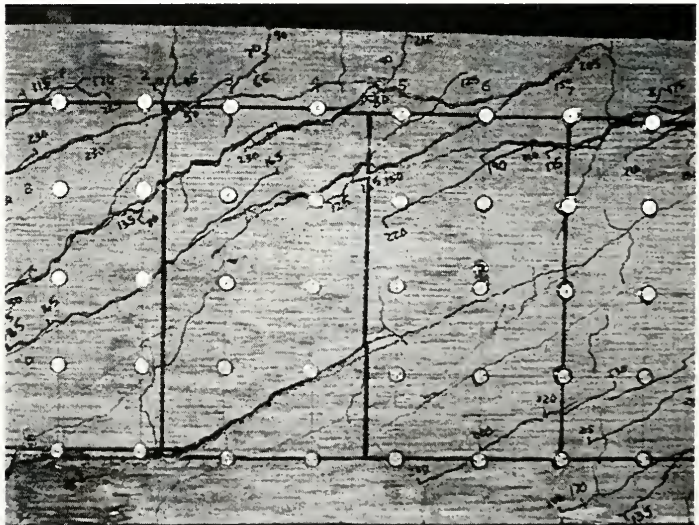


Figure 6.346 Specimen 6-LWLB at Failure (Part 2 of 4)

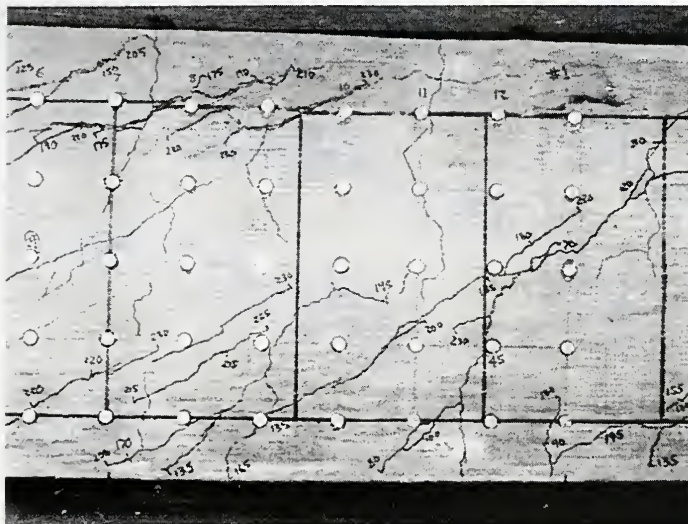


Figure 6.347 Specimen 6-LWLB at Failure (Part 3 of 4)

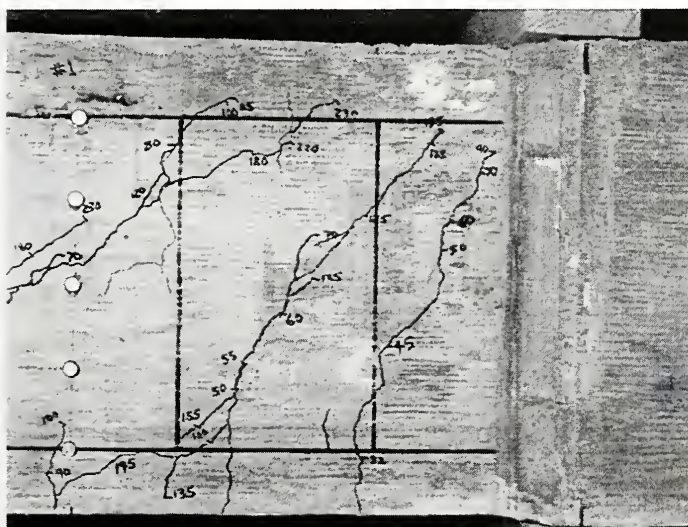


Figure 6.348 Specimen 6-LWLB at Failure (Part 4 of 4)



Figure 6.349 Specimen 7-LWLC at Failure (Part 1 of 3)

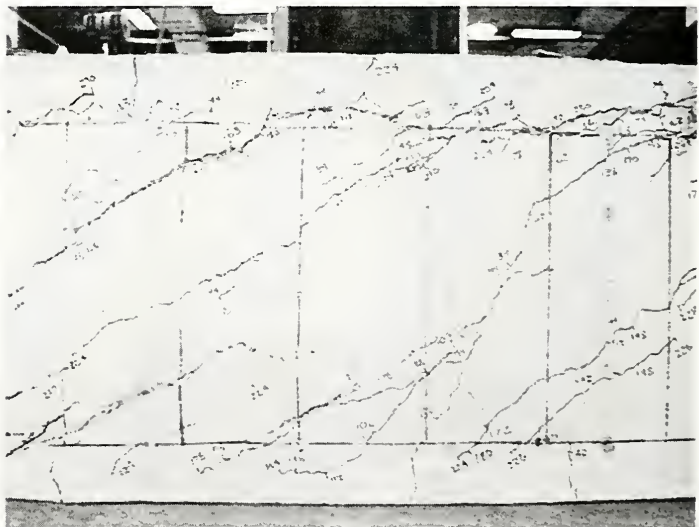


Figure 6.350 Specimen 7-LWLC at Failure (Part 2 of 3)

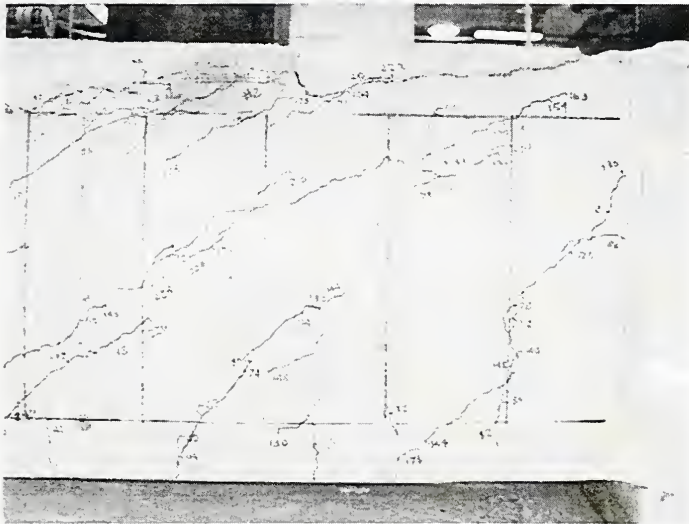


Figure 6.351 Specimen 7-LWLC at Failure (Part 3 of 3)

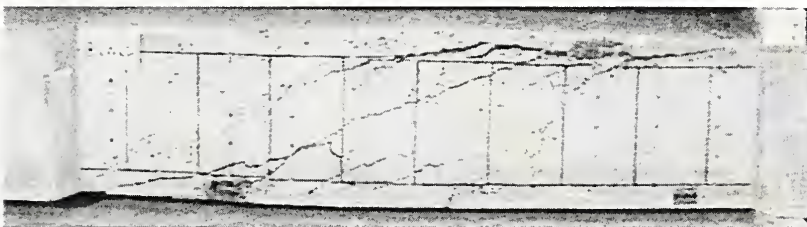


Figure 6.352 Specimen 8-LWLD at Failure

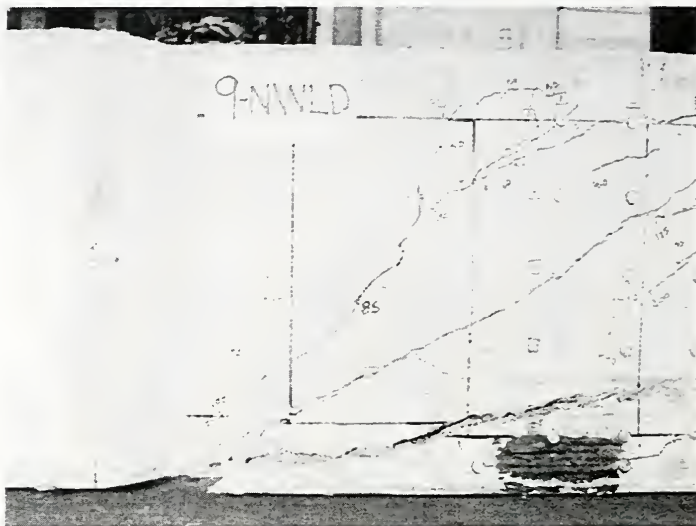


Figure 6.353 Specimen 9-NWLD at Failure (Part 1 of 4)



Figure 6.354 Specimen 9-NWLD at Failure (Part 2 of 4)

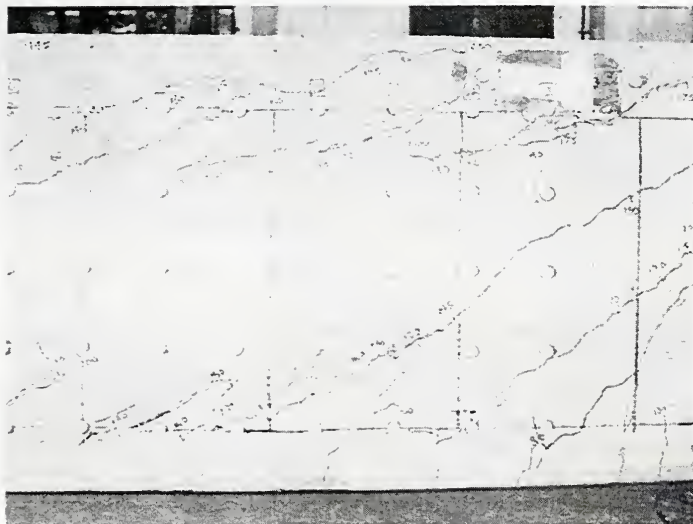


Figure 6.355 Specimen 9-NWLD at Failure (Part 3 of 4)

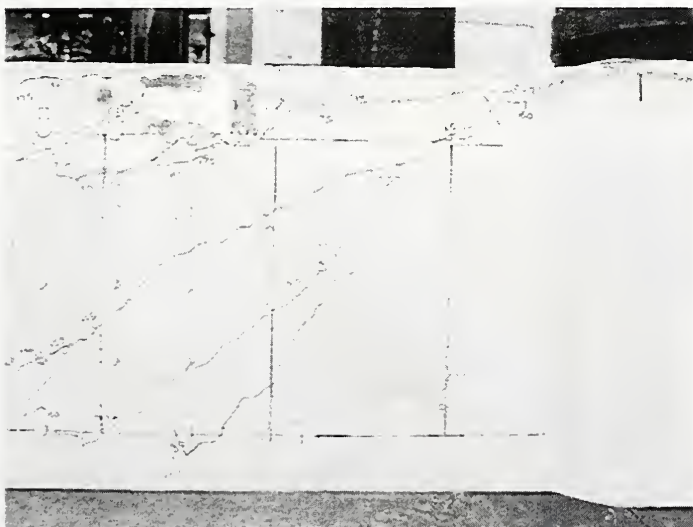


Figure 6.356 Specimen 9-NWLD at Failure (Part 4 of 4)



Figure 6.357 Specimen 10-NWHD at Failure

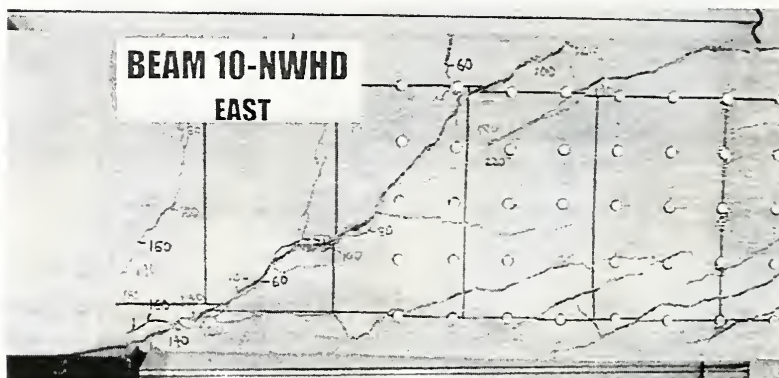


Figure 6.358 Specimen 10-NWHD at Failure (Part 1 of 2)

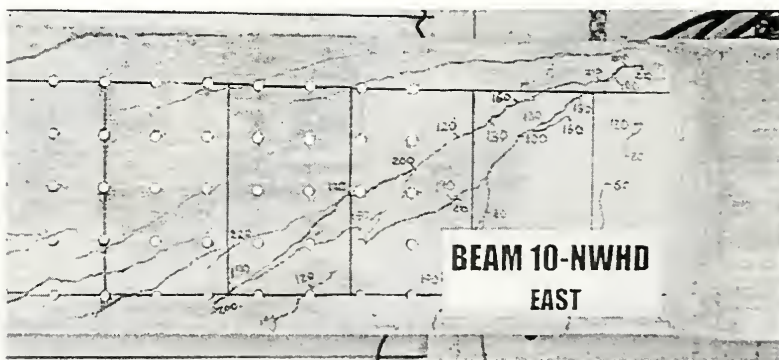


Figure 6.359 Specimen 10-NWHD at Failure (Part 2 of 2)

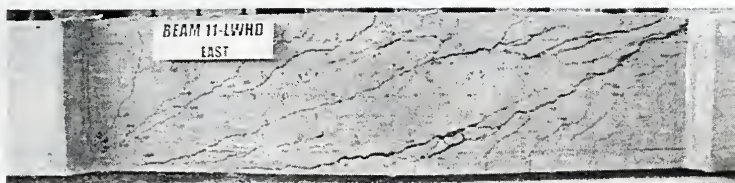


Figure 6.360 Specimen 11-LWHD at Failure

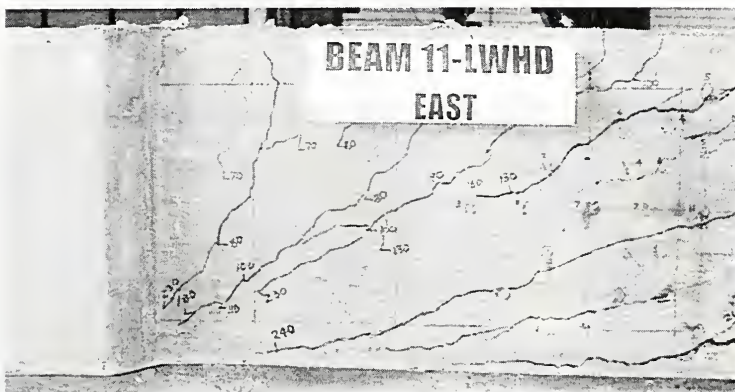


Figure 6.361 Specimen 11-LWHD at Failure (South Test Region)

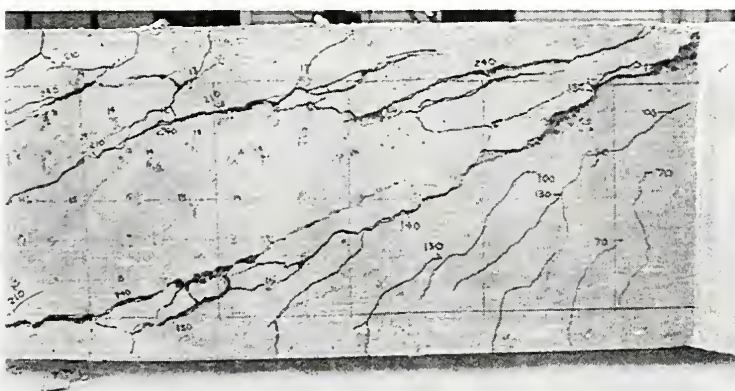


Figure 6.362 Specimen 11-LWHD at Failure (North Test Region)

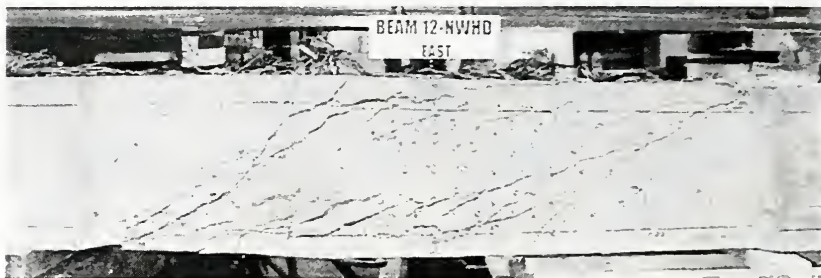


Figure 6.363 Specimen 12-NWHD at Failure

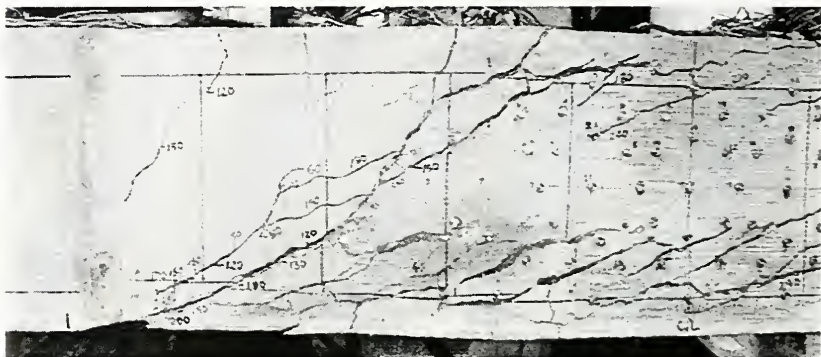


Figure 6.364 Specimen 12-NWHD at Failure (South Test Region)

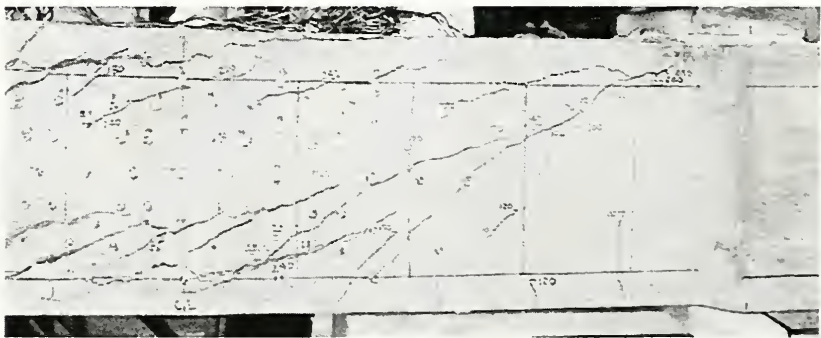


Figure 6.365 Specimen 12-NWHD at Failure (North Test Region)

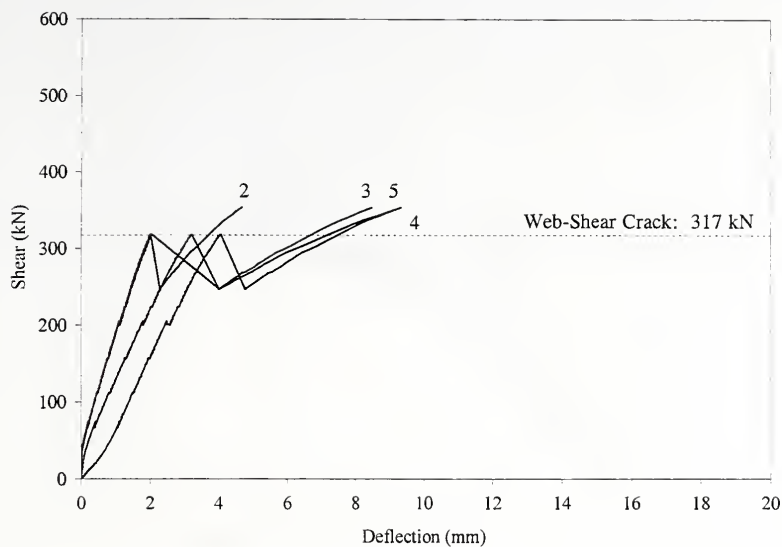


Figure 6.366 Shear-Deflection Relationship for Specimen PC6N

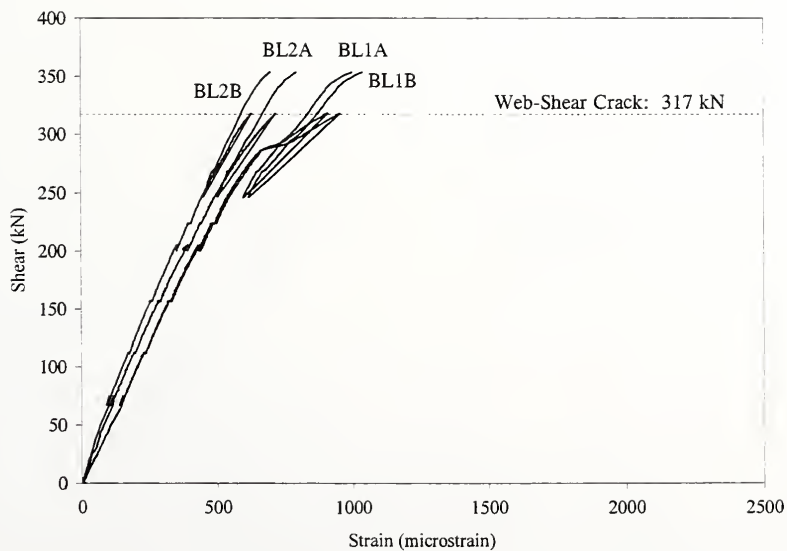


Figure 6.367 Shear-Longitudinal Steel Strain Relationship for Specimen PC6N

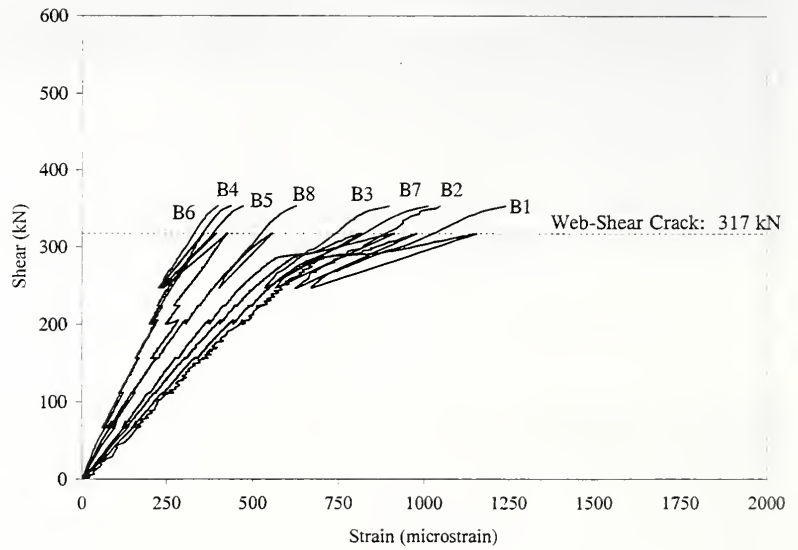


Figure 6.368 Shear-Strand Strain Relationship for Specimen PC6N

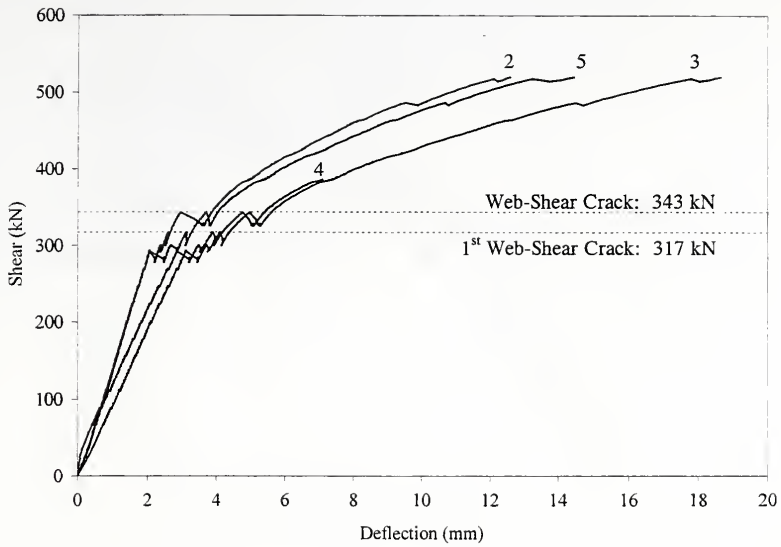


Figure 6.369 Shear-Deflection Relationship for Specimen PC6S

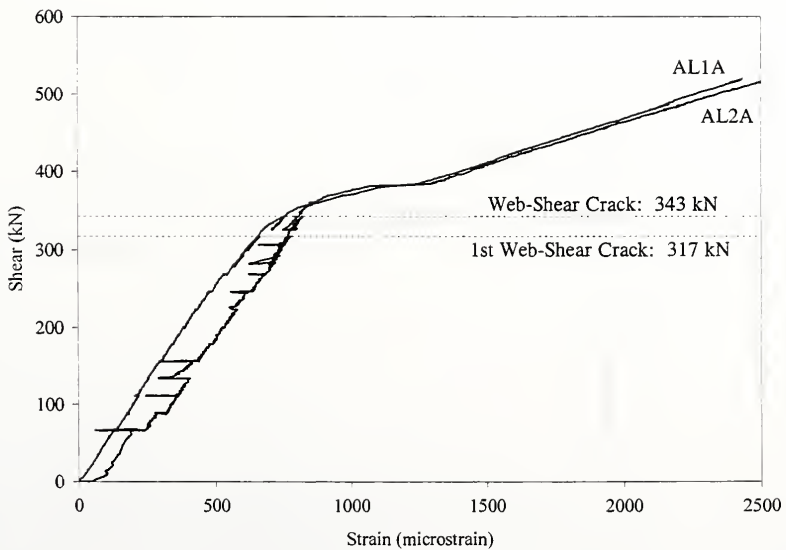


Figure 6.370 Shear-Longitudinal Steel Strain Relationship for Specimen PC6S

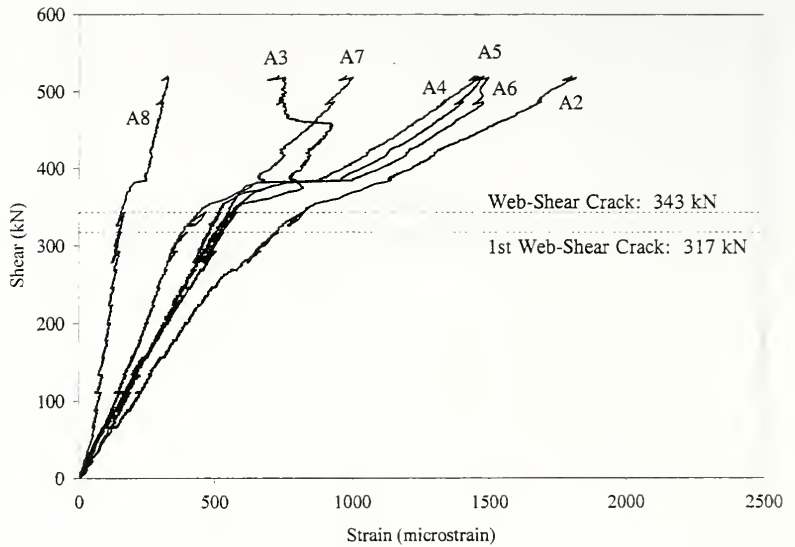


Figure 6.371 Shear-Strand Strain Relationship for Specimen PC6S

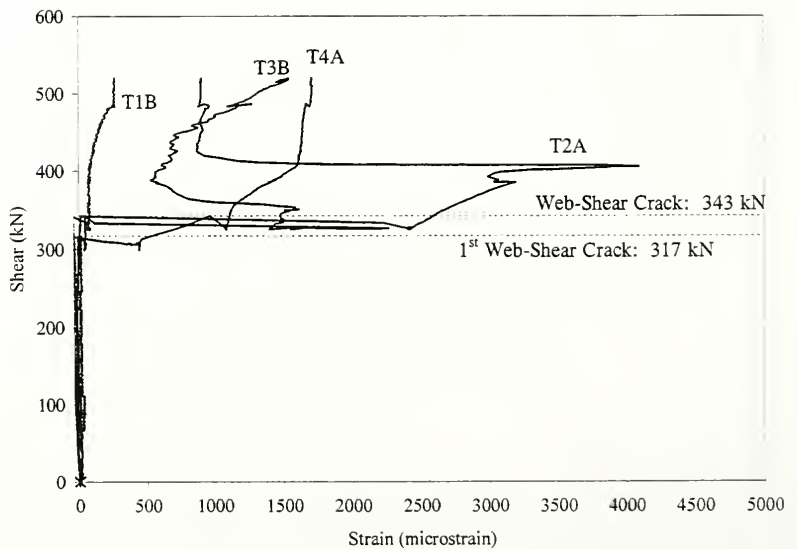


Figure 6.372 Shear-Stirrup Strain Relationship for Specimen PC6S, Stirrups T1-T5

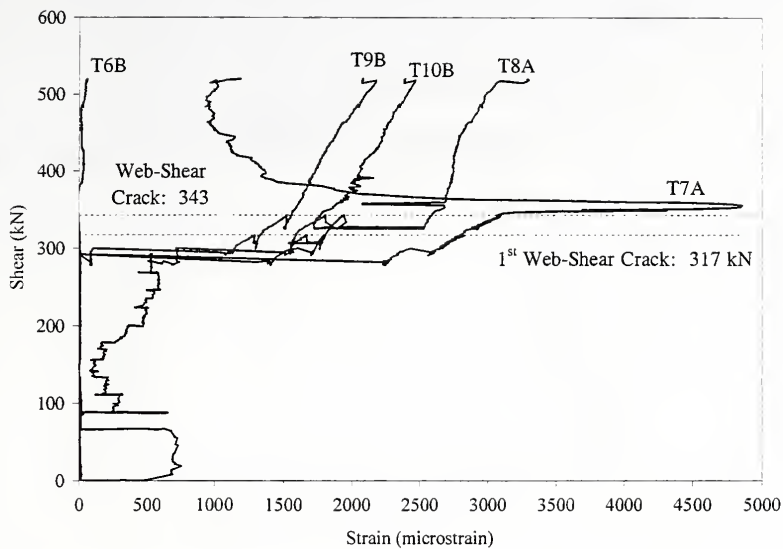


Figure 6.373 Shear-Stirrup Strain Relationship for Specimen PC6S, Stirrups T6-T10

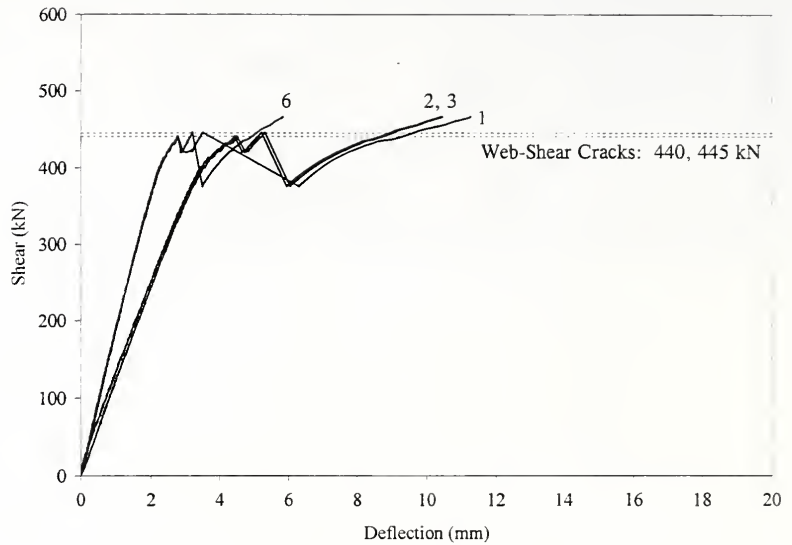


Figure 6.374 Shear-Deflection Relationship for Specimen PC10N

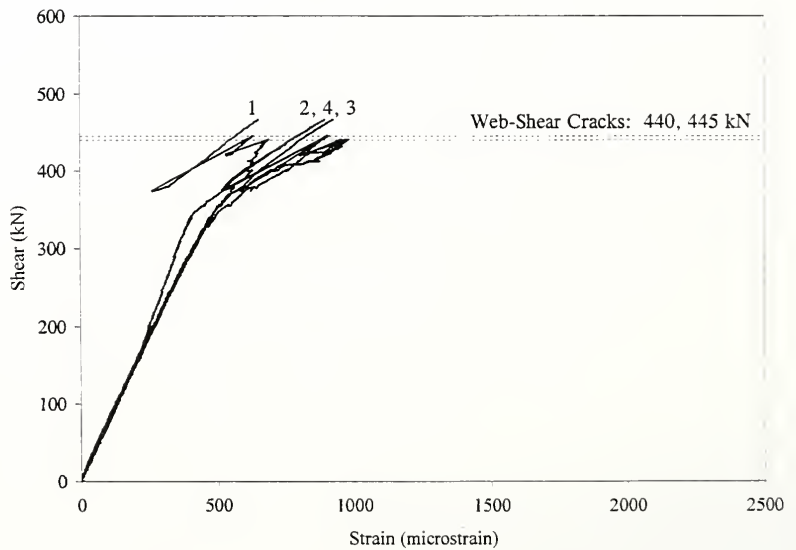


Figure 6.375 Shear-Longitudinal Steel Strain Relationship for Specimen PC10N

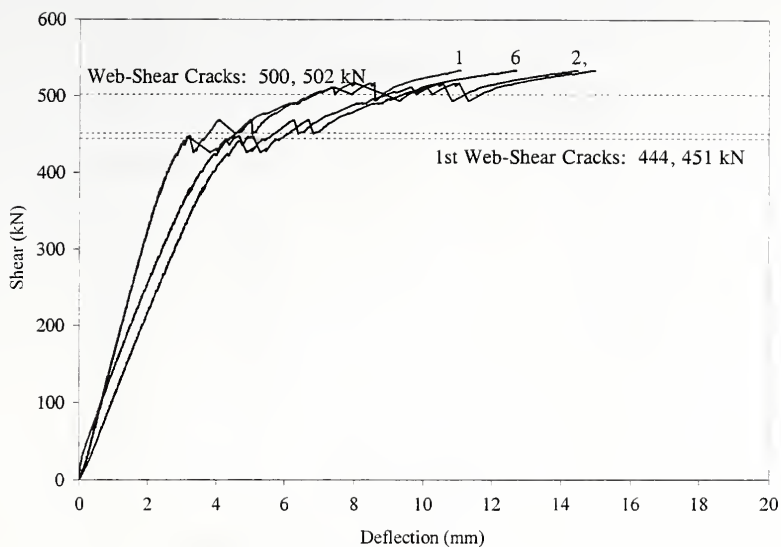


Figure 6.376 Shear-Deflection Relationship for Specimen PC10S

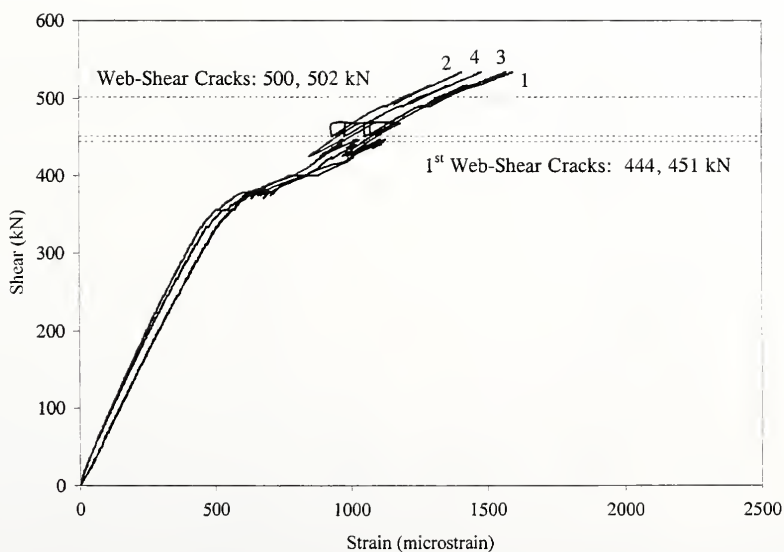


Figure 6.377 Shear-Longitudinal Steel Strain Relationship for Specimen PC10S

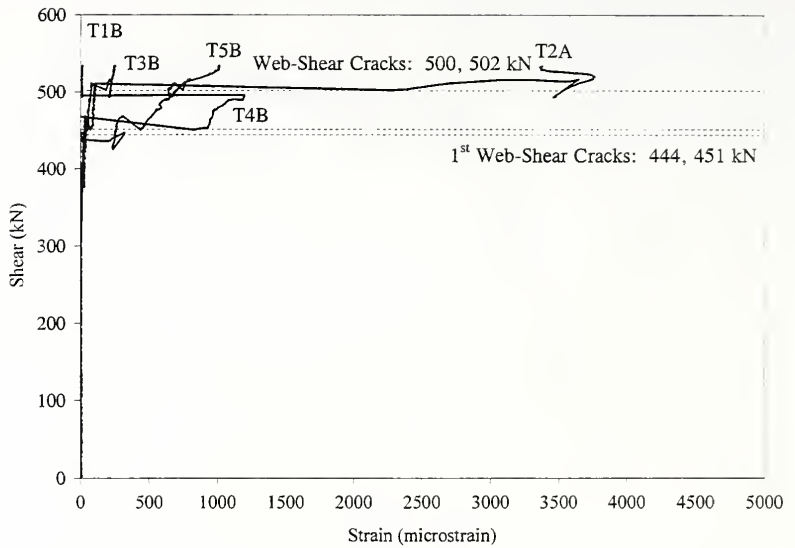


Figure 6.378 Shear-Stirrup Strain Relationship for Specimen PC10S, Stirrups T1-T5

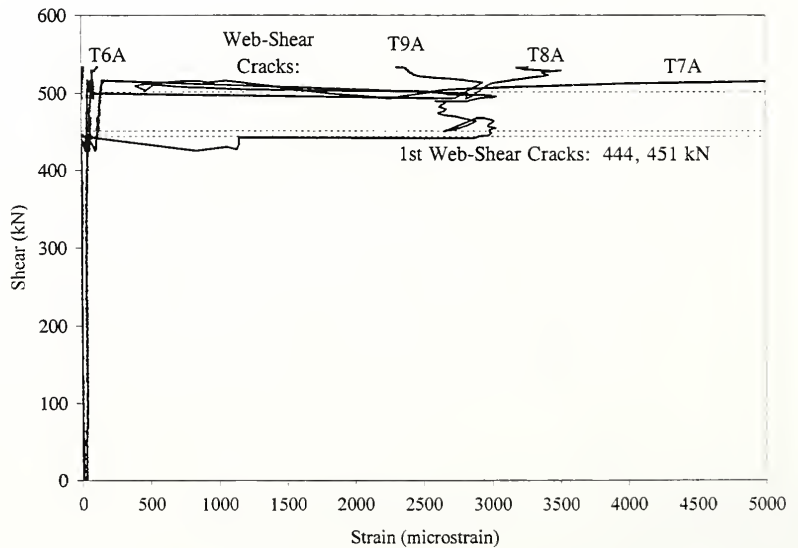


Figure 6.379 Shear-Stirrup Strain Relationship for Specimen PC10S, Stirrups T6-T10

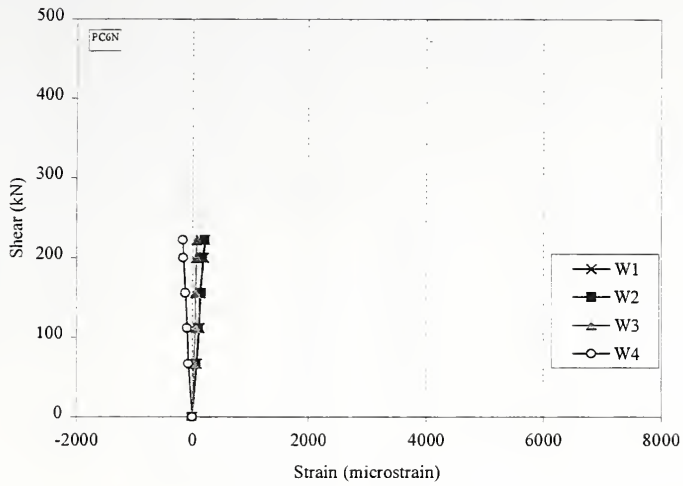


Figure 6.380 Shear-Strain Relationship, Whittemore Strains, Rosette 1, Specimen PC6N

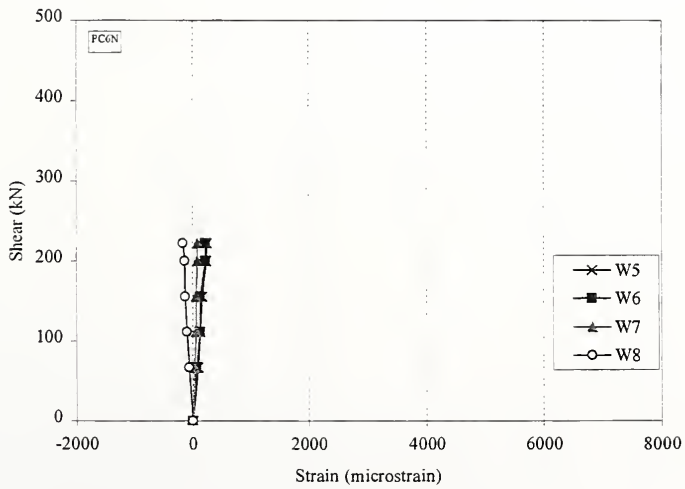


Figure 6.381 Shear-Strain Relationship, Whittemore Strains, Rosette 2, Specimen PC6N

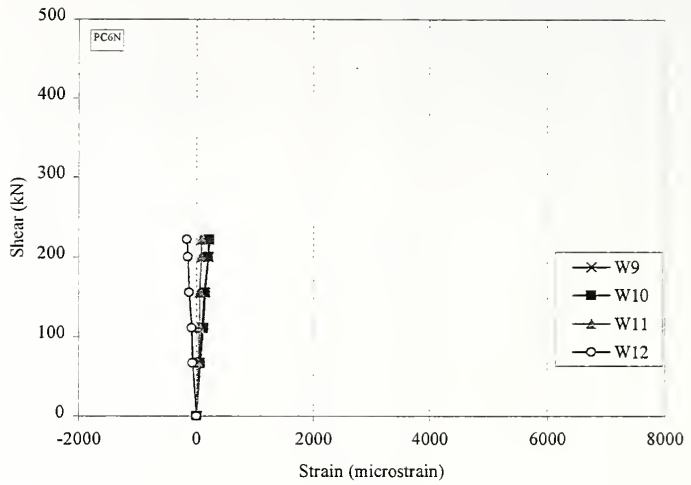


Figure 6.382 Shear-Strain Relationship, Whittemore Strains, Rosette 3, Specimen PC6N

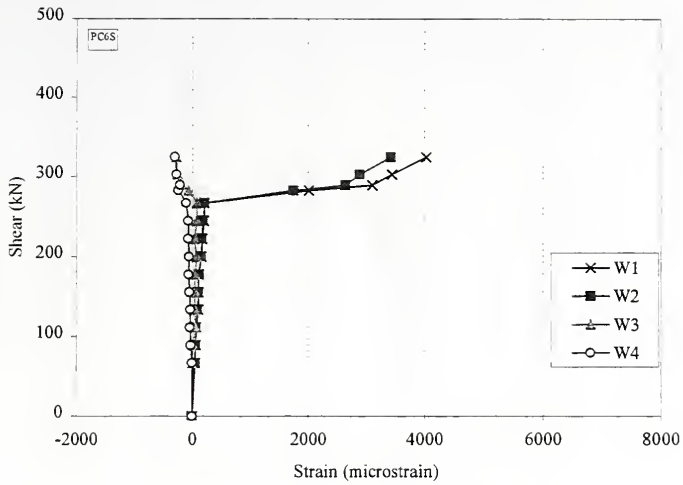


Figure 6.383 Shear-Strain Relationship, Whittemore Strains, Rosette 1, Specimen PC6S

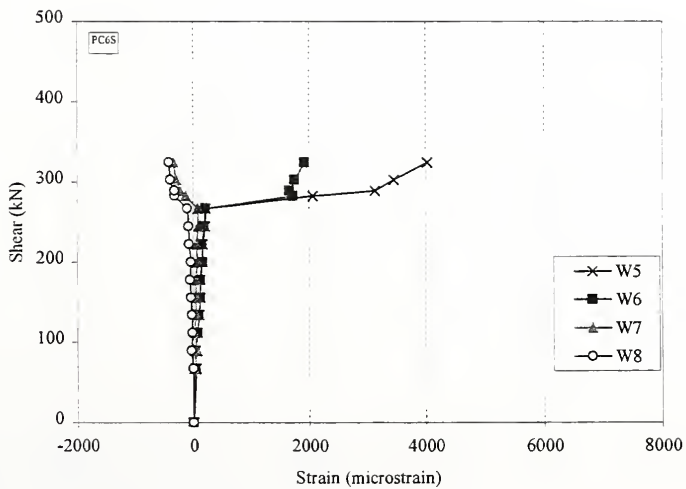


Figure 6.384 Shear-Strain Relationship, Whittemore Strains, Rosette 2, Specimen PC6S

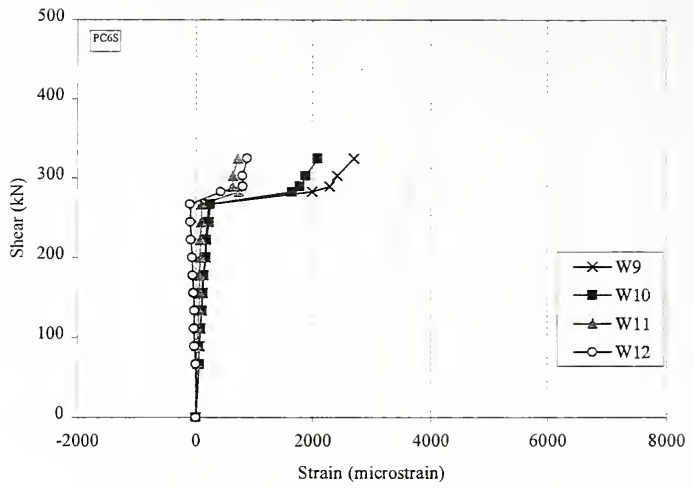


Figure 6.385 Shear-Strain Relationship, Whittemore Strains, Rosette 3, Specimen PC6S

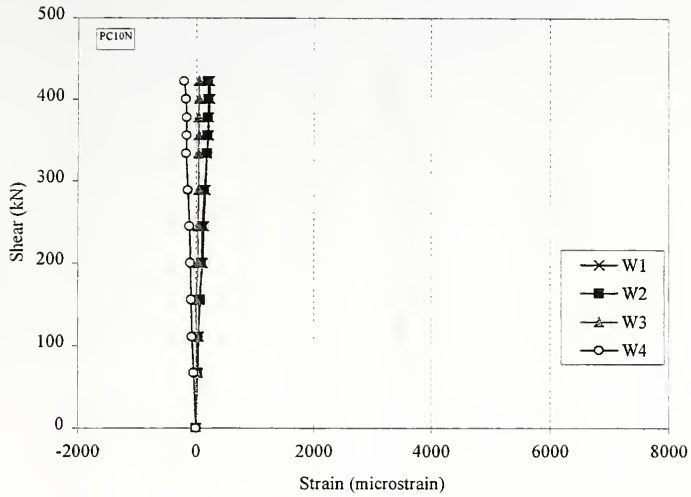
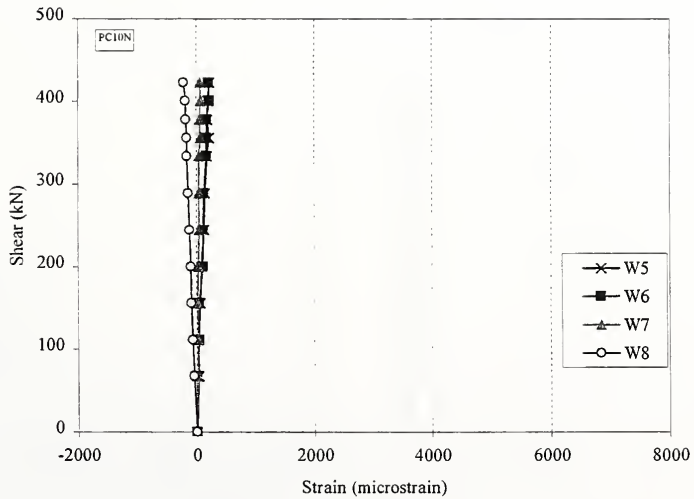


Figure 6.386 Shear-Strain Relationship, Whittemore Strains, Rosette 1, Specimen PC10N



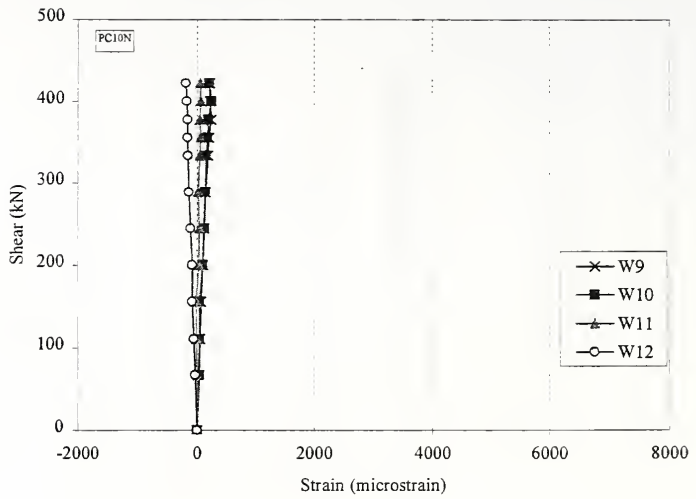


Figure 6.388 Shear-Strain Relationship, Whittemore Strains, Rosette 3, Specimen PC10N

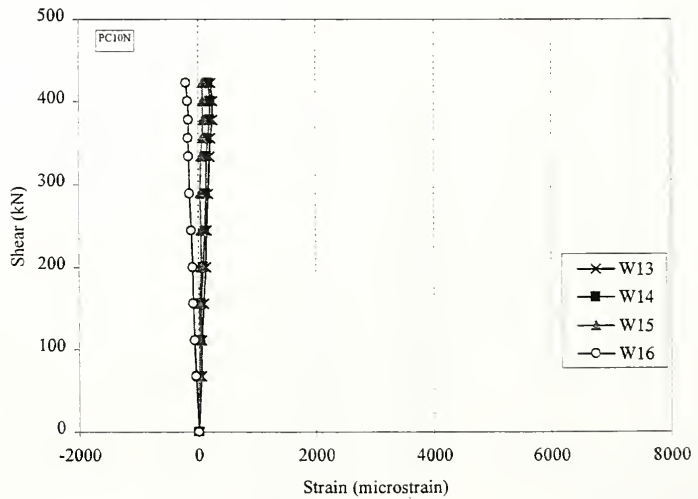


Figure 6.389 Shear-Strain Relationship, Whittemore Strains, Rosette 4, Specimen PC10N

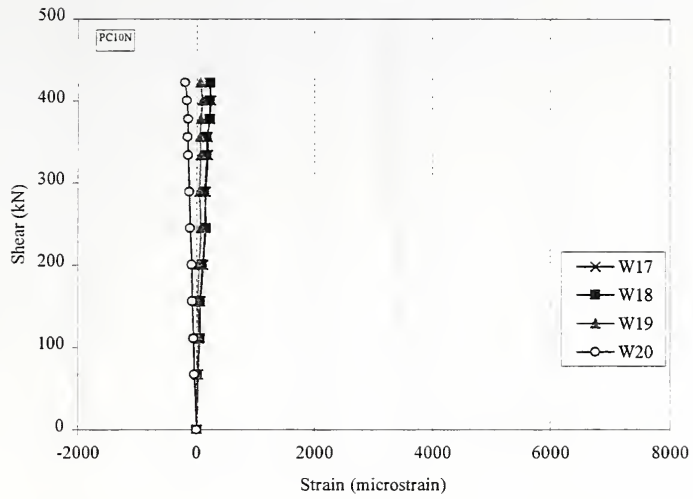


Figure 6.390 Shear-Strain Relationship, Whittemore Strains, Rosette 5, Specimen PC10N

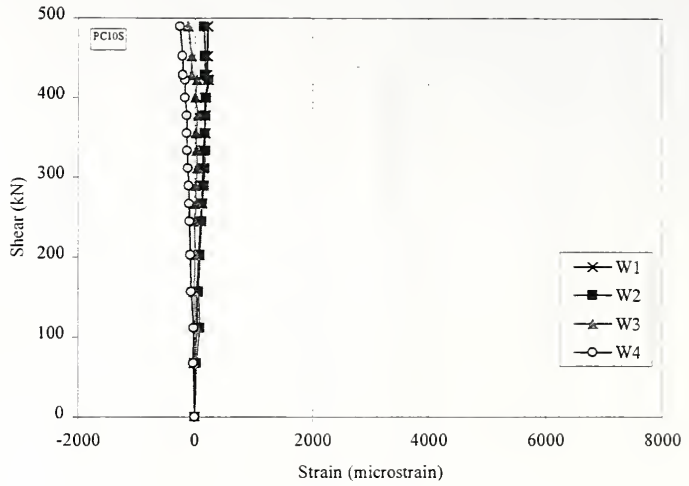


Figure 6.391 Shear-Strain Relationship, Whittemore Strains, Rosette 1, Specimen PC10S

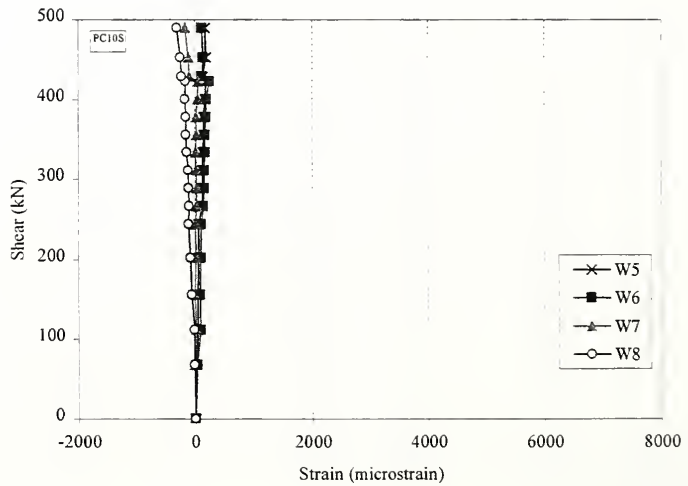


Figure 6.392 Shear-Strain Relationship, Whittemore Strains, Rosette 2, Specimen PC10S

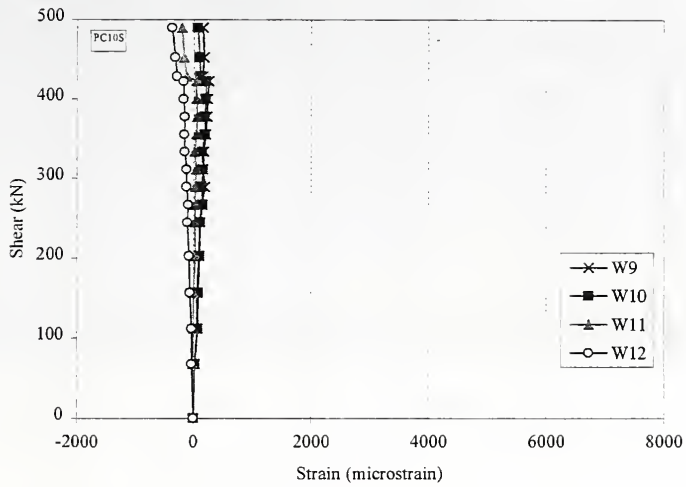


Figure 6.393 Shear-Strain Relationship, Whittemore Strains, Rosette 3, Specimen PC10S

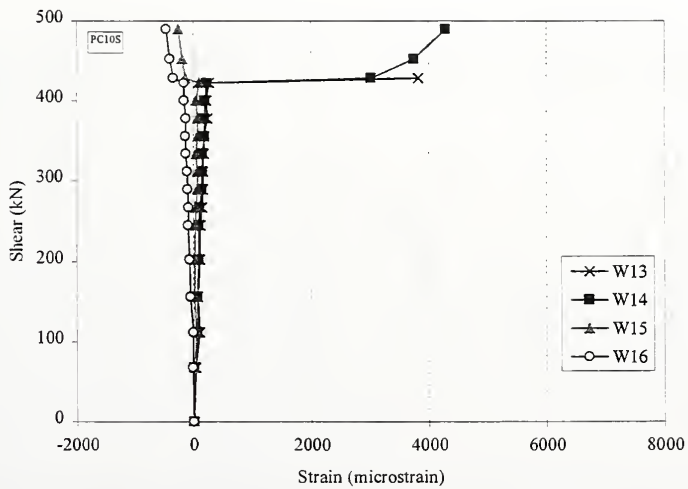


Figure 6.394 Shear-Strain Relationship, Whittemore Strains, Rosette 4, Specimen PC10S

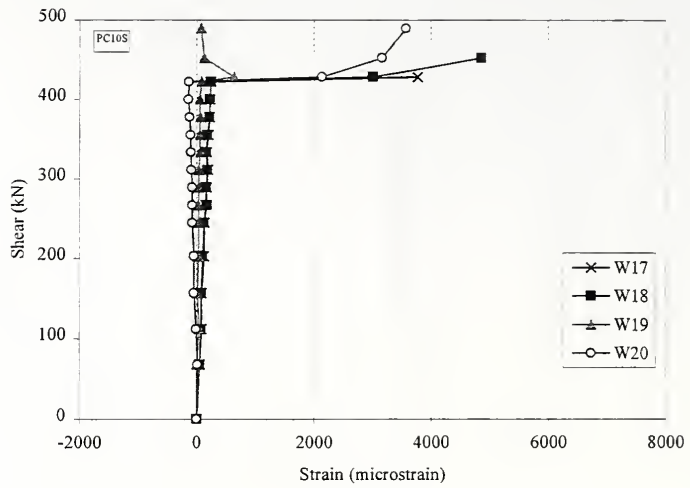


Figure 6.395 Shear-Strain Relationship, Whittemore Strains, Rosette 5, Specimen PC10S



Figure 6.396 Failure Crack in North Shear Span, Specimen PC6N



Figure 6.397 Spalling of Web in North Shear Span, Specimen PC6N

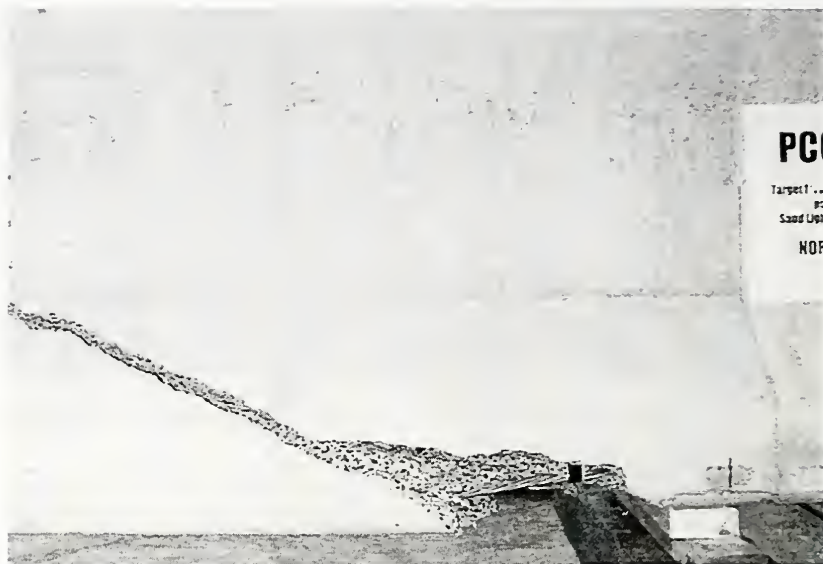


Figure 6.398 Failure Crack Extending to Face of Support, Specimen PC6N



Figure 6.399 Web-Shear Crack in South Shear Span at Failure, Specimen PC6N

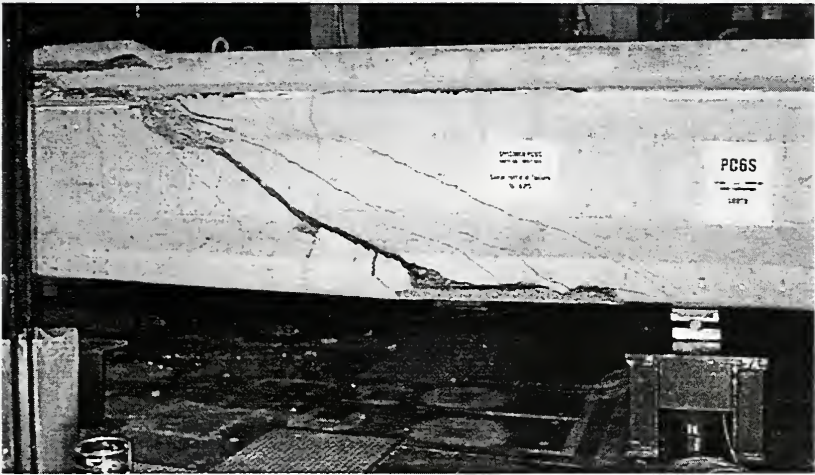


Figure 6.400 Failure Crack in South Shear Span, Specimen PC6S

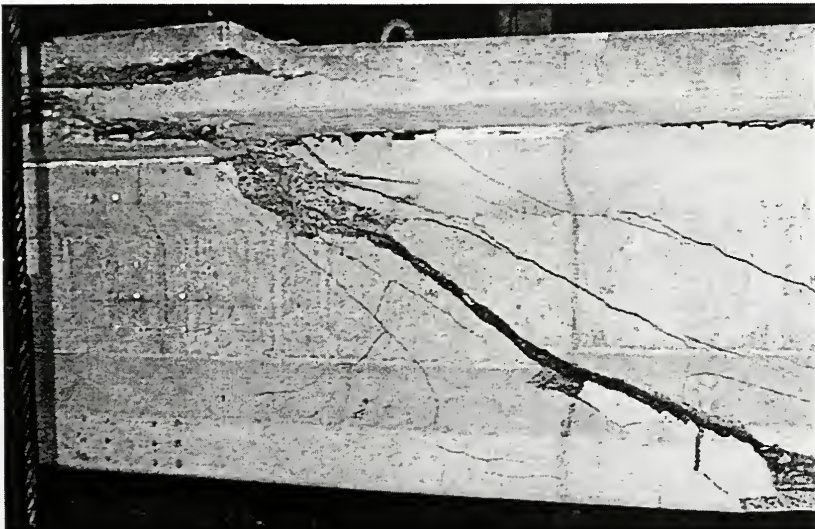


Figure 6.401 Crushing of Top Flange, Specimen PC6S



Figure 6.402 Splitting Crack Along Prestressing Reinforcement, Specimen PC6S

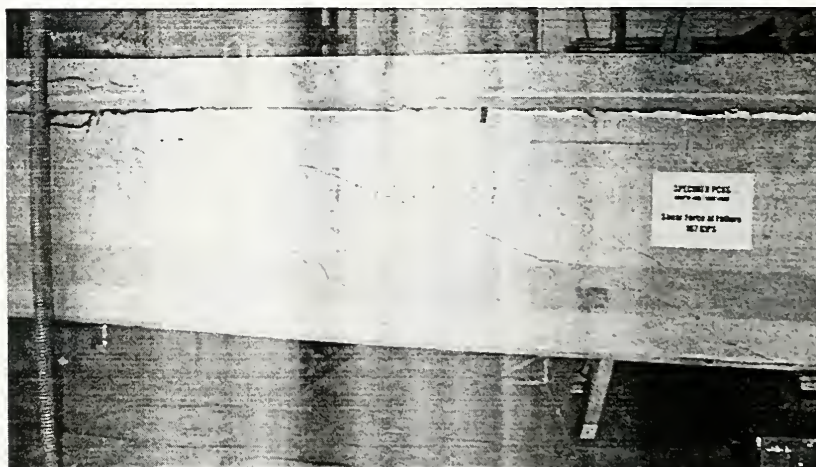


Figure 6.403 Web-Shear Crack in North Shear Span, Specimen PC6S



Figure 6.404 Major Web-Shear Crack in North Shear Span, Specimen PC10N

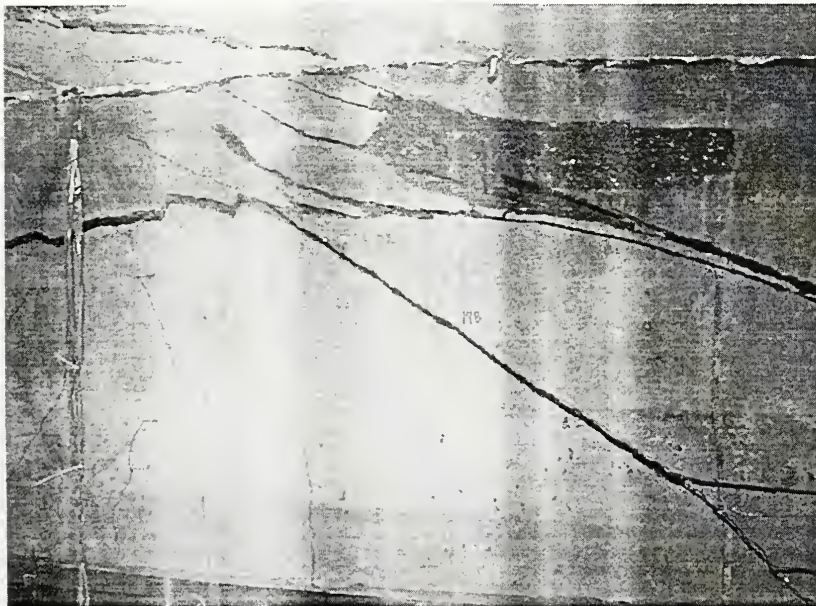


Figure 6.405 Crushing of Upper Flange near Midspan, Specimen PC10N

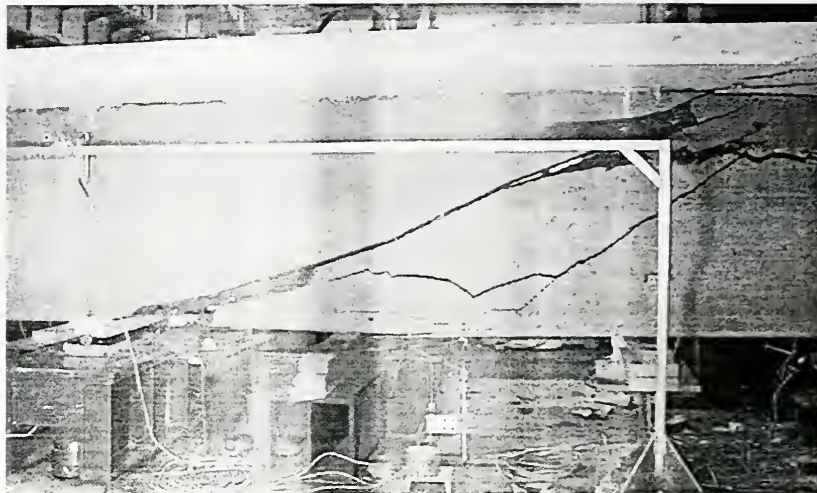


Figure 6.406 Web-Shear Crack in North Shear Span, Specimen PC10N

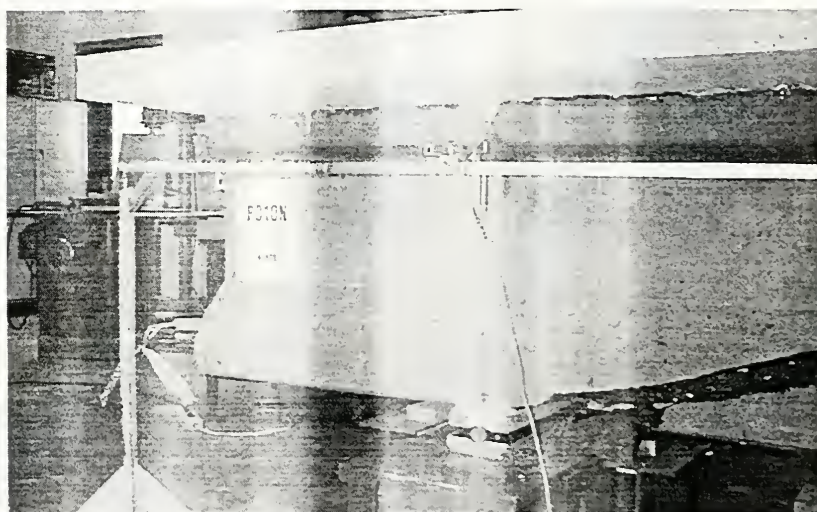


Figure 6.407 Undamaged Transfer Length Zone Behind Support, Specimen PC10N

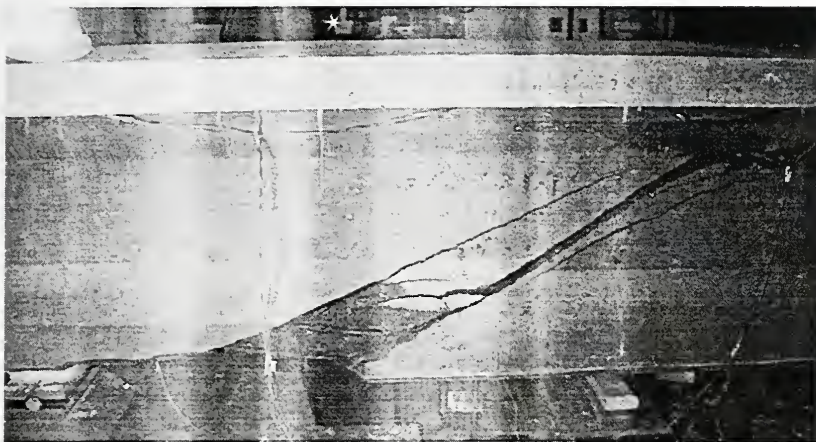


Figure 6.408 Web-Shear Crack in South Shear Span, Specimen PC10S, East Side

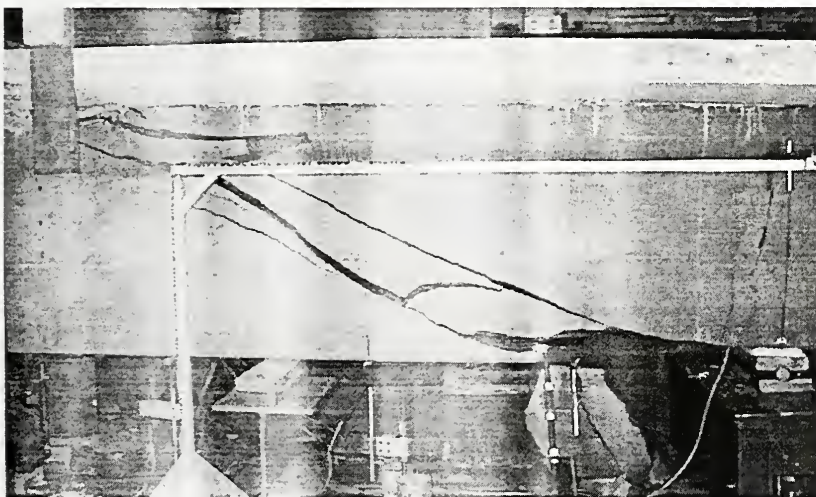


Figure 6.409 Web-Shear Crack in South Shear Span, Specimen PC10S, West Side

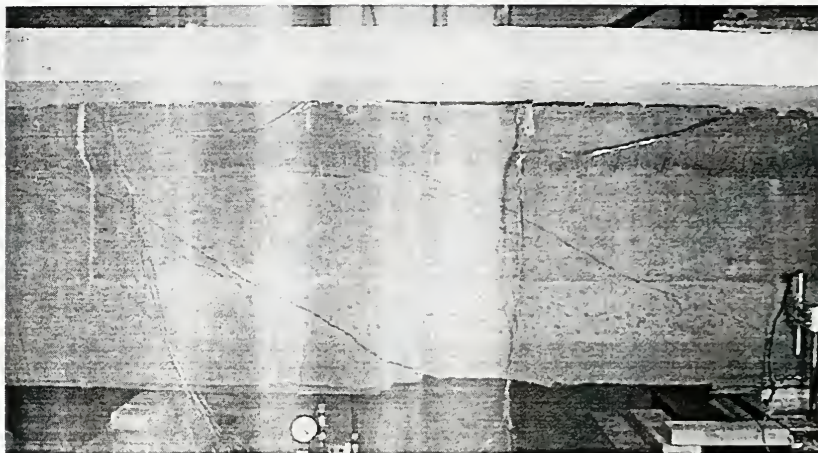


Figure 6.410 Web-Shear Cracks in North Shear Span, Specimen PC10S



Figure 6.411 Crushing of Upper Web and Flange near Midspan, Specimen PC10S

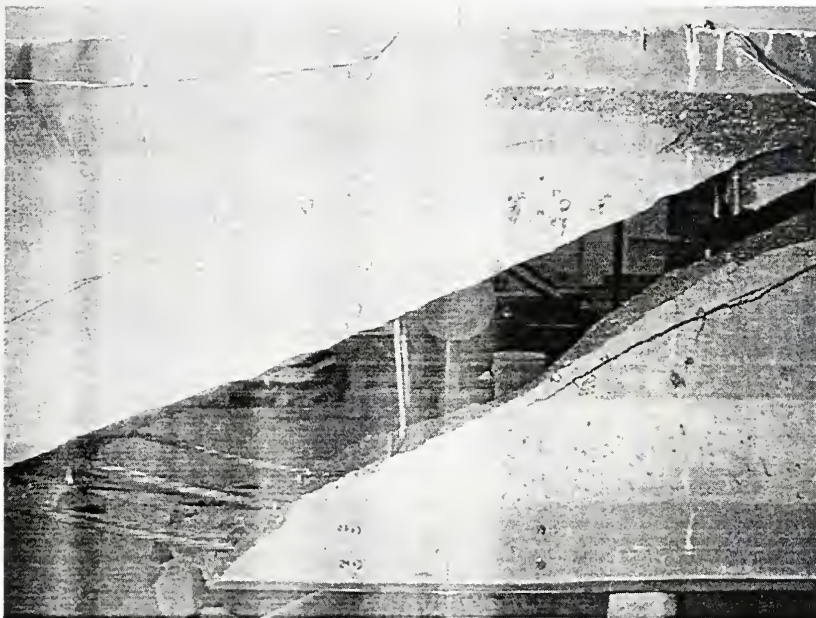


Figure 6.412 Ruptured Stirrups after Removal of Web Concrete, Specimen PC10S

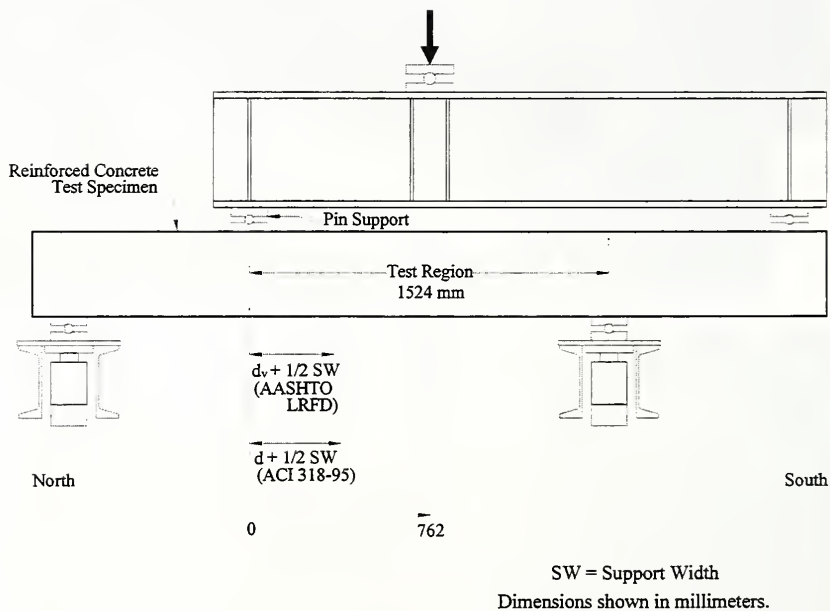


Figure 6.413 Locations of Critical Sections for Shear, Reinforced Concrete Specimens

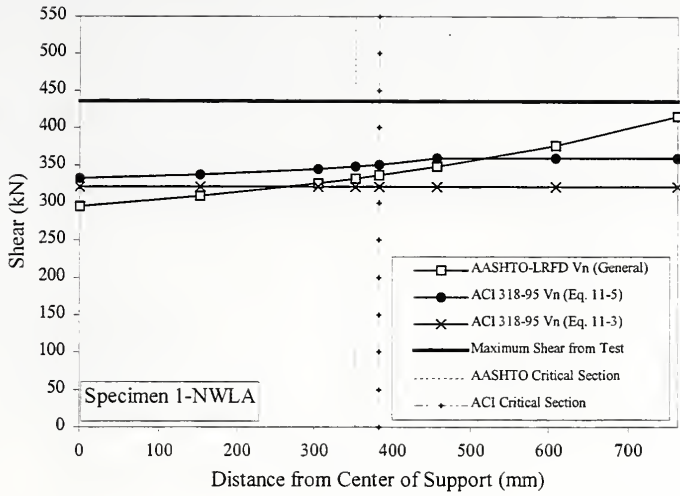


Figure 6.414 Comparison of Measured Shear Capacity and Code-Estimated Shear Capacities, Specimen 1-NWLA

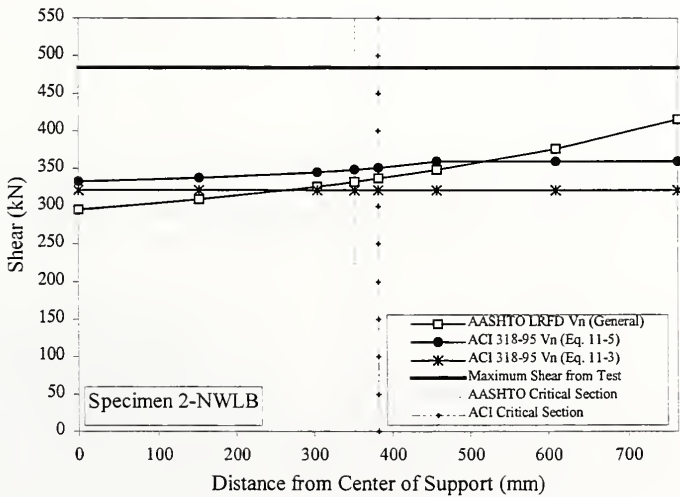


Figure 6.415 Comparison of Measured Shear Capacity and Code-Estimated Shear Capacities, Specimen 2-NWLB

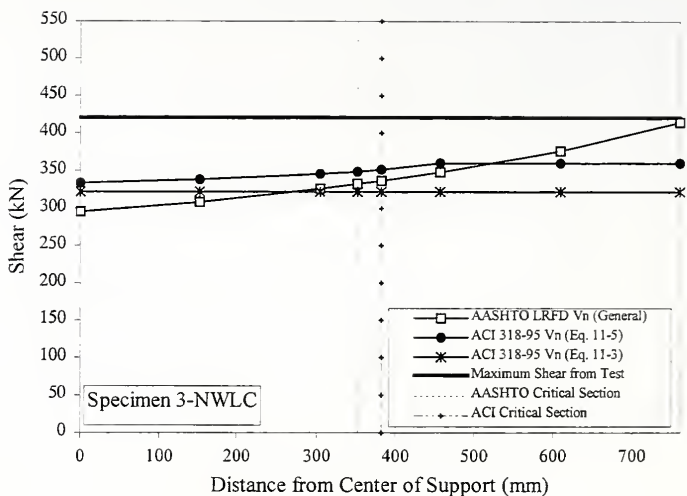


Figure 6.416 Comparison of Measured Shear Capacity and Code-Estimated Shear Capacities, Specimen 3-NWLC

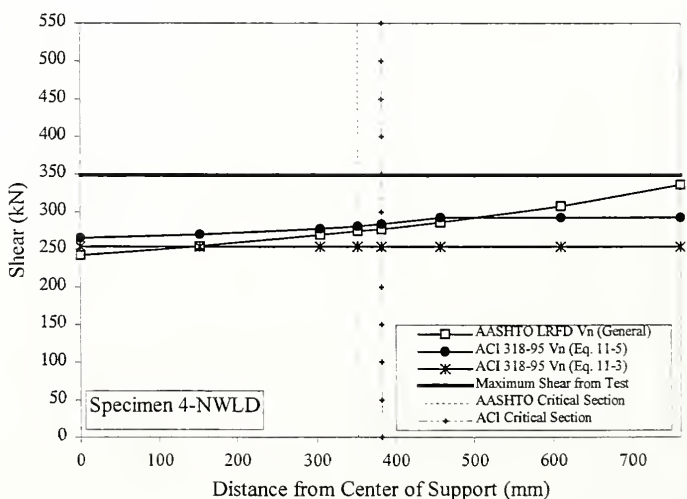


Figure 6.417 Comparison of Measured Shear Capacity and Code-Estimated Shear Capacities, Specimen 4-NWLD

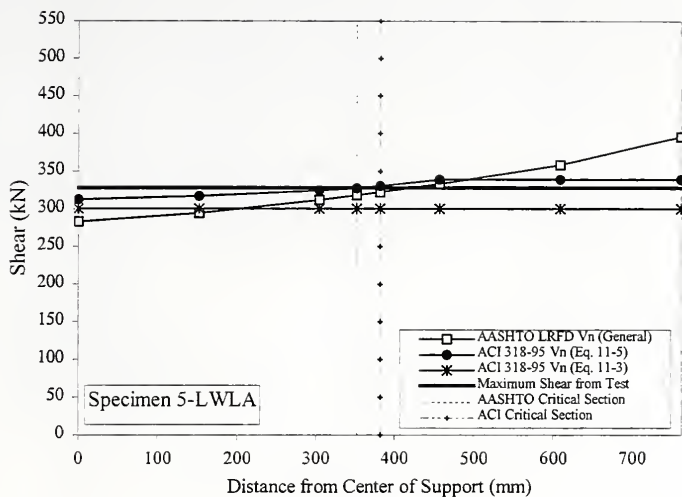


Figure 6.418 Comparison of Measured Shear Capacity and Code-Estimated Shear Capacities, Specimen 5-L WLA

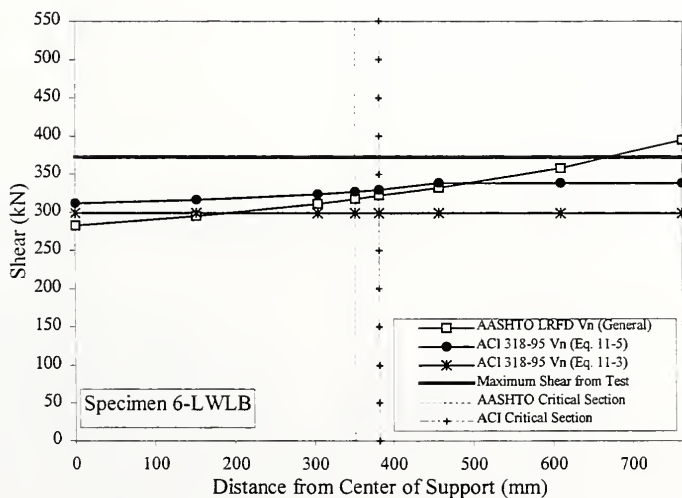


Figure 6.419 Comparison of Measured Shear Capacity and Code-Estimated Shear Capacities, Specimen 6-L WLB

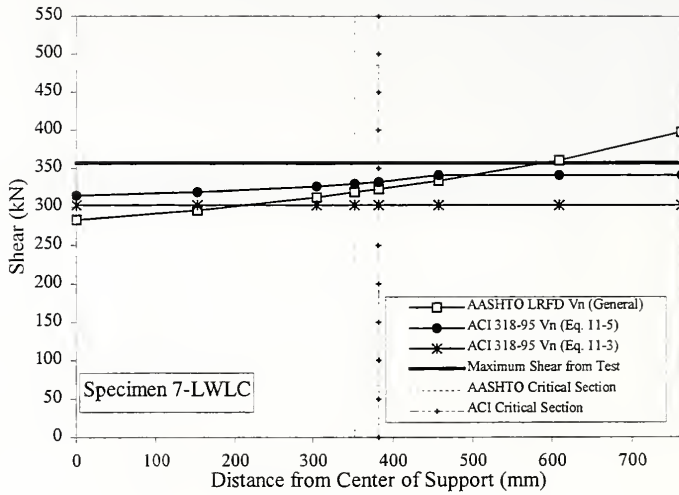


Figure 6.420 Comparison of Measured Shear Capacity and Code-Estimated Shear Capacities, Specimen 7-LWLC

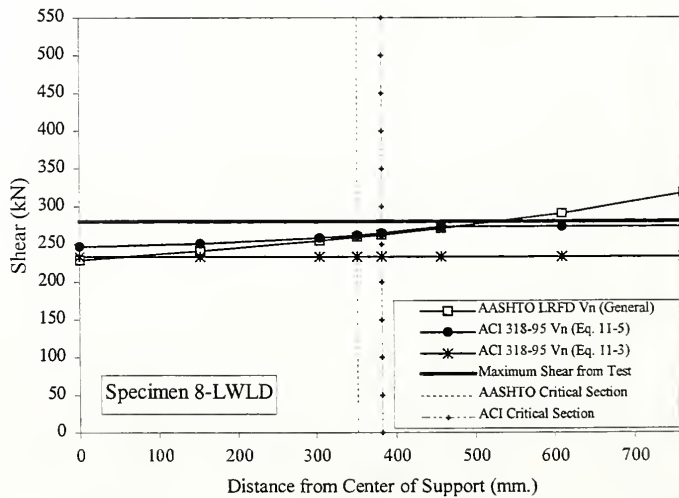


Figure 6.421 Comparison of Measured Shear Capacity and Code-Estimated Shear Capacities, Specimen 8-LWLD

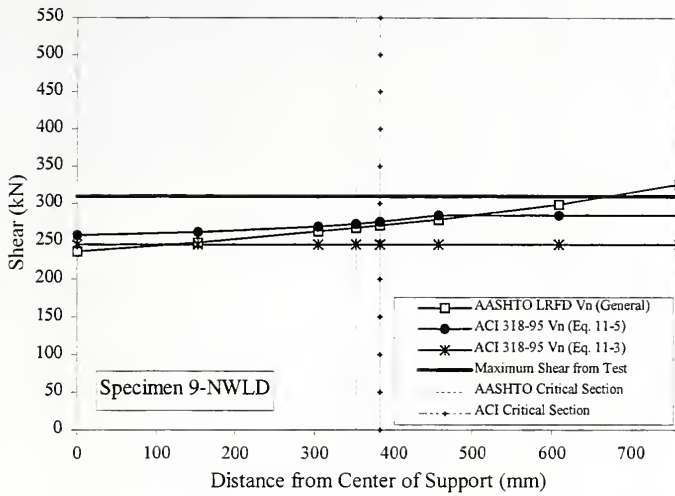


Figure 6.422 Comparison of Measured Shear Capacity and Code-Estimated Shear Capacities, Specimen 9-NWLD

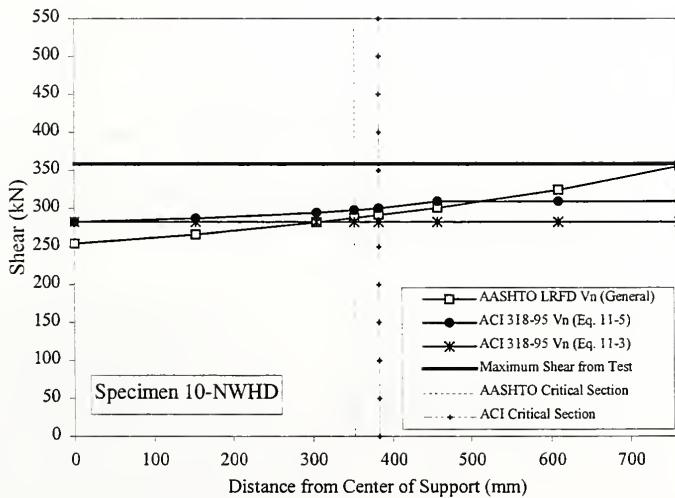


Figure 6.423 Comparison of Measured Shear Capacity and Code-Estimated Shear Capacities, Specimen 10-NWHD

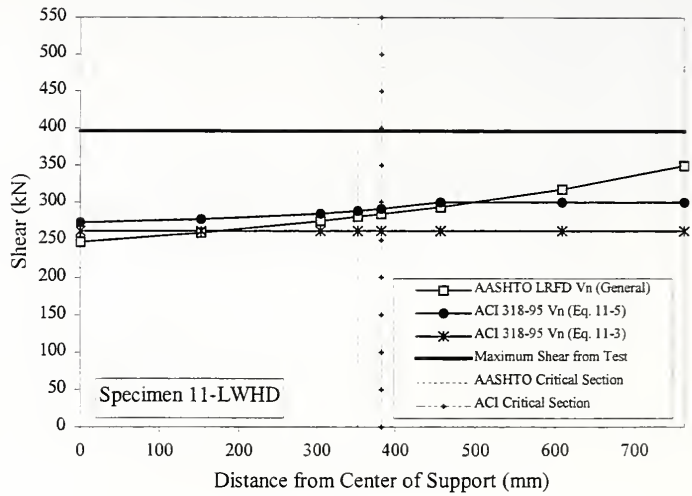


Figure 6.424 Comparison of Measured Shear Capacity and Code-Estimated Shear Capacities, Specimen 11-LWHD

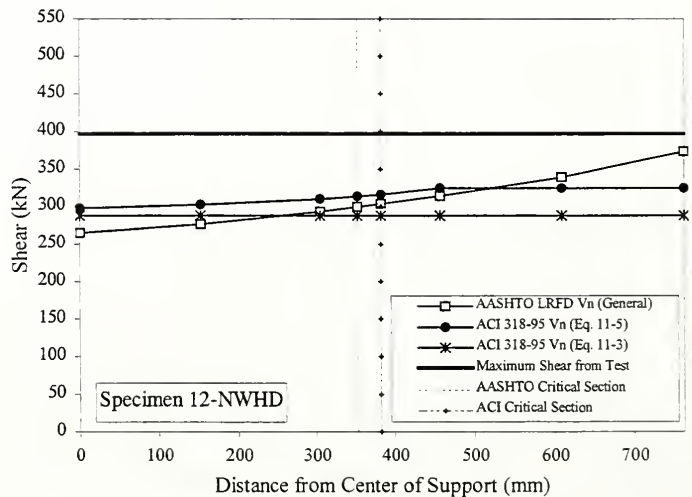


Figure 6.425 Comparison of Measured Shear Capacity and Code-Estimated Shear Capacities, Specimen 12-NWHD

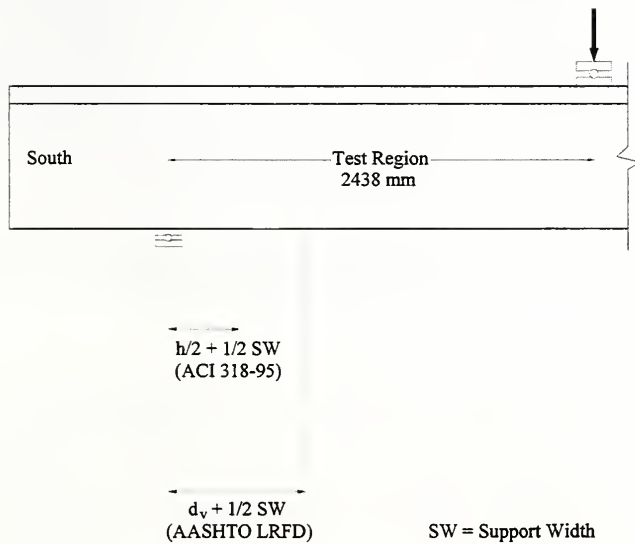


Figure 6.426 Locations of Critical Sections for Shear, Prestressed Concrete Specimens

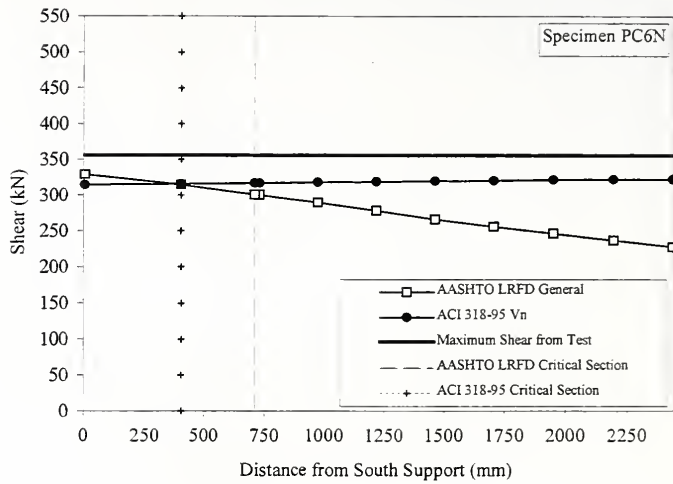


Figure 6.427 Comparison of Measured Shear Capacity and Code-Estimated Shear Capacities, Specimen PC6N

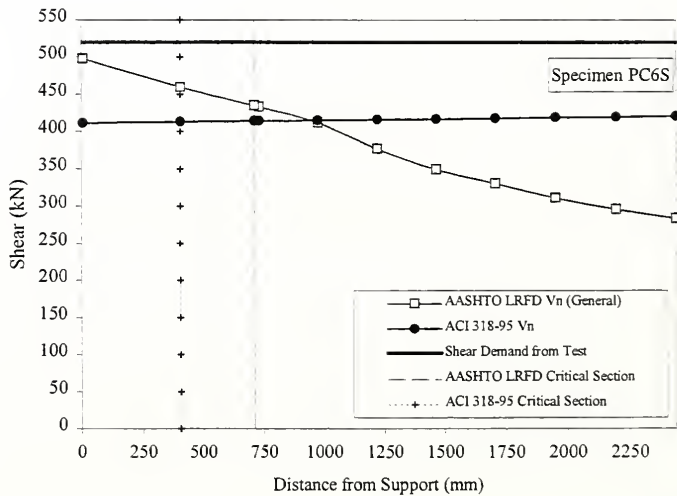


Figure 6.428 Comparison of Measured Shear Capacity and Code-Estimated Shear Capacities, Specimen PC6S

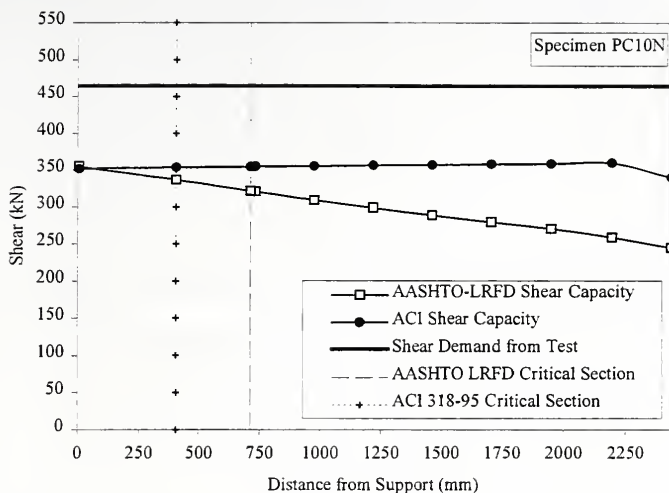


Figure 6.429 Comparison of Measured Shear Capacity and Code-Estimated Shear Capacities, Specimen PC10N

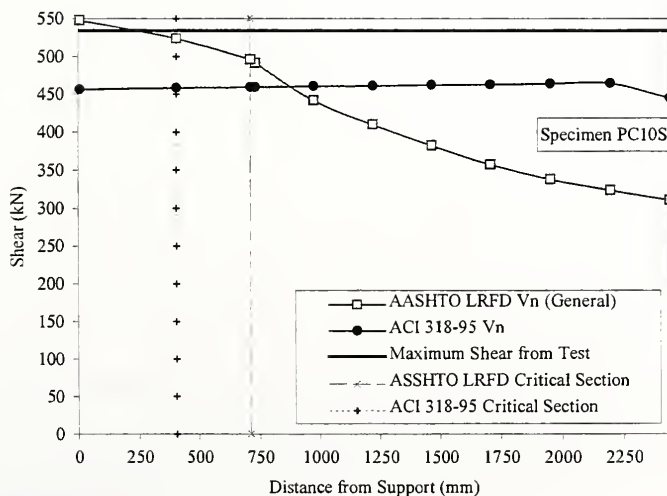


Figure 6.430 Comparison of Measured Shear Capacity and Code-Estimated Shear Capacities, Specimen PC10S

CHAPTER 7. SUMMARY, CONCLUSIONS AND RECOMMENDATIONS

7.1 Summary

7.1.1 Material Issues

This research investigation was carried out to evaluate the material aspects of the utilization of lightweight aggregate concrete in bridge decks and girders. In particular, the research was focused on evaluating the suitability of Indiana sources of LWA for the development of 42 MPa and 69 MPa (6000 psi and 10,000 psi) LWC for use in bridge girders and 31 MPa (4500 psi) LWC for use in bridge decks.

A procedure of mixture proportioning based on water-cement ratio was used in this research to better control the amount of total water in the mix. Compared to the volumetric method of mixture proportioning that is preferred, the water-cement ratio method produced better concrete strength and overall performance. There were some problems related to the difficulty of producing the 69 MPa (10,000 psi) LWC at the plant. An extensive experimental program was conducted to resolve the problems of flash setting and the incompatibility of cement and chemical admixtures at the plant.

The target compressive strengths were achieved using LWC and the proposed concrete showed good workability, had mechanical properties comparable to that of NWC, and had excellent durability properties. LWC tested in this research had far better freezing and thawing resistance than that of NWC made with the Lafayette source of normal weight aggregate.

7.1.2 Beam Shear Strength

In order for structural engineers to safely implement the use of LWC in bridge applications, information pertinent to the strength and behavior of LWC beams needs to be developed. This research study provided information regarding the shear strength of reinforced concrete beams with minimum and up to 1.62 MPa shear reinforcement amounts, and prestressed lightweight aggregate concrete beams with low amounts of shear reinforcement. Measurements during the beam tests and observations of the structural behavior also enabled the evaluation of the ACI 318-95, AASHTO Standard (1995), and AASHTO LRFD (1994) shear design methods for the types of beams tested.

7.1.2.1 Reinforced Concrete Specimens

An experimental program consisting of twelve reinforced concrete beams tested in shear was completed. The program included five sand-lightweight aggregate concrete beams and seven normal weight aggregate concrete beams. All specimens were rectangular in cross-section and contained equal amounts of tensile and compressive reinforcement. Moderate strength concrete ($40.0 \text{ MPa} < f'_c < 46.6 \text{ MPa}$) was used in nine of the beams. The remaining three beams were made of high-strength concrete ($60.1 \text{ MPa} < f'_c < 75.2 \text{ MPa}$). All beams contained at least the minimum transverse reinforcement that is required by the ACI 318-95.

For each beam, the strains on the transverse reinforcement, longitudinal reinforcement, and concrete surface were measured. Applied load and deflections were also measured for each test.

All specimens experienced shear-compression failures. The predominant type of cracking was flexure-shear cracking. All but one specimen (2-NWLB) failed without yielding the longitudinal reinforcement. All lightweight aggregate concrete specimens and the two normal weight high-strength concrete specimens had smooth crack surfaces.

After testing the beams, the measured shear capacity of each beam was compared with the code/specification-estimated shear capacity. In all cases, the measured shear capacities exceeded the code/specification-estimated shear capacities.

A second experimental program was conducted to study shear strength of prestressed concrete beams. This program comprised four sand-lightweight aggregate concrete prestressed I-girders. Moderate strength concrete ($44.8 \text{ MPa} < f'_c < 48.5 \text{ MPa}$) was used in two of the beams. The remaining two were made of high-strength concrete (69.6 MPa). Two beams were tested without stirrups, and two beams contained the minimum amount of transverse reinforcement required by the AASHTO LRFD. These beams would also meet minimum requirements for shear reinforcement in the AASHTO Standard Specifications / ACI 318-95 Code.

For each beam, the strains on the transverse reinforcement, longitudinal reinforcement, prestressed reinforcement and concrete surface were measured. Load and deflection were also measured for each test.

All specimens experienced web-shear failures. The two specimens without transverse reinforcement (PC6N and PC10N) developed one major web-shear crack in each shear span prior to collapse. The remaining two specimens with minimum amount of transverse reinforcement (PC6S and PC10S) developed three major web-shear cracks and minor flexure-shear cracks in each shear span prior to failure. No slip of the

prestressed reinforcement was measured at the ends. An approximately 1-meter overhang was provided behind the support centerline to provide additional anchorage to the prestressing steel. All specimens had smooth crack surfaces.

A comparison of the measured shear capacity with code/specification-estimated shear capacities (AASHTO LRFD and ACI 318-95/AASHTO Standard) for each specimen was conducted. In all cases, the measured shear capacities exceeded the code/specification-estimated capacities.

7.2 Conclusions

7.2.1 Material Issues

Based on the results obtained in this research the following can be concluded:

1. Good quality concrete can be produced using Haydite and Minergy aggregates.
2. Haydite aggregate concrete produced higher strengths than Minergy aggregate.
3. An adequate procedure for pre-conditioning of LWA is necessary for the production of good quality concrete.
4. The water-cement ratio based method of mixture proportioning of LWC is far superior than the volumetric method.
5. When developing LWC with strengths in the 69 MPa (10,000 psi) range, proper control of water-cementitious ratio was critical.
6. Compressive strengths of 69 MPa (10,000 psi) can be achieved by replacing all coarse aggregate with lightweight aggregate and using natural sand as a fine aggregate.

7. Partial replacement of LWA with crushed limestone can be a good alternative to concrete with all LWA as coarse aggregate.
8. The newly developed LWC deck concrete performed much better than the reference concrete mixes.
9. Silica fume LWC performed better than LWC made with fly ash.
10. The compressive, tensile, and flexural strengths of LWC are comparable to that of concrete made with NWC. The static modulus of elasticity, dynamic modulus of elasticity, and Poisson's ratio for LWC were lower than the values for NWC.
11. The freezing and thawing resistance of LWC performed better than NWC used in this research.
12. LWC performed better when allowed a period of drying before subjecting the concrete to cycles of freezing and thawing. The test results indicated that excellent freezing and thawing resistance was achieved by allowing 14 days of air-drying.
13. LWC has excellent resistance to rapid chloride ion penetration, especially when made with a mineral admixture such as silica fume. Haydite aggregate concrete had better resistance to chloride ion penetration than Minergy aggregate concrete.
14. The resistance to scaling of LWC was satisfactory.
15. The high cement content in the high strength LWC did not result in higher than normal temperatures during the hydration period.

7.2.2 Beam Shear Strength

7.2.2.1 Reinforced Concrete Specimens

Based on the results of reinforced concrete specimens tested in this study, the following conclusions can be made:

1. Considering Specimens 1-8, the measured shear capacities (normalized to the square root of the compressive strength) of the sand-lightweight aggregate concrete beams (Specimens 5-8) were, on average, 82 % of the measured shear capacities of the companion normal-weight concrete beams (Specimens 1-4). The 0.85 reduction factor used by the current specifications does not adequately account for the reduction of shear strength in sand-lightweight aggregate concrete beams. The observed trend is important especially for the case of beams with low to minimum amounts of shear reinforcement where the concrete contribution is a larger fraction of the total shear strength. However, even Specimens 5-8 had higher measured shear capacities than those calculated using code/specification methods considered in this report.
2. The measured shear capacity (normalized to the square root of the compressive strength) of the high-strength sand-lightweight aggregate concrete beams (11-LWHD) was, 2 % larger than the measured shear capacity of the companion high-strength normal-weight concrete specimens (12-NWHD). As the concrete compressive strength increases in the range considered in this study (up to 69 MPa), the behavioral difference between lightweight aggregate concrete beams and normal weight aggregate beams decreases.

3. The AASHTO LRFD (General Method) provided conservative estimates of the shear strength for the twelve beams tested in this series. The mean ratio of measured shear capacity to estimated shear capacity was 1.24 with a standard deviation of 0.13.
4. The AASHTO LRFD (General Method) provided more conservative estimates of the shear strength of the normal weight aggregate concrete beams (Specimens 1-4 and 9: mean ratio of 1.29, standard deviation of 0.11) than the sand-lightweight aggregate concrete beams (Specimens 5-8: mean ratio of 1.1, standard deviation of 0.06).
5. The ACI 318-95/AASHTO (Simple Method) provided conservative estimates of the shear strength for the twelve beams tested in this series. The mean ratio of measured shear capacity to estimated shear capacity was 1.31 with a standard deviation of 0.13.
6. The ACI 318-95/AASHTO (Simple Method) provided more conservative estimates of the shear strength of the normal weight aggregate concrete beams (Specimens 1-4 and 9: mean ratio of 1.36, standard deviation of 0.09) than the sand-lightweight aggregate concrete beams (Specimens 5-8: mean ratio of 1.18, standard deviation of 0.06). Hence, the degree of conservatism in the calculated capacities decreases for moderate-strength lightweight aggregate concrete beams.
7. In all twelve cases, the ACI 318-95/AASHTO (Simple Method) produced estimates of shear strength 6% more conservative than did the AASHTO LRFD (General Method).

7.2.2.2 Prestressed Concrete Specimens

Based on the results of prestressed concrete specimens tested in this study, the following conclusions can be made:

1. The beams without stirrups had the same failure crack pattern. The failure pattern was represented by a major web-shear crack extending from the point of application of load towards the support. The first web-shear crack appeared at a shear of 317 kN for Specimen PC6N and 440 kN for Specimen PC10N. The failure shears were 356 kN and 465 kN, respectively. Therefore, the concrete contribution increased with the concrete compressive strength and the measured shear capacities were higher than the calculated values.
2. The measured shear capacities of specimen PC6S and PC10S were nearly equal. Therefore, the minimum amount of transverse reinforcement prescribed by the AASHTO LRFD did not provide the same level of conservatism for the high-strength beams (69.6 MPa).
3. The AASHTO LRFD (General Method) produced conservative estimates of the shear strength of the four beams tested. The mean ratio of measured shear capacity to estimated shear capacity was 1.23 with a standard deviation of 0.15.
4. The ACI 318-95/AASHTO (Simple Method) provided conservative estimates of the shear strength for the four beams tested in this series. The mean ratio of measured shear capacity to estimated shear capacity was 1.22 with a standard deviation of 0.09.
5. In general, the degree of conservatism afforded by the AASHTO LRFD and the ACI 318-85/AASHTO were nearly equal.

7.3 Recommendations

7.3.1 Material Issues

LWC has not been widely used in bridge construction although it provides technological and economical benefits. The author hopes that this report will give information that would eventually result in more wide spread use of Haydite and Minergy aggregate in the state of Indiana. The recommendations for future use of LWC include the following:

1. Mixture proportioning should be done using the water-cementitious ratio method. Quality control of LWC is critical in order to successfully obtain high strength concrete. Accurate knowledge of the actual water cement-ratio is necessary.
2. Trial mixes should always be done at the concrete mixing facility before actually proceeding with actual construction. Of importance is the transfer of knowledge about proper batching procedures to the technicians at mix producing facility. This information would go a long way in ensuring that quality control is at an optimum level and the technicians are comfortable using the material.
3. If high performance concrete is desired, LWC containing silica fume is a viable alternative to NWC. In the case of bridge deck concrete, a water-cementitious ratio above 0.42 is not recommended. High range water reducers or normal range water reducers can be used to produce adequate workability without any significant loss of slump.

4. LWC concrete should be allowed to dry before being exposed to cycles of freezing and thawing immediately.

7.3.2 Beam Shear Strength

The following recommendations are made regarding the use of lightweight aggregate concrete beams:

1. The ACI 318-95/AASHTO procedures and the AASHTO LRFD (General Method) procedure to estimate the shear capacity were shown conservative for LWC reinforced and prestressed beams. For the reinforced concrete specimens, AASHTO LRFD allows the engineer to use the simplified procedure to estimate shear strength. This simplified procedure is nearly identical to that of ACI 318-95/AASHTO. The degree of conservatism for the AASHTO LRFD and the ACI 318-95/AASHTO Standard Specifications is essentially the same.
2. More research is needed in the area of high-strength, lightweight aggregate prestressed beams, especially with regard to the minimum amount of transverse reinforcement needed. This is proposed because the same minimum amount results in a lower ratio of measured/calculated capacity as the concrete compressive strength is increased. The limited number of tests in this study does not permit to make a concrete proposal at this time.
3. All the prestressed specimens had additional 1-meter anchorages of the prestressing steel behind the centerline of the support. All the observations presented in this study regarding shear strength and behavior of this type of member are contingent on providing an adequate amount and proper anchorage of

longitudinal tension reinforcement at the support. The AASHTO LRFD Specifications provide guidelines regarding the calculation of the proper amount of tension reinforcement required for shear. Regarding the anchorage of mild reinforcement, the AASHTO LRFD Specifications account for LWC in the development length calculations. However, this is not the case for bonded prestressing strand. It is recommended that a study be conducted to assess a possible reduction in bond strength with sand-lightweight aggregate concrete.

LIST OF REFERENCES

LIST OF REFERENCES

AASHTO. LRFD Standard Specifications for Highway Bridges. First Edition. The American Association of State Highway and Transportation Officials. Washington, D.C., 1994.

AASHTO. Standard Specifications for Highway Bridges. Fifteenth Edition. The American Association of State Highway and Transportation Officials. Washington, D.C., 1992.

AASHTO. Standard Specifications for Highway Bridges. Sixteenth Edition. The American Association of State Highway and Transportation Officials. Washington, D.C., 1995.

ACI Committee 318, "Building Code Requirements for Reinforced Concrete (ACI 318-89) and Commentary – ACI 318 R-89," American Concrete Institute, Detroit, 1989, 353 pp.

ACI Committee 318, "Building Code Requirements for Structural Concrete (ACI 318-95) and Commentary – ACI 318 R-95," American Concrete Institute, Detroit, 1989, 369 pp.

ACI 116 R –90, "Cement and Concrete Terminology," American Concrete Institute, Detroit Michigan, 1990.

ACI 211.2-91, "Standard Practice for Selecting Proportions for Structural Lightweight Concrete," American Concrete Institute, Detroit MI, 1991, 14 pp.

ACI 213R-87, "Guide for Structural Lightweight Aggregate Concrete," American Concrete Institute, Detroit MI. 1987, 27 pp.

ACI-ASCE Committee 326, "Shear and Diagonal Tension ACI-ASCE Committee 326 Report, 1960, 124 pp.

ACI-ASCE Committee 426, "Shear Strength of Reinforced Concrete Members," Journal of the Structural Division, ASCE, Vol. 99, No. ST6, June 1973, pp.1091-1187.

Advanced Building Technologies-Autoclaved Aerated Concrete, "Advanced Technologies for Buildings," <http://www.advancedbuildings.org/aerocon.htm>

Standard Practice for Selecting Proportions for Structural Lightweight Concrete. ACI 211.2-91.

Guide for Structural Lightweight Aggregate Concrete. ACI 213R-87.

Ahmad, Shuaib H., and Barker, Roy, "Flexural Behavior of Reinforced High-Strength Lightweight Concrete Beams," ACI Structural Journal, January-February 1991, pp. 69-77.

Ahmad, S.H.; Xie, Y.; and Yu, T., "Shear Strength of Reinforced Lightweight Concrete Beams of Normal and High Strength Concrete," Magazine of Concrete Research, Vol. 46, No. 166, March 1994, pp. 57-66.

Caltrans and Pacific Custom Materials, "International Symposium on Lightweight Concrete Bridges", Sacramento, California, September 10, 1996, 9 pp.

CEB-FIP, Model Code for Concrete Structures: CEB-FIP International Recommendations, 3rd Ed., Comité Euro-International du Béton, Paris, 1978, 348 pp.

Collins, M.P., and Mitchell, D., *Prestressed Concrete Structures*, Prentice-Hall, Inc., Englewood Cliffs, N.J., 1991, 766 pp.

Department of Commerce. "Creep and Drying Shrinkage of Lightweight and Normal Weight Concretes", National Bureau of Standards, NBS Monograph 74, 1974, 30 pp.

Diamond, S., Huang, J. The Interfacial Transition Zone: Reality or Myth? Rilem 2nd International Conference on the Interfacial Zone in Cementitious Composites, Haifa, Israel, 1998.

Elzanaty, A.H.; Nilson, A.H.; and Slate, F.O., "Shear Capacity of Prestressed Beams Using High-Strength Concrete," ACI Journal, May-June 1986, pp.359-368.

Environmental Building News. "Autoclave Aerated Concrete: Is North America Finally Ready," Vol. 5, No.2 March/April 1996.

Expanded Shale, Clay and Slate Institute. Back-Up Statistics to Building Bridges. Information Sheet # 470.4, Salt Lake City, Utah, 16 pp.

Expanded Shale, Clay and Slate Institute. "Building Bridges with Structural Lightweight Aggregate Concrete" Salt Lake City, Utah, 6 pp.

Expanded Shale Clay and Slate Institute. Lightweight Concrete: History, Application, Economics. National Press Building, Washington, D.C., 1971, 44 pp.

Expanded Shale, Clay and Slate Institute. Rotary Kiln Produced Lightweight Aggregate for Geotechnical Applications. Publication # 6600, Salt Lake City, Utah, 4 pp.

Fergestad, S., Jordet, E. A., Nielsen, K. H., Walstad, T. An Evaluation of the Economical and Technical Potential of High-Strength Concrete in Long-Span Concrete Bridge Construction. Nordisk Betong, 1988.

Grutzeck, M., "AAC at Penn State," <http://www.personal.psu.edu/faculty/g/u/gul>

Hamadi, Y.D., and Regan, P.E., "Behaviour in Shear of Beams with Flexural Cracks," Magazine of Concrete Research, Vol. 32, No. 111, June 1980, pp. 67-78.

Harding, M. A., Structural Lightweight Aggregate Concrete. Concrete Construction, July 1995.

Holm., Thomas A. Lightweight Concrete and Aggregate. Standard Technical Publication 169C. American Society of Testing and Materials.

Holm, T., A., "Structural Lightweight Concrete Bridge Redecking", *Concrete Construction*, August, 1985, 4 pp.

Holm, T., A., "Physical Properties of High Strength Lightweight Aggregate Concretes," Second International Congress on Lightweight Concrete, London U.K., April 1980, 10 pp.

Holm, Thomas A., and Bremmer, T. W., De Souza, H. Aggregate-Matrix Interaction in Concrete Subjected to Severe Exposure. Proceedings of The FIP/CPCI Symposia, Canada, August 25-31, 1984.

Holm, Thomas A., and Bremmer, T. W., Newman, J. B. Lightweight Concrete Subject to Severe Weathering. Concrete International, ACI, June 1984.

Holm, Thomas A., and Vaysburd, A. M., Structural Lightweight Aggregate Performance. ACI SP-136, 1992, 424 pp.

Hwang, Jiann-Yang, and Song, M., X., "Replacing Al Powder with Al Slag or Recycled Foil in Cellular Concrete," *JOM*, Vol. 49 n8, August 1997, pp 29-30.

Hydraulic Press Brick Company. "The Production Process: The Haydite Story. From Raw Shale to Consumer Product", Data Sheet. Brooklyn, IN, 2 pp.

The Indian Concrete Journal, "Foamed Concrete Becomes Popular," Notes of The Month, Vol. 63, No. 4, April 11, 1989, pp 169-170.

Kaufman, K.M., and Ramirez, J.A., "Re-evaluation of the Ultimate Shear Behavior of High-Strength Concrete Prestressed I-Beams," ACI Structural Journal, May-June 1988, pp. 295-303.

Kong, P.Y.L., and Rangan, B.V., "Studies on Shear Strength of High Performance Concrete Beams," Research Report No. 2/97, School of Civil Engineering, Curtin University of Technology, Perth, Western Australia, March 1997, 163 pp.

Latona, M., C., Neufeld, R., D., Vallejo, and L., E., Brandon, D., "Leachate and Radon Production from Fly Ash Autoclaved Cellular Concrete", *Journal of Energy Engineering*, Vol. 123, No. 2, August 1997, pp 55-67.

MacGregor, J.G.; Sozen, M.A.; and Siess, C.P., "Strength of Prestressed Concrete Beams with Web Reinforcement," *Journal of the American Concrete Institute*, December 1965, pp. 1503-1518.

Mehta, P., K., and Monteiro, P. J. M. *Concrete: Structure, Properties, and Materials*, Second Edition. Prentice Hall, 1993.

Mindness, S., Young, J. *Concrete*. Prentice-Hall, Inc. 1982.

Lightweight Aggregate from Fly Ash and Waste Water Sludges. Minergy Corporation, Wisconsin Energy Corporation. Internet Website.

Minergy Corporation, "Lightweight Aggregate From Fly Ash and Waste Water Sludges," Wisconsin Energy Corporation, <http://www.minerals.com/minergy/>

Minergy Corporation. "Minergy Lightweight Aggregate", Data Sheet, Wisconsin Energy Corporation, Milwaukee, WI, 2 pp.

Mor, Avi, "Steel-Concrete Bond in High-Strength Lightweight Concrete," *ACI Materials Journal*, January-February 1992, pp. 76-82.

Murillo, S., Thoman, S., Smith, D. Lightweight Concrete for a Segmental Bridges. *Civil Engineering*, ASCE, Vol. 65, No. 5, May 1994.

Neville, A.M., *Properties of Concrete*, John Wiley and Sons, Inc., 605 Third Avenue, New York, N.Y., 1997, 844 pp.

Raithby, K. D., Lydon, F. D. Lightweight Concrete in Highway Bridges. *The International Journal of Cement Composites and Lightweight Concrete*. Vol. 2, No. 3, May 1981.

Roberts, J. E. "Structural Lightweight Concrete Bridges". *American Segmental Bridges Institute*, Vol. 37, Fall 1997, 16 pp.

Salandra, M.A., and Ahmad, S.H. "Shear Capacity of Reinforced Lightweight High-Strength Concrete Beams," *ACI Structural Journal*, November-December 1989, pp.697-704.

Sarkar, S., L., Chandra, S., and Berntsson, L., "Interdependence of Microstructure and Strength of Structural Lightweight Aggregate Concrete", *Cement and Concrete composites*, Vol. 14, 1992, pp. 239-248.

Solis, M., "Autoclaved Cellular Concrete for Residential Construction," *Concrete International: Design and Construction*, Vol. 12, No. 9, September, 1990, pp 41-44.

Swamy, R., N., and Lambert, G., H., "The Microstructure of Lytag aggregate." *The International Journal of Cement Composites and Lightweight Concrete*, Vol. 3, No. 4, Nov. 1981.

U.S. Department of Transportation. Criteria For Designing Lightweight Concrete Bridges, Report No. FHWA/RD-85/045, 1988, 146 pp.

Vecchio, F.J., and Collins, M.P., "The Modified Compression Field Theory for Reinforced Concrete Elements Subjected to Shear," *ACI Journal*, Vol. 83, No. 2, Mar.-Apr. 1986, pp. 219-231.

Vecchio, F.J., and Collins, M.P., "The Response of Reinforced Concrete To In-Plane Shear and Normal Stresses," Publication No. 82-03, Department of Civil Engineering, University of Toronto, Mar. 1982, 332 pp.

Walraven, J., and Al-Zubi, N., "Shear Capacity of Lightweight Concrete Beams with Shear Reinforcement," *International Symposium on Structural Lightweight Concrete*, Sandefjord, Norway, June 20-24, 1995, pp. 94-104.

Wasserman, R. and Bentur, A., "Interfacial Interactions in Lightweight Aggregate Concrete and Their Influence on the Concrete Strength", *Cement and Concrete Composites*, Vol. 18, 1996, pp 67-76.

Zhang, Min-Hong, and Gjorv, O., E., "Microstructure of The Interfacial Zone Between Lightweight Aggregate and Cement Paste", *Cement and Concrete Research*, Vol. 20, 1990, pp. 610-618.

Zhang, Min-Hong, Gjorv, O., E., "Pozzolanic Reactivity of Lightweight Aggregates," *Cement and Concrete Research*, Vol. 20, 1990, pp. 884-890.

Zhang, M., and Gjörv, O. E., "Characteristics of Lightweight Aggregates for High-Strength Concrete", *ACI Materials Journal*, March-April, 1991, pp. 150-158.

Zhang, M., and Gjorv, O., E. "Penetration of Cement Paste Into Lightweight Aggregate," *Cement and Concrete Research*, vol. 22, 1992, pp 47-55.

Zhang, M. H., Gjorv, O. E. "Development of High-Strength Lightweight Concrete". ACI SP 121-32, American Concrete Institute, Detroit, MI, pp. 667-681.

APPENDICES

Appendix A. AASHTO LRFD Tables

Table A.1 Reproduction of Table 5.8.3.4.2-1 of 1994 AASHTO LRFD with 1997
Interim Revisions

$\frac{\nu}{f'_c}$	$\epsilon_x \times 1,000$										
	-0.2	-0.15	-0.1	0	0.125	.25	0.5	0.75	1	1.5	2
≤ 0.05	27.0 6.78	27.0 6.17	27.0 5.63	27.0 4.88	27.0 3.99	28.5 3.49	29.0 2.51	33.0 2.37	36.0 2.23	41.0 1.95	43.0 1.72
0.075	27.0 6.78	27.0 6.17	27.0 5.63	27.0 4.88	27.0 3.65	27.5 3.01	30.0 2.37	33.5 2.33	36.0 2.23	40.0 1.90	42.0 1.65
0.1	23.5 6.50	23.5 5.87	23.5 5.31	23.5 3.26	24.0 2.61	26.5 2.54	30.5 2.41	34.0 2.28	36.0 2.16	38.0 1.72	39.0 1.45
0.125	20.0 2.71	21.0 2.71	22.0 2.71	23.5 3.26	26.0 2.57	28.0 2.50	31.5 2.37	34.0 2.18	36.0 2.09	37.0 1.60	38.0 1.35
0.15	22.0 2.66	22.5 2.61	23.5 2.61	25.0 2.55	27.0 2.50	29.0 2.45	32.0 2.28	34.0 2.06	36.0 2.01	36.5 1.50	37.0 1.24
0.175	23.5 2.59	24.0 2.58	25.0 2.54	26.5 2.50	28.0 2.41	30.0 2.39	32.5 2.20	34.0 1.95	35.0 1.74	35.5 1.35	36.0 1.11
0.2	25.0 2.55	25.5 2.49	26.5 2.48	27.5 2.45	29.0 2.37	31.0 2.33	33.0 2.10	34.0 1.82	34.5 1.58	35.0 1.21	36.0 1.00
0.225	26.5 2.45	27.0 2.38	27.5 2.43	29.0 2.37	30.5 2.33	32.0 2.27	33.0 1.92	34.0 1.67	34.5 1.43	36.5 1.18	39.0 1.14
0.25	28.0 2.36	28.5 2.36	29.0 2.32	30.0 2.30	31.0 2.28	32.0 2.01	33.0 1.64	34.0 1.52	35.5 1.40	38.5 1.30	41.5 1.25

Table A.2 Reproduction of Table 5.8.3.4.2-2 of 1994 AASHTO LRFD with 1997
Interim Revisions

s_x	$\epsilon_x \times 1,000$								
	-0.2	-0.1	0	0.25	0.5	0.75	1	1.5	2
≤ 130	26.0 6.90	26.0 5.70	27.0 4.94	29.0 3.78	31.0 3.19	33.0 2.82	34.0 2.56	36.0 2.19	38.0 1.93
250	27.0 6.77	28.0 5.53	30.0 4.65	34.0 3.45	37.0 2.83	39.0 2.46	40.0 2.19	43.0 1.87	45.0 1.65
380	27.0 6.57	30.0 5.42	32.0 4.47	37.0 3.21	40.0 2.59	43.0 2.23	45.0 1.98	48.0 1.65	50.0 1.45
630	8.0 6.24	31.0 5.36	35.0 4.19	41.0 2.85	45.0 2.26	48.0 1.92	51.0 1.69	54.0 1.40	57.0 1.18
1270	31.0 5.62	33.0 5.24	38.0 3.83	48.0 2.39	53.0 1.82	57.0 1.50	59.0 1.27	63.0 1.00	66.0 0.83
2500	35.0 4.78	35.0 4.78	42.0 3.47	55.0 1.88	62.0 1.35	66.0 1.06	69.0 0.87	72.0 0.65	75.0 0.52
5000	42.0 3.83	42.0 3.83	47.0 3.11	64.0 1.39	71.0 0.90	74.0 0.66	77.0 0.53	80.0 0.37	82.0 0.28

Appendix B. Derivation of AASHTO LRFD Equations

The ASSHTO LRFD general procedure for determining the shear strength of reinforced and prestressed concrete beams is derived in this section. The AASHTO LRFD equations are derived from the modified compression field theory. These equations will be summarized first. Modified compression field theory equations necessary to derive the AASHTO LRFD equations will be introduced (Collins and Mitchell, 1991). Equations referenced from Collins and Mitchell are identified with numbers in brackets.

The AASHTO LRFD estimates the nominal shear resistance of a reinforced or prestressed concrete beam as

$$V_n = V_c + V_s + V_p , \quad (\text{B.1})$$

where V_c is the nominal shear strength provided by the tensile stresses in the concrete; V_s is the nominal shear strength provided by the transverse reinforcement; and V_p is the nominal shear strength provided by the component in the direction of the applied shear, of the force in the longitudinal prestressing tendons.

The concrete contribution is calculated as

$$V_c = 0.083 \beta \sqrt{f'_c} b_v d_v , \quad (\text{B.2})$$

where the term β is a factor indicating the ability of the diagonally cracked concrete to transmit tension; f'_c is the concrete compressive strength in MPa; b_v is the effective web width; and d_v is the effective shear depth.

The steel contribution is calculated as

$$V_s = \frac{A_v f_y d_v \cot \theta}{s} , \quad (\text{B.3})$$

where A_v is the area of transverse reinforcement; f_y is the yield strength of the transverse reinforcement; d_v is the effective shear depth; θ is the angle of inclination of diagonal compressive stresses; and s is the spacing of the transverse reinforcement.

The values of θ and β to be used in Equations B.2 and B.3 are determined from AASHTO LRFD Tables 5.8.3.4.2-1 and 5.8.3.4.2-2, reproduced in this appendix as Tables A.1 and A.2. These values are functions of the concrete compressive strength,

fN_c , the factored shear stress at the section, v , and the longitudinal strain in the flexural tension reinforcement, ε_x . The factored shear stress is defined as

$$v = \frac{V_u - \phi V_p}{\phi b_v d_v}, \quad (B.4)$$

where V_u is the factored shear force at the section and ϕ is the resistance factor. The resistance factor for shear is 0.9 for normal-weight concrete and 0.7 for lightweight concrete.

The strain in the reinforcement on the flexural tension side of the beam is calculated as

$$\varepsilon_x = \frac{\frac{M_u}{d_v} + 0.5 N_u + 0.5 V_u \cot \theta - A_{ps} f_{po}}{E_s A_s + E_p A_{ps}}, \quad (B.5)$$

where M_u is the factored moment at the section; N_u is the axial force; A_{ps} is the area of prestressing steel on the flexural tension side of the member; f_{po} is the stress in the prestressing steel when the stress in the surrounding concrete is zero; E_s is the modulus of elasticity of the mild longitudinal steel; A_s is the area of mild longitudinal steel on the flexural tension side of the member; and E_p is the modulus of elasticity of the prestressing steel.

If the value of ε_x , calculated from Equation (B.5), is negative, the value shall be modified by multiplying by the factor F_ε calculated as

$$F_\varepsilon = \frac{E_s A_s + E_p A_{ps}}{E_c A_c + E_s A_s + E_p A_{ps}}, \quad (B.6)$$

where E_c is the modulus of elasticity of the concrete and A_c is the area of the concrete on the flexural tension side of the member. The preceding AASHTO LRFD equations are derived in the next part of this section.

The form of Equation (B.1) was chosen to resemble the traditional expressions for shear strength. These expressions usually contain contributions to the shear strength from the concrete, transverse reinforcement, and the prestressing force. In order to apply the modified compression field theory to design, a number of simplifying assumptions need to be made.

In order to derive the concrete contribution given in Equation (B.2), the following equation developed in the modified compression field theory is considered:

$$V = f_1 b_w j d \cot \theta + \frac{A_v f_v}{s} j d \cot \theta. \quad [7-28]$$

where f_1 is the principal tensile stress in the concrete; b_w is the width of the web; jd is the flexural arm; θ is the angle of inclination of principal compressive stress (or assumed angle of crack inclination); A_v is the area of web reinforcement; f_v is the stress in the web reinforcement; and s is the spacing of the web reinforcement. Equation [7-28] is an expression for the shear resistance of a reinforced concrete member. The concrete contribution is taken as the first component of Equation [7-28]:

$$V_c = f_1 b_w j d \cot \theta, \quad (B.7)$$

where the principal tensile stress in the concrete is calculated as

$$f_1 = \frac{\alpha_1 \alpha_2 f_{cr}}{1 + \sqrt{500 \varepsilon_1}}, \quad [7-31]$$

where α_1 and α_2 are factors accounting for the bond characteristics of the reinforcement and the type of loading; f_{cr} is the concrete cracking stress; and ε_1 is the principal tensile strain. Assuming that the cracking stress, f_{cr} , equals $0.33 \sqrt{f'_c}$ MPa, then Equation [7-31] becomes

$$f_1 = \frac{\alpha_1 \alpha_2 0.33 \sqrt{f'_c}}{1 + \sqrt{500 \varepsilon_1}}. \quad (B.8)$$

Substituting the value of f_1 from Equation (B.8) into Equation (B.7) results in

$$V_c = \frac{\alpha_1 \alpha_2 0.33 \cot \theta}{1 + \sqrt{500 \varepsilon_1}} b_w j d \sqrt{f'_c}, \quad (B.9)$$

where it is assumed that

$$0.083 \beta = \frac{\alpha_1 \alpha_2 0.33 \cot \theta}{1 + \sqrt{500 \varepsilon_1}}. \quad (B.10)$$

Assuming that $b_w = b_v$ and $jd = d_v$, the concrete contribution may now be rewritten as

$$V_c = 0.083 \beta \sqrt{f'_c} b_v d_v, \quad (B.11)$$

which is the AASHTO LRFD equation for the shear strength provided by the concrete given in Equation (B.2).

The AASHTO LRFD steel contribution to the shear strength may be derived from Equation [7-28] shown above in which the steel contribution is taken as

$$V_s = \frac{A_v f_v}{s} j d \cot \theta. \quad (\text{B.12})$$

Assuming that the stirrups yield at failure ($f_v = f_{vy}$) and that $j d = d_v$, the following equation is derived:

$$V_s = \frac{A_v f_y d_v \cot \theta}{s}, \quad (\text{B.13})$$

which is the AASHTO LRFD equation for the shear strength provided by the transverse reinforcement given in Equation (B.3).

The values of θ and β are determined from the AASHTO LRFD tables reproduced in this appendix as Tables A.1 and A.2. The derivation of the values used for β is the subject of the next part of this section. Solving for β in Equation (B.10) results in

$$\beta = \frac{\alpha_1 \alpha_2 4 \cot \theta}{1 + \sqrt{500 \varepsilon_1}}. \quad (\text{B.14})$$

As the principal tensile strain increases, the value of β decreases. However, the rate of decrease of β is not only a function of the principal tensile strain. If the inclined cracks are too wide, the average tension in the concrete will be limited by the mechanisms that transmit the forces across the cracks (i.e. aggregate interlock). In particular, the shear stress along the crack surfaces, v_{ci} , become critical. To avoid such crack slipping failures β must be limited. The following equations will be used to derive this limit to the value of β :

$$V_c = f_1 b_w j d \cot \theta, \quad (\text{B.7})$$

$$v_{ci} \leq \frac{0.18 \sqrt{f'_c}}{0.3 + \frac{24 w}{a + 16}}, \quad [7-32b]$$

$$f_1 = v_{ci} \tan \theta + \frac{A_v}{s b_v} (f_{vy} - f_v), \text{ and} \quad [7-33]$$

$$w = \varepsilon_1 s_{m\theta}, \quad [7-34]$$

where v_{ci} is the limiting value of the local shear stress; w is the average crack width in millimeters; $s_{m\theta}$ is the average crack spacing in millimeters; and a is the maximum aggregate size in millimeters.

Assuming that the stirrups yield at failure ($f_v = f_{vy}$), Equation [7-33] becomes

$$f_1 = v_{ci} \tan \theta. \quad (B.15)$$

Under the assumptions that $b_w = b_v$ and $jd = d_v$, combining Equations (B.7) and (B.2) results in

$$f_1 b_v d_v \cot \theta = 0.083 \beta \sqrt{f'_c} b_v d_v. \quad (B.16)$$

Solving Equation (B.16) for β results in

$$\beta = \frac{f_1 \cot \theta}{0.083 \sqrt{f'_c}}. \quad (B.17)$$

Substituting Equation (B.15) into Equation (B.17) results in

$$\beta = \frac{v_{ci}}{0.083 \sqrt{f'_c}}. \quad (B.18)$$

Substituting Equation [7-34] into [7-32b] results in

$$v_{ci} \leq \frac{0.18 \sqrt{f'_c}}{0.3 + \frac{24 \varepsilon_1 s_{m\theta}}{a + 16}}. \quad (B.19)$$

Substituting Equation (B.19) into Equation (B.18) results in

$$\beta \leq \frac{2.16}{0.3 + \frac{24 \varepsilon_1 s_{m\theta}}{a + 16}}, \quad (B.20)$$

which is the upper limit to the value of β . Therefore, the complete expression for β is calculated by the following expression:

$$\beta = \frac{\alpha_1 \alpha_2 4 \cot \theta}{1 + \sqrt{500 \varepsilon_1}} \leq \frac{2.16}{0.3 + \frac{24 \varepsilon_1 s_{m\theta}}{a + 16}}. \quad (B.21)$$

Based on Equations (B.13) and (B.19), the value of β , and therefore the value of the V_c , decrease as the principal tensile strain, ϵ_1 , increases. In order to calculate β , ϵ_1 needs to be determined. Consider the following equations:

$$\tan^2 \theta = \frac{\epsilon_x - \epsilon_2}{\epsilon_t - \epsilon_2} \quad \text{and} \quad [7-23]$$

$$\epsilon_t = \epsilon_x + \epsilon_t - \epsilon_2, \quad [7-24]$$

where ϵ_x is taken as the longitudinal strain in the flexural tension reinforcement; ϵ_2 is the principal compressive strain; and ϵ_t is the average strain in the transverse direction.

Solving for ϵ_t in Equation [7-23] results in

$$\epsilon_t = \epsilon_1 + \epsilon_2 - \epsilon_x. \quad (B.22)$$

Substituting ϵ_t into Equation [7-24] results in

$$\tan^2 \theta = \frac{\epsilon_x - \epsilon_2}{\epsilon_1 + \epsilon_2 - \epsilon_x - \epsilon_2} = \frac{\epsilon_x - \epsilon_2}{\epsilon_1 - \epsilon_x}. \quad (B.23)$$

Solving for ϵ_1 in Equation (B.23) results in

$$\epsilon_1 = \epsilon_x + (\epsilon_x - \epsilon_2) \cot^2 \theta. \quad (B.24)$$

The principal tensile strain is now a function of the longitudinal strain, principal compressive strain, and the angle of inclination of principal compressive stresses.

The principal compressive strain, ϵ_2 , depends on the magnitude of the principal compressive stress, f_2 . The magnitude of the principal compressive stress can be conservatively estimated as

$$f_2 = (\tan \theta + \cot \theta) v, \quad (B.25)$$

where the principal tensile stresses are taken equal to zero ($f_1 = 0$).

The following expression is suggested to represent the stress-strain relationship of diagonally cracked concrete (Collins and Mitchell, 1991):

$$f_2 = f_{2\max} \left[2 \left(\frac{\epsilon_2}{\epsilon'_c} \right) - \left(\frac{\epsilon_2}{\epsilon'_c} \right)^2 \right]. \quad [7-26]$$

Assuming that the compressive strain, ϵ'_c , at which the concrete reaches its peak stress is equal to -0.002 , Equation [7-26] can be rearranged to give

$$\frac{f_2}{f_{2\max}} = 2\left(\frac{\varepsilon_2}{-0.002}\right) - \left(\frac{\varepsilon_2}{-0.002}\right)^2. \quad (\text{B.26})$$

Solving Equation (B.26) for ε_2 results in

$$\varepsilon_2 = -0.002\left(1 - \sqrt{1 - \frac{f_2}{f_{2\max}}}\right), \quad (\text{B.27})$$

where

$$f_{2\max} = \frac{f'_c}{0.8 + 170\varepsilon_1}. \quad (\text{B.28})$$

Equation (B.28) was suggested as a maximum value to the principal concrete compressive stress (Collins and Mitchell, 1991).

If we substitute the expression for ε_2 given by Equation (B.28) into Equation (B.24), the following equation is obtained:

$$\varepsilon_1 = \varepsilon_x + \left[\varepsilon_x + 0.002\left(1 - \sqrt{1 - \frac{f_2}{f_{2\max}}}\right) \right] \cot^2 \theta. \quad (\text{B.29})$$

If we now substitute the expressions for f_2 and $f_{2\max}$ from Equations (B.25) and (B.26) into Equation (B.29), we obtain the following quadratic equation for ε_1 :

$$\varepsilon_1 = \varepsilon_x + \left[\varepsilon_x + 0.002\left(1 - \sqrt{1 - \frac{v}{f'_c}(\tan\theta + \cot\theta)(0.8 + 170\varepsilon_1)}\right) \right] \cot^2 \theta. \quad (\text{B.30})$$

If the values ε_x , θ , and $\frac{v}{f'_c}$ are known, than the value of ε_1 is calculated from Equation (B.30).

Because the AASHTO LRFD is a design code, to be conservative, the longitudinal strain, ε_x , is taken as the strain at the level of the flexural tension reinforcement. The location of ε_x is shown in Figure B.1 (similar to AASHTO LRFD Figure 5.8.3.4.2-3). The strain depends on the flexural moment, axial force, shear force and prestressing force, as well as the amount of mild and prestressing longitudinal reinforcement. The flexural force is a function of the flexural moment and the effective depth. Half of the axial force is assumed resisted by the longitudinal reinforcement in the flexural tension side of the member. The value of the longitudinal strain is calculated by

$$\varepsilon_x = \frac{\frac{M_u}{d_v} + 0.5 N_u + 0.5 V_u \cot \theta - A_{ps} F_{po}}{E_s A_s + E_p A_{ps}}. \quad (\text{B.31})$$

If the value of ε_x given by Equation (B.30) is negative, the value shall be modified by multiplying by the factor F_ε calculated as

$$F_\varepsilon = \frac{E_s A_s + E_p A_{ps}}{E_c A_c + E_s A_s + E_p A_{ps}}. \quad (\text{B.32})$$

A negative value of ε_x indicates compression at the level of the tension reinforcement. Equation (B.31) neglects the stiffness of the concrete assuming that ε_x is tensile and the concrete is cracked. Ignoring the stiffness of the concrete in compression will lead to an overestimation of the compressive strain at the level of flexural tension reinforcement. This overestimation is unconservative as it will overestimate β and V_c . In order to account for the concrete stiffness in compression, a reduction factor is introduced. Equation (B.32) is simply a ratio of the stiffness provided by the steel alone to the stiffness provided by the steel and concrete. The value of ε_x is multiplied by the reduction factor.

The modified (if necessary) value of ε_x and the factored shear stress given by

$$v = \frac{V_u - \phi V_p}{\phi b_v d_v} \quad (\text{B.4})$$

are used to determine the value of θ and β . These values enable the designer to determine the steel and concrete contributions to the shear strength of reinforced and prestressed concrete beams.

Collins and Mitchell have produced tables similar to those in AASHTO LRFD to determine the values of θ and β . These tables are reproduced as Tables B.1 and B.2. For members with transverse reinforcement, the following values are assumed for the values in Table B.1: $\alpha_1 \alpha_2 = 1.0$, $s_{m\theta} = 305 \text{ mm}$, and $a = 19 \text{ mm}$.

The values of θ in Table B.1 “have been chosen to ensure that, for highly stressed members, the compressive stress in the concrete, f_2 , does not exceed the crushing strength, $f_{2 \text{ max}}$ and that the strain in the web reinforcement, ε_t , is at least equal to 0.002.

Within the possible range of values for θ , the values chosen will result in close to the minimum amount of shear reinforcement” (Collins and Mitchell, 1991).

For members without transverse reinforcement, the values of θ and β are functions of the longitudinal strain, ϵ_x , and the crack spacing parameter, s_{mx} . As in the case of a beam with transverse reinforcement, $\alpha_1\alpha_2$ is taken equal to 1.0 and a is taken equal to 19 mm.

The spacing of inclined cracks, $s_{m\theta}$, can be determined by

$$s_{m\theta} = \frac{1}{\left(\frac{\sin\theta}{s_{mx}} + \frac{\cos\theta}{s_{mv}} \right)}, \quad [7-35]$$

where s_{mx} and s_{mv} are the crack spacings in the longitudinal and transverse directions, respectively. If there is no transverse reinforcement, s_{mv} becomes infinity. Equation [7-35] becomes

$$s_{m\theta} = \frac{s_{mx}}{\sin\theta}, \quad (B.33)$$

where s_{mx} is the spacing of the vertical cracks.

The values of θ given in Table B.2 “are those that result in the highest value of β ” (Collins and Mitchell, 1991).

Table B.1 Reproduction of Table 7-3 of Collins and Mitchell
Values of θ and β for Members with Web Reinforcement

Shear Stress v/f N_c		Longitudinal Strain $\epsilon_x \times 1,000$									
		0	0.25	0.50	0.75	1.00	1.50	2.00	2.50	3.00	5.00
≤ 0.050	θ	28.0	31.0	34.0	36.0	38.0	41.0	43.0	45.0	46.0	56.0
	β	5.24	3.70	3.01	2.62	2.33	1.95	1.72	1.54	1.39	0.92
0.075	θ	28.0	30.0	30.0	34.0	36.0	40.0	42.0	43.0	43.0	56.0
	β	4.86	3.31	2.48	2.37	2.15	1.90	1.65	1.44	1.25	0.92
0.100	θ	22.0	26.0	30.0	34.0	36.0	38.0	38.0	38.0	38.0	55.0
	β	2.71	2.42	2.31	2.27	2.08	1.72	1.39	1.16	1.00	0.95
0.125	θ	23.0	27.0	31.0	34.0	36.0	36.0	36.0	36.0	36.0	55.0
	β	2.40	2.33	2.29	2.16	2.00	1.52	1.23	1.03	0.88	0.94
0.150	θ	25.0	28.0	31.0	34.0	34.0	34.0	34.0	34.0	35.0	55.0
	β	2.53	2.25	2.13	2.06	1.73	1.30	1.04	0.85	0.77	0.94
0.175	θ	26.0	29.0	32.0	32.0	32.0	32.0	34.0	36.0	38.0	54.0
	β	2.34	2.19	2.11	1.69	1.40	1.01	0.94	0.91	0.88	0.96
0.200	θ	27.0	30.0	33.0	34.0	34.0	34.0	37.0	39.0	41.0	53.0
	β	2.34	2.13	2.09	1.82	1.52	1.08	1.11	1.04	0.99	0.98
0.225	θ	28.0	31.0	34.0	34.0	34.0	37.0	39.0	42.0	44.0	-
	β	1.97	2.07	2.08	1.67	1.35	1.29	1.17	1.16	1.09	-
0.250	θ	30.0	32.0	34.0	35.0	36.0	39.0	42.0	45.0	49.0	-
	β	2.26	2.00	1.87	1.63	1.45	1.37	1.32	1.28	1.24	-

Table B.2 Reproduction of Table 7-4 of Collins and Mitchell
Values of θ and β for Members without Web Reinforcement

Spacing Parameter s_{mx} , mm		Longitudinal Strain $\epsilon_x \times 1,000$									
		0	0.25	0.50	0.75	1.00	1.50	2.00	2.50	3.00	5.00
125	θ	27.0	30.0	32.0	33.0	34.0	36.0	38.0	39.0	40.0	43.0
	β	4.89	3.74	3.19	2.81	2.55	2.19	1.95	1.77	1.63	1.27
250	θ	30.0	34.0	37.0	39.0	41.0	43.0	45.0	47.0	48.0	52.0
	β	4.65	3.40	2.83	2.46	2.21	1.87	1.64	1.48	1.35	1.03
380	θ	32.0	37.0	41.0	43.0	45.0	48.0	50.0	52.0	53.0	58.0
	β	4.47	3.15	2.59	2.23	1.99	1.67	1.45	1.30	1.17	0.87
630	θ	35.0	42.0	46.0	49.0	51.0	54.0	57.0	59.0	61.0	65.0
	β	4.24	2.82	2.27	1.90	1.70	1.39	1.19	1.05	0.94	0.67
1270	θ	38.0	48.0	53.0	57.0	60.0	64.0	66.0	69.0	70.0	75.0
	β	3.90	2.39	1.82	1.50	1.28	1.01	0.84	0.72	0.63	0.41
2540	θ	42.0	56.0	62.0	66.0	69.0	73.0	75.0	77.0	78.0	81.0
	β	3.55	1.87	1.35	1.06	0.88	0.65	0.52	0.43	0.37	0.23
5080	θ	46.0	64.0	71.0	74.0	77.0	80.0	82.0	83.0	84.0	85.0
	β	3.19	1.39	0.90	0.66	0.53	0.37	0.29	0.23	0.20	0.12

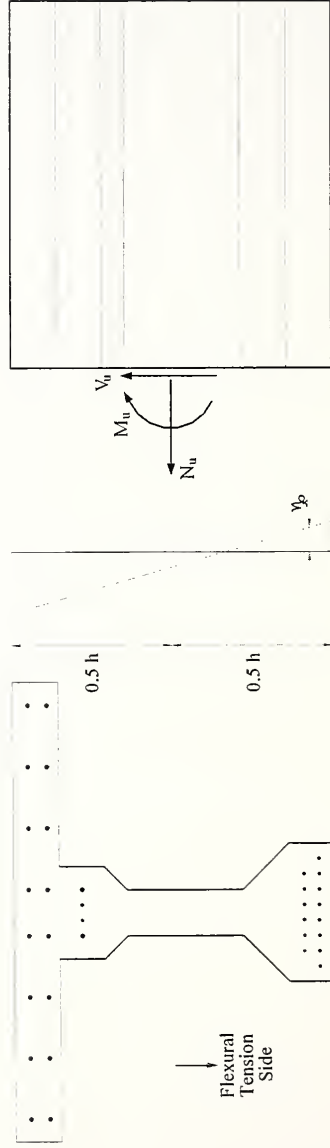


Figure B.1 Free Body Diagram of Beam (AASHTO LRFD Method)

